METAMORPHISM IN THE NORTHERN FRONT RANGE, COLORADO

Barbara J. Munn

Dissertation submitted to the Faculty of the Virginia Polytechnic Institute and State University in partial fulfillment of the requirements for the degree of

Doctor of Philosophy
in
Geological Sciences

Robert J. Tracy, Chair
Robert J. Bodnar
David A. Hewitt
Richard D. Law
Spencer Cotkin

August 20, 1997
Blacksburg, VA

Keywords:
Metamorphic Petrology, Precambrian, Anatexis, Cordierite

Metamorphism in the Northern Front Range, Colorado

Barbara J. Munn

(ABSTRACT)

Thermobarometry, detailed petrography, electron microprobe analysis and fluid inclusion microthermometry were used to quantify the history of a high grade Proterozoic terrane exposed within the northeastern Colorado Front Range. Pressure-temperature calculations identified two blocks from different crustal levels exposed adjacent to one another within the Poudre Canyon west of Fort Collins. They are the eastern, higher pressure, block (HPB; 734°C, 7.1 kbar) and the western, lower pressure, block (LPB; 655°C, 5.2 kbar). The blocks followed a clockwise uplift path and were juxtaposed by ductile shear near the end of the decompressive stage of uplift. Final assembly of the separate blocks to the same crustal level was constrained by mineralogic and textural considerations and by the isochores of identical low density CO_2 inclusions trapped by both blocks. Both blocks experienced peak metamorphism within the sillimanite-K-feldspar zone accompanied by partial melting, are characterized by stromatic migmatites, and show textural evidence for localized reactions related to decompression and cooling. Differences between the blocks include the type of melt-generating reactions and the pronounced late muscovite in the LPB. Gibbs' Method calculations indicate that local (outcrop scale) textural and mineralogical differences between HPB Mg-enriched pelites are caused by small differences in bulk composition and locally variable H_2O content. The quartzo-feldspathic biotite gneisses in the LPB generated migmatites by wet melting, whereas the pelitic schists and gneisses in the HPB generated migmatites by dehydration melting of muscovite and biotite. Biotite dehydration melting enriched the leucosomes in HPB pelitic migmatites in K-feldspar and garnet. The minor presence of late muscovite in the HPB relative to the LPB was controlled by the different positions of their uplift paths relative to the muscovite breakdown reaction.

This work received support from the Geological Society of America, Sigma Xi, the Colorado Scientific Society, and NSF grant EAR-9205823.

DEDICATION

This work is dedicated to my grandfather, John Pier Munn Jr. (1899-1992). He supported my every endeavor, large or small, and knew how to have a good laugh.

AUTHOR'S ACKNOWLEDGEMENTS

Primary thanks go to my husband, Ron Wirgart, for his technical support and for making so many sacrifices for me to complete this degree. I could not have done it without him. Thanks also to my son, Devin Wirgart, who kept me smiling as I finished writing the dissertation. I would like to acknowledge my committee members, Bob Tracy, Bob Bodnar, Dave Hewitt, Rick Law and Spencer Cotkin, for ushering me through the doctoral program. I would especially like to thank Bob Tracy for financially supporting this project, lending me his petrologic expertise, and making editorial comments on the first draft of the dissertation. Thanks also to Bob Bodnar who allowed me free use of the Fluid Inclusion Research Facility and to Brenda Kutz and Sarah Beutner who were so helpful in every way. Todd Soldberg deserves credit for the garnet X-ray and CL maps. Finally, I would like to acknowledge Tom Armstrong, Matt Nyman, Ron Sheets, Charlie Oakes, Jane Selverstone, Colin Shaw and Eileen McLellan who all gave me extra insights into this research.

TABLE OF CONTENTS

FIGURES

TABLES

I. INTRODUCTION

Objectives

The Front Range is the easternmost range of the Rocky Mountains and exposes Proterozoic age igneous and high grade metamorphic rocks (Figure 1). These rocks reveal a complex history of deformation, plutonism and metamorphism. The metamorphism reached sillimanite-K–feldspar grade and was accompanied by migmatization (Tweto, 1960, Sims et al., 1963; Hedge et al., 1967). This study seeks to answer questions about the conditions governing upper amphibolite to lower granulite facies metamorphism: (1) what were the pressures and temperatures of peak metamorphism, (2) did partial melting produce the migmatites, and (3) what type of fluids were present at that time? A fourfold approach was taken in addressing these questions, using northern Front Range rocks exposed in the Cache la Poudre River canyon (Figure 1, inset). First, detailed petrography and analysis of mineral chemistry were used to determine which minerals co-existed at peak metamorphism. Second, thermobarometric calculations were used to establish a pressure-temperature framework for the northern Front Range metamorphism. Third, field relations of the migmatites and analysis of their compositions were used to elucidate migmatite genesis. Fourth, fluid inclusion analysis was used to explore the fluid history of the area.

Regional Geology

Introduction

The Front Range forms part of the Proterozoic age Colorado province that was accreted to the Archean Wyoming province during the Early Proterozoic (Condie, 1982; Bickford et al., 1986; Reed et al., 1987). Metavolcanic and metasedimentary rocks of the Colorado province accumulated between 1700 and 1780 Ma in a probable volcanic arc or back-arc geologic setting (Bickford and Boardman, 1984; Bickford et al., 1986; Reed et al., 1987). Tectonic convergence along a southeast-dipping subduction zone thrust these rocks onto the margin of the Archean Wyoming province (Hills and Houston, 1979; Condie, 1982; Duebendorfer and Houston, 1987). The convergent zone is marked by extensive ductile shearing in the Cheyenne Belt of southern Wyoming (see Figure 1; Karlstrom and Houston, 1984). The late synkinematic Sierra Madre Granite, exposed within and just south of this suture, allows a minimum age of 1753±16 Ma to be assigned to the convergence near the Cheyenne Belt (Reed et al., 1987; Duebendorfer and Houston, 1987). Farther to the south, in the central Front Range, deformation is bracketed between 1.70 and 1.67 Ga (Reed et al., 1987; Reed et al., 1993). Thus, deformation in the northern Front Range occurred between 1.75 and 1.70 Ga. During this Early Proterozoic tectonism, the northern Front Range underwent extensive deformation, metamorphism, and igneous intrusion. The timing of the known geologic events in the northern Front Range is summarized in Table 1.

Plutonism

The Front Range rocks experienced three episodes of magmatism during the Proterozoic. The resultant plutons were grouped and renamed by Tweto (1987); his terminology is adopted here.

1.7 Ga Routt Plutonic Suite

This suite comprises the Boulder Creek Granodiorite, Rahwah Batholith, and associated plutons. In the central Front Range, the Boulder Creek Granodiorite yielded a U-Pb zircon age of 1714±6 Ma (Premo and Van Schmus, 1989) and a Rb-Sr age of 1665±40 Ma (Peterman et al., 1968). In the northern Front Range, the Rahwah Batholith (Figure 1, inset) yielded a U–Pb zircon age of 1720±8 Ma (Premo and Van Schmus, 1989). The calc-alkalic rocks of the Routt Plutonic Suite were emplaced during the deformation associated with peak metamorphism (Hedge, 1972;

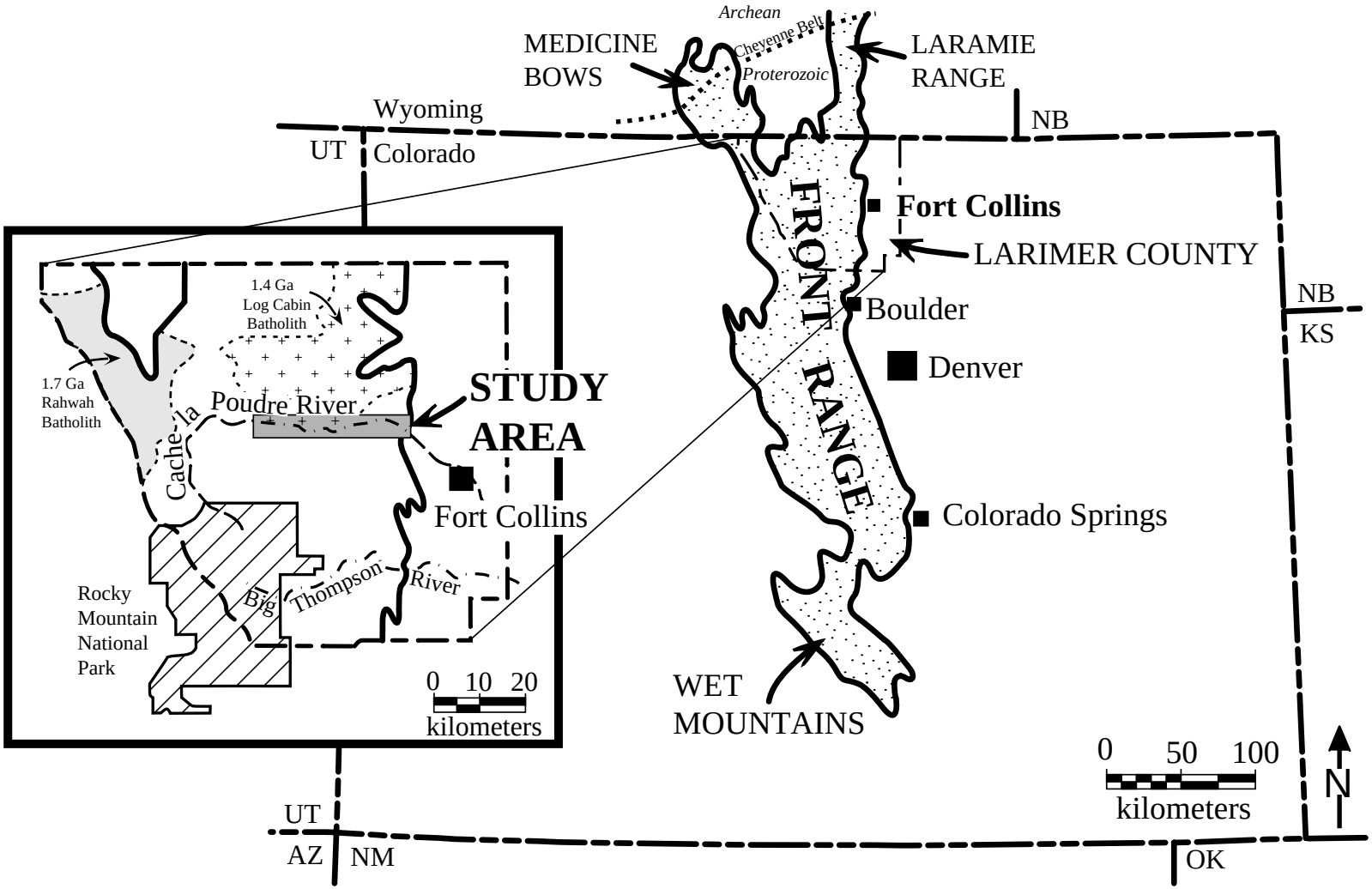

Figure 1 Map of Colorado showing the location of Precambrian exposures (stippled) in the Front Range and contiguous mountains (adapted from Sims and Sheridan, 1964). Larimer County inset shows the study area location, including the locations of significant batholiths (after Reed et al., 1993).

Peterman et al., 1968; Aleinikoff et al., 1993). These syntectonic plutons are structurally concordant, extensively foliated and lack contact aureoles. They also contain sillimanite grade xenoliths, some of which are migmatites. Therefore, migmatization must have occurred during peak metamorphism (Hedge, 1972). Wobus and Hutchinson (1988) suggested that the Routt Plutonic Suite was emplaced at depths exceeding 16 km (>4.5 kbar) in the central Front Range.

Table 1 TIMING OF EVENTS IN THE NORTHERN FRONT RANGE

~ 70 Ma	Laramide Orogeny: brittle faulting
~320 Ma	Uplift of Ancestral Rockies Onlap of Pennsylvanian sediments (major unconformity)
~500-400 Ma	Repeated epeirogenic uplift (recognized by deposition and erosion in the sedimentary record)
1.0 Ga	Pike's Peak Batholith (southern Front Range) Anorogenic; emplacement depth: 5.4 km (~1.5 kbar); 700°C
1.2 ± 0.2 Ga	Ductile shearing (Skin Gulch Shear Zone) Local recrystallization to form andalusite ± cordierite
1.4 Ga	Berthoud Plutonic Suite Discordant, generally non-foliated Emplacement depth: 9.7-11.2 km (~3 kbar); 740-760°C K-Ar ages of older rocks reset → reheating event Post-peak development of cross-muscovite and cross-biotite?
1.7 Ga	Peak metamorphism (upper amphibolite facies) Migmatization Routt Plutonic Suite (syntectonic) Structurally concordant, extensively foliated Emplacement depth exceeded 16 km (>4.5 kbar)

Sources: *Abbott, 1976; Anderson and Thomas, 1985; Barker et al., 1975; Braddock et al., 1988a; De Voto, 1980; Nesse, 1977; Peterman et al., 1968; Peterman and Hedge, 1967; Premo and Van Schmus, 1989; Ross and Tweto, 1980; Tweto, 1980a, 1980b, 1980c, 1987; Wobus and Hutchinson, 1988.*

1.4 Ga Berthoud Plutonic Suite

The Berthoud Plutonic Suite lies within a regionally extensive belt of ±1.4 Ga plutons that extends from Labrador to southern California (Anderson, 1983). In Colorado, the 1.4 Ga plutons are grouped into the Berthoud Plutonic Suite, comprising the Silver Plume Granite, Sherman Granite, and related plutons. The ages of these plutonic rocks, using Rb-Sr systematics, are as follows: Silver Plume in the type area, 1410±30 Ma (Peterman et al., 1967), Silver Plume in the Log Cabin Batholith (Figure 1, inset), 1392±30 Ma (Peterman et al., 1968), and Sherman Granite, 1430±20 Ma (Zielinski et al., 1981). In general, rocks of the Berthoud Plutonic Suite are

nonfoliated and clearly discordant with the metamorphic rocks. Some are associated with local folding (Abbott, 1970) whereas others possess a flow foliation or were foliated by intrusion along active ductile shear zones (Abbott, 1970, Graubard, 1991, and Aleinikoff et al., 1993). In a kinematic study of 1.4 Ga plutons from Arizona to Colorado, Nyman et al. (1994) suggest that these plutons represent magmatism associated with contractional or transpressional orogeny at the southern margin of Laurentia. The 1.4 Ga plutons have a crustal source (DePaolo, 1981) and their emplacement depth is believed to be shallower than that of the Routt Plutonic Suite. Anderson and Thomas (1985) suggested that the Silver Plume Granite in the central Front Range was emplaced at depths of 9.7-11.2 km (2.7-3.1 kbar) at 740-760°C.

1.0 Ga Pikes Peak Batholith

The Pikes Peak Batholith was emplaced at shallower depths than the Berthoud Plutonic Suite (~5.5 km or 1.5 kbar) in a 1020 Ma episode of anorogenic plutonism (Barker et al., 1975; Wobus and Hutchinson, 1988). The 1.0 Ga plutonism is limited to the Pikes Peak area (west of Colorado Springs) and is not observed in the northern Front Range. The successively shallower emplacement depths of the Front Range plutons demonstrate that this area was being actively uplifted and eroded from 1.7 to 1.0 Ga.

Metamorphism and Deformation

Peak metamorphism in the Front Range reached the upper amphibolite to granulite facies and has been dated at 1713±30 Ma based on whole rock Rb-Sr systematics for central Front Range schists and gneisses (Peterman and Hedge, 1967; Steiger and Jager, 1977; Braddock et al., 1988a). Synchronous deformation produced multiple episodes of folding (Abbott, 1970, 1976; Hedge et al., 1967; Peterman and Hedge, 1968; Nesse, 1984). The migmatites are stromatic with layer-parallel leucosomes (quartzo-feldspathic segregations) conformable with the foliation. Moreover, many leucosomes are folded and the axial planes of the folds are parallel to the dominant foliation. This implies a peak metamorphic origin of the migmatites because the deformation is documented as synmetamorphic (Hedge, 1969 and 1972; Abbott, 1970; Olsen, 1982). On a regional scale the foliations in the Front Range do not follow a clear penetrative pattern. The complexity of the foliations suggests that the deformation associated with metamorphism was not due to simple compression during accretionary tectonism (Reed et al., 1987). Reed et al. (1987) proposed that rising magmas of the Routt Plutonic Suite provided much of the heat for the metamorphism and profoundly influenced the character of the deformation as they penetrated the crust.

Following the 1.7 Ga event, no further geologic activity is evident in the area until intrusion of the 1.4 Ga Berthoud Plutonic Suite (Peterman et al., 1967). The local production of secondary muscovite in sillimanite-K-feldspar bearing pelites around some of these plutons is attributed to fluid released during emplacement (Wobus and Hutchinson, 1988). This thermal event may be more pervasive than indicated by mineralogic and textural observations of the metamorphic rocks because the K-Ar isotopic systems of older rocks are reset to the 1.4 Ga age (Tweto, 1987; Reed and Snee, 1991). In addition, recent $^{40}Ar/^{39}Ar$ thermochronology on muscovite, biotite, and K-feldspar mineral separates from samples collected in the Big Thompson Canyon (see Figure 1, inset) and the Idaho Springs-Ralston Zone (in the central Front Range) yield ages ranging from 1.3 to 1.4 Ga (Shaw, 1995 and Shaw et al., 1995). Ages on hornblende from the same area range from 1.5 to 1.6 Ga. Shaw et al. (1995) suggested that the mica and feldspar data are consistent with a regional-scale change in thermal conditions around 1.4 Ga. Microtextures observed by Selverstone et al. (1995) in samples from the Big Thompson Canyon corroborate a change in thermal conditions. Selverstone et al. (1995) observed peak metamorphic staurolite that was pseudomorphically replaced by chlorite + muscovite ± cordierite and then overprinted by euhedral garnet and staurolite. They interpreted the new garnet-staurolite growth as a thermal pulse

subsequent to the 1.7 Ga peak metamorphism; the 1.3 to 1.4 Ga $^{40}Ar/^{39}Ar$ dates are believed to correspond to the cooling phase of this thermal pulse. Current interpretation of the $^{40}Ar/^{39}Ar$ data is that uplift and cooling followed the 1.7 Ga peak metamorphism and then, at 1.4 Ga, a thermal pulse was initiated to at least 500-550°C (Selverstone et al., 1995). Shaw et al. (1995) suggested that this thermal pulse was short in duration and was followed by rapid cooling, as the $^{40}Ar/^{39}Ar$ hornblende data were not completely reset.

Sometime between 1400 and 1000 Ma, an extensive episode of ductile shearing affected the entire Front Range (Wells et al., 1964; Abbott, 1976; Graubard, 1991) and may explain the rapid cooling recorded by the $^{40}Ar/^{39}Ar$ data. These shear zones may have developed along crustal weaknesses originally generated during the 1.7 Ga deformation (Nesse, 1977). During this event, the rocks in the shear zones were locally recrystallized (Wells et al., 1964) producing lower grade andalusite±cordierite assemblages along the shear zones (Abbott, 1970, 1976 and Nesse, 1977). There is no evidence for any regional-scale metamorphism since the Proterozoic (Hart, 1964). However, fault reactivation during the Late Cretaceous to Eocene Laramide uplift produced cataclastic textures that overprinted the Precambrian ductile event.

The Study Area

Introduction

The Cache la Poudre River flows in an east-west trending canyon that transects the Front Range northwest of Fort Collins in Larimer County, Colorado (Figure 1, inset). The majority of the canyon lies within the Roosevelt National Forest and is traversed by Colorado Highway 14 that parallels the river. The nearly 50 kilometer stretch of highway within the study area provides access to fresh exposures across the eastern half of the northern Front Range. The study area is a geologic traverse across the following 1:24000 geologic quadrangle maps (from east to west): LaPorte (Braddock et al., 1988a), Poudre Park (Braddock et al., 1988b), Big Narrows (Abbott, 1976), and Rustic (Shaver et al., 1988). Complete descriptions of the rock units exposed in the Poudre Canyon can be found in Abbott (1970, 1972).

Metamorphic Rocks

Figure 2 is a highly generalized sketch map of the study area based on the geologic quadrangle maps mentioned above. The metamorphic rocks (unpatterned) were mapped on the basis of lithology and were not assigned a formation name (Abbott, 1976; Braddock et al., 1988a, 1988b; Shaver et al., 1988). They are predominantly interlayered migmatitic schists and gneisses with minor amphibolite and rare calc-silicate rocks and marbles. The entire area lies within the sillimanite-K-feldspar zone. Mineral assemblages observed in 115 thin sections from 51 different outcrops along Highway 14 are tabulated in Table A-1, Appendix A; outcrop locations are shown in Figure A-1, Appendix A. In general, pelites predominate down-canyon (eastward) whereas the up-canyon exposures are more quartzo-feldspathic. Migmatites occur in both schistose and gneissic host rocks throughout the canyon. They are stromatic with layer-parallel leucosomes (quartzo-feldspathic segregations), as shown in Figure 3. Tightly folded leucosomes with axial planes parallel to the primary foliation (see Figure 4), rootless leucosome folds, and boudinaged leucosomes all attest to the strong deformation experienced by the migmatites, presumably after crystallization of the leucosomes.

Igneous Rocks

Foliated granodioritic rocks, believed to be part of the syntectonic 1.7 Ga Routt Plutonic Suite (shaded in Figure 2) occur in the western and central portions of the study area. Exposures of the non-foliated 1.4 Ga Berthoud Plutonic Suite (coarsely stippled in Figure 2), most of which belong

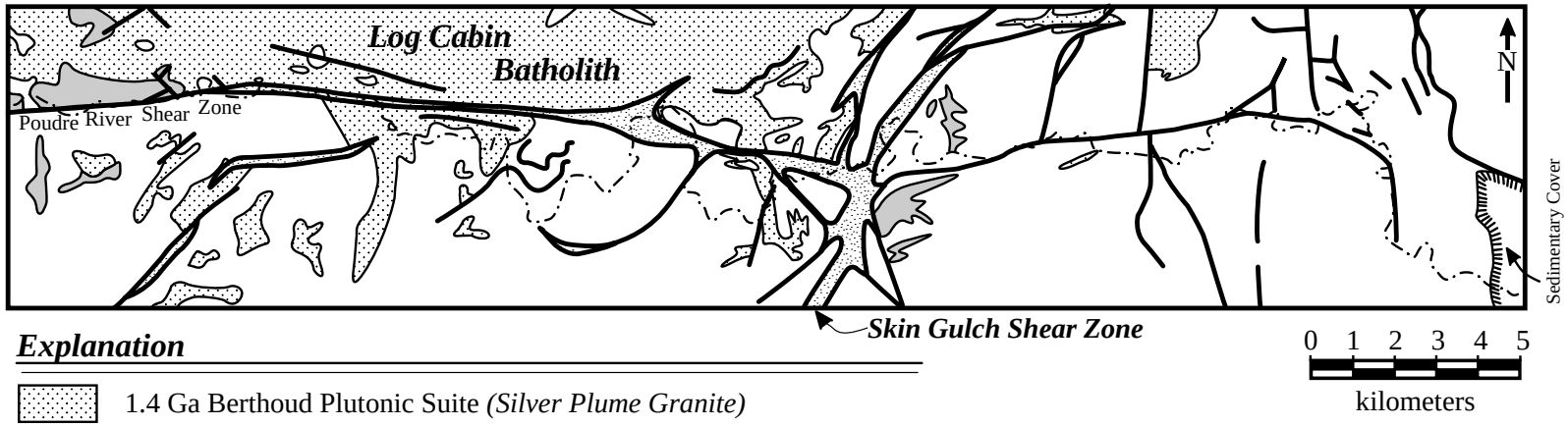

Figure 2 Geologic sketch map of the study area showing the general distribution of rock types and shear zones. *Adapted from Abbott (1976), Braddock et al. (1988a, 1988b) and Shaver et al. (1988).*

Figure 3 A typical stromatic migmatite in the Poudre Canyon. Coarse-grained quartz+feldspar segregations (leucosomes) are aligned parallel to the foliation; photograph #5-10-91, locality 107 (Figure A-1, Appendix A).

Figure 4 An isoclinally folded leucosome in the Poudre Canyon; the axial planes of these folds are parallel to the primary foliation; photograph #7-17-90, locality 110 (Figure A-1, Appendix A).

to the Log Cabin Batholith, are especially voluminous up-canyon (westward) and are clearly discordant, as shown in Figure 5. However, folded granitic veins emanating from these igneous exposures indicate that some deformation was associated with the emplacement of the 1.4 Ga plutons. Abbott (1970) identified F4 crinkle folds in this area that he attributed to a renewed compressive stress created by the 1.4 Ga plutonism.

Figure 5 The 1.4 Ga Log Cabin Batholith as exposed in the Poudre Canyon. Note the clearly discordant nature of the contact between the granitic intrusion and the gneissic country rock; photograph #8-13-90, locality 39 (Figure A-1, Appendix A).

At least two generations of pegmatites occur in the field area: early concordant pegmatites and later discordant ones. Figure 6 is a field photograph of an early, near-vertical concordant pegmatite (center of photograph) that is cross-cut by a later sub-horizontal pegmatite. The early pegmatites are commonly deformed (boudinaged as in Figure 6) whereas later pegmatites show no signs of deformation. Neither pegmatite type has been age-dated.

Figure 6 Field photograph of a boudinaged, near-vertical pegmatite (in center) that is crosscut by a later, subhorizontal pegmatite. The early pegmatite is clearly concordant with the surrounding gneiss, schist and amphibolite; photograph #8-22-90, locality 111 (Figure A-1, Appendix A).

Faulting

Fault zones criss-cross the study area, as shown in Figure 2. The amount of relative displacement along these faults is unknown. The generally north-south striking shear zones are mostly Proterozoic age ductile faults, the east-west striking shear zones are later brittle faults. Ductile

shear along the Skin Gulch Shear Zone (labeled in Figure 2) was dated by Abbott (1970, 1972) using whole rock Rb-Sr techniques at 1178±220 Ma (recalculated according to Steiger and Jager,1977). According to Nesse (1995), the sense of movement along the Skin Gulch Shear Zone is southeast side up and the net slip was probably substantial. In the field, the Skin Gulch Shear Zone is recognized by the alignment of the near vertical foliations parallel to the fault zone (S5 of Abbott, 1970). In addition, synchronous folding produced folds with axial planes parallel to the fault zone (Abbott, 1970). Mylonitic fabrics are present, especially in the coarser-grained, conformable pegmatites. However, in finer-grained rocks appreciable recovery via recrystallization is evident. Consequently, the lateral extent of the shear zone can not be delineated by simple inspection of crystal-plastic fabrics; instead it appears to be gradational.

The major east-west trending shear zone that bisects the study area [labeled the Poudre River Shear Zone (Abbott, 1976) in Figure 2] is a brittle fault related to the Laramide uplift. Whether or not the Poudre River Shear Zone is a reactivated Proterozoic structure is unknown. Other Laramide-related faulting is apparent throughout the study area in the form of largely low angle (10-20°), brittle faults, as shown in Figures 7a and 7b. These faults show small apparent relative displacements (9-20 cm), and were avoided when sampling.

Previous P-T Estimates

Previous pressure-temperature estimates for peak metamorphism in the Front Range cluster between 630-670°C and 3-4.5 kbar as shown in Figure 8 (Abbott, 1970; Nesse, 1977 and Olsen, 1987). The following observations indicate that the peak pressure may be higher than previously estimated for the northern Front Range.

(1) Emplacement depth for the synkinematic Boulder Creek Granodiorite is believed to have been greater than 16 km (Wobus and Hutchinson, 1988). This indicates that pressures probably exceeded 4.5 kbar.

(2) Lower-pressure minerals such as andalusite and cordierite are extremely rare. Porphyroblastic andalusite was observed by both Abbott (1970, 1976) and Nesse (1977) in areas localized along the Skin Gulch Shear Zone. They suggested that this andalusite was the product of local metamorphism associated with the 1.2±0.2 Ga shearing event rather than the product of peak metamorphism. This would be especially feasible if shearing occurred around the time of the 1.4 Ga thermal pulse identified by Selverstone et al.. (1995). On the other hand, anhedral corroded grains of andalusite and cordierite were interpreted by Abbott (1970) as relicts of the pre-peak, prograde path followed by the northern Front Range.

(3) The P-T estimates lie marginally within the range of the granite minimum melt (Figure 8). If the migmatites formed by wet melting under these conditions, then an H_2O-dominated fluid must have been present. However, CO_2-rich fluid inclusions are common in these and other Front Range migmatites (Munn, this study; Olsen, 1988), suggesting that x_{H2O} was less that 1.0 during anatexis. As x_{CO2} increases (or x_{H2O} decreases), wet melting only will occur at higher pressures and/or temperatures (Kerrick, 1972; Ohmoto and Kerrick, 1977). On the other hand, if the primary mechanism of migmatization was by dehydration melting of muscovite, then the pressure must have been greater than 3.5 kbar.

Figure 7a Outcrop 134 (Figure A-1, Appendix A) viewed generally across strike of dominant metamorphic foliation; down canyon is toward the right. A low angle brittle fault that dips down canyon is apparent in the up canyon portion of the outcrop; photograph #11-24-91.

Figure 7b A view of the gouge found in the low angle brittle fault shown in Figure 7a. The apparent offset on this fault is approximately 8.5 cm; photograph #8-24-91.

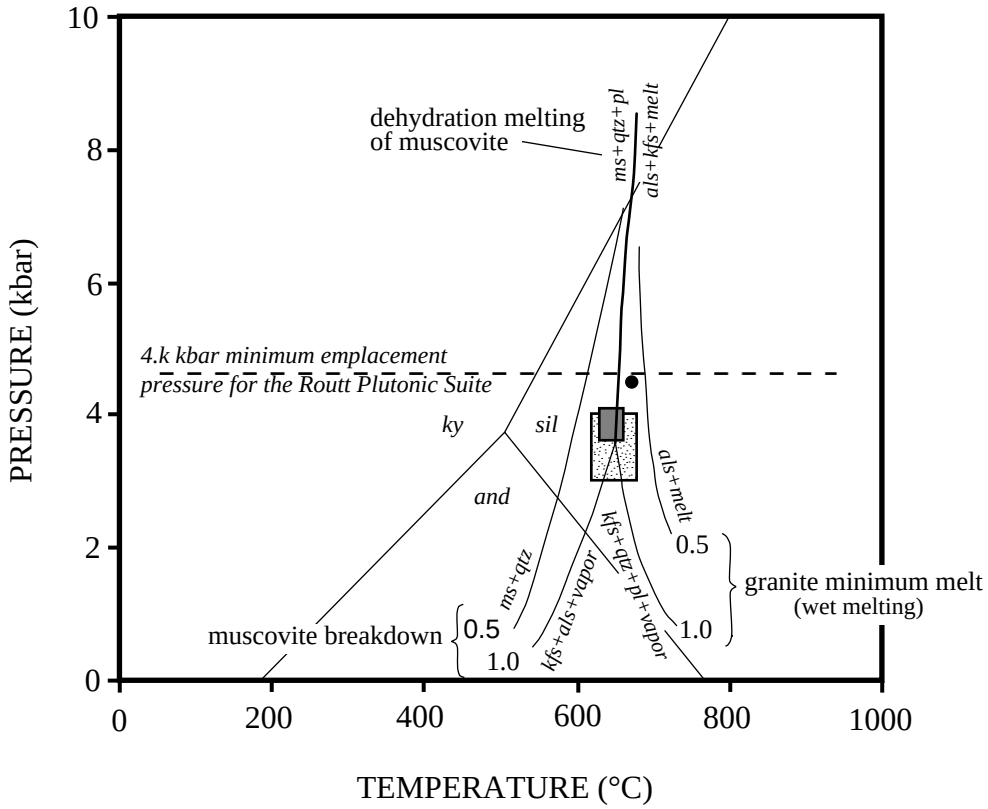

Figure 8 P-T diagram showing previous pressure-temperature estimates for peak metamorphism in the Front Range; solid circle: Abbott, 1970; stippled rectangle: Nesse, 1977; shaded rectangle: Drexler & Braddock via Olsen, 1987. Reactions are shown for x_{H_2O} = 0.5 and 1.0. Adapted from Kerrick, 1972; Holdaway and Mukhopadhyay, 1993.

II. PETROGRAPHY

Garnet-Bearing Pelites and Semi-Pelites

Peak Assemblage

Modes for the pelites and semi-pelites selected for thermobarometry are presented in Tables 2a and 2b. The stable peak assemblage for the pelites is *grt-bt-sil-kfs-qtz-pl±ilm*; the less aluminous semi-pelites lack sillimanite. Sillimanite is generally fibrolitic and associated with red brown biotite; both phases define the dominant foliation. Garnet varies from 0.1 mm to greater than 5 cm in diameter. Commonly, it is stretched parallel to the foliation (Figure 9) and may be distributed along the limbs of folds (Figure 10), indicating garnet growth prior to or during folding. In thin section, garnet shows irregular grain boundaries with embayed edges (Figure 11). It is typically poikiloblastic, containing mineral inclusions characterizing *only* the peak assemblage. For example, Figure 12 shows biotite, quartz, and sillimanite inclusions in garnet, all of which occur in the matrix of the sample. K-feldspar, plagioclase, and, in places, high density fluid inclusions (possibly CO_2) also occur in garnet. No garnets show any inclusion record of lower grade assemblages, which suggests that garnet grew at high temperature, perhaps continuously re-equilibrating up to peak conditions.

Figure 9 Sillimanite (white) and garnet (reddish) stretched out along the foliation at locality 113 (Figure A-1, Appendix A); photograph #7-6-91.

Post-Peak Reactions

Peak metamorphism was followed by garnet resorption and local production of fine-grained reaction coronas of biotite, quartz, and plagioclase (Figure 13). Sillimanite does not occur in these coronas. This texture suggests retrograde formation by a composite of the following reactions:

[grossular + 2sillimanite + quartz = 3anorthite]
+ [garnet (alm-py) + K-feldspar + H_2O = sillimanite + biotite + 2quartz]
garnet + sillimanite + K-feldspar + H_2O = plagioclase + biotite + quartz

Biotite provides additional evidence for post-peak activity. It is red-brown in the matrix but, where directly adjacent to garnet rims or along garnet fractures, biotite is green, as in Figure 14. The embayed nature of the garnet grain boundaries, the garnet reaction coronas and the association of green biotite with garnet indicates that these rocks were subject to local post-peak discontinuous reactions and retrograde ion exchange between garnet and biotite.

Cordierite-Bearing Pelites

Cordierite was identified only at outcrop 128 (Figure A-1) where it occurs in the garnet-free assemblage, *crd-bt-sil-qtz-pl* (samples 128/10b and 128/6, Table A–1) and the garnet-bearing

Table 2a: Modes of Pelites and Semi-Pelites Used for Thermobarometry

	50E	**66A**	**86D**	**93A**	**104F**	**109A**	**110A**	**111A**	**113/4a**	**113C**	**113E**	**116/3a**	**119A**	**128/10a**	**128/10c**	**133A**	**134D**
quartz	32	49	38	50	53	54	46	41	31	31	41	58	61	61	42	30	37
plagioclase	26	10	36	22	11	28	27	33	16	11	6	8	12	5	24	39	3
*An Content**	*.33-.38*	*.27-.32*	*.23-.28*	*.37-.40*	*.20-.23*	*.25-.32*	*.32-.39*	*.34-.37*	*.22-.27*	*.21-.27*	*.21-.27*	*.20-.23*	*.25-.29*	*.33-.34*	*.34-.38*	*.23-.28*	*.26-.28*
K-feldspar	7	13	3	1	1	-	4	4	13	16	tr	10	6	8	-	5	-
biotite	26	21	14	23	26	16	20	15	30	24	32	13	15	20	23	19	43
garnet	7	3	8	2	9	1	2	7	4	10	9	6	2	1	3	6	1
sillimanite	-	tr	-	-	-	tr	-	-	6	7	11	4	4	4	5	-	15
cordierite	-	-	-	-	-	-	-	-	-	-	-	-	-	-	3	-	-
zircon	tr	tr	tr	tr	tr	tr	tr	tr	tr	tr	tr	tr	tr	tr	tr	tr	tr
opaques	1	tr	1	tr	tr	tr	tr	tr	-	-	tr	1	-	-	tr		tr
apatite	-	tr	-	tr	-	-	tr	tr	-	tr	tr	-	-	-	-	tr	-
muscovite	-	3	-	2	-	-	-	-	-	-	-	-		1	-	-	-
sericite	-	-	-	-	-	-	-	tr	-	-	-	-	-	-	tr	-	-
chlorite	-	-	-	tr	-	-	-	tr	-	-	-	-	tr	-	-	-	-
epidote	-	tr	-	tr	-	-	-	-	-	-	-	-	-	-	-	-	-
total	*99*	*99*	*100*	*100*	*100*	*99*	*99*	*100*	*100*	*99*	*99*	*100*	*100*	*100*	*100*	*99*	*99*
# grts per thin section	**7**	**18**	**2**	**8**	**±75**	**3**	**22**	**10**	**9**	**13**	**9**	**10**	**12**	**5**	**5**	**13**	**2**
grt size (mm)	1-8	0.5-1	1-8	0.5-3	0.5	0.5	0.5-1.5	0.5-7	0.5-4	2-6.5	1-6.5	1-6	0.2-3.5	0.5-2	1-4.5	1-4	1.5-9
*raw grt:bt***	*0.27*	*0.14*	*0.57*	*0.09*	*0.35*	*0.06*	*0.10*	*0.47*	*0.13*	*0.42*	*0.28*	*0.46*	*0.13*	*0.05*	*0.13*	*0.32*	*0.02*
*raw grt:pl***	*0.27*	*0.30*	*0.22*	*0.09*	*0.82*	*0.04*	*0.07*	*0.21*	*0.25*	*0.91*	*1.50*	*0.75*	*0.17*	*0.20*	*0.13*	*0.15*	*0.33*
garnet inclusions	qtz, pl, op, bt	pl, bt rare	qtz, pl, op, bt	qtz, pl bt	qtz, bt zr(?)	qtz, fib	qtz, bt	qtz, bt	qtz	qtz, bt fib	qtz, bt fib	qtz, fib	qtz, bt fib	none	qtz, bt fib	qtz, pl, op, bt	qtz, fib

* *total range in mole fraction anorthite from microprobe analysis*

** *raw ratios are effectively reduced in samples with fewer, larger garnets because only the rims of large garnets are available for reaction*

Table 2b: Modes of Migmatites Used for Thermobarometry

HOST	**19D**	**68A**	**88A**	**104E**	**108C**
quartz	16	38	27	33	33
plagioclase	6	11	20	2	32
An Content	*.25-.28*	*.31-.34*	*.32-.36*	*.18-.22*	*.28-.32*
K-feldspar	-	4	-	5	-
biotite	7	20	12	25	27
garnet	tr	8	-	2	1
sillimanite	-	-	tr	3	-
zircon	tr	tr	tr	tr	tr
opaques	1	1	tr	tr	tr
apatite	tr	tr	tr	-	tr
muscovite	4	-	-	-	-
sericite	-	-	-	-	tr
epidote	tr	-	-	-	-
chlorite	-	-	tr	-	tr
total	*34*	*82*	*59*	*70*	*93*

LEUCOSOME

Table 2b: Modes of Migmatites Used for Thermobarometry

*An Content**	*.25-.34*	*.25-.32*	*.32-.37*	*N/A*	*N/A*
K-feldspar	-	4	-	18	-
biotite	tr	tr	1	1	tr
garnet	-	-	3	-	-
opaques	tr	-	-	-	-
muscovite	tr	-	-	-	-
chlorite	tr	-	-	-	-
total	*0*	*4*	*4*	*19*	*0*
# grts per thin section	**53**	**122**	**34‡**	**6**	**11**
grt size (mm)	0.1-1.2	0.2-1.5	0.5-1.5	0.5-3.5	0.5-3
*raw grt:bt***	*0.14*	*0.40*	*0.23*	*0.08*	*0.04*
*raw grt:pl***	*####*	*0.73*	*0.15*	*1.00*	*0.03*
garnet inclusions	qtz, bt CO2	qtz, bt, pl, kfs	qtz, fib bt	qtz, fib bt	qtz, bt pl

* *total range in mole fraction An from microprobe analysis*

** *these raw ratios are effectively reduced in samples with fewer, larger garnets since only the rims of large garnets are available for reaction*

‡ *all garnets are isolated within the leucosome*

Figure 10 Garnet (reddish) distributed along the limbs and around the hinge of a fold at locality 113 (figure A-1, Appendix A); sillimanite (white) is also folded. Garnet and sillimanite growth must predate or be synchronous with the folding; photograph #7-4-91.

Figure 11 Photomicrograph of a garnet (high relief, center) with irregular, embayed grain boundaries. Garnet is associated with red-brown biotite (bt) and fibrolite (fib); foliation is horizontal in this view. Field of view is 4.8 mm (longest dimension); plane light; sample 113C.

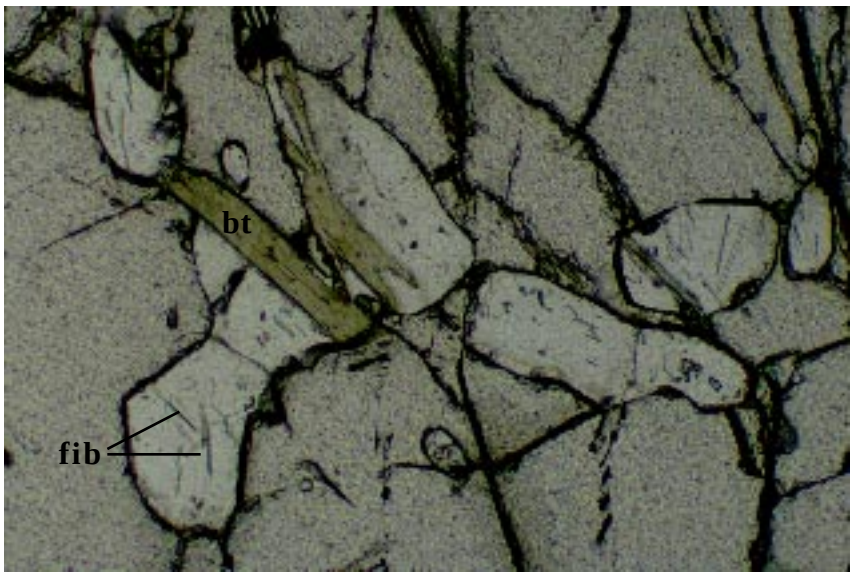

Figure 12 Photomicrograph of inclusions of quartz (white, low relief), fibrolite (fib) and biotite (bt) in garnet. Field of view is 1.2 mm (longest dimension); plane light; sample 113C.

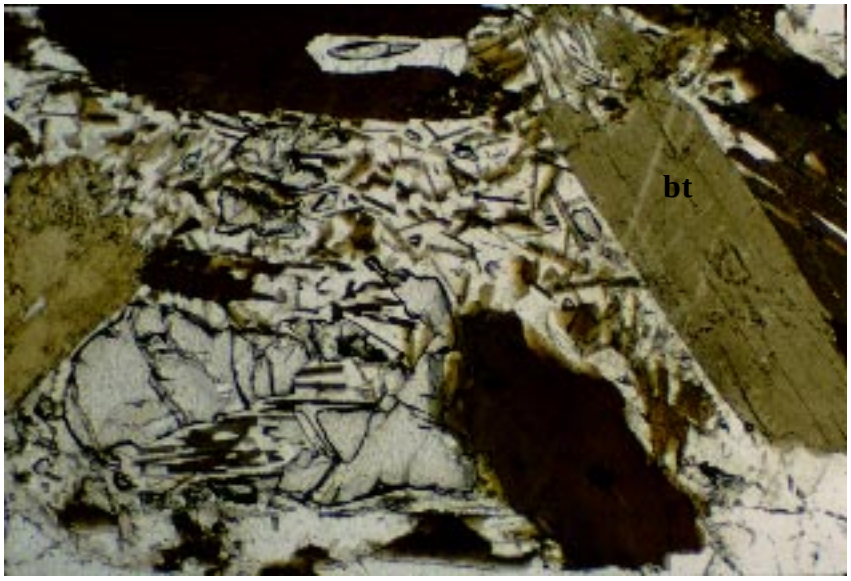

Figure 13 Photomicrograph of coarse-grained biotite (bt) surrounding remnants of garnet in the midst of fine grained biotite, quartz, and plagioclase. Field of view is 2.4 mm (longest dimension); plane light; sample 104E.

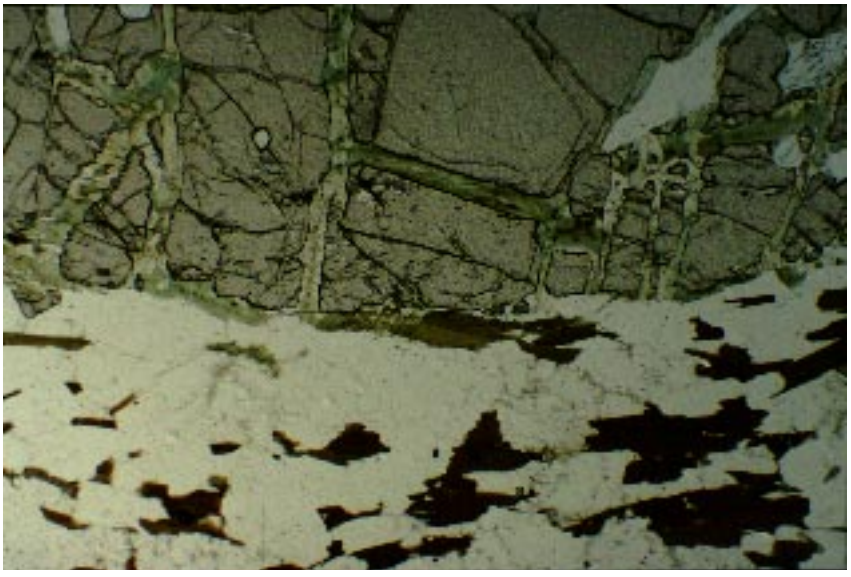

Figure 14 Photomicrograph showing green biotite in garnet fractures and immediately adjacent to the garnet (top half of photograph). Redbrown biotite occurs within millimeters of the garnet in the bottom half of the photograph. Field of view is 4.8 mm (longest dimension); plane light; sample 128/5.

assemblage, *crd-grt-bt-sil-qtz-pl* (sample 128/10c, Table A-1). Optically, cordierite is identified by its highly pinitized grain boundaries and fracture surfaces; polysynthetic twinning is rare.

Crd-Bt-Sil-Qtz-Pl Assemblage (Sample 128/10b)

In the garnet-free samples, the cordierite is irregularly-shaped and overgrown by later phases. Two textural overgrowths occur, each of which suggest a different cordierite breakdown reaction. The first, shown in Figure 15, involves cordierite overgrown by subhedral, red-brown biotite and euhedral, prismatic sillimanite. This texture implies the reaction,

$$cordierite + K\text{-}feldspar + H_2O = sillimanite + biotite + quartz,$$

labeled reaction 1 in Figure 16. The coarse-grained nature of the biotite and the prismatic, euhedral nature of the sillimanite imply growth at near-peak metamorphic temperatures. The red-brown color of the biotite is caused by the addition of titanium (presumably by the breakdown of ilmenite or rutile) and is directly correlated with increasing metamorphic grade (Guidotti et al., 1977; Spear, 1993). Thus, cordierite probably formed as part of the prograde assemblage (perhaps by the breakdown of staurolite) and then, with the addition of water, reacted to form the biotite and sillimanite. Prograde dehydration reactions (muscovite breakdown, for example) could provide the water necessary to drive reaction (1), as could the synmetamorphic Routt Plutonic Suite or the crystallizing leucosomes of the migmatites. Concrete evidence for the presence of a fluid near the peak of metamorphism lies in the folded, concordant nature of quartz veins unique to this outcrop. A sketch of one of these syntectonic quartz veins is shown in Figure 17. The ductile shear zone near outcrop 128 (see Figure A-1, Appendix A) may have been the conduit for the near peak fluids.

The second overgrowth texture involves the replacement of cordierite by randomly oriented muscovite and pale green biotite (Figure 18). The two micas are intimately intergrown, commonly appearing to be part of a single grain. The pale green color of the biotite is attributed to the near absence of titanium suggesting that these micas are not part of the prograde assemblage. The late, retrograde nature of the muscovite and pale green biotite is supported by their random orientation and by the additional presence of trace amounts of chlorite elsewhere in this sample. The overgrowth texture shown in Figure 18 implies reaction (2) in Figure 16,

$$cordierite + K\text{-}feldspar + H_2O = muscovite + biotite + quartz.$$

Cross-cutting pegmatites such as the ones shown in Figure 19 could have been a source for the fluids. K–feldspar, which is now absent from this sample (see Table A-1; Appendix A), may have been completely exhausted by the retrograde mica production, thus preserving the remaining cordierite.

Crd-Grt-Bt-Sil-Qtz-Pl Assemblage (Sample 128/10c)

In samples that contain cordierite and garnet, three textural varieties of cordierite are evident: matrix cordierite, cordierite-sillimanite mats in garnet pressure shadows and cordierite-quartz symplectites.

Matrix Cordierite

In the matrix, cordierite occurs as anhedral grains removed from garnet and associated with red-brown biotite and prismatic sillimanite. Reaction 1 in Figure 16 may be responsible for this association. However, the occasional presence of red brown biotite and sillimanite *between* garnet and cordierite, as shown in Figure 20, suggests that reaction 3 in Figure 16,

$$cordierite + garnet + K\text{-}feldspar + H_2O = sillimanite + biotite$$

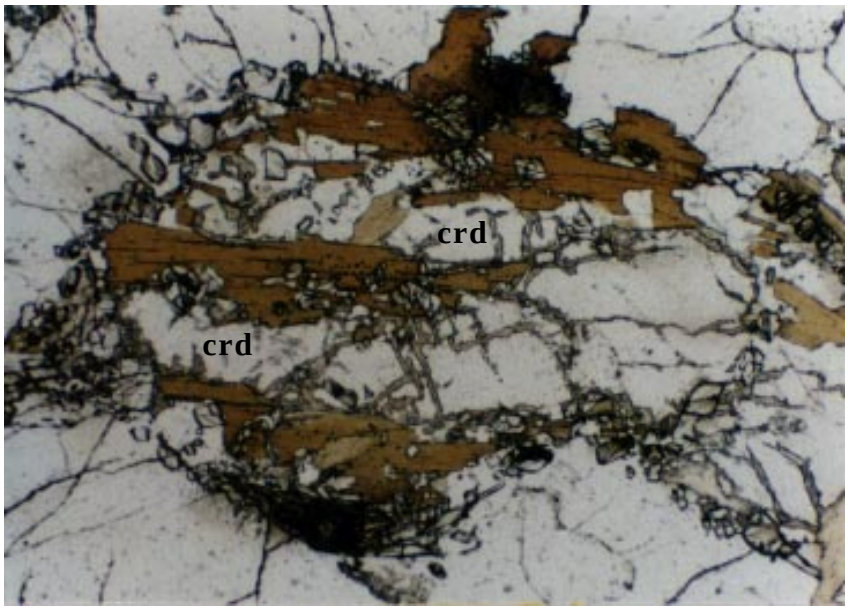

Figure 15a Photomicrograph of resorbed cordierite (crd) over grown by red-brown biotite and prismatic sillimanite (higher relative relief). Field of view is 2.4 mm (longest dimension); plane light; sample 128/10b.

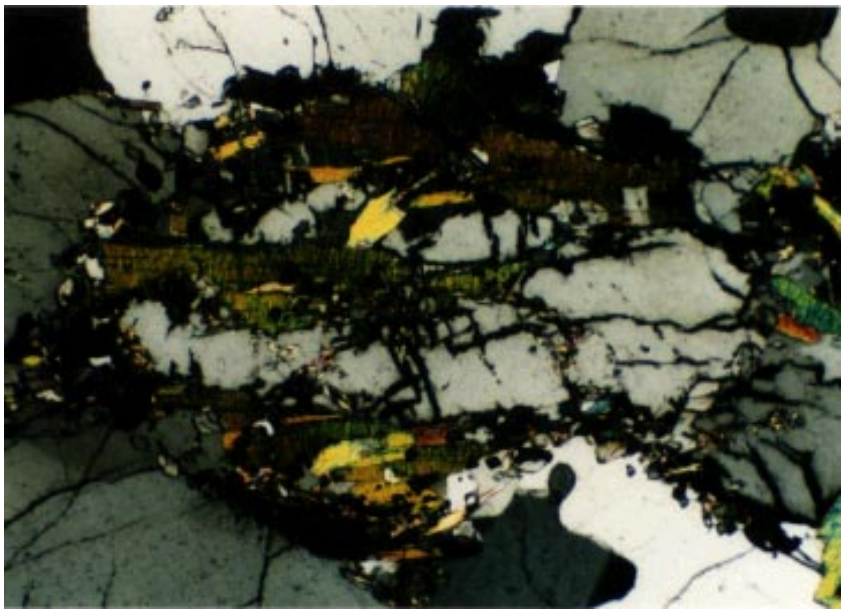

Figure 15b Same view as 15a, with crossed polars.

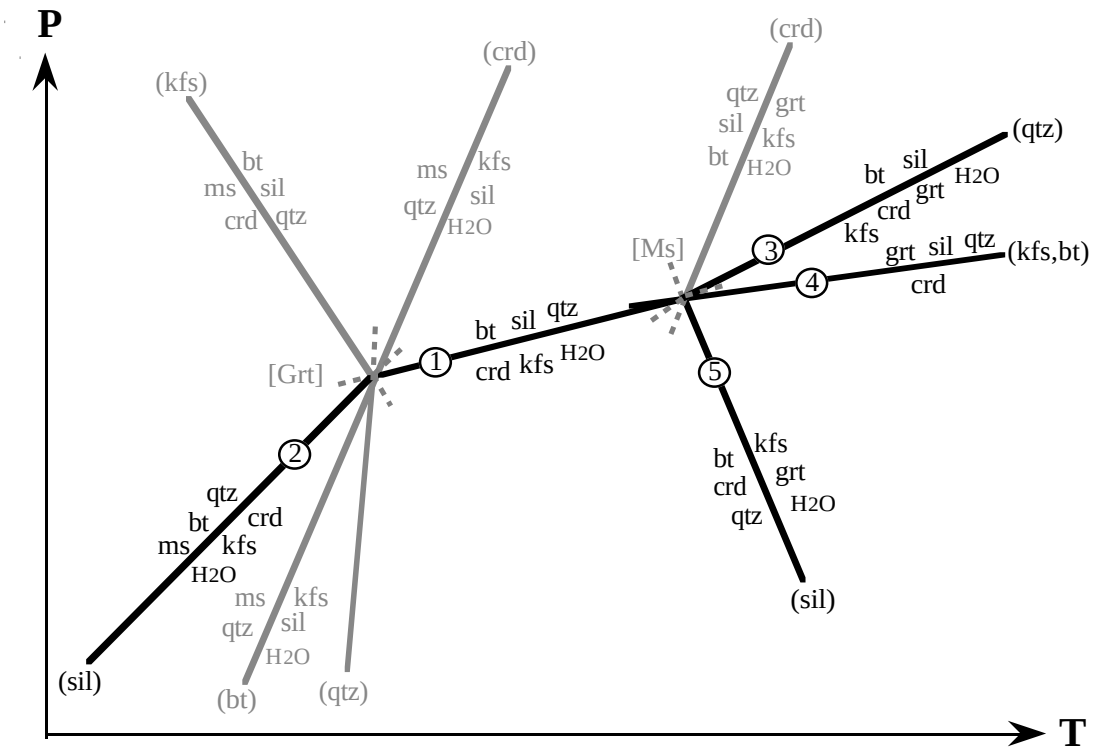

Figure 16 Schreinemaker's construction for reactions involving biotite (bt), cordierite (crd), K-feldspar (kfs), muscovite (ms), sillimanite (sil), quartz (qtz), and H_2O (after Thompson, 1976; Mukhopadhyay and Holdaway, 1994)

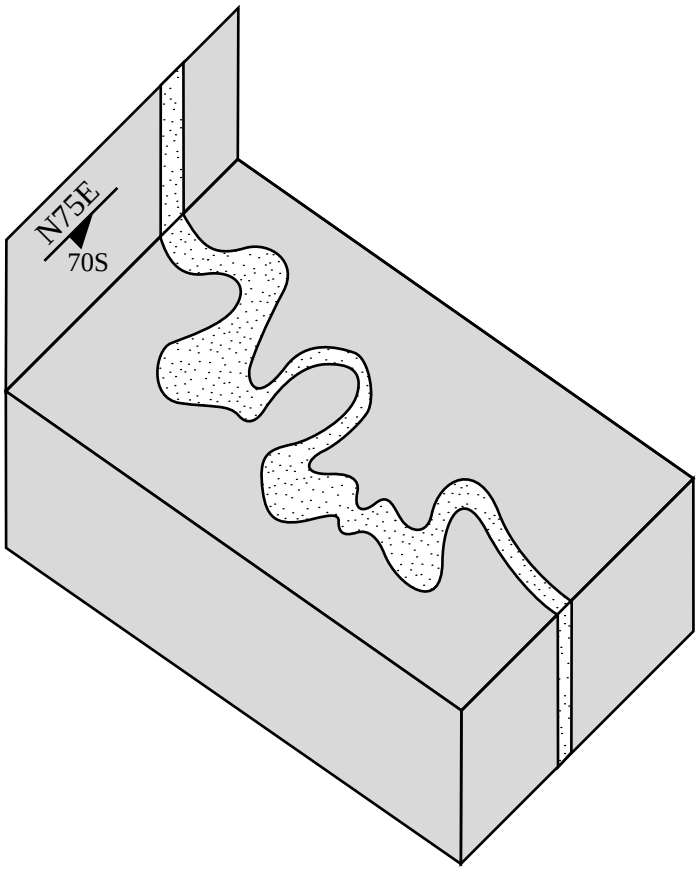

Figure 17 Sketch of a folded quartz vein (stippled) in outcrop 128; 1-2cm thick. Folds are generally axial planar to the dominant foliation (~N75E/70°S).

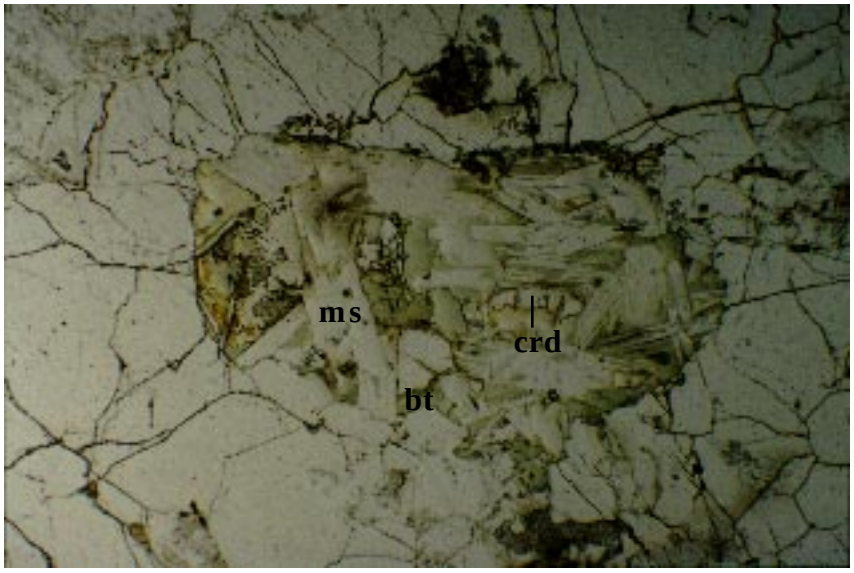

Figure 18 Photomicrograph of cordierite pseudomorphically replaced by muscovite (ms) and pale green biotite (bt). A remnant of the cordierite (crd) is still visible. Field of view is 4.8 mm (longest dimension); plane light; sample 128/10b.

Figure 19 Field photograph of a pegmatite in outcrop 128 (see Figure A-1, Appendix A) that cuts the foliation at a slight angle; photograph #2-3-93.

also may have occurred. Again, the red-brown color of the biotite suggests the breakdown of a titanium-rich phase, such as ilmenite, during prograde metamorphism. The red-brown color and coarse-grained nature of the biotite and the prismatic, euhedral nature of the sillimanite suggest formation at near peak conditions using the same fluid which promoted the near peak reactions in sample 128/10b.

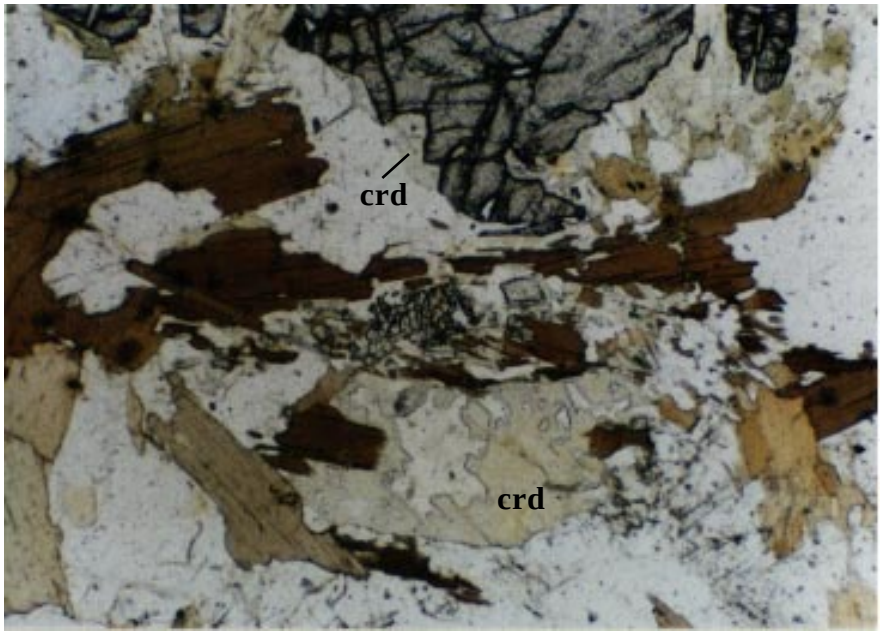

Figure 20 Photomicrograph of cordierite separated from garnet by red-brown biotite and prismatic sillimanite. Field of view 2.4 mm (longest dimension); plane light; sample 128/10c.

Cordierite-Sillimanite Mats

Within garnet pressure shadows, cordierite is coarse-grained, optically continuous, and encloses thick mats of both fibrolitic and prismatic sillimanite (Figure 21). The precipitation of cordierite in the low strain regions of the pressure shadow suggests growth of cordierite at the expense of garnet, perhaps by reaction 4 in Figure 16,

garnet + sillimanite + quartz = cordierite.

This reaction has a shallow positive slope in pressure-temperature space (Figure 16; Mukhopadhyay and Holdaway, 1994) and proceeds with increasing temperature or decreasing pressure; as the cordierite grew it enclosed nearby sillimanite mats. This texture, similar to the classic cordierite pressure shadows on garnet observed by Hollister (1977), commonly is attributed to decompression following peak metamorphism. Cordierite-sillimanite mats also occur in the matrix (Figure 22). Although physically separated from garnet, their shape and texture are reminiscent of the garnet pressure shadows. Hence, these isolated, oblate cordierite-sillimanite mats are interpreted as pseudomorphs after garnet in which the garnet was consumed completely in reaction 4 (Figure 16).

Cordierite-Quartz Symplectites

Immediately adjacent to the garnet grain boundary and within through-going fractures, a sillimanite-absent, cordierite-quartz symplectite occurs in association with fine-grained red brown biotite, as shown in Figure 23. Similarly, in Figure 24 garnet relicts lie within a cordierite-quartz-biotite reaction corona *without* sillimanite. Thus, reaction 5 in Figure 16 also may have allowed cordierite to grow at the expense of garnet,

$$garnet + K\text{-}feldspar + H_2O = cordierite + quartz + biotite,$$

producing the observed reaction coronas and symplectites.

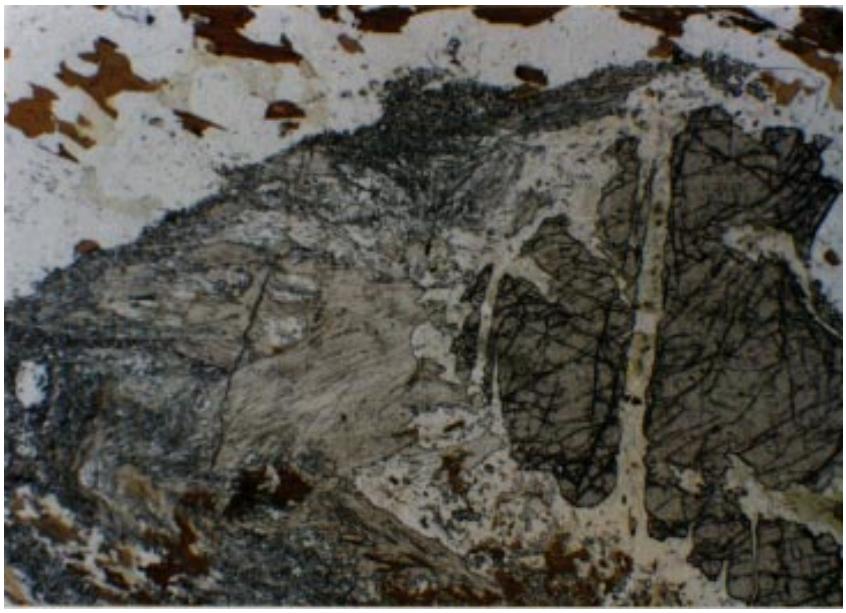

Figure 21a Photomicrograph of optically continuous cordierite surrounding garnet and enveloping a mat of sillimanite. Field of view is 4.8 mm (longest dimension); plane light; sample 128/10c.

Figure 21b Same view as above with crossed polars, cordierite shows gray birefringence and twinning.

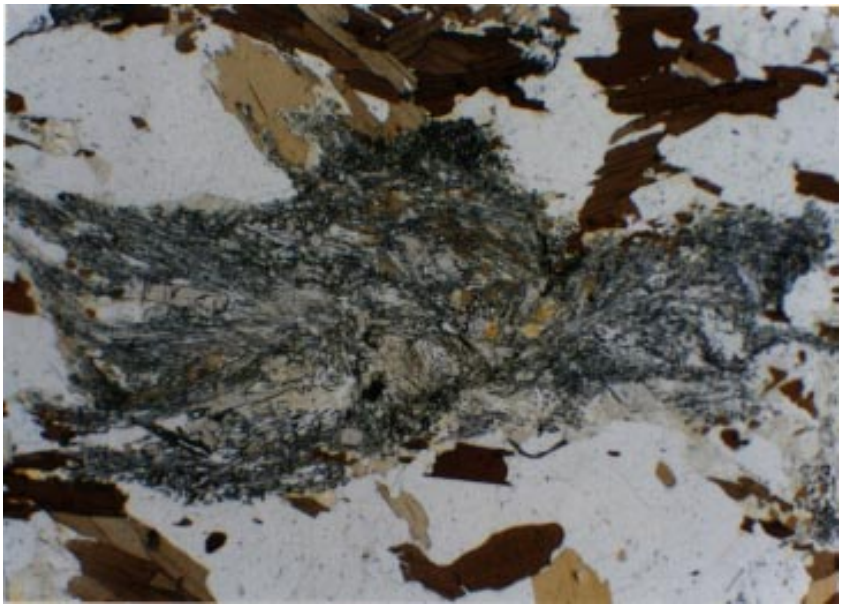

Figure 22 Photomicrograph of optically continuous cordierite (brownish yellow from pinitization) growing within sillimanite mats to form an apparent pseudomorph after garnet. Field of view 4.8 mm (longest dimension); plane light; sample 128/10c.

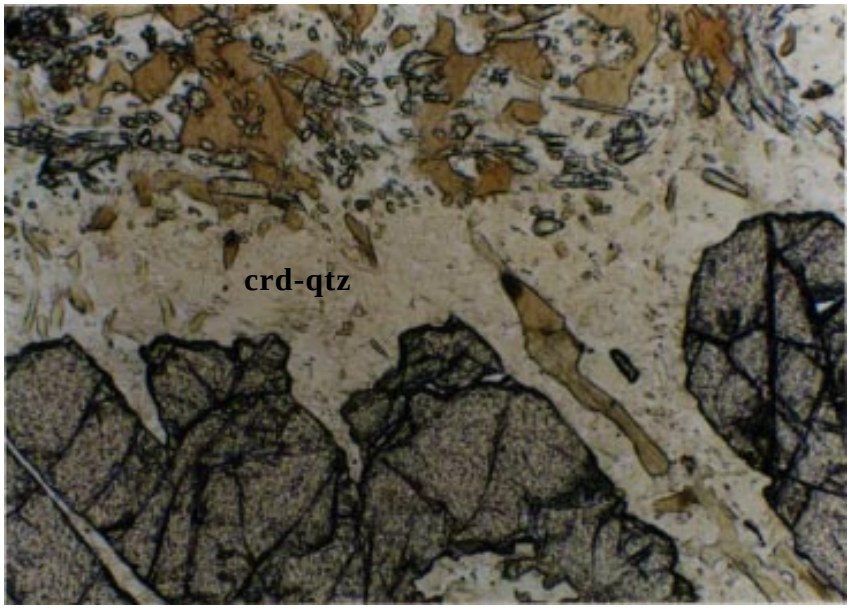

Figure 23a Photomicrograph of cordierite-quartz symplectite (crd-qtz) adjacent to garnet. Field of view is 1.2 mm (longest dimension); plane light; sample 128/10c.

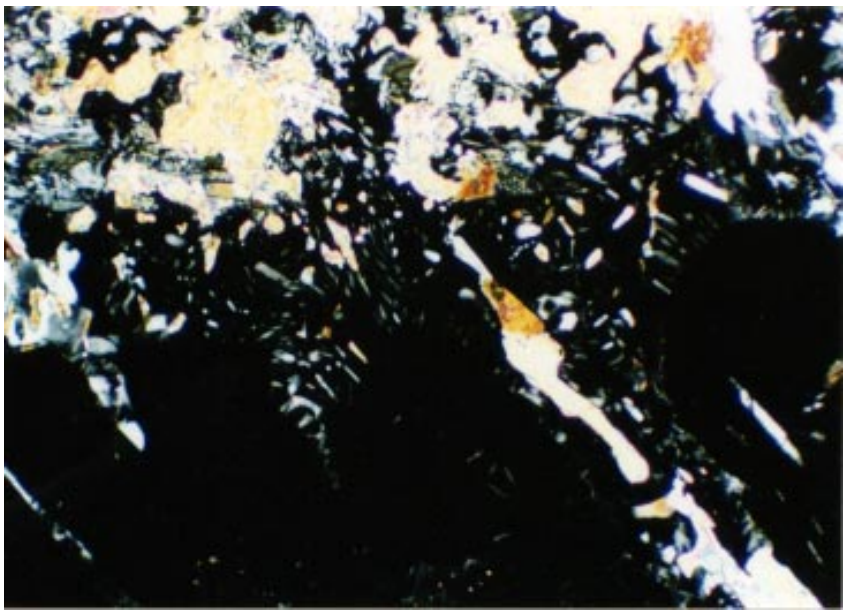

Figure 23b Same view as above, crossed polars.

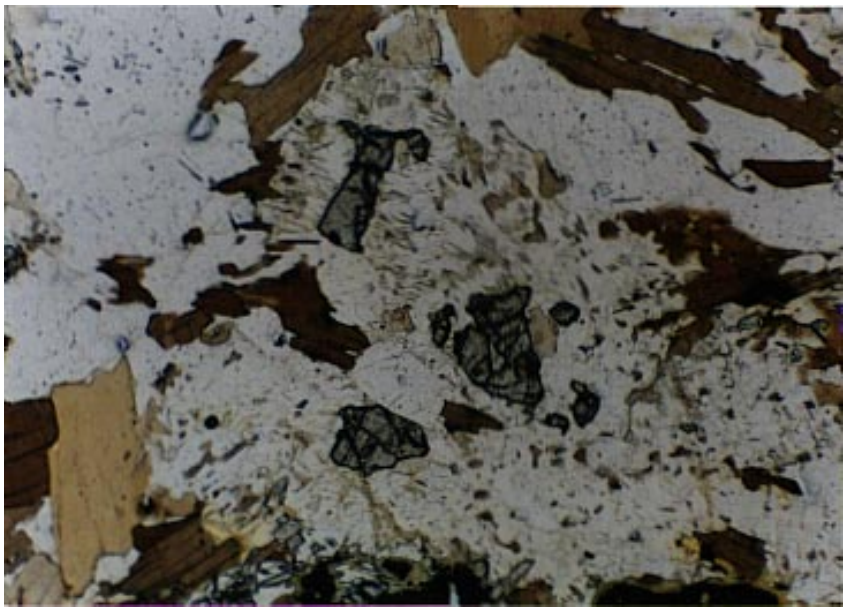

Figure 24 Photomicrograph of relict garnet within an aggregate of cordierite + biotite + quartz *without* sillimanite. Field of view is 2.4 mm (longest dimension); plane light; sample 128/10c.

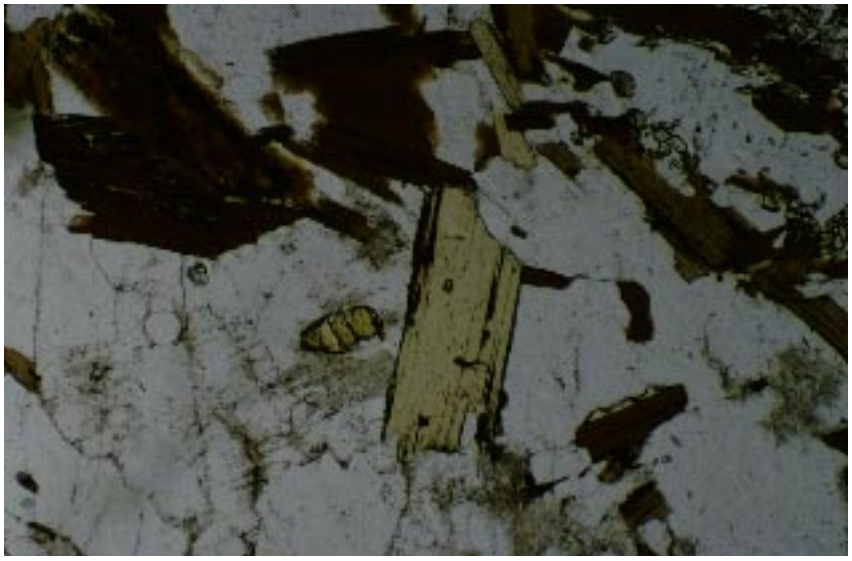

Figure 25 Photomicrograph of a rounded relict staurolite (center) enclosed within a plagioclase grain. Field of view is 2.4 mm (longest dimension); plane light; sample 128/6.

K-Feldspar

Like the garnet-absent sample 128/10b, this sample also lacks K–feldspar (see Table A-1, Appendix A) and cordierite likely persisted because K–feldspar was exhausted in reactions 1, 3, or 5. Unlike the garnet-absent sample 128/10b, this sample does not show the retrograde formation of muscovite and pale green biotite on cordierite. This indicates that the late-stage fluid infiltration was localized closer to sample 128/10b, leaving other areas of the outcrop unaffected.

Relict Staurolite

Cordierite-bearing rocks contain the only observed staurolite, preserved as rare rounded inclusions within plagioclase grains (Figure 25). Staurolite is completely absent from all samples except those containing cordierite, and is interpreted as a relict of the prograde path followed by the Poudre Canyon rocks. Indeed, the peak assemblage in the lower grade Big Thompson Canyon just south of the Poudre Canyon (see Figure 1, inset) includes garnet and staurolite (Selverstone et al., 1995). Woodsworth (1977) attributed the persistence of staurolite to higher grades in upper amphibolite facies cordierite-bearing rocks in British Columbia to the reaction,

$$stt + qtz = grt + crd + sil + \text{more zincian } stt + H_2O.$$

Although no chemical analyses were obtained on the Poudre Canyon relict staurolite, it is possible that similar enrichment in some extra component preserved the staurolite in these cordierite-bearing pelites.

Pelites and Semi-Pelites Containing Secondary Muscovite

Introduction

The peak metamorphic assemblages in several samples are locally overprinted by retrograde muscovite. This late muscovite occurs in four general forms: 1) as well-formed grains that may be mistaken for primary muscovite; 2) as grains that commonly cross-cut the dominant foliation (cross muscovite); 3) as porphyroblastic grains that cross-cut the dominant foliation; and 4) as muscovite clots that appear to be pseudomorphic. The secondary muscovite is best developed in the semi-pelites and biotite gneisses up-canyon (westward) and is less apparent in the pelites that predominate down-canyon (eastward). The diversity of muscovite forms suggests more than one origin. The muscovite-forming reaction(s) must have occurred while the rocks were hot enough to produce coarse grains and at a time when water was present to drive the reaction(s).

Well-Formed, Coarse-Grained Muscovite

Some muscovite in the Poudre Canyon samples is well-formed and intergrown with similar-sized biotite. Microtextures suggest a secondary, post-peak origin for this coarse-grained muscovite. Muscovite may be intergrown with biotite and aligned parallel to the foliation, however, elsewhere optically continuous, equally large and well-formed muscovite completely overgrows the same foliation (Figure 26). Other samples contain muscovite-quartz symplectites overgrowing fibrolite and in contact with microcline. Such textures, as shown in Figure 27, suggests formation by the retrograde reaction

$$\textit{K-feldspar} + \textit{sillimanite} + H_2O = \textit{muscovite} + \textit{quartz} + \textit{albite}$$

Therefore, the coarse-grained, well-formed muscovite is likely a product of post-peak metamorphism.

Cross-Muscovite

Figure 28 shows the typical development of cross muscovite. The randomly oriented, fine-grained

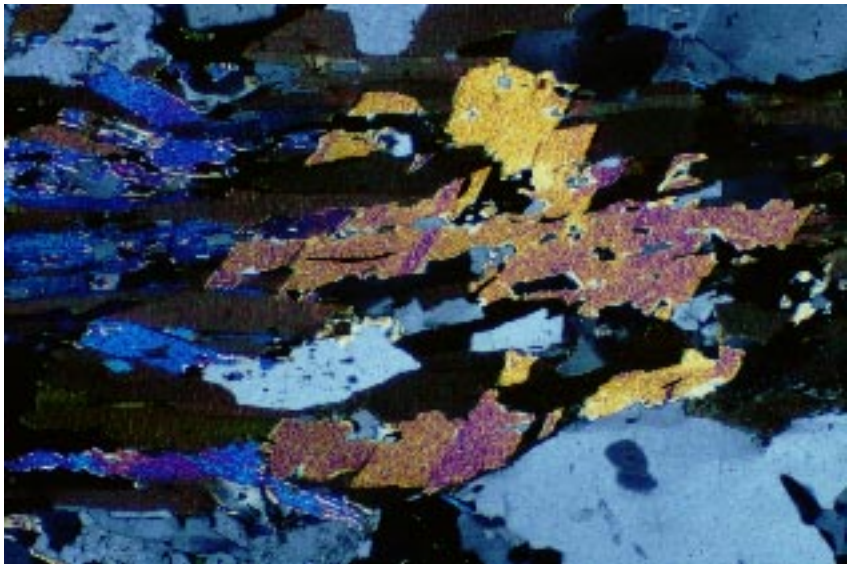

Figure 26 Photomicrograph well-formed muscovite (to the left) intergrown with biotite and aligned parallel to the foliation; optically continuous late muscovite (center) completely overgrows the same foliation. Field of view is 2.4 mm (longest dimenstion); crossed polars; sample 108/2.

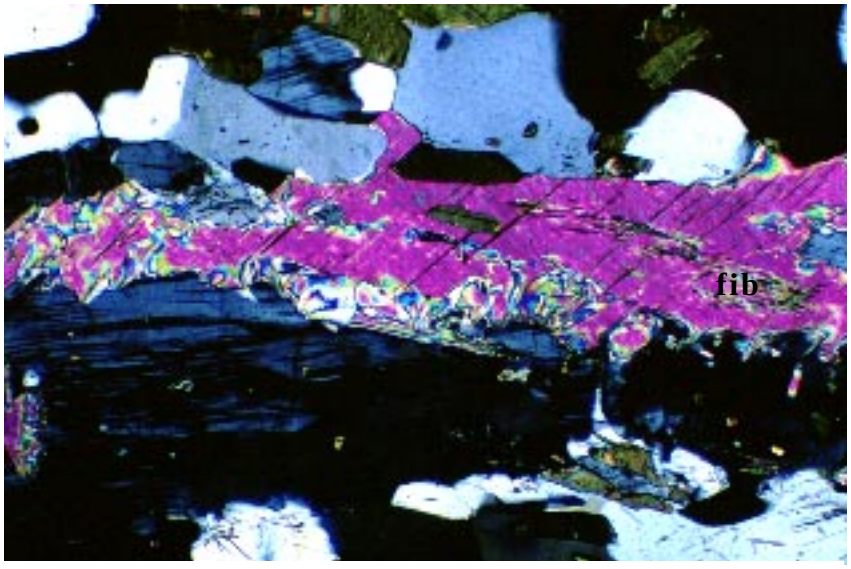

Figure 27 Photomicrograph of a muscovite-quartz symplectite (center of photograph) overgrowing fibrolite (fib) and in contact with microcline (lower left). Field of view is 1.2 mm (longest dimension); crossed polars; sample 99/1.

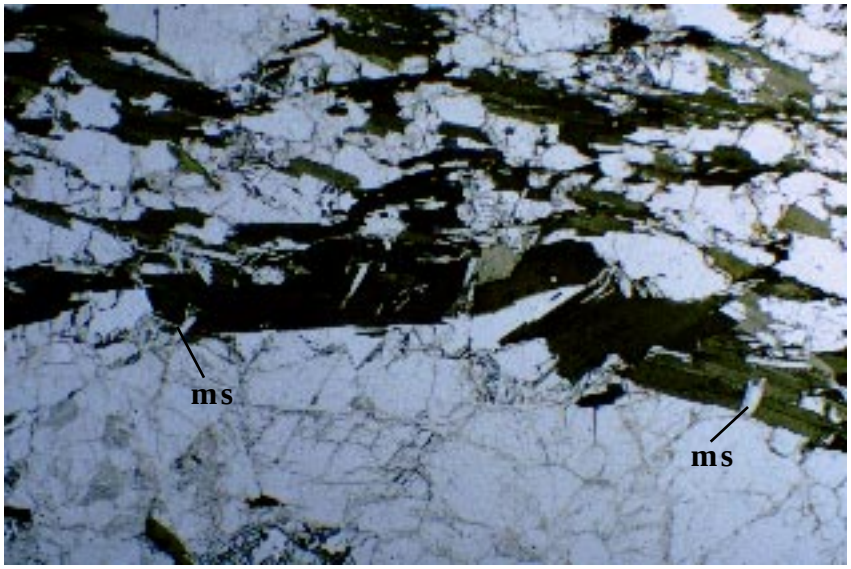

Figure 28 Photomicrograph showing fine-grained secondary muscovite (ms) crosscutting larger biotite grains that define the dominant foliation. Field of view is 2.4 mm (longest dimension); plane light; sample 13G.

muscovite grains clearly cross-cut the primary foliation defined by the coarser-grained biotite. The likely explanation for this post-peak metamorphic muscovite is the rehydration of K-feldspar, as discussed above. Figure 29 shows muscovite enveloping K-feldspar and texturally supports this

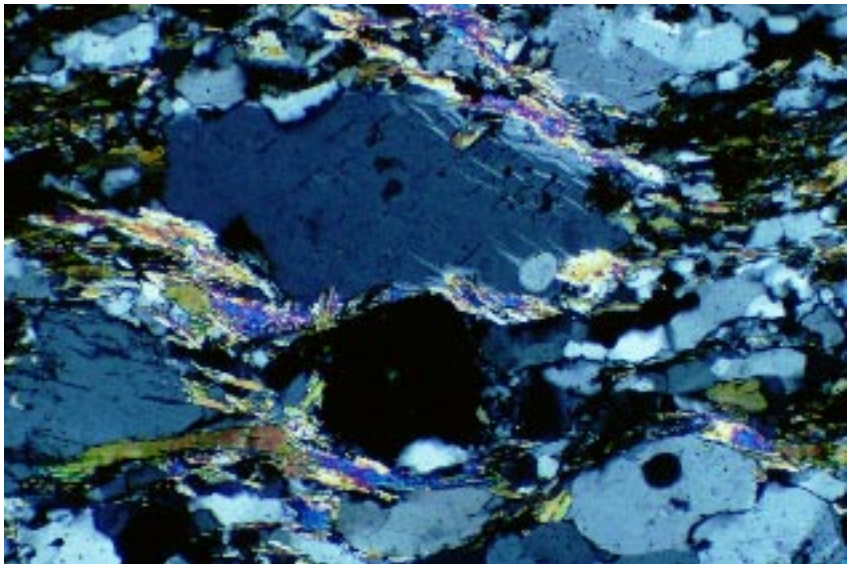

Figure 29 Photomicrograph of muscovite surrounding K-feldspar (center). Field of view is 1.2 mm (longest dimension); crossed polars; sample 79A.

conclusion. Elsewhere, remnants of garnet in the midst of an aggregate of biotite, muscovite, quartz, and plagioclase (Figure 30) indicates that

garnet+ K-feldspar+ plagioclase + H_2O = biotite + muscovite + more calcic plagioclase + quartz

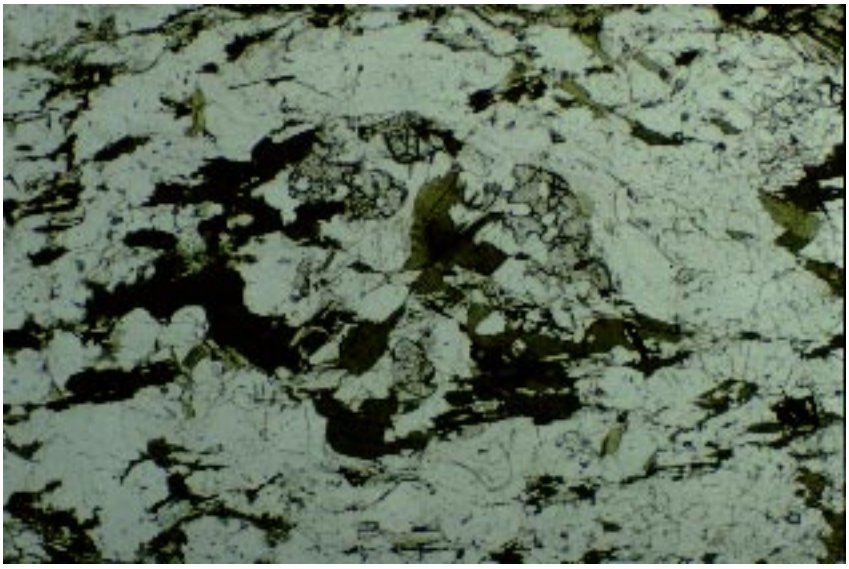

Figure 30 Photomicrograph of garnet relicts (high relief) in a clot of biotite (dark grains), muscovite (colorless, moderate relief), plagioclase, and quartz. Field of view is 2.4 mm (longest dimension); plane light; sample19D.

may be operating. Finally, Figure 31 shows both muscovite *and* biotite cutting the primary foliation. The synchronous retrograde development of both muscovite and biotite suggests the reaction

garnet + K-feldspar + H_2O = biotite + muscovite + quartz;

no garnet remains in this sample. The growth of cross-muscovite (and cross-biotite) at a random yet high angle to the primary foliation (see Figures 28 and 31), suggests static crystallization sometime after peak metamorphism. Figure 32 shows cross-muscovite and biotite (post-1.7 Ga) that are plastically deformed into closer alignment with each other within the Skin Gulch Shear Zone (1.2 Ga). Microtextures such as these confine cross-mica production to some time after 1.7 Ga peak metamorphism and prior to or during 1.2±0.2 Ga ductile shearing.

Porphyroblastic Muscovite

Late muscovite also occurs as large porphyroblasts that grow across the dominant foliation. Figure 33 shows a muscovite porphyroblast (center right) overgrowing an open fold defined by biotite and fibrolite. Muscovite-quartz symplectites associated with K–feldspar, as shown in Figure 34, indicate that the primary reaction responsible for the porphyroblastic muscovite is

K-feldspar + sillimanite + H_2O = muscovite + quartz + albite.

Porphyroblastic muscovite occurs in sillimanite-bearing samples, and commonly envelops fibrolite (see Figures 27 and 33). As with cross-muscovite, muscovite porphyroblasts show little evidence of deformation, except in the vicinity of ductile faults. Figure 35 shows plastically deformed muscovite "fish" from a sample within the Skin Gulch Shear Zone. Hence, muscovite

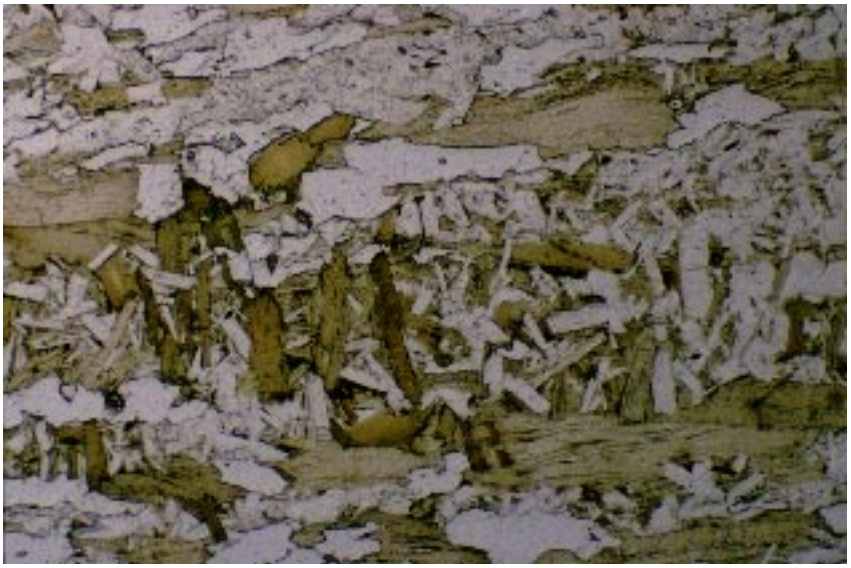

Figure 31 Photomicrograph showing late muscovite and biotite cross-cutting the primary foliation (horizontal in this view). Field of view is 2.4 mm (longest dimension); plane light; sample 83A.

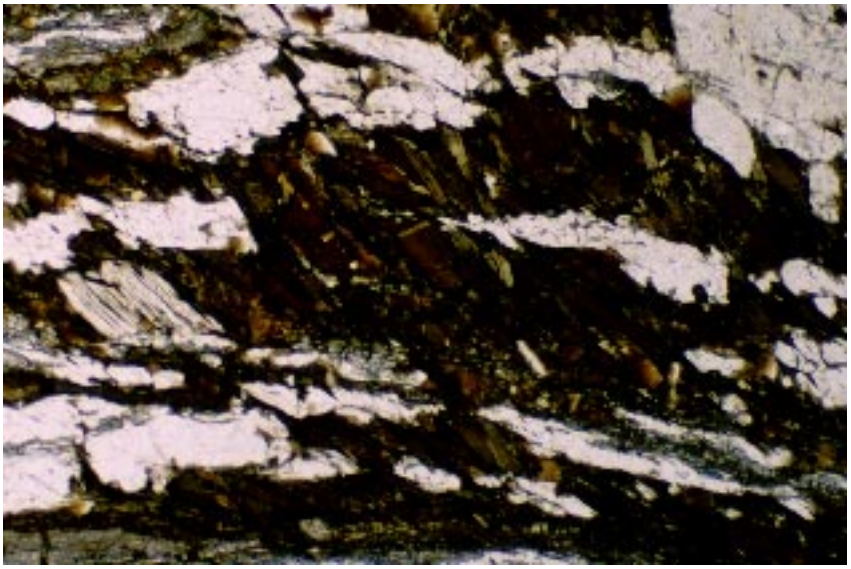

Figure 32 Photomicrograph of aligned cross-biotite and cross-muscovite from a sample within the Skin Gulch Shear Zone, compare to Figure 31. Field of view is 2.4 mm (longest dimension); plane light; sample 67C.

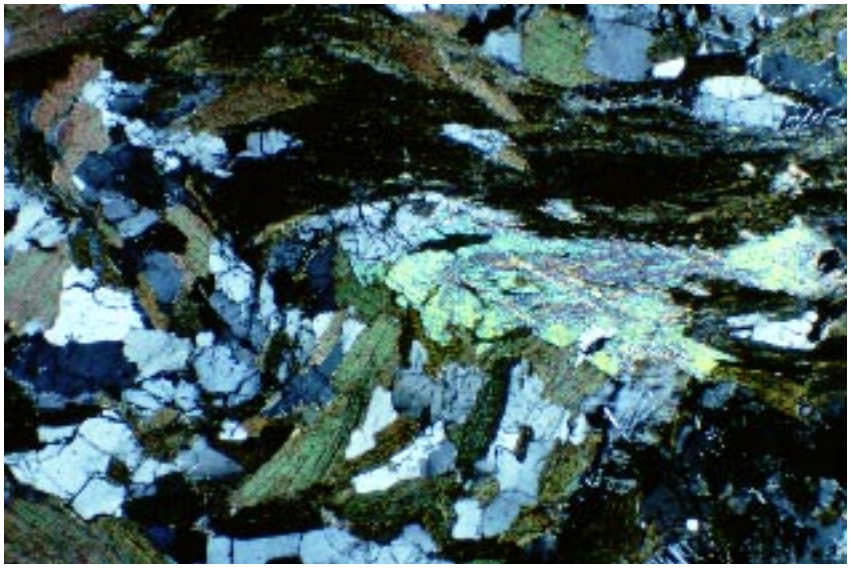

Figure 33 Photomicrograph of porphyroblastic muscovite (pale green) overgrowing an open fold defined by fibrolite and biotite. Field of view is 4.8 mm (longest dimension); crossed polars; sample 11C.

Figure 34 Photomicrograph of muscovite + quartz symplectite on microcline. Field of view is 1.2 mm (longest dimension) crossed polars, sample 57B.

porphyroblasts grew prior to, or synchronous with, the ductile deformation.

Figure 35 Photomicrograph of porphyroblastic muscovite (center) plastically deformed into mica fish in the Skin Gulch Shear Zone. Note the fibrolite inclusions in the muscovite. Field of view is 2.4 mm (longest dimension); plane light; sample 61A.

Muscovite Clots

Secondary muscovite more rarely takes the form of spheroidal aggregates of muscovite (Figure 36). The shape of these aggregates suggests a pseudomorph; however, no remnants of the original mineral remain. Hence, their origin remains speculative. Macroscopically, the pseudomorphs appear as rounded silvery white clots within the foliation plane surrounded by a darker biotite halo (Figure 37).

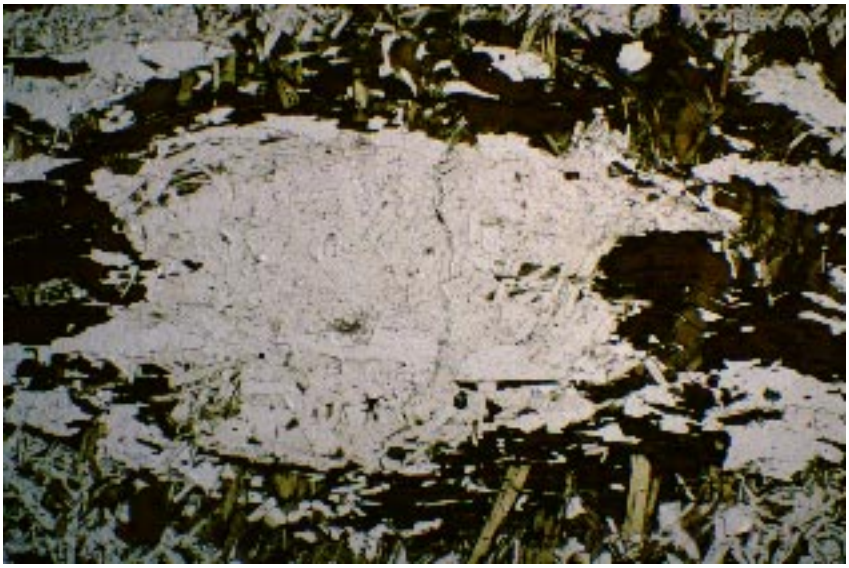

Figure 36 Photomicrograph of a clot of intergrown muscovite grains (colorless center of photograph) surrounded by biotite. The morphology of the muscovite clot suggests that it may be a pseudomorph. Field of view is 4.8 mm (longest dimension); plane light; sample 83A.

Figure 37 Field photograph of silvery white muscovite clots developed within the foliation plane; note the darker biotite halos; photograph #3-7-93, locality 83 (see Figure A-1, Appendix A).

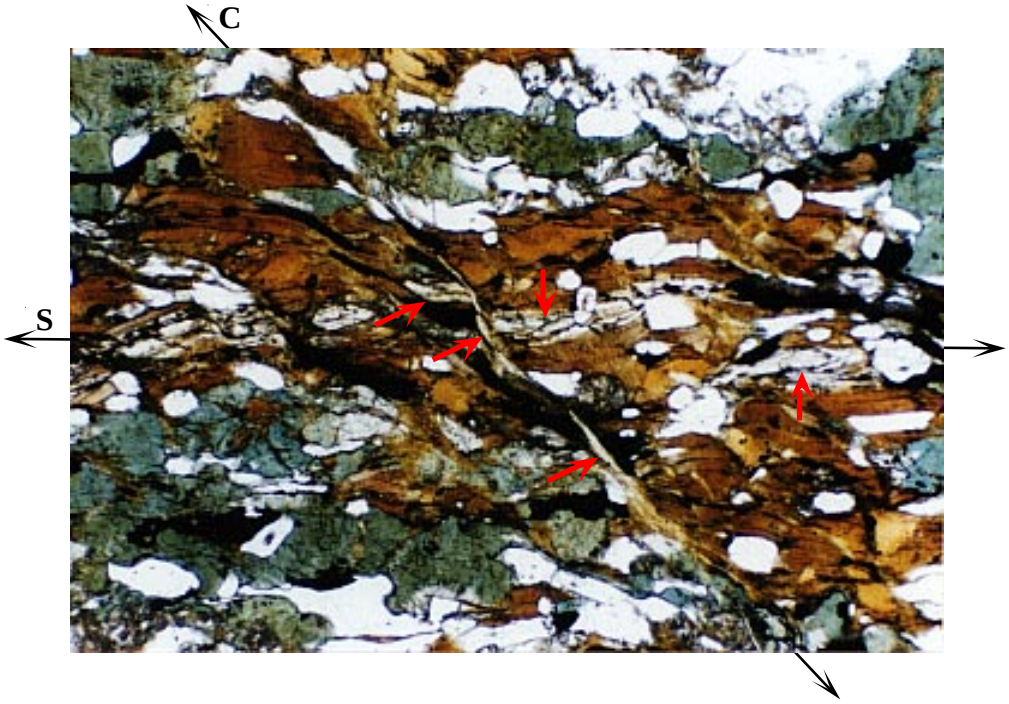

Figure 38 Photomicrograph showing prehnite (red arrows) developed parallel to both S and C surfaces. Field of veiw is 2.4 mm (longest dimension); plane light; sample 80/1.

Amphibolites

Amphibolites normally contain *hbl-pl-qtz-ilm±di±ap±py* (see samples 19C, 50A, 62A, 70D, 85A, 91C,104D and 113K, Table A-1, Appendix A); less typically they contain biotite and garnet as well. The modes for garnet-bearing amphibolite samples selected for thermobarometry are presented in Table 3. Garnet is irregularly shaped and biotite is red-brown. The hornblende is sub- to anhedral and is pleochroic from olive green to straw yellow to bluish green. Both samples contain ilmenite and lack titanite. Upper amphibolite facies conditions are suggested by the absence of titanite, which is favored by low temperature, high pressure, and high oxygen fugacity (Spear, 1981). Alteration generally is restricted to the formation of epidote, clinozoisite, and/or chlorite.

Table 3 Modes of amphibolites used for thermobarometry.

	80B	**107F**
plagioclase *An content**	tr *.91-.96‡*	32 *.40-.59*
quartz	18	35
hornblende	32	27
biotite	21	5
garnet	7	1
ilmenite	7	2
apatite	3	tr
zircon	tr	tr
allanite	-	tr
clinozoisite	2	-
prehnite	8	-
sericite	1	-
total	*99*	*100*
# grts per thin section	**±12**	**4**
garnet inclusions	*qtz, bt, ilm, ap*	*bt, pl, ilm,qtz, ap*

** total range in An content from microprobe analysis.*
‡ does not represent primary plagioclase

Sample 80 contains prehnite, a secondary mineral observed nowhere else in the study area. Prehnite is a low temperature mineral stable in the zeolite and greenschist facies; its upper stability limit is about 400°C (Liou, 1971). The prehnite in sample 80 is colorless with a micaceous habit and moderate to high relief; it is biaxial (+), length fast, shows patchy near-parallel extinction, and has a maximum birefringence of 0.021. The presence of prehnite was confirmed by microprobe analysis (discussed in the next chapter). Sample 80 is further distinguished by the rarity of plagioclase. This suggests that plagioclase breakdown, in the presence of water at low temperatures, ultimately produced prehnite (and clinozoisite). Outcrop 80 is located near the Skin Gulch and Poudre River Shear Zones (see Figure A-1, Appendix A) and shows well-developed S-C surfaces. Prehnite is intergrown with biotite aligned parallel to the schistosity (S), but also is well-developed within the *cisaillement* (or shear) surfaces (C) as shown in Figure 38. Hence, the prehnite either pre-dates or is synchronous with the ductile shearing. The low proportion of plagioclase (including its alteration products), the high proportion of biotite, and the presence of aluminous phases such as prehnite, clinozoisite, and garnet suggests that the probable protolith of sample 80 was a marl.

III. MINERAL CHEMISTRY

Microprobe Analyses

In order to perform thermobarometric calculations, the mineral composition in the equilibrium assemblages must be determined. However, minerals commonly vary in composition, even within a single thin section. This makes it difficult to assess which minerals or portions of minerals represent the peak metamorphic equilibrium assemblage (or closest approximation thereof). Therefore, careful analysis of mineral compositions across a thin section must be combined with petrographic observations in order to choose the most appropriate compositions for the pressure-temperature calculations.

Polished thin sections were analyzed using the CAMECA SX-50 microprobe at Virginia Tech. The quantitative analyses were collected using an accelerating potential of 15 kV and a beam current of 20 nA. These analyses are reported in Appendix B (Tables B-1 - B-8); data from representative garnet traverses are plotted as compositional profiles in Appendix C. Qualitative images of representative garnets in the form of X-ray maps also were collected. These were constructed by accumulating X-ray counts keyed to the X-Y positions within a 512 x 512 grid. The electron beam was defocussed to approximate the selected step size within this 512 x 512 grid. Accelerating potential for the X-ray mapping was 25 kV with a beam current of 500 nA. Counts for Mg, Ca, Mn, and Fe were simultaneously collected. The final garnet X-ray images are presented in Appendix D as false-color analog representations of the distribution of Mn, Mg, Ca, and Fe concentrations based on the X-ray intensities.

Pelites and Semi-Pelites

Garnet

Complete garnet analyses are presented in Table B-1, Appendix B. Garnets are zoned, with rims enriched in iron and manganese and depleted in magnesium relative to the core compositions. The zoning is shown by the typical Mg and Mn X-ray images in Figure 39 and the corresponding traverses for these images in Figure 40. Sample 113E, profile GT6 is typical; almandine increases incrementally from the core toward the rim, whereas the pyrope component decreases concomitantly. This incremental change suggests continued garnet growth as the rocks began to cool. Within 0.1 to 0.2 mm of the rim, the profile becomes significantly steeper. This steepening effect is especially pronounced where the rim is adjacent to biotite (compare the left and right sides of profile 113E, Figure 40). Spessartine also increases at the rims, but the change is less conspicuous because spessartine base levels are low. Grossular compositions show little variation from core to rim. The changes in almandine, pyrope, and spessartine observed at the garnet rim also occur where fractures cut through garnet interiors, as shown by the X-ray images for 88A (Figure 39) and by traverse GT2 (Figure 40). Similar changes in spessartine and almandine in upper amphibolite facies garnets have been documented elsewhere (e.g., Grant and Weiblen, 1971; Hess, 1971; Loomis, 1975; Ashworth and Chinner, 1978; Tracy and Dietsch, 1982). All agree that late retrograde activity in the form of garnet resorption and cation exchange with biotite can produce pronounced increases in almandine and spessartine at the rim and along through-going fractures. Garnet becomes iron-enriched as secondary biotite fractionates magnesium, resulting in magnesium-depleted garnet rims. Because manganese is not compatible in the surrounding mineral phases, it becomes progressively concentrated in garnet rims as resorption progresses (Grant and Weiblen, 1971; Bethune and Laduron, 1975, Woodsworth, 1977).

Tables 4a and 4b list the average Fe/(Fe+Mg) ratios and spessartine values for different locations within analyzed garnets. These tables show that Fe/(Fe+Mg) and spessartine are higher at the garnet rim and that the highest values typically occur where garnet lies directly adjacent to biotite

Figure 39 Typical false color images of the distribution of Mg and Mn concentrations in garnet based on X-ray intensities; solid lines represent garnet traverses shown in Figure 40.

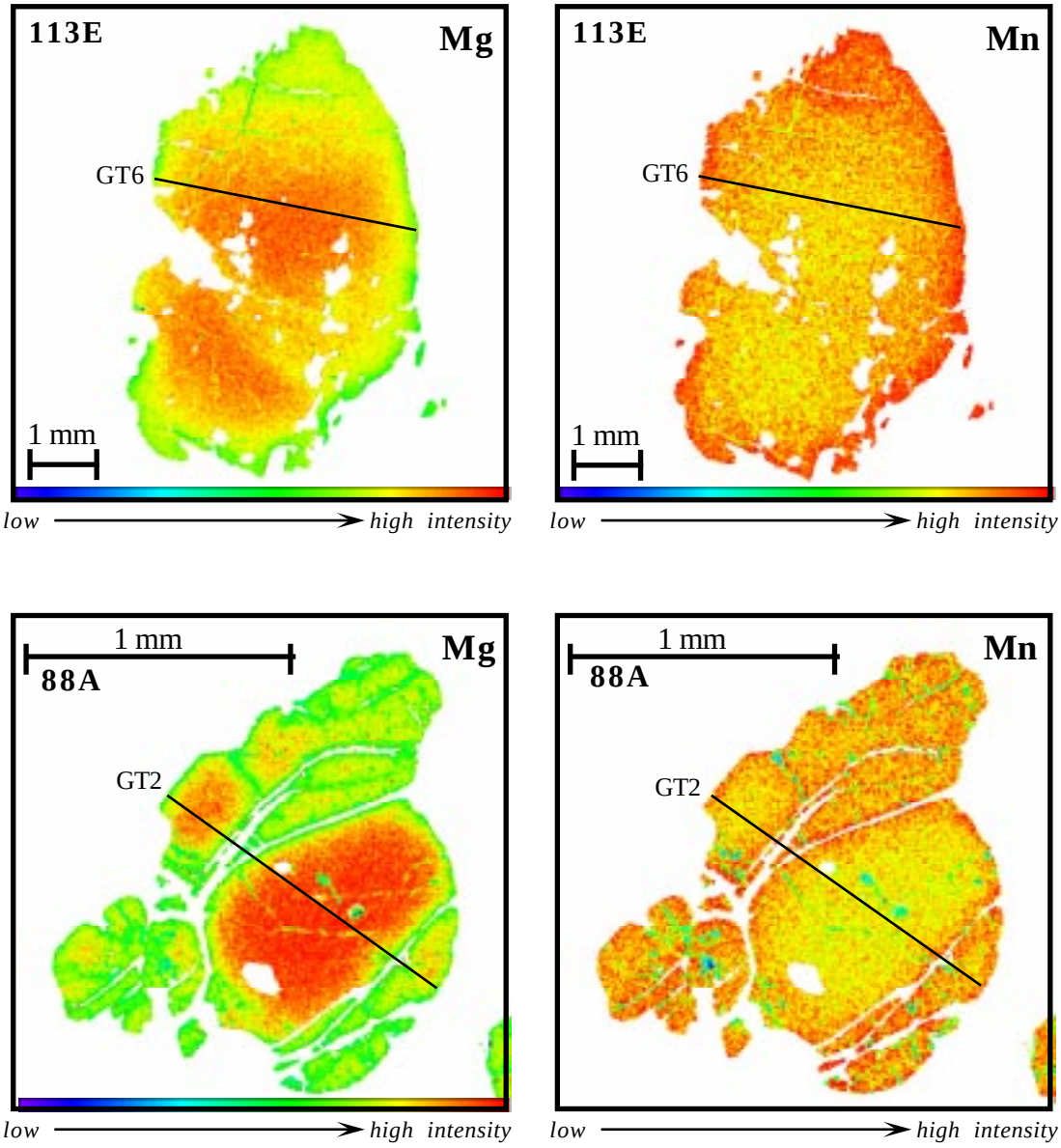

Mg depletion at the rims ***Mn enrichment at the rims***

Figure 40 Typical garnet profiles (pelites/semi-pelites); dashed lines represent uniform core compositions (see Figure 39 for traverse locations).

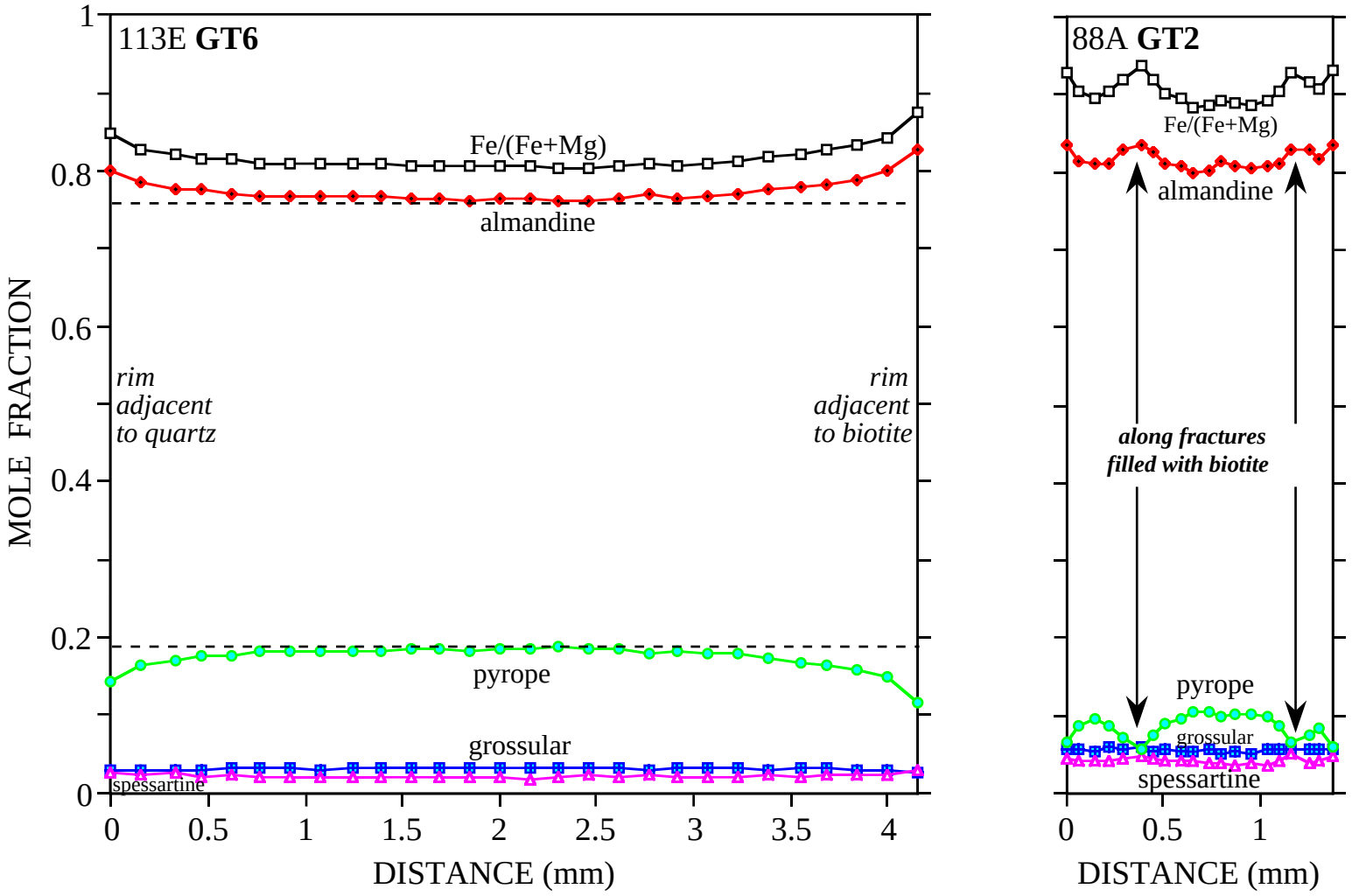

Table 4a Average Fe/(Fe+Mg) values for analyzed garnets; pelites and semi-pelites (listed from west to east)*

sample #	interior	rim adj bt	adj fract, bt-filled	rim adj qtz	rim adj pl	rim adj crd	adj bt inclusion
50E	0.815	0.866		0.857	0.861		
19D	0.951	0.964	0.969	0.960	0.964		
68A	0.933	0.949	0.950	0.947	0.945		0.959
66A	0.935	0.965	0.954	0.951			
88A	0.887	0.929	0.927	0.920	0.914		
86D	0.906	0.941	0.934	0.924	0.924		
93A	0.938	0.944	0.950				0.953
104E	0.856	0.890	0.898	0.873	0.881		
104F	0.863	0.896		0.871			
108C	0.853	0.897	0.891		0.890		
109A	0.883	0.885	0.908		0.880		
110A	0.905	0.921		0.914			
111A	0.868	0.892	0.893	0.880			0.899
113(4a)	0.833	0.878		0.850	0.847		
113C	0.837	0.864		0.851	0.857		
113E	0.813	0.873		0.842			0.828
116(3a)	0.812	0.863		0.842			
119A	0.805	0.864		0.838			
128(10a)	0.799	0.887					
128(10c)	0.791					0.855	
133A	0.840	0.866		0.851			
134D	0.828	0.875					

Table 4b Average spessartine values for analyzed garnets; pelites and semi-pelites (listed from west to east)*

sample #	interior	rim adj bt	adj fract, bt-filled	rim adj qtz	rim adj pl	rim adj crd	adj bt inclusion
50E	0.071	0.106		0.100	0.095		
19D	0.194	0.265	0.281	0.241	0.257		
68A	0.026	0.034	0.030	0.032	0.029		0.034
66A	0.119	0.198	0.177	0.156			
88A	0.040	0.049	0.050	0.045	0.045		
86D	0.057	0.063	0.064	0.062	0.086		
93A	0.132	0.160	0.161				0.170
104E	0.038	0.055	0.059	0.055	0.053		
104F	0.036	0.049		0.042			
108C	0.064	0.109	0.075		0.103		
109A	0.068	0.070	0.072		0.068		
110A	0.077	0.092		0.087			
111A	0.022	0.032	0.028	0.027			0.028
113(4a)	0.021	0.029		0.023	0.022		
113C	0.023	0.030		0.026	0.029		
113E	0.021	0.030		0.026			0.022
116(3a)	0.036	0.049		0.044			
119A	0.036	0.052		0.047			
128(10a)	0.020	0.061					
128(10c)	0.045					0.077	
133A	0.030	0.039		0.032			
134D	0.047	0.061					

** abbreviations used: adj = adjacent; bt = biotite; fract = fracture; pl = plagioclase; qtz = quartz*

(compare to values adjacent to quartz or plagioclase). In addition, analytical points of the garnet interior that are adjacent to biotite inclusions show elevated Fe contents relative to other interior points. These data support the case for Fe-Mg exchange between garnet and biotite and further imply that the cation exchange was localized in the vicinity of neighboring garnet-biotite pairs.

Biotite

Biotite was analyzed both adjacent to garnet or cordierite (contact biotite) and in areas as far removed from garnet or cordierite as possible within each thin section (matrix biotite). The complete analyses are presented in Table B-2, Appendix B. Biotite exhibits generally uniform compositions within a single thin section *except* where it is in direct contact with garnet or cordierite. Tables 5a and 5b list the average Fe/(Fe+Mg) and Ti values for matrix biotite and contact biotite. These data are presented graphically in Figures 41a and 41b by plotting the values of Fe/(Fe+Mg) and Ti/6, respectively, for matrix biotite versus contact biotite. A dotted 1:1 line is indicated in each plot. Samples that fall on, or near, this line show no significant compositional differences between matrix and contact biotites. On the other hand, samples that lie above the line show decreased Fe or Ti content in contact biotite, whereas those below the line show an analogous increase. The majority of the samples show lower levels of both Fe and Ti in contact biotites. The lower Ti content explains the greenish color observed in contact biotites (see Figure 14). According to Rossman (1984), green biotites always have low Ti contents whereas high Ti contents characterize red-brown biotite (as found in the matrix biotites). The lower Fe levels in contact biotite and associated Fe-enrichment of the garnet rims would be expected from retrograde Fe-Mg exchange between garnet and biotite. The distribution coefficient (K_D) for Fe-Mg exchange between garnet and biotite is:

$$K_D = \frac{\left(\frac{Mg}{Fe+Mg}\right)^{grt}}{\left(\frac{Fe}{Fe+Mg}\right)^{grt}} \frac{\left(\frac{Fe}{Fe+Mg}\right)^{bt}}{\left(\frac{Mg}{Fe+Mg}\right)^{bt}}$$

At the reduced temperatures of retrogression, the minerals are less tolerant of Fe or Mg substitution and K_D is lowered (Yardley, 1989). A lower K_D necessitates Fe-enrichment in the garnet rims and Mg-enrichment (or Fe depletion) in the contact biotite.

The samples that have equivalent or increased Fe/(Fe+Mg) in contact biotite relative to matrix biotite (1) contain a large number of garnet grains per thin section (filled symbols, Figure 41a) or, (2) contain a few large, highly fragmented garnets (cross symbols, Figure 41a). Assuming that reaction took place along the *exterior surfaces* of the garnet, the presence of numerous garnets (as opposed to a few large garnets of equivalent volume) increased the amount of garnet available for reaction with biotite. Similarly, the surface area available for potential reaction with nearby biotite was dramatically increased in highly fragmented large garnets. Both situations increase the effective ratio of garnet to biotite such that the correspondingly larger bulk change in Fe/(Fe+Mg) ratio must be spread over a larger proportion of the biotite (Tracy et al., 1976; Ferry and Spear, 1978).

Sample 88A, labeled in Figure 41, is an exception to this phenomenon. This sample contains a large number of garnet grains, yet shows a marked decrease in Fe/(Fe+Mg) (and Ti) contents in the contact biotites where a more even distribution would be expected. Unlike garnet in the other samples, those in sample 88A, a migmatite, are isolated within the leucosome whereas the matrix biotites lie within the surrounding host. The textural and compositional information from sample 88A suggest that the leucosome insulated the garnets from late ion exchange with the biotites in the surrounding host area. In this way, contact biotite compositions remained distinctly different from the matrix biotite. Alternatively, it may be that the secondary biotite in sample 88A arrived later

Table 5a Fe/(Fe+Mg) values for analyzed biotites; pelites and semi-pelites (listed from west to east)

sample #	matrix	adjacent garnet	fracture fill	garnet corona	adjacent cordierite	pale green, on cordierite
50E	0.515	0.492				
19D	0.741*	0.747				
68A	0.733	0.746				
66A	0.772	0.805				
88A	0.675‡	0.575	0.553			
86D	0.675	0.582				
93A	0.702	0.730				
104E	0.600	0.556		0.587		
104F	0.615	0.598				
108C	0.637	0.637		0.588		
109A	0.578	0.588				
110A	0.643	0.663				
111A	0.641	0.637				
113(4a)	0.577	0.535				
113C	0.575	0.532				
113E	0.580	0.530				
116(3a)	0.561	0.525				
119A	0.574	0.511				
128(10a)	0.579	0.560				
128(10b)	0.437				0.387	0.339
128(10c)	0.461		0.382		0.481	
133A	0.579	0.569				
134D	0.590	0.511				

** values for the "right" side of the leucosome; left side = 0.766*

Table 5b Ti/6 values for analyzed biotites; pelites and semi-pelites (listed from west to east)

sample #	matrix	adjacent garnet	fracture fill	garnet corona	adjacent cordierite	pale green, on cordierite
50E	0.040	0.032				
19D	0.043*	0.053				
68A	0.045	0.041				
66A	0.045	0.020				
88A	0.068‡	0.001	0.001			
86D	0.067	0.008				
93A	0.057	0.024				
104E	0.068	0.026		0.051		
104F	0.048	0.036				
108C	0.071	0.066		0.053		
109A	0.057	0.057				
110A	0.069	0.049				
111A	0.066	0.075				
113(4a)	0.072	0.041				
113C	0.073	0.054				
113E	0.071	0.066				
116(3a)	0.064	0.048				
119A	0.067	0.028				
128(10a)	0.065	0.019				
128(10b)	0.041				0.027	0.000
128(10c)	0.059		0.003		0.050	
133A	0.072	0.066				
134D	0.061	0.013				

** values for the "right" side of the leucosome; left side = 0.066*

Figure 41a Plot of Fe/(Fe+Mg) for matrix biotite versus contact biotite.

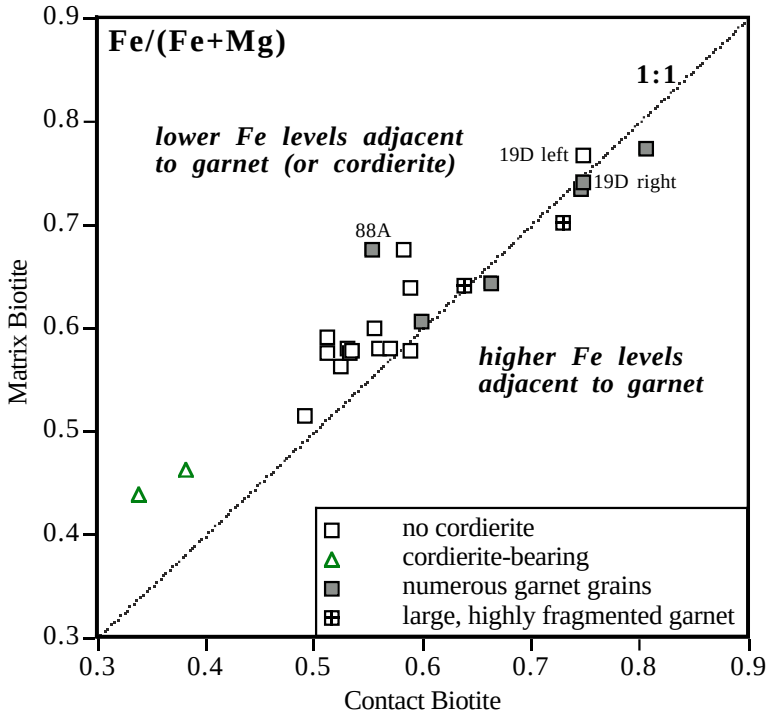

Figure 41b Plot of Ti/6 for matrix biotite versus contact biotite

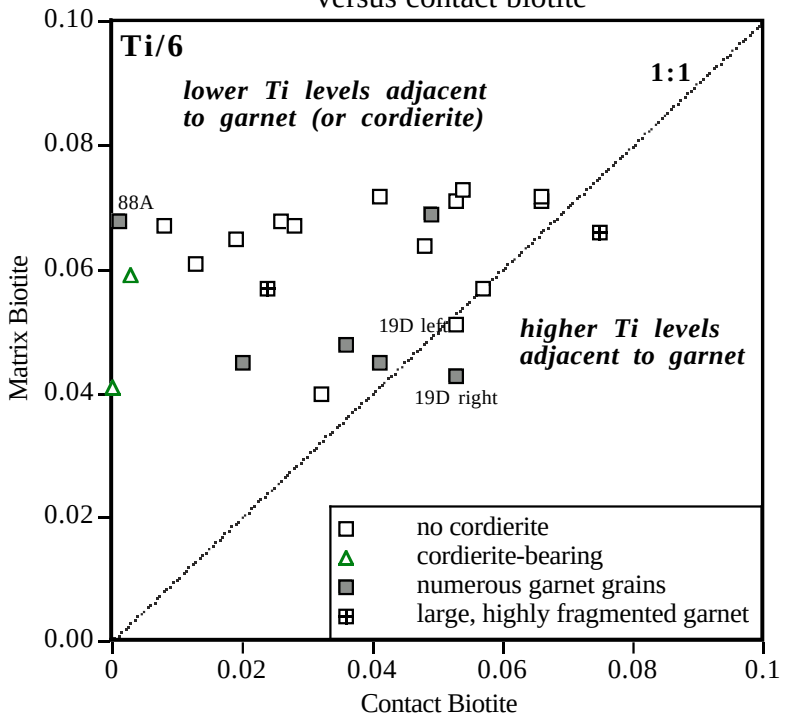

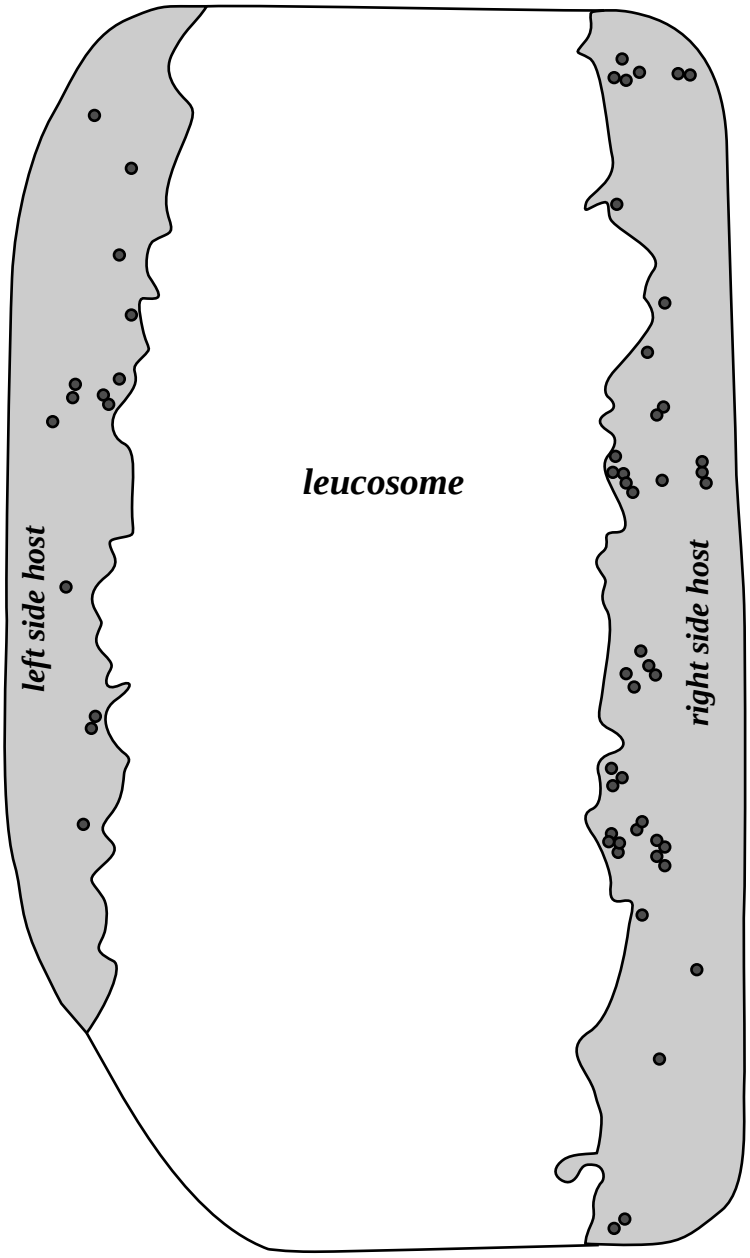

Figure 42 Full thin section sketch of sample 19D; leucosome is shown in white and the surrounding host in gray. Garnet locations are shown by the circles. Note that the majority of the garnets are located within the host on the *right hand side* of the leucosome.

(and at a lower temperature) than in the other samples.

The ability of the leucosome to provide local insulation from retrograde reactions is further illustrated by sample 19D, another migmatite. Figure 42 is a sketch showing where the garnets are located in thin section 19D. The majority of the garnets in this sample (circles) occur within the host on the right hand side of the leucosome in this sketch. Average Fe/(Fe+Mg) for right-side matrix biotite, labeled '19D right' in Figure 41a, is 0.747, essentially equivalent to the Fe/(Fe+Mg) for contact biotite (0.741). On the other hand, the Fe/(Fe+Mg) ratio for matrix biotite on the lefthand side (where far fewer garnet grains are found) is 0.766, a marked increase over the contact biotite value (see '19D left' in Figure 41a). This suggests that the left-side matrix biotite remained isolated from the high effective garnet:biotite ratios which modified the matrix biotite compositions on the righthand side of the leucosome.

Cordierite

Pelitic samples collected from outcrop 128 contained three different assemblages: *grt-bt-sil-qtz-pl-kfs* (128/10a), *crd-bt-sil-qtz-pl* (128/10b), and *crd-grt-bt-sil-qtz-pl* (128/10c). K-feldspar is assumed to have been present in the peak assemblages of 128/10b and 128/10c but was exhausted during later post-peak reactions (see Chapter II). The occurrence of a given assemblage appears to be related to bulk composition, as illustrated in the AFM diagram in Figure 43. Note that grt-bt-sil characterizes the most iron-rich bulk composition and the most magnesian yields crd-bt-sil; the intermediate bulk compositions contain grt-crd-bt. Thus, the persistence of cordierite in 128/10b and 128/10c is attributed to their more magnesian bulk compositions. The complete cordierite analyses for samples 128/10b and 128/10c are presented in Table B-3, Appendix B.

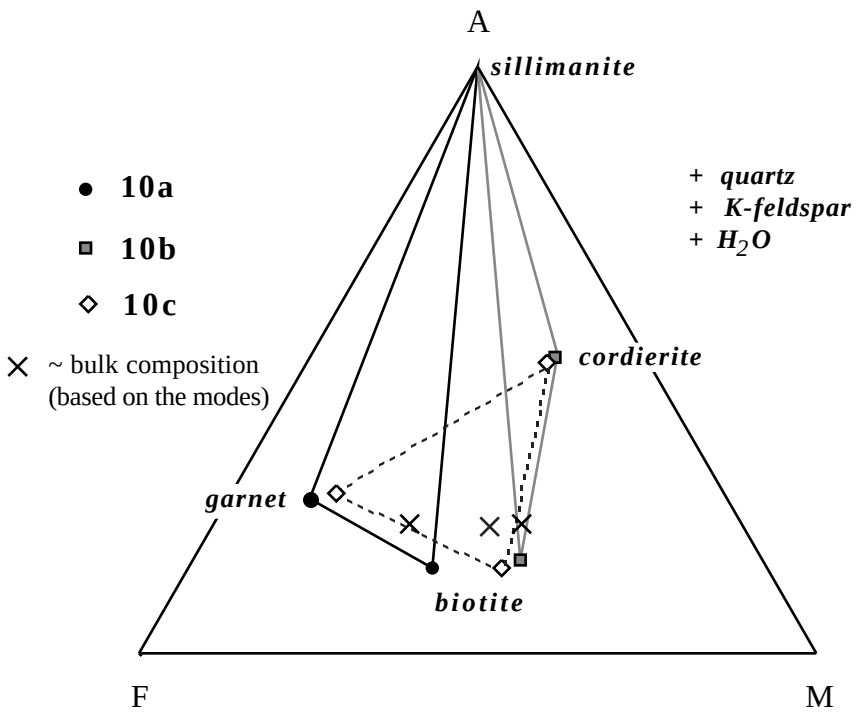

Figure 43 AFM diagram projected through K-feldspar for all the approximate peak metamorphic assemblages observed in pelites from outcrop 128.

Garnet-Free Sample

Figure 44 is a Fe/(Fe+Mg) profile across the least altered cordierite grain from sample 128/10b (no garnet in the assemblage). The location of this traverse is indicated on the sketch in Figure 45. The core compositions exhibit a fairly uniform

Fe/(Fe+Mg) ratio of 0.273. Within approximately 0.2 millimeters of the rim, the Fe/(Fe+Mg) ratio decreases to an approximate value of 0.262 at the rim.

Flat interior profiles commonly are attributed to diffusional homogenization during peak metamorphism (Young, 1989). Therefore, the homogeneous cordierite interior is assumed to represent peak compositions created by wholesale chemical diffusion within cordierite. These compositions are assumed to be in equilibrium with the matrix biotite. The decline in Fe/(Fe+Mg) values toward the cordierite rim (Figure 44) suggests reactions at lower temperature with more sluggish chemical diffusion. Assuming that biotite and cordierite remained in reaction equilibrium, Fe-Mg exchange between coexisting cordierite and biotite would shift cordierite and nearby biotite toward Mg-enrichment as the temperature continued to fall. This shift in the crd-bt-sil three phase triangle toward more magnesian compositions is indicated on the AFM diagram in Figure 46 and is demonstrated by the arrows in the T-X_{Fe-Mg} plot in Figure 47a. Increasing μ_{H2O} produces a similar result as will be demonstrated by applying the Gibbs' Method to these data in Chapter V.

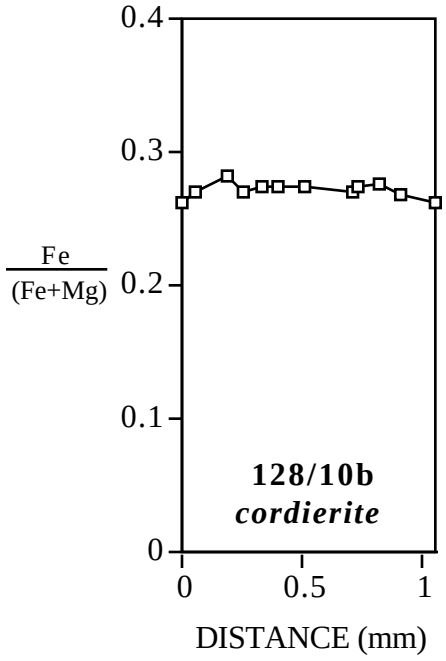

Figure 44 Compositional profile for garnet-free sample 128/10b.

The cordierite in sample 10b is associated with both biotite and muscovite, a retrograde assemblage attributed to the breakdown of cordierite. Most cordierite grains in sample 128/10b show a high degree of resorption and replacement by biotite and muscovite. The cordierite grain depicted in Figure 45 is one of the best preserved grains in this sample. Fe/(Fe+Mg) ratios for biotite grains surrounding this cordierite are indicated in Figure 45. Clearly, green biotite nearest to the cordierite has a lower Fe/(Fe+Mg), 0.39, than the more distant red brown biotite grains, 0.42. Across the thin section, matrix biotite has the highest Fe/(Fe+Mg), 0.44, whereas biotite analyzed adjacent to cordierite pseudomorphs (see Figure 18) has the lowest value, 0.34. It can be inferred that resorption of the relatively Mg-rich cordierite during retrogression caused the newly forming green biotite to become correspondingly enriched in magnesium, thus lowering its Fe/(Fe+Mg) ratio. The retrogressive change in biotite composition can be seen in the AFM diagram in Figure 46.

Cordierite + Garnet Assemblage

The Fe/(Fe+Mg) values for cordierite in the garnet-bearing sample (128/10c) are higher than those in the garnet-free sample (128/10b), as are summarized in Table 6. In sample 128/10c, the highest Fe/(Fe+Mg) occurs in cordierite adjacent to garnet, whereas the lowest value occurs in

Table 6
Average Fe/(Fe+Mg) ratios for analyzed cordierites

128/10b - *cordierite, no garnet*

rim	interior
0.262	0.273

128/10c - *cordierite co-existing with garnet*

adjacent garnet		**matrix**	**pseudomorph**
rim	interior	interior	near rim
0.330	0.338	0.295	0.303

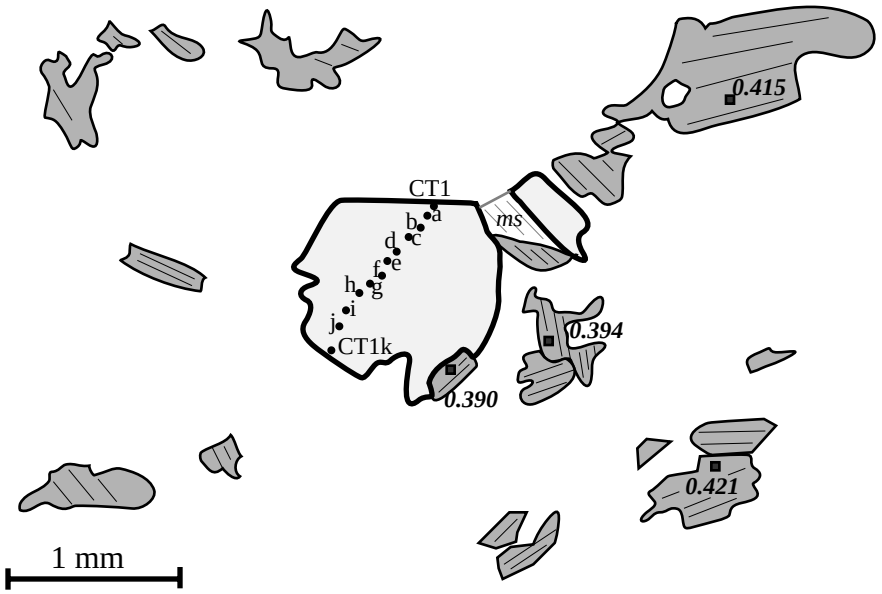

Figure 45 Sketch from a photomicrograph of sample 128/10b showing cordierite (bold outlines) and biotite (gray). Labeled circles indicate the location of points along the cordierite traverse. The square symbols indicate analyzed biotite points and their associated Fe/(Fe+Mg) ratios.

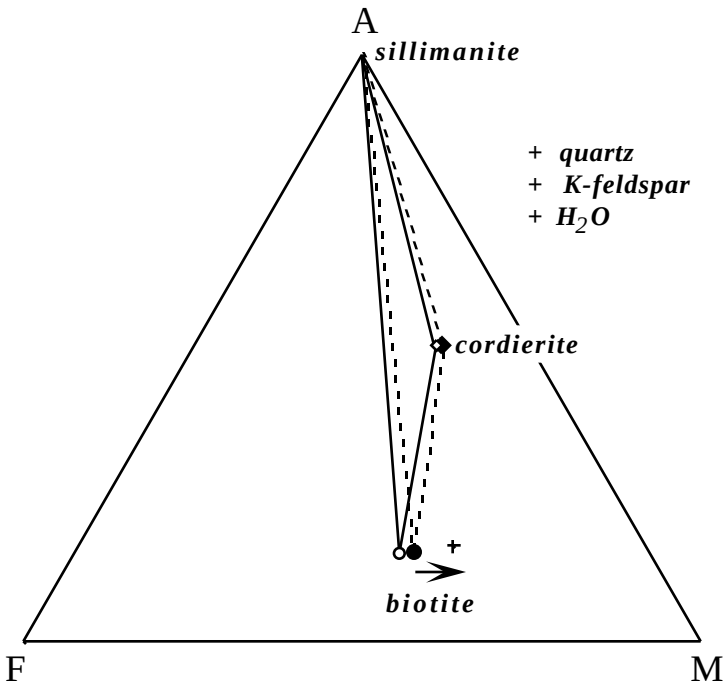

Figure 46 AFM diagram projected through K-feldspar showing cordierite and biotite compositions analyzed for the garnet-free sample, 128/10b. Open symbols (probable peak conditions): interior cordierite-matrix biotite; filled symbols: cordierite rims-nearby red-brown biotite; plus symbol: pale green biotite pseudomorph of cordierite. Note the shift of the crd-bt-sil triangle toward Mg-enrichment (dashed tie lines). The arrow indicates the retrograde change of biotite toward lower Fe/(Fe+Mg) as cordierite is resorbed.

matrix cordierite. The lower Fe/(Fe+Mg) ratio of the matrix cordierite and its texturally different appearance all suggest that the Mg-enriched matrix cordierite still may represent near-peak metamorphic conditions. The higher Fe/(Fe+Mg) of cordierite adjacent to garnet is consistent with breakdown of garnet to form cordierite. Textures indicate that garnet broke down via retrograde reactions 5 (*grt + kfs + H_2O = crd + bt + qtz*) and 4 (*grt + sil + qtz = crd*) in Figure 16, probably during decompression and cooling. Reaction 5 is the continuous reaction depicted by the grt-bt-crd loop in the T–$X_{Fe–Mg}$ and P–X_{Fe-Mg} diagrams in Figure 47a and 47b. If biotite, cordierite, and garnet remained in equilibrium, then with decreasing pressure coexisting garnet, biotite, and cordierite would move along the reaction loop, becoming enriched in Fe (see arrows in Figure 47b). This trend is supported by (1) the higher Fe/(Fe+Mg) values in cordierite adjacent to garnet, (2) the higher Fe/(Fe+Mg) in biotite adjacent to cordierite (0.483, see Table 5a) compared to matrix biotite (0.461), and (3) the Fe-enriched rims of garnet adjacent to cordierite, as depicted by the compositional profiles in Figure 48. A similar result is produced by decreasing the μ_{H2O} (see Chapter V). The AFM diagram in Figure 49 shows the shift in the near-peak three phase triangle (solid tie lines) toward the Fe corner (dotted tie lines). Further retrogression in the form of late cation exchange between biotite and garnet is evident in the low Fe/(Fe+Mg) ratio of green biotites found along garnet fractures (0.382; plus symbol in Figure 49).

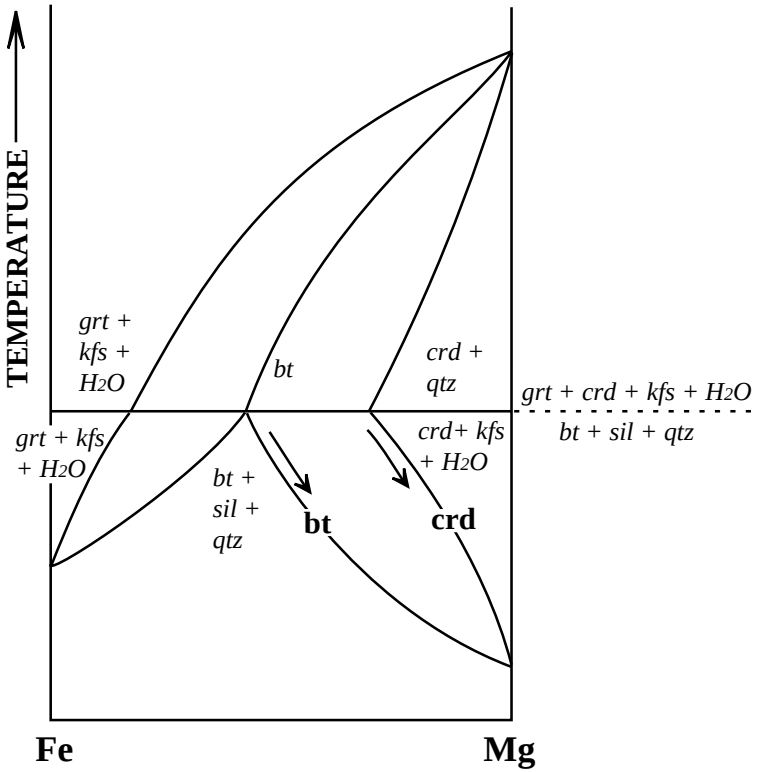

Figure 47a Schematic T-X(Fe-Mg) plot for continuous and discontinuous reactions involving grt-bt-crd-sil-kfs-qtz-H_2O (after Thompson, 1976a). Note that on cooling, coexisting biotite and cordierite become more Mg-rich (arrows).

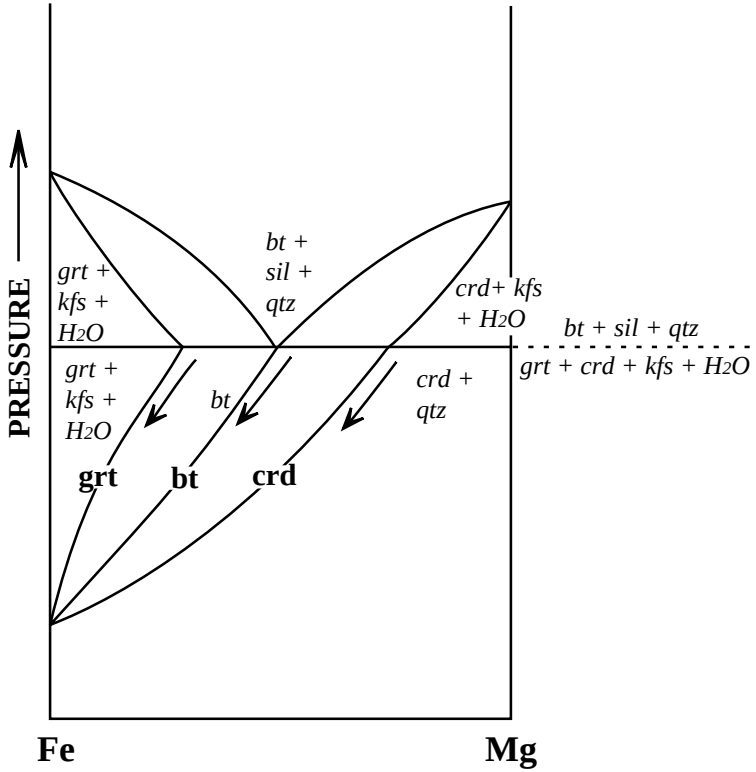

Figure 47b Schematic P-X(Fe-Mg) plot for continuous and discontinuous reactions involving grt-bt-crd-sil-kfs-qtz-H_2O (after Thompson, 1976a). Note that on decompression, coexisting garnet, biotite, and cordierite become more Fe-rich (arrows).

Figure 48 Compositional profiles for adjacent cordierite (crd1) and garnet (grt1) in sample 128/10c.

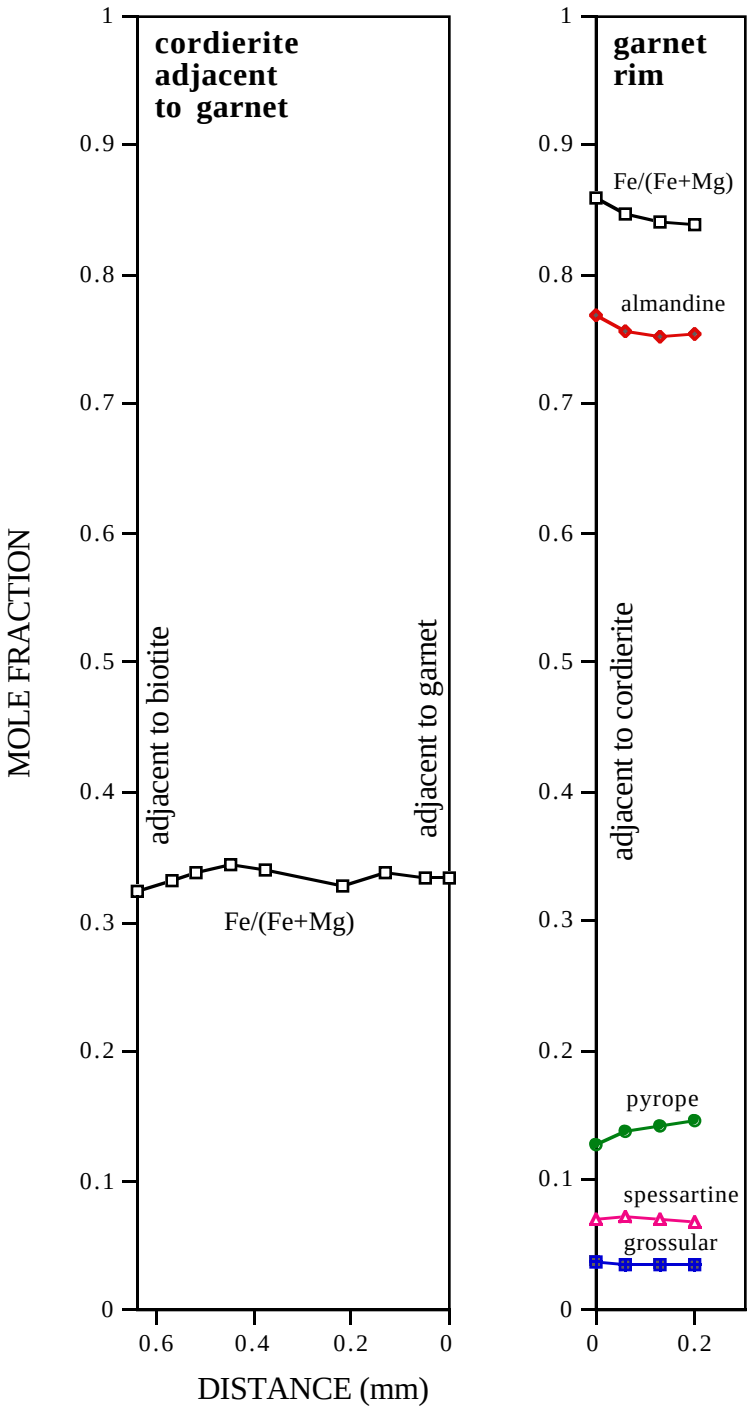

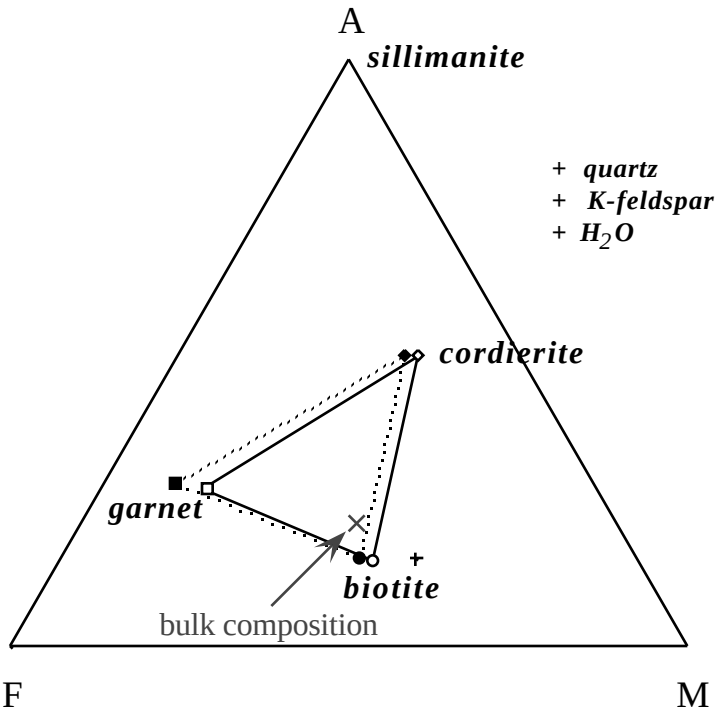

Figure 49 AFM diagram projected through K-feldspar showing garnet, biotite, and cordierite compositions analyzed for sample 128/10c. Open symbols (probable peak conditions): interior garnet-matrix cordierite-matrix biotite; filled symbols: garnet rims-adjacent cordierite-adjacent biotite; plus symbol: biotite in garnet fracture. Note the shift of the grt-crd-bt triangle toward Fe-enrichment.

Plagioclase

Rims and interior portions of plagioclase grains were analyzed both adjacent to garnet (contact plagioclase) and in areas as far removed from garnet as possible within each thin section (matrix plagioclase) (Table B-4, Appendix B; Table 7). Of the samples that show zoned matrix plagioclase, sillimanite-bearing pelites contain normally zoned plagioclase and sillimanite-free semi-pelites contain reversely zoned plagioclase. This is shown graphically in Figure 50 in which the average anorthite content of matrix plagioclase interiors is plotted against the rims. The dashed 1:1 line indicates plagioclase that shows no compositional variation from core to rim. Above this line interiors are enriched in calcium (normal zoning), and below it rims are enriched in calcium (reverse zoning). All but one sillimanite-bearing sample (squares) fall within the normally zoned area of the graph whereas all but one of the semi-pelites (circles) fall within the reversely zoned area of the graph.

For those samples in which plagioclase and garnet are the only Ca-bearing phases, garnet growth typically produces normal zoning in plagioclase. Most garnet growth involves plagioclase consumption (Spear et al., 1990). The anorthite component in the dissolving plagioclase contributes grossular to the garnet, and new, more albitic plagioclase forms, producing normally

Table 7 Average Mole Fraction Anorthite (pelites and semi-pelites)

Sample	Matrix			Adjacent Garnet			Garnet Corona	Leucosome		
	rim	interior	zoning*	rim	interior	zoning*		rim	interior	zoning*
50E	0.363	0.355	*R*	0.356			*(inclusion =0.373)*			
19D	0.267	0.254	*R*	0.278	0.264	*R*		0.258	0.256	
68A	0.329	0.315	*R*	0.330				0.322	0.286	*R*
66A**	0.300	0.314	*N*	N/A						
88A**	0.329	0.335	*N*	N/A	0.331			0.354	0.361	*N*
86D	0.261	0.259		0.279						
93A	0.387	0.372	*R*	N/A						
104E**	0.196	0.204	*N*	0.194	0.190		0.210			
104F	0.215	0.219		0.229	0.222	*R*				
108C	0.291	0.284	*R*	0.288			0.306			
109A**	0.251	0.265	*N*	0.302	0.318	*N*				
110A	0.333	0.328		0.333	0.332		0.378			
111A	0.363	0.352	*R*	0.363	0.357	*R*				
113(4a)**	0.227	0.253	*N*	N/A						
113C**	0.238	0.264	*N*	0.236			0.253			
113E**	0.240	0.253	*N*	0.223	0.235	*N*				
116(3a)**	0.208	0.221	*N*	N/A						
119A**	0.286	0.280	*R*	0.285						
128(10a)**	0.336			N/A						
128(10C)‡	0.369	0.347	*R*	N/A						
113A	0.257	0.240	*R*	0.261						
134D**	0.267	0.269		0.280						

* *R = reverse zoning; N = normal zoning*

** *samples that contain sillimanite*

‡ *sample contains both sillimanite and cordierite*

zoned plagioclase. Thus, near-peak metamorphic compositions would be represented by the *rims* of normally zoned plagioclase. Conversely, plagioclase that exhibits reverse zoning suggests garnet resorption. As garnet dissolves, the grossular component reacts to form anorthite-enriched plagioclase rims. Thus, near-peak metamorphic compositions would be represented by the *interiors* of reversely zoned plagioclase.

Under upper amphibolite facies conditions, garnet resorption commonly is ascribed to the reaction

grossular + sillimanite + quartz = anorthite

which occurs with decompression following peak metamorphism. In semi-pelitic rocks, any sillimanite that may have been present would be consumed in this reaction. Garnet textures and biotite compositions previously discussed indicate garnet resorption occurred in *all* garnet-bearing assemblages. However, in sillimanite-bearing samples, plagioclase compositions from garnet

Figure 50 Mole fraction anorthite for matrix plagioclase interiors versus rims.

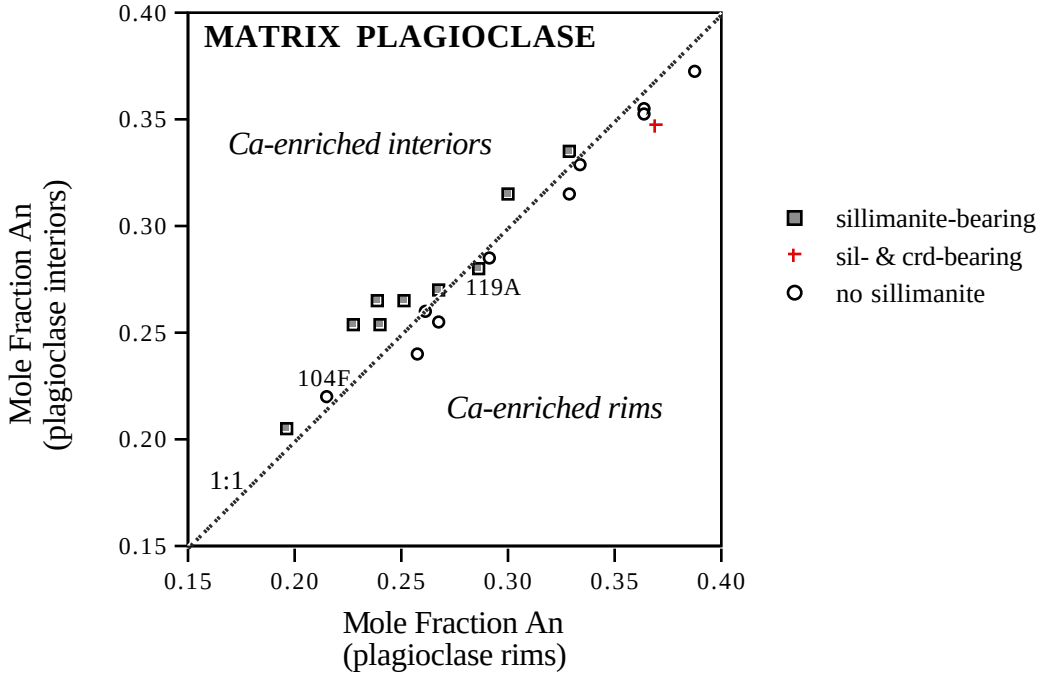

Figure 51 Mole fraction anorthite for contact plagioclase (adjacent garnet or in garnet corona) versus near-peak matrix plagioclase (rim for normal zoning, interior for reverse zoning); corona data was not available for sample 113E.

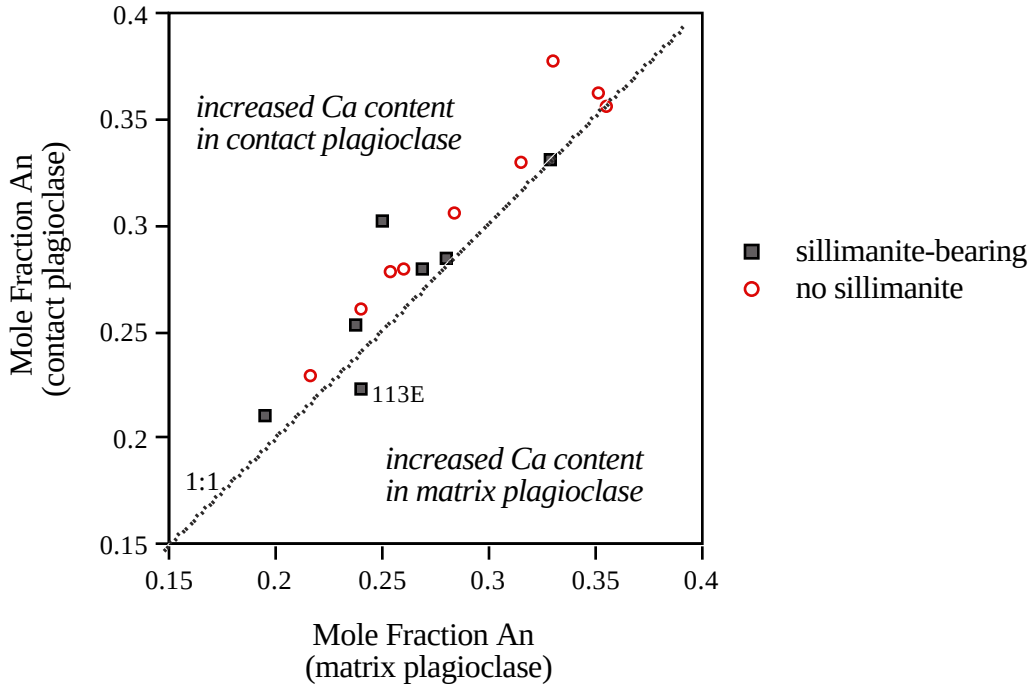

coronas, as shown in Table 7, are always more anorthitic than matrix plagioclase. Furthermore, where no corona data are available, plagioclase adjacent to garnet is typically more anorthitic than matrix plagioclase compositions that represent near-peak conditions. This evidence suggests that the more calcic plagioclase that must result from garnet resorption is localized adjacent to the garnets in the sillimanite-bearing samples (rather than as anorthite-enriched rims on all plagioclase grains). Figure 51 is a plot of the anorthite contents of contact plagioclase versus near-peak matrix plagioclase. This figure demonstrates that plagioclase from both pelites and semi-pelites becomes more anorthitic in the vicinity of garnet, as would be expected given pervasive post-peak garnet resorption.

Muscovite

Muscovite was analyzed from eight samples (Table B-5, Appendix B). Table 8 summarizes the average compositions for each sample. The range in compositions probably represents the broad range of bulk compositions exhibited by these samples (see Table A-1, Appendix A for the modes). There does not appear to be any appreciable difference between various types of muscovite within a single sample. For example, both cross muscovite and muscovite clots were analyzed in sample 83A and both types of post-peak muscovite exhibit similar compositions (see Table 8).

Table 8 Average compositions of analyzed muscovite grains.
$x_i = i / (Fe+Mg+Mn+Ti+Al^{vi})$

Sample	Na/Na+K	xFe	xMg	xTi	xAl^{vi}	Fe/(Fe+Mg)
19D	0.046	0.110	0.029	0.012	0.848	0.793
66A	0.026	0.147	0.055	0.016	0.781	0.725
83A*	0.111	0.039	0.025	0.011	0.925	0.607
83A**	0.113	0.042	0.025	0.016	0.916	0.620
84C	0.081	0.047	0.025	0.005	0.922	0.652
93A	0.030	0.121	0.055	0.020	0.803	0.688
128(10a)	0.056	0.059	0.034	0.001	0.905	0.638
128(10b)^	0.093	0.044	0.040	0.002	0.913	0.524
128(10b)^^	0.090	0.042	0.036	0.031	0.890	0.535
131(2)	0.074	0.093	0.033	0.022	0.852	0.738

* muscovite clot
** cross muscovite
^ muscovite adjacent to cordierite, intergrown with green biotite
^^ muscovite intergrown with red biotite, removed from cordierite

Variable amounts of octahedral Fe, Mg, and Ti occur in muscovite from each specimen. The titanium content appears to correlate with the neighboring phases. For example, muscovite intergrown with red-brown biotite in sample 128/10b has a much higher X_{Ti} than does muscovite associated with green, Ti-poor biotite in cordierite overgrowths (see Table 8). Fe/(Fe+Mg) appears to reflect the bulk composition of each specimen. For example, sample 128/10b is

cordierite-bearing (Mg-enriched bulk composition) and the constituent muscovite has the lowest Fe/(Fe+Mg) ratio. The presence of Fe and Mg in the octahedral site suggests that deviations from ideal muscovite composition involve tschermak substitution, $(Fe^{2+},Mg)Si = Al^{vi}Al^{iv}$, toward a more phengitic composition. Figure 52 is a ternary plot of the octahedral constituents, Fe_{total}+Mg+Mn+Ti, versus octahedral and tetrahedral aluminum. If tschermak substitution produced the deviations, then the samples should plot on a line between phengite, $K_2(Fe,Mg)Al_3AlSi_7O_{20}(OH)_4$, and muscovite, $K_2Al_4Al_2Si_6O_{20}(OH)_4$. Instead, the samples fall along a line between muscovite and the Fe_{total}+Mg+Mn+ Ti apex. This indicates that phengite substitution may be accompanied by substitution of Fe^{3+} for Al^{vi} (Guidotti, 1984). Unfortunately, microprobe analysis can not distinguish between iron oxidation states. According to Guidotti (1984), the presence of Fe^{3+} in muscovite inhibits the substitution of Na for K. Therefore, as Fe^{3+} content increases, the Na/(Na+K) ratio should decrease. Accordingly, the samples with the highest X_{Fe} (66A, 93A, 19D), also have the lowest Na/(Na+K) values. Further support for the presence of Fe^{3+} is found in the presence of green muscovite in sample 128/10a. The muscovite envelops garnet and is green enough to be mistaken optically for contact biotite. Studies of green muscovite (Finch et al., 1982) indicate that the greenest muscovite correspond with the highest Fe^{3+} content. Green color also may result from high chromium content (Rossman, 1984); however, the Cr content of 128/10a muscovite is no different than that of the other analyzed muscovites (Table B-5, Appendix B).

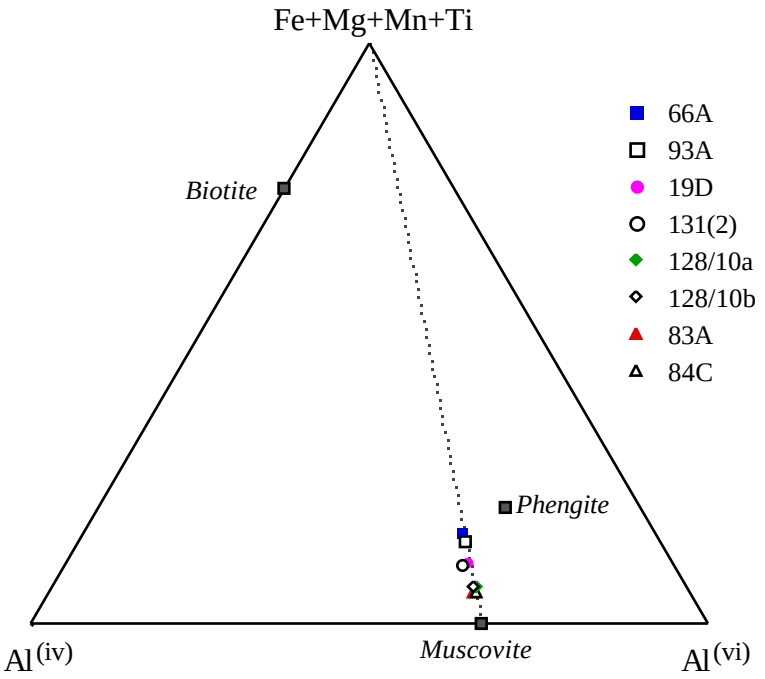

Figure 52 Ternary plot of muscovite (averaged for each sample) in terms of Fe+Mg+Mn+Ti, tetrahedral Al (8 - Si), and octahedral Al. The dashed line represents a constant ratio of Al(iv):Al(vi).

Amphibolites

Garnet

Two amphibolite samples were used for thermobarometry (80B and 107F, see Table 3 for the modes). These samples are distinguished from other amphibolites in the Poudre Canyon by the presence of garnet and biotite, perhaps representing aluminous impurities within the mafic protolith. As with garnet in pelites and semi-pelites, these garnets are zoned, showing Mg-depletion and Mn-enrichment at the rims. However,they show higher concentrations of grossular and lower concentrations of almandine and pyrope than do the pelite and semi-pelite garnets. Figure 53 shows some typical compositional profiles (compare to Figure 40) for the X-ray images that are displayed in Figures D-6 and D-7, Appendix D. The average values of Fe/(Fe+Mg), spessartine, and grossular are given in Table 9. Both Fe/(Fe+Mg) and spessartine content is lower in the garnet interior than at the garnet rims or along fractures. Furthermore, the highest

Figure 53 Typical garnet profiles for amphibolites used for thermobarometry. See figures D-6 and D-7, Appendix D for traverse locations.

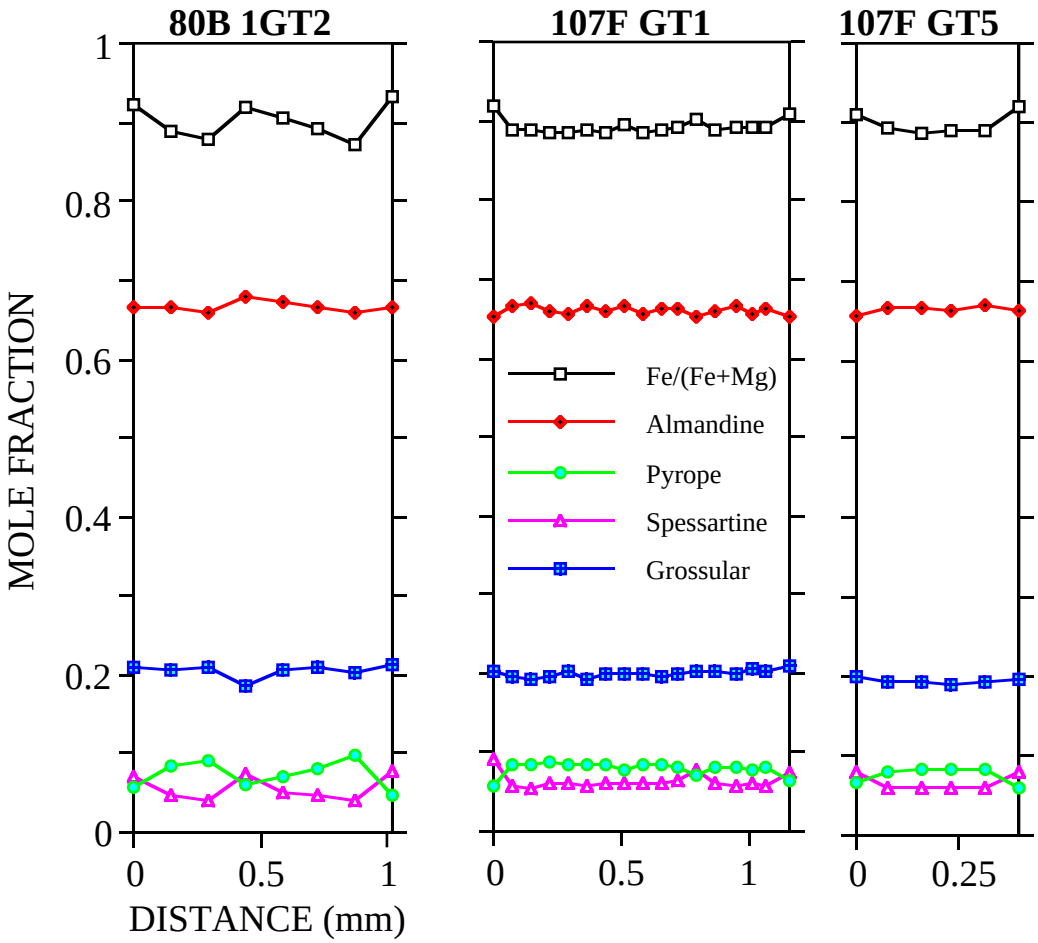

Table 9 Average Fe/(Fe+Mg), spessartine and grossular values for garnet in amphibolite samples.

	garnet interior	garnet rim adjacent bt	garnet rim adjacent hbl	garnet rim adjacent qtz	adjacent fracture
Fe/(Fe+Mg)					
80B	0.877	0.925	0.908	0.913	0.920
107F	0.889		0.914	0.912	0.903
Spessartine					
80B	0.046	0.066	0.059	0.057	0.067
107F	0.059		0.089	0.079	0.067
Grossular					
80B	0.218	0.205	0.207	0.203	0.207
107F	0.196		0.194	0.203	0.198

Fe/(Fe+Mg) and spessartine values are found where garnet rims are in direct contact with biotite, suggesting that garnet resorption and cation exchange with biotite occurred in amphibolite samples.

Hornblende

Hornblende was analyzed both in the vicinity of garnet and in matrix areas of each sample; all of the analyses are presented in table B-6, Appendix B. Table 10 summarizes the average total Na+K, Ti, and Fe+Mg for hornblende found in the matrix and adjacent to garnet. Note that the Na+K and Ti values are highest in sample 107F. The presence of a greater pargasitic component, $NaCa_2(Fe,Mg)_4AlAl_2Si_6O_{22}(OH)_2$, distinguishes sample 107F hornblende from that of sample 80B, as demonstrated by the plot of $(Na+K)^A$ versus Si in Figure 54a. Based on Fe/(Fe+Mg), the hornblende can be further classified as ferro-pargasitic hornblende in 107F and ferro-hornblende in sample 80B (see Figure 54b; after Leake, 1978). Na+K and Ti content are thought to increase with increasing temperature (Raase, 1974; Robinson et al., 1982; Spear, 1993). The greater Na+K and Ti values in 107F suggest that this sample formed at higher temperatures than did 80B. Furthermore, within each sample, Ti and Na+K are lower in hornblende adjacent to garnet than in the matrix (see Table 11 for complete representative analyses for matrix grains and for grains adjacent to garnet.). Thus, apparent lower

Table 10 Average hornblende compositions measured adjacent to garnet and in the matrix.

Sample	Location	Na+K	Ti	Fe+Mg
80B	*adjacent grt*	0.353	0.055	0.652
	aligned with C–surfaces	0.336	0.057	0.363
	matrix aligned with S-surfaces	0.393	0.089	0.650
107F	*adjacent grt*	0.478	0.114	0.706
	matrix	0.574	0.136	0.696

Figure 54a Na+K in the *A* site versus Si atoms for analyzed amphiboles (after Deer et al., 1992).

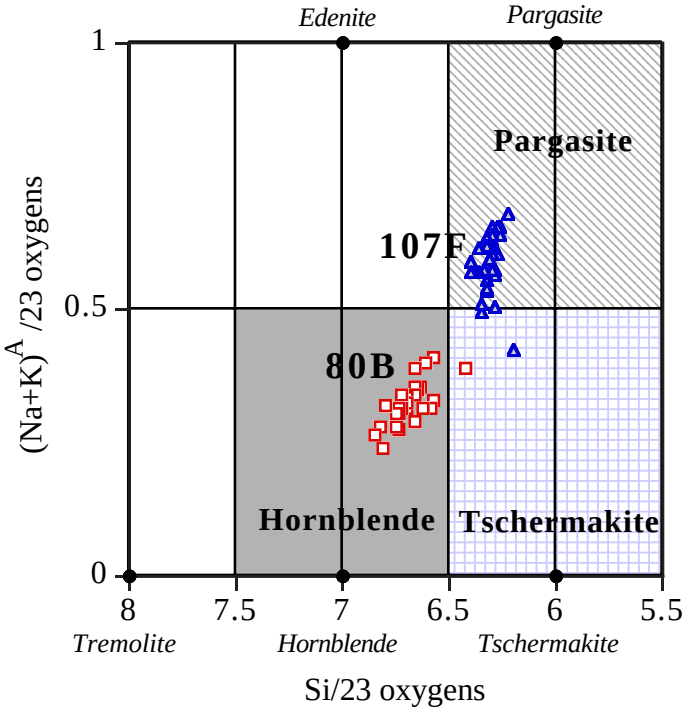

Figure 54b Fe/(Fe+Mg) ratio versus Si atoms for analyzed amphiboles (after Leake, 1978).

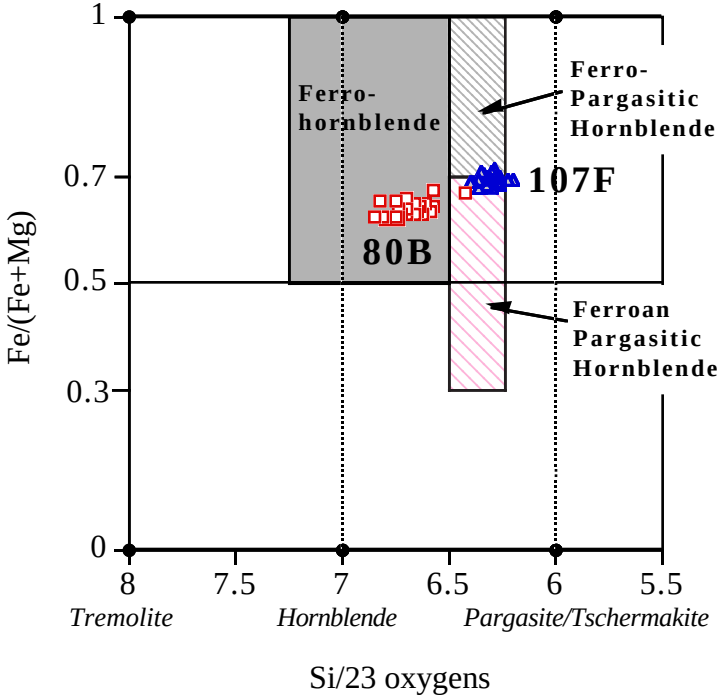

temperature changes in hornblende composition are localized in the vicinity of garnet.

Sample 80B shows considerable evidence for post-peak alteration in the form of ductile deformation (see Figure 38) and extensive development of secondary phases (clinozoisite and prehnite). If peak compositions remain, they would be in hornblende aligned parallel to the primary schistosity (S–surfaces), whereas post-peak compositions would most likely form in hornblende grains within the C–surfaces. Hornblende grains aligned with the S-surfaces should (and do) have correspondingly higher Na+K and Ti contents than hornblendes aligned with the C-surfaces, as demonstrated in Table 10. Therefore, hornblende grains aligned with the primary schistosity may retain compositions representative of peak metamorphism.

Table 11 Representative Analyses for Hornblende Composition

PC-80B		*S-Surface*	*C-Surface*	***P-C-107F***	
	Adj Grt	**Matrix**	**Matrix**	**Adj Grt**	**Matrix**
WEIGHT PERCENT OXIDES					
SiO_2	43.77	43.91	44.98	41.03	40.99
Al_2O_3	12.81	11.58	11.81	13.42	12.68
TiO_2	0.48	0.79	0.55	0.99	1.17
MgO	6.60	6.84	7.20	5.79	5.86
FeO	22.09	22.64	22.39	24.74	23.92
MnO	0.22	0.26	0.27	0.22	0.28
CaO	11.48	11.14	11.46	11.03	11.63
Na_2O	0.86	0.88	0.83	0.94	1.19
K_2O	0.53	0.71	0.49	1.03	1.12
Cl	0.01	0.01	0.02	0.00	0.01
F	0.08	0.10	0.08	0.00	0.05
TOTAL	*98.93*	*98.85*	*100.08*	*99.18*	*98.90*
-O = Cl	-0.00	-0.00	-0.01	-0.00	-0.00
-O = F	-0.03	-0.04	-0.03	-0.00	-0.02
TOTAL	98.90	98.80	100.04	99.18	98.88
CATIONS RECALCULATED TO 23 OXYGENS					
Si	6.58	6.64	6.69	6.28	6.31
Al	2.27	2.06	2.07	2.42	2.30
Ti	0.06	0.09	0.06	0.11	0.14
Mg	1.48	1.54	1.60	1.32	1.34
Fe	2.78	2.86	2.78	3.17	3.08
Mn	0.03	0.03	0.03	0.03	0.04
Ca	1.85	1.80	1.82	1.81	1.92
Na	0.25	0.26	0.24	0.28	0.35
K	0.10	0.14	0.09	0.20	0.22
TOTAL	**15.40**	**15.43**	**15.38**	**15.63**	**15.69**

Plagioclase

Plagioclase grains in sample 80B are small (<0.25 mm in length), exist only in trace amounts and have an average anorthite mole fraction of 0.95. The small size and high anorthite content suggests that this plagioclase does *not* represent peak conditions, but rather some product of a late retrogressive reaction (perhaps involving the breakdown of garnet or hornblende). The high proportion of clinozoisite and prehnite in 80B (11% of the mode) suggests that any plagioclase present during peak metamorphism completely broke down to form these lower temperature phases, leaving no traces of the original peak plagioclase.

In sample 107F, plagioclase in the matrix is reversely zoned with an average anorthite mole fraction of 0.425 in plagioclase interiors and 0.448 at plagioclase rims. Matrix plagioclase has a substantially lower anorthite content than the plagioclase adjacent to garnet (0.556). The resorbed nature of garnet (see Figure D-7) suggests that garnet breakdown occurred, released grossular, and produced the local calcium-enrichment in adjacent plagioclase.

Prehnite and Clinozoisite

Both prehnite and clinozoisite are found throughout sample 80B. Prehnite is intimately intergrown with biotite; clinozoisite occurs as distinct anhedral grains commonly associated with (but not intergrown with) prehnite. Microprobe analyses for prehnite and clinozoisite are presented in Table B-7, Appendix B; the average chemical composition for each mineral is presented in Table 12. Chemical variability in the clinozoisite is restricted to substitution of Fe^{3+} for Al. The prehnite also exhibits appreciable substitution of Fe^{3+} for octahedral Al. Figure 55 is a Fe_2O_3-Al_2O_3-CaO ternary plot for both clinozoisite and prehnite. The substitution of Fe^{3+} for aluminum is represented on this plot by movement away from the ideal aluminum-only composition toward the Fe-end members (arrows on Figure 55).

Table 12 Average clinozoisite and prehnite analyses of sample 80B.

	Clinozoisite	**Prehnite**
Weight Percent Oxides		
SiO_2	39.24	42.81
Al_2O_3	31.04	23.13
TiO_2	0.01	0.49
Fe_2O_3	4.88	3.83
MgO	0.00	0.61
FeO	**	**
MnO	0.04	0.02
CaO	24.07	25.22
BaO	0.00	0.02
Na_2O	0.00	0.03
K_2O	0.00	0.04
TOTAL	**99.28**	**96.20**
Cations Recalculated to 25 Oxygens		
Si	5.97	5.90
Al	5.56	3.77
Ti	0.00	0.05
Fe^{3+}	0.52	0.40
Mg	0.00	0.13
Fe^{2+}	**	**
Mn	0.00	0.00
Ca	3.92	3.72
Ba	0.00	0.00
Na	0.00	0.01
K	0.00	0.01
TOTAL	**15.98**	**13.99**

*** all Fe reported as ferric iron*

Solid solution between $Ca_2Al(AlSi_3O_{10})(OH)_2$ and $Ca_2Fe^{3+}(AlSi_3O_{10})(OH)_2$ is common in prehnite (Hashimoto, 1964; Liou, 1971; Liou and Maruyama, 1983; Deer et al., 1992) whereas the presence of components other than Fe_2O_3 is unusual (Deer et al., 1962b, 1992). The prehnite from this study shows slightly more variation in the amounts of Mg and Ti than exhibited by the published analyses. In addition, deviations of the prehnite analyses away from the solid solution line in Figure 55 suggests that some of the Fe_2O_3 may be FeO. The "excess" Fe, Mg and Ti may reflect the biotite with which the prehnite is invariably intergrown. Both prehnite and clinozoisite are assumed to be related to the retrograde breakdown of original peak plagioclase. The upper limit of prehnite stability is defined by the continuous reaction

$$prehnite_{s.s} + iron\ oxide = epidote_{s.s} + garnet_{s.s} + H_2O$$

which occurs at about 400°C (Liou and Maruyama, 1983). Figure 56 shows the experimentally determined equilibria for prehnite and epidote at the f_{O2} of the QMF buffer (Liou and Maruyama, 1983). These data suggest that clinozoisite could have formed first through the breakdown of anorthite and grossular. Then, at still lower temperatures (about 400°C), the clinozoisite reacted with the grossular component of the

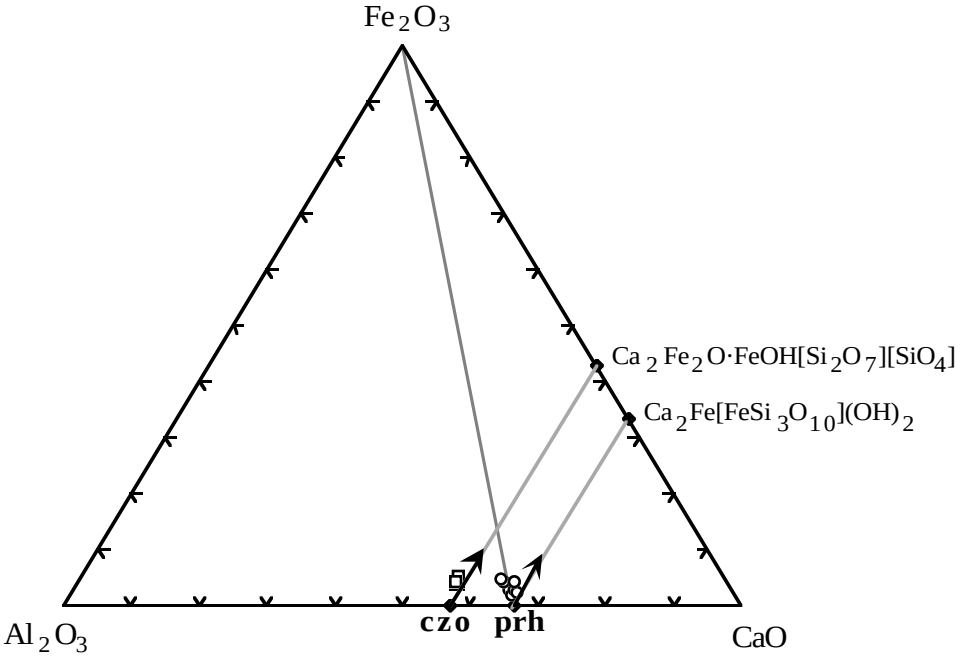

Figure 55 Fe_2O_3-Al_2O_3-CaO ternary plot for clinozoisite (czo) and prehnite (prh) in sample 80B. Arrows indicate direction of solid solution toward the Fe-end members (after Liou and Shigenori, 1983).

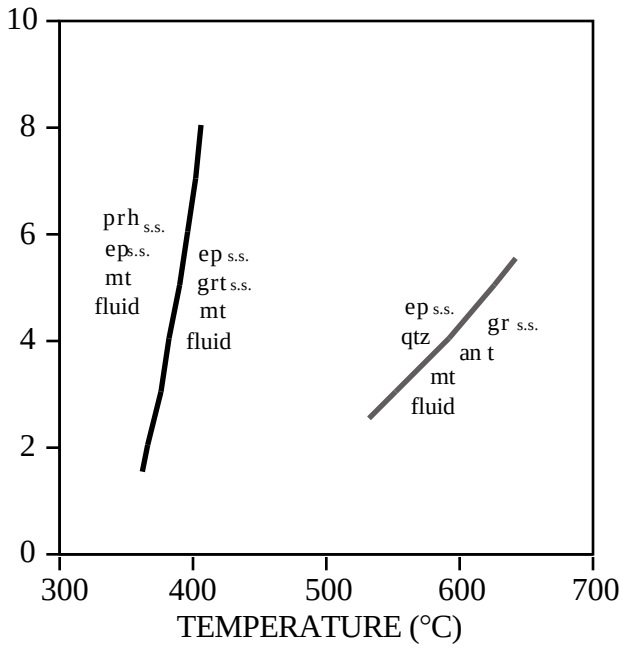

Figure 56 P-T diagram for prehnite and epidote stability (after Liou and Maruyama, 1983).

garnet to form prehnite. Biotite, which also was involved in reactions involving garnet resorption, may have served as a convenient mica template for prehnite growth, thus producing the observed intergrowths.

Synthesis of Observations

Reconstructing the early (pre-peak) history of these rocks is difficult because prograde assemblages were almost completely destroyed. Garnet, the usual repository for relict phases, lacks such inclusions and does not exhibit the growth zoning signatures typical of lower grades. The only data relevant to the pre-peak assemblages is the rare relict staurolite found exclusively in cordierite-bearing rocks. It is likely that some of the garnet growth was driven by staurolite breakdown as metamorphism progressed to higher temperatures and pressures. The presumably prolonged high temperatures that followed caused garnet to re-equilibrate continuously to peak conditions of the sillimanite-K-feldspar zone. This explains why the garnet, although poikiloblastic, only contains inclusions related to peak metamorphism. A weak compositional zoning developed in the garnet as cooling proceeded and was intensified by retrograde activity.

Retrograde chemical alteration at garnet rims and among surrounding plagioclase, biotite, or hornblende indicates an episode of garnet resorption and localized Fe-Mg exchange. The embayed, irregular habit of garnet and the fine-grained reaction coronas support this conclusion. The production of biotite in the reaction coronas indicates that the resorption involved the addition of H_2O and K_2O. Formation of more anorthitic plagioclase in garnet coronas and of cordierite rims on garnet suggest that retrogression occurred during decompression. Further post-peak hydration reactions produced the static growth of muscovite (and biotite) in numerous samples. In calcium-rich mafic rocks, local hydration produced prehnite, epidote and clinozoisite. Ductile deformation of cross-muscovite and cross-biotite along the Skin Gulch Shear Zone indicates that mica-producing hydration reactions occurred prior to or during this 1.2±0.2 Ga event.

IV. PRESSURE-TEMPERATURE CALCULATIONS

Introduction

Good geothermometers are highly sensitive to temperature changes and relatively insensitive to pressure changes. The geothermometers used in this study involve Fe-Mg exchange between co-existing garnet-biotite, garnet-hornblende, and garnet-cordierite pairs (Ferry and Spear, 1978; Graham and Powell, 1984; Bhattacharya et al., 1988; Berman, 1990). Exchange reactions between cations of similar size and charge, such as Mg^{2+} and Fe^{2+}, involve very little difference in the volume of the reactants and products. Therefore, theoretically the pressure term can be ignored, and, by determining the distribution coefficient using the electron microprobe, temperature can be calculated.

Good geobarometers are highly sensitive to pressure changes and relatively insensitive to temperature changes. Consequently, the common geobarometers are net transfer reactions involving a large change in volume (Wood and Fraser, 1976). Unfortunately, the P-dependency of the geobarometers is less complete than the T-dependency of the geothermometers. Hence, geobarometers necessitate an independent temperature estimate in order to calculate pressure. The geobarometers used in this study are net transfer reactions involving garnet-sillimanite-quartz-plagioclase (GASP), garnet-plagioclase-biotite-quartz, and garnet-plagioclase-hornblende-quartz (Koziol and Newton, 1988; Koziol, 1989; Hoisch, 1990; Kohn and Spear, 1990). Given the inhomogeneous composition of many of the key phases for thermobarometry, the petrographic and chemical information from each sample must be carefully interpreted in order to select the compositions most representative of peak metamorphic conditions.

Choosing the Appropriate Mineral Compositions for Thermometry

All of the thermometers used in this study involve garnet, and all of the garnets are zoned. Therefore, the garnet zoning history must be understood in order to choose the appropriate garnet composition (if any) for pressure-temperature calculations. Zoning depends on temperature (which controls diffusivity), the duration of metamorphism, and the volume of garnet through which ions must move. Homogenization of garnet compositions is common in the upper amphibolite faces due to the characteristically high temperatures (Woodsworth, 1977; Tracy, 1982; Spear, 1988; Selverstone and Chamberlain, 1990; Spear, 1991; Florence and Spear, 1991). However, the extent of homogenization depends on the size of the garnet. Florence and Spear (1991) suggested that large garnets (radii greater than 1 mm) may preserve some of the growth history, whereas smaller garnets experience continuous homogenization as they grow. Garnet from the Poudre Canyon displays two basic profile types that reflect differences in grain size. Large garnets (greater than 2 mm in diameter) show a slightly convex interior with steepened rims (e.g., Figure 40). Small garnets (less than 2 mm in diameter) show a flat interior profile with or without steepened rims (see 109A and 110A, Appendix C). Highly fragmented, albeit large, garnets (as in sample 86D, Appendix C) also show relatively flat profiles. These size-related differences in zoning necessitate different garnet composition choices for thermobarometry.

Figure 57 presents an interpretative history for garnets with a diameter greater than 2 mm using x_{py} as an example. Garnet equilibrated at the high temperatures associated with peak metamorphism. With slight, slow cooling, continuous Fe-Mg exchange between garnet and biotite produced the broad, shallow convex upward profile shown in Figure 57a. The temperature still was hot enough to allow pervasive diffusion to and from biotite so that the matrix biotite achieved equilibrium with the garnet rims. These modified garnet rims and re-equilibrated matrix biotite compositions reflect "near-peak" compositions. The biotite composition that once co-existed with the garnet interiors at the highest temperatures of peak metamorphism no longer exists. Late resorption coupled with *localized* ion exchange and subsequent diffusion, steepened the garnet profile at its rim as shown in

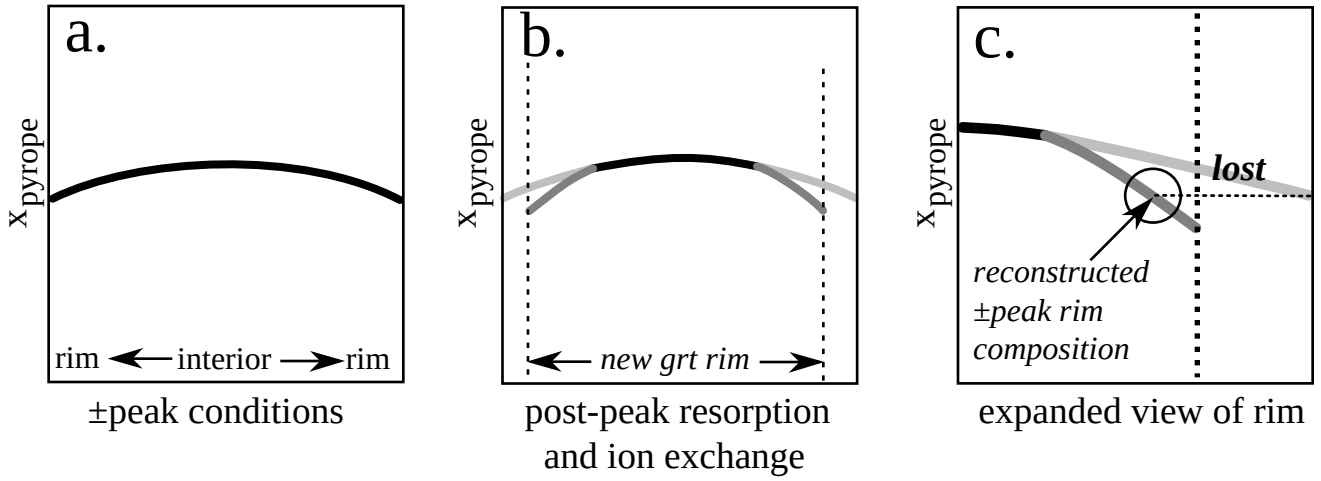

Figure 57 Interpretative history of Poudre Canyon garnets greater than 2 mm in diameter using the mole fraction of pyrope as an example. (**a**) Garnet re-equilibration up to peak temperature conditions; slight cooling accompanied by continuous Fe-Mg exchange between garnet and biotite produced a broad convex upward profile. Garnet rims are in equilibrium with all biotite. (**b**) Post-peak resorption coupled with *localized*, late ion exchange steepened the garnet profile (dark gray) at its new rim position. Matrix biotite retains its peak composition but is no longer in equilibrium with garnet rims. (**c**) Expanded view of the garnet rim shows the lost portion of the garnet profile (light gray) and a method for reconstructing the near-peak garnet rim composition.

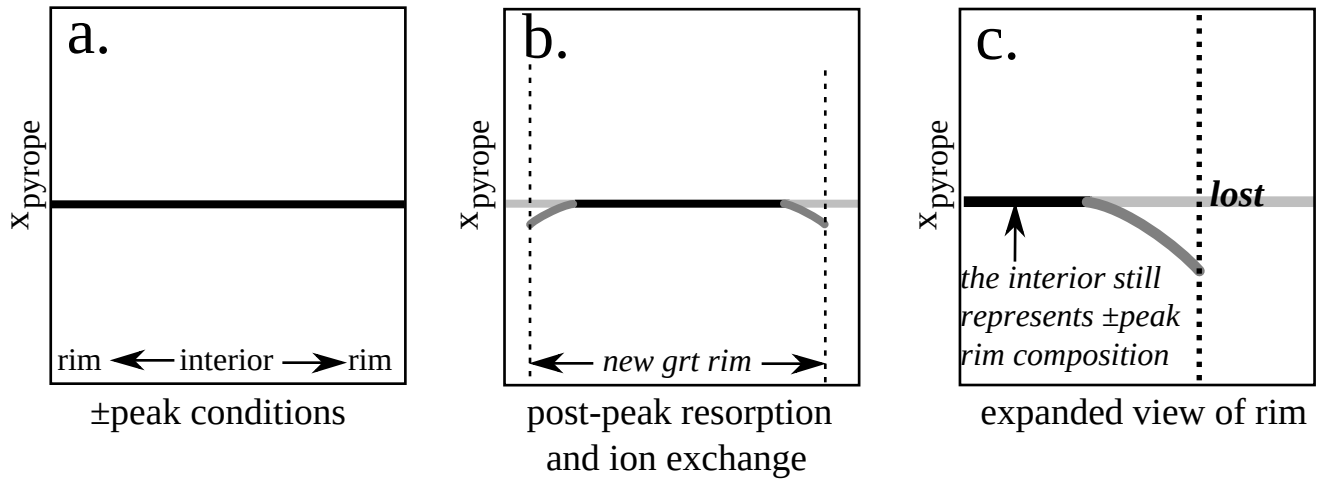

Figure 58 Interpretative history of Poudre Canyon garnets less than 2 mm in diameter using the mole fraction of pyrope as an example. (**a**) Garnet re-equilibration up to peak temperature conditions and during slight cooling accompanied by continuous Fe-Mg exchange between garnet and biotite. The resultant homogenized garnet is in equilibrium with all biotite. (**b**) Post-peak resorption coupled with *localized*, late ion exchange steepened the garnet profile (dark gray) at its new rim position. Matrix biotite retains its peak composition but is no longer in equilibrium with garnet rims. (**c**) Expanded view of the garnet rim shows the lost portion of the garnet profile (light gray). The garnet interior is still in equilibrium with the matrix biotite.

Figure 57b. The newly modified garnet rims are no longer in equilibrium with the matrix biotite. However, given a low effective ratio of garnet to biotite, the matrix biotite still records the "near-peak" composition (Ferry and Spear, 1978; Tracy, 1982; Spear 1991). Therefore, if the near-peak garnet rim composition can be reconstructed, then it can be paired with the matrix biotite to calculate a temperature that is as close as possible to peak conditions. Figure 57c demonstrates how the near-peak garnet rim composition is reconstructed by choosing points on the garnet profile just in from the garnet rim. Although not perfect, this reconstruction is a reasonable approximation of the garnet composition that once co-existed with the matrix biotite close to peak metamorphism.

Figure 58 presents an interpretative history for garnets with a diameter less than 2 mm using x_{py} as an example. Garnet equilibrated at the high temperatures associated with peak metamorphism. Although the slow cooling that followed produced a slightly convex profile in the large garnets, diffusion in the smaller garnets kept pace with the slight temperature changes. The resultant flat profile shown in Figure 58a shows a garnet whose entire composition is in equilibrium with the surrounding biotite at near-peak metamorphic conditions. Late resorption, localized ion exchange with nearby biotite and subsequent diffusion steepened the garnet profile at its rim as shown in Figure 58b. The near-peak garnet composition that was in equilibrium with the matrix biotite in this case is represented by the garnet interior as shown in Figure 58c. Thus, by pairing garnet interiors with matrix biotite, the near-peak conditions can be calculated.

Based on the interpretation of garnet zoning presented in Figures 57 and 58, temperatures were calculated using near-rim compositions of garnet larger than 2 mm in diameter, and interior compositions of garnet smaller than 2 mm in diameter (or of highly fragmented garnet). The composition choices are specified for each sample in Appendix E. All of the garnet compositions were paired with matrix biotite, hornblende, or cordierite compositions. Where possible, samples were chosen with a low effective modal percentage of garnet:biotite, garnet:cordierite, or garnet:hornblende (see Table 2 for raw grt:bt ratios). This minimizes the compositional effects of late changes in the garnet rim on the matrix biotite. Although present, biotite was not used for thermometry in the amphibolites because there is (1) a high grossular component in the garnets (not accounted for in garnet-biotite thermometry) and (2) a much higher modal percentage of hornblende (maintaining a low effective ratio of garnet to hornblende).

Choosing the Appropriate Mineral Compositions for Barometry

The same garnet, biotite, and hornblende compositions used for calculating near peak temperature were applied to the pressure calculations. Plagioclase composition also is needed in order to calculate the K_D of the barometric reactions. However, the compositional variation exhibited by plagioclase in all of these samples necessitates a careful analysis before choosing the compositions most representative of peak conditions. Plagioclase adjacent to garnet was avoided as the generally higher mole percentage of anorthite in this plagioclase probably reflects late garnet resorption reactions. In the matrix, plagioclase was either normally zoned (sillimanite-bearing pelites) or reversely zoned (sillimanite-absent semi-pelites and amphibolites). In general, normal zoning is associated with the prograde process of garnet growth whereas reverse zoning results from the retrograde process of garnet resorption. Therefore, the rims of normally zoned plagioclase and the interiors of reversely zoned plagioclase were chosen as most representative of the near-peak plagioclase compositions. In addition, where possible, samples were chosen with a low effective modal percentage of garnet:plagioclase (see Table 2 for raw grt:pl ratios). This minimizes the compositional effects of late changes in the garnet rim on the matrix plagioclase (Spear et al., 1990).

Thermometry

Garnet-Biotite Thermometry

Substitutions in Garnet

The garnet-biotite thermometer is based on the equilibrium,*almandine + phlogopite = annite + pyrope*, (Ferry and Spear, 1978) and was applied using Berman's (1990) data on the mixing properties of Ca, Mg, Fe, and Mn in garnet. Geothermometry is confounded by the effects of additional components on the Fe-Mg exchange between garnet and co-existing ferromagnesian minerals (biotite, cordierite and hornblende). Ferry (1980) observed that temperatures calculated using the Ferry-Spear calibration of the garnet-biotite thermometer are too low when there are substantial amounts of grossular and/or spessartine in the garnet ($x_{gr} > 0.10$ and $x_{gr}+x_{sp} > 0.30$). Octahedral substitutions of the larger Ca and Mn^{2+} cations in garnet produces localized structural expansions such that Fe^{2+} would be preferred over the smaller Mg (Dallmeyer, 1974). Such an increase in the iron content of garnet results in a lower K_D value and yields a calculated temperature which is too low. Table 13 is a summary table showing the x_{gr} and $x_{gr}+x_{sp}$ values for compositions used in garnet-biotite thermometry. The grossular contents of samples 66A and 93A are nearly twice as high as the maximum suggested x_{gr}. Hence, the temperatures calculated from these samples should be treated with suspicion. The garnet compositions of all of the other samples are well within acceptable ranges for garnet-biotite thermometry. Substitutions of Fe^{3+} in garnet also may affect the calculated K_D value in garnet-based Fe-Mg exchange thermometers (Goldman and Albee, 1977). Unfortunately, analysis by the electron microprobe does not allow for distinction between oxidation states of Fe.

Table 13
Average values of grossular, grossular + spessartine, and octahedral Al+Ti in biotite for points used in garnet-biotite thermometry. Compositions that fall outside of the range of acceptable values are in bold type; samples with unacceptable garnet *and* biotite values are in bold italics.

Sample #	Garnet		Biotite
	x_{gr}	$x_{gr}+x_{sp}$	$(Al^{vi}+Ti)/(Fe+Mg+Al^{vi}+Ti)$
recommended values	*< 0.10*	*< 0.30*	*< 0.15*
50E	0.06	0.13	0.14
19D	0.06	0.23	**0.17**
66A	***0.20***	***0.32***	***0.16***
68A	0.05	0.08	**0.19**
86D	0.04	0.10	**0.20**
108C	0.03	0.12	**0.18**
109A	0.03	0.10	**0.17**
110A	0.06	0.14	**0.17**
88A	0.06	0.10	**0.20**
93A	***0.18***	***0.31***	***0.16***
104E	0.02	0.07	**0.19**
104F	0.02	0.06	**0.17**
111A	0.05	0.08	**0.21**
113/4a	0.03	0.05	**0.17**
113C	0.03	0.06	**0.18**
113E	0.03	0.05	**0.18**
116/3a	0.02	0.06	**0.18**
119A	0.03	0.07	**0.19**
128/10a	0.04	0.08	**0.20**
133A	0.04	0.07	**0.20**
134D	0.03	0.09	**0.19**

Substitutions in Biotite

The distribution coefficient also is affected by substitutions in biotite of Ti, Al, and Fe^{3+} for Mg and Fe^{2+} (Guidotti, 1984). In the simplest situation, the presence of these smaller, more highly charged cations causes the octahedral layer of biotite to decrease in size and increase its positive charge. The excess positive charge is accommodated by unoccupied octahedral sites and by the tetrahedral substitution of Al^{3+} for Si^{4+} (Dallmeyer, 1974). Because Al is larger than Si, the tetrahedral layer becomes correspondingly larger. To compensate for these structural distortions, the larger Fe^{2+} cation is preferred over Mg (Dallmeyer, 1974). This response is particularly noticeable with Ti substitution due to the large charge difference between Ti^{4+} and the divalent Mg and Fe (Thompson, 1976b). By increasing the ratio of ferrous iron to magnesium in biotite, the K_D value will increase such that the calculated temperature will be too high. Given these problems, Ferry and Spear (1978) suggest that biotite with $(Al^{vi}+Ti)/(Fe+Mg+Al^{vi}+Ti) < 0.15$ produces the best results for garnet-biotite thermometry. As shown in Table 13, all but one sample contained mole fractions of octahedral Al + Ti in excess of 0.15 (ranging from 0.14 to 0.21). Although not a large deviation from the recommended values, it should be noted that the temperatures calculated here may be slightly high and, thus, represent maximum possible temperatures. The ideality of the Fe^{2+}-Mg exchange (and hence the K_D value) also may be affected by substitutions of Na and Mn^{2+} in biotite (Goldman and Albee, 1977). However, the amounts of Na and Mn in these samples is negligible and, thus, their effects were ignored (see Table B-2, Appendix B).

Garnet-Hornblende Thermometry

The garnet-hornblende thermometer is an empirical thermometer calibrated against garnet-clinopyroxene thermometry for rocks in the amphibolite and granulite facies (Graham and Powell, 1984, Ellis and Green, 1979). The thermometer is based on the Fe-Mg exchange equilibrium

ferro-pargasite + pyrope = pargasite + almandine.

A regular solution model for mixing of Ca in garnet is incorporated into the $\ln K_D$ expression. All Fe is assumed to be present as Fe^{2+} in calculating K_D; however, Graham and Powell (1984) note that significant temperature overestimates may occur if the amphibole is unusually rich in ferric iron or Ca. They suggest that Na(M4) should be greater than 0.09 for the best results. In addition, x_{sp} in garnet should be less than 0.1, because the non-ideality associated with mixing of Mn in garnet is not taken into account. Table 14 lists the average values of x_{sp} in garnet and Na(M4) in amphiboles used for garnet-hornblende thermometry. Both samples comply with the optimum values suggested by Graham and Powell (1984) for garnet-hornblende thermometry.

Table 14 Average values of x_{sp} in garnet and Na(M4) in amphibole samples used for garnet-hornblende thermometry.

Sample Number	x_{sp}	Na(M4)*
recommended values	*< 0.1*	*> 0.09*
80B	0.04	0.20
107F	0.06	0.11

**Na(M4) = 2-Ca*

Garnet-Cordierite Thermometry

The cordierite-garnet thermometer is based on the equilibrium

$$1/3\ Fe_3Al_2Si_3O_{12} + 1/2\ Mg_2Al_4Si_5O_{18} = 1/3\ Mg_3Al_2Si_3O_{12} + 1/2\ Fe_2Al_4Si_5O_{18}$$

and was refined by using natural samples to extract data on Fe-Mg mixing in cordierite in terms of

the change in free energy, ΔG, and the Margules parameter, $W_{Fe\text{-}Mg}$ (Bhattacharya et al., 1988). These data then were used to derive a geothermometric expression for the garnet-cordierite exchange reaction. This expression was calibrated against independent estimates of temperature for the same natural samples; the resultant calculated temperatures were within ±30°C of the published temperatures.

Because the garnet-cordierite thermometer is based on a calibration with natural samples, it would seem appropriate to use garnet and cordierite compositions that fall within the range of compositions used in the calibration. Table 15 compares sample 128/10c from this study with the range of sample compositions used for the Bhattacharya et al. (1988) calibration. The compositions of 128/10c fall well within the range of compositions for which this thermometer was derived.

Table 15 Average garnet and cordierite compositions used for grt–crd thermometry

	128/10c	**Range used in Bhattacharya et al. (1988) calibration**
GARNET		
almandine	0.73	0.492-0.899
pyrope	0.19	0.077-0.426
spessartine	0.04	0.004-0.059
grossular	0.04	0.006-0.054
CORDIERITE		
x_{Fe}	0.30	0.120-0.617
x_{Mg}	0.70	0.501-0.880

Barometry

GASP Barometry

Koziol and Newton (1988a) experimentally determined the position of the plagioclase breakdown reaction

3 anorthite = grossular + 2 kyanite + quartz.

Koziol (1989) then recalibrated the GASP barometer based on this experimental data and an empirical asymmetric model of the activity of grossular in garnet (Koziol and Newton, 1988b). Difficulties associated with applying the GASP barometer include: (1) the unknown effect of andradite on the activity of grossular and (2) the strong dependence of the barometer on the assumed temperatures (Essene, 1982). The effect of Mn in garnet on these calculations is not known. However, Newton and Haselton (1981) suggested that garnets with Mn < 1/3Mg should be chosen for the best results. Table 16 presents the average values of Mn and Mg in the garnet points used for GASP barometry. All but four samples (shown in italics) comply with the suggested values of Mn. Of these four, sample 66A shows the largest deviation from

Table 16
Average values for Mn and Mg used in GASP Barometry (optimally, Mn should be less than 1/3 Mg). Samples that fall outside of the recommended range are italicized.

Sample #	**Mn**	**Mg**	**1/3 Mg**
66A	*0.36*	*0.13*	*0.04*
109A	*0.20*	*0.33*	*0.11*
88A	*0.12*	*0.30*	*0.10*
104E	0.13	0.39	0.13
113/4a	0.07	0.45	0.15
113C	0.08	0.43	0.14
113E	0.07	0.46	0.15
116/3a	0.11	0.52	0.17
119A	0.13	0.47	0.16
128/10a	0.11	0.40	0.13
128/10c	0.14	0.59	0.20
134D	*0.17*	*0.42*	*0.14*

the recommended values of Mn (Mn is 9 times higher than 1/3Mg).

Garnet-Plagioclase-Biotite-Quartz Barometry

The garnet-plagioclase-biotite-quartz barometer is an empirical barometer calibrated against the GASP barometer by Hoisch (1990). It is based on the following exchange reactions:

1/3 pyrope + 2/3 grossular + eastonite + 2 quartz = 2 anorthite + phlogopite

and

1/3 almandine + 2/3 grossular + siderophyllite + 2 quartz = 2 anorthite + annite.

Hoisch (1990) recommended that this barometer's use be restricted to biotites that fall within the range of compositions used for the calibration (in terms of octahedral Mg, Fe, Al, and Ti). These ranges and the corresponding composition values for the Poudre Canyon samples are shown in Table 17. All compositions for Ti and Al^{vi} fall within the recommended values. However, only two samples (50E and 133A) contain Mg and Fe compositions that fall within the range of values used for the Hoisch (1990) calibration. Of the remaining samples, 19D, 68A, 86D, and 93A are the furthest outside of the recommended Mg and Fe composition range (italicized in Table 17).

Table 17
Average octahedral values for Mg, Fe, Ti and Al in biotites used for garnet-plagioclase-biotite-quartz barometry as compared to the values recommended by Hoisch (1990).

	50E	***19D***	***68A***	***86D***	**108C**	**110A**	***93A***	**104F**	**111A**	**133A**	**Hoisch Range**
Mg/6	0.40	*0.18*	*0.21*	*0.24*	0.29	0.28	*0.24*	0.31	0.27	0.32	0.319-0.417
Fe/6	0.42	*0.61*	*0.57*	*0.50*	0.49	0.51	*0.56*	0.49	0.48	0.43	0.339-0.443
Ti/6	0.04	0.05	0.04	0.07	0.07	0.07	0.06	0.04	0.07	0.07	0.024-0.073
Al^{vi}/6	0.10	0.11	0.13	0.12	0.10	0.09	0.10	0.12	0.13	0.11	0.089-0.170

Garnet-Plagioclase-Hornblende-Quartz Barometry

The garnet-plagioclase-hornblende quartz barometer involves the following end member reactions:

6 anorthite + 3 tremolite = 2 grossular + pyrope + 3 tschermakite + 6 quartz

and

6 anorthite + 3 Fe-actinolite = 2 grossular + almandine + 3 Fe-tschermakite + 6 quartz

(Kohn and Spear, 1990). The pressure equations were calibrated using natural samples with well-constrained pressure and temperature information. Kohn and Spear (1990) strongly recommended that this barometer only be applied to assemblages that fall within the compositional range of the data set used for the calibration. Table 18 compares data from sample 107F to Kohn and Spear's compositional criteria. This barometer was not applied to sample 80B since there was apparently no peak plagioclase remaining in the sample. Although the hornblende, garnet and plagioclase compositions from sample 107F largely met the Kohn and Spear criteria for this geobarometer, the Fe/(Fe+Mg) ratio in hornblende was slightly higher than the recommended value.

Results of the Thermobarometric Calculations

A total of 24 specimens (pelites, semi-pelites, migmatites, and amphibolites) from 19 different locations throughout the Poudre Canyon were used for thermobarometry. Their modes are presented in Tables 2a,b and 3. The thermometers and barometers were applied using the

Table 18
Average cation values for hornblende, garnet and plagioclase compared to Kohn and Spear's (1990) criteria for use in the grt-hbl-pl-qtz barometer.

	Kohn & Spear's composition criteria (given in cations)	**107F**
AMPHIBOLE (recalculated to 23 ox)		
Al	1.9-3.75	2.28
Ti	< 0.25	0.14
Ca	< 1.5	1.89
Na	0.3 - 0.6	0.39
K	< 0.4	0.23
Fe/(Fe+Mg)	preferably 0.4 - 0.6	0.70
GARNET (recalculated to 12 oxygens)		
Mn	< 0.45	0.18
PLAGIOCLASE (recalculated to 8 ox)		
Ca	preferably 0.15 - 0.7	0.42

Table 19
Thermobarometric Calculations
(standard deviations represent the averaging process only)

Sample	T (°C)	P (kbar)
50E	**663**±12	5.5±0.5
19D	**622**±16	5.3±0.1
66A	**812**±13	**16.0**±0.4
68A	**667**±22	5.3±0.4
80B	*660±18*	N/A
86D	**662**±23	4.7±0.2
108C	**682**±6	4.3±0.1
109A	**596**±25	**4.5**±0.2
110A	**623**±23	5.2±0.2
88A	**760**±31	**8.3**±0.2
93A	**619**±11	8.7±0.1
104E	**703**±30	**6.4**±0.5
104F	**728**±15	5.7±0.3
107F	*690±19*	*7.2±0.1*
111A	**712**±15	6.0±0.2
113/4a	**727**±18	**7.3**±0.3
113C	**721**±13	**6.9**±0.4
113E	**767**±20	**7.9**±0.3
116/3a	**780**±11	**7.6**±0.2
119A	**769**±25	**7.3**±0.2
128/10a	**773**±23	**7.6**±0.5
128/10c	***707±10***	**6.1**±0.1
133A	**698**±19	6.4±0.6
134D	**728**±30	**6.8**±0.2

TEMPERATURES
grt-bt = in bold
grt-hbl = in plain italics
grt-crd = in bold italics

PRESSURES
GASP = in bold
grt-bt-pl-qtz = in plain
grt-hbl-pl-qtz = in plain italics

compositions obtained from microprobe analysis (see Appendix B) and the program "Thermobarometry" developed by Spear and Kohn (1990) for the Macintosh. Multiple temperatures and pressures were calculated for each sample using every possible combination of the chosen mineral compositions. Averages of these permutations are presented in Table 19. Standard deviations given in this table are based only on the statistics of the calculated results; the systematic error in the calibrations is excluded. Peak pressure is assumed to occur where the calculated temperature reaction line intersects that of the calculated pressure reaction line. However, barometric reactions (involving recrystallization of plagioclase via net transfer of cations) may close sooner than the Fe-Mg exchange thermometric reactions (Frost and Chacko, 1989; Selverstone and Chamberlain, 1990; Spear and Florence, 1992). Thus, pressures reported here may actually be *minimum* pressures for the calculated temperatures. The calculated temperature and pressure reaction lines for each sample are presented in Appendix F.

Figure 59 is a P-T plot of all the calculated temperatures and pressures. The majority of the pressure-temperature results correspond well with the observed mineral assemblages, plotting within the sillimanite field. On the other hand, samples 66A and 93A plot within the kyanite field, although there is no kyanite in either sample. Not surprisingly, the mineral compositions in both

Figure 59
P-T plot of calculated temperatures and pressures in the Poudre Canyon (see Table 19). Alumino-silicate phase relations after Holdaway and Mukhopadhyay, 1993.

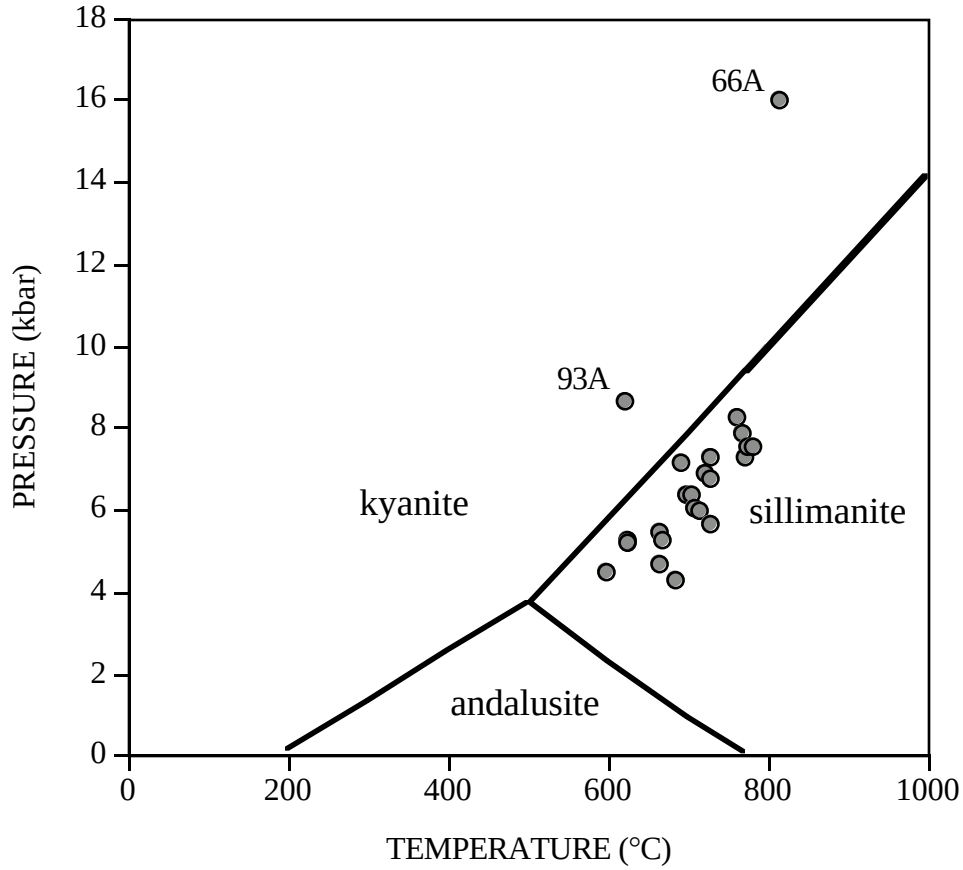

samples were unsuitable for the available thermometers and barometers (see Tables 13, 15, and 17). Therefore, the calculated temperatures and pressures for these errant samples are rejected here. The remaining samples yield petrographically reasonable temperatures and pressures. Multiple samples were analyzed for outcrops 104, 113, and 128 and the resultant calculated temperatures and pressures for each outcrop agree fairly well (see Table 19). Identical thermometers and barometers were applied to the samples from outcrop 113 (grt-bt and GASP). The calculated temperatures and pressures lie within 30° and 0.5 kbar of the average near peak conditions (738°C and 7.4 kbar) for this outcrop. However, the calculated conditions for sample 113/4a are more representative of the outcrop than is the average because samples 113C and 113E have high garnet:plagioclase ratios. Of the two samples from outcrop 104, 104F also has a high garnet:plagioclase ratio (containing nearly 75 small garnet grains in a single thin section). Therefore, the P-T results for sample 104E are considered to be more reliable. Different thermometers were applied to the two samples from outcrop 128: (garnet-biotite in 128/10a and garnet-cordierite in 128/10c). Because the garnet-biotite thermometer is the most widely used and respected thermometer, and considering the temperature-dependent nature of the pressure calculations, the results from sample 128/10a are preferred here.

Table 20 The most reliable pressure-temperature calculations for samples from the Poudre Canyon.

Sample	T (°C)	P (kbar)
DOWN CANYON		
88A	760	8.3
104E	703	6.4
107F	690	7.2
111A	712	6.0
113/4a	727	7.3
116/3a	780	7.6
119A	769	7.3
128/10a	773	7.6
133A	698	6.4
134D	728	6.8
GRABEN		
108C	682	4.3
109A	596	4.5
110A	623	5.2
UP CANYON		
50E	663	5.5
19D	622	5.3
68A	667	5.3
80B	660	n/a
86D	662	4.7

Table 20 presents the most reliable pressure-temperature calculations for the Poudre Canyon. These data are plotted in pressure-temperature space in Figure 60 where they are separated based on pressure and location within the canyon. The thermobarometric results define two adjacent fault-bound blocks: an eastern higher-pressure block down canyon (HPB; averaging 734°C and 7.1 kbar) and a western, lower pressure block up canyon (LPB; averaging 655°C and 5.2 kbar). Lower pressures also are recorded for a small, fault-bound region within the higher pressure block (averaging 634°C and 4.7 kbar), here interpreted as a graben. Figure 61 shows the location of each sample in Table 20 and their corresponding pressures and temperatures. The HPB, LPB, and graben and their respective average temperatures and pressures are further delineated in Figure 62. The pressures and temperatures for all three blocks reflect the observed sillimanite zone mineralogy. These blocks seem to be distinguished by the relative amounts of late muscovite present in each. In the HPB, late muscovite occurs sporadically and only in trace to accessory amounts (see Table A-1, Appendix A). However, in the lower pressure regions (LPB and graben) late muscovite is more widespread and much better developed; multiple samples contain minor to major amounts of late muscovite in their modes (see Table A-1, Appendix A). This suggests that

the lower pressure areas were more susceptible to the effects of the retrograde event that produced secondary muscovite. This information may be useful in interpreting the uplift paths followed by each block and will be expanded upon in later chapters.

Figure 60
P-T plot of the most acceptable calculated pressures and temperatures (see Table 20). Alumino-silicate phase relations after Holdaway and Mukhopadhyay, 1993.

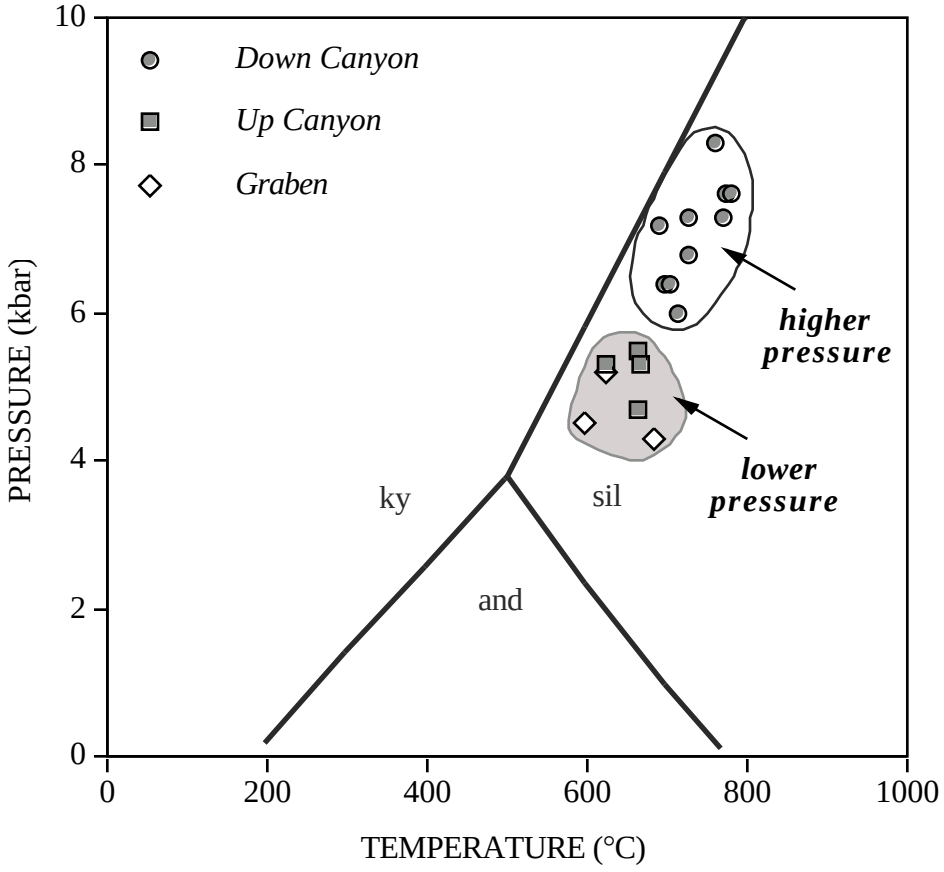

Figure 61 Map showing the most reliable calculated T (°C) and P (kbar) for samples collected for thermobarometry.

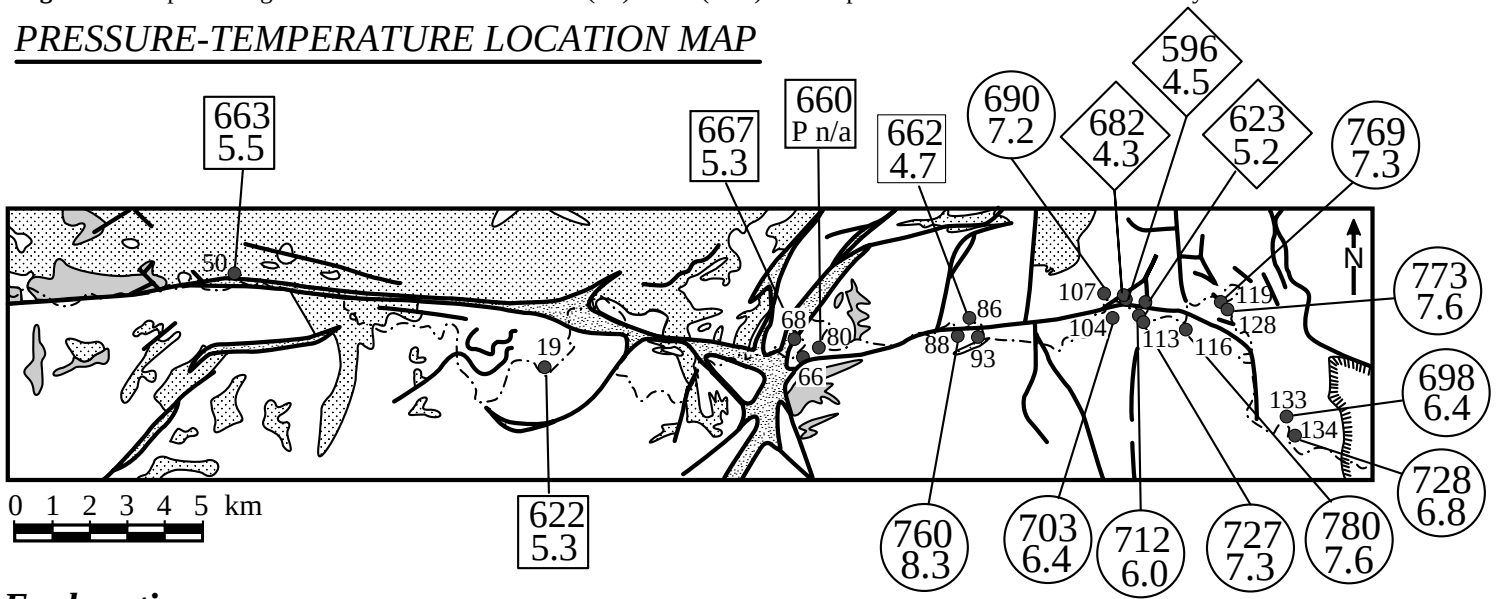

Explanation

- 1.7 Ga Amphibolite Facies Metamorphic Rock *(undifferentiated)*
- 1.7 Ga Routt Plutonic Suite *(Boulder Creek Granodiorite)*
- 1.4 Ga Berthoud Plutonic Suite *(Silver Plume Granite)*
- Fault Zones *(ductile and brittle)*
- Cache la Poudre River
- 119 ***Sample location with calculated T (°C) & P (kbar):***
  - ○ *down canyon higher pressure block*
  - □ *up canyon lower pressure block*
  - ◇ *graben*

Figure 62 Map showing averaged P-T data for the Higher Pressure Block, Lower Pressure Block (diagonal lines), and Graben (shaded).

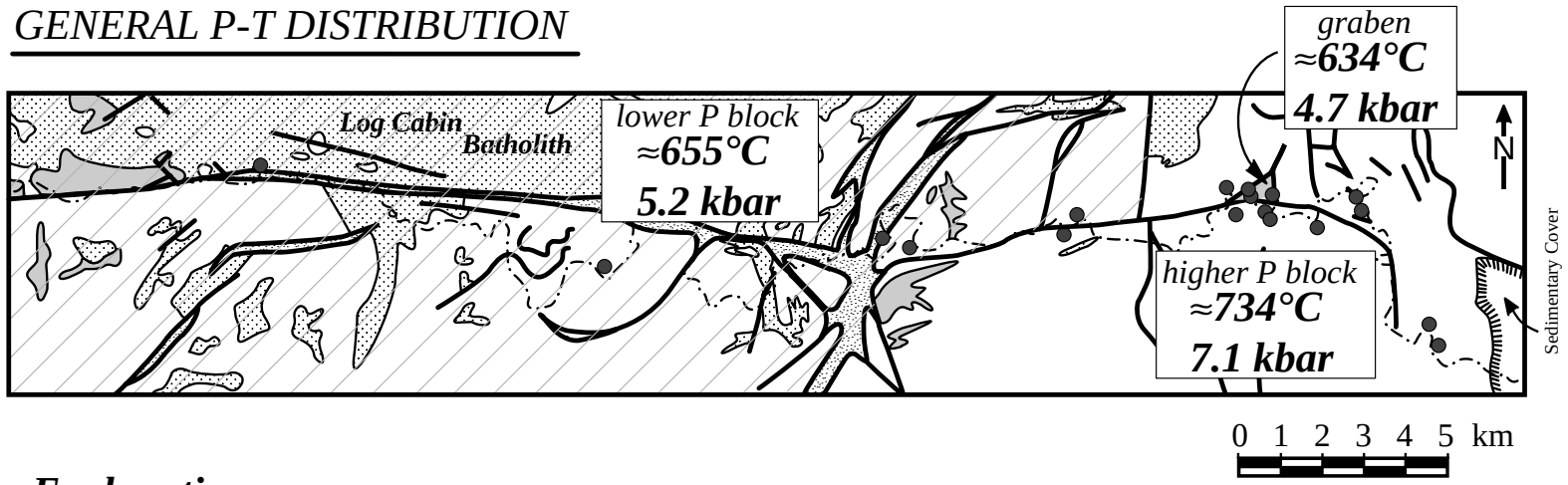

V. MORE ON CORDIERITE: THE GIBBS' METHOD

Introduction

The presence of syntectonic quartz veins in the cordierite-bearing outcrop 128 (Figure 17) suggests that μ_{H2O} must be considered along with pressure and temperature as a potential intensive variable in analyzing the origin of the diverse textures and compositions observed in the pelites from outcrop 128. The Gibbs' Method uses simultaneous linear equations to describe the variance of a system (Spear et al., 1982) and can be applied to derive equations that relate changes in μ_{H2O} to changing X_{Fe} of ferro-magnesian phases such as garnet, cordierite, and biotite.

Review of Petrographic and Chemical Observations

Sample 128/10a

Sample 128/10a is typical of the pelites throughout the Poudre Canyon. It contains a peak metamorphic assemblage of grt-bt-sil-qtz-pl-kfs; there is no cordierite in this sample. Thermobarometric calculations involving near-rim garnet, matrix biotite, and matrix plagioclase compositions indicate that near peak metamorphism occurred at 773 °C (grt-bt) and 7.6 kbar (GASP). Late retrograde activity is indicated by the marked increase in almandine and spessartine and decrease in pyrope along the garnet rims (see garnet profile, Appendix C). Furthermore, garnet is resorbed and surrounded by green biotite and muscovite (Figure 18), suggesting that later retrogression progressed via reaction

garnet + K-feldspar + H_2O = biotite + muscovite + quartz.

Sample 128/10b

The peak metamorphic assemblage in sample 128/10b is crd-bt-sil-qtz-pl-kfs. The cordierite appears to be a product of prograde metamorphism. The presence of coarse-grained biotite and sillimanite overgrowing cordierite suggest that under peak conditions the reaction

cordierite + K-feldspar + H_2O = sillimanite + biotite + quartz

was operative. The syntectonic quartz veins represent a channelized source for H_2O during metamorphism that may have driven this reaction. Cordierite compositions (Figure 44) display a fairly uniform interior composition with a decrease in Fe/(Fe+Mg) toward the rim. The interior compositions (paired with matrix biotite) are regarded as representative of peak metamorphism. On the other hand, the rim compositions, in conjunction with lower Fe/(Fe+Mg) values of biotite near to the cordierite, represent continuous Fe-Mg exchange between the cordierite and biotite following peak metamorphism . Evidence for later retrograde reaction is apparent in cordierite grains that are overgrown by randomly oriented muscovite and pale green biotite.

Sample 128/10c

There are three generations of cordierite in sample 128/10c. The first is the prograde cordierite in the peak metamorphic assemblage grt-crd-bt-sil-qtz-pl-kfs. Coarse-grained sillimanite and biotite occur between nearby garnet and cordierite (Figure 20), suggesting that the reaction

cordierite + garnet + K-feldspar + H_2O = sillimanite + biotite + quartz

was operating at peak metamorphic conditions. Thermobarometric calculations involving interior garnet, matrix cordierite, and matrix plagioclase compositions indicate that near peak metamorphism occurred at 707 °C (grt-crd) and 6.1 kbar (GASP).

The second generation of cordierite occurs in cordierite + quartz symplectites immediately adjacent to garnet and in cordierite-biotite-quartz reaction coronas surrounding relict garnet (see Figure 23). Changing conditions (a drop in temperature, pressure, or μ_{H2O}) caused garnet to break down via

the reaction

garnet + K-feldspar + H_2O = cordierite + quartz + biotite.

The third generation of cordierite occurs in cordierite-sillimanite mats within garnet pressure shadows (Figure 21). This cordierite is attributed to decompression via the reaction

garnet + sillimanite + quartz = cordierite.

The Gibbs' Method Calculations for Peak Metamorphism

Introduction

This outcrop can be treated as a six component system (FeO-MgO-Al_2O_3-SiO_2-K_2O-H_2O), all other components are neglected for the purposes of the Gibbs' calculation. Three different peak phase assemblages derived from these components are represented in this outcrop:

- 128/10a: grt-bt-sil-qtz-pl-kfs
- 128/10b: crd-bt-sil-qtz-pl-kfs
- 128/10c: grt-crd-bt-sil-qtz-pl-kfs.

The prograde reactions ascribed to the peak assemblage of each sample are:

(1) 128/10a: *sillimanite + biotite + quartz = garnet + K-feldspar + H_2O*
(2) 128/10b: *sillimanite + biotite + quartz = cordierite + K-feldspar + H_2O*
(3) 128/10c: *sillimanite + biotite + quartz = garnet + cordierite + K-feldspar + H_2O.*

Given that $P_{H2O} = P_S$, then the phase rule dictates that reactions (1) and (2), which involve six components and six phases, would be continuous, or divariant. Thus, coexisting garnet-biotite or cordierite-biotite (which involve Fe-Mg solid solution) in these reactions change composition with changing temperature or pressure. On the other hand, reaction (3), which involves six components and seven phases, would be discontinuous, or univariant, and the phases involved would maintain fixed compositions if either T or P was specified. At peak metamorphism, both T and P are fixed and the co-existing Fe-Mg phases presumably would have compositions corresponding to the P-T conditions of their given reaction assemblages. However, if μ_{H2O} is not constant across the outcrop, then its effects on the reactions must be considered along with that of T and P. Thus, even at the specified T and P of peak metamorphism, reactions (1) and (2) will continue to show compositional changes with variable μ_{H2O} whereas reaction (3) will occur at a fixed μ_{H2O}.

Using the Gibbs' Method, garnet, cordierite, and biotite compositions can be used to track changes in μ_{H2O} at the metamorphic conditions calculated in Chapter IV. Matrix equations were constructed for the peak metamorphic assemblages, and consisted of the pertinent reactions (1, 2, and 3) and the equations of homogeneous and heterogeneous equilibria for each assemblage. These matrix calculations resulted in equations describing $d\mu_{H2O}/dX_{Fe}$ in terms of X_{Fe} and T at constant P. The complete Gibbs' Method calculation for this outcrop is given in Appendix G. Both X_{Fe} and T are known from microprobe analysis and thermobarometry, respectively. A temperature of 775°C, which corresponds to the garnet-biotite temperature calculated for sample 128/10a, was used in the calculations, as were the compositions used for thermobarometry for samples 128/10a and 128/10c. Matrix biotite and interior cordierite points were assumed to correspond to peak cordierite-biotite compositions in sample 128/10b. Table 21 lists the peak Fe/(Fe+Mg) ratios for garnet, cordierite, and biotite that were used in the Gibbs' calculations. Numerically integrating the solutions for $d\mu_{H2O}/dX_{Fe}$ at varying X_{Fe} provided the information needed to construct a quantitative $\Delta\mu_{H2O}$–X_{Fe} diagram (see Appendix G for the integration).

Results

Figure 63 is the $\Delta\mu_{H2O}$–X_{Fe} diagram calculated for outcrop 128. Reactions (1) and (2) generated continuously varying loops for each Fe-Mg mineral because they behave divariantly, producing changes in mineral composition with changing μ_{H2O} at constant T and P. On the other hand, reaction (3) appears as a line of constant μ_{H2O} in Figure 63 because it behaves univariantly such that all of the phases coexist at a single μ_{H2O} at constant T and P. By setting $\Delta\mu_{H2O} = 0$ for reaction (3),

Table 21 Fe/(Fe+Mg) ratios for peak garnet, biotite and cordierite compositions in outcrop 128.

	Reaction (1) **128/10a**	Reaction (2) **128/10b**	Reaction (3) **128/10c**
garnet	0.860		0.791
cordierite		0.273	0.296
biotite	0.579	0.437	0.461
	near rim grt matrix bt	*interior crd matrix bt*	*interior grt matrix crd matrix bt*

Figure 63
$\Delta\mu_{H2O}$ vs X_{Fe} for the system grt-crd-bt-sil-qtz-kfs-H_2O (circled numbers refer to reactions described in the text). Observed compositions of equilibrium assemblages are indicated by gray tie lines. Values for the changing ratio of fugacity of H_2O (fi/f3) are given for comparison.

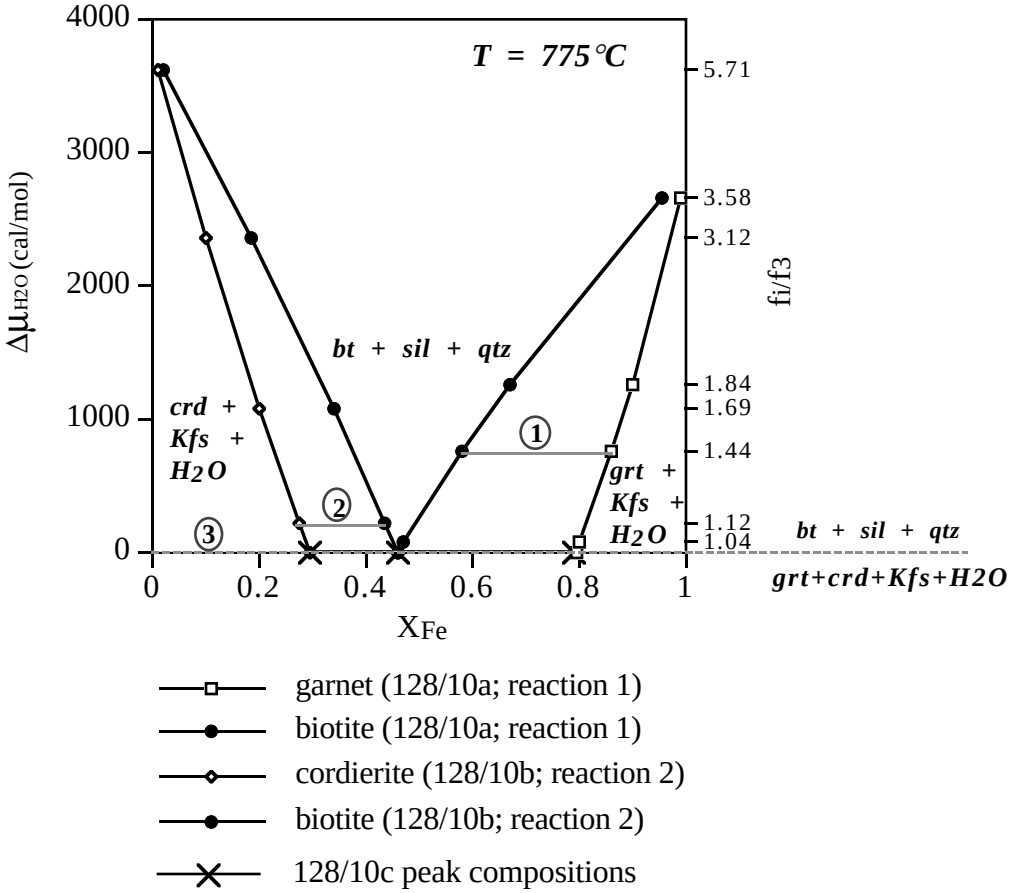

the divariant reaction loops can be depicted in terms of how much μ_{H2O} of each varies from that of the univariant reaction. The observed peak compositions for coexisting cordierite, biotite, and garnet in sample 128/10c (reaction 3) are indicated by the "X" symbols. The match between the expected compositions for each reaction loop and the observed compositions at $\Delta\mu_{H2O} = 0$ is excellent, as shown in Figure 63 and by the data in Table 22. The observed peak X_{Fe} of coexisting cordierite-biotite and garnet-bioite in samples 128/10b and 128/10a are connected by solid gray lines and correspond to a $\Delta\mu_{H2O}$ of 227 cal/mol for 128/10b (reaction 2) and 758 cal/mol for 128/10a (reaction 1). Thus, the μ_{H2O} in sample 128/10b exceeds that of sample 128/10c by 0.23 kcal/mol, whereas that of sample 128/10a exceeds that of sample 128/10c by 0.76 kcal/mol.

Table 22 Observed peak X_{Fe} for grt-crd-bt of reaction (3) and the *calculated* X_{Fe} for grt-bt and crd-bt of reactions (1) and (2) at $\Delta\mu_{H2O}$=0

	X_{Fe} observed at $\Delta\mu_{H2O} = 0$	*X_{Fe} calculated at $\Delta\mu_{H2O} = 0$*	
	Reaction (3) **128/10c**	Reaction (1) **128/10a**	Reaction (2) **128/10b**
garnet	0.791	0.793	
cordierite	0.296		0.293
biotite	0.461	0.461	0.461

Using the definition of μ_{H2O} for real gases, $\Delta\mu_{H2O}$ can be reformulated in terms of change in fugacity of H_2O relative to reaction (3):

$$\mu_{H_2O} = \mu^{o}_{H_2O} + RT \ln \frac{f_{H_2O}}{f^{o}_{H_2O}};$$ where: $\mu^{o}_{H_2O}$ = standard state of H_2O at T, 1 bar

f_{H_2O} = fugacity of water

$f^{o}_{H_2O}$ = standard – state fugacity of water

R = the gas constant.

The standard-state fugacity of water (pure water at 1 bar and temperature of interest) is assumed to be 1 bar (Nordstrom and Munoz, 1986). The change in μ_{H2O} is defined as $\mu_i - \mu_3$:

$$\Delta\mu_{H_2O} = \mu_i - \mu_3 = \mu^{o}_{1bar,T} - \mu^{o}_{1bar,T} + RT\ln f_i - RT\ln f_3$$

Because all of the calculations were done at the same temperature (775°C), $\Delta\mu_{H2O}$ can be written as:

$$\Delta\mu_{H_2O} = RT\ln(f_i / f_3) \quad \text{and} \quad \frac{f_i}{f_3} = e^{\left[\frac{\Delta\mu_{H_2O}}{RT}\right]}.$$

The fugacity ratios for the $\Delta\mu_{H2O}$ data points are indicated on the right hand y-axis in Figure 63 and tabulated for each reaction in Appendix G. Because $\Delta\mu_{H2O} = 0$ for the peak conditions of sample 128/10c (reaction 3), $f_i/f_3 = f_3/f_3 = 1$ for this reaction. In Figure 63, the f_i/f_3 ratio tracks the change in f_{H2O} with changing composition relative to reaction (3). The observed peak X_{Fe} of coexisting cordierite-biotite and garnet-bioite in samples 128/10b and 128/10a correspond to f_i/f_3 of 1.12 for 128/10b (reaction 2) and 1.44 cal/mol for 128/10a (reaction 1). Thus, sample 128/10a represents a 44% increase of f_{H2O} above the conditions of sample 128/10c, whereas f_{H2O} of sample 128/10b exceeds that of 128/10c by only 12%.

The Waning Stages of Peak Metamorphism

Introduction

The reduced Fe/(Fe+Mg) ratios at cordierite rims in sample 128/10b and the crd-qtz symplectites/crd-qtz-bt coronas on garnet in 128/10c appear to predate more obviously late retrograde textures such as the pale green biotite and muscovite overgrowths on cordierite in 128/10b and the cordierite pressure shadows in 128/10c. The Gibbs' Method can be used to test the possibility that these post-peak chemical and textural changes are due to reactions produced by changes in μ_{H2O} during the waning stages of peak metamorphism rather than some much later retrogression.

Sample 128/10b

The observed X_{Fe} of coexisting cordierite rims and nearby red-brown biotite are plotted on the $\Delta\mu_{H2O}$–X_{Fe} diagram in Figure 64 (dotted tie line) and correspond to a $\Delta\mu_{H2O}$ of 354 cal/mol (f_2/f_3 = 1.19). The observed X_{Fe} for the apparent post-peak cordierite-garnet pair are compared to those calculated by the Gibbs' Method in Table 23. The match is very good and suggests that the change in composition may have occurred by continuous reaction simply by increasing μ_{H2O} by 0.13 kcal/mol (or f_{H2O} by 7%) beyond that of the peak compositions in this sample. This moves coexisting cordierite and biotite along the divariant loop to lower X_{Fe} and accounts for the shift in the cordierite-biotite- sillimanite three phase field to higher Mg contents in Figure 46.

Table 23 Observed X_{Fe} for cordierite rim-nearby red-brown biotite pairs in sample 128/10b (reaction 2) compared to *calculated* X_{Fe} for this reaction.

	cordierite	**biotite**
Observed X_{Fe}	0.262	0.418
Calculated X_{Fe}	0.262	0.423

Sample 128/10c

The Gibbs' Method also can be used to compare μ_{H2O} to X_{Fe} in coexisting cordierite, biotite, and garnet found in the crd-qtz-bt coronas and cordierite-quartz symplectites around garnet in sample 128/10c. The reaction responsible for this texture,

garnet + K-feldspar + H_2O = cordierite + biotite + quartz,

is a continuous reaction represented by a divariant cordierite-biotite-garnet loop on a $\Delta\mu_{H2O}$–X_{Fe} diagram (reaction 4). Assuming that this reaction followed peak metamorphism in a continuum, then the calculated data can be incorporated with that already calculated for the peak conditions. The complete calculation for reaction (4) is given in Appendix G. Table 24 compares the observed X_{Fe} for the peak cordierite-biotite-garnet assemblage from reaction (3) at $\Delta\mu_{H2O}$=0 (column 1) to those calculated by the Gibbs' Method for reaction (4) at $\Delta\mu_{H2O}$=0 (column 2). Cordierite rims adjacent to garnet, biotite adjacent to both garnet and cordierite, and garnet near-rim compositions were used to calculate the cordierite-biotite-garnet X_{Fe} reported in column 2 of Table 24. The data diverge somewhat for garnet suggesting that the near-rim garnet composition used in the

Table 24 Observed peak X_{Fe} for grt-crd-bt of reaction (3) and the *calculated* X_{Fe} for grt-crd-bt of reaction (4) at $\Delta\mu_{H2O}$=0 for sample 128/10c

	X_{Fe} observed at $\Delta\mu_{H2O}$ = 0	*X_{Fe} calculated at $\Delta\mu_{H2O}$ = 0*	*X_{Fe} calculated using grt rims at $\Delta\mu_{H2O}$ = 0*
	Reaction (3)	**Reaction (4)**	***Reaction (4)***
garnet	0.791	0.816	*0.842*
cordierite	0.296	0.301	*0.314*
biotite	0.461	0.461	*0.461*

Figure 64 $\Delta\mu_{H2O}$ vs X_{Fe} for the system grt-crd-bt-sil-kfs-H_2O. Observed compositions of peak equilibrium assemblages are indicated by the solid gray tie lines. Observed apparent post-peak crd-bt compositions are indicated by the dotted black tie line. Values for the changing ratio of fugacity of H_2O (fi/f3) are given for comparison.

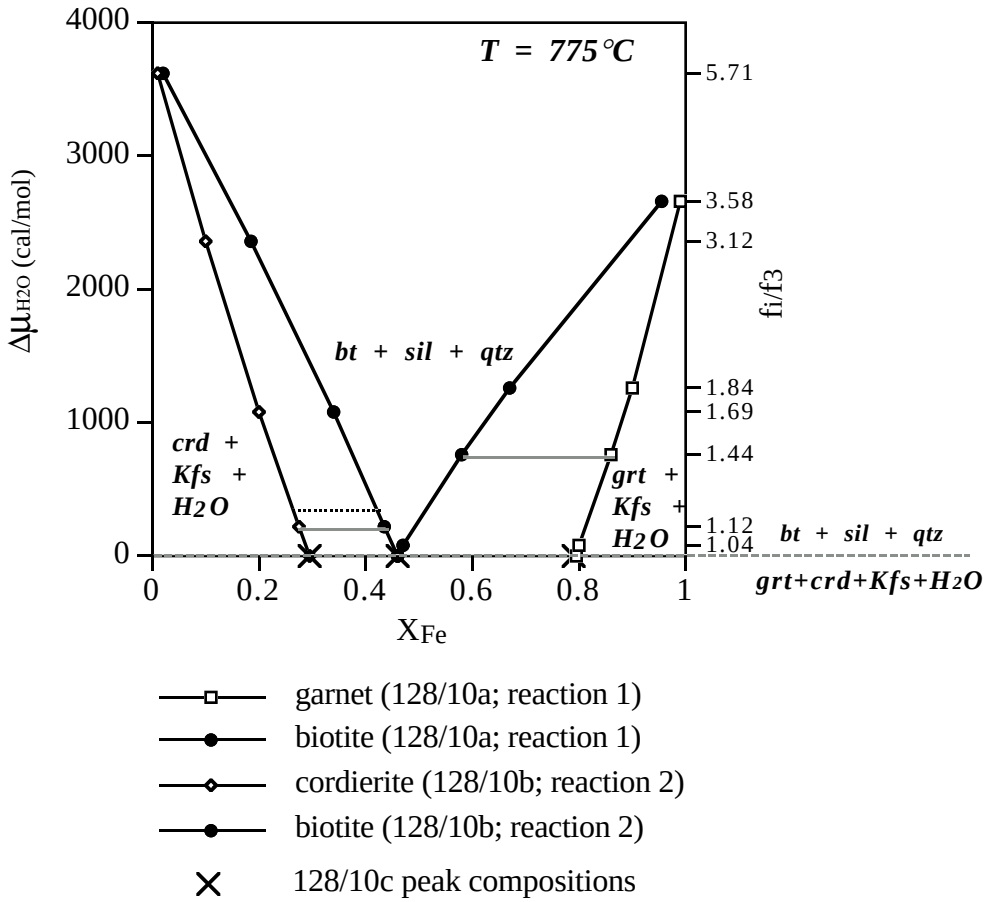

calculation was not a perfect choice, although it was the best available. Near-rim garnet compositions were chosen because a much larger mismatch between observed and calculated X_{Fe} resulted when the garnet rim compositions were used, as shown in column 3 of Table 24. This mismatch is attributed to the change in garnet rim compositions created by the decompression reaction that produced later cordierite from garnet. Therefore, near-rim garnet compositions are taken as the best approximation of the garnet that was in equilibrium with cordierite during reaction (4).

Figure 65 incorporates the data from reaction (4) into the $\Delta\mu_{H2O}$–X_{Fe} diagram for outcrop 128. The observed X_{Fe} of coexisting cordierite, biotite, and garnet are connected by the dashed tie line and correspond to a $\Delta\mu_{H2O}$ of -320 cal/mol (14% reduction in f_{H2O}). Thus, unlike samples 128/10a and 128/10b, sample 128/10c experienced a *loss* of water during peak metamorphism that

Figure 65 $\Delta\mu_{H2O}$ vs X_{Fe} for the system grt-crd-bt-sil-qtz-kfs-H_2O (circled numbers refer to reactions described in the text). Observed compositions of peak equilibrium assemblages are indicated by the gray tie lines. The dotted and dashed tie lines represent assemblages present during the waning stages of metamorphism. Values for the changing ratio of fugacity of H_2O (fi/f3) are given for comparison.

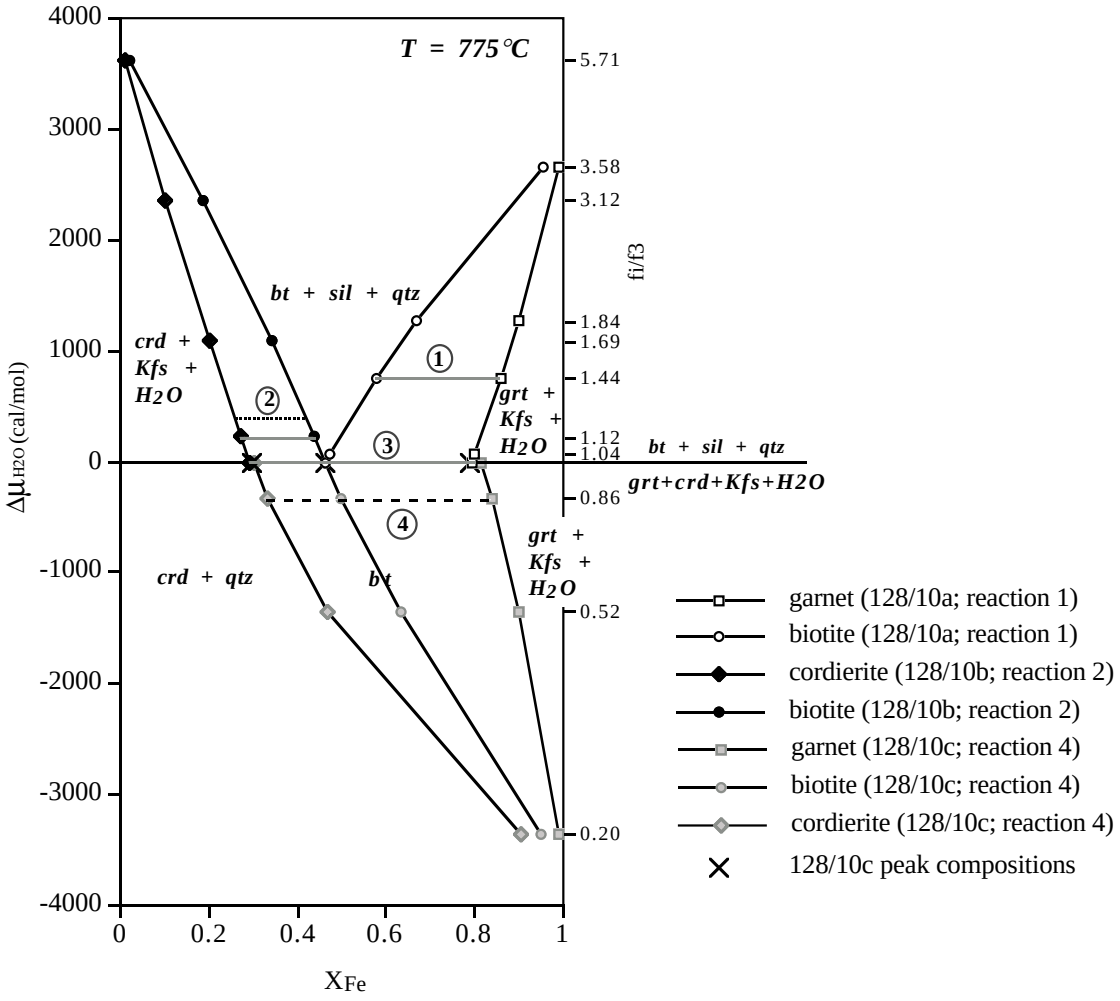

reduced the μ_{H2O} and interrupted the progress of reaction (3). A decline of 0.32 kcal/mol in μ_{H2O} moved the remaining cordierite, biotite, and garnet compositions along the divariant loop of reaction (4) toward higher X_{Fe}. This accounts for the shift in the cordierite-bioite-garnet three phase field to higher Fe contents seen in Figure 49. This reaction ceased when K-feldspar was depleted.

Interpretation

The AFM diagrams in Figure 66 portray the reactions involved in peak metamorphism of samples from outcrop 128. The prograde assemblages differ due to differences in bulk composition as indicated in Figure 66A (grt-bt-kfs-qtz for sample 128/10a, crd-bt-kfs-qtz for sample 128/10b, and grt-crd-bt-kfs-qtz for sample 128/10c). During peak metamorphism, H_2O entered the area represented by outcrop 128. This fluid influx is believed to have been channelized rather than pervasive based on the presence of distinct syntectonic quartz veins in the outcrop. Furthermore, the absence of syntectonic quartz veins elsewhere in the study area suggest that the fluid influx was a local phenomenon. Sample 128/10a, which showed the largest μ_{H2O}, must have been more accessible to the fluid than sample 128/10c, which showed the smallest μ_{H2O}.

The introduction of H_2O to this system drove reactions that changed the topology of the AFM diagram and consequently changed the equilibrium assemblages in each sample. The change in topology was caused by reaction (3),

garnet + cordierite + K-feldspar + H_2O = biotite + sillimanite + quartz.

This reaction produced the coarse-grained biotite and sillimanite observed between nearby garnet and cordierite in sample 128/10c ("***c***" in Figure 66B). However, reaction 3 obviously did not go to completion because garnet and cordierite are preserved. The arrested nature of this reaction is attributed to the limited availability of μ_{H2O}; the μ_{H2O} needed to drive the reaction was not maintained suggesting that sample 128/10c was less accessible to the H_2O source. Instead, reduced levels of μ_{H2O} shifted coexisting cordierite, biotite, and garnet to higher X_{Fe} along divariant reaction (4),

garnet + K-feldspar + H_2O = cordierite + biotite + quartz.

Reaction (4) produced cordierite-quartz symplectites and cordierite-biotite-quartz reaction coronas adjacent to garnet, then ceased when K-feldspar was depleted. Garnet breakdown to cordierite in sample 128/10c was reinitiated during decompression via the K-feldspar-absent reaction

garnet + sillimanite + quartz = cordierite.

Elevated μ_{H2O} placed sample 128/10a ("***a***" in Figure 66B) in the grt-bt-sil three phase field, presumably producing Fe-enrichment in coexisting garnet and biotite as the continuous reaction

garnet + K-feldspar + H_2O = biotite + sillimanite + quartz

proceeded. On the other hand, the more magnesian bulk composition of sample 128/10b placed this sample ("***b***" in Figure 66B) in the crd-bt-sil three phase field. Mg-enrichment in coexisting cordierite and biotite followed as the continuous reaction

cordierite + K-feldspar + H_2O = biotite + sillimanite + quartz

proceeded. Thus, the textural and mineralogical differences between the samples 128/10a, 128/10b, and 128/10c can be attributed to differences in μ_{H2O} coupled with differences in bulk composition.

Figure 66 AFM diagrams projected through K-feldspar depicting the peak metamorphic assemblages. The letter symbols ***a***, ***b*** and ***c***, refer to bulk compositions for samples 128/10a, 128/10b and 128/10c, respectively.

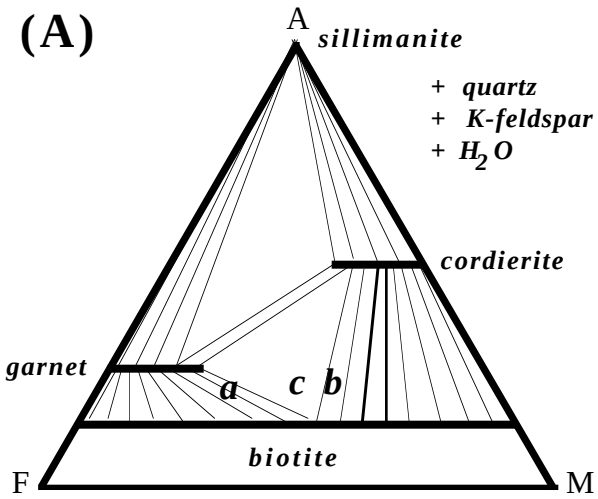

Original prograde assemblages:

128/10a = grt-bt-kfs-qtz
128/10b = crd-bt-kfs-qtz
128/10c = grt-crd-bt-kfs-qtz

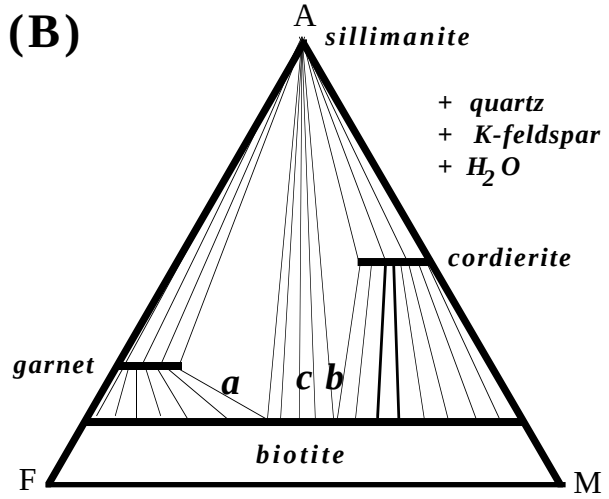

Increase μ_{H_2O} at peak metamorphism:

128/10a = grt-bt-sil-kfs-qtz *grt + kfs + H_2O = bt + sil*
128/10b = crd-bt-sil-kfs-qtz *crd + kfs + H_2O = bt + sil*
128/10c = development of bt + sil where garnet and cordierite are in contact.
grt + crd+ kfs + H_2O = bt + sil + qtz
(this sample shows the least change in μ_{H_2O})

VI. MIGMATITE GENESIS

Introduction

High grade metamorphic terranes supply much of the available data about geological processes which occur at depth in the crust. Prominent among these processes is migmatization. Migmatization is widely attributed to partial melting via wet or dehydration melting (von Platen, 1965; Mehnert, 1968; Grant, 1973; Tracy, 1978; Thompson and Tracy, 1979; Thompson, 1982; McLellan, 1983; Johannes, 1984; Clemens and Vielzeuf, 1987; Le Breton & Thompson, 1988, Thompson, 1990; Brown, 1994). Other mechanisms may be actively involved in migmatization, either separate from, or in concert with, anatexis. These other mechanisms include subsolidus differentiation, metasomatism, and magmatic injection (Olsen, 1984; Grant, 1985; Johannes, 1988). Clarifying the origin of migmatites in basement rocks (such as occur in the Poudre Canyon) will improve our understanding of the petrogenesis of the deeper crust. In this chapter, the factors which affected the development of migmatites in the Poudre Canyon are addressed through field observations and petrography combined with modal and compositional analyses.

Previous Work on Front Range Migmatites

Migmatites from the central Front Range (west of Golden, Colorado) have been studied by Hedge (1969, 1972) and Olsen (1982, 1984, 1985). Hedge (1969) observed that the migmatites occur in both schists and gneisses but are best developed in the schists. The migmatites consist of a quartzo-feldspathic portion (the *leucosome*) with a mafic selvage (the *melanosome*). The leucosomes are contorted yet roughly conformable with the primary foliation, suggesting a syn-deformational origin (Hedge, 1972). Migmatite xenoliths occur in the 1.7 Ga Boulder Creek Granodiorite member of the Routt Plutonic Suite (Hedge 1969, 1972). Therefore, the migmatites must have formed at the height of regional metamorphism prior to the emplacement of the syntectonic Boulder Creek Granodiorite (Hedge, 1972), part of the Routt Plutonic Suite. Hedge (1972) ruled out granitic injection as a mechanism since the migmatites (1) bear no spatial relationship to the Routt Plutonic Suite and (2) appear to pre-date the Routt Plutonic Suite. He further observed that feldspar compositions, including trace elements, do not vary from leucosome to melanosome (Hedge, 1969). Hedge (1969) concluded that the migmatites originated either by anatexis or by some unspecified subsolidus metamorphic process.

Olsen (1982, 1984) and Olsen and Grant (1991) studied migmatitic gneisses from the same area as Hedge (between Golden and Idaho Springs, Colorado) and applied mass-balance analyses to further elucidate the migmatite genesis. Olsen compared net compositions of leucosome + melanosome to the "unmigmatized" portion of the rock (the *paleosome*). She concluded that several different simultaneously operating processes generated the migmatites. Some migmatites formed by the injection of melt and the interaction of that melt with the wall rocks (Olsen, 1982). Others formed by partial melting accompanied by metasomatism. In these migmatites, water-rich fluid infiltrated along subparallel channels, metasomatized the rock and initiated partial melting to form the leucosomes (Olsen, 1984). Still other migmatites formed by a combination of subsolidus reactions and partial melting (Olsen, 1985). According to Olsen, biotite breakdown,

$$biotite + 6H^{+} = microcline + 3(Fe,Mg) + 4H_2O,$$

produced H_2O which led to wet melting of the albite, K-feldspar and quartz components in the rock, forming the leucosome. Partial melting reduced the a_{H2O} and led to more biotite breakdown and the excess Fe and Mg reacted with microcline to form the biotite-rich selvage, or melanosome (Olsen, 1985). The metamorphic differentiation was driven by the gradient of f_{H2O} between the leucosome and the paleosome. Olsen's work demonstrates that migmatite genesis is not a simple matter and that no single mechanism can account for the migmatites in the central Front Range.

Figure 67 Migmatite Outcrop Location Map

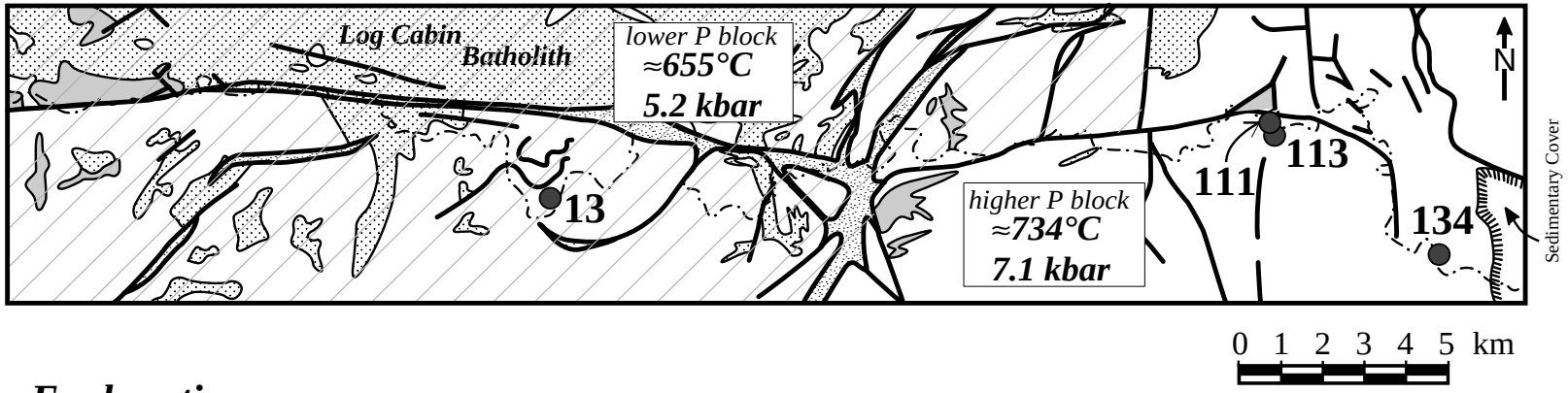

Explanation

- 1.7 Ga Amphibolite Facies Metamorphic Rock *(undifferentiated)*
- 1.7 Ga Routt Plutonic Suite *(Boulder Creek Granodiorite)*
- 1.4 Ga Berthoud Plutonic Suite *(Silver Plume Granite)*
- Fault Zones *(ductile and brittle)*
- Cache la Poudre River
- **13** Outcrop location

Lithologies and shear zones adapted from Abbott (1976), Braddock et al (1988a, 1988b) and Shaver et al (1988).

Table 25: Modes of Migmatite Thin Sections

								selvage							
HOST	**13G**	**13G-1**	**13I**	**13I-1**	**111I****	**111I-1A****	**113B**	**113B†**	**113M-2**	**134E-1**	**134E-2**	**134E-2A‡**	**134M-1**	**134M-1A‡‡**	**134M-2**
quartz	41	36	45	40		70	55	31	63	69	73	64	54	20	50
plagioclase	12	23	26	33		10	12	10	6	9	7	6	28	55	32
*An Content**	*.18-.20*	*.23-.24*	*.33-.34*	*.33-.33*		*.20-.21*	*.21-.26*	*N/A*	*.22-.24*	*.24-.27*	*.24-.28*	*.23-.27*	*.26-.28*	*.27-.27*	*.27-.28*
microcline	13	16	11	6		2	6	-	1	tr	-	1	-	-	-
biotite	30	23	15	18		13	21	45	15	20	18	26	16	24	15
garnet	-	-	-	-		1	1	9	4	-	-	-	-	-	tr
sillimanite	-	-	-	-		3	4	4	10	-	-	-	-	-	-
zircon	tr	tr	tr	tr		tr	tr	tr	tr	tr	tr	tr	tr	tr	tr
opaques	tr	tr	tr	tr		tr	tr	-	tr	1	1	2	1	tr	2
apatite	tr	tr	tr	tr		-	-	-	-	-	-	-	-	tr	-
muscovite	2	1	2	1		-	-	-	-	-	tr	-	-	-	-
sericite	tr	tr	tr	tr		-	tr	tr	-	-	-	-	tr	-	-
chlorite	-	-	-	-		tr	-	-	-	-	-	-	-	-	-
total	*98*	*99*	*99*	*98*		*99*	*99*	*99*	*99*	*99*	*99*	*99*	*99*	*99*	*99*
avg grain size	0.2	0.2	0.2	0.2		0.3	0.3	0.8	0.3	0.3	0.3	0.4	0.2	0.3	0.3
LEUCOSOME															
quartz	29	30	51	45	22		13		17	23	34		55		44
plagioclase	31	16	42	35	17		2		2	17	40		42		55
*An Content**	*.22-.24*	*.18-.24*	*.34-.34*	*.32-.33*	*.03-.14*		*.21-.24*		*.22-.25*	*.23-.27*	*.24-.28*		*.27-.28*		*.26-.28*
microcline	35	52	3	13	60		84		80	57	25		-		-
biotite	3	1	3	6	-		tr		tr	2	tr		2		tr
opaques	-	-	-	tr	-		-		-	-	tr		-		-
muscovite	tr	-	tr	-	-		-		-	-	-		-		-
sericite	1	1	tr	tr	1		tr		tr	1	1		tr		tr
chlorite	-	-	-	-	-		-		-	tr	-		-		-
total	*99*	*100*	*99*	*99*	*100*		*99*		*99*	*100*	*100*		*99*		*99*
average grain size (mm)	2.0	2.0	1.0	1.0	5.0		5.0		4.0	5.0	5.0		1.0		1.0
leuco thick-ness (mm)	*6*	*10*	*8*	*7*	*23*		*15*		*18*	*15*	*16*		*3*		*5*

** total range in mole fraction An from microprobe analysis (rim to interior)*
*** 111I is all leucosome and is contiguous with 111I-1A which is all host*
† this mode is for the approxiamtely 1 cm thick selvage adjacent to the leucosome
‡ 134E-2A is all host and is contiguous with the leucosome in 134E-2
‡‡ 134M-1A is all host and is contiguous with the leucosome in 134M-1

Observations of Migmatites in the Poudre Canyon

Introduction

Examination of migmatite exposures in the Poudre Canyon, where the pressure-temperature regimes are well-defined (Munn, this study), may help to clarify the conditions surrounding migmatite genesis in the northern Front Range. As in the central Front Range, the northern Front Range migmatites are deformed and conformable with the primary foliation. Unlike the central Front Range, no migmatitic xenoliths were observed in the syntectonic Routt Plutonic Suite nor were there any observable contacts between migmatites and the 1.7 Ga intrusive rocks in this study area. However, according to Abbott (1970), gradational contacts make it difficult to distinguish between the intrusive Routt Plutonic Suite and migmatitic biotite schists in the northern Front Range. Therefore, the migmatites must have formed during the deformation which accompanied peak metamorphism synchronous with the intrusion of the Routt Plutonic Suite. Four migmatitic outcrops from across the study area were chosen for detailed study, PC–13, -111, -113, and -134. The locations of these outcrops are shown in Figure 67. PC–13 is a gneissic migmatite and is located in the lower pressure block (up canyon; 655°C, 5.2 kbar). PC–111, -113, and -134 are interbedded migmatized schists and gneisses from the higher pressure block (down canyon; 734°C, 7.1 kbar).

The modes for thin sections of migmatite samples taken from these outcrops are presented in Table 25. Modes are recorded for both the host and the leucosome portions of each sample. The term *host* refers to the rock in which the leucosome occurs, excluding the melanosome. The host may or may not have been involved in the migmatization process, hence, this non-genetic term is preferred over that of paleosome. Melanosomes (or mafic selvages) are thin, dark biotite-rich zones which may envelop the leucosomes. They are common in outcrops 13 and 113 but are unusual in outcrops 111 and 134. The K-feldspar and plagioclase compositions for host and leucosome were analyzed using the electron microprobe. All of the K-feldspar is microperthitic and was analyzed using an enlarged electron beam. Table 26 summarizes the feldspar compositions; the complete analyses are presented in Appendix H.

Outcrop Descriptions

Outcrop 13

Outcrop 13 is comprised of migmatized fine- to medium-grained quartzo-feldspathic biotite gneiss, mapped as *Xqs* by Abbott (1976). The leucosomes range up to 9 centimeters in thickness and are composed of medium-grained quartz, plagioclase and microcline (see Table 25). The leucosomes comprise approximately 28% of the outcrop, and commonly are enveloped by 0.1 to 2 mm thick biotite-rich selvages. These selvages generally increase in thickness in proportion to the leucosome thickness, as shown in Figure 68. In

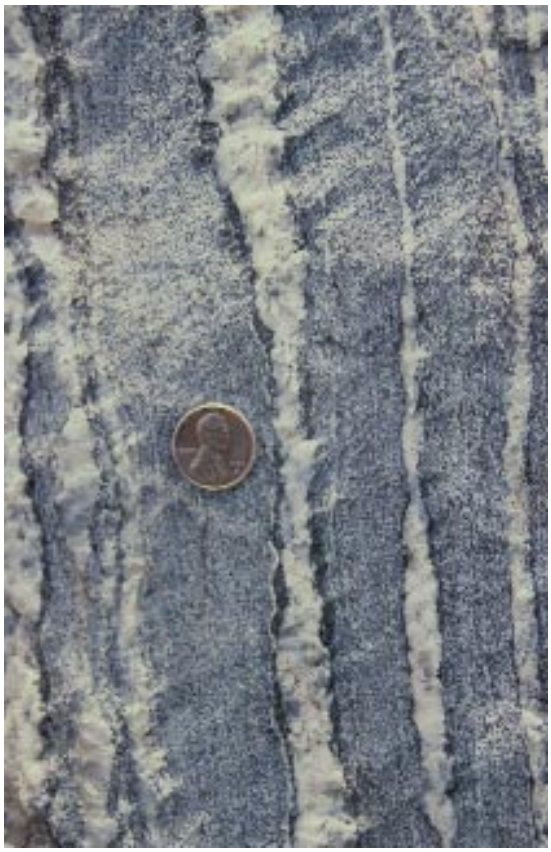

Figure 68 Field photograph of outcrop 13 showing the development of thin biotite-rich selvages (black) adjacent to the leucosomes (white); photograph #9-11-91.

Table 26 Average Feldspar Compositions for Migmatites (mole fraction anorthite for plagioclase, pl, and mole fraction orthoclase and albite for K-feldspar)

Sample Number	LEUCOSOME			HOST		
	pl rim	*pl interior*	*K-feldspar*	*pl rim*	*pl interior*	*K-feldspar*
13G	0.216	0.237	$Or_{93}Ab_{7}$	0.184	0.200	$Or_{93}Ab_{7}$
13G-1	0.180	0.239	$Or_{93}Ab_{7}$	0.227	0.235	$Or_{92}Ab_{8}$
13I	0.335	0.339	$Or_{92}Ab_{8}$	0.329	0.337	$Or_{94}Ab_{6}$
13I-1	0.315	0.334	$Or_{93}Ab_{7}$	0.330	0.330	$Or_{93}Ab_{7}$
111I	0.025	0.142	$Or_{77}Ab_{22}An_{01}$	*leucosome contiguous with host in 111I-1A*		
111I-1A	*host contiguous with leucosome in 111I*			0.205	0.213	$Or_{87}Ab_{13}$
113B	0.211	0.244	$Or_{88}Ab_{12}$	0.209	0.257	$Or_{86}Ab_{14}$
113M-2	0.217	0.253	$Or_{78}Ab_{21}An_{01}$	0.243	0.266	$Or_{76}Ab_{24}$
134E-1	0.234	0.273	$Or_{79}Ab_{21}$	0.243	0.266	$Or_{85}Ab_{15}$
134E-2	0.239	0.279	$Or_{88}Ab_{12}$	0.243	0.278	*not available*
134E-2A	*host contiguous with leucosome in 134E-2*			0.234	0.268	$Or_{85}Ab_{15}$
134M-1	0.267	0.280	*no K-feldspar*	0.256	0.276	*no K-feldspar*
134M-1A	*host contiguous with leucosome in 134E-1*			0.275	0.274	*no K-feldspar*
134M-2	0.265	0.281	*no K-feldspar*	0.267	0.277	*no K-feldspar*

thin section, the average grain size of the host is 0.2 mm whereas that of the leucosome is 2 mm (10 times larger). Grains within the leucosome typically exhibit irregular to serrated grain boundaries. In addition, undulatory extinction is common in the quartz and grain boundary recrystallization is observed around the feldspars, as shown in Figure 69. This solid state deformation obscures any earlier textures related to the migmatization.

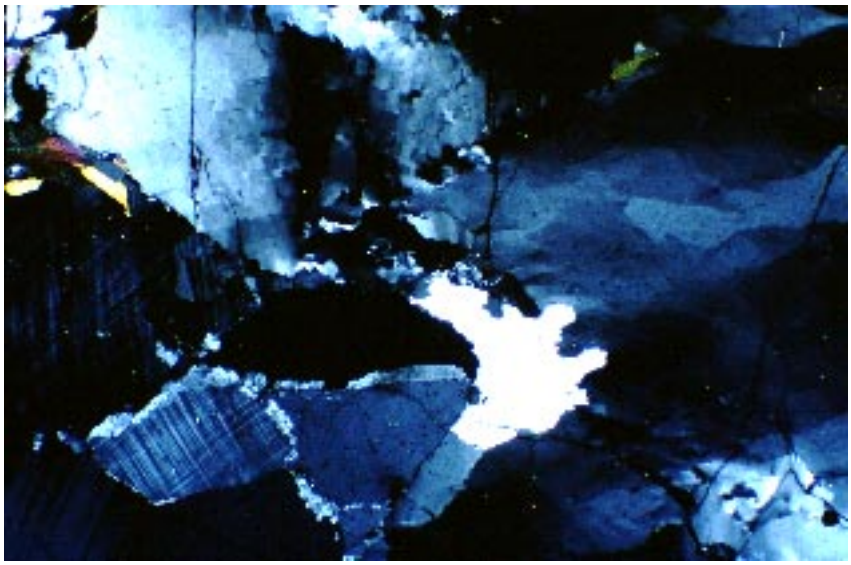

Figure 69 Photomicrograph of sample 13G-1 showing undulose extinction in quartz, grain boundary recrystallization around feldspar, and irregular to serrated grain boundaries all of which typify the leucosomes in outcrop 13. Field of view 4.8 mm (longest dimension); crossed polars.

Individual plagioclase grains are either slightly

Figure 70 Sketch of outcrop 13, a stromatic migmatite.

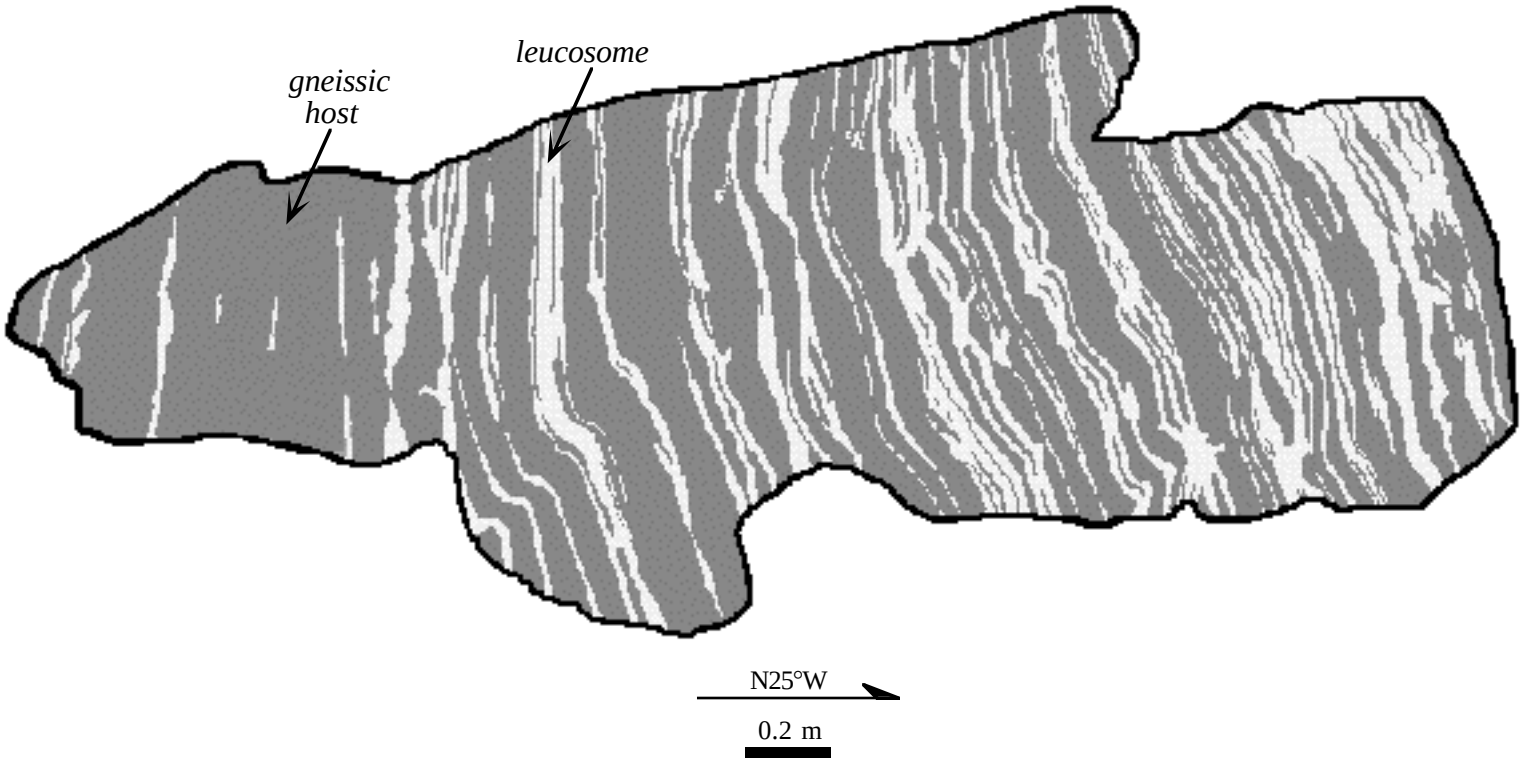

normally zoned or show no appreciable change from core to rim (see Table 26). In addition, there is very little difference in plagioclase, or K-feldspar, composition between the host and the leucosome (see Table 26). Hosts containing sizeable amounts of microcline relative to plagioclase (13G and 13G-1, Table 25) have leucosomes enriched in microcline and a mole fraction of 18 to 24% anorthite in the plagioclase. On the other hand, plagioclase- and quartz-enriched hosts with relatively less microcline in the host mode (13I and 13I-1, Table 25) have a higher mole fraction of anorthite in the plagioclase (An_{32} to An_{34}) and low modal percentages of microcline in the leucosomes.

The leucosomes are continuous across outcrop 13, and are generally concordant with the primary foliation (N62°E/88°NW). This layer-parallel, or stromatic, character is evident in the outcrop sketch in Figure 70, and is typical of all of the migmatites in the Poudre Canyon. The leucosomes may be boudinaged or exhibit pinch and swell texture with elongation parallel to the dominant foliation, as shown in Figures 71a and 71b. The leucosomes also exhibit a variety of fold types, including

Figure 71b Pinch and swell structure in a cut slab from outcrop 13.

Figure 71a Boudinaged leucosome extended parallel to the dominant foliation in outcrop 13; photograph #8-34-91.

disharmonic folds (Figures 72a and 72b), intrafolial isoclinal folds (Figure 72c), and parallel harmonic folds (Figure 72d). According to McLellan (1989), deformation of partially molten material should produce noncylindrical folds (Figures 72a and 72b) whereas deformation of wholly solid material produces regular harmonic folds (Figure 72d).

Figures 72c and 72d also show a texture specific to this outcrop in which separate leucosomes appear to coalesce to form leucocratic clots which cross-cut the otherwise continuous layer-parallel leucosomes. The clots always extend across several leucosomes, are slightly coarser-grained than these leucosomes, and appear to have similar mineralogy. The compositional similarity of the clots

Figure 72b Disharmonically folded leucosome from outcrop 13; photograph #9-5-91.

Figure 72a Disharmonically folded leucosome from outcrop 13; photograph #10-5-91.

Figure 72d Parallel, harmonic folds in outcrop 13. Note the large leucocratic clot to the left of the penny; photograph #9-9-91.

Figure 72c Intrafolial isoclinal fold in outcrop 13. Note the leucocratic clots to the left of the penny; photograph #9-18-91.

to the layer-parallel leucosomes and the restriction of the clots to the vicinity of the leucosomes suggests a common source for both. The outward appearance of the clots suggests a blending together of the leucosomes which they cross-cut. This implies that the leucosomes were less viscous (molten?) than the surrounding material.

Outcrop 111

Outcrop 111 consists of migmatized, interlayered, fine- to medium-grained quartzo-feldspathic biotite gneiss and sillimanite-biotite schist, mapped as *Xqs* by Braddock et al. (1988a). This outcrop is part of the large road cut shown in Figure 6 (the migmatized exposure investigated here is located to the left of the near-vertical pegmatite). It is a stromatic migmatite in which the leucosomes are more or less continuous and conformable with the dominant foliation (N75°E/84°SE). Figure 73 is a field sketch of this outcrop. The leucosomes (white in Figure 73) range up to 9 cm in thickness and comprise 23% of the outcrop. Some leucosomes are folded

Figure 73 Sketch of outcrop 111. The area of the field photograph shown in Figure 75 is outlined.

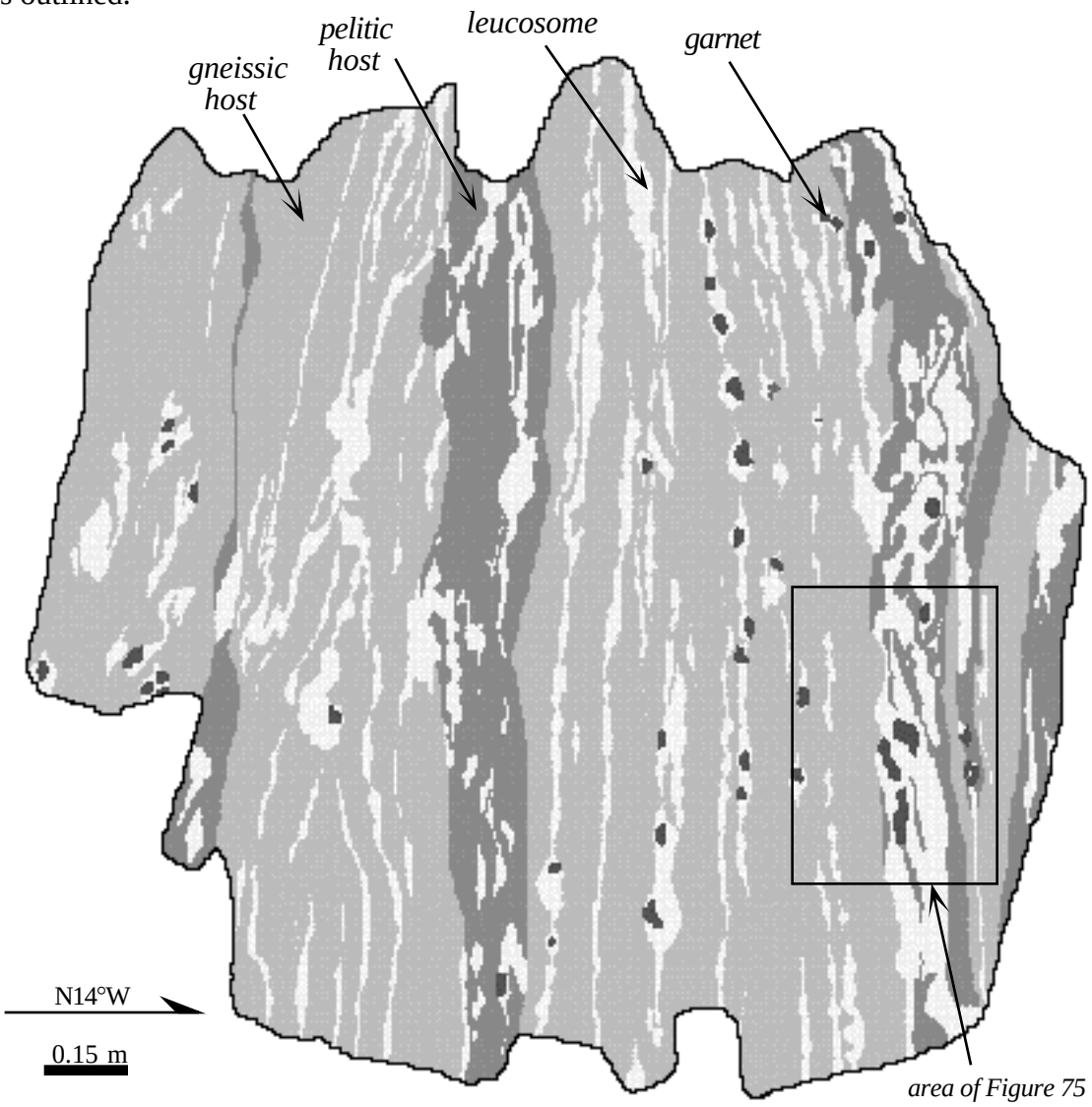

(disharmonic and harmonic) whereas others exhibit boudinage and pinch and swell textures, shown in Figure 74. Figure 73 shows the interlayered nature of this migmatite (quartzo-feldspathic biotite gneiss in light gray and sillimanite-biotite schist in darker gray). Both rock types host leucosomes, however, the leucosomes are more concentrated in the pelitic layers. Figure 75 is a field photograph showing the contrast between the pelitic and gneissic layers: the leucosomes are densely packed within the pelitic layer whereas they have a more dispersed distribution within the gneiss. This texture suggests that dehydration melting of the micas within the pelitic layers played an important part in the migmatization of the outcrop.

Figure 74 Field photograph of a stromatic migmatite in outcrop 111 showing pinch and swell texture in the leucosomes. Note the biotite-rich selvage enveloping the leucosome to the left of the penny (a rare occurrence in this outcrop); photograph #11-13-91.

Figure 75 Typical field photograph of migmatitic outcrop 111 showing interlayered pelitic (to the right) and gneissic (to the left) host rock. The leucosomes are densely packed in the pelite whereas they are more widely dispersed in the gneiss. Also, note the large garnet porphyroblasts within the leucosomes in the pelitic layer; photograph #11-17-91.

The leucosomes in outcrop 111 consist of quartz, plagioclase, and microcline, with or without garnet (see Table 25). Where present, garnet is poikiloblastic and individual grains can be quite large, ranging up to 2.5 cm in width and 5 cm in length, as in Figure 75. Garnets are elliptically shaped with their long axes extended parallel to the dominant foliation. Figure 76 shows one of these large poikiloblastic garnets within a leucosome boudin, suggesting that the origin of these garnets is related to the migmatization process. Leucosome plagioclase is normally zoned and is more sodic (An_{2-14}) than in the host (An_{21}). Microcline also is more sodic in the leucosome ($Or_{78}Ab_{22}$) than in the host ($Or_{87}Ab_{13}$). The *average* leucosome grain size is 5 mm, however, microcline is typically much coarser grained than quartz or plagioclase (up to 3.5 cm in length). In thin section, quartz and feldspar have irregular grain boundaries and show interlocking textures that are more igneous than metamorphic in appearance, as shown in Figure 77. Microtextures within the host differ greatly from those of the leucosome. The average host grain size is much smaller, 0.3 mm, and quartz and feldspar exhibit granoblastic-polygonal texture (grain boundaries meet at triple junctions with interfacial angles of 120°). This texture is typical of high grade metamorphic rocks that have achieved textural equilibrium by minimizing grain boundary energy (Barker, 1989).

Figure 76 Field photograph of outcrop 111 showing a large poikiloblastic garnet within a leucosome boudin; photograph #11-9-91.

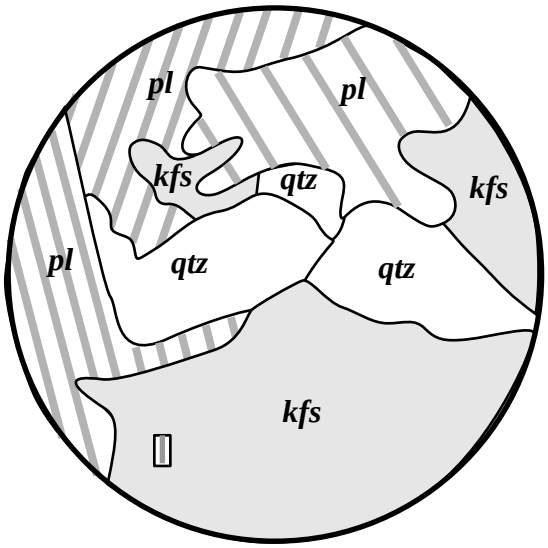

Figure 77 Micrographic sketch of the leucosome in sample 111I (4x objective; field of view = 3.6 mm). Note the irregular grain shapes and interlocking crystal texture which suggests an igneous origin (crystallization from a melt) for this leucosome.

Outcrop 113

The migmatized host rock in outcrop 113 is mapped as *Xks* (knotted schist) by Braddock et al. (1988a) and shows a gradational change from highly pelitic garnet-sillimanite-biotite schist to semi-pelitic garnet-biotite quartzo-feldspathic gneiss. Figures 9 and 10 show the schistose and gneissic host rock. Figure 78 is an outcrop sketch showing the leucosomes (white) and host rock (light gray). The leucosomes comprise approximately 24% of the outcrop, range in thickness up to 10

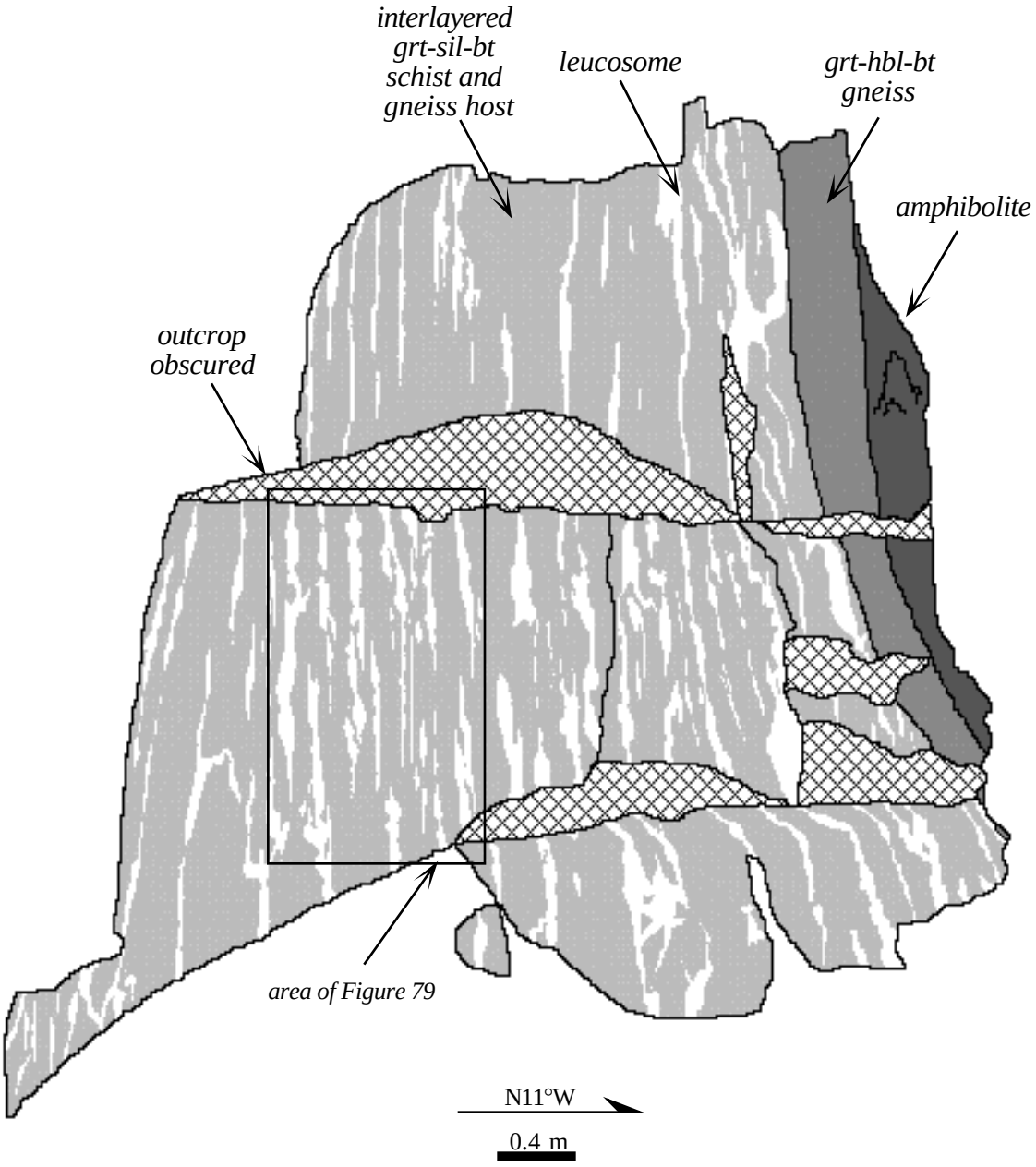

Figure 78 Sketch of outcrop 113. The area of the field photograph shown in Figure 79 is outlined.

centimeters, and are concordant with the primary foliation (N79°E/85°SE). Figure 79, a typical view of this stromatic migmatite, shows that the leucosomes are more concentrated in the pelitic layers (darker host rock) than in the gneiss. As is common throughout the Poudre Canyon, leucosomes may be folded, boudinaged or exhibit pinch and swell texture (see Figures 78 and 79). The intensity of the deformation that affected the Poudre Canyon migmatites is suggested by structural features such as the rootless fold in Figure 80.

Figure 79 Typical field photograph of the stromatic migmatite exposed at outcrop 113. Leucosomes (white) are hosted by interlayered gray garnet-biotite quartzo-feldspathic gneiss and garnet-sillimanite-biotite schist. Note that the leucosomes tend to be concentrated within the darker, more pelitic layers; photograph #6-34-91.

Figure 80 Rootless fold in outcrop 113; photograph #6-30-91.

The leucosomes consist of quartz, plagioclase, and microcline, with or without garnet or biotite (see Table 25 for the modes); their grain size is at least twice that found in the host rock. The average grain size of the leucosome is 5 mm, however, as in outcrop 111, microcline is normally 4 to 20 times larger than plagioclase or quartz and dominates the mode (see Table 25). Plagioclase in both the host and leucosome is normally zoned (see Table 26); the overall range of plagioclase composition varies from An_{21} (rim) to An_{27} (interior). There is very little difference in plagioclase or K-feldspar composition between the host and the leucosome (see Table 26). In thin section, larger quartz grains in the leucosomes exhibit undulatory extinction whereas smaller, recrystallized

polygonal quartz grains occur between feldspars as shown in Figure 81a. Figure 81b shows additional evidence for solid state modification of leucosome grains in the form of grain boundary recrystallization around larger feldspars, similar to that observed in outcrop 13.

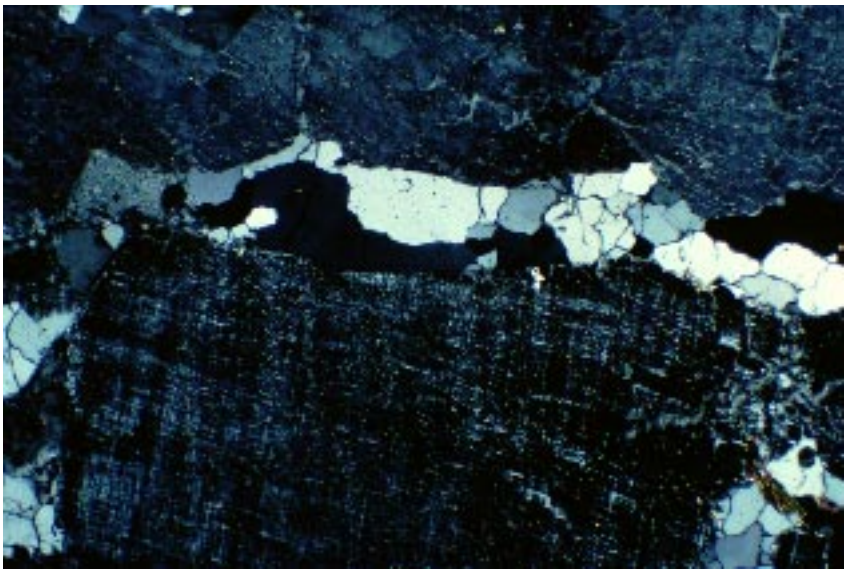

Figure 81a Photomicrograph of the leucosome in sample 113B showing finer-grained polygonal quartz grains that have recrystallized between larger microcline grains. Field of view 4.8 mm (longest dimension); crossed polars.

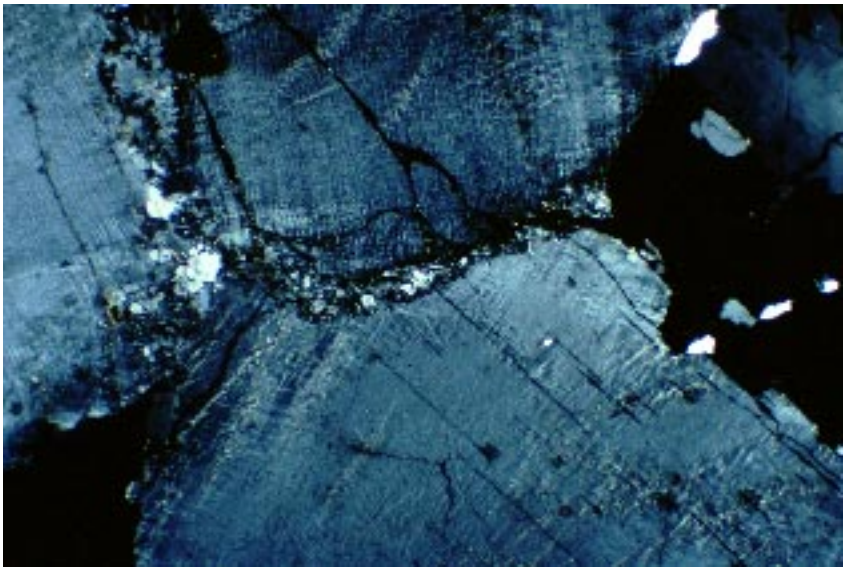

Figure 81b Photomicrograph of the leucosome in sample 113M-2 showing grain boundary recrystallization around microcline. Field of view 4.8 mm (longest dimension); crossed polars.

Biotite-rich selvages ranging in thickness from 0.1 to 1 cm commonly envelop the leucosomes. The selvage mode given in Table 25 (sample 113B) is enriched in biotite and garnet and depleted in K-feldspar relative to the host rock. In general, selvages may be difficult to recognize, due to their thin nature. In addition, the garnet-sillimanite-biotite mineralogy in the more aluminous host rock may camouflage the selvages, or suggest selvages where none may exist.

Outcrop 134

Outcrop 134 is a migmatized, interbedded fine- to medium-grained quartzo-feldspathic biotite gneiss and sillimanite-biotite schist (knotted schist) mapped as *Xks* by Braddock et al. (1988b). As in outcrops 111 and 113, leucosomes are present in both host rocks yet are more concentrated in the schist, as shown in Figure 82 (knotted schist to the left and biotite gneiss to the right). The knotted schist in outcrop 134 contains much less garnet than was observed in outcrop 113 and is characterized by clots of fibrolitic sillimanite, rather than disseminated fibrolite. These fibrolite clots appear as thin lenses when viewed across strike (see Figure 83a) and as flattened and stretched out disks when viewed within the foliation plane (see Figure 83b). The mineral lineation created by these elongated sillimanite knots plunges 31° at S84°W which is sub-parallel to the strike (N87°W/68°SW) and parallel to the orientation of the fold axes (S89°W/20°). Folding is common and is observed most easily in the leucosomes, as in Figure 83a and Figure 84.

Figure 82 Typical field photograph of outcrop 134 showing the sillimanite-biotite schist host (to the left) and quartzo-feldspathic biotite gneiss host (to the right) for this migmatite; photograph #3-15-91.

Figure 83a Field photograph of outcrop 134 showing the fibrolitic sillimanite knots which appear as thin white lenses when viewed across strike (to the right of the penny and below the pink folded leucosome); photograph #1-20-93.

Figure 83b Field photograph of outcrop 134 showing the white fibrolitic sillimanite knots which appear as large elongate disks flattened and stretched out within the foliation plane; photograph #3-25-91.

Figure 84 Field photograph of outcrop 134 showing a rootless fold (pink leucosome) the axial plane of which is parallel to the dominant foliation as defined by the white sillimanite knots; photograph #3-14-91. This photograph is a close up of the view shown in Figure 82.

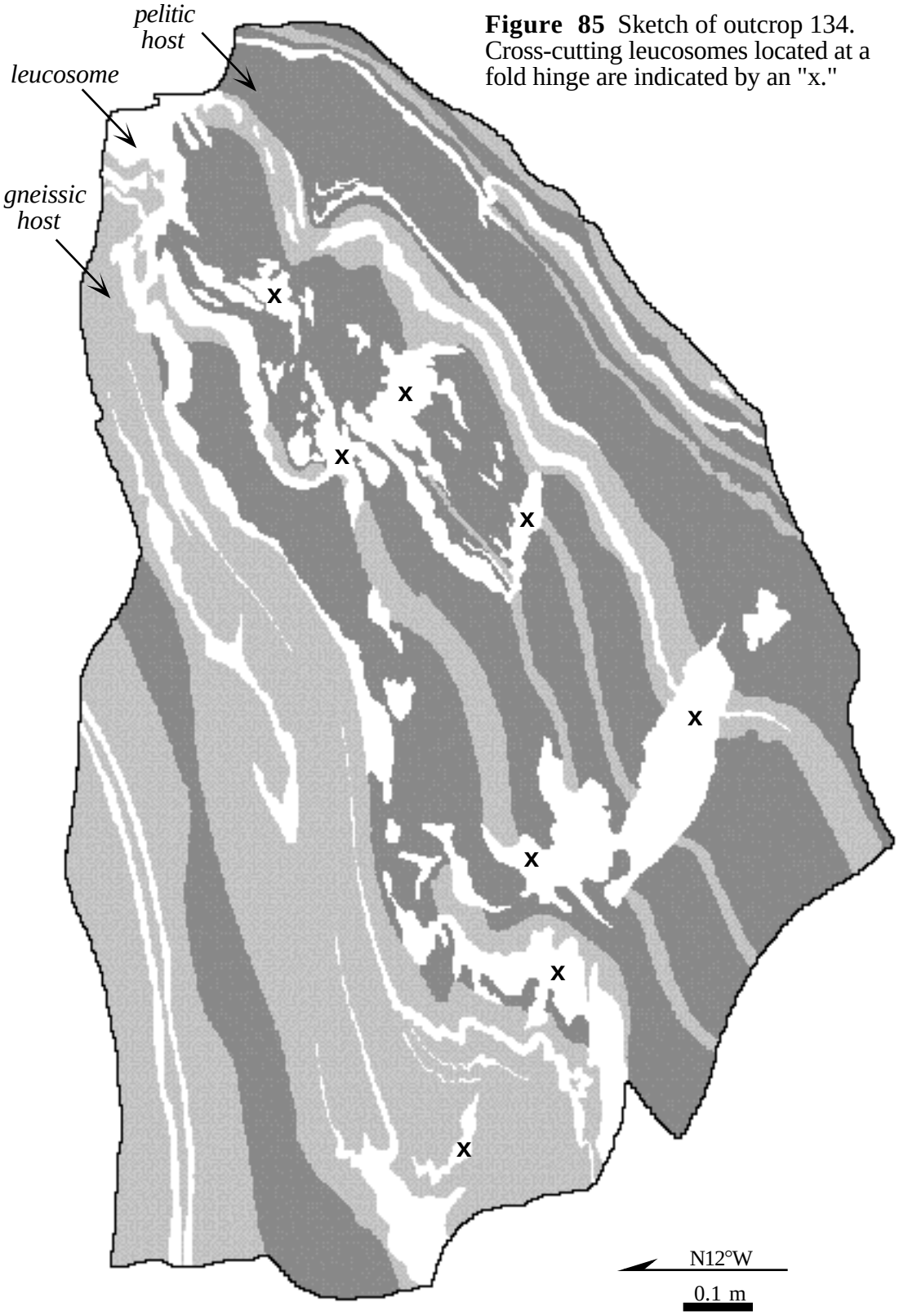

Figure 85 Sketch of outcrop 134. Cross-cutting leucosomes located at a fold hinge are indicated by an "x."

Figure 85 is an outcrop sketch of one exposure of this migmatite. The leucosomes are shown in white and comprise 15% of the outcrop; the gneissic and pelitic host rocks are shown in light and dark gray, respectively. The leucosomes take on two different orientations, concordant and cross-cutting, shown in Figures 86a and 86b, respectively. Concordant (stromatic) leucosomes are conformable with the dominant foliation and exhibit boudinage and pinch and swell texture (see Figure 86a). Two different compositions are observed in concordant leucosomes (a) quartz-plagioclase-microperthitic microcline (qtz-pl-kfs; 134E-1, -2, and -2A, Table 25) and (b) quartz-plagioclase (qtz-pl; 134M-1,-1A, and -2, Table 25). The average grain size of the qtz-pl-kfs leucosomes (5 mm) is 5 times larger than that of the qtz-pl leucosomes (1 mm) and over 15 times larger than that of the host rock (0.3 mm). The photomicrograph in Figure 87 shows the irregular, interlocking grain boundaries which typify the coarser-grained qtz-pl-kfs leucosomes, an igneous texture. On the other hand, the finer-grained qtz-pl leucosomes more commonly exhibit granoblastic-polygonal (i.e. metamorphic) texture. The constituent quartz and feldspar of the host rock for both leucosome composition types also exhibit granoblastic-polygonal texture. In all of the analyzed leucosomes, plagioclase is normally zoned, ranging in composition from An_{23} at the rim to An_{28} in the interior (see Table 26). Neither plagioclase, nor K-feldspar (when present) show any appreciable difference in composition between the host and the leucosome.

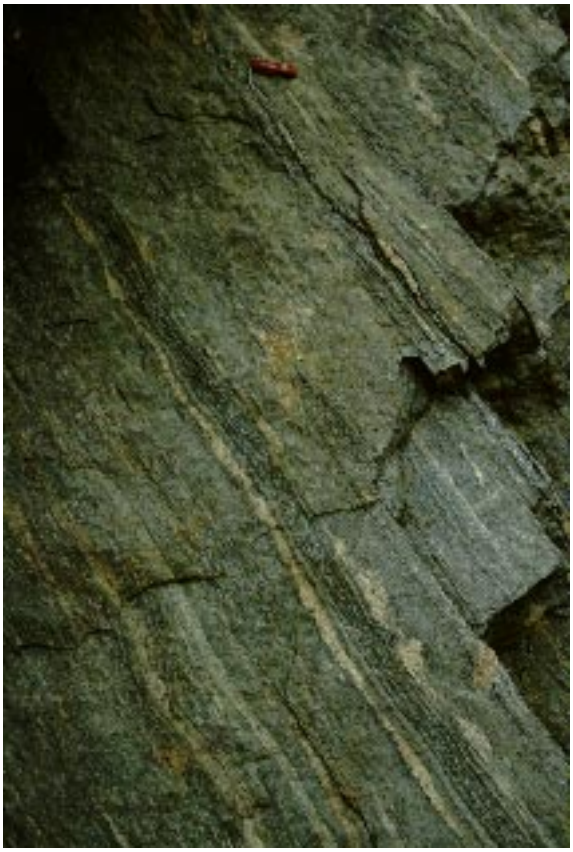

Figure 86a Typical conformable leucosomes (white) in outcrop 134; photograph #8-19-91.

Figure 86b Typical cross-cutting, irregularly-shaped leucosome in outcrop 134 (hand lens for scale); photograph #8-19-91.

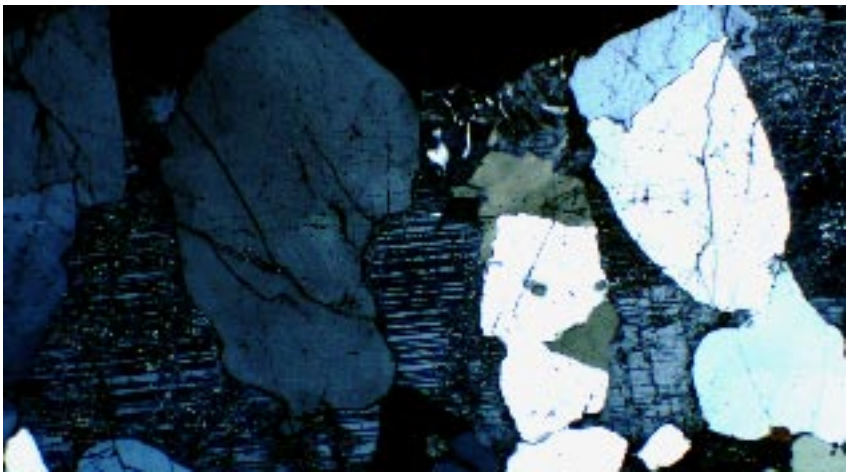

Figure 87 Photomicrograph of the leucosome in sample 134E-1 showing rounded quartz grains enveloped by optically continuous plagioclase at the edge of a large microcline (extinct grain at the top of the photo). Field of view 4.8 mm (longest dimension); crossed polars.

Figure 86b is a field photograph of one of the cross-cutting leucosomes. These coarse-grained, irregularly-shaped bulbous masses always show the qtz-pl-kfs assemblage. Cross-cutting leucosomes are easily seen in Figure 85 where they stretch across the pelitic and gneissic host rocks and the concordant leucosomes. Figure 85 also clearly shows that the cross-cutting leucosomes coincide with fold hinges (marked by "x's"). Similar accumulation of magma along the axial planes of folds has been reported in other migmatized terranes (McLellan, 1984; Hand and Dirks, 1992; Collins and Sawyer, 1996). The larger-scale open folds associated with cross-cutting leusocomes in outcrop 134 have not been observed in any other outcrop in the study area. Closer examination reveals that many of the conformable qtz-pl-kfs leucosomes are continuous with the cross-cutting leucosomes with only a slight increase in grain size and no change in composition. Figure 88 is a field photograph which displays the continuity between conformable (to the left of the penny) and cross-cutting (at the top of the photograph) leucosomes. These observations suggest a single origin for the concordant and cross-cutting qtz-pl-kfs leucosomes.

Figure 88 Field photograph of outcrop 134 showing conformable (vertical orientation) and cross-cutting (upper left hand corner) leucosomes. The leucocratic material (pink) is continuous from one leucosome orientation to the other, with no real difference in grain size or composition; photograph #1-16-93.

Leucosome Modes

Methodology

Modal analysis of the leucosomes using thin sections is not necessarily representative due to the coarse grain size of the leucosomes. Therefore, slab-cut samples from outcrops 13, 113, and 134 were used to calculate the modal percentages of quartz, feldspar, and plagioclase in the leucosomes more accurately. These slabs were stained using sodium cobaltinitrate to turn the K–feldspar a bright yellow; the plagioclase took on a powder white color and the quartz remained a vitreous gray. The distribution of K-feldspar, plagioclase, and quartz within each leucosome were traced, scanned and imported into *Image 1.47*, an image processing and analysis program developed for the Macintosh at the National Institute of Health. The quartz, K-feldspar, and plagioclase grains within each leucosome were color-coded by assigning them a set pixel value on a scale of 1 to 256. Figure 89 shows one of these stained slabs with four different layer-parallel leucosomes, labeled A, B, C and D. Figure 90 is the resultant gray scale image for these same leucosomes. Using the histogram function in *Image 1.47*, the number of pixels corresponding to each color value were counted. These counts were used to calculate the modal proportions of quartz, K-feldspar, and plagioclase in each leucosome; the resultant modes are presented in Table 27. Figures 91, 92 and 93 plot these data on quartz-plagioclase-K-feldspar ternary diagrams for outcrops 13, 134 and 113, respectively.

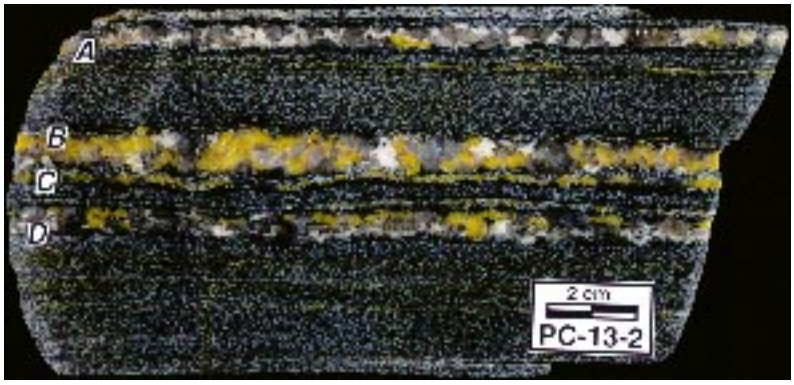

Figure 89 Photograph of cut slab 13-2 that was stained for feldspar content; K-feldspar: bright yellow, plagiocalse: powder white, quartz: vitreous gray. Lettered leucosomes correspond to the modes listed for 13-2 in Table 27.

Layer Parallel Leucosomes

Inspection of Table 27 and Figures 91, 92 and 93 reveals a considerable spread in leucosome compositions for each outcrop (multiple leucosomes from the same sample have a common symbol), and significant compositional overlap between all three outcrops, despite their different peak pressure-temperature conditions. In general, leucosomes from outcrops 13 (650°C, 5 kbar) and 134 (730°C, 7 kbar) can be grouped into quartz-plagioclase (qtz-pl) and quartz-plagioclase-K-feldspar (qtz-pl-kfs) compositions, as indicated in Figures 91 and 92. Some of the modes from outcrop 113 (730°C, 7 kbar) also fall within the qtz-pl-kfs grouping and the remainder have a significant K–feldspar component, as indicated in Figure 93. Closer examination of the host composition within and between individual samples from all three outcrops reveals that the leucosome diversity within individual samples, as well as the observed compositional overlap between different outcrops, are directly related to the host rock which surrounds each leucosome.

Figure 90 Gray scale image of the leucosomes (A,B,C,D) in slabbed sample 13-2; quartz: black, K-feldspar: dark gray, plagioclase: light gray.

Table 27 Leucosome modes [volume percent plagioclase (pl), K-feldspar (kfs) and quartz (qtz)] based on stained slabs. Multiple leucosomes from the same slab are grouped between heavy black lines and are differentiated by letter designations appended to the sample number.

OUTCROP 13				OUTCROP 113				OUTCROP 134			
Sample	pl	kfs	qtz	*Sample*	pl	kfs	qtz	*Sample*	pl	kfs	qtz
13-1 A	51	14	35	*113-1*	8	65	27	*134A A*	28	3	69
13-1 B	56	0	44	*113-2 A*	16	49	35	*134A B*	28	23	49
13-2 A	21	15	64	*113-2 B*	4	75	21	*134A C*	22	30	48
13-2 B	26	35	39	*113G A*	42	16	42	*134C*	19	38	43
13-2 C	13	35	52	*113G B*	32	36	32	*134E*	42	17	41
13-2 D	35	8	57	*113G C/D*	6	63	31	*134M*	22	0	78
13-3A clot	16	40	44	*113G E*	22	24	54	*134-1*	18	18	64
13-3 A1	33	34	32	*113U A*	5	86	9				
13-3 A2	44	24	31	*113U B*	1	76	23				
13-3 A3	42	3	55								
13-3 B clot	26	30	43								
13-3 B1	44	17	38								
13-3 B2	44	14	42								
13-3B3	42	14	44								
13-3 C	55	0	45								
13-3 D	32	18	50								
13-3 E	30	32	38								
13-4	50	14	36								
13B A	39	1	60								
13B B	47	1	52								
13B C clot	50	5	45								
13B C1	52	1	47								
13B C2	41	1	58								
13B D	57	0	43								
13B E	63	0	37								
13B F	59	0	41								

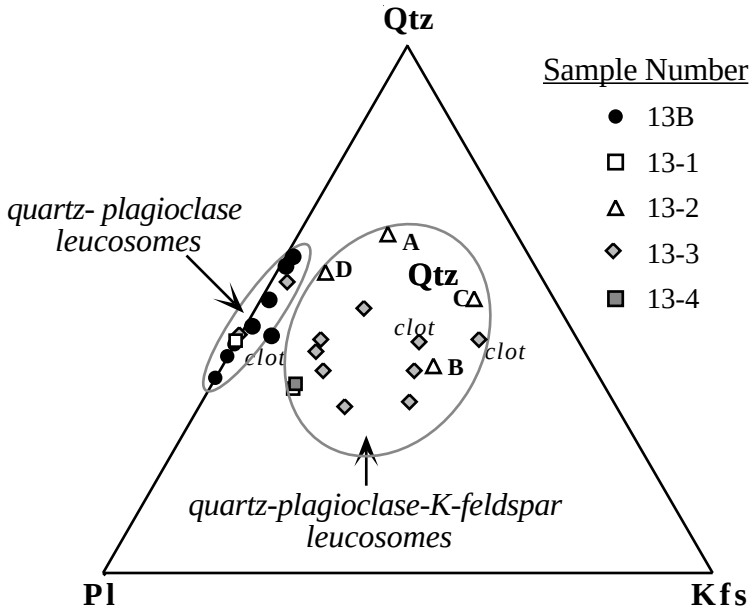

Figure 91 Quartz-plagioclase-K-feldspar ternary plot of the leucosome modes (volume percent) calculated from slabbed samples from outcrop 13; all are layer parallel except for those labeled "clot."

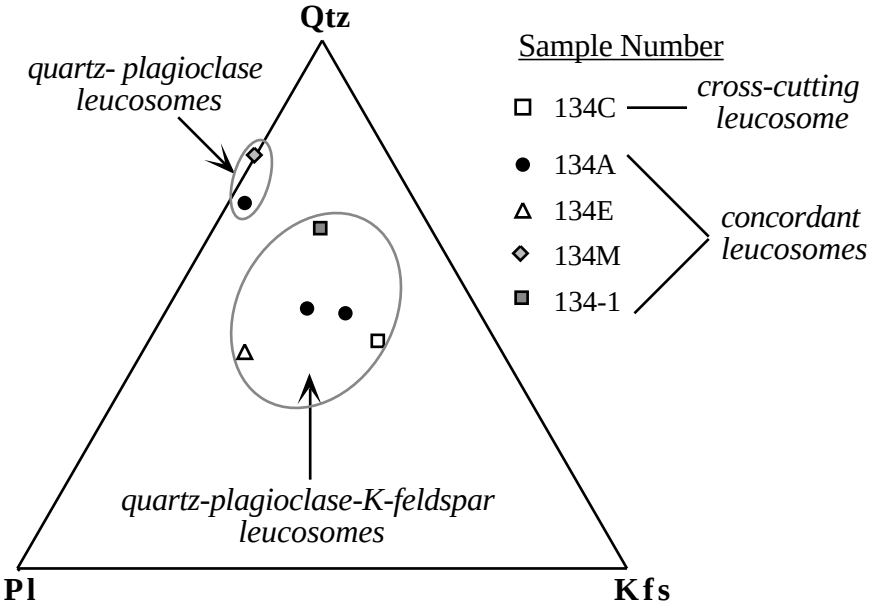

Figure 92 Quartz-plagioclase-K-feldspar ternary plot of the leucosome modes (volume percent) calculated from slabbed samples from outcrop 134.

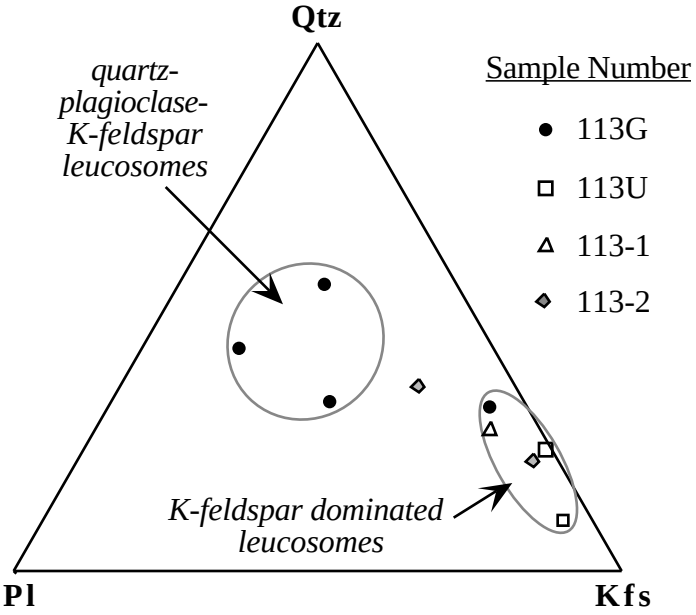

Figure 93 Quartz-plagioclase-K-feldspar ternary plot of the leucosome modes (volume percent) calculated from slabbed samples from outcrop 113.

The qtz-pl leucosomes from outcrops 13 and 134 occur in quartzo-feldspathic biotite gneiss hosts that are enriched in plagioclase versus microcline (see 13I, 134M–1, 134 M-2, Table 25). On the other hand, the qtz-pl-kfs leucosomes from outcrops 13 and 113 occur in low-Al semi-pelitic biotite gneiss hosts. Sillimanite is generally absent and garnet is a minor component in these rocks. The qtz-pl-kfs leucosomes in outcrop 134 occur in a sillimanite-biotite schist. However, garnet is scarce in these schistose layers and the sillimanite is segregated into areas removed from the leucosomes. Thus, the host rock in direct contact with the leucosomes in the schistose layers in outcrop 134 is more semi-pelitic than pelitic. The K-feldspar-dominated leucosomes found in outcrop 113 are surrounded by pelitic schist host that contains garnet, sillimanite, and biotite (see 111-IA, 113B, Table 25). Neither outcrop 13 nor outcrop 134 possess typical pelitic schist host rock and, hence, contain no K-feldspar-dominated leucosomes. Conversely, outcrop 111 does contain highly pelitic host rock, and thin section analysis indicates that the leucosomes of such host rock also are enriched in K–feldspar (see Table 25). Thus, the gross compositional groupings of the leucosomes in the Poudre Canyon migmatites are tied to their immediate host rocks and not to a particular outcrop or pressure-temperature condition.

The local nature of the diversity of the layer parallel leucosome compositions is apparent within individual hand samples. For example, the compositions of the four leucosomes in sample 13-2 shown in Figure 89 are indicated by the triangle symbols in Figure 91 (lettered A, B, C and D). The average distance between neighboring leucosomes within this and the other stained samples is given in Table 28. Notice that the 13-2 leucosomes show markedly different compositions yet are separated from their nearest leucosome neighbors by only 0.1 to 2 centimeters. Leucosomes in samples 13-1 and 13–3 show a similar diversity as do multiple leucosomes from slabbed samples in outcrops 134 and 113 (see Figures 92 and 93). The short range differences observed in this study suggests that changes in composition between small scale layers within each outcrop control the actual composition of the leucosome. Johannes (1988) suggests that pre-existing

Table 28 Average distances between leucosomes within each slab; see Table 27 for the modes.

Sample Number	Neighboring Leucosomes	Distance (cm)
13-1	A-B	1.5
13-2	A-B	0.5
	B-C	0.1
	C-D	2.0
13-3	A1-A2	<0.1
	A2-A3	0.1
	A3-B1	0.2
	B1-B2	<0.1
	B2-B3	0.2
	B3-C	1.0
	C-D	0.7
	D-E	<0.1
13B	A-B	0.2
	B-C1	2.0
	C1-C2	0.1
	C2-D	0.7
	D-E	<0.1
	E-F	<0.1
113-2	A-B	2.5
113G	A-B	0.5
	B-C/D	0.5
	D-E	1.5
113U	A-B	8.5
134A	A-B	7.5
	B-C	0.2

compositional heterogeneities tend to favor the development of stromatic migmatites. Certainly, the compositionally diverse leucosomes in the Poudre Canyon migmatites reflect differences in the host rock which occur over short distances (0.1-2 cm) across strike.

Cross-Cutting Leucosomes

Three leucocratic clots from outcrop 13 (labeled clot, Figure 91) and one cross-cutting leucosome from outcrop 134 (134C, open square, Figure 92) were analyzed for modal composition. The layer parallel leucosome which was continuous with sample 134C was not analyzed. However, the cross-cutting leucosome plots within the qtz-pl-kfs grouping, as would be expected, and is slightly more K-feldspar enriched than the concordant leucosomes analyzed from outcrop 134 (see Figure 92). Figure 94 is a ternary plot showing the leucocratic clots from outcrop 13 (filled symbols) and the associated sets of layer parallel leucosomes cut by these clots (open symbols); sample 134C is shown for comparison (plus symbol). The clot that cuts qtz-pl leucosomes (triangles) is much closer in composition to its associated leucosomes than it is to the clots that cut qtz-pl-kfs leucosomes (filled square and circle). Thus, this figure shows that the leucocratic clots are generally related in composition to the stromatic leucosomes that they cut, and to their respective host rocks. Interestingly, although the clots that cut qtz-pl-kfs leucosomes fall within the qtz-pl-kfs compositional grouping, they are much closer in composition to each other (and to that of sample 134C) than they are to the leucosomes that they cut.

Evidence for Partial Melting

Textures

If the leucosomes formed by crystallizing from a melt, then they should be coarser grained than the surrounding host rock and contain igneous fabrics such as irregular, interlocking grain boundaries. The average grain size of the leucosomes (except for the quartz-plagioclase leucosomes in outcrop 134) is 10 to 17 times larger than that of the corresponding host rocks (see Table 25). Furthermore, irregular, interlocking grain boundaries are observed in the qtz-pl-kfs leucosomes of outcrop 134 (Figure 87) and in all of the leucosomes in outcrop 111 (Figure 77). Unfortunately, any igneous fabrics that may have been present in the 13 and 113 leucosomes, are obscured by subsequent solid state deformation (Figures 69 and 81).

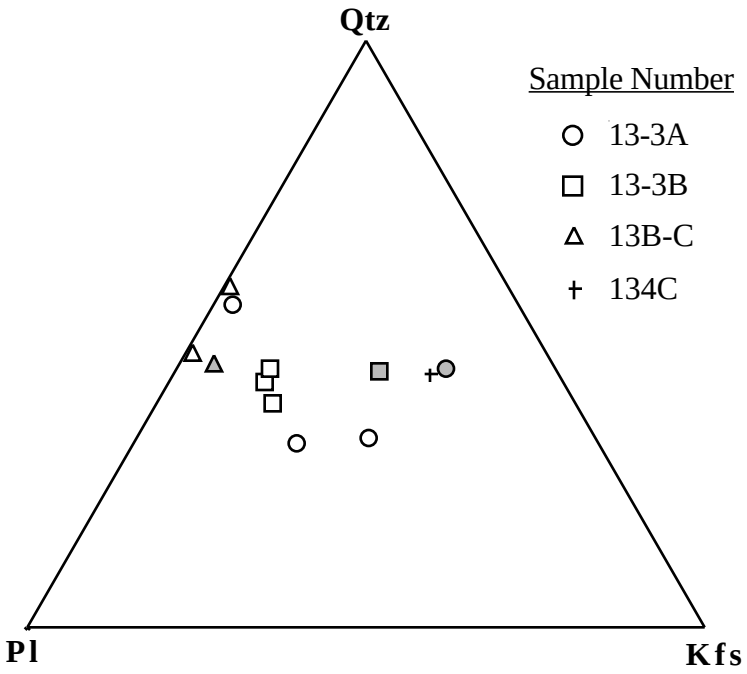

Figure 94 Quartz-plagioclase-orthoclase ternary plot of the layer parallel leucosomes (open symbols) from outcrop 13 slabbed samples that are cut by leucocratic clots (filled symbols). The composition of the cross-cutting leucosome in outcrop 134 is indicated by the plus symbol.

Disharmonically folded leucosomes in all of the outcrops suggests a mechanical contrast between the less competent leucosomes and the surrounding host rock during deformation (McLellan, 1989). These fold styles indicate that the leucosomes were once less viscous than the surrounding host rock, perhaps in a molten state. On the other hand, boudinage, pinch and swell textures, parallel harmonic folds and the microtextural evidence for solid state deformation suggest that the leucosomes also were more competent than the surrounding host rock during the deformation. These seemingly contradictory observations can be resolved by concluding that the leucosomes once were partially molten and that the deformation proceeded during the partial melting event and continued after the leucosomes had fully crystallized.

The leucocratic clots in outcrop 13 and the irregularly-shaped, cross-cutting leucosomes in outcrop 134 are further evidence for the probable molten behavior of the leucosomes. In a discussion of deformation-assisted melt segregation, Sawyer (1994) noted that deformation of anisotropic rocks (compositionally layered such as in outcrop 13) with viscosity contrasts (layer-parallel melt fractions represented by the leucosomes in outcrop 13) produces strain instabilities that can create dilational structures such as shear bands, tension gashes and boudins (Platt and Vissers, 1980). Figure 95 is a field photograph of a portion of outcrop 13 in which numerous clots occur. Several of these appear to be located in the necks of boudins. Similar leucosomal concentrations in boudin necks were observed by Collins and Sawyer (1996) and by Brown (1994) and were attributed to melt accumulation driven by a pressure gradient from the high stress regions of the flank into low pressure, dilatant regions of the neck. Leucosomes located along fold hinges, as in outcrop 134 (Figure 85), may have accumulated in a similar manner by migrating away from high stress limbs and pooling in dilatant hinge regions.

Figure 95 Field photograph of a portion of outcrop 13 showing numerous cross-cutting leucosomal clots. Several of these appear to be located within the necks of incipient boudins (arrows).

Overall, the micro- and macrotextures of the majority of the leucosomes support an origin by crystallization from a melt, with the exception of the qtz-pl leucosomes of outcrop 134. These qtz-pl leucosomes are only 3 to 5 times coarser-grained than the surrounding host rock, exhibit metamorphic microtextures and are never found in the cross-cutting orientation. In addition, they are more quartz-enriched than those in outcrop 13 (compare Figure 92 to Figure 91), suggesting the least correspondence with the eutectic composition expected from partial melting. Therefore, these leucosomes are more likely the result of metamorphic subsolidus differentiation and will be disregarded in the remaining discussion of partial melting.

Granite Minimum Melt Compositions

The granite minimum melt represents the minimum pressure-temperature condition for ternary melting of quartz, albite and orthoclase. If the migmatites in either block formed by partial melting, the initial melt would have been a ternary eutectic (or minimum) composition. Depending on the composition of the source rock, the melt would have evolved away from the ternary eutectic along the cotectic lines of the liquidus surface. If the original host rock is K-feldspar-absent (as in the quartzo-feldspathic gneiss host rocks), then the minimum melt would correspond to the binary eutectic composition in the quartz-plagioclase system. Figure 96 shows the leucosome modes from this study superimposed on the haplogranite system (excluding the qtz-pl leucosomes from outcrop 134). The filled symbols are leucosomes which formed at 5 kbar whereas the open symbols are those that formed at 7 kbar. The majority of the compositions lie within the quartz field of this phase diagram. Only two of the leucosomes plot in the vicinity of the qtz-ab-or *or* qtz-ab eutectics, and only a few plot along the quartz-K-feldspar cotectic. If the system was not

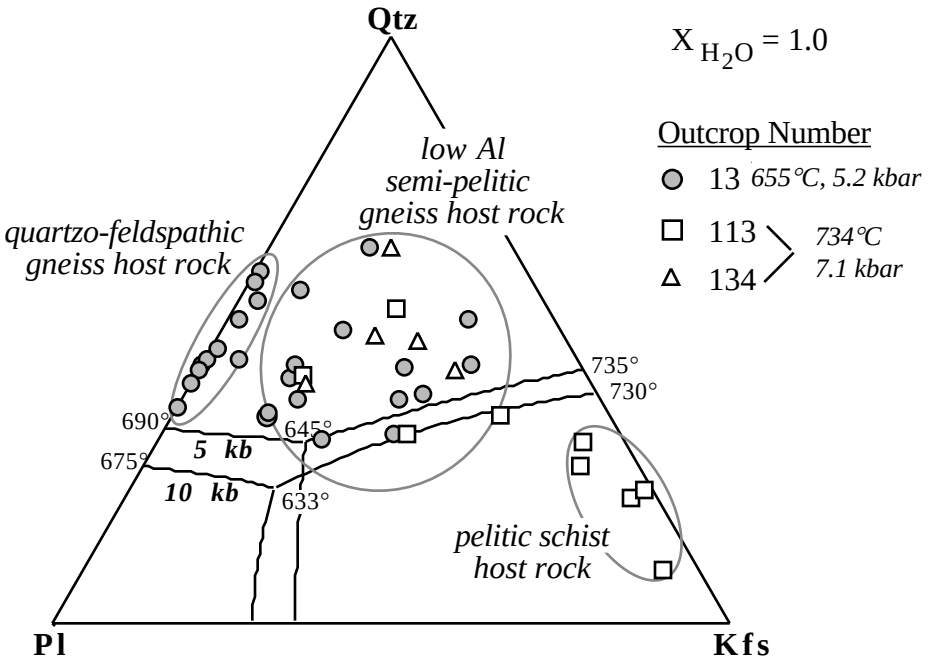

Figure 96 Leucosome modes calculated from slabbed samples (volume percent) superimposed on the liquidus phase relations in the water-saturated qtz-ab-or system (after Johannes, 1984, Johannes and Holtz, 1990 and Holtz et al., 1992).

saturated in H_2O, then the position of the ternary eutectics would shift to the right with decreasing X_{H2O}, as shown in Figure 97 (Johannes and Holtz, 1990; Holtz et al., 1992). Thus, given $X_{H2O}<1.0$, some of the leucosome compositions more closely approximate the ternary eutectic and cotectic compositions; all of these are hosted by the low Al semi-pelitic gneiss. The addition of an anorthite component in plagioclase will shift the position of the binary eutectic toward the quartz corner, and the ternary eutectic up and to the right into the quartz field as shown by the arrows in Figure 98 (Luth, 1976). This would allow more of the leucosomes to be considered as near eutectic or cotectic in composition.

Considering the anorthite component and allowing for limited evolution of the melts away from their respective eutectics, two different melt-forming reactions appear to be operating: one at the ternary minimum for the low-Al semi-pelite and one at the qtz-pl binary minimum for the quartzo-feldspathic gneiss. Simple melting could not have generated the leucosomes hosted by pelitic schists since none of these fall within the range of the ternary minimum. However, the K-feldspar-enrichment of these leucosomes can be explained by dehydration melting. They may not resemble a granite minimum melt because dehydration reactions also form solid products (such as K-feldspar) which may become mixed in with the melt (Mehnart, 1968). Therefore, most of the spread in the leucosome compositions can be accounted for by simple ternary melting in the semi-pelites, binary melting in the gneisses and dehydration melting in pelitic host rocks. The divergence of the other leucosomes from the minimum melt compositions could be attributed to a number of different processes. First, the leucosome components may have an inhomogeneous distribution such that the slabbed samples may not have been large enough to get an accurate mode for every leucosome. Second, the composition could reflect a combination of partial melting with

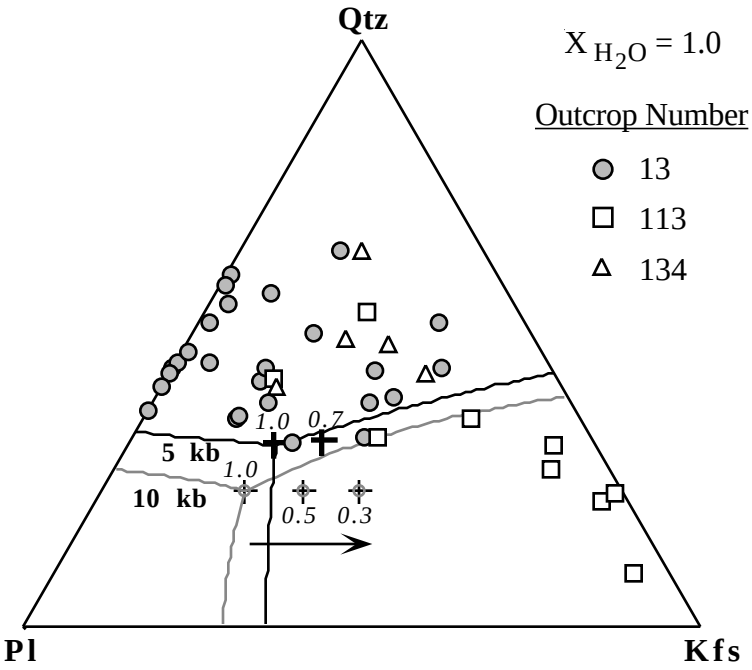

Figure 97 Leucosome modes calculated from slabbed samples (volume percent) superimposed on the liquidus phase relations in the haplogranite system. Cross symbols and associated italic numbers indicate the changing positions of the ternary eutectics for 5 and 10 kbar with changing X_{H_2O} (after Johannes and Holtz, 1990 and Holtz et al., 1992).

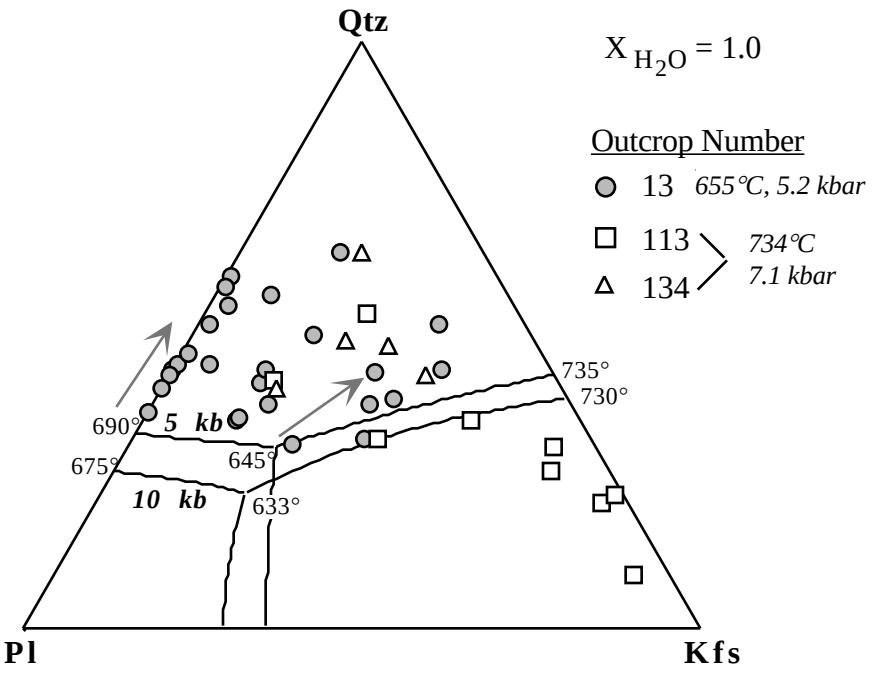

Figure 98 Leucosome modes calculated from slabbed samples (volume percent) superimposed on the liquidus phase relations in the water-saturated qtz-ab-or system (after Johannes, 1984, Johannes and Holtz, 1990 and Holtz et al, 1992). The arrows represents the general direction that the minimum ternary and binary melts will move as more anorthite component is added to the system (after Luth, 1976 and von Platen 1964).

other migmatite-forming mechanisms as suggested by Olsen (1982, 1984 , 1985) for migmatites in the central Front Range. Third, the leucosomes could have been modified by post-peak events.

Plagioclase Composition

If the migmatites formed by partial melting, then phase relations dictate that plagioclase compositions be more sodic in the leucosome than in the host. Outcrop 111 is the only analyzed migmatite with leucosome plagioclase (An_{02}, rim) more sodic than host plagioclase (An_{20}, rim). Given that outcrop 111 apparently underwent partial melting, then the normal zoning observed in the leucosome plagioclase can be attributed to disequilibrium crystallization upon cooling. All of the other outcrops (13, 113 and 134) show no appreciable difference in plagioclase composition between the leucosomes and the host rock, a common observation in migmatites (Johannes, 1988; Ashworth, 1979, 1985). Ashworth suggested that subsequent to crystallization the leucosome plagioclase re–equilibrated with the surrounding metamorphic rock producing a homogeneous plagioclase composition in the migmatite. Given the high peak metamorphic temperatures and a probable history of slow cooling, this is a reasonable scenario. It is unclear why the plagioclase from outcrop 111 does not exhibit the same degree of re-equilibration.

Origin of the Migmatites

Introduction

The textural and compositional evidence suggest that the dominant process for generating the Poudre Canyon migmatites is partial melting. Injection is not a major contributor since there are no traceable field relations between the leucosomes in the analyzed outcrops and the granitic intrusions (pegmatites, Routt or Berthoud Plutonic Suites). In addition, the diverse compositions exhibited by the leucosomes over short distances argue against a common intrusive source. Subsolidus differentiation probably produced the qtz-pl leucosomes in outcrop 134 which are finer grained than the other leucosomes and exhibit granoblastic polygonal textures. In addition, subsolidus differentiation may have contributed to the layered heterogeneities in the rock, and thus controlled the composition of the leucosomes ultimately produced through partial melting. Fluid-driven metasomatism also may have influenced the final leucosome composition, helped to coarsen the grain size and, most importantly, initiated the partial melting. Quantification of the interaction between partial melting and metasomatism and/or subsolidus differentiation would require additional chemical information and is beyond the scope of this study. Therefore, the remainder of this chapter will concentrate on partial melting as the dominant migmatite-forming mechanism in the Poudre Canyon rocks.

Melt-Generating Reactions

Wet Melting

Wet melting takes place when the melting point of a rock is lowered through the addition of H_2O. Wet melting is only possible if H_2O is introduced into the system (Tuttle and Bowen, 1958). According to Thompson and Connolly (1990), what little grain boundary fluids there are in the lower crust would produce less than 3% melt at the water-saturated solidus. If the leucosomes in the Poudre Canyon represent melt, then, based on the proportion of leucosomes versus host, 15-28% of these migmatitic outcrops once was partially molten. Therefore, if wet melting occurred, there must have been an additional external source for the H_2O in order to produce this much melt. One possible source of H_2O would be fluids emanating from the syntectonic Routt Plutonic Suite. If no external source of water was available, then melting could have occurred via dehydration melting.

Dehydration Melting

During dehydration, or fluid-absent, melting the breakdown of hydrous mineral phases releases H_2O which goes directly into generating a melt (Grant, 1985). The muscovite- and biotite-dehydration reactions commonly invoked to explain migmatite production in amphibolite facies pelitic rocks are:

ms + qtz + ab = kfs + sil + melt (Ashworth, 1985) and

bt + pl + sil + qtz = kfs + grt + melt (Clemens and Wall, 1981).

In both wet and dehydration melting, the initial melt would be a granite minimum melt and may evolve away from the minimum as quartz or feldspar is used up (Ashworth, 1985). In addition, any of the products of dehydration melting may become entrained by the melt to become part of the leucosome after crystallization.

Higher Pressure Block - Outcrops 111, 113 and 134

Figure 99 is a plot of the average peak pressure-temperature conditions for the higher pressure block (circle) superimposed on the reactions for wet melting and muscovite and biotite dehydration melting. The two curves for the biotite breakdown reaction in this figure are based on calculated (1a; Clemens and Wall, 1981) and experimental (1b; Le Breton and Thompson, 1988) data. The pressure-temperature conditions of the higher pressure block fall within the range of wet melting, muscovite dehydration and possibly biotite dehydration (depending on which reaction curve is used). The semi-pelitic gneiss layers in outcrops 111, 113 and 134 contain no muscovite or sillimanite. Therefore, only wet melting could account for the qtz-pl-kfs leucosomes found in these layers. Leucosomes are far more abundant in the schistose layers of these outcrops, suggesting that the hydrous phases associated with these

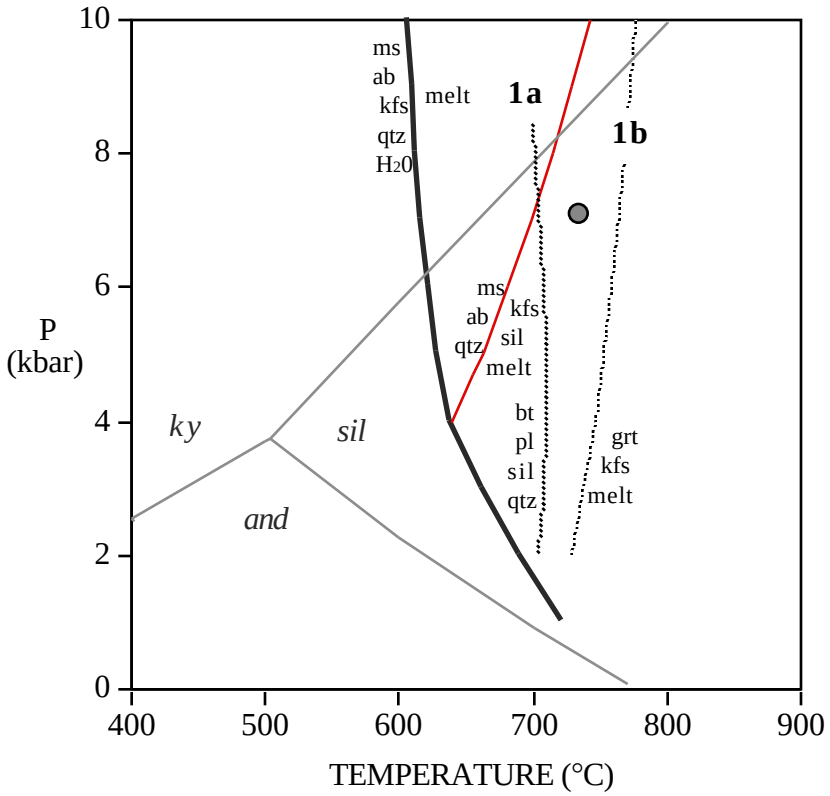

Figure 99 Average pressure-temperature conditions for the higher pressure block (filled circle) superimposed on the aluminosilicate fields (Holdaway and Mukhopadhyay, 1993), the granite minimum melt (Thompson and Tracy, 1979), muscovite dehydration melting (Thompson and Tracy, 1979), and biotite dehydration melting (**1a**: Clemens and Wall, 1981 and **1b**: LeBreton and Thompson, 1988). Note that P_{H2O} = P for the experimentally determined reactions.

layers generated most of the leucosomes in the higher pressure block by dehydration melting. The pressure-temperature conditions fall well within the range of muscovite dehydration melting. Moreover, the presence of garnet within the leucosomes in outcrops 111 and 113 implies that biotite dehydration melting also must have occurred, producing garnet as a product phase. Work by Powell and Downes (1990) on garnet-bearing leucosomes in Broken Hill, Australia suggested that the presence of large garnet poikiloblasts similar to those observed in outcrop 111 is due to incongruent melting involving biotite dehydration. Similar observations were made by Brown (1994). Although not as coarse-grained as in outcrop 111, garnet in outcrop 113 is abundant in and around all of the leucosomes within pelitic layers. On the other hand, garnet is rarely observed near the leucosomes in outcrop 134, implying that biotite dehydration did not occur in the schistose layers of this outcrop.

Dehydration melting of muscovite and biotite can be invoked to explain the K-feldspar enrichment of samples from outcrops 111 and 113 and the extraordinarily coarse-grained nature of this K–feldspar. Both of these reactions produce K-feldspar as well as a melt. An in-situ melt would aid cation diffusion thus allowing the K-feldspar reaction products to grow large. As the rock cooled, the K-feldspar component in the melt would crystallize as overgrowths on the solid state K-feldspar and the quartz and plagioclase would crystallize as interstitial material. The resultant leucosome would contain coarsened K-feldspar and would plot toward the K-feldspar corner of the ternary.

The leucosomes in outcrop 134 do not show the same K-feldspar-enrichment or association with garnet as is seen in outcrops 113 and 111. In addition, the amount of melting which took place in outcrop 134 is nearly half that of the other two outcrops, suggesting that this outcrop did not experience as much partial melting as in other areas of the Poudre Canyon. It can be concluded that outcrop 134 did not undergo biotite dehydration melting, hence the reduced degree of melting and rarity of garnet. The presence of sillimanite and the predominance of leucosomes within schistose layers does suggest that muscovite dehydration did occur. The sillimanite must have been concentrated into the sillimanite clots prior to reaching the temperatures of the biotite dehydration reaction. In this way the sillimanite was removed from interaction with plagioclase and biotite in these layers, thus preventing biotite dehydration. The absence of K–feldspar enrichment in the 134 leucosomes suggests that entraining and coarsening K-feldspar was a more significant process in biotite dehydration than it was in muscovite dehydration.

Overall it appears that the higher pressure block experienced three stages of melting during prograde metamorphism. The small proportion of leucosomes in the semi-pelitic gneiss of outcrops 111, 113 and 134 indicates that wet melting occurred first, but was limited in extent by the availability of water. As prograde metamorphism proceeded, muscovite dehydration produced a second melt within the pelitic layers. Finally, biotite dehydration added still more melt to the pelitic layers within outcrops 111 and 113. The melts from the muscovite and biotite dehydration reactions combined to form the leucosomes ultimately observed in these pelitic layers. In all of these outcrops small-scale folding occurred during or after the dehydration melting reactions, while the leucosomes were still molten. Slight cooling caused the melt to completely crystallize into the leucosomes while deformation continued to proceed, causing the harmonic folds, boudins and pinch and swell textures. Only in outcrop 134 were large-scale folds observed which were synchronous with the melting event. The large scale folding and lineated sillimanite clots observed in outcrop 134 suggests that the rocks exposed in this outcrop experienced a slightly different stress regime which forced much of the melt from the limbs into the dilatant zones of the fold hinges.

Lower Pressure Block - Outcrop 13

Figure 100 is a plot of the average peak pressure-temperature conditions for the lower pressure block (square) superimposed on the reactions for wet melting and muscovite and biotite dehydration melting. The pressure-temperature conditions of the lower pressure block fall within the range of wet melting and muscovite dehydration (given error associated with calculating the P-T conditions). If melting proceeded via muscovite dehydration, then sillimanite should form as a reaction product. However, no sillimanite was observed anywhere in outcrop 13, although it is present elsewhere in the lower pressure block. The bulk composition of outcrop 13 appears to preclude the possibility of dehydration melting. Therefore, wet melting must be responsible for the leucosomes in outcrop 13. The leucosomes make up 28% of this outcrop, representing the highest melt proportion in all of the analyzed outcrops. This much melt could only be generated via wet melting if there was an appreciable external source of H_2O, more than that apparently available in the higher pressure block. If the source was the Routt Plutonic Suite then this block may have had more of these igneous fluids passing through it than through the higher pressure block because the lower pressure block lay at shallower depths.

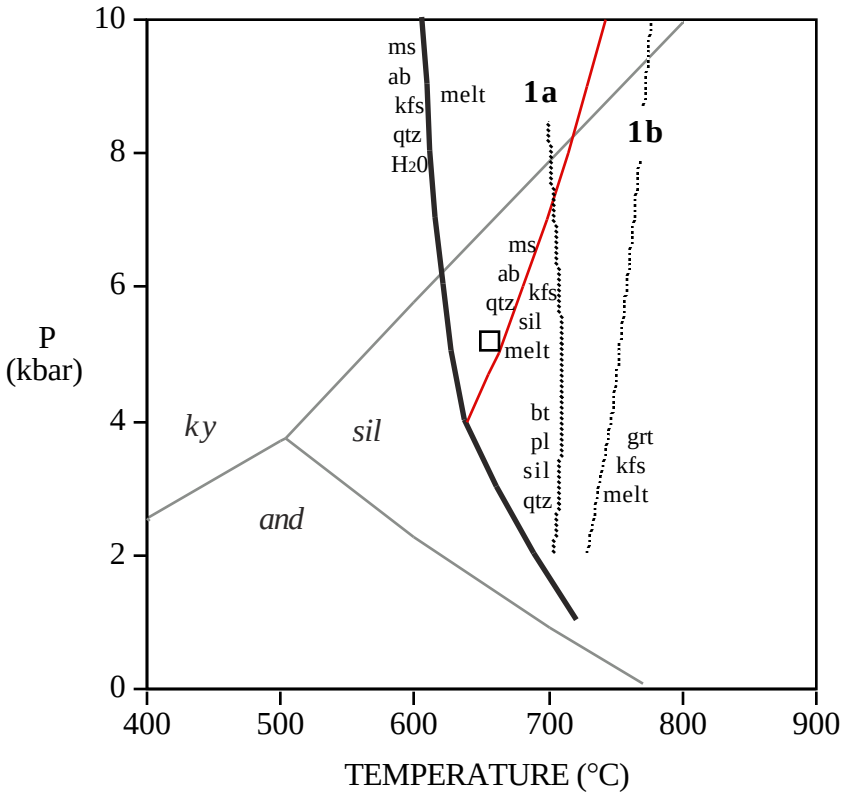

Figure 100 Average pressure-temperature conditions for the lower pressure block (square) superimposed on the aluminosilicate fields (Holdaway and Mukhopadhyay, 1993), minimum wet melting (Thompson and Tracy, 1979), muscovite dehydration melting (Thompson and Tracy, 1979), and biotite dehydration melting. The biotite breakdown curves are based on calculated (**1a**: Clemens and Wall, 1981) and experimental (**1b**: LeBreton and Thompson, 1988) data. Note that $P_{H2O} = P$ for the experimentally determined reactions.

Two different host rocks in outcrop 13 yielded two different leucosome types, qtz-pl-kfs leucosomes in low-Al semipelites and qtz-pl leucosomes in quartzo-feldspathic gneisses. This suggests that anatexis occurred in stages as successive melt reactions were reached in P-T space. First, the ternary melts formed in the semi-pelitic gneisses followed by binary melting in the quartzo-feldspathic gneisses. Following or during melting, deformation produced dilational structures which cut across the segregated melts allowing them to intermingle to form the clots (Sawyer, 1994). Alternatively, Rubie and Brearly (1990) have suggested that since melting reactions involve an increase in volume, then rapid melting could result in hydraulic fracturing of the surrounding material by the newly molten material. Thus, if the more competent host rock could not keep pace with the rapidly expanding molten material, then the layers containing the melt could fracture causing the melt to accumulate in cross-cutting pockets, the observed clots. Similar hydraulic fracturing may not have occurred in the higher pressure block because melt accumulation was more incremental as smaller volumes of melt were created with each melting reaction. As in the higher pressure block, the leucosomes crystallized before the deformation event ended.

Summary

Field and microtextural evidence indicates that the dominant process in generating the Poudre Canyon migmatites was partial melting. Several different melt-forming reactions must have operated based on the correspondence between leucosome composition and host rock type. In this scenario, pre-existing layered heterogeneities in the rock were susceptible to different melt-forming reactions thus producing different melt compositions. In the lower pressure block, semi-pelitic layers melted first via wet melting at the ternary eutectic followed by higher temperature quartz-plagioclase melting in the quartzo-feldspathic gneiss layers. In the higher pressure block, wet melting was initiated first in the gneissic layers but was limited by the availability of water. As prograde metamorphism proceeded melting began in the pelitic layers first by muscovite dehydration followed by biotite dehydration. Biotite dehydration melting produced K-feldspar-enriched leucosomes closely associated with garnet. In both blocks, folding occurred while the leucosomes were still molten and continued after they had completely crystallized.

VII. FLUID INCLUSION ANALYSIS

Introduction

Within the last two decades, petrologists have directed increasing attention to the role of fluids in metamorphic terranes. Fluids actively participate in prograde and retrograde reactions and also function as a medium to aid diffusion and enhance chemical reactions. Amphibolite facies fluids are composed predominantly of H_2O diluted by CO_2 and CH_4, N_2 and/or CO (Ohmoto and Kerrick, 1977; Grant, 1985; Touret and Olsen, 1985). Water is especially important in high grade metamorphic environments because it can lower a rock's melting point. Moreover, water controls the amount of melt produced (Arzi, 1978; Ashworth, 1979). Where present, preserved, intact, peak metamorphic fluid inclusions offer an opportunity to examine paleofluids directly. Of particular interest to this study is the composition of the fluid present when migmatites were produced; i.e. was an H_2O-rich fluid responsible for initiating melting? Of additional interest are the trapping conditions of any secondary fluids that infiltrated the area following peak metamorphism. Such secondary fluid inclusion data may help to delineate the path followed by this terrane during decompression and cooling. Table 1 summarizes the events affecting the northern Front Range. Plutons emplaced to successively shallower levels over time mark the uplift that followed peak metamorphism. Post-peak reaction-controlled microtextures such as resorbed garnets surrounded by coronas containing calcium-enriched plagioclase (Figure 13) or cordierite (Figure 21) suggest that significant decompression was associated with this uplift. Isochores calculated for secondary fluid inclusions can constrain the positions of decompression and subsequent cooling in pressure-temperature space. In order to determine the composition of the peak fluid, identify the secondary fluids, and constrain the uplift path, migmatitic samples from two different outcrops were prepared for fluid inclusion microthermometry. The locations of these outcrops, one from the higher pressure block (113M) and one from the lower pressure block (13I), are shown in Figure 67.

Analytical Procedure

Sample Preparation

Preliminary examination of thin sections from each outcrop revealed that the majority of the fluid inclusions are trapped in quartz and rarely exceed 15 μm in size with an average of two to three microns. Consequently, fluid inclusion sections were made as thin as possible (approximately 50 μm) to maximize optical clarity. Each sample was chosen so that both leucosome (coarse-grained leucocratic material representing partial melt) and enclosing host could be covered in a standard thin section. The sections were doubly polished and temporarily mounted on a glass slide for initial petrographic examination. Once petrographic documentation was complete, the sections were removed from the glass slides for microthermometry.

Microthermometry

Sample PC-113M

Sample 113M was analyzed in 1992 using a gas flow heating and cooling stage at the Fluid Inclusion Research Lab at Virginia Tech. The stage was mounted on a petrographic microscope equipped with a 40x objective. Microthermometry was performed on isolated fluid inclusions, and fluid inclusion assemblages in clusters and along fractures in both leucosome and host quartz grains. These fluid inclusions ranged in size from 3 to 15 μm in the longest dimension and were much more common in the leucosome. Eutectic, melting and homogenization temperatures were measured on a total of 85 fluid inclusions, 67 from the leucosome and 18 from the host. The heating and freezing measurements are reported in Appendix I (Tables I-1, I-2, I-3). Fluid inclusions along individual fracture planes were examined for generally similar homogenization behavior prior to making exact measurements. It was assumed that if the fluid inclusion data are

not consistent within a single fracture, then the probability is high that incomplete post-entrapment modification occurred such that the fracture no longer contains a meaningful homogeneous fluid (Goldstein and Reynolds, 1994). Therefore, measurements for fluid inclusions along fractures which showed widely varying homogenization temperatures are not included in this data set.

Sample PC-13I

Sample 13I was prepared and analyzed in 1994 at the Fluid Inclusion Research Lab at Virginia Tech. Inclusion microthermometry was performed on seven chips using a LINKAM TMS600 heating-freezing stage mounted on a petrographic microscope equipped with a 100x objective. Based on the preliminary data from the earlier analysis of 113M, only inclusions along fractures within leucosome quartz were analyzed in 13I. Prior to analysis, a photomontage was created as a permanent record of the fracture orientations relative to the thin section. One end of the fluid inclusion section was arbitrarily designated as "north" and all of the orientations of the fluid inclusion trails within the section are given relative to this arbitrary north. The paragenesis of the fractures was explored through cathodoluminescence (CL) maps. These maps were constructed using the CL mode of the Cameca SX 50 electron microprobe at Virginia Tech with an accelerating potential of 15 kV and a beam current of 30 nA. Once documented, the thin section was cut into approximate 0.5 x 0.5 cm chips and the location of each chip was noted on the photomontage. Careful records were kept to assure that each inclusion trail was referenced to its respective fracture on the photomontage. Measurements of eutectic, melting and homogenization temperatures were collected for 135 fluid inclusions ranging in size from 2 to 10 μm in the longest dimension. The heating and freezing measurements are reported in Appendix I (Tables I-4, I-5). Measurements for fluid inclusions along fractures which showed widely varying homogenization temperatures are not included in this data set.

Isochore, Density, and Salinity Calculations

H_2O-salt and CO_2 were the two dominant fluid types present in both samples. Isochores and densities for aqueous inclusions were calculated using the PVT properties of NaCl-H_2O along the liquid-vapor curve and the slopes of iso-homogenization temperature lines determined using synthetic fluid inclusions (Bodnar and Vityk, 1994). Isochores and densities for CO_2 fluid inclusions were calculated using the equation of state of Bottinga and Richet (1981). Both the NaCl-H_2O and CO_2 isochore calculations were completed using the program MacFlinCor (version 0.92) developed for MacIntosh computers by Brown and Hagemann (1994). Measurements of fluid inclusions from fluid inclusion assemblages (fractures or clusters) were averaged to yield a single data set per assemblage prior to calculating the isochores (see Appendix I).

NaCl-Equivalent salinities for undersaturated aqueous fluid inclusions with ice melting between 0°C and the NaCl-H_2O eutectic temperature (-21.2°C) were determined from freezing point depressions (Bodnar, 1993). If a daughter mineral was present, salinities were calculated using the salinity equation presented by Bodnar and Vityk (1994) based on the halite solubility data of Sterner et al. (1988). These salinities pertain to homogenization along the liquid-vapor-halite curve (i.e. simultaneous liquid-vapor homogenization and halite dissolution). However, in both samples the halite dissolved after the liquid and vapor had homogenized. Therefore, salinities calculated using this method are approximate (roughly ±3 weight percent; Bodnar and Vityk, 1994). Even more approximate are the salinities obtained for aqueous inclusions with final ice melting lower than -21.2°C but with no daughter mineral. These inclusions showed initial ice melting temperatures of -71 to -40°C and final ice melting from -32.7 to -21.6°C. These ranges of initial and final ice melting are typical of the NaCl-$CaCl_2$-H_2O system (Vanko et al., 1988; Oakes et al., 1992). The isotherms in the ice field of this system are more or less parallel to the NaCl-$CaCl_2$ join of the ternary, therefore, the liquidus surface (after Oakes et al., 1990) was used to estimate

roughly the total salinity (but not the relative proportions of NaCl and $CaCl_2$).

Sample 113M

Petrography

Outcrop 113 lies within the higher pressure block which experienced peak metamorphism at approximately 735°C and 7 kbar. This outcrop consists of migmatites hosted by gradationally interlayered garnet-sillimanite-biotite schist and garnet-biotite quartzo-feldspathic gneiss. The migmatites are in contact with garnet-hornblende gneiss and amphibolite as shown in Figure 78. Table 29 presents the mode for sample 113M, a migmatitic pelitic schist. Although initiated by wet melting, migmatization in outcrop 113 occurred predominantly by muscovite and biotite dehydration melting. The dehydration-melting reactions produced solid K-feldspar in addition to K-feldspar dissolved in the melt, thus enriching the leucosome in microcline (Table 29). The majority of the fluid inclusions are trapped in quartz grains within the leucosome; far fewer were found in the surrounding host. In the leucosome, quartz occurs as large grains with undulose extinction and subgrain development. It also occurs as recrystallized grains between coarser-grained microcline as shown in Figure 81a. Quartz commonly reacts to an imposed stress by recrystallizing which explains its smaller size relative to the microcline in this figure (Spry, 1969; Berthé et al., 1979, Dixon and Williams, 1983). In the host, quartz is even finer-grained and more polygonal in shape than in the leucosome. This suggests that recrystallization was more intense in the host. Because recrystallization tends to wipe out early-formed fluid inclusions (Kerrich, 1976; Roedder, 1981), it may explain the relative paucity of host fluid inclusions.

Table 29 Fluid inclusion thin section mode

	Sample 113M	
	Leucosome	Host
quartz	27	51
microcline	69	2
plagioclase	3	4
biotite	1	24
garnet	-	2
fibrolite	-	16
zircon	-	tr
sericite	tr	-
total	100	99

The majority of the fluid inclusions in both the host and the leucosome occur along healed fracture planes. In general, these inclusion trails extend either from one grain boundary into the quartz interior, as shown in Figure 101, or they extend across the entire quartz grain from one boundary to another. The few that can be traced through several different quartz grains are certainly secondary in nature. Tracing the trails into neighboring non-quartz grains is difficult. Occasionally, fluid inclusions are found concentrated along lobate grain boundaries between adjacent quartz grains. Presumably, these were swept into the grain boundaries as irregularly shaped subgrains developed in strained quartz. Fluid inclusions also may occur in shapeless clusters and even more rarely as isolated inclusions which show no obvious spatial relation to any other fluid inclusion. The origin of the isolated and clustered inclusions is uncertain. They may have formed by migrating away from fracture planes with increasing maturity (Roedder, 1981; Johnson and Hollister, 1995). Alternatively, they may have originated as decrepitation clusters similar to those described by Sterner and Bodnar (1989). Microthermometry identifies three general fluid compositions in sample 113M: H_2O–CO_2, CO_2, and H_2O-salt.

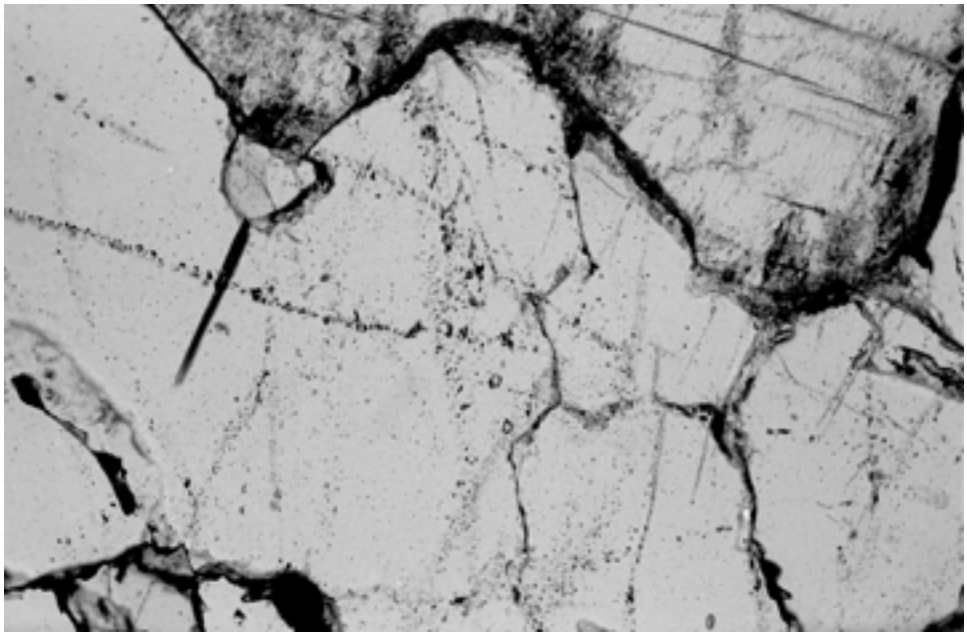

Figure 101a Photomicrograph of a portion of the leucosome in sample 113M showing abundant fluid inclusion trails trapped in quartz. Field of view is 1.2 mm (longest dimension); plane light.

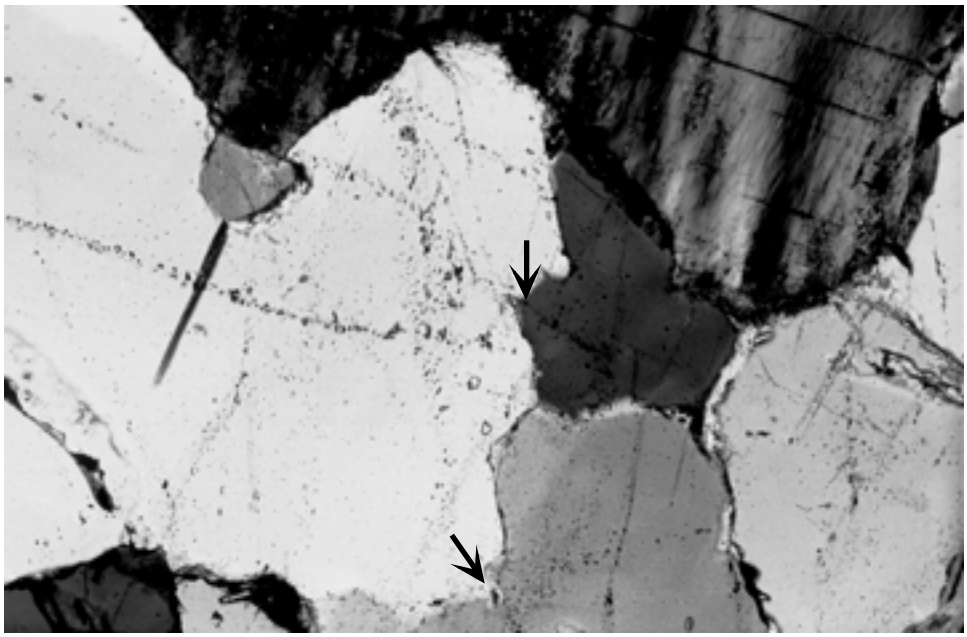

Figure 101b Crossed nicols view of same. Note that a few inclusion trails cross boundaries between different quartz grains (arrows), however, it is difficult to trace the trails into microcline (top of the photomicrograph).

Microthermometric Data

H_2O-CO_2

H_2O-CO_2 fluid inclusions are rare in this sample. Where present, they occur in clusters or as relatively large, irregularly shaped, isolated inclusions. At room temperature they contain two or three fluid phases. Microthermometric data were collected for only two of these inclusions, one in the leucosome and one in the host. The H_2O-CO_2 data are reported in Appendix I, Table I-3. Isochores for the H_2O-CO_2 inclusions were not calculated due to the incomplete nature of the data and their uncertain paragenesis.

CO_2

CO_2 fluid inclusions are more common in the leucosome than in the host. At room temperature the CO_2 fluid inclusions normally contain two fluid phases (liquid and vapor) and invariably possess negative crystal shapes with dark outlines as shown in Figure 102. Microthermometry was performed on thirty-one CO_2 fluid inclusions in the leucosome (six were isolated inclusions and the rest were concentrated along seven different fractures) and six in the host (five along two different fractures and one isolated inclusion). The results are summarized in Table 30. The CO_2 melting temperatures (Tm) ranged from -57.7 to –56.8°C . The depressed melting points are likely due to calibration error in the thermocouple. A second, more recently calibrated stage in the same laboratory consistently recorded room temperature readings 0.7-1.1°C higher than the stage used to collect this data set. Therefore, the visible phases in these inclusions are believed to be pure CO_2.

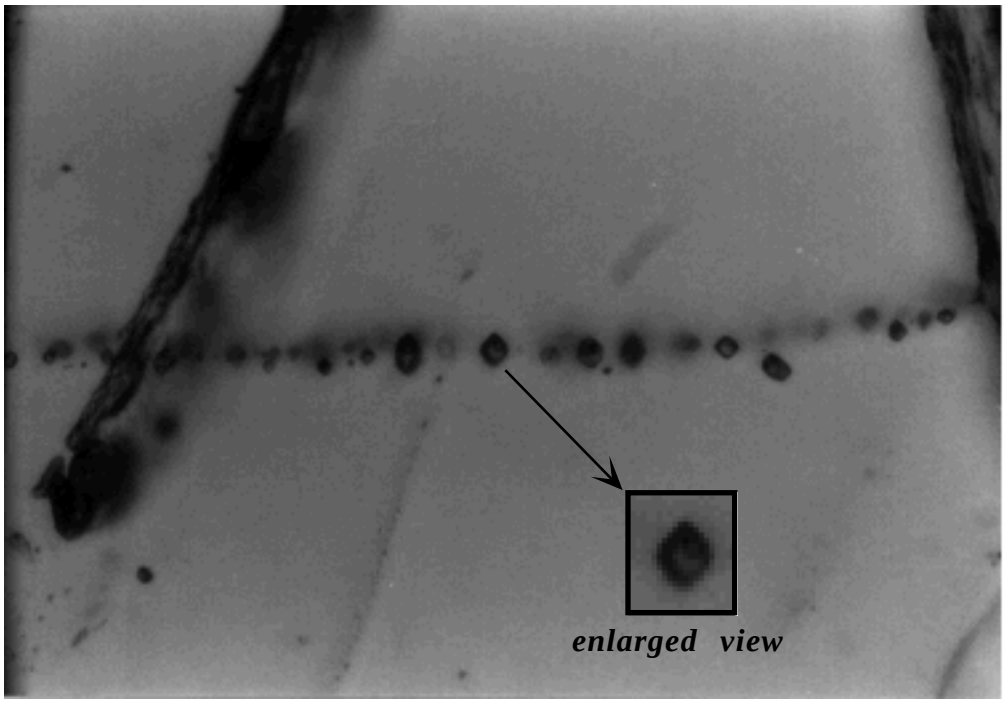

Figure 102 Photomicrograph of a typical CO_2 fluid inclusion trail in sample 113M. Note darkly outlined negative crystal shapes and two-phase nature (liquid + vapor bubble). Field of view is 0.3 mm in the longest dimension.

Table 30 Data for CO_2 Fluid Inclusions, Sample 113M

LEUCOSOME				*HOST*		
Fractures				*Fractures*		
Tm (°C)	**Th L (°C)**	**Th V (°C)**	**Density (g/cc)**	**Tm (°C)**	**Th L (°C)**	**Density (g/cc)**
-57.4	22.5		0.745	-57.6	26.1	0.692
-57.3	22.9		0.740	-57.4	26.5	0.685
-57.0	25.2		0.707			
-57.0	26.9		0.678	*Isolated*		
-57.1	27.9		0.657	-57.7	12.6	0.841
-57.1	28.5		0.642			
-57.0	28.7		0.637			
Isolated						
-57.6	11.6		0.849			
-57.4		28.0	0.290			
-57.1	12.4		0.843			
-56.8		21.7	0.209			
-57.3	16.2		0.811			
-57.0	23.5		0.732			

The CO_2 fluid inclusions that lie along fractures, whether in the leucosome or the host, exhibit remarkably consistent behavior (Table 30). All homogenize to the liquid phase at temperatures between 22.5 and 28.6°C with densities ranging from 0.64 to 0.74 g/cm^3. The isochores for the CO_2 fractures are plotted in Figure 103a. The behavior of the isolated CO_2 inclusions is much less predictable. These fluid inclusions homogenize to either the liquid or the vapor phase and they show a much larger range in homogenization temperature (Th) and density (Table 30), with only one conforming to the inclusion behavior observed in the fractures. The isochores for isolated CO_2 inclusions are plotted in Figure 103b. Figure 104 superimposes the isolated and clustered inclusion data on the fracture data (shown by the gray area). Peak metamorphism is indicated by the circle and the solid black arrow shows nearly isothermal decompression of the rocks following peak metamorphism. None of the isochores pass through the peak pressure and temperature, thus, the low density CO_2 fluid inclusions in this sample cannot represent peak conditions.

The consistency of the CO_2 trapped by fractures in both the host and the leucosome indicate a major fluid event, either permeation of the sample by a new fluid or re-equilibration of an old (peak) fluid to the new pressure-temperature conditions. The latter is considered to be more likely because CO_2 is frequently present during high grade metamorphism and re-equilibration (stretching and leaking) is a common phenomenon in rocks which undergo isothermal decompression (Hollister, 1988; Bodnar et al., 1989; Sterner and Bodnar, 1989; Hall and Sterner, 1993; Vityk et al., 1994). However, the original primary fluid inclusions could not have been *pure* CO_2, because (1) H_2O is routinely released by dehydration reactions during prograde metamorphism of pelitic rocks and so should be present in the grain boundary fluid, and (2) H_2O must have been present at least in some areas to initiate wet melting. Thus, it is more likely that both H_2O and CO_2 coexisted as a single supercritical fluid during peak metamorphism. Recent field and experimental studies attribute the presence of low-density CO_2 inclusions in high grade metamorphic rocks to leakage of H_2O during re-equilibration of H_2O-CO_2 primary fluid inclusions (Barker, 1995; Johnson and Hollister, 1995; Bakker and Jansen, 1994; Hall and Sterner, 1993; Craw and Norris, 1993; Hollister, 1988; Crawford and Hollister, 1986). Experimental work by Bakker and Jansen (1994)

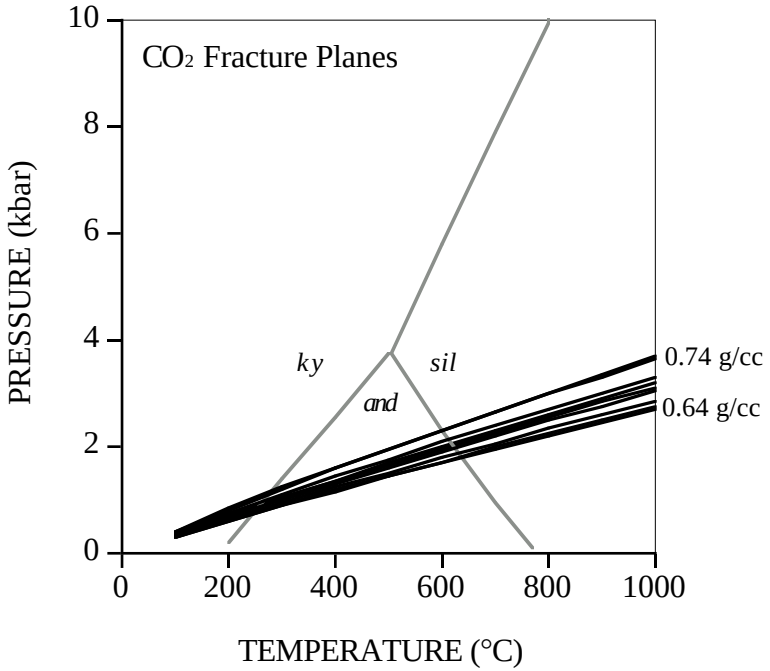

Figure 103a Pressure-temperature plot of the isochores for fluid inclusions which lie along fracture planes in both the leucosome and the host in sample 113M (aluminosilicate fields after Holdaway and Mukhopadhyay, 1993).

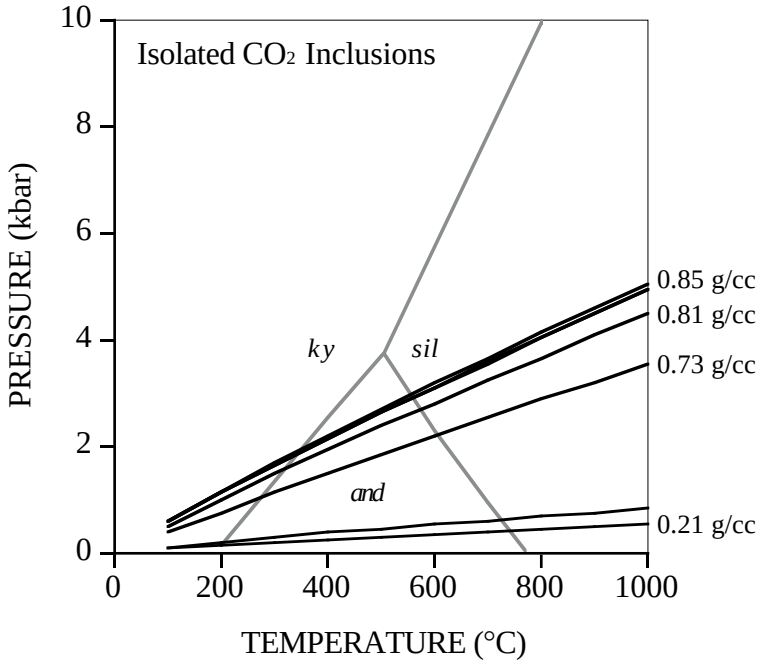

Figure 103b Pressure-temperature plot of the isochores for isolated fluid inclusions in both the leucosome and the host in sample 113M (aluminosilicate fields after Holdaway and Mukhopadhyay, 1993).

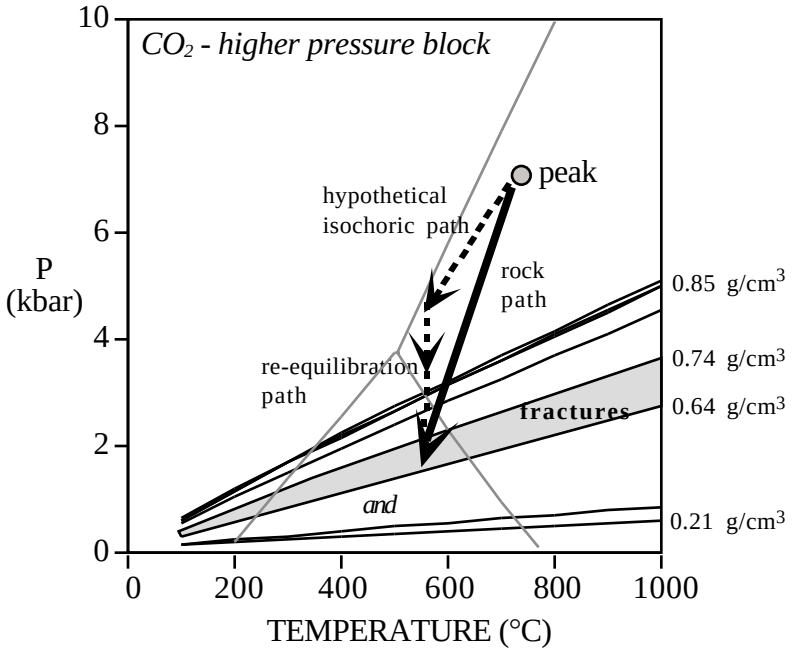

Figure 104 Pressure-temperature plot of all of the CO isochores for sample 113M. Isochores for inclusions which lie along fracture planes are restricted to the area shaded in gray, the remaining isochores are for isolated inclusions. The peak metamorphic conditions are indicated by the filled circle. The solid arrow shows a possible nearly isothermal decompression path taken by the rocks following peak metamorphism. The dashed arrow shows the hypothetical path followed by the primary fluid inclusions during this decompression.

indicate that preferential leakage of H_2O from H_2O-CO_2 inclusions occurs under supercritical conditions. Thus, it is probable that the CO_2 fluid inclusions trapped in sample 113M originated in a similar manner. Although an origin by re-equilibration of peak fluids is preferred here, it should be noted that Lamb (1990) and Lamb et al. (1987) have proposed that CO_2-rich fluid inclusions in granulite facies rocks in the Adirondacks originated from a late influx of a secondary H_2O-CO_2 fluid that became enriched in CO_2 through retrograde hydration reactions within the host rock.

The dashed black arrows in Figure 104 show a hypothetical path followed by the proposed peak H_2O-CO_2 inclusions during decompression. During uplift and cooling, the path taken by a fluid inclusion is constrained to its isochore as long as the inclusion remains a closed system. Under conditions of isothermal decompression, the internal pressure (P_i) within a fluid inclusion will exceed the confining pressure (P_c) as P_c is reduced. This creates a situation of internal overpressure ($P_i > P_c$) which , if large enough, can lead to re-equilibration of the fluid inclusions (Bodnar et al., 1989). The most recent data suggest that overpressures of 1.2 kbar can lead to re-equilibration (Bodnar, R.J., 1997 personal communication). The isochoric path shown in Figure 104 is completely hypothetical yet illustrates the potential for high internal overpressures in primary fluid inclusions of this sample. Assuming that the CO_2 fluid inclusions re-equilibrated from peak conditions, then internal overpressures of at least 2 to 3 kbars (as indicated by the length of the re-equilibration path in Figure 104) are likely given the relatively high peak pressures and the shallow slope of the CO_2 isochores. Once re-equilibration begins, the primary fluid inclusions move off of the original isochores, lose H_2O, and complete re-equilibration to lower pressure conditions.

Experimental work by Hall and Sterner (1993) indicated that loss of H_2O from inclusions may be driven by diffusion along a gradient of f_{H2O}. They suggest that isothermal decompression lowers the f_{H2O} of grain boundary fluids thus providing a driving force for H_2O loss from inclusions. TEM observations by Bakker and Jansen (1994) clearly showed that synthetic H_2O-CO_2 fluid inclusions trapped in quartz become surrounded by abundant crystal defects after being subjected to internal overpressures or underpressures. These defects provide pathways for diffusional loss of H_2O from H_2O-CO_2 fluid inclusions (Bakker and Jansen, 1994). In sample 113M, post-peak hydration reactions may have enhanced H_2O diffusion by maintaining a gradient in f_{H2O}. Garnet resorption and local production of fine-grained reaction coronas of biotite, quartz and plagioclase (Figure 13) suggest that H_2O-consuming reactions such as

$$grt + sil + Kfs + H_2O = pl\ (Ca\text{-}enriched) + bt + qtz$$

were operating during decompression (see Chapter II). The loss of H_2O from the grain boundary fluid to fuel hydration reactions reduces f_{H2O} which causes further diffusive loss of H_2O from the H_2O-CO_2 fluid inclusions. Thus, not only would it be possible to preferentially remove H_2O from the inclusions, much of it could be consumed in these post-peak reactions. In this way, both the fluid inclusions and the remaining grain boundary fluid could become enriched in the CO_2 component.

The isochores for the majority of the isolated CO_2 inclusions shown in Figure 104 appear to track the re-equilibration down to the conditions recorded by the fluids in the fracture planes. In this scenario, the higher-density, isolated and clustered inclusions did not completely re-equilibrate to the new conditions, thus retaining densities corresponding to conditions along the decompression path. The extremely low-density, isolated inclusions underwent further density reduction either through later changes in volume (stretching) or fluid leakage as the rocks continued to be exhumed.

H_2O-Salt

At room temperature, the H_2O-salt inclusions contain a liquid and a vapor phase with or without a daughter mineral. The mean size of the measured inclusions in both the host and the leucosome is about 6 microns. The majority of the inclusions are round to ellipsoidal shapes; four exhibit negative crystal shapes and three show irregular morphologies. Where present, the daughter minerals exhibit both square and rectangular crystal habits. Halite is suspected in most cases based on crystal habit and similar index of refraction to that of quartz. Microthermometric measurements were made on 46 H_2O-salt inclusions, 35 from the leucosome (three isolated, two in clusters and 30 along 19 different fractures), and 11 from the host (seven along five different fractures, three in clusters and one isolated inclusion). These data are summarized in Table 31. The small size of the inclusions prevented observation of hydrohalite.

Figure 105 is a histogram of the homogenization temperatures for aqueous fluid inclusions trapped in fracture planes. This figure illustrates the diverse assortment of aqueous fluid inclusions present in the leucosome (black) as opposed to the more uniform fluid behavior in the host (gray). Fractures within the leucosome trapped fluids that homogenize to the liquid phase at temperatures ranging from 63 to 393°C and possess NaCl-

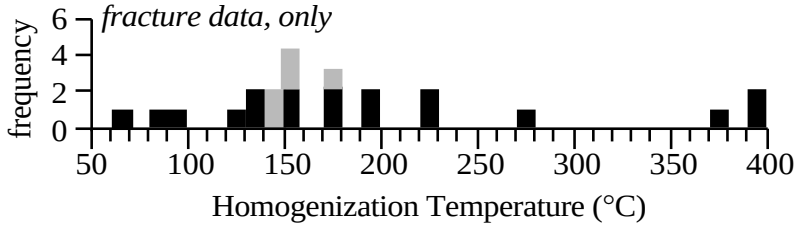

Figure 105 Histogram of homogenization temperatures (L+V=L) for aqueous inclusions along fracture planes; black: leucosome, gray: host.

Table 31 Data for H2O-salt Fluid Inclusions, Sample 113M

~Te (°C)	Tm ice (°C)	Th L (°C)	Tm salt (°C)	NaCl Equivalent Salinity (wt %)	Density (g/cm³)	Sample Number
LEUCOSOME						
Fractures						
-43	-10.5	63	-	14	1.07	2-1
-49	-24.7	84	-	24	1.14	3-1
-56	-21.4	98	-	22	1.13	4-3
-66	-39.4	125	167	30	1.17	4-1
-67	-32.7	138	-	27	1.10	2-8
-55	-22.1	139	-	22	1.10	4-4
-69	-22.4	151	-	22	1.09	4-6
-52	-22.7	157	-	23	1.08	2-2
-22	-17.4	172	-	21	1.04	2-4
-45	-32.4	172	-	26	1.07	2-7
-29	-16.7	193	-	20	1.02	2-9
-23	-10.5	230	-	14	0.95	1-4
-24	-10.0	232	-	14	0.94	1-6
-4	-0.5	273	-	1	0.76	3-2
-40	-23.9	370	-	23	0.87	1-5
-	-6.6	391	-	10	0.66	2-5
-63	-31.9	393	-	26	0.84	1-3b
-30	-23.2	*Td = 448*				3-3
-65	-31.7	*Td = 482*		26		1-3a
Clusters						
-27	-12.2	235	-	16	0.96	2-9b/a
-25	-9.9	386	-	14	0.74	2-9a/a
Isolated						
-36	-14.5	243	-	18	0.96	2-10a
-37	-17.3	384	-	20	0.94	2-8a
-28	-17.5	decrep.	354	45		2-2b
HOST						
Fractures						
-	-	140	196	32	1.17	10-4
-	-	148	191	31	1.16	10-3
-40	-11.4	151	-	15	1.02	9-7
-90	-44.0	152	180	31	1.15	8-1
-72	-43.0	170	184	31	1.14	9-4
Clusters						
-	-22.0	139	194	32	1.17	10-2
-	-	151	181	31	1.16	10-1
Isolated						
-41	-11.6	150	-	16	1.02	9-2

equivalent salinities from 1 to 30 weight percent (Table 31). Although fewer fluid inclusions were measured from the host, those that were present along fractures trapped aqueous fluids with a much narrower range of Th (140 to 170°C) and salinity (15 to 32 weight percent NaCl equivalent, Table 31).

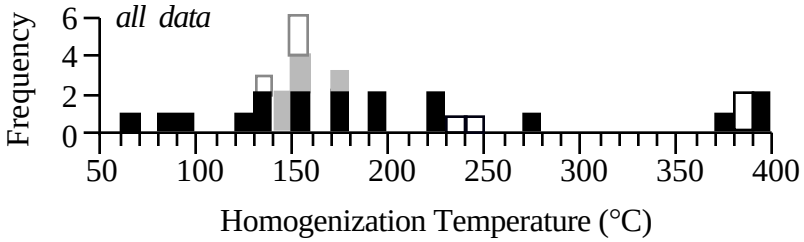

Figure 106 Histogram of homogenization temperatures (L+V=L) for all the aqueous fluids measured in sample 113M; solid black: leucosome fractures, solid gray: host, black outline: leucosome isolated/clusters, gray outline: host isolated/clusters.

In Figure 106, Th for fluids found in isolated and clustered inclusions have been added to the fracture data. Note that the isolated and clustered inclusions within the host (gray outline) trap the same fluid found in the host fractures (solid gray). On the other hand, the isolated and clustered inclusions in the leucosome (black outline) exhibit more diverse behavior. The data indicate that the host trapped a single aqueous fluid, here called fluid A. Fluid A also was trapped by numerous fractures within the leucosome and together with the host they form a prominent maximum at about 150°C on the histogram (Figure 106). The extensive recrystallization in the finer-grained host probably destroyed all traces of early-formed fluid inclusions and, thus is responsible for the lower variability of the host fluids. Any remnants of early fluids in the host were completely re-equilibrated to the trapping conditions of fluid A. This fluid undoubtedly represents a significant secondary fluid event associated with or post-dating the recrystallization. The leucosome still contains coarse-grained minerals related to peak metamorphism. Thus, a wider variety of fluid species representing the long history of this sample still remain trapped within the leucosome.

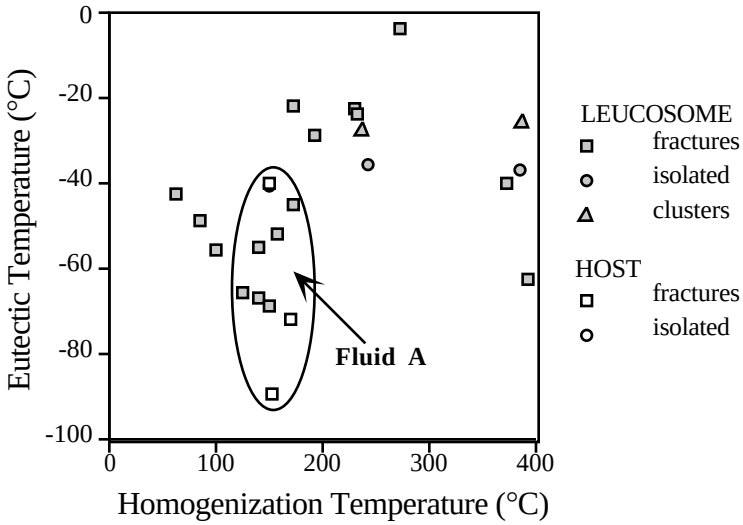

Figure 107 Plot of eutectic temperature versus homogenization temperature for aqueous fluid inclusions in sample 113M.

Figure 107 is a plot of eutectic temperature (Te) versus Th for all of the fluids in sample 113M. Fluid A shows low Te from -90 to -40°C, most being lower than -52°C. The low first melting temperatures indicate the probable presence of $CaCl_2$ and NaCl, although other salts such as $MgCl_2$ or $FeCl_2$ may be present as well (Roedder, 1984; Vanko et al., 1988). The ternary eutectic for the NaCl-$CaCl_2$-H_2O system is -52.0°C (Crawford, 1981; Vanko et al.,1988; Oakes et al., 1990). Eutectics lower than the expected -52°C in this system are due to metastable behavior. Experimental work in the NaCl-$CaCl_2$-H_2O system records initial melting as low as -85°C and is attributed to a metastable ice-halite-

$CaCl_2 \cdot nH_2O$ eutectic (Davis et al., 1990, Oakes et al., 1992). Eutectics higher than the expected -52°C may reflect the difficulties associated with recognizing and accurately measuring initial melting in small fluid inclusions. One fluid inclusion (sample 2-4, Th = 172°C) had an unexpectedly high Te (-22°C) suggesting that if this was part of the same fluid event, then more than one composition fluid may have been present. Most of the fluid inclusions or inclusion assemblages with Th greater than 170°C (see Figure 107) show Te ranging from -40 to -22°C indicating that $CaCl_2$ is not present in these fluids. Eutectic temperatures in this range suggest NaCl-KCl-H_2O fluids with possible additional $FeCl_2$ or $MgCl_2$ (Roedder, 1984; Barker, 1995). It should be noted that although the eutectic temperature of the NaCl-KCl-H_2O system is –22.9°C, Davis et al. (1990) report initial melting in this system as low as –40°C.

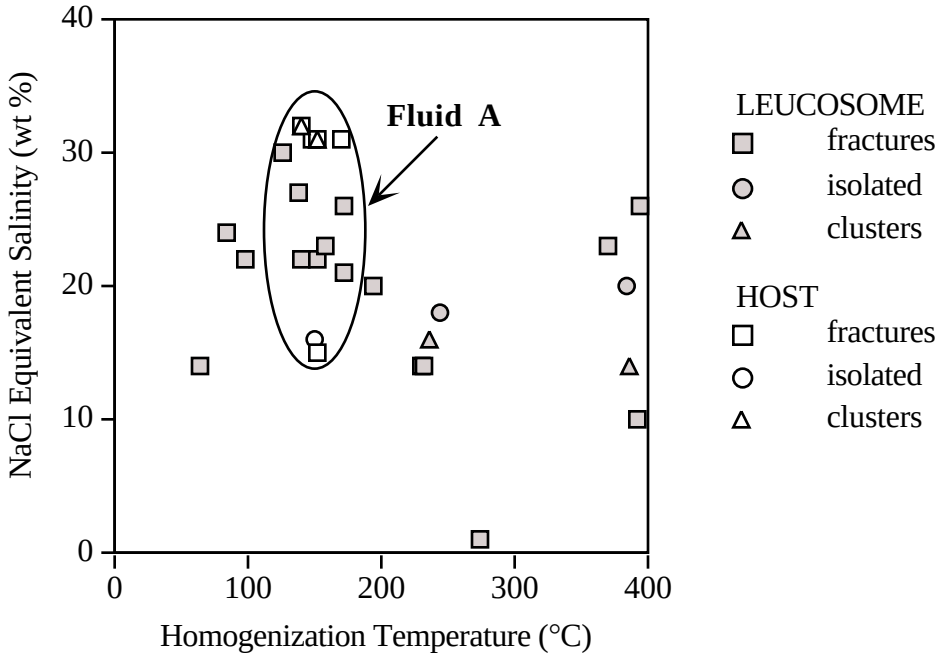

Figure 108 Plot of NaCl equivalent salinity versus homogenization temperature for aqueous fluid inclusions in sample 113M.

Figure 108 is a plot of NaCl-equivalent salinity versus homogenization temperature. Fluid A is the highest salinity fluid trapped in this sample, most with NaCl equivalent salinities ranging from 22 to 32 weight percent. Two samples of fluid A did exhibit notably lower salinities (15 to 16 wt%, Figure 108; 9-7 and 9-2, Table 31). However, if the observed final ice melting of these fluids (–11°C) was actually final hydrohalite melting, then their compositions should plot in the hydrohalite field with a significantly higher salinity. Figure 109 shows the location of the hydrohalite field in the NaCl-$CaCl_2$-H_2O system. Note that fluids without a halite daughter mineral and with final hydrohalite melting of –11°C would have a salinity of around 25 weight percent total salt. All of the fluid inclusions with daughter minerals belong to fluid A. Figure 109 also plots the approximate compositions of the these saturated fluid inclusions using the method described by Vanko et al. (1988) and Williams-Jones and Samson (1990). Because hydrohalite dissolution often cannot be measured, compositions in the halite field can be estimated using ice

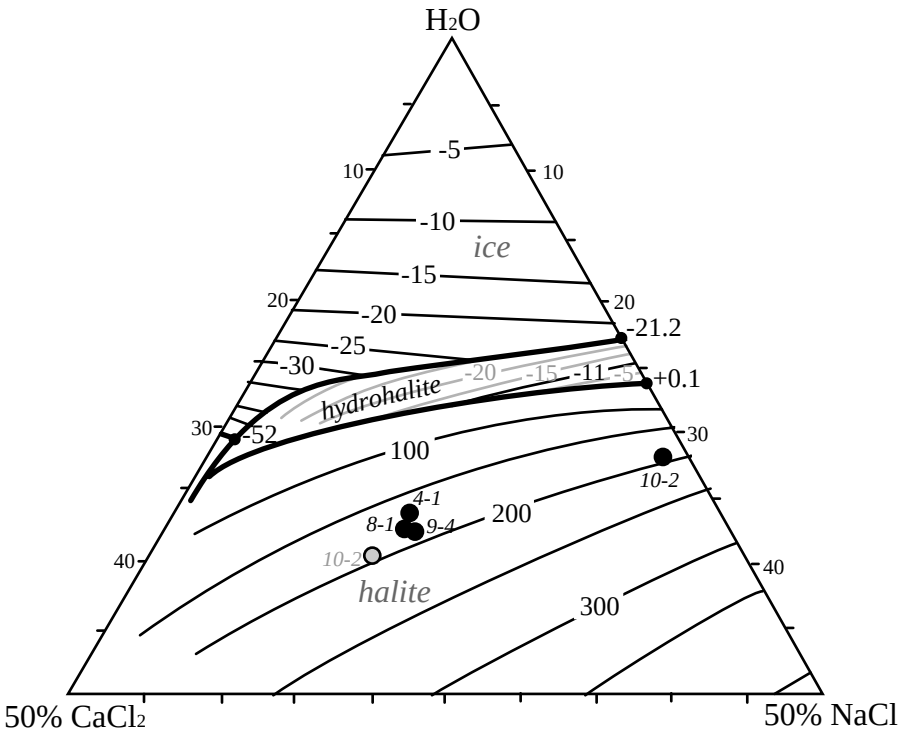

Figure 109 Phase diagram showing the liquidus surface in a portion of the NaCl-$CaCl_2$-H_2O system (after Vanko et al., 1988; Oakes et al., 1990, and Oakes et al., 1992). The total salinity for fluids with final hydrohalite melting of -11°C in the hydrohalite field is approximately 25 weight percent. The approximate compositions of the saturated aqueous fluid inclusions from sample 113M are plotted based on final melting temperatures of ice and halite (black circles; see Vanko et al., 1988 and Williams-Jones and Samson, 1990 for plotting method). The gray circle represents a plot of inclusion 10-2 assuming final melting of hydrohalite was observed rather than that of ice.

melting and halite dissolution temperatures (see Williams-Jones and Samson, 1990, for a thorough discussion). The saturated fluids in this sample plot around a composition of 21 weight percent $CaCl_2$, 16 weight percent NaCl and 63 weight percent H_2O, except for sample 10-2. If it is assumed that the final ice melting temperature of the fluid in 10-2 (–22°C) was actually final hydrohalite melting, then its composition would plot much closer to that of the other saturated inclusions (gray circle in Figure 109). The high proportion of $CaCl_2$ in these fluids (about 60% of the total salt content) suggests that the fluid composition was influenced by the more calcic phases of the amphibolite unit in this outcrop.

The remaining fluids found in the leucosome are more dilute than fluid A (see Figure 108), ranging from 10 to 25 weight percent (NaCl equivalent) except for one fracture that trapped nearly pure H_2O (1 wt %; sample 3-2, Table 31). In general, the aqueous component of peak metamorphic fluids in pelitic schists and gneisses is fairly dilute (2-6 weight percent; Crawford and Hollister, 1986; Crawford, 1981). Thus, all but one of the aqueous fluids trapped in this sample contain higher salinities than expected for peak metamorphism. If the peak metamorphic fluid was a supercritical miscible H_2O-CO_2 fluid, then no aqueous fluid, no matter what its salinity, could be trapped independent of CO_2 at the peak conditions. Thus, it is probable that all of the aqueous fluid inclusions in this sample are secondary in nature. Despite its secondary nature, the 1 weight percent fluid still may record the composition, if not the density of the aqueous component of the peak fluid as it was released during re-equilibration. Re-equilibration experiments (Hall and Sterner, 1993) on saline synthetic fluid inclusions trapped in quartz showed that isothermal decompression with internal overpressures of 2 kbar produced salinity increases of 2 to 22 weight percent. Moreover, they found that the highest-salinity changes are recorded in the smallest inclusions. Crawford et al. (1979) reported a similar salinity increase of 5 to 10 weight percent in late fluids observed in natural samples. Hall and Sterner (1993) attributed increased salinities to preferential diffusional loss of H_2O during re-equilibration, whereas Crawford et al. (1979) suggested that retrograde hydration reactions concentrated the salts in the fluids. Thus, the high salinities measured in the bulk of the aqueous fluid inclusions in sample 113M (all of which are small) may be due to multiple processes operating during re-equilibration. In addition, if the 1 weight percent fluid does represent the aqueous component of the peak fluid, then it must have been trapped early in the re-equilibration process before the fluid became more saline.

Figure 110 is a pressure-temperature plot of the isochores for all of the aqueous fluids observed in sample 113M. Also shown in Figure 110 are the CO_2 isochores, the conditions of peak metamorphism (gray circle), the decompression path (solid black arrow), and the probable cooling path (solid dark gray arrow) that followed decompression. The aqueous isochores appear to fall into five general fluid groups, labeled A-E in Figure 110. None of the isochores pass through the peak conditions, although fluid B comes close. Given a homogeneous H_2O-CO_2 peak fluid, and the fairly high salinities of fluid B (14-18 weight percent, Figure 110), fluid B probably is secondary. In fact, it is unlikely that any primary fluid inclusions survived the extreme internal overpressures produced by the decompression of these rocks. Fluids C (the 1 weight percent fluid) and D intersect the nearly isothermal decompression path interpreted for this area and, thus, may represent re-equilibrated peak fluids. During decompression the H_2O-CO_2 fluid inclusions initially followed their isochores through pressure-temperature space (dashed arrow, completely hypothetical) until internal overpressures were too high and H_2O began to leak out. The wetting characteristics of H_2O allowed it to form an interconnected fluid network along dislocations, microfractures and grain boundaries (Watson and Brennan, 1987) whereas the much larger CO_2 molecules were left behind in the fluid inclusions. As predicted, the isochore for fluid C (1 weight percent) is the first to be crossed by the decompression path and, thus, may mark the early stages of H_2O leakage. As decompression and re-equilibration continued, more H_2O was released from the primary inclusions and became involved in retrograde hydration reactions. The loss of H_2O by

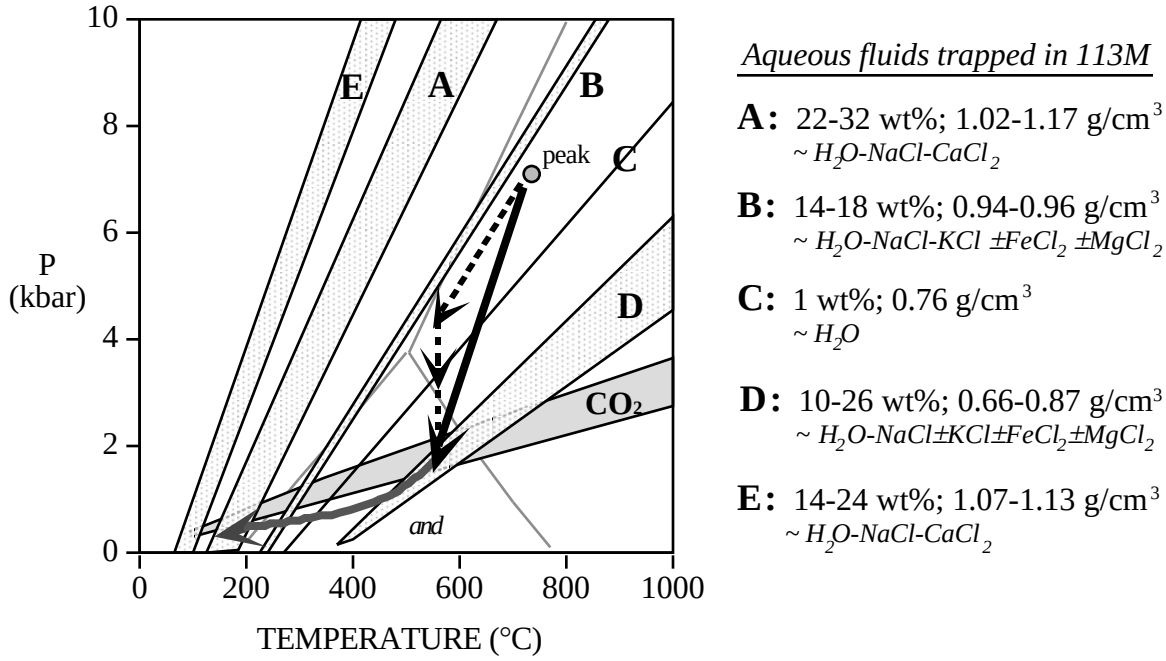

Figure 110 Pressure-temperature plot showing the isochores for all of the aqueous fluid inclusions (fractures, clusters and isolated inclusions) in sample 113M. The isochores are grouped according to their location in P-T space and labeled A-E (gray stippled regions between high and low isochores). The region of the re-equilibrated CO_2 isochores are shown for reference. Also shown are the peak metamorphic conditions, the nearly isothermal decompression path (solid black arrow) and the nearly isobaric cooling path (solid dark gray arrow) interpreted for this area. The dashed arrow indicates the hypothetical path taken by the peak metamorphic fluid.

leakage and rehydration caused the fluid remaining within the inclusions to become more saline and more enriched in CO_2. The increased salinity and CO_2 content enlarges the H_2O-CO_2 immiscibility field causing the two phases to separate. Thermodynamic calculations by Bowers and Helgeson (1983) indicate that increasing the salinity in the H_2O-CO_2-NaCl system produces vapor-liquid immiscibility at pressures and temperatures in excess of 2 kbar and 550°C. The highest salinities in their calculations was approximately 12 weight percent, with the mole fraction of CO_2 being 0.10. Hence, the generally more saline fluid D (10-26 weight percent, Figure 110) could represent the re-equilibrated remnants of the aqueous component of the peak fluid which became immiscible during decompression. Rehealed fractures retained the pure re-equilibrated CO_2 inclusions and aqueous fluid D was trapped in new fractures, both fluids equilibrated to the same pressure-temperature conditions, shown in Figure 110 where the two isochores cross (approximately 560°C and 1.7 kbar).

There is no evidence for any significant reheating events after peak metamorphism in this study area. Because the CO_2 fluid inclusions show no further evidence for re-equilibration, their internal fluid pressure must have remained nearly equal to the confining pressure. This is only possible if the cooling segment of the uplift path is restricted to near parallelism with the CO_2 isochores, as shown in Figure 110. Thus, dominantly isobaric cooling probably followed dominantly

isothermal decompression. The fluid inclusions and fluid inclusion assemblages (FIA's) trapping fluid D, experienced underpressures of less than 1 kbar during isobaric cooling. It is unknown whether underpressures of this magnitude can cause re-equilibration. Vityk et al. (1994) report no morphological changes for experimental underpressures of 1 kbar. Vityk and Bodnar (1995) observed morphological changes in large fluid inclusions for underpressures of 1.2 kbar but found no change in medium and small inclusions, such as those which dominate this sample. However, if small scale stretching and leakage is possible, then fluid B, which is compositionally similar to fluid D, could represent incomplete re-equilibration of fluid D.

As discussed above, fluid A, the high salinity, NaCl-$CaCl_2$-H_2O fluid which homogenizes at approximately 150°C, is believed to represent a major fluid event in this sample. All of the aqueous fluid inclusions in the host and many of those in the leucosome trap fluid A. The presence of appreciable amounts of $CaCl_2$ (about 20 wt % $CaCl_2$, 15 wt % NaCl in the saturated inclusions) in this fluid suggests that it is fundamentally different from fluids B, C, and D. Therefore, fluid A is interpreted as a late fluid which infiltrated the area at low pressure and temperature (approximately 1 kbar and 200°C, see Figure 110). Fluid E, which is compositionally similar to fluid A but homogenizes to lower temperatures, may be related to this fluid event. However, why fluids originally trapped during the fluid A event should re-equilibrate to the fluid E conditions is not understood.

Summary

Although no primary fluid inclusions remain in sample 113M, the original peak fluid is interpreted to have been a homogeneous H_2O-CO_2 mixture. An intense episode of nearly isothermal decompression led to post-entrapment modification of the primary fluid inclusions, however, remnants of the peak fluid can be found in re-equilibrated aqueous and pure CO_2 inclusions. There is some suggestion that the aqueous component of the peak fluid was fairly dilute (about 1 weight percent, NaCl equivalent). However, most of the aqueous fluids became enriched in salts as H_2O was taken up in post-peak hydration reactions during the decompression. The fluid inclusion data from sample 113M reveal two major post-peak fluid events. The first occurred at pressures and temperatures of approximately 1.5 to 2 kbar and 550 to 600°C, trapping a 10-26 wt % NaCl-KCl-H_2O fluid with a fairly high homogenization temperature (370 to 393°C) and retaining pure CO_2 in the original peak fluid inclusions. The 10-26 wt % NaCl-KCl-H_2O fluid is found only in the leucosome, presumably because subsequent intense recrystallization within the finer-grained host wiped out all evidence of this early aqueous fluid. The second major fluid event trapped a high salinity NaCl-$CaCl_2$-H_2O fluid which infiltrated the area at pressures and temperatures of approximately 0.5 kbar and 150 to 200°C.

Sample 13I

Petrography

Outcrop 13 lies within the lower-pressure block which experienced peak metamorphism at approximately 650°C and 5 kbar. The migmatites in this outcrop were generated during peak metamorphism by wet melting processes. The host rocks are finely interlayered quartzo-feldspathic biotite gneisses and low-Al semi-pelitic gneisses. These gneisses are identified based on their plagioclase composition and the relative proportions of plagioclase and microcline in the leucosomes that they enclose. The quartzo-feldspathic biotite gneiss host rocks, of which sample 13I is one, are enriched in plagioclase over microcline and their leucosomes contain very little to no microcline. The mode for sample 13I is given in Table 32 and shows that the leucosome contains 42% plagioclase and only 3% microcline. The mole fraction of anorthite in both the host and leucosome plagioclase is 33% (Table 25). The semi-pelitic gneisses (e.g. sample 13G, Table 25)

enclose leucosomes that are more enriched in microcline and contain less calcic plagioclase (An20). Typically, the leucosomes associated with the two gneisses are separated by distances of only 0.1 to 1.5 cm, emphasizing the finely layered character of this outcrop.

Table 32 Fluid Inclusion Thin Section Mode

	Sample 13I	
	Leucosome	Host
quartz	51	45
microcline	3	11
plagioclase	42	26
biotite	3	15
zircon	-	tr
sericite	tr	tr
muscovite (retrograde)	tr	2
total	99	99

The presence of trace to minor amounts of cross-cutting secondary muscovite grains in almost all of the samples from outcrop 13 (Table 32, Table A-1, Appendix A, and Figure 28) indicates a retrograde event involving the hydration of K-feldspar not seen in outcrop 113. Microtextural evidence (Figures 31 and 32) suggests that cross-cutting muscovite was produced sometime after 1.7 Ga peak metamorphism and prior to 1.2±0.2 Ga ductile shearing. Late solid state deformation of the leucosomes is evident in grain boundary recrystallization around leucosome microcline (Figure 69), and undulose extinction and subgrain development in irregularly shaped leucosome quartz. Within the host, quartz is fine-grained, relatively unstrained, and inclusion-free. This suggests that recrystallization was more complete in the finer-grained host than it was in the leucosome. The solid state deformation evident in this sample must have preceded the late hydration event because secondary muscovite grains show no evidence of strain or preferred orientation.

The majority of the fluid inclusions in sample 13I are trapped within healed fracture planes in the coarser grained leucosome quartz. Figure 111 is a photomicrograph showing numerous diversely oriented fluid inclusion trails typical of the leucosome quartz. Most of the inclusion trails contain small (1-5 μm), rounded fluid inclusions. Other trails contain larger (up to 20 μm in the longest dimension), irregularly shaped inclusions, many of which are decrepitated. As can be seen in Figure 111, the inclusion trails are more or less continuous across the entire quartz grain. Some cross the boundary between adjacent quartz grains (A, Figure 111), and others appear to project into cleavage planes of adjacent non-quartz grains (B, Figure 111). Although the majority of the fluid inclusions lie in well-defined fractures, some seemingly unstructured groups of fluid inclusions appear to have been swept into subgrain boundaries as shown in Figure 112. Unlike sample 113M, this sample is distinguished further by the presence of large annular fluid inclusions that cut across healed fracture planes (see

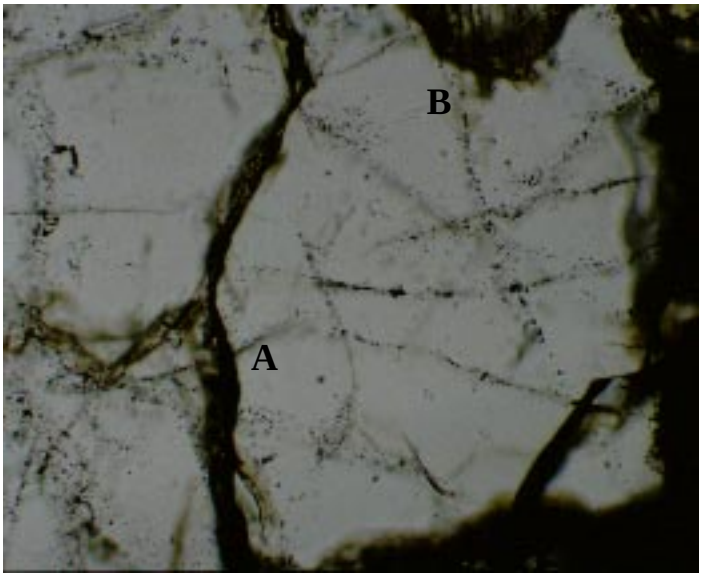

Figure 111 Photomicrograph of a leucosome quartz grain in sample 13I cut by numerous inclusion trails. Some cross the boundary between adjacent quartz grains (A), and others appear to project into cleavage planes of adjacent non-quartz grains (B). Field of view is 4 mm in the longest dimension; plane light.

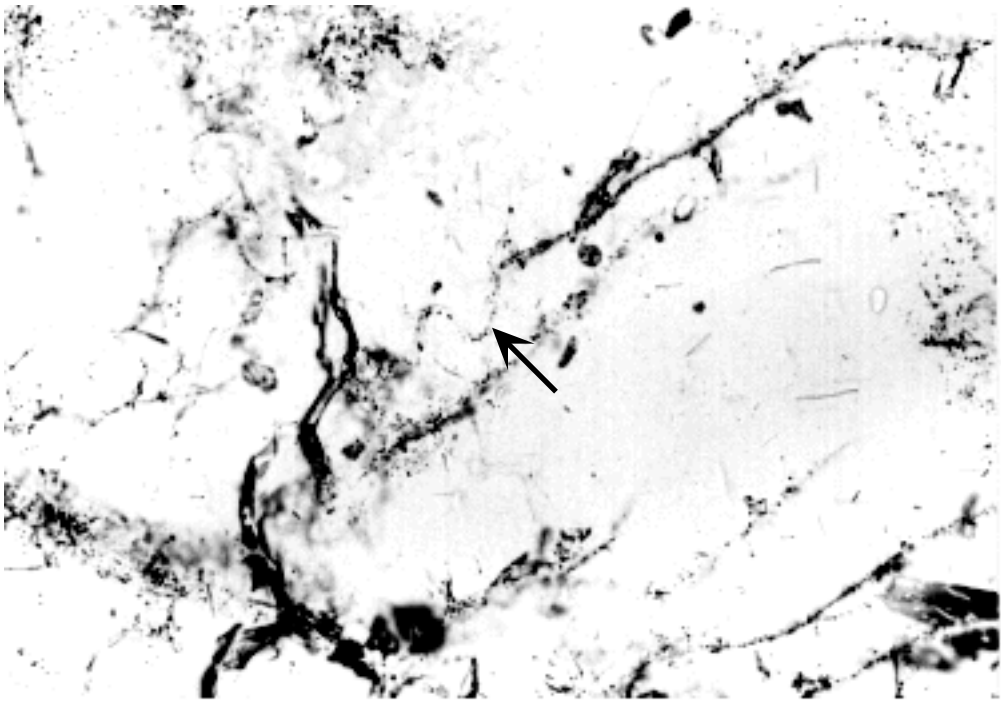

Figure 112a Photomicrograph showing fluid inclusions that appear to have been swept into subgrain boundaries (arrow). Field of view is 1.2 mm in the longest dimension, plane light.

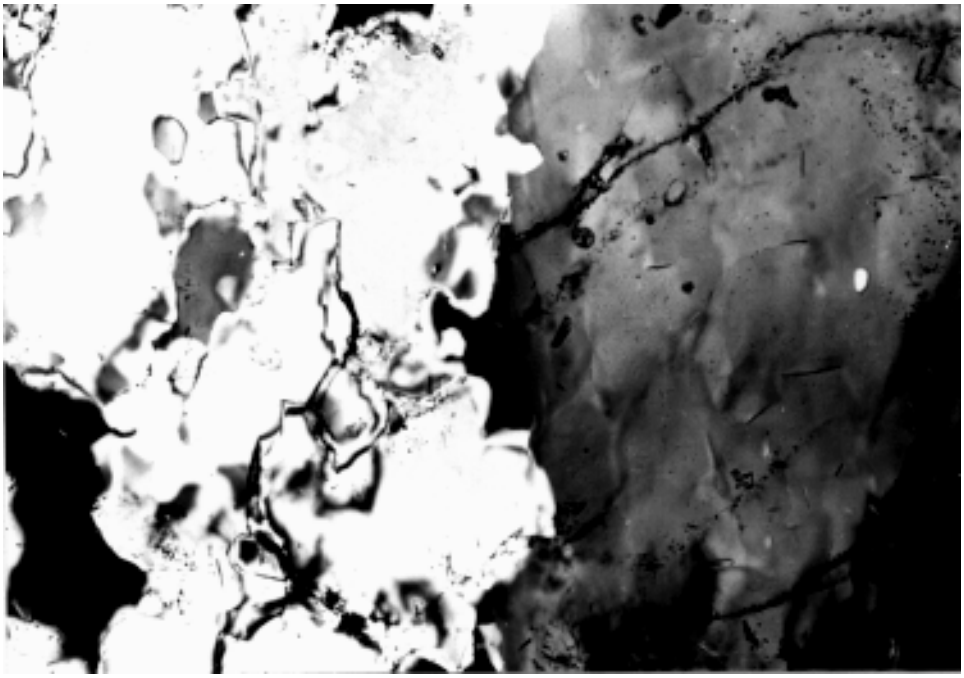

Figure 112b Same view, crossed polars.

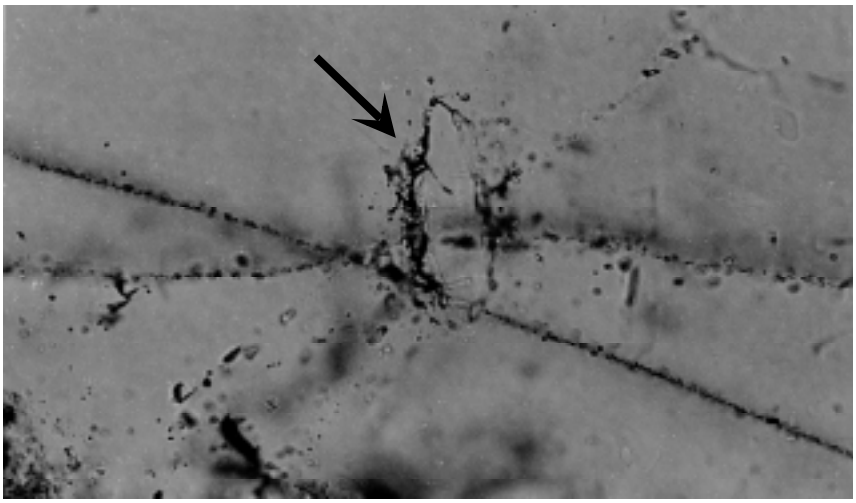

Figure 113 Photomicrograph of an approximately 90μm long annular fluid inclusion (arrow) cutting across two fluid inclusion trails. Field of view is 0.3 mm (longest dimension), plane light.

Figure 113). Experimentally produced annular inclusions have been attributed to conditions involving internal underpressure (Pêcher, 1981; Vityk and Bodnar, 1995). Boullier et al. (1991) observed natural annular inclusions from the structurally highest regions sampled in the High Himalaya. They attributed the annular texture to a sudden loading event which led to an anisotropic increase in confining pressure. Vityk and Bodnar (1995) experimentally reproduced compressive loads of about 2 kbar to form annular inclusions and found that an anisotropic stress field was not necessary to produce annular textures.

Microthermometry in sample 13I was limited to fluid inclusion trails in the leucosome. Four basic types of trails can be identified in this specimen: *type 1* trails cross boundaries between adjacent quartz grains, *type 2* trails are continuous across a single quartz grain but do not appear to extend beyond the grain boundaries, *type 3* trails project from (but do not cross) the grain boundary into the interior of a single quartz grain, and *type 4* trails are wholly restricted to the interior of a single quartz grain, usually truncated by other fractures. The type 1 inclusion trails are the only unambiguous secondary fractures since they traverse grain boundaries. The luminescent properties of quartz were used to resolve the cross-cutting relationships between all of the fracture types. Figures 114, 115, 116 and 117 are cathodoluminescent (CL) images of intersecting inclusion trails in sample 13I. Examination of the intersections between the inclusion trails in Figures 114, 115 and 117 suggests the following order of formation: type 3 formed first followed by type 2 and finally by type 1. A single fracturing event appears to have generated both the type 3 and 4 inclusion trails since each type can be seen to overprint the other in Figure 116. It should be noted that since type 2 and type 3 inclusion trails do reach the grain boundaries, it is possible that at least some of them belong to the same fracturing event that produced the continuous type 1 inclusions trails. Moreover, the same could be true of the type 4 inclusion trails since it was not possible to view their behavior in the third dimension. Figure 117 is a CL image of an annular inclusion which clearly overprints type 2 and type 3 fractures, suggesting a late formation. The annular inclusion shown in the photomicrograph in Figure 113 appears to crosscut a type 2 trail (horizontal in the photograph) and a type 1 trail (upper left to lower right in the photograph). This implies that the annular inclusions were the last to form, post-dating types 1, 2 and 3 inclusion trails. The late generation of the annular inclusions is further substantiated by their large size and non-equilibrium shape (Boullier et al., 1991).

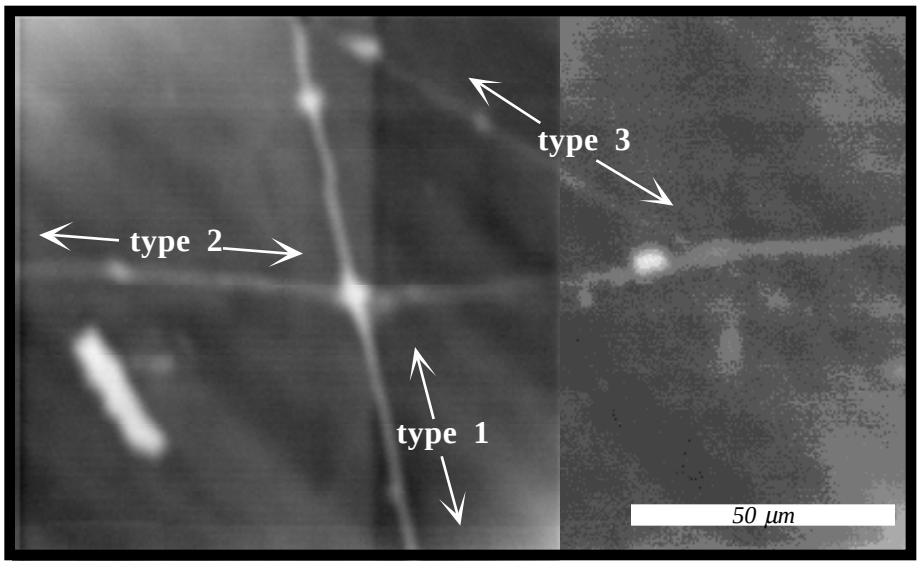

Figure 114 Cathodoluminescent image showing three different fluid inclusion trails. The type 1 trail is the most recent fracture in this image. It overprints the type 2 trail which in turn overprints the type 3 trail. The arbitrary north end of the thin section is toward the top of this image.

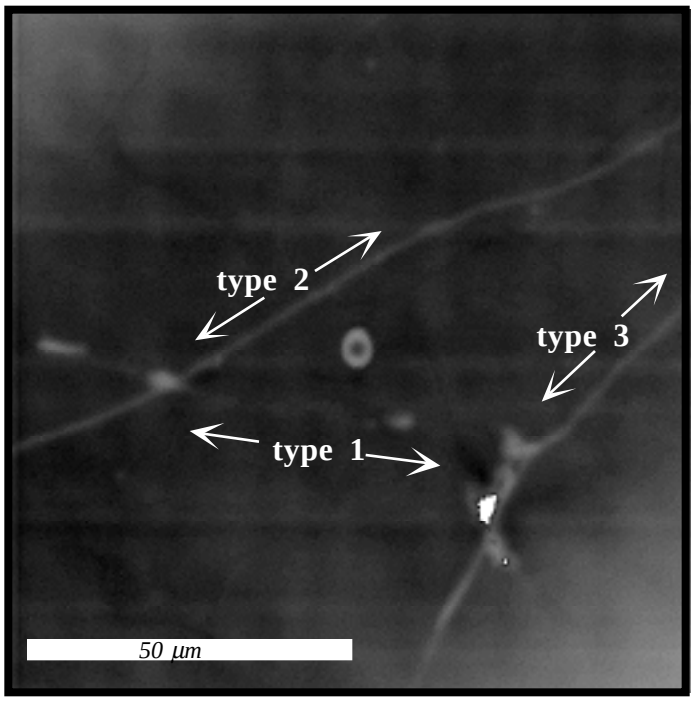

Figure 115 Cathodoluminescent image showing a type 1 fluid inclusion trail overprinting type 2 and type 3 fluid inclusion trails. The arbitrary north end of the thin section is toward the top of this image.

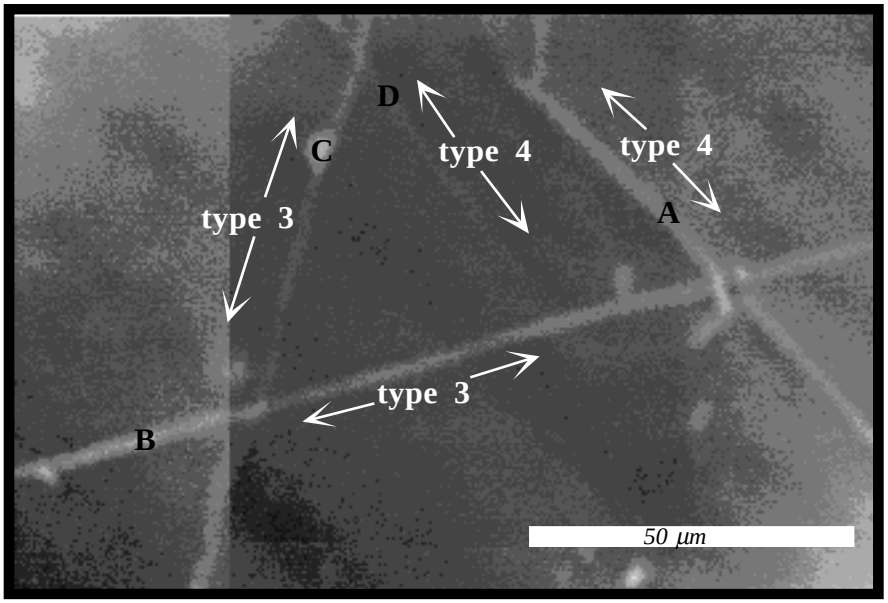

Figure 116 Cathodoluminescent image showing the cross-cutting relationships between types 3 and 4 inclusion trails. In this case, inclusion trail A (type 4) appears to overprint inclusion trail B (type 3) which in turn overprints both trail C (type 3) and trail D (type 4); inclusion trail C overprints D. Thus, a type 4 (D) healed first, was cut by a type 3 (C) that was cut by another type 4 (B) that was cut by another type 3. This suggests probable simultaneous generation of type 3 and 4 inclusion trails. The arbitrary north end of the thin section is toward the top of this image.

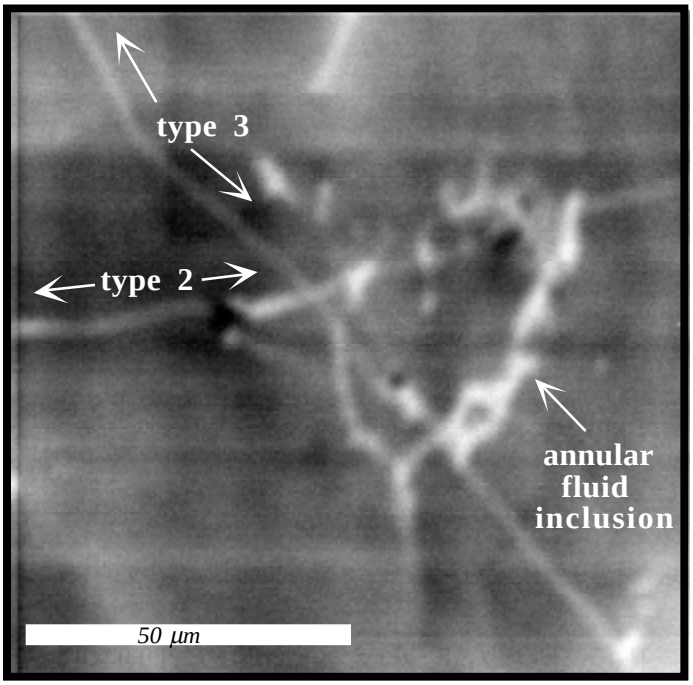

Figure 117 Cathodoluminescent image showing an annular fluid inclusion overprinting a type 2 fluid inclusion trail that overprints a type 3 fluid inclusion trail. The arbitrary north end of the thin section is toward the top of this image.

Microthermometric Data

The primary fluids analyzed in sample 13I are H_2O-salt and CO_2. H_2O-CO_2 inclusions are present but extremely rare and never occur along continuous fracture planes. Where present, they occur at the intersections between CO_2 and aqueous fluid inclusion trails, suggesting mixing of CO_2 and H_2O-salt fluids.

CO_2

CO_2 inclusions are less frequently observed in this sample than in sample 113M. As in sample 113M, they contain a liquid and a vapor phase at room temperature and exhibit a negative crystal shape. The average size of the measured CO_2 inclusions is about 4 μm. Microthermometry was performed on eight CO_2 inclusions spread over six different fractures. The results are presented in Table 33 along with inclusion trail type and orientation of the fractures relative to the arbitrary north end of the thin section. All of the inclusions trapped pure CO_2, based on the melting temperatures which range from -56.6 to –56.0°C. The inclusions homogenize to the liquid phase at temperatures from 22 to 30°C. Four of the six analyzed fractures had an E-W orientation relative to the thin section, however this is not statistically significant since so few CO_2 inclusion trails were analyzed. The type 1 and 2 CO_2 inclusion trails show the highest homogenization temperatures (28.5 to 30.0°C) corresponding to an average density of 0.62 g/cm^3. The remaining measured CO_2-bearing inclusions in types 3 and 4 trails have an average density of 0.74 g/cm^3. The composition and range of Th and density are nearly identical to the CO_2 data for fractures in sample 113M (compare to Table 30). The isochores and their corresponding densities for CO_2-bearing inclusions are presented in Figure 118 along with the peak pressure-temperature conditions for sample 13 (filled square), the probable path of nearly isothermal decompression (solid arrow) and the hypothetical path followed by fluid inclusions originally trapped under peak metamorphic conditions (dashed arrow). This hypothetical fluid path suggests that the primary fluid inclusions could easily have experienced the minimum 1.2 kbar of overpressures needed to promote re-equilibration during decompression. As in sample 113M, none of the CO_2 isochores intersect the pressure-temperature conditions of peak metamorphism. Following the same reasoning proposed for sample 113M, the CO_2 inclusions in sample 13I are interpreted as secondary inclusions originally trapped near peak conditions which re-equilibrated with H_2O-loss during isothermal decompression.

Table 33 Data for CO_2 Fluid Inclusion Trails, Sample 13I

Fracture Number	Tm (°C)	Th L (°C)	Density (g/cc)	Orientation (to thin sect)	inclusion trail type
Y2C-12	-56.2	22.0	0.751	NNE	3
Y2C-14	-56.0	22.0	0.751	ENE	4
Y2C-9	-56.4	23.5	0.732	E-W	4
V2W-2	-56.4	28.5	0.642	E-W	1
V2W-3	-56.6	29.0	0.628	E-W	2
V2W-1	-56.6	30.0	0.592	E-W	1

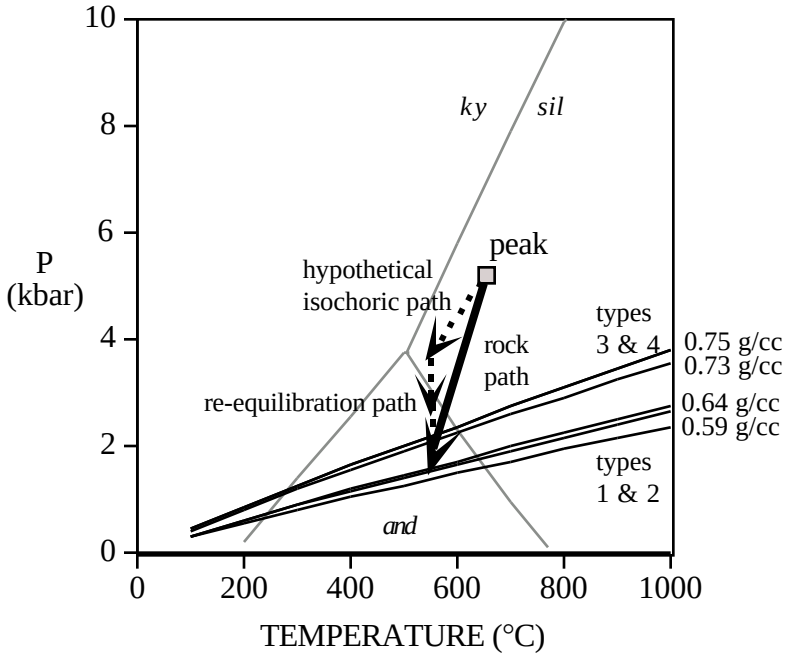

Figure 118 Pressure-temperature plot of the CO_2 isochores for sample 13I. The peak metamorphic conditions are indicated by the filled square. The solid arrow shows a possible nearly isothermal decompression path taken by the rocks following peak metamorphism. The dashed arrow shows the hypothetical path followed by the primary fluid inclusions during uplift.

H_2O-salt

H_2O-salt is the volumetrically most important fluid in this sample. 125 aqueous inclusions spread over 45 different fractures were analyzed. The averaged data for each fracture are presented in Table 34, the complete data set is given in Appendix I, Table I-4. At room temperature, the aqueous fluid inclusions contain a liquid and a vapor phase with or without a daughter mineral. With heating, they all homogenize to the liquid phase. Where present, the daughter minerals exhibit a square crystal habit and a similar index of refraction to that of the enclosing quartz. This suggests that the daughter minerals are halite. No evidence for more than one daughter mineral in a given inclusion was found. The mean size of the measured aqueous fluid inclusions was 4 μm. The majority possessed round to ellipsoidal shapes; 21 possessed negative crystal shapes and four had more irregular shapes. The small size of the inclusions prevented recognition of hydrohalite.

Examination of Table 34 shows that none of the fracture types are limited to a particular orientation within the thin section, nor do the orientations appear to coincide with a specific fluid behavior. Figure 119 is a histogram of the homogenization temperatures (Th) for the aqueous fluid inclusions in sample 13I arranged by fracture orientation relative to the arbitrary north end of the thin section. Unlike sample 113M, the data from this sample are more tightly grouped producing a unimodal distribution of homogenization temperature with a maximum of approximately 173°C (compare to Figure 105). Figure 120 presents this same data broken down by fracture type. The fluids trapped in the late type 1 fractures show the tightest clustering of Th with a unimodal peak of 168°C.

Table 34 Averaged data for H_2O-Salt fluid inclusions trails, sample PC-13I leucosome

~Te (°C)	Tm ice (°C)	Th L (°C)	Tm salt (°C)	NaCl Equivalent Salinity (wt %)	density (g/cm^3)	Orientation (re: thin sect)	Sample Number	Fracture Type
-71	-21.6	147	-	22	1.09	E-W	Z2E1 5	1
-74	-17.0	152	-	20	1.05	E-W	Z2E1 2	1
-37	-18.5	158	-	21	1.06	NNE	V2W 4	1
-55	-24.4	158	177	31	1.15	E-W	Z2E1 8	1
-52	-11.0	164	-	15	1.00	NE	V2W 10	1
-44	-22.5	165	-	22	1.08	NE	V2W 9	1
-60	-11.0	167	-	15	1.00	NE	V2W 7	1
-53	-13.9	168	-	18	1.02	NE	Z2W 4	1
-63	-30.6	168	169	30	1.14	NE	Z2E2 11	1
-27	-10.3	174	-	14	0.99	NE	Z2E2 5	1
-67	-24.7	174	-	24	1.07	E-W	Z2E1 7	1
-36	-8.7	176	-	12	0.98	E-W	Z2E2 4a-b	1
-	-24.0	186	185	31	1.13	ENE	W2W 8	1
-39	-17.0	189	-	20	1.02	NE	W2W 9	1
-48	-9.0	120	-	13	1.02	E-W	Z2E1 6	2
-44	-13.2	125	-	17	1.05	ENE	Z2E2 6	2
-51	-16.5	164	-	20	1.04	NE	V2W 5	2
-	-	165	178	31	1.14	NNE	Y2C 11	2
-	-20.8	168	-	23	1.07	E-W	Z2E1 9	2
-	-8.5	169	N/A	-		NE	Z2E2 1	2
-63	-25.5	173	-	24	1.07	E-W	W2W 2	2
-41	-16.5	174	-	20	1.03	NE	Y2W 4	2
-	-6.0	174	154	30	1.13	E-W	W2W 13	2
-	-	175	-	-		NNE	Y2C 2	2
-33	-9.1	176	-	13	0.98	ENE	Z2W 1	2
-	-10.0	177	166	30	1.13	NNE	W2W 1	2
-34	-16.5	177	192	31	1.14	ENE	W2W 7	2
-27	-9.5	180	-	14	0.98	NE	Z2E2 7	2
-67	-26.8	181	-	24	1.06	ENE	Z2E2 10	2
-67	-23.9	182	-	23	1.06	ENE	Z2E2 12	2
-41	-13.5	183	-	17	1.01	ENE	W2W 5	2
-55	-15.0	186	-	19	1.01	E-W	W2W 4	2
-41	-6.5	102	-	10	1.01	NE	Y2W 2	3
-34	-16.0	147	-	19	1.05	ENE	Y2W 3	3
-	0.0	160	-	0	0.91	NNW	Y2C 5	3
-51	-6.5	169	-	10	0.97	NNE	V2W 8	3
-	-	174	-	-		NE	Y2C 13	3
-43	-8.3	179	-	12	0.97	E-W	Z2E2 8	3
-37	-8.2	186	-	12	0.97	E-W	Z2E2 3	3
-40	-13.0	190	-	17	1.00	NNE	Y2C 4	3
-	-0.5	191	-	1	0.88	ENE	Y2C 1	3
-48	-7.8	193	-	11	0.96	N-S	Z2E2 9	3
-40	-22.0	193	-	22	1.05	E-W	W2W 6	3
-54	-15.0	168	-	19	1.03	NNE	Z2W 3	4
-	-	178	-	-		N-S	Y2C 10	4

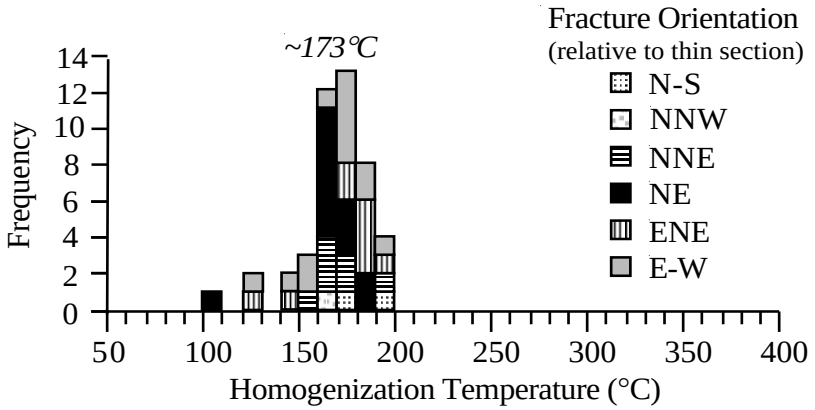

Figure 119 Histogram of homogenization temperatures (L+V=L) for aqueous inclusions along fracture planes in sample 13I.

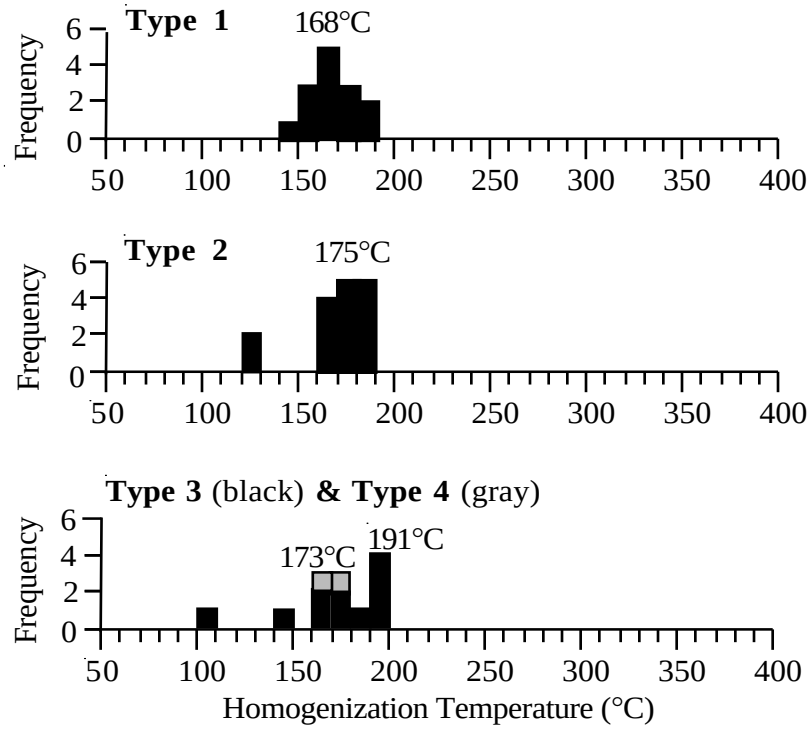

Figure 120 Histograms of homogenization temperature for inclusion trails that cross grain boundaries (*type 1*), trails that span and entire single grain (*type 2*), trails that project from a grain boundary into the grain interior (*type 3*) and grains that are restricted to the interior only (*type 4*).

Because these are the most recent fractures, they would be expected to show the least post-entrapment modification and, therefore, the most uniform behavior. Type 2 fractures show more spread but the peak at 175°C is similar to that of the type 1 inclusion trails. Type 3 and 4 fractures, grouped together as the earliest generation of fractures, yield the greatest spread in data and an apparent bimodal distribution with peaks at 173°C (similar to type 1) and 191°C. The similarity between the maxima for each fracture type (168, 175, 173°C) suggests that the same aqueous fluid was trapped by the majority of the fracture planes in this sample.

Eutectic temperatures (Te) for this fluid ranges from -74 to –27°C. The large range in initial ice melting indicates that although this fluid homogenizes to the same temperature, it has a variable composition. The composition of the two fluids trapped in the inclusion trails can be modeled by the NaCl-$CaCl_2$-H_2O system (Te = -52°C) and by the NaCl-KCl-H_2O system (Te = -22.9°C). As discussed earlier, the spread in the reported Te about the actual Te's for these systems is attributed to metastable behavior and to difficulties recognizing and measuring initial melting in small inclusions (Davis et al., 1990, Oakes et al., 1992).

Figure 121 plots the approximate compositions of the saturated probable NaCl-$CaCl_2$-H_2O fluid inclusions using the method described by Vanko et al. (1988) and Williams-Jones and Samson (1990). Since hydrohalite dissolution often cannot be measured, compositions in the halite field can be estimated using ice melting and halite dissolution temperatures (see Williams-Jones and Samson, 1990, for a thorough discussion). The reported final ice melting temperatures of the fluid in fractures W2W-1 and W2W-13 (-10 and -6.0°C, respectively) were assumed to be final hydrohalite melting for this plot (gray circles). Although the total salt content is fairly consistent (31 to 34 weight percent), the amount of $CaCl_2$ varies from 6 to 16 weight percent which corresponds to $CaCl_2$ to total salt ratios of 19 to 47%. As discussed previously, this outcrop is characterized by small scale compositional heterogeneities, especially in the relative proportions of the feldspars and the plagioclase composition. The variability in $CaCl_2$ observed in the fluid inclusions is somewhat consistent with the shifting plagioclase composition observed in the gneissic laminae. Indeed, considering that the gneissic layering is oriented approximately N-S relative to the arbitrary north end of the fluid inclusion thin section, the fractures trapping fluids with low proportions of $CaCl_2$ (19%, 22% and 23%) exhibit orientations which go across the foliation (E-W and ENE) suggesting connection with nearby lamina containing plagioclase of lower anorthite content (An20). On the other hand, the fractures with higher proportions of $CaCl_2$ (36% and 47%) have orientations which are generally parallel to the gneissic layering (NNE and NE). Therefore, the more calcic fluids in these fractures could reflect the higher anorthite content of the plagioclase in the layer represented by this sample (An33).

Figure 122 is a plot of NaCl equivalent salinity versus homogenization temperature for the fluids trapped by each fracture type. Two of the type 3 fractures have extremely low salinities unlike any of the other fluids. Based on their dilute nature and relatively early fracture genesis, these are the most likely to represent the composition (but not the density) of the aqueous component of the peak metamorphic fluid. The remainder of the inclusions plotted in Figure 122 have higher salinities (NaCl-equivalent) varying from 10 to 31 weight percent. The lower salinity inclusions (10 to 18 weight percent, NaCl-equivalent) in Figure 122 have final ice melting temperatures of –13.9 to –6.0°C. If the observed final ice melting of these fluids was actually final hydrohalite melting, then their compositions would plot in the hydrohalite field with a salinity of around 25 weight percent. Given the difficulty identifying hydrohalite in these small inclusions (average size 4 μm), it is possible that all of the aqueous inclusions presented in Figure 122 have a relatively high salinity.

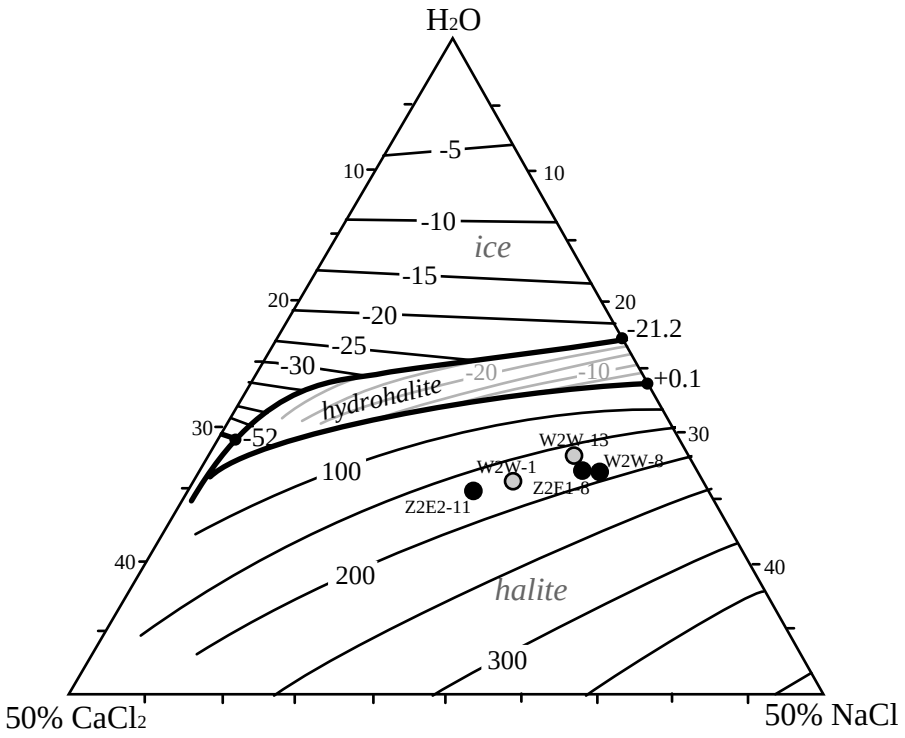

Figure 121 Phase diagram showing the liquidus surface in a portion of the NaCl-$CaCl_2$-H_2O system (after Vanko et al., 1988, Oakes et al., 1990, and Oakes et al., 1992). The approximate compositions of the saturated aqueous fluid inclusions trapped in types 1 and 2 fractures in sample 13I are plotted based on final melting temperatures of ice and halite (black circles) or by assuming that final melting of hydrohalite was observed rather than that of ice (gray circles).

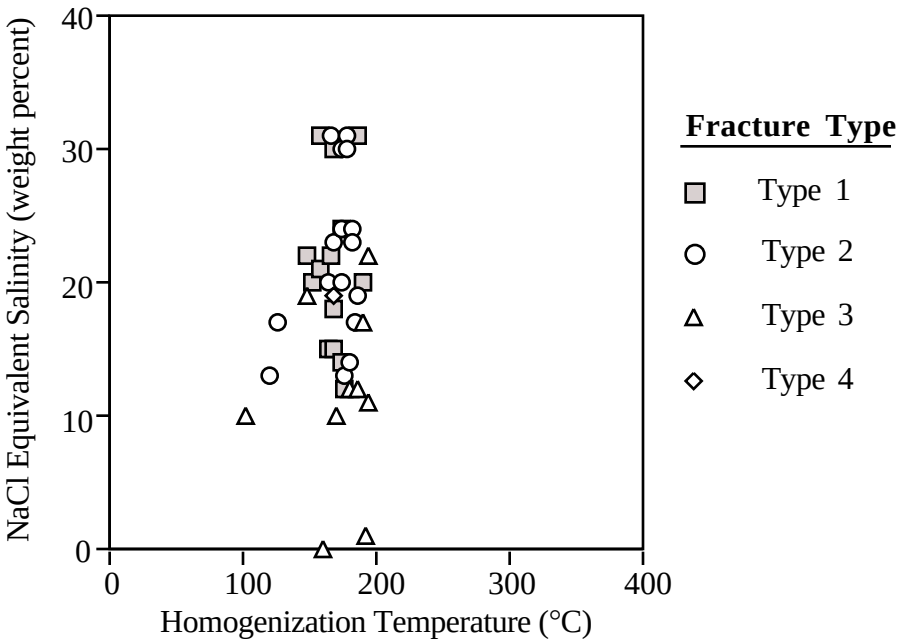

Figure 122 Plot of NaCl equivalent salinity versus homogenization temperature for aqueous fluids trapped in the different fracture types in sample 13I.

Figure 123 is a plot of the isochores for the aqueous and CO_2 inclusions from this sample along with the peak metamorphic conditions, the isothermal decompression path (black arrow), and the isobaric cooling path (gray arrow). The location of the aqueous isochores is nearly identical to those calculated for the type A fluids in sample 113M. However, unlike sample 113M, this sample shows no evidence for the high Th fluids whose isochores intersect the decompression path. This suggests that re-equilibration of the peak fluid was more extensive in sample 13I. The presence of two aqueous fluids ($NaCl\text{-}CaCl_2\text{-}H_2O$ and $NaCl\text{-}KCl\text{-}H_2O$) with the same homogenization temperature indicates that there may be two aqueous fluid sources. The first would be the same externally derived high salinity $NaCl\text{-}CaCl_2\text{-}H_2O$ fluid proposed for sample 113M (fluid A). The second would be the remnants of the peak fluid ($NaCl\text{-}KCl\text{-}H_2O$) which re-equilibrated to the pressure-temperature conditions of the fluid A event. The fairly high salinities of this fluid were produced by concentrating the salt species in the fluid as the retrograde hydration of K-feldspar to muscovite proceeded. If the atypical low salinity fluid inclusions trapped in some type 3 fractures represent the composition of the aqueous component of the peak fluid, then they must have somehow survived fairly intact along the bulk of the uplift path. How this could have occurred is not clear, however, the possibility can not be ruled out.

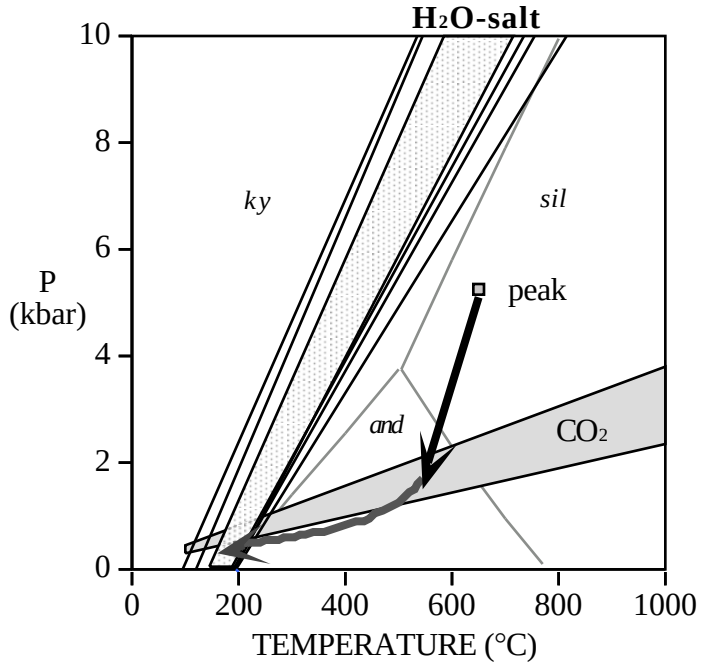

Figure 123 Pressure-temperature plots of the isochores for aqueous fluid inclusions in sample 13I. The majority of the isochores range in density from 1.00 to 1.15 g/cm (stippled region). Individual isochores which do not fall within the majority range are plotted also. Peak metamorphic conditions and the location of the CO_2 isochores for this sample are shown for reference along with the interpreted isothermal decompression and isobaric cooling paths.

Summary

As in sample 13I, the original primary fluid inclusions are interpreted to have been a homogeneous mixture of H_2O and CO_2. Remnants of this fluid can be found in the re-equilibrated low density CO_2 fluid inclusions and possibly in the low salinity (0 to 1 weight percent) aqueous inclusions. These two fluid phases separated from each other primarily through leakage of H_2O during decompression. Much of the H_2O was taken up into hydrous retrograde phases, causing the remaining aqueous fluid to become more enriched in NaCl and KCl. During isobaric cooling, the aqueous inclusions trapped in fractures continued to re-equilibrate. However, since the cooling path generally paralleled the CO_2 isochores, the CO_2 inclusions remained intact. The fluid inclusion data reveal the same major post-peak fluid events identified in sample 113M. The first is represented by the re-equilibrated CO_2 inclusions and the second by the high salinity NaCl-$CaCl_2$-H_2O inclusions.

Synthesis

Migmatites from both the lower and higher pressure blocks trapped two major secondary fluids: (1) low density CO_2 and (2) high salinity NaCl-$CaCl_2$-H_2O. The secondary origin of these fluids is supported by the evidence for recrystallization in both samples, the preponderance of fluid

inclusions in fractures, many of which are clearly secondary, and the lack of correspondence between the peak metamorphic conditions and the calculated fluid inclusion isochores. The absence of consistently identifiable primary fluid inclusions suggests that the fluids trapped during peak metamorphism were modified or lost during this area's long geologic history. Although no primary fluid inclusions were observed to document the fluid present during migmatization, it is likely that some of the secondary fluid inclusions still retain peak fluid compositions albeit recycled to lower pressure-temperature conditions. The probable re-equilibrated peak fluid inclusions include the pure CO_2 inclusions and the rare 0-1 weight percent aqueous inclusions. Based on the composition of the observed secondary fluid inclusions and the fluids appropriate to amphibolite facies metamorphism in migmatized pelitic schists and gneisses, the original fluid present during peak metamorphism, 1.7 Ga ago, is speculated to be H_2O-CO_2. Fluid inclusions trapping this peak fluid experienced high internal overpressures during isothermal decompression causing them to re-equilibrate. The nature of the decompression and subsequent isobaric cooling can be more fully interpreted by combining the fluid inclusion data with the known metamorphic, magmatic and tectonic history of this area (see Table 1).

Figure 124 shows the pressure-temperature conditions of peak metamorphism for both blocks and the proposed uplift path followed by each. The isochores for the major secondary CO_2 and late aqueous fluids trapped by both samples show substantial overlap and thus are combined in Figure 124. This suggests that both blocks trapped the same post-metamorphic fluids. Although these two blocks are now exposed next to each other at the surface, during peak metamorphism the higher pressure block lay at a level six to seven kilometers below that of the lower pressure block. The nearly identical nature of the secondary fluids trapped by these rocks suggests that the higher and lower pressure blocks were in their current, juxtaposed configuration (or nearly so) prior to trapping the secondary fluids. The sequence of events described by Figure 124 begins with peak metamorphism at 1.7 Ga. At this time, the higher pressure block lay six to seven kilometers below the lower pressure block. Migmatites in the lower pressure block formed by wet melting processes, only, whereas those in the higher pressure block formed initially by wet-melting followed by more substantial anatexis via dehydration melting. Some H_2O (presumably more in the lower pressure block) must have been present to initiate wet melting. Nearly isothermal decompression followed peak metamorphism, as indicated by the steep, identical paths depicted for each block in Figure 124. Continued decompression was accompanied by re-equilibration of the primary fluid inclusions as higher and higher internal pressures were attained. At 1.4 Ga voluminous amounts of the Berthoud Plutonic Suite intruded the lower pressure block in the form of the Log Cabin Batholith (Figures 1, 2, and 63). The Berthoud Plutonic Suite was emplaced to depths of about 10 to 11 km (~ 3 kbar of pressure; Anderson and Thomas, 1985), suggesting a 2.5 kbar reduction in pressure for the lower pressure block by the time the Log Cabin Batholith was emplaced. Since the two blocks must move as a single package (albeit starting at different depths), a similar uplift was experienced by the higher pressure block. Given conditions of nearly isothermal decompression between 1.7 and 1.4 Ga, the overpressure experienced by primary fluid inclusions in these rocks over this period of time was approximately 2.5 kbar. Sterner and Bodnar (1989) conducted experimental simulations of internal overpressure using synthetic aqueous fluid inclusions and concluded that fluid inclusions are unlikely to maintain their original densities given overpressures of 1 to 1.5 kbar. Thus, sometime between 1.7 and 1.4 Ga the primary fluid inclusions began to re-equilibrate.

By 1.4 Ga the lower pressure block had reached the emplacement depth of the Berthoud Plutonic Suite and was invaded by large volumes of hot magma (emplacement temperature estimated to be

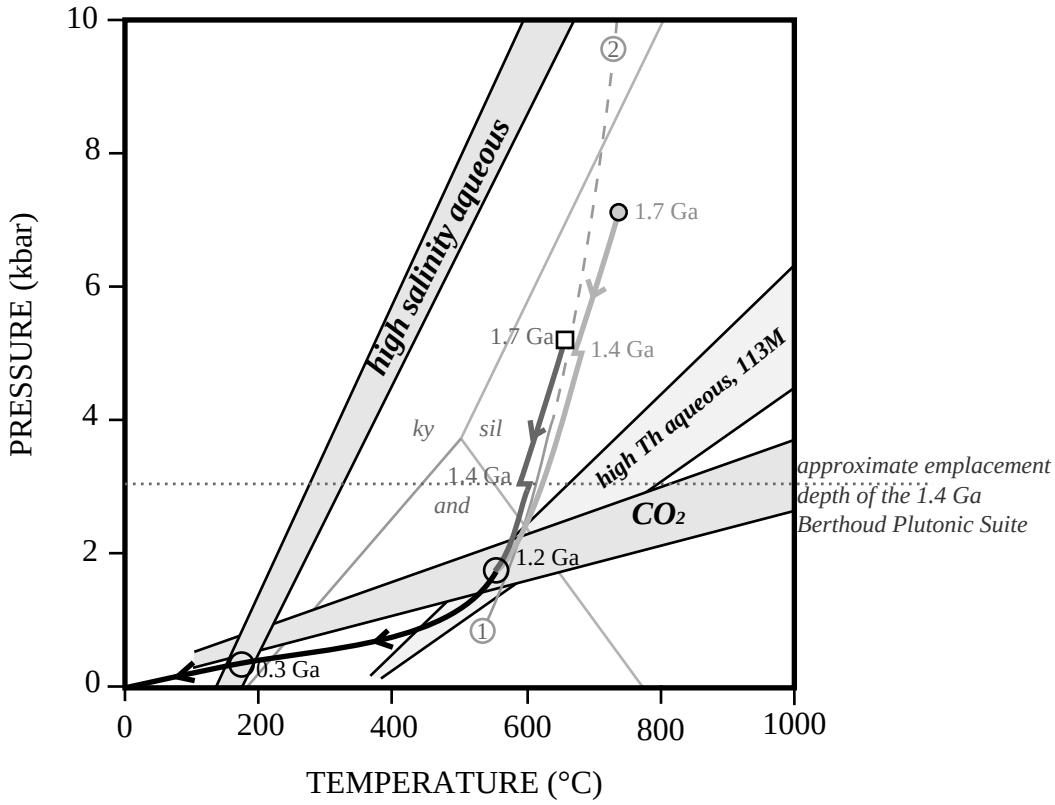

Figure 124 Pressure-temperature plot showing the uplift paths followed by the higher pressure block (filled circle) and the lower pressure block (square). Episodes of fluid-trapping are circled. The univariant reaction curves for muscovite breakdown (1 and 2) are after Thompson and Tracy (1979). The aluminosilicate fields are after Holloway and Mukhopadhyay (1993).

about 750°C, Anderson and Thomas, 1985). The slight heat pulse accompanying intrusion reset K-Ar ages (Tweto, 1987 and Reed and Snee, 1991), and initiated some of the recrystallization textures observed in the migmatites, destroying more fluid inclusions. Stretching and leakage of the primary fluid inclusions released H_2O back in to the interstitial fluid. The H_2O allowed the retrograde hydration of K–feldspar to form the secondary muscovite common in the lower pressure block. The position of the retrograde reaction,

$$K\text{-}feldspar + aluminosilicate + H_2O = muscovite + albite + quartz$$

is indicated on Figure 124 (reaction 1). Note that the uplift path taken by the lower pressure block allowed it to overstep this reaction. Thus, local addition of water could easily cause the retrograde formation of muscovite. On the other hand, the proposed uplift path taken by the higher pressure block keeps to the high temperature side of the reaction during much of the isothermal decompression. This explains why secondary muscovite is relatively rare in the higher pressure block.

Uplift, internal overpressuring and re-equilibration continued until 1.2±0.2 Ga when an extensive episode of ductile shearing affected the entire Front Range. At this time the rocks in the active shear zones were locally recrystallized and retrogressed to andalusite-cordierite assemblages (Wells et al., 1964; Abbott, 1970, 1976; Nesse, 1977). Thus, the uplift path must have crossed into the andalusite field, as shown in Figure 124. By this time hydration reactions had caused the remaining aqueous fluid to became more saline. The increased salinity caused the two phase H_2O-CO_2 field to enlarge producing immiscible fluids at the conditions proposed for ductile shearing. The pure CO_2 inclusions (remnants of the peak metamorphic fluid) most likely were trapped in both blocks at this time, implying near juxtaposition of the two blocks by 1.2 Ga, as indicated by the converging uplift paths (Figure 124). The location of this trapping event in pressure-temperature space is further constrained to approximately 560°C and 1.7 kbar by the high Th, 10-26 weight percent aqueous fluids which were trapped in sample 113M along with CO_2.

Subsequent to ductile shearing, the northern Front Range remained tectonically quiescent and followed an isobaric cooling path, subparallel to the CO_2 isochores, as shown in Figure 124. Renewed uplift began in the Pennsylvanian (0.3 Ga) when the Ancestral Rockies were built. This period of active mountain building is recognized by thick accumulations of clastic sediment (DeVoto, 1980). The major uncomformity related to this tectonism can be observed in the southeastern corner of the study area where the Upper Pennsylvanian age Fountain Formation overlies the Precambrian basement rocks of the higher pressure block (labeled “sedimentary cover” in Figure 2; Braddock et al., 1988b). The high salinity NaCl-$CaCl_2$-H_2O fluid probably was trapped at this time, as indicated in Figure 124. Since the rocks now lay at fairly shallow depths, these fluids may have been surface-derived, perhaps infiltrating down to deeper levels during Pennsylvanian tectonism. In addition, some of the fluid could represent the re-equilibrated aqueous component of the metamorphic fluids that became more saline by losing H_2O during uplift (Crawford et al., 1979; Touret, 1981).

The latest mountain-building episode in the Front Range was the Late Cretaceous to Eocene Laramide Orogeny which brought these basement rocks to their present position. In the vicinity of the Poudre Canyon, the Laramide structures are characterized by a series of northeast-dipping faults which bring the basin side of the orogen up relative to the mountains (Erslev et al., 1988). This counter-intuitive observation is explained by Erslev et al. (1988) as a series of backthrusts which lie above a westward dipping master thrust that remains unexposed in this region of the

Front Range (see Erslev et al., Figure 9). The presence of annular inclusions in the lower pressure block appears to justify an interpretation of a late, westward-directed loading event in this area. Thus, the annular inclusions may record the back thrusting associated with the Laramide Orogeny in which portions of the higher pressure block were thrust to the west over the lower pressure block to bring the two blocks to their final relative positions. This interpretation awaits analysis of the Laramide structures which is beyond the scope of the original intent of this study.

VIII. CONCLUSIONS

Estimates of peak metamorphic conditions in the northern Front Range by previous authors (630-670°C and 3-4.5 kbar; Abbott, 1970; Nesse, 1977; Olsen 1987) have been confined to fairly low pressure conditions in keeping with the cordierite commonly observed in amphibolite facies pelites west of Golden, Colorado (Gable and Sims, 1969; Tweto, 1987). However, none of the rocks in the Poudre Canyon display the extensive development of cordierite in pelitic rocks observed farther south in the central Front Range. In the Poudre Canyon, cordierite only occurs in rare magnesium-enriched pelite bulk compositions. This suggests that metamorphism of the northern Front Range may be fundamentally different from that of the central Front Range, and indeed, the results of this study indicate higher pressure conditions for metamorphism of the Poudre Canyon rocks.

By combining thermobarometric calculations with detailed petrography and fluid inclusion analysis, the peak and post-peak history of this high-grade metamorphic terrane was successfully quantified. Pressure-temperature calculations identify the presence of two major blocks within the Poudre Canyon, the down canyon (eastern) higher pressure block (HPB; 734°C, 7.1 kbar) and the up canyon (western) lower pressure block (LPB; 655°C, 5.2 kbar). Both blocks experienced peak metamorphism within the sillimanite-K-feldspar zone and underwent partial melting. Both show evidence for localized reactions related to decompression and cooling. The differences between the two blocks lie in the melting reactions which led to anatexis in each, and in the more pronounced evidence for late static crystallization of muscovite in the LPB. These differences appear to be related to the position of the blocks in pressure-temperature space both during peak metamorphism and during subsequent uplift and cooling.

Figures 125 and 126 show the proposed uplift paths for the LPB and HPB in pressure-temperature and pressure-time space, respectively. Although originally metamorphosed at different depths, both blocks belong to the same terrane and, hence, initially followed similar paths while maintaining their separate positions in the crust. Little is known about the prograde portion of the path, the hypothetical position of which is dashed in Figure 125. Garnet, the usual source of information about prograde metamorphism, shows no evidence for lower grade inclusions or appreciable growth zoning in either block. Textural and chemical evidence suggest that garnet grew at high temperature, continuously re-equilibrating up to peak conditions. Rare grains of relict staurolite preserved in plagioclase suggest that some of the garnet growth was driven by staurolite breakdown.

At 1.7 Ga, peak regional metamorphism produced the upper amphibolite facies assemblages observed in the rocks from both blocks. Both blocks underwent partial melting which was controlled by rock type and by their respective pressure-temperature positions relative to the melt-forming reactions (Figure 125). The LPB, composed largely of quartzo-feldspathic biotite gneisses, generated migmatites primarily by wet melting processes. Muscovite dehydration was possible in the less common pelites in this block, however, the pressure-temperature conditions of peak metamorphism precluded melting by biotite dehydration. The HPB, which experienced peak metamorphism at higher temperatures and pressures and in which pelitic schists and gneisses are more common, generated migmatites primarily by dehydration melting of both muscovite and biotite. As a result, many of the leucosomes found in HPB pelites are enriched in K-feldspar and garnet, the byproducts of biotite dehydration.

Sillimanite zone metamorphism accompanied by anatexis and followed by nearly isothermal decompression fits the pattern predicted for a terrane thickened by a collisional orogeny and exhumed by subsequent uplift and erosion (England and Thompson, 1984; Thompson and England, 1984; Brown 1994). The collision in this case was between the Archean Wyoming

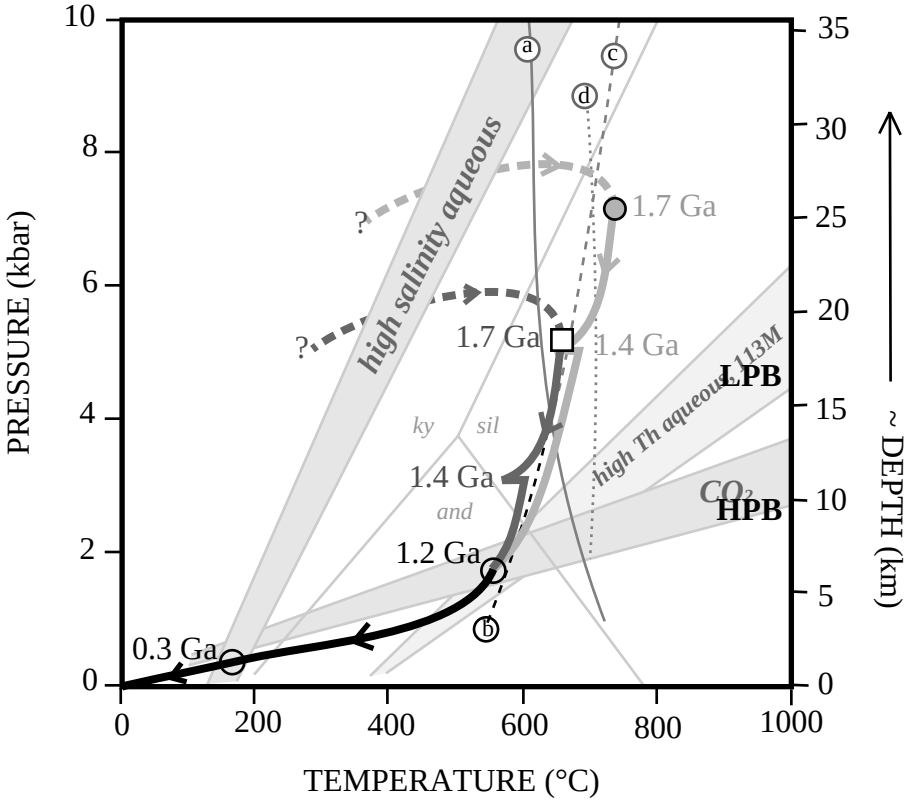

Figure 125 Pressure-temperature plot showing the uplift path followed by each block (thick lines; dark gray: lower pressure block, light gray: higher pressure block). The isochores for CO_2 and aqueous fluid inclusions trapped in major fluid trapping events (circled) are shown. The reactions for granite minimum melting (a), muscovite breakdown (b), muscovite dehydration melting (c) are after Thompson and Tracy (1979). Biotite dehydration (d) is after Clemens and Wall (1981) and the aluminosilicate univariant reaction lines are after Holdaway and Mukhopadhyay, 1993).

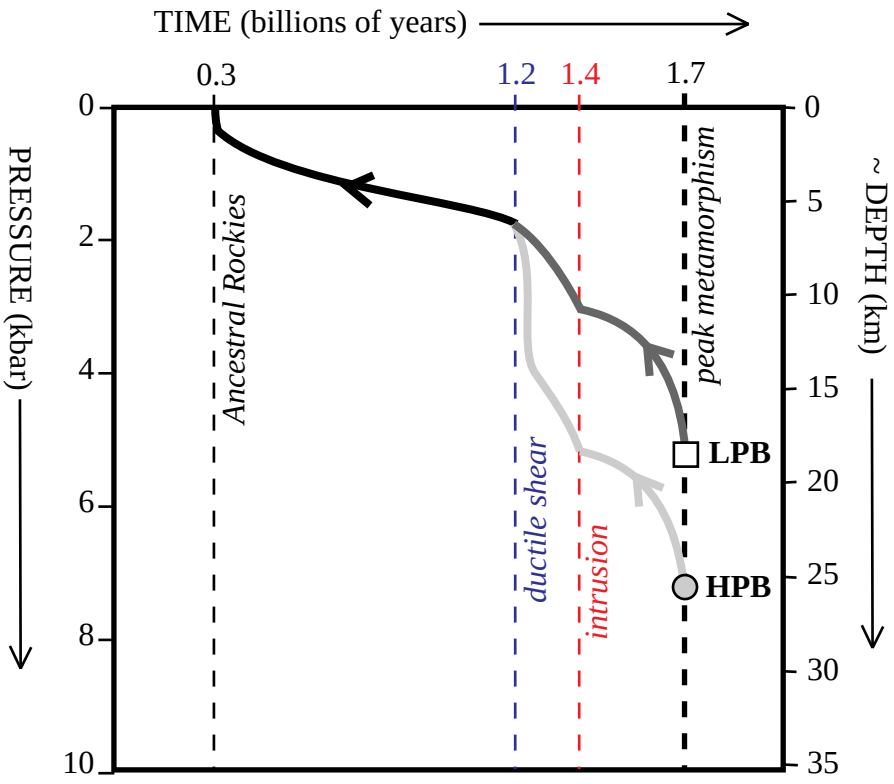

Figure 126 Pressure-time plot showing the schematic uplift paths followed by the lower pressure (LPB) and higher pressure (HPB) blocks.

terrane and the Colorado Province (Condie, 1982; Bickford et al., 1986; Reed et al., 1987). Isostatic rebound of the thickened orogenic belts led to erosion which perturbed the pre-collisional geotherm. In other words, erosion moved hot rocks toward the surface, producing higher temperatures than normal for a given depth. Consequently, sillimanite zone metamorphism and partial melting became possible (England and Richardson, 1977; England and Thompson, 1984). Calculations suggest that 15 to 30% of the migmatites in the Poudre Canyon were partially molten at peak metamorphism and that deformation accompanied anatexis and continued after the magma crystallized. The presence of a sizeable melt fraction would have softened the crust, perhaps intensifying the deformation experienced by these rocks. This intensified deformation produced the diverse fold types, necking and boudinage features, and cross-cutting leucosomes observed. Brown (1994) indicated that partial melting of strongly foliated, compositionally layered source rocks coupled with anisotropic stress regimes (as would likely be present in a collisional tectonic setting) would facilitate deformation-enhanced melt segregation leading to the formation of stromatic migmatites. Thus, the layer-parallel nature of the Poudre Canyon migmatites may be tied both to the heterogeneous nature of the source rocks, as documented by this study, and to the intense deformation experienced by this terrane.

The fluid present during peak metamorphism was probably a supercritical mixture of H_2O and CO_2. No primary fluid inclusions have been found and apparently none are preserved in these rocks due to the high internal overpressures produced in the fluid inclusions during decompression. However, isochores for pure CO_2 and dilute aqueous fluids cross the decompression path suggesting that these fluids are the re-equilibrated remnants of the peak fluid. The presence of a greater number of CO_2 inclusions in the HPB sample (113M) suggests that if the CO_2 does represent recycled peak fluid, then there may have been more CO_2 in the HPB fluid than in the LPB fluid. A higher proportion of CO_2 would mean a lower activity of H_2O and, thus, may explain, in part, why much of the anatexis in the HPB sample occurred by dehydration melting rather than wet melting.

Subsequent to peak metamorphism both blocks underwent a period of nearly isothermal decompression (Figures 125 and 126). Isothermal decompression of thickened orogenic belts results from uplift and erosion that take place faster than the rocks can cool down. Evidence for decompression in the Poudre Canyon includes resorbed garnets surrounded by coronas of anorthite-enriched plagioclase in average pelites and coronas of cordierite in Mg-enriched pelites. England and Thompson (1984) suggested that mountain chains are eroded within 50 to 200 million years. Assuming a maximum of 200 million years, then by 1.5 Ga, rapid decompression would have largely ended and cooling would have become dominant, as indicated in Figures 125 and 126 by the curvature of the paths prior to 1.4 Ga. Decompression and cooling was accompanied by localized cation exchange between ferromagnesian phases such as garnet and biotite and localized hydration reactions. The hydration reactions produced biotite and quartz (in addition to plagioclase) in garnet reaction coronas and muscovite (from K-feldspar). The source of the H_2O appears to be the aqueous component of the primary fluid inclusions. These fluid inclusions would have experienced almost two kbar of internal overpressure in both blocks by the time cooling began, leading to preferential leakage of H_2O (Vityk et al., 1994; Bakker and Jansen, 1993; Hall and Sterner, 1993). Cross muscovite probably began to form in the LPB at this time. The muscovite breakdown reaction is indicated for reference in Figure 125 (black dashed reaction curve, labeled *b*). Note that the uplift path for the HPB remains on the high temperature side of the reaction. Thus, as late muscovite began to form in the LPB, the H_2O released in the HPB was used not to form muscovite, but instead to form biotite in garnet reaction coronas.

At 1.4 Ga, the Berthoud Plutonic Suite intruded the rocks of the present Front Range with an approximate emplacement pressure of 3 kbar (Anderson and Thomas, 1984). Since the LPB was

intruded by large volumes of this magma, the uplift path for the LPB is positioned at three kilobars 1.4 Ga ago (Figures 125 and 126). Intrusion at 1.4 Ga produced a slight thermal pulse, indicated by the horizontal movement of the uplift paths in Figure 125 toward higher temperature. The intrusion of such a voluminous body of hot magma must have thickened the crust and made it more buoyant. The consequent isostatic readjustment led to increased rates of erosion and renewed isothermal decompression (Figure 125). During decompression, internal overpressure within the remaining primary fluid inclusions continued to build. As more H_2O leaked out, garnet continued to be resorbed to form plagioclase-biotite-quartz coronas, and more secondary muscovite was formed in the LPB. The HPB still lay on the high temperature side of the muscovite breakdown reaction, thus, muscovite formation remained restricted to the LPB.

Rocks in both the HPB and the LPB trap equally dense CO_2 inclusions, believed to be the re-equilibrated remnants of the CO_2 component of the peak metamorphic fluid. Since the densities of these inclusions are identical, the two blocks must have been juxtaposed by the time of the final re-equilibration (thus enabling them to re-equilibrate the remnant CO_2 to the same conditions). In order for this to occur, the HPB must have moved upward relative to the LPB. The bulk of the HPB is separated from the LPB by the Skin Gulch Shear Zone (see Figure 62). This ductile shear zone is dated at 1.2±0.2 Ga and has a southeast side up sense of movement (Nesse, 1995). This sense of movement corroborates upward movement of the HPB relative to the LPB. Late production of andalusite is localized within portions of the Skin Gulch Shear Zone (Abbott, 1970, 1976; Nesse, 1977) suggesting that ductile shear occurred under andalusite zone conditions. In addition, the cross muscovite observed in the LPB is deformed within the Skin Gulch Shear Zone. Given these constraints, the uplift paths of the LPB and HPB must converge in the andalusite field on the low temperature side of the muscovite breakdown reaction by 1.2 Ga. It is likely that the high-Th aqueous fluid inclusions preserved in the sample from the HPB were trapped at the same conditions of final re-equilibration experienced by the CO_2 inclusions. Therefore, the convergence of the uplift path is restricted further to the intersection between the CO_2 isochores and the isochores for the high Th aqueous inclusions, as shown in Figure 125.

By 1.2 Ga, the rate of erosion of the orogen was substantially reduced. In addition, thermal relaxation of the geotherm, originally perturbed during collisional orogeny at 1.7 Ga and then perturbed again by the intrusion of the 1.4 Ga magmas, allowed cooling processes to control the position of the now combined uplift path. The cooling-decompression path must have been nearly parallel to the CO_2 isochores, as shown in Figure 125, thus allowing these fluid inclusions to maintain their densities as the rocks cooled. The proposed uplift paths delineated in Figure 125 show that the HPB crosses to the low temperature side of the muscovite breakdown reaction as significant decompression ceased, hence, late muscovite could begin to form in the HPB. Note that production of muscovite in the HPB was possible over a much shorter time span than in the LPB. Moreover, given the uplift path in Figure 125, the HPB cooled approximately 130°C between 1.4 and 1.2 Ga whereas the LPB only cooled about 50°C over the same period of time. Thus, the HPB experienced a cooling rate more than twice as fast as the LPB as it moved into position adjacent to the LPB. Consequently, it is possible that the HPB crossed the muscovite forming reactions too quickly to record extensive retrograde effects. The temporally limited presence of the HPB on the low temperature side of the muscovite breakdown reaction and the faster cooling rate experienced by the HPB may explain the limited development of muscovite in this block.

Following their assembly at 1.2 Ga, the combined blocks experienced a protracted period of cooling. The movement of the terrane to lower temperatures preserved the sillimanite zone assemblages and blocked further retrograde reaction. Final exposure of the two blocks at the surface occurred at about 320 Ma when the Ancestral Rockies were formed (DeVoto, 1980). A

high salinity NaCl-$CaCl_2$ aqueous fluid infiltrated the area and was trapped in both blocks at this time, as shown in Figure 125. At the time of Pennsylvanian tectonism the terrane lay at a depth of approximately 1 to 1.5 kilometers, therefore, these fluids probably were derived from the surface. As the fluid interacted with the rocks, the proportion of $CaCl_2$ within the fluid changed to reflect the rock chemistry prior to entrapment. The presence of late annular fluid inclusions in the LPB sample indicates that the LPB experienced an episode of compressive loading not apparent in the HPB. It may be that portions of the HPB were thrust over the LPB as part of a series of back thrusts similar to those proposed by Erslev et al. (1988) for the Late Cretaceous to Eocene Larimide Orogeny in the northern Front Range.

This study determined the pressure-temperature conditions of peak metamorphism and further identified the presence of blocks from two different crustal levels now exposed adjacent to one another. Anatexis of the blocks was controlled by pressure-temperature conditions, rock type, and availability of H_2O. Partial melting softened the crust and intensified the deformation. Decompression followed at high temperatures and is marked by reaction textures involving garnet. Primary fluid inclusions were completely re-equilibrated to lower pressure conditions during decompression, yet, the re-equilibrated fluid inclusions still retain compositional information about the peak metamorphic fluids. Fluids trapped subsequent to peak metamorphism (either as re-equilibrated fluids or as newly introduced fluids) were exceptionally helpful in accurately locating the uplift path in pressure-temperature space. This research also underscores the extreme care that must be used in applying thermobarometry to upper amphibolite facies metamorphic rocks. Detailed chemical analyses must be made in order to ascertain zoning patterns in individual minerals and changes in mineral compositions across a thin section. Differences in composition and zoning patterns may be related to late, localized exchange with neighboring phases, to the size and shape (intact or fragmented) of the phases (especially garnet) and to modal abundances of the key phases from sample to sample, or even from one part of a thin section to another. Finally, application of the Gibbs' Method can explain variable, or even seemingly contradictory, localized textures and mineral assemblages. Although not easy, studies of complex high grade metamorphic terranes, such as is exposed in the Poudre Canyon, can yield useful information about the processes affecting mid- to lower crustal basement rocks.

REFERENCES

Abbott, J.T., 1970, Geology of Precambrian Rocks and Isotope Geochemistry of Shear Zones in the Big Narrows Area, Northern Front Range, Colorado: *PhD Thesis, Univ. Colorado, Boulder*, 239p.

Abbott, J.T., 1976, Geologic map of the Big Narrows quadrangle, Larimer County, Colorado: *USGS Geologic Quadrangle*, GQ-1323, 1:24000.

Anderson, J.L., 1983, Proterozoic anorogenic granite plutonism of North America; *GSA Memoir 161*, 133-154.

Anderson, J.L. and Thomas, W.M., 1985, Proterozoic anorogenic two-mica granites: Silver Plume and St. Vrain batholiths of Colorado: *Geology*, 13, 177-180.

Arzi, A.A., 1978, Fusion kinetics, water diffusion and electrical conductivity in melting rock, interrelated: *J. Petrology*, 19, 153-169.

Ashworth, J.R., 1979, Comparative petrography of deformed and undeformed migmatites from the Grampian Highlands of Scotland: *Geological Magazine*, 116, 445-456.

Ashworth, J.R., 1985, Introduction, *in* Ashworth, J.R., ed., Migmatites: *Blackie*, London, 1-35.

Ashworth, J.R. and Chinner, G.A., 1978, Coexisting garnet and cordierite in migmatites from the Scottish Caledonides: *Contrib. Mineral. Petrol.*, 65, 370-394.

Bakker, R.J. and Jansen, J.B.H., 1994, A mechanism for preferential H_2O leakage from fluid inclusions in quartz, based on TEM observations: *Contrib. Mineral. Petrol.*, 116, 7-20.

Barker, A.J., 1989, Introduction to Metamorphic Textures and Microstructures: *Blackie*, London, p.38-39.

Barker, A.J., 1995, Post-entrapment modification of fluid inclusions due to overpressure: evidence from natural samples: *J. Metamorphic Geology*, 13, 737-750.

Barker, F., Wones, D.R., Sharp, W.N. and Desborough, 1975, The Pikes Peak batholith, Colorado Front Range, and a model for the origin of the gabbro-anorthosite-syenite-potassic granite suite: *Precambrian Research*, 2, 97-160.

Barr, D., 1985, Migmatites in the Moines, *in* Ashworth, J.R., ed., Migmatites: *Blackie*, London, 225-264.

Berman, R.G., 1990, Mixing properties of Ca-Mg-Fe-Mn garnets: *Am. Mineralogist*, 75, 328-344.

Berthé, D., Choukroune, P. and Jegouzo, P., 1979, Orthogneiss, mylonite and non-coaxial deformation of granites: The example of the South Armorican Shear Zone: *J. Structural Geol.*, 1, 31-42.

Bethune, P. de and Laduron, D., 1975, Diffusion processes in resorbed garnets: *Contrib. Mineral. Petrol.*, 50, 197-204.

Bhattacharya, A., Mazumdar, A.C. and Sen, S.K., 1988, Fe-Mg mixing in cordierite: Constraints from natural data and implications for cordierite-garnet geothermometry in granulites: *Am. Mineralogist*, 73, 338-344.

Bickford, M.E. and Boardman, S.J., 1984, A Proterozoic volcano-plutonic terrane, Gunnison and Salida areas, Colorado: *J. Geology*, 92, 657-666.

Bickford, M.E., Van Schmus, W.R. and Zietz, I., 1986, Proterozoic history of the midcontinent region of North America: *Geology*, 14, 492-496.

Bodnar, R.J., 1993, Revised equation and table for determining the freezing point depression of H_2O-NaCl solutions: *Geochim. Cosmochim. Acta*, 57, 683-684.

Bodnar, R.J., Binns, P.R. and Hall, D.L., 1989, Synthetic fluid inclusions - VI. Quantitative evaluation of the decrepitation behavior of fluid inclusions in quartz at one atmosphere confining pressure: *J. Metamorphic Geol.*, 7, 229-242.

Bodnar, R.J. and Vityk, M.O., 1994, Interpretation of microthermometric data for H_2O-NaCl fluid inclusions, *in*, De Vivo and Fezzotti, eds., Fluid Inclusions in Minerals: Methods and Applications: *Short Course of the Working Group (IMA) "Inclusions in Minerals,"* 117-130.

Borisenko, A.S., 1977, Study of the salt composition of solutions of gas-liquid inclusions in minerals by the cryometric method: *Geologiya i Geofizika*, 18, 16-27.
Bottinga, Y. and Richet, P., 1981, High pressure and temperature equation of state and calculation of the thermodynamic properties of gaseous carbon dioxide: *Am. J. Science*, 281, 615-660.
Boullier, A., France-Lanord, C., Dubessy, J., Adamy, J. and Champenois, M., 1991, Linked fluid and tectonic evolution in the High Himalaya mountains (Nepal): *Contrib. Mineral. Petrol.*, 107, 358-372.
Bowers, T.S. and Helgeson, H.C., 1983, Calculation of the thermodynamic and geochemical consequences of nonideal mixing in the system H_2O-CO_2-NaCl on phase relations in geologic systems: metamorphic equilibria at high pressures and temperatures: *Am. Mineralogist*, 68, 1059-1075.
Braddock, W.A., Abbott, J.T., Connor, J.J. and Swann, G.A., 1988a, Geologic map of the Poudre Park quadrangle, Larimer County, Colorado: *USGS Geologic Quadrangle*, GQ-1620, 1:24000.
Braddock, W.A., Connor, J.J, Swann, G.A. and Wohlford, D.D., 1988b, Geologic map of the LaPorte Quadrangle, Larimer County, Colorado: *USGS Geologic Quadrangle*, GQ-1621, 1:24000.
Brown, M., 1994, The generation, segregation, ascent and emplacement of granite magma: The migmatite-to-crustally-derived granite connection in thickened orogens: *Earth-Science Reviews*, 36, 83-130.
Brown, P.E. and Hagemann, S.G., 1994, MacFlinCor: A computer program for fluid inclusion data reduction and manipulation, *in*, De Vivo and Fezzotti, eds., Fluid Inclusions in Minerals: Methods and Applications: *Short Course of the Working Group (IMA) "Inclusions in Minerals,"* 231-250.
Burnham, D.W. and Davis, N.F., 1971, The role of H_2O in silicate melts I. P-V-T relations in the system $NaAlSi_3O_8$-H_2O to 10 kilobars and 1000°C: *Am. J. Science*, 270, 54-79.
Clemens, J.D. and Vielzeuf, D., 1987, Constraints on melting and magma production in the crust: *Earth & Planetary Sci. Letters*, 86, 287-306.
Clemens, J.D. and Wall, V.J., 1981, Origin and crystallization of some peraluminous (S-type) granitic magmas: *Can. Mineralogist*, 19, 111-131.
Collins, W.J. and Sawyer, E.W., 1996, Pervasive granitoid magma transfer through the lower-middle crust during non-coaxial compressional deformation: *J. Metamorphic Geology*, 14, 565-579.
Condie, K.C., 1982, Plate-tectonics model for Proterozoic continental accretion in the southwestern United States: *Geology*, 10, 37-42.
Crawford, M.L., 1981, Phase equilibria in aqueous fluid inclusions, *in*, Hollister,L.S. and Crawford, M.L., eds., A Short Course in Fluid Inclusions: Applications to Petrology: *Mineralogical Assoc. Canada*, Short Course Handbook 6, 75-100.
Crawford, M.L., Filer, J. and Wood, C., 1979, Saline fluid inclusions associated with retrograde metamorphism: *Bull. Minéral.*, 102, 562-568.
Crawford, M.L. and Hollister, L.S., 1986, Metamorphic fluids: the evidence from fluid inclusions, *in* Walther, J. and Wood, B.J., eds., Fluid-Rock Interactions during Metamorphism (Advances in Geochemistry, vol. 5): *Springer Verlag*, New York, 1-35.
Dallmeyer, R.D., 1974, The role of crystal structure in controlling the partitioning of Mg and Fe^{2+} between coexisting garnet and biotite: *Am. Mineralogist*, 59, 201-203.
Davis, D.W., Lowenstein, T.K., and Spencer, R.J., 1990, Melting behavior of fluid inclusions in laboratory-grown halite crystals: *Geochim. Cosmochim. Acta*, 54, 591-602.
Deer, W.A., Howie, R.A. and Zussman, J., 1962a, The Rock-Forming Minerals, vol. 1, Ortho- and Ring Silicates: *John Wiley and Sons*, 183-210.
Deer, W.A., Howie, R.A. and Zussman, J., 1962b, The Rock-Forming Minerals, vol. 3, Sheet Silicates: *John Wiley and Sons*, 263-266.

Deer, W.A., Howie, R.A. and Zussman, J., 1992, An Introduction to the Rock-Forming Mineral, Second Edition: *Longman Scientific & Technical*, 696p.
De Paolo, D.J., 1981, Neodymium isotopes in the Colorado Front Range and crust-mantle evolution in the Proterozoic: *Nature*, 291, 193-196.
De Voto, R.H., 1980, Pennsylvanian stratigraphy and history of Colorado, *in* Kent, H.C. and Porter, K.W., eds., Colorado Geology: *Rocky Mountain Assoc. Geologists*, Denver, 71-101.
Dixon, J. and Williams, G.D., 1983, Brittle-ductile processes in granitoid mylonites: *J. Geol. Soc. London*, 140, 841.
Duebendorfer, E.M. and Houston, R.S., 1986, Kinematic history of the Cheyenne Belt, Medicine Bow Mountains, southeastern Wyoming: *Geology*, 14, 171-174.
Ellis, D.J. and Green, D.H., 1979, An experimental study of the effect of Ca upon garnet-clinopyroxene Fe-Mg exchange equilibria: *Contrib. Min. Petrol.*, 71, 13-22.
England, P.C. and Richardson, S.W., 1977, The influence of erosion upon the mineral facies of rocks from different metamorphic environments: *J. Geol. Soc. London*, 134, 201-213.
England, P.C. and Thompson, A.B., 1984, Pressure-temperature-time paths of regional metamorphism I. Heat transfer during the evolution of regions of thickened continental crust: *J. Petrology*, 25, 894-928.
Erslev, E.A., Rogers, J.L. and Harvey, M., 1988, The northeastern Front Range revisited: Horizontal compression and crustal wedging in a classic locality for vertical tectonics, *in* Holden, G.S., ed., Geological Society of America Fieldtrip Guidebook: *Professional Contributions - Colorado School of Mines*, number 12, 122-133.
Essene, E.J., 1982, Geologic thermometry and barometry, *in*, Ferry, J.M., ed., Characterization of Metamorphism through Mineral Equilibria: *MSA Reviews in Mineralogy*, 10, 153-206.
Ferry, J.M., 1980, A comparative study of geothermometers and geobarometers in pelitic schists from south-central Maine: *Am. Mineralogist*, 65, 720-732.
Ferry, J.M. and Spear, F.S., 1978, Experimental calibration of the partitioning of Fe and Mg between biotite and garnet: *Contrib. Mineral. Petrol.*, 66, 113-117.
Finch, J., Gainsford, A.R., and Tennant, W.C., 1982, Polarized optical absorption and ^{57}Fe Mössbauer study of pegmatitic muscovite: *Am. Mineralogist*, 67, 59-68.
Florence, F.P. and Spear, F.S., 1991, Effects of diffusional modification of garnet growth zoning on P-T path calculations: *Contrib. Mineral. Petrol.*, 107, 487-500.
Frost, B.R. and Chacko, T., 1989, The granulite uncertainty principle: limitations on thermobarometry in granulites: *J. Geology*, 97, 435-450.
Frost, B.R. and Tracy, R.J., 1991, P-T paths from zoned garnets: some minimum criteria: *Am. J. Science*, 291, 917-939.
Goldman, D.S. and Albee, A.L., 1977, Correlation of Mg/Fe partitioning between garnet and biotite with $^{18}O/^{16}O$ partitioning between quartz and magnetite: *Am. J. Science*, 277, 750-767.
Goldstein, R.H. and Reynolds, T.J., 1994, Systematics of Fluid Inclusions in Diagenetic Minerals: *SEPM Short Course 31*, 199 pp.
Graham, C.M. and Powell, R., 1984, A garnet-hornblende geothermometer: Calibration, testing, and application to the Pelona Schist, southern California: *J. Metamorphic Geology*, 2, 13-31.
Grant, J.A., 1973, Phase equilibria in high-grade metamorphism and partial melting of pelitic rocks: *Am. J. Science*, 273, 289-317.
Grant, J.A., 1985, Phase equilibria in partial melting of pelitic rocks, *in* Ashworth, J.R., ed., Migmatites: *Blackie*, London, 86-144.
Grant, J.A. and Weiblen, P.W., 1971, Retrograde zoning in garnet near the second sillimanite isograd: *Am. J. Science*, 270, 281-196.
Graubard, C., 1991, Extension in a transpressional setting; Emplacement of the Mid-Proterozoic Mt. Evans batholith, central Front Range, Colorado: *GSA Abs/Prog.*, 23, p.27.

Guidotti, C.V., 1984, Micas in metamorphic rocks, *in*, Bailey, S.W., ed., Micas: *Reviews in Mineralogy*, 13, 357-418.
Guidotti, C.W., Cheney, J.T. and Guggenheim, S., 1977, Distribution of titanium between coexisting muscovite and biotite in pelitic schists from northwestern Maine: *Am. Mineralogist*, 62, 438-448.
Hall, D.L., Sterner, S.M. and Bodnar, R.J., 1988, Freezing point depression of NaCl-KCl-H_2O solutions: *Economic Geology*, 83, 197-202.
Hall, D.L. and Sterner, S.M., 1993, Preferential water loss from synthetic fluid inclusions: *Contrib. Mineral. Petrol.*, 114, 489-500.
Hand, M. and Dirks, P.H.G.M., 1992, The influence of deformation on the formation of axial-planar leucosomes and the segregation of small melt bodies within the migmatitic Napperby Gneiss, Central Australia: *J. Structural Geology*, 14, 591-604.
Hart, S.R., 1964, The petrology and isotopic-mineral age relations of a contact zone in the Front Range, Colorado: *J. Geology*, 72, 493-525.
Hashimoto, M., 1964, The chemistry and optics of prehnite: *J. Geol. Soc. Japan*, 70, 180-183.
Hedge, C.E., 1969, Petrogenetic and Geochronological Study of Migmatites and Pegmatites in the Central Front Range: *PhD Thesis, Colorado School of Mines.*
Hedge, C.E., 1972, Source of leucosomes of migmatites in the Front Range, Colorado: *GSA Memoir 132*, 65-72.
Hedge, C.E., Peterman, Z.E. and Braddock, W.A., 1967, Age of the major Precambrian regional metamorphism in the northern Front Range, Colorado: *GSA Bulletin*, 78, 551-558.
Hess, P.C., 1971, Prograde and retrograde equilibria in garnet-cordierite gneisses in south-central Massachusetts: *Contrib. Mineral. Petrol.*, 30, 177-195.
Hills, F.A. and Houston, R.S., 1979, Early Proterozoic tectonics of the central Rocky Mountains, North America: Contributions to Geology, Univ. Wyoming, 17, 89-109.
Hoisch, T.D., 1990, Empirical calibration of six geobarometers for the mineral assemblage quartz+muscovite+biotite+plagioclase+garnet: *Contrib. Mineral. Petrol.*, 104, 225-234.
Holdaway, M.J. and Lee, S.M., 1977, Fe-Mg cordierite stability in high-grade pelitic rocks based on experimental, theoretical, and natural observations: *Contrib. Mineral. Petrol.*, 63, 175-198.
Holdaway, M.J. and Mukhopadhyay, B., 1993, A reevaluation of the stability relations of andalusite: Thermochemical data and phase diagram for the aluminum silicates: *Am. Mineralogist*, 78, 298-315.
Hollister, L.S., 1977, The reaction forming cordierite from garnet, the Khtada Lake Metamorphic Complex, British Columbia: *Can.Mineralogist*, 15, 217-229.
Hollister, L.S., 1988, On the origin of CO_2-rich fluid inclusions in migmatites: *J. Metamorphic Geol.*, 6, 467-474.
Hollister, L.S., 1990, Enrichment of CO_2 in fluid inclusions in quartz by removal of H_2O during crystal-plastic deformation: *J. Structural Geol.*, 12, 895-901.
Holtz, F., Pichavant, M., Barbey, P. and Johannes, W., 1992, Effects of H_2O on liquidus phase relations in the haplogranite system at 2 and 5 kbar: *Am. Mineralogist*, 77, 1223-1241.
Johannes, W., 1984, Beginning of melting in the granite system Az-Or-Ab-An-H2O: *Contrib. Mineral. Petrol.*, 86, 264-273.
Johannes, W., 1985, The significance of experimental studies for the formation of migmatites, *in* Ashworth, J.T., ed., Migmatites: *Blackie*, London, 36-85.
Johannes, W., 1988, What controls partial melting in migmatites?: *J. Metamorphic Geology*, 6, 451-465.
Johannes, W. and Holtz, F., 1990, Formation and composition of H_2O-undersaturated granitic melts, *in* Ashworth, J.R. and Brown, M., High-temperature Metamorphism and Crustal Anatexis: *Mineralogical Society Great Britain and Ireland, series 2*, London, 87-104.

Johnson, E.L. and Hollister, L.S., 1995, Syndeformational fluid trapping in quartz: determining the pressure-temperature conditions of deformation from fluid inclusions and the formation of pure CO_2 fluid inclusions during grain-boundary migration: *J. Metamorphic Geol.*, 13, 239-249.

Karlstrom, K.E. and Houston, R.S., 1984, The Cheyenne Belt: Analysis of a Proterozoic suture in southern Wyoming: *Precambrian Research*, 25, 415-446.

Kerrich, R., 1976, Some effects of tectonic recrystallization on fluid inclusions in vein quartz: *Contrib. Mineral. Petrol.*, 59, 195-202.

Kerrick, D.M., 1972, Experimental determination of muscovite + quartz stability with $P_{H2O}=P_{total}$: *Am. J. Science*, 272, 946-958.

Kohn, M.J. and Spear, F.S., 1990, Two new geobarometers for garnet amphibolites, with applications to southeastern Vermont: *Am. Mineralogist*, 75, 89-96.

Koziol, A.M., 1989, Recalibration of the garnet-plagioclase-Al_2SiO_5-quartz (GASP) geobarometer and application to natural parageneses: *EOS, Trans. Am. Geophys. Union*, 70, p.493.

Koziol, A.M. and Newton, R.C., 1988a, Redetermination of the anorthite breakdown reaction and improvement of the plagioclase-garnet-Al_2SiO_5-quartz geobarometer: *Am. Mineralogist*, 73, 216-233.

Koziol, A.M. and Newton, R.C., 1988b, The activity of grossular in ternary (Ca, Mg, Fe) garnet determined by reversed phase equilibrium experiments at 1000°C and 900°C: *GSA Abs/Prog.*, 20, A191.

Lamb, W.M., 1990, Fluid inclusions in granulites: Peak vs. retrograde formation, *in* Vielzeuf, D. and Vidal, Ph., eds., Granulites and Crustal Evolution: *Kluwer Academic Publishers*, The Netherlands, 419-433.

Lamb, W.M., Valley, J.W. and Brown, P.E., 1987, Post metamorphic CO_2-rich fluid inclusions in granulites: *Contrib. Mineral. Petrol.*, 96, 485-495.

Leake, B.E., 1978, Nomenclature of amphiboles: *Canadian Mineralogist*, 16, 501-520.

Le Breton, N. and Thompson, A.B., 1988, Fluid-absent (dehydration) melting of biotite in metapelites in the early stages of crustal anatexis: *Contrib. Mineral. Petrol.*, 99, 226-237.

Liou, H.S.K. and Maruyama, S., 1983, Prehnite-epidote equilibria and their petrologic applications: *J. Petrology*, 24, 321-342.

Liou, J.G., 1971, Synthesis and stability relations of prehnite, $Ca_2Al_2Si_3O_{10}(OH)_2$: *Am. Mineralogist*, 56, 507-531.

Loomis, T.P., 1975, Reaction of zoning of garnet: *Contrib. Mineral. Petrol.*, 52, 285-305.

Luth, W.C., 1976, Granitic Rocks, *in* Bailey, D.K. and MacDonald, R., The Evolution of Crystalline Rocks: *Academic Press*, New York, p.335-417.

McLellan, E.L., 1983, Contrasting textures in metamorphic and anatectic migmatites: an example from the Scottish Caledonides: *J. Metamorphic Geol.*, 1, 241-262.

McLellan, E.L., 1984, Deformational behavior of migmatites and problems of structural analysis in migmatite terrains: *Geol. Magazine*, 121, 339-345.

McLellan, E.L., 1989, Sequential formation of subsolidus and anatectic migmatites in response to thermal evolution, eastern Scotland: *J. Geology*, 97, 165-182.

Mehnert, K.R., 1968, Migmatites and the Origin of Granitic Rocks: *Elsevier Publishing Company*, New York, 405p.

Mukhopadhyay, B. and Holdaway, M.J., 1994, Cordierite-garnet-sillimanite-quartz equilibrium: I. New experimental calibration in the system FeO-Al_2O_3-SiO_2-H_2O and certain P-T-x_{H2O} relations: *Contrib. Mineral. Petrol.*, 116, 462-472.

Nesse, W.D., 1977, Geology and Metamorphic Petrology of the Pingree Park Area, Northeast Front Range, Colorado: *PhD thesis, Univ. Colorado, Boulder*, 214p.

Nesse, W.D., 1984, Metamorphic petrology of the northeast Front Range, Colorado: The Pingree Park area: *GSA Bulletin*, 95, 1158-1167.

Nesse, W.D., 1995, Sense of movement on Precambrian shear zones, northeast Front Range, Colorado: *GSA Abs/Prog.*, 27, 49-50.
Newton, R.C., 1966, Some calc-silicate equilibrium relations: *Am. J. Science*, 264, 204-222.
Newton, R.C. and Haselton, H.T., 1981, Thermodynamics of the garnet-plagioclase-Al_2SiO_5-quartz geobarometer, *in*, Newton, R.C. et al, eds., Thermodynamics of Minerals and Melts: *Springer Verlag*, New York, 131-147.
Nordstrom, D.K. and Munoz, J.L., 1986, Geochemical Thermodynamics: *Blackwell Scientific Publications*, Palo Alto, 477p.
Nyman, M.W., Karlstrom, K.E., Kirby, E. and Graubard, C.M., 1994, Mesoproterozoic contractional orogeny in western North America: Evidence from ca. 1.4 Ga plutons: *Geology*, 22, 901-904.
Oakes, C.S., Bodnar, R.J. and Simonson, J.M., 1990, The system NaCl-$CaCl_2$-H_2O: I. The ice liquidus at 1 atm total pressure: *Geochim Cosmochim. Acta*, 54, 603-610.
Oakes, C.S., Sheets, R.W., Bodnar R.J., and Simonson, J.M., 1992, (NaCl + $CaCl_2$){aq}: Phase equilibria and volumetric properties: *Fourth Pan-American Conference on Research on Fluid Inclusions Program and Abstracts*, Lake Arrowhead, California.
Ohmoto, H. and Kerrick, D., 1977, Devolatilization equilibria in graphitic systems: *American J. Science*, 277, 1013-1044.
Olsen, S.N., 1982, Open- and closed-system migmatites in the Front Range, Colorado: *Am. J. Science*, 282, 1596-1622.
Olsen, S.N., 1984, Mass-balance and mass-transfer in migmatites from the Colorado Front Range: *Contrib. Mineral. Petrol.*, 85, 30-44.
Olsen, S.N., 1985, Mass balance in migmatites, *in* Ashworth, J.R., ed., Migmatites: *Blackie*, London, 145-179.
Olsen, S.N., 1987, The composition and role of the fluid in migmatites: A fluid inclusion study of the Front Range rocks: *Contrib. Mineral. Petrol.*, 96, 104-120.
Olsen, S.N., 1988, High-density CO_2 inclusions in the Colorado Front Range: *Contrib. Mineral. Petrol.*, 100, 226-235.
Olsen, S,.N. and Grant, J.A., 1991, Isocon analysis of migmatization in the Front Range, Colorado, USA: *J. Metamorphic Geol.*, 9, 151-164.
Pêcher, A., 1981, Experimental decrepitation and reequilibration of fluid inclusions in synthetic quartz: *Tectonophysics*, 78, 567-584.
Peterman, Z.E. and Hedge, C.E., 1967, Chronology of Precambrian events in the Front Range, Colorado: *Can. J. Earth Sci.*, 5, 749-756.
Peterman, Z.E., Hedge, C.E. and Braddock, W.A., 1968, Age of Precambrian events in the northeastern Front Range, Colorado: *J. Geophys. Research*, 73, 2277-2296.
Platt, J.P. and Vissers, R.L.M., 1980, Extensional structures in anisotropic rocks: *J. Structural Geology*, 2, 397-410.
Powell, R., 1983, Processes in granulite-facies metamorphism, *in* Atherton, M.P. and Gribble, C.D., eds., Migmatites, Melting and Metamorphism: *Shiva Publishing Limited*, Cheshire, 127-139.
Powell, R. and Downes, J., 1990, Garnet porphyroblast-bearing leucosomes in metapelites: mechanisms, phase diagrams, and an example from Broken Hill, Australia, *in*, Ashworth, J.R. and Brown, M., eds., High-Temperature Metamorphism and Crustal Anatexis: *Mineralogical Society of Great Britain and Ireland*, London, 105-123.
Premo, W.R. and Van Schmus, W.R., 1989, Zircon geochronology of Precambrian rocks in southeastern Wyoming and northern Colorado, *in* Grambling, J.A., and Tewksbury, B.J., eds., Proterozoic geology of the southern Rocky Mountains: *GSA Special Paper 235*, 13-32.
Raase, P., 1974, Al and Ti contents of hornblende, indicators of pressure and temperature of regional metamorphism: *Contrib. Mineral. Petrol.*, 45, 231-236.

Reed, J.C., Jr., Bickford, M.E., Premo, W.R., Aleinikoff, J.N. and Pallister, J.S., 1987, Evolution of the Early Proterozoic Colorado province: Constraints from U-Pb geochronology: *Geology*, 15, 861-865.

Reed, J.C., Jr., Bickford, M.E. and Tweto, O., 1993, Proterozoic accretionary terranes of Colorado and southern Wyoming, *in* Reed, J.C., Jr, Bickford, M.E., Houston, R.S., Link, P.K., Rankin, D.W., Sims, P.K. and Van Schmus, W.R., eds., Precambrian: Conterminous U.S., The Geology of North America, v.C-2: *The Geological Society of America, Inc.*, 211-228.

Reed, J.C., Jr. and Snee, L.W., 1991, 1.4-Ga deformational and thermal events in the central Front Range, Colorado: *GSA Abs/Prog.*, 23, p.58.

Robinson, P., Spear, F.S., Schumacher. J.C., Laird, J., Klein, C., Evans, B.W. and Doolan, B.L., 1982, Phase relations of metamorphic amphiboles: natural occurrence and theory, *in*, Veblen, D.R. and Ribbe, P.H., eds., Amphiboles: Petrology and Experimental Phase Relations: *MSA Reviews in Mineralogy*, 9B, 1–228.

Roedder, E., 1981, Origin of fluid inclusions and changes that occur after trapping, *in*, Hollister, L.S. and Crawford, M.J., eds., Fluid Inclusions: Applications to Petrology: *Mineralogical Association of Canada Short Course Handbook*, 6, 101-137.

Roedder, E., 1984, Fluid Inclusions: *Mineralogical Society of America Reviews in Mineralogy*, 12, 361-380.

Ross, R.J., Jr. and Tweto, O., 1980, Lower Paleozoic sediments and Tectonics in Colorado: *in* Kent, H.C. and Porter, K.W., eds., Colorado Geology: *Rocky Mountain Assoc. Geologists*, Denver, 47-56.

Rossman, G.R., 1984, Spectroscopy of micas, *in* Bailey, S.W., ed., Micas: *MSA Reviews in Mineralogy*, 13, 145-181.

Rubie, D.C. and Brearley, A.J., 1990, A model for rates of disequilibrium melting during metamorphism, *in* Ashworth, J.R. and Brown, M., High-temperature Metamorphism and Crustal Anatexis: *Mineralogical Society Great Britain and Ireland, series 2*, London, 57-86.

Sawyer, E.W., 1994, Melt segregation in the continental crust: *Geology*, 22, 1019-1022.

Selverstone, J. and Chamberlain, C.P., 1990, Apparent isobaric cooling paths from granulites: Two counterexamples from British Columbia and New Hampshire: *Geology*, 18, 307-310.

Selverstone, J., Hodgins, M. and Shaw, C.A., 1995, 1.4 versus 1.7 Ga metamorphism in the northern Colorado Front Range: A repeated history of post-accretion midcrustal heating: *GSA Abs/Prog*, National Meeting in New Orleans.

Shaver, K.C., Nesse, W.D. and Braddock, W.A., 1988, Geologic map of the Rustic quadrangle, Larimer County, Colorado: *USGS Geologic Quadrangle*, GQ-1619, 1:24000.

Shaw, C. A., 1995, $^{40}Ar/^{39}Ar$ Thermochronologic Constraints on the Middle Proterozoic Geologic History of the Big Thompson Canyon area, Colorado Front Range: *MS Thesis, Univ. Colorado, Boulder*.

Shaw, C. A., Snee, L.W., Reed, J.C., Jr. and Selverstone, J., 1995, $^{40}Ar/^{39}Ar$ data identify transient ~1.4 Ga thermal event related to mid-Proterozoic metamorphism in the Colorado Front Range: *GSA Abs/Prog*, National Meeting in New Orleans.

Sims, P.K. and others, 1963, Geology of uranium and associated ore deposits central part of the Front Range mineral belt, Colorado: *USGS Prof. Paper 371*, 119pp.

Sims,P.K. and Sheridan, D.M., 1964, Geology of uranium deposits in the Front Range, Colorado: *USGS Bulletin*, 1159, 116pp.

Spear, F.S., 1981, An experimental study of hornblende stability and compositional variability in amphibolite: *Am. J. Science*, 281, 697-734.

Spear, F.S., 1988, Metamorphic fractional crystallization and internal metasomatism by diffusional homogenization of zoned garnets: *Contrib. Mineral. Petrol.*, 99, 507-517.

Spear, F.S., 1991, On the interpretation of peak metamorphic temperatures in light of garnet diffusion during cooling: *J. Metamorphic Geology*, 9, 379-388.

Spear, F.S., 1993, Metamorphic Phase Equilibria and Pressure-Temperature-Time Paths: *MSA Monograph Series*, 1, 799pp.
Spear, F.S., Ferry, J.M. and Rumble III, D., 1982, Analytical formulation of phase equilibria: The Gibbs' Method, *in*, Ferry, J.M., ed., Characterization of Metamorphism through Mineral Equilibria: *MSA Reviews in Mineralogy*, 10, 105-152.
Spear, F.S., Kohn, M.J., Florence, F.P. and Menard, T., 1990, A model for garnet and plagioclase growth in pelitic schists: implications for thermobarometry and P-T path determinations: *J. Metamorphic Geology*, 8, 683-696.
Spear, F.S. and Florence, F.P., 1992, Thermobarometry in granulites: pitfalls and new approaches: *Precambrian Research*, 55, 209-241.
Spry, A., 1969, Metamorphic Textures: *Pergamon Press*, London, 350p.
Steiger, R.H. and Jager, E., 1977, Subcommission on Geochronology - Convention and use of decay constants in geo- and cosmochronology: *Earth and Planetary Sci. Letters*, 36, 359-362.
Sterner, S.M. and Bodnar, R.J., 1989, Synthetic fluid inclusions VII. Re-equilibration of fluid inclusions in quartz during laboratory-simulated metamorphic burial and uplift: *J. Metamorphic Geol.*, 7, 243-260.
Sterner, S.M., Hall, D.L. and Bodnar, R.J., 1988, Synthetic fluid inclusions: V. solubility relations in the system NaCl-KCl-H_2O under vapor-saturated conditions: *Geochim. Cosmochim. Acta*, 52, 989-1006.
Thompson, A.B., 1976a, Mineral reactions in pelitic rocks: I. Prediction of P-T-x(Fe-Mg) phase relations: *Am. J. Science*, 276, 401-424.
Thompson, A.B., 1976b, Mineral reactions in pelitic rocks: II. Calculation of some P-T-x(Fe-Mg) phase relations: *Am. J. Science*, 276, 425-454.
Thompson, A.B., 1982, Dehydration melting of pelitic rocks and the generation of H_2O-undersaturated granitic liquids: *Am. J. Science*, 282, 1567-1595.
Thompson, A.B., 1990, Heat, fluids, and melting in the granulite facies, *in*, Vielzeuf, D. and Vidal, Ph., eds, Granulites and Crustal Evolution: *Kluwer*, 37-57.
Thompson, A.B. and Connolly, J.A.D., 1990, Crustal anatexis in orogenic belts: modeling constraints on fluid behavior and melt generation: *EOS Trans., Am. Geophys. Union*, 71, p.650.
Thompson, A.B. and England, P.C., 1984, Pressure-temperature-time paths of regional metamorphism II. Their influence and interpretation using mineral assemblages in metamorphic rocks: *J. Petrology*, 25, 929-955.
Thompson, A.B. and Tracy, R.J., 1979, Model systems for anatexis of pelitic rocks, II. Facies series melting and reactions in the system CaO-$KAlO_2$-$NaAlO_2$-Al_2O_3-H_2O: *Contrib. Mineral. Petrol.*, 70, 429-438.
Touret, J., 1981, Fluid inclusions in high grade metamorphic rocks, *in* Hollister.L.S. and Crawford, M.L., eds., A Short Course in Fluid Inclusions: Applications to Petrology: *Mineralogical Assoc. Canada*, Short Course Handbook 6, 182-208.
Touret, J. and Olsen, S.N., 1985, Fluid inclusions in migmatites, *in* Ashworth, J.R., ed., Migmatites: *Blackie*, London, 265-288.
Tracy, R.J., 1978, High grade metamorphic reactions and partial melting in pelitic schist, west-central Massachusetts: *Am. J. Science*, 278, 150-178.
Tracy, R.J., 1982, Compositional zoning and inclusions in metamorphic minerals, *in*, Ferry, J.M., ed., Characterization of Metamorphism through Mineral Equilibria: *MSA Reviews in Mineralogy*, 10, 355-397.
Tracy, R.J. and Dietsch, C.W., 1982, High-temperature retrograde reactions in pelitic gneiss, central Massachusetts: *Canadian Mineralogist*, 20, 425-437.
Tracy, R.J., Robinson, P. and Thompson, A.B., 1976, Garnet composition and zoning in the determination of temperature and pressure of metamorphism, central Massachusetts: *Am. Mineralogist*, 61, 762-775.

Tuttle, O.F. and Bowen, N.L., 1958, Origin of granite in the light of experimental studies in the system $NaAlSi_3O_8$-$KAlSi_3O_8$-SiO_2-H_2O: *GSA Memoir 74*, 153p.
Tweto, O., 1960, Scheelite in the Precambrian gneisses of Colorado: *Economic Geology*, 55, 1406-1428.
Tweto, O., 1980a, Tectonic history of Colorado, *in* Kent, H.C. and Porter, K.W., eds., Colorado Geology: *Rocky Mountain Assoc. Geologists*, Denver, 5-9.
Tweto, O., 1980b, Precambrian Geology of Colorado, *in* Kent, H.C. and Porter, K.W., eds., Colorado Geology: *Rocky Mountain Assoc. Geologists*, Denver, 37-46.
Tweto, O., 1980c, Summary of Laramide Orogeny in Colorado, *in* Kent, H.C. and Porter, K.W., eds., Colorado Geology: *Rocky Mountain Assoc. Geologists*, Denver, 129-134.
Tweto, O., 1987, Rock units of the Precambrian basement in Colorado: *USGS Prof. Paper 1321-A*, 54p.
Vanko, D.A., Bodnar, R.J. and Sterner, S.M., 1988, Synthetic fluid inclusions: VIII. Vapor-saturated halite solubility in part of the system NaCl-$CaCl_2$-H_2O, with application to fluid inclusions from oceanic hydrothermal systems: *Geochim. Cosmo. Acta*, 52, 2451-2456.
Vityk, M.O. and Bodnar, R.J., 1995, Textural evolution of synthetic fluid inclusions in quartz during reequilibration, with applications to tectonic reconstructions: *Contrib. Mineral. Petrol.*, 121, 309-323.
Vityk, M.O., Bodnar, R.J. and Schmidt, C.S., 1994, Fluid inclusions as tectonothermo-barometers: Relation between pressure-temperature history and reequilibration morphology during crustal thickening: *Geology*, 22, 731-734.
von Platen, H., 1965, Experimental anatexis and genesis of migmatites, *in* Pitcher, W.S. and Flynn, G.W., eds., Controls of Metamorphism: *John Wiley & Sons, Inc.I, New York*, 203-218.
Watson, E.B. and Brenan, J.M., 1987, Fluids in the lithosphere, 1. Experimentally-determined wetting characteristics of CO_2-H_2O fluids and their implications for fluid transport, host-rock physical properties, and fluid inclusion formation: *Earth and Planetary Science Letters*, 85, 497-515.
Wells, J.D., Sheridan, D.M. and Albee, A.L., 1964, Relationship of Precambrian quartzite-schist sequence along Coal Creek to Idaho Springs Formation, Front Range, Colorado: *USGS Prof. Paper 454-O*, 25p.
Williams-Jones, A.E. and Samson, I.M., 1990, Theoretical estimation of halite solubility in the system NaCl-$CaCl_2$-H_2O: applications to fluid inclusions: *Canadian Mineralogist*, 28, 299-304.
Wobus, R.A. and Hutchinson, R.M., 1988, Proterozoic plutons and pegmatites of the Pikes Peak region, Colorado, *in* Holden, G.S., ed., GSA Fieldtrip Guidebook: *Prof. Contrib. - Colorado School of Mines*, 12, 35-42.
Wood, B.J. and Fraser, D.G., 1976, Elementary Thermodynamics for Geologists: *Oxford University Press*, 303p.
Woodsworth, G.J., 1977, Homogenization of zoned garnets from pelitic schists: *Can. Mineralogist*, 15, 230-242.
Yoder, H.S., 1968, Albite-anorthite-quartz-water at 5 kbar: *Yb. Carnegie Inst. Wash.*, 66, 477-478.
Yardley, B.W.D., 1989, An Introduction to Metamorphic Petrology: *Longman Scientific & Technical*, Essex, 248p.
Young, E. D., 1989, Petrology of biotite-cordierite-garnet gneiss of the McCullough Range, Nevada II. P-T-a_{H2O} path and growth of cordierite during late stages of low-P granulite-grade metamorphism: *J. Petrology*, 30, 61-78.
Zielinski, R.A., Peterman, Z.E, Stuckless, J.S., Rosholt, J.N. and Nkomo, I.T., 1981, The chemical and isotopic record of rock-water interaction in the Sherman Granite, Wyoming and Colorado: *Contrib. Mineral. Petrol.*, 78, 209-219.

APPENDIX A

Sample Locations
Mineral Assemblages

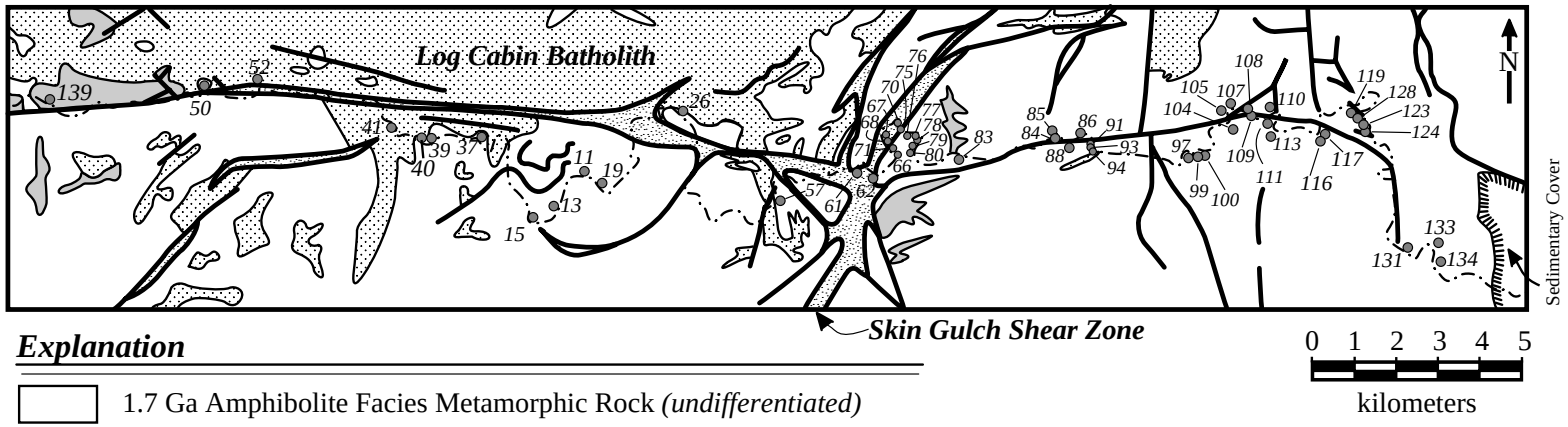

Figure A-1 Geologic sketch map of the study area showing the sample locations. *Map adapted from Abbott (1976), Braddock et al (1988a, 1988b) and Shaver et al (1988).*

TABLE A-1: Mineral Assemblages for Poudre Canyon thin sections

	11C	**13B**	**13F**	**13G**	**13H**	**13I**	***13K***	**13M**	**13N**	**13O**	**15A**	**19A**	***19C***	**19D**	**26B**	**37A**	**39A**	**41A**	***50A***	**50D**	**50E**	***52A***	***57A***	**57B**	**61A**	***62A***	**66A**
quartz	M	M	M	M	M	M	M	M	M	M	M	M	M	M	M	M	M	M	tr	m	M	m	M	m	M	a	M
plagioclase	m	M	M	M	M	M	m	M	*(ser)*	m	m	M	m	M	M	a	M	M	M	M	M	M	m	m	m	M	m
K-feldspar	m	-	-	M	M	m	-	tr	-	a	-	a	-	-	a	-	m	-	-	-	m	-	-	M	m	-	m
biotite	M	M	M	M	M	m	a	M	M	M	M	m	-	m	M	M	M	M	-	m	M	m	a	M	M	-	M
garnet	-	-	tr	-	-	-	-	-	-	-	-	-	-	tr	-	-	-	-	-	m	m	-	-	-	-	-	a
sillimanite	m	-	-	-	-	-	-	-	-	-	-	-	-	-	-	m	-	-	-	-	-	-	-	-	tr	-	tr
cordierite	-	-	-	-	-	-	-	-	-	-	-	-	-	-	-	-	-	-	-	-	-	-	-	-	-	-	-
relict staurolite	-	-	-	-	-	-	-	-	-	-	-	-	-	-	-	-	-	-	-	-	-	-	-	-	-	-	-
late muscovite	m	a	tr	tr	tr	a	-	-	-	a	a	-	-	a	-	a	tr	tr	-	-	-	-	-	m	a	-	a
late biotite	-	-	-	-	-	-	-	-	-	-	-	tr	-	-	-	-	-	-	-	-	-	-	-	a	-	-	-
opaques	tr	tr	tr	tr	tr	a	a	tr	a	tr	tr	-	tr	a	a	tr	a	-	tr	tr	a	a	tr	-	tr	a	tr
zircon	tr	tr	tr	tr	tr	tr	tr	tr	-	tr	tr	tr	-	tr	tr	tr	-	tr	-	-	tr	-	tr	tr	tr	-	tr
apatite	-	tr	a	tr	tr	tr	tr	tr	tr	tr	tr	tr	-	tr	-	-	tr	tr	-	tr	-	-	tr	-	-	tr	tr
rutile	-	-	-	-	-	-	-	-	-	-	-	-	-	-	-	-	-	-	-	-	-	-	-	-	-	-	-
hornblende	-	-	-	-	-	-	M	-	a	-	-	-	M	-	-	-	-	-	M	-	-	M	m	tr	-	M	-
diopside	-	-	-	-	-	-	-	-	-	-	-	-	-	-	-	-	-	-	-	-	-	-	-	-	-	m	-
titanite	-	-	-	-	-	-	tr	-	tr	-	-	-	tr	-	-	-	-	-	-	-	-	tr	a	-	-	a	-
primary calcite	-	-	-	-	-	-	-	-	-	-	-	-	-	-	-	-	-	-	-	-	-	-	-	-	-	-	-
allanite	-	-	-	-	-	-	-	-	-	-	-	-	-	-	-	-	-	-	-	-	-	-	-	-	-	-	-
clinozoisite	-	-	-	-	-	-	-	-	-	-	-	-	a	-	-	-	-	-	-	-	-	-	-	-	-	-	-
epidote	-	-	tr	-	-	-	tr	tr	a	-	tr	-	tr	tr	-	-	tr	-	-	-	-	tr	m	-	-	tr	tr
chlorite	a	-	-	-	-	-	-	-	-	-	m	tr	tr	tr	-	-	-	tr	-	-	-	-	-	-	-	-	-
actinolite	-	-	-	-	-	-	-	-	-	-	-	-	-	-	-	-	-	-	-	-	-	-	tr	-	-	-	-
prehnite	-	-	-	-	-	-	-	-	-	-	-	-	-	-	-	-	-	-	-	-	-	-	-	-	-	-	-
margarite?	-	-	-	-	-	-	-	-	-	-	-	-	-	-	-	-	-	-	-	-	-	-	-	-	-	-	-
sericite	-	-	tr	tr	tr	tr	tr	tr	m	tr	a	tr	tr	-	-	-	-	-	a	-	-	tr	a	-	-	a	tr
2ndy calcite	-	-	-	-	-	-	-	-	-	-	-	-	tr	-	-	-	-	-	-	-	-	-	a	-	-	a	tr

M=major (>10%) m=minor (≤10%) a=accessory (<5%) tr=trace (<0.5%) See figure A-1 for sample locations.

TABLE A-1 (continued): Mineral Assemblages for Poudre Canyon thin sections

	66C	**66D**	**67B**	**67C**	**68A**	***70D***	**71A**	**71B**	**75(9)**	**75A**	**76A**	**77B**	**78A**	**79A**	**80**	**83/1**	**83A**	**84B**	**84C**	***85A***	**86A**	**86D**	**88A**	**88B**	***91C***	**91D**	**93A**
quartz	M	M	M	M	M	a	M	M	M	M	M	M	M	M	M	M	M	M	M	m	M	M	M	M	a	M	M
plagioclase	M	m	M	tr	M	*(ser)*	m	a	a	m	a	a	*(ser)*	m	tr	tr	a	M	m	m	M	M	M	M	M	m	M
K-feldspar	m	m	-	a	m	-	-	-	-	-	m	-	m	M	-	-	-	-	a	-	-	a	-	-	-	M	a
biotite	M	m	m	M	M	-	M	m	M	m	M	-	m	m	M	M	M	m	M	-	m	m	m	M	-	a	M
garnet	a	-	m	-	m	-	a	m	-	-	-	-	-	-	m	-	-	-	-	-	m	m	a	a	-	-	a
sillimanite	-	-	a	m	-	-	-	-	m	-	-	-	-	-	-	a	tr	-	m	-	-	-	tr	-	-	-	-
cordierite	-	-	-	-	-	-	-	-	-	-	-	-	-	-	-	-	-	-	-	-	-	-	-	-	-	-	-
relict staurolite	-	-	-	-	-	-	-	-	-	-	-	-	-	-	-	-	-	-	-	-	-	-	-	-	-	-	-
late muscovite	tr	tr	a	a	-	-	tr	-	M	-	tr	-	tr	a	-	m	M	tr	m	-	-	-	-	-	-	-	a
late biotite	-	-	m	M	-	-	-	-	m	-	-	-	a	-	-	m	m	-	m	-	-	-	-	-	-	-	a
opaques	tr	tr	tr	tr	a	a	tr	tr	tr	a	tr	tr	tr	tr	m	tr	tr	tr	-	a	tr	a	tr	tr	a	tr	tr
zircon	tr	tr	tr	tr	tr	-	tr	tr	tr	tr	tr	tr	tr	tr	tr	tr	tr	tr	tr	tr	tr	tr	tr	tr	-	tr	tr
apatite	a	tr	-	-	tr	-	tr	-	-	-	-	-	tr	a	-	-	tr	-	tr	tr	-	tr	tr	-	tr	tr	
rutile	tr?	-	-	-	-	-	-	-	-	-	-	-	-	-	-	tr	-	-	-	-	-	-	-	-	-	-	-
hornblende	-	-	-	-	-	M	-	-	-	-	-	-	-	-	M	-	-	-	-	M	-	-	-	-	M	a	-
diopside	-	-	-	-	-	tr	-	-	-	-	-	-	-	-	-	-	-	-	-	-	-	-	-	-	m	m	-
titanite	-	-	-	-	-	a	-	-	-	-	-	a	tr	-	-	-	-	-	-	-	-	-	-	-	tr	a	-
primary calcite	-	-	-	-	-	-	-	-	-	-	-	-	-	-	-	-	-	-	-	-	-	-	-	-	m	-	-
allanite	-	-	-	-	-	-	-	-	-	-	-	-	-	-	-	-	-	-	-	-	-	-	-	-	-	-	-
clinozoisite	-	-	-	-	-	-	-	-	-	-	-	-	-	-	a	-	-	-	-	-	-	-	-	-	tr	tr	-
epidote	tr	tr	-	-	-	a	tr	-	-	-	-	M	a	-	-	-	-	-	-	-	-	-	-	-	-	-	tr
chlorite	-	-	-	-	-	-	-	-	-	-	-	-	-	-	-	-	tr	m	-	-	tr	-	tr	tr	-	-	tr
actinolite	-	-	-	-	-	-	-	-	-	-	-	m	-	-	-	-	-	-	-	-	-	-	-	-	-	-	-
prehnite	-	-	-	-	-	-	-	-	-	-	-	-	-	-	m	-	-	-	-	-	-	-	-	-	-	-	-
margarite?	-	-	-	-	-	-	-	-	-	-	-	-	-	-	-	-	-	-	-	-	-	-	-	-	-	-	-
sericite	tr	-	tr	tr	tr	M	a	tr	a	M	tr	tr	m	tr	a	a	-	tr	a	a	tr	-	-	tr	a	-	a
2ndy calcite	-	-	-	-	-	tr	-	-	-	-	-	a	a	-	-	-	-	-	-	-	-	-	-	-	-	tr	-

M=major (>10%) m=minor (≤10%) a=accessory (<5%) tr=trace (<0.5%) See figure A-1 for sample locations.

TABLE A-1 (continued): Mineral Assemblages for Poudre Canyon thin sections

	111I	13(4a	13(4b	113A	113B	113C	113E	113G	*113K*	113M	113P	113S	16(3a	16(3b	16(3c	116B	117A	119/5	119A	119B
quartz	M	M	M	M	M	M	M	M	m	M	M	m	M	M	M	M	M	M	M	M
plagioclase	M	M	m	a	m	m	m	m	M	a	M	M	m	M	a	M	-	M	m	m
K-feldspar	M	M	M	M	M	M	tr	a	-	M	-	-	m	a	M	a	-	-	m	m
biotite	m	M	M	m	M	M	M	M	-	M	M	a	m	m	m	M	-	M	M	M
garnet	tr	a	m	a	a	m	m	tr	-	a	m	-	m	a	a	m	-	-	a	a
sillimanite	a	m	m	a	m	m	m	a	-	m	-	-	a	-	a	-	-	-	a	m
cordierite	-	-	-	-	-	-	-	-	-	-	-	-	-	-	-	-	-	-	-	-
relict staurolite	-	-	-	-	-	-	-	-	-	-	-	-	-	-	-	-	-	-	-	-
late muscovite	tr	-	-	-	-	-	-	tr	-	-	-	-	-	-	-	-	-	tr	-	-
late biotite	-	-	-	-	-	-	-	tr	-	-	-	-	-	-	-	-	-	-	-	-
opaques	tr	-	tr	tr	tr	-	tr	tr	tr	tr	a	a	a	tr	-	tr	tr	tr	-	-
zircon	tr	tr	tr	tr	tr	tr	tr	tr	tr	tr	tr	tr	tr	tr	tr	tr	-	tr	tr	tr
apatite	-	-	-	-	-	tr	tr	tr	-	-	tr	tr	-	-	-	tr	-	tr	-	-
rutile	-	-	-	-	-	-	-	-	-	-	-	-	-	-	-	-	-	-	tr	-
hornblende	-	-	-	-	-	-	-	-	M	-	m	M	-	-	-	-	a	-	-	-
diopside	-	-	-	-	-	-	-	-	a	-	-	-	-	-	-	-	tr	-	-	-
titanite	-	-	-	-	-	-	-	-	-	-	-	-	-	-	-	-	-	-	-	-
primary calcite	-	-	-	-	-	-	-	-	-	-	-	-	-	-	-	-	M	-	-	-
allanite	-	-	-	-	-	-	-	-	-	-	-	-	-	-	-	-	-	-	-	-
clinozoisite	-	-	-	-	-	-	-	-	-	-	-	-	-	-	-	-	-	-	-	-
epidote	-	-	-	-	-	-	-	-	-	-	-	tr	-	-	-	-	m	-	-	-
chlorite	tr	-	-	tr	tr	-	-	tr	-	-	-	tr	-	-	-	tr	tr	tr	tr	tr
actinolite	-	-	-	-	-	-	-	-	-	-	-	-	-	-	-	-	-	-	-	-
prehnite	-	-	-	-	-	-	-	-	-	-	-	-	-	-	-	-	-	-	-	-
margarite?	-	-	-	-	-	-	-	-	-	-	-	tr	-	-	-	-	-	-	-	-
sericite	tr	-	tr	tr	tr	-	-	a	tr	tr	a	-	a	-	a	-	a	-	tr	
2ndy calcite	-	-	-	-	-	-	-	-	tr	-	-	-	-	-	-	-	-	-	-	-

M=major (>10%) m=minor (≤10%) a=accessory (<5%) tr=trace (<0.5%) See figure A-1 for sample locations.

TABLE A-1 (continued): Mineral Assemblages for Poudre Canyon thin sections

	123A	124/2	8(10	8(10	28(10	128/2	128/5	128/6	31(2	133A	34(1a	34(1b	134A	134D	134E	134G	134J	134L	134M
quartz	m	M	M	M	M	M	M	M	M	M	M	M	M	M	M	M	M	M	M
plagioclase	M	M	m	M	M	M	M	M	m	M	tr	a	M	a	M	m	a	m	M
K-feldspar	-	-	m	-	-	-	-	-	a	-	-	M	-	-	M	m	-	-	-
biotite	a	M	M	M	M	m	M	M	M	M	M	M	M	M	m	M	M	M	M
garnet	-	a	a	-	a	m	a	-	-	m	-	a	tr	a	-	-	-	M	tr
sillimanite	-	-	a	m	m	-	m	a	m	-	m	a	a	M	-	M	M	M	tr
cordierite	-	-	-	m	a	-	-	a	-	-	-	-	-	-	-	-	-	-	-
relict staurolite	-	-	-	tr	-	-	-	tr	-	-	-	-	-	-	-	-	-	-	-
late muscovite	-	-	a	a	-	-	-	a	a	-	a	tr	-	-	tr	-	-	-	-
late biotite	-	-	-	-	-	-	-	-	-	-	-	-	-	-	-	-	-	-	-
opaques	a	a	-	tr	tr	a	tr	tr	a	tr	a	a	a	tr	tr	a	tr	a	a
zircon	tr	tr	tr	tr	tr	tr	tr	tr	tr	tr	tr	tr	tr	tr	tr	tr	tr	tr	tr
apatite	tr	a	-	-	tr	tr	tr	tr	-	tr	-	-	tr	-	-	-	-	-	tr
rutile	-	-	-	tr	-	-	-	tr	-	-	-	-	-	-	-	-	-	-	-
hornblende	M	-	-	-	-	-	-	-	-	-	-	-	-	-	-	-	-	-	-
diopside	-	-	-	-	-	-	-	-	-	-	-	-	-	-	-	-	-	-	-
titanite	-	-	-	-	-	-	-	-	-	-	-	-	-	-	-	-	-	-	-
primary calcite	-	-	-	-	-	-	-	-	-	-	-	-	-	-	-	-	-	-	-
allanite	-	-	-	-	-	-	-	-	-	-	-	-	-	-	-	-	-	-	-
clinozoisite	-	-	-	-	-	-	-	-	-	-	-	-	-	-	-	-	-	-	-
epidote	tr	-	-	-	-	-	-	-	-	-	-	-	-	-	-	-	-	-	-
chlorite	tr	tr	tr	-	-	-	-	tr	-	-	-	-	-	-	tr	-	-	-	-
actinolite	-	-	-	-	-	-	-	-	-	-	-	-	-	-	-	-	-	-	-
prehnite	-	-	-	-	-	-	-	-	-	-	-	-	-	-	-	-	-	-	-
margarite?	-	-	-	-	-	-	-	-	-	-	-	-	-	-	-	-	-	-	-
sericite	tr	tr	tr	tr	tr	tr	tr	tr	-	tr	-	-	tr	-	tr	-	tr	-	tr
2ndy calcite	-	-	-	-	-	-	-	-	-	-	-	-	-	-	-	-	-	-	-

M=major (>10%) m=minor (≤10%) a=accessory (<5%) tr=trace (<0.5%) See figure A-1 for sample locations.

APPENDIX B

Quantitative Analysis for Mineral Compositions

Garnet
Biotite
Cordierite
Plagioclase
Muscovite
Hornblende
Prehnite
Clinozoisite
Ilmenite

Abbreviations used for analysis location:

bt	*biotite*	adj	*adjacent to*
crd	*cordierite*	-	*which is adjacent to*
grt	*garnet*	rm	*garnet rim*
hb	*hornblende*	nr	*near (within 0.15 mm of the rim)*
il	*ilmenite*	±nr	*±near (0.15 to 0.30mm of the rim)*
kfs	*K-feldspar*	fract	*fracture in the garnet*
ms	*muscovite*	frag	*garnet fragment*
qz	*quartz*	incl	*inclusion*
op	*opaque*	hst	*host (region surrounding leuco)*
pl	*plagioclase*	leuco	*leucosome*
sil	*sillimanite*	mtrx	*matrix (removed from the garnet)*
		psdmrph	*pseudomorph*
		emb	*garnet embayment*

TABLE B-1: Quantitative Microprobe Analysis for Garnet Compositions

PC-19D

	GT1a	GT1b	GT1c	GT1d	GT1e	GT1f	GT1g	GT1h	GT1i	GT2a	GT2b	GT2c	GT2d	GT3a	GT3b	GT3c	GT3d	GT4a
WEIGHT PERCENT OXIDES																		
SiO2	36.911	37.698	37.877	37.478	37.389	37.534	38.172	37.456	37.490	38.178	37.240	37.691	37.969	37.229	38.180	37.759	38.434	37.725
Al2O3	21.004	21.442	20.822	21.108	20.904	21.020	21.148	21.247	21.500	21.272	21.104	21.691	21.252	21.087	21.026	21.231	21.546	20.662
TiO2	0.006	0.006	0.020	0.000	0.000	0.009	0.000	0.000	0.000	0.083	0.009	0.000	0.020	0.100	0.014	0.066	0.000	0.063
Fe2O3	0.359	0.000	1.025	0.240	0.813	0.578	0.750	0.157	0.000	0.520	0.452	0.000	0.406	0.283	0.841	0.547	0.267	0.832
MgO	0.759	0.969	0.988	0.979	1.074	0.970	0.964	0.841	0.751	0.745	1.018	1.090	1.022	0.637	1.006	0.991	0.863	0.556
FeO	31.600	33.600	33.778	32.963	33.343	33.748	33.270	32.892	32.464	31.460	33.788	34.265	33.776	30.103	33.334	34.358	33.211	29.036
MnO	10.737	7.841	8.154	8.315	8.004	7.947	8.710	9.126	10.195	10.872	8.122	7.845	7.663	12.343	8.353	8.223	9.216	12.462
CaO	1.422	1.748	1.378	1.519	1.952	1.598	1.548	1.428	1.426	1.649	1.646	1.600	1.749	1.507	1.532	1.413	1.384	1.56:
TOTAL	**102.798**	**103.304**	**104.042**	**102.602**	**103.479**	**103.404**	**104.562**	**103.147**	**103.826**	**104.779**	**103.379**	**104.182**	**103.857**	**103.289**	**104.286**	**104.588**	**104.921**	**102.906**
CATIONS RECALCULATED TO 12 OXYGENS																		
Si	2.962	2.989	2.993	2.993	2.971	2.983	2.996	2.983	2.971	2.993	2.965	2.968	2.995	2.970	3.002	2.972	3.002	3.011
Al	1.986	2.003	1.939	1.987	1.958	1.969	1.956	1.994	2.008	1.965	1.980	2.013	1.976	1.983	1.949	1.970	1.984	1.943
Ti	0.000	0.000	0.001	0.000	0.000	0.001	0.000	0.000	0.000	0.005	0.001	0.000	0.001	0.006	0.001	0.004	0.000	0.004
Fe3+	0.022	0.000	0.061	0.014	0.049	0.035	0.044	0.009	0.000	0.031	0.027	0.000	0.024	0.017	0.04:	0.032	0.016	0.050
Mg	0.091	0.115	0.116	0.117	0.127	0.115	0.113	0.09:	0.089	0.087	0.121	0.128	0.120	0.076	0.118	0.116	0.101	0.066
Fe2+	2.121	2.228	2.232	2.202	2.216	2.243	2.184	2.191	2.152	2.063	2.250	2.257	2.228	2.009	2.192	2.262	2.170	1.938
Mn	0.730	0.527	0.546	0.563	0.539	0.535	0.579	0.616	0.684	0.722	0.548	0.523	0.512	0.834	0.556	0.548	0.610	0.842
Ca	0.122	0.148	0.117	0.130	0.166	0.136	0.130	0.122	0.121	0.139	0.140	0.135	0.148	0.129	0.129	0.119	0.116	0.134
TOTAL	**8.034**	**8.009**	**8.006**	**8.006**	**8.026**	**8.015**	**8.003**	**8.015**	**8.025**	**8.004**	**8.031**	**8.025**	**8.004**	**8.024**	**7.997**	**8.023**	**7.998**	**7.989**
Fe/Fe+Mg	*0.959*	*0.951*	*0.950*	*0.950*	*0.946*	*0.951*	*0.951*	*0.956*	*0.960*	*0.959*	*0.949*	*0.946*	*0.949*	*0.964*	*0.949*	*0.951*	*0.956*	*0.967*
Alm	0.692	0.738	0.741	0.731	0.727	0.741	0.727	0.723	0.706	0.685	0.736	0.742	0.741	0.659	0.732	0.743	0.724	0.650
Py	0.02:	0.038	0.039	0.039	0.042	0.038	0.038	0.033	0.029	0.029	0.03:	0.042	0.040	0.025	0.039	0.038	0.034	0.022
Sp	0.238	0.175	0.181	0.187	0.177	0.177	0.193	0.203	0.225	0.240	0.179	0.172	0.170	0.274	0.186	0.180	0.204	0.283
Gr	0.03:	0.049	0.039	0.043	0.055	0.045	0.043	0.040	0.03:	0.046	0.046	0.044	0.049	0.042	0.043	0.039	0.039	0.045
(Ca+Mn)/(Mg+Ca+Mn+Fe)	0.278	0.224	0.220	0.230	0.231	0.222	0.236	0.244	0.264	0.286	0.225	0.216	0.219	0.316	0.229	0.219	0.242	0.328
X	-63.10	-62.59	-62.20	-61.65	-60.58	-59.95	-59.52	-58.69	-57.48	-61.18	-61.16	-61.14	-61.12	-62.08	-61.59	-61.11	-60.63	-64.91
Y	272.74	271.99	271.23	270.48	269.71	268.97	268.22	267.47	265.96	272.68	272.21	271.73	271.26	211.31	212.16	213.22	213.87	179.58
x-axis mm	0.00	0.09	0.18	0.27	0.40	0.50	0.58	0.70	0.89	0.00	0.05	0.0:	0.14	0.00	0.0:	0.21	0.30	0.00
location	*rim adj qz*	*adj qz incl*	*adj qz incl*	*adj qz incl*	*±interior*	*±near rim*	*±near rim*	*near rim*	*rim adj qz*	*rim adj bt*	*nr rm - bt*	*nr rm - bt*	*adj qz incl*	*rim adj bt*	*nr rm - bt*	*nr rm - qz*	*rim adj qz*	*rim adj bt*

TABLE B-1: Quantitative Microprobe Analysis for Garnet Compositions

PC-19D (continued)

	GT4b	**GT4c**	**GT4d**	**GT4e**	**GT4f**	**GT5a**	**GT5b**	**GT5c**	**GT5d**	**GT5e**	**GT5f**	**GT6a**	**GT6b**	**GT6c**	**GT6d**	**GT6e**
WEIGHT PERCENT OXIDES																
SiO2	37.741	38.198	38.012	38.257	37.954	37.977	38.249	37.815	38.035	38.005	38.091	37.853	38.324	38.012	38.153	37.58:
Al2O3	21.058	21.291	21.606	20.972	21.049	20.740	20.494	20.874	20.645	21.219	20.772	20.840	21.045	20.664	20.899	20.340
TiO2	0.029	0.040	0.000	0.089	0.000	0.085	0.077	0.034	0.000	0.043	0.000	0.000	0.029	0.000	0.034	0.077
Fe2O3	0.409	0.335	0.255	0.792	0.538	1.142	1.328	0.777	1.098	0.571	0.974	0.627	0.987	1.264	1.005	0.952
MgO	0.954	0.743	0.985	0.866	0.678	0.608	0.956	0.524	0.931	0.960	0.620	0.647	0.822	0.917	0.642	0.629
FeO	32.493	31.598	33.336	32.949	30.008	30.065	32.427	28.893	31.494	33.082	29.870	29.281	31.947	32.324	30.758	28.910
MnO	8.601	10.202	9.092	8.902	11.752	12.165	8.507	12.567	8.82:	8.778	11.397	11.983	9.980	9.314	11.382	11.135
CaO	1.700	1.638	1.781	1.398	1.516	1.653	1.526	2.084	2.085	1.747	1.862	1.536	1.850	1.506	1.648	1.964
TOTAL	**102.985**	**104.045**	**105.067**	**104.225**	**103.495**	**104.435**	**103.564**	**103.568**	**103.118**	**104.405**	**103.586**	**102.767**	**104.984**	**104.001**	**104.521**	**101.597**
CATIONS RECALCULATED TO 12 OXYGENS																
Si	3.001	3.008	2.972	3.010	3.008	2.995	3.025	2.000	3.018	2.988	3.016	3.018	2.998	3.003	3.002	3.028
Al	1.973	1.976	1.991	1.945	1.966	1.928	1.910	1.951	1.930	1.966	1.938	1.958	1.93:	1.924	1.938	1.931
Ti	0.002	0.002	0.000	0.005	0.000	0.005	0.005	0.002	0.000	0.003	0.000	0.000	0.002	0.000	0.002	0.005
Fe3+	0.025	0.01:	0.015	0.047	0.032	0.068	0.079	0.046	0.066	0.034	0.058	0.038	0.058	0.075	0.059	0.058
Mg	0.113	0.087	0.115	0.102	0.080	0.072	0.113	0.062	0.110	0.113	0.073	0.077	0.096	0.108	0.075	0.076
Fe2+	2.161	2.081	2.180	2.168	1.989	1.983	2.145	1.917	2.08:	2.175	1.978	1.952	2.090	2.136	2.024	1.947
Mn	0.579	0.680	0.602	0.593	0.789	0.813	0.56:	0.844	0.593	0.585	0.764	0.809	0.661	0.623	0.758	0.760
Ca	0.145	0.138	0.149	0.118	0.129	0.140	0.129	0.177	0.177	0.147	0.158	0.131	0.155	0.127	0.139	0.170
TOTAL	**7.998**	**7.992**	**8.025**	**7.988**	**7.993**	**8.002**	**7.976**	**7.999**	**7.984**	**8.00:**	**7.986**	**7.984**	**8.001**	**7.997**	**7.998**	**7.973**
Fe/Fe+Mg	*0.950*	*0.960*	*0.950*	*0.955*	*0.961*	*0.965*	*0.950*	*0.969*	*0.950*	*0.951*	*0.964*	*0.962*	*0.956*	*0.952*	*0.964*	*0.963*
Alm	0.721	0.697	0.716	0.727	0.666	0.660	0.725	0.639	0.703	0.720	0.665	0.657	0.696	0.713	0.675	0.660
Py	0.038	0.029	0.038	0.034	0.027	0.024	0.038	0.021	0.037	0.037	0.025	0.026	0.032	0.036	0.025	0.026
Sp	0.193	0.228	0.198	0.199	0.264	0.270	0.193	0.281	0.200	0.194	0.257	0.272	0.220	0.208	0.253	0.257
Gr	0.048	0.046	0.049	0.03:	0.043	0.046	0.044	0.059	0.05:	0.049	0.053	0.044	0.052	0.043	0.046	0.057
(Ca+Mn)/(Mg+Ca+Mn+Fe)																
	0.242	0.274	0.247	0.239	0.307	0.317	0.236	0.340	0.259	0.242	0.310	0.317	0.272	0.251	0.299	0.315
X	-64.41	-63.91	-63.41	-62.91	-62.41	-50.05	-50.82	-51.71	-52.35	-53.12	-53.88	-200.94	-200.84	-200.75	-200.86	-200.55
Y	180.56	181.29	182.52	183.50	184.48	156.13	157.00	158.11	158.75	159.63	160.50	361.19	360.00	358.82	357.63	356.44
x-axis mm	0.11	0.20	0.33	0.44	0.55	0.00	0.12	0.26	0.35	0.47	0.58	0.00	0.12	0.24	0.36	0.48
location	*nr rm - bt*	*adj fract*	*±near rim*	*nr rm - qz*	*rim adj qz*	*rim adj bt*	*nr rm - bt*	*adj fract*	*±near rim*	*nr rm - pl*	*rim adj pl*	*rim adj qz*	*nr rm - qz*	*±near rim*	*nr rm - bt*	*rim adj bt*

TABLE B-1: Quantitative Microprobe Analysis for Garnet Compositions

PC-50E

	G1 ref	G1 ref	G2	G3	G4	G5	GT1a	GT1b	GT1c	GT1d	GT1e	GT1f	GT1g	GT1h	GT1i	GT1j	GT1k	GT1l
WEIGHT PERCENT OXIDES																		
SiO2	38.416	38.689	38.416	37.966	38.523	37.726	38.162	39.411	38.195	38.486	38.646	38.226	38.615	38.037	38.281	38.329	38.268	38.342
Al2O3	20.971	21.112	21.237	21.329	21.364	21.182	21.357	22.547	21.552	21.505	21.569	21.424	21.497	21.458	21.515	21.841	21.662	21.514
TiO2	0.000	0.000	0.035	0.000	0.040	0.109	0.046	0.000	0.084	0.026	0.000	0.000	0.026	0.035	0.012	0.073	0.044	0.000
Fe2O3	0.887	0.947	0.510	0.216	0.482	0.185	0.365	0.000	0.132	0.306	0.257	0.300	0.369	0.331	0.444	0.000	0.027	0.370
MgO	4.145	4.052	2.785	2.645	3.269	2.780	3.083	3.846	4.026	4.007	4.002	4.082	4.128	4.035	4.129	4.101	4.098	4.174
FeO	31.963	32.506	32.927	33.102	33.053	33.104	33.621	33.930	33.027	32.901	32.702	32.273	32.515	33.153	32.838	32.879	33.109	33.041
MnO	3.312	3.558	4.976	4.888	4.222	4.873	3.983	3.344	3.307	3.256	3.102	3.115	3.359	3.243	3.299	3.118	3.165	3.241
CaO	1.886	1.731	1.868	2.024	1.962	1.750	2.046	1.760	1.933	1.916	2.104	2.322	1.954	2.028	2.246	2.009	1.872	1.832
TOTAL	**101.580**	**102.595**	**102.754**	**102.170**	**102.915**	**101.709**	**102.663**	**104.838**	**102.256**	**102.403**	**102.382**	**101.742**	**102.463**	**102.320**	**102.764**	**102.350**	**102.245**	**102.514**
CATIONS RECALCULATED TO 12 OXYGENS																		
Si	3.020	3.017	3.015	3.001	3.009	2.996	2.996	3.003	2.991	3.005	3.013	3.001	3.009	2.981	2.984	2.991	2.993	2.994
Al	1.943	1.941	1.964	1.987	1.967	1.983	1.976	2.025	1.989	1.979	1.982	1.982	1.975	1.982	1.977	2.009	1.997	1.980
Ti	0.000	0.000	0.002	0.000	0.002	0.007	0.003	0.000	0.005	0.002	0.000	0.000	0.002	0.002	0.001	0.004	0.003	0.000
Fe3+	0.053	0.056	0.030	0.013	0.028	0.011	0.022	0.000	0.008	0.018	0.015	0.018	0.022	0.01:	0.026	0.000	0.002	0.022
Mg	0.486	0.471	0.326	0.312	0.381	0.329	0.361	0.437	0.46:	0.466	0.465	0.478	0.480	0.471	0.480	0.477	0.478	0.486
Fe2+	2.101	2.120	2.161	2.188	2.159	2.199	2.208	2.162	2.163	2.149	2.132	2.119	2.119	2.173	2.141	2.146	2.166	2.157
Mn	0.221	0.235	0.331	0.327	0.279	0.328	0.265	0.216	0.219	0.215	0.205	0.207	0.222	0.215	0.218	0.206	0.210	0.214
Ca	0.159	0.145	0.157	0.171	0.164	0.149	0.172	0.144	0.162	0.160	0.176	0.195	0.163	0.170	0.188	0.168	0.157	0.153
TOTAL	**7.982**	**7.985**	**7.986**	**7.999**	**7.991**	**8.001**	**8.002**	**7.985**	**8.006**	**7.995**	**7.988**	**7.999**	**7.991**	**8.016**	**8.014**	**8.001**	**8.005**	**8.006**
Fe/Fe+Mg	*0.812*	*0.818*	*0.869*	*0.875*	*0.850*	*0.870*	*0.860*	*0.832*	*0.821*	*0.822*	*0.821*	*0.816*	*0.815*	*0.822*	*0.817*	*0.818*	*0.819*	*0.816*
Alm	0.708	0.714	0.726	0.730	0.724	0.732	0.735	0.731	0.718	0.718	0.716	0.707	0.710	0.717	0.707	0.716	0.719	0.717
Py	0.164	0.159	0.110	0.104	0.128	0.110	0.120	0.148	0.156	0.156	0.156	0.159	0.161	0.156	0.159	0.159	0.159	0.161
Sp	0.074	0.079	0.111	0.109	0.094	0.109	0.088	0.073	0.073	0.072	0.069	0.069	0.074	0.071	0.072	0.069	0.06:	0.071
Gr	0.054	0.049	0.053	0.057	0.055	0.04:	0.057	0.049	0.054	0.054	0.059	0.065	0.055	0.056	0.062	0.056	0.052	0.051
(Ca+Mn)/(Mg+Ca+Mn+Fe)	0.128	0.128	0.164	0.166	0.149	0.159	0.145	0.122	0.127	0.126	0.128	0.134	0.129	0.127	0.134	0.125	0.122	0.122
X	-119.57	-119.57	-124.99	-119.46	-111.90	-115.58	-128.99	-128.25	-127.33	-126.77	-126.05	-125.31	-124.57	-123.84	-123.10	-122.47	-121.63	-120.89
Y	106.22	106.22	121.19	115.96	98.21	87.22	88.46	89.13	90.20	90.39	91.13	91.79	92.46	93.03	93.79	94.45	95.12	95.78
x-axis mm	0.00	0.10	0.24	0.30	0.40	0.50	0.60	0.69	0.80	0.89	0.00	1.0:						
location	*interior*	*interior*	*rim adj bt*	*rim adj bt*	*rim adj bt*	*rim adj bt*	*rim adj pl*	*nr rm - pl*	*±near rim*	*±near rim*	*interior*	*interior*	*interior*	*interior*	*interior*	*interior*	*interior*	*interior*

TABLE B-1: Quantitative Microprobe Analysis for Garnet Compositions

PC-50E (continued)

	GT1m	GT1n	GT1o	GT1p	GT1q	GT1r	GT1s	GT1t	GT1u	GT1v	GT1w	GT1x	GT1y	GT2a	GT2b	GT2c	GT2d	GT2e
WEIGHT PERCENT OXIDES																		
SiO2	38.923	38.081	38.214	38.559	38.333	38.527	38.051	34.500	38.008	38.583	38.110	37.920	38.481	37.236	38.056	38.558	38.321	38.431
Al2O3	21.660	21.476	21.221	21.540	21.597	21.852	21.511	21.196	21.534	21.793	21.453	21.584	21.888	20.745	21.455	21.490	21.655	21.223
TiO2	0.012	0.000	0.000	0.047	0.026	0.000	0.015	0.000	0.000	0.000	0.000	0.026	0.119	0.081	0.000	0.000	0.061	0.000
Fe2O3	0.337	0.049	0.638	0.222	0.137	0.202	0.132	0.000	0.174	0.000	0.358	0.000	0.000	0.349	0.251	0.231	0.163	0.700
MgO	4.217	4.164	4.295	4.263	4.262	4.331	3.708	3.427	3.759	3.775	3.326	3.385	3.047	2.769	3.655	4.086	4.182	4.241
FeO	32.556	32.432	32.125	32.493	32.882	33.312	33.210	31.466	32.991	32.614	33.186	33.424	34.117	31.913	32.967	32.466	33.282	32.544
MnO	3.052	3.071	3.278	3.102	2.927	3.159	3.230	3.310	3.551	3.623	4.473	4.118	4.702	4.874	3.578	3.267	3.328	3.191
CaO	2.194	1.899	2.065	1.913	1.929	2.053	2.148	2.301	2.165	2.270	1.914	1.812	1.619	1.996	2.166	1.810	1.740	1.817
TOTAL	**102.951**	**101.172**	**101.836**	**102.139**	**102.093**	**103.436**	**102.005**	**96.200**	**102.182**	**102.658**	**102.820**	**102.269**	**103.973**	**99.963**	**102.128**	**101.908**	**102.732**	**102.147**
CATIONS RECALCULATED TO 12 OXYGENS																		
Si	3.014	3.003	2.999	3.00:	2.998	2.981	2.991	2.892	2.985	3.005	2.987	2.985	2.986	3.004	2.991	3.018	2.987	3.007
Al	1.977	1.996	1.963	1.982	1.991	1.993	1.993	2.094	1.993	2.000	1.982	2.002	2.002	1.972	1.987	1.982	1.989	1.957
Ti	0.001	0.000	0.000	0.003	0.002	0.000	0.001	0.000	0.000	0.000	0.000	0.002	0.007	0.005	0.000	0.000	0.004	0.000
Fe3+	0.01:	0.003	0.038	0.013	0.008	0.012	0.008	0.000	0.010	0.000	0.021	0.000	0.000	0.021	0.015	0.014	0.00:	0.041
Mg	0.487	0.490	0.502	0.496	0.497	0.500	0.435	0.428	0.440	0.438	0.389	0.397	0.353	0.333	0.428	0.477	0.486	0.495
Fe2+	2.108	2.139	2.108	2.121	2.151	2.155	2.183	2.206	2.167	2.124	2.175	2.200	2.214	2.153	2.167	2.125	2.170	2.130
Mn	0.200	0.205	0.218	0.205	0.194	0.207	0.215	0.235	0.236	0.239	0.297	0.275	0.309	0.333	0.238	0.217	0.220	0.211
Ca	0.182	0.160	0.174	0.160	0.162	0.170	0.181	0.207	0.182	0.189	0.161	0.153	0.135	0.173	0.182	0.152	0.145	0.152
TOTAL	**7.988**	**7.997**	**8.001**	**7.990**	**8.001**	**8.017**	**8.007**	**8.061**	**8.013**	**7.995**	**8.012**	**8.013**	**8.006**	**7.994**	**8.008**	**7.984**	**8.00:**	**7.994**
Fe/Fe+Mg	*0.812*	*0.814*	*0.808*	*0.810*	*0.812*	*0.812*	*0.834*	*0.837*	*0.831*	*0.829*	*0.848*	*0.847*	*0.863*	*0.866*	*0.835*	*0.817*	*0.817*	*0.811*
Alm	0.708	0.714	0.702	0.711	0.716	0.711	0.724	0.717	0.716	0.710	0.720	0.727	0.736	0.720	0.719	0.715	0.718	0.713
Py	0.164	0.164	0.167	0.166	0.165	0.165	0.144	0.139	0.145	0.147	0.129	0.131	0.117	0.111	0.142	0.161	0.161	0.166
Sp	0.067	0.069	0.073	0.069	0.065	0.068	0.071	0.076	0.078	0.07:	0.098	0.091	0.103	0.111	0.079	0.073	0.073	0.071
Gr	0.061	0.054	0.058	0.054	0.054	0.056	0.060	0.067	0.060	0.063	0.053	0.051	0.045	0.058	0.061	0.051	0.048	0.051
(Ca+Mn)/(Mg+Ca+Mn+Fe)																		
0.128	0.122	0.130	0.122	0.118	0.124	0.131	0.144	0.138	0.143	0.151	0.141	0.147	0.169	0.139	0.124	0.121	0.122	
X	-120.72	-119.85	-118.68	-118.19	-117.21	-116.47	-115.67	-115.00	-114.27	-113.68	-112.47	-112.06	-111.32	-125.80	-124.93	-123.87	-123.30	-122.56
Y	96.40	97.31	97.78	98.45	99.11	99.78	100.57	101.11	101.77	102.44	103.42	103.77	104.43	123.96	124.10	124.33	124.36	124.50
x-axis mm	1.16	1.29	1.42	1.50	1.62	1.72	1.83	1.91	2.01	2.10	2.26	2.31	2.41	0.00	0.09	0.20	0.25	0.33
location	*interior*	*interior*	*interior*	*interior*	*interior*	*interior*	*interior*	*interior*	*±near rim*	*±near rim*	*nr rm - bt*	*nr rm - bt*	*rim adj pl*	*rim adj qz*	*nr rm - qz*	*±near rim*	*±near rim*	*interior*

TABLE B-1: Quantitative Microprobe Analysis for Garnet Compositions

PC-50E (continued)						*PC-66A*												
	GT2f	**GT2g**	**GT2h**	**GT2i**	**GT2j**	**GT1a**	**GT1b**	**GT1c**	**GT1d**	**GT1e**	**GT1f**	**GT1g**	**GT1h**	**GT1i**	**GT1j**	**GT2a**	**GT2b**	**GT2c**
WEIGHT PERCENT OXIDES																		
SiO2	38.150	38.213	38.636	38.336	37.602	38.236	38.309	38.058	38.405	38.299	38.078	39.018	38.250	38.267	38.405	38.271	37.873	38.288
Al2O3	21.582	21.271	21.222	21.480	21.485	21.059	20.763	20.982	20.763	21.063	20.696	20.547	21.124	20.708	20.552	20.535	20.571	20.447
TiO2	0.064	0.000	0.032	0.104	0.052	0.009	0.138	0.073	0.012	0.114	0.056	0.012	0.038	0.000	0.117	0.000	0.076	0.067
Fe2O3	0.202	0.591	0.870	0.277	0.000	1.098	1.243	0.919	1.679	1.044	1.445	2.085	1.195	1.391	1.703	1.653	1.558	1.580
MgO	4.134	4.006	4.085	3.705	3.278	0.518	1.069	1.093	1.167	1.110	0.806	1.106	1.200	1.067	0.890	0.436	0.670	0.712
FeO	33.058	32.685	32.721	33.400	32.424	25.023	29.070	28.881	29.850	29.310	26.812	28.813	30.230	28.229	28.258	23.219	28.207	26.840
MnO	3.498	3.326	3.443	3.568	3.912	9.294	5.515	5.863	5.058	5.736	6.768	5.375	5.401	5.605	6.398	9.215	7.151	7.970
CaO	1.853	2.058	1.930	1.862	2.153	8.539	7.133	7.111	7.314	7.247	8.520	7.527	7.072	7.601	7.457	9.512	7.379	6.970
TOTAL	**102.541**	**102.150**	**102.939**	**102.732**	**100.906**	**103.776**	**103.240**	**102.980**	**104.248**	**103.923**	**103.181**	**104.483**	**104.510**	**102.868**	**103.780**	**102.841**	**103.485**	**102.874**
CATIONS RECALCULATED TO 12 OXYGENS																		
Si	2.982	2.997	3.006	2.995	2.990	2.986	3.002	2.990	2.988	2.985	2.988	3.019	2.971	3.005	3.000	3.006	2.979	3.016
Al	1.988	1.966	1.946	1.978	2.014	1.938	1.917	1.943	1.904	1.935	1.914	1.874	1.934	1.917	1.892	1.901	1.907	1.898
Ti	0.004	0.000	0.002	0.006	0.003	0.001	0.008	0.004	0.001	0.007	0.003	0.001	0.002	0.000	0.007	0.000	0.005	0.004
Fe3+	0.012	0.035	0.051	0.016	0.000	0.065	0.073	0.054	0.098	0.061	0.085	0.121	0.06:	0.082	0.100	0.098	0.092	0.094
Mg	0.482	0.468	0.474	0.432	0.389	0.060	0.125	0.128	0.135	0.129	0.094	0.128	0.139	0.125	0.104	0.051	0.079	0.084
Fe2+	2.161	2.143	2.129	2.182	2.157	1.634	1.905	1.898	1.942	1.910	1.759	1.864	1.964	1.854	1.846	1.525	1.856	1.768
Mn	0.232	0.221	0.227	0.236	0.264	0.615	0.366	0.390	0.333	0.379	0.450	0.352	0.355	0.373	0.423	0.613	0.476	0.532
Ca	0.155	0.173	0.161	0.156	0.183	0.714	0.599	0.599	0.610	0.605	0.716	0.624	0.589	0.640	0.624	0.801	0.622	0.588
TOTAL	**8.015**	**8.003**	**7.994**	**8.002**	**7.000**	**8.012**	**7.995**	**8.007**	**8.011**	**8.011**	**8.00:**	**7.983**	**8.024**	**7.995**	**7.997**	**7.995**	**8.016**	**7.984**
Fe/Fe+Mg	*0.818*	*0.821*	*0.818*	*0.835*	*0.847*	*0.964*	*0.938*	*0.937*	*0.935*	*0.937*	*0.949*	*0.936*	*0.934*	*0.937*	*0.947*	*0.968*	*0.959*	*0.955*
Alm	0.713	0.713	0.712	0.726	0.721	0.540	0.636	0.630	0.643	0.632	0.583	0.628	0.645	0.620	0.616	0.510	0.612	0.595
Py	0.159	0.156	0.158	0.144	0.130	0.01:	0.042	0.043	0.045	0.043	0.031	0.043	0.046	0.042	0.035	0.017	0.026	0.028
Sp	0.076	0.074	0.076	0.079	0.088	0.203	0.122	0.129	0.110	0.125	0.149	0.119	0.117	0.125	0.141	0.205	0.157	0.179
Gr	0.051	0.058	0.054	0.052	0.061	0.236	0.200	0.199	0.202	0.200	0.237	0.210	0.193	0.214	0.208	0.268	0.205	0.198
(Ca+Mn)/(Mg+Ca+Mn+Fe)	0.128	0.131	0.130	0.130	0.149	0.440	0.322	0.328	0.312	0.325	0.386	0.329	0.310	0.338	0.349	0.473	0.362	0.377
X	-121.63	-120.72	-119.96	-119.22	-118.29	-159.38	-159.85	-160.52	-160.66	-161.21	-161.91	-162.50	-162.68	-163.15	-163.62	-162.45	-162.34	-160.96
Y	124.63	124.77	124.90	125.04	125.17	-343.24	-342.33	-341.42	-340.51	-339.87	-338.31	-337.79	-336.88	-335.97	-335.14	-343.85	-343.14	-342.38
x-axis mm	0.42	0.51	0.59	0.67	0.76	0.00	0.10	0.22	0.31	0.39	0.56	0.64	0.73	0.84	0.93	0.00	0.07	0.23
location	*interior*	*±near rim*	*±near rim*	*nr rm - qz*	*rim adj qz*	*rim ad bt*	*nr rm - bt*	*±near rim*	*±near rim*	*adj fract*	*adj fract*	*±near rim*	*±near rim*	*nr rm - qz rim adj qz? rim adj bt*			*nr rm - bt*	*adj fract*

TABLE B-1: Quantitative Microprobe Analysis for Garnet Compositions

PC-66A (continued)

	GT2d	GT2e	GT2f	GT2g	GT2h	GT3a	GT3b	GT3c	GT3d
WEIGHT PERCENT OXIDES									
SiO2	38.586	37.985	38.111	38.133	37.779	38.705	37.841	38.181	38.205
Al2O3	21.033	20.783	20.899	20.807	20.932	20.944	20.812	20.543	20.664
TiO2	0.053	0.100	0.070	0.023	0.091	0.029	0.006	0.000	0.000
Fe2O3	1.405	1.430	1.270	1.328	1.027	1.473	1.301	1.762	1.551
MgO	1.125	1.150	0.771	0.904	0.620	0.497	0.487	1.180	0.711
FeO	28.905	29.914	27.583	28.211	26.806	25.044	25.159	28.863	26.607
MnO	5.681	5.190	7.997	6.374	8.807	8.716	8.742	5.361	7.775
CaO	7.849	7.303	7.297	7.603	7.422	9.026	8.891	7.459	7.897
TOTAL	**104.637**	**103.855**	**103.998**	**103.383**	**103.484**	**104.434**	**103.239**	**103.349**	**103.410**
CATIONS RECALCULATED TO 12 OXYGENS									
Si	2.986	2.971	2.979	2.989	2.971	2.999	2.975	2.993	2.996
Al	1.918	1.916	1.925	1.922	1.93:	1.912	1.928	1.898	1.909
Ti	0.003	0.006	0.004	0.001	0.005	0.002	0.000	0.000	0.000
Fe3+	0.082	0.084	0.075	0.078	0.061	0.086	0.077	0.104	0.092
Mg	0.130	0.134	0.08:	0.106	0.073	0.057	0.057	0.138	0.083
Fe2+	1.870	1.957	1.803	1.850	1.763	1.623	1.654	1.892	1.745
Mn	0.372	0.344	0.529	0.423	0.587	0.572	0.582	0.356	0.516
Ca	0.651	0.612	0.611	0.639	0.625	0.749	0.749	0.626	0.663
TOTAL	**8.012**	**8.023**	**8.017**	**8.009**	**8.024**	**8.000**	**8.022**	**8.007**	**8.004**
Fe/Fe+Mg	*0.935*	*0.936*	*0.953*	*0.946*	*0.960*	*0.966*	*0.967*	*0.932*	*0.955*
Alm	0.619	0.642	0.594	0.613	0.578	0.541	0.544	0.628	0.580
Py	0.043	0.044	0.02:	0.035	0.024	0.019	0.019	0.046	0.028
Sp	0.123	0.113	0.175	0.140	0.192	0.191	0.191	0.118	0.172
Gr	0.215	0.201	0.201	0.212	0.205	0.250	0.246	0.208	0.221
(Ca+Mn)/(Mg+Ca+Mn+Fe)	0.338	0.314	0.376	0.352	0.398	0.440	0.438	0.326	0.392
X	-160.41	-159.64	-158.86	-158.08	-157.30	-160.58	-159.98	-159.52	-158.99
Y	-341.63	-340.87	-340.12	-339.36	-338.61	-345.45	-346.45	-347.44	-348.36
x-axis mm	0.32	0.43	0.54	0.65	0.76	0.00	0.12	0.23	0.33
location	*±near rim*	*±near rim*	*adj fract*	*nr rm - bt*	*rim adj bt*	*rim adj bt*	*nr rm - bt*	*nr rm - qz*	*rim adj qz*

PC-68A

	G1	G1a	GT1a	GT1b	GT1c	GT1d	GT1e	GT1f	GT1g
WEIGHT PERCENT OXIDES									
SiO2	37.851	38.224	38.206	36.945	37.981	37.646	37.562	38.419	37.827
Al2O3	21.378	21.544	21.342	20.649	21.315	20.951	21.188	20.982	21.164
TiO2	0.000	0.075	0.063	0.000	0.052	0.057	0.000	0.014	0.012
Fe2O3	0.362	0.285	0.338	0.591	0.447	0.708	0.485	0.882	0.683
MgO	1.487	1.531	1.169	1.264	1.282	0.977	1.190	1.355	1.676
FeO	40.092	40.463	40.002	38.814	40.455	40.509	40.510	39.384	39.687
MnO	1.285	1.201	1.563	1.276	1.327	1.534	1.356	1.290	1.220
CaO	1.605	1.516	1.528	1.842	1.532	1.424	1.538	1.625	1.726
TOTAL	**104.060**	**104.839**	**104.211**	**101.381**	**104.391**	**103.806**	**103.829**	**103.951**	**103.995**
CATIONS RECALCULATED TO 12 OXYGENS									
Si	2.979	2.984	3.001	2.986	2.984	2.984	2.974	3.018	2.978
Al	1.983	1.982	1.976	1.967	1.974	1.957	1.977	1.943	1.964
Ti	0.000	0.004	0.004	0.000	0.003	0.003	0.000	0.001	0.001
Fe3+	0.021	0.017	0.020	0.036	0.026	0.042	0.029	0.052	0.041
Mg	0.174	0.178	0.137	0.152	0.150	0.115	0.140	0.159	0.197
Fe2+	2.639	2.641	2.628	2.624	2.658	2.686	2.682	2.588	2.613
Mn	0.086	0.079	0.104	0.087	0.088	0.103	0.091	0.086	0.081
Ca	0.135	0.127	0.129	0.160	0.129	0.121	0.130	0.137	0.146
TOTAL	**8.018**	**8.013**	**7.997**	**8.012**	**8.013**	**8.012**	**8.023**	**7.983**	**8.019**
Fe/Fe+Mg	*0.938*	*0.937*	*0.950*	*0.945*	*0.947*	*0.959*	*0.950*	*0.942*	*0.930*
Alm	0.870	0.873	0.877	0.868	0.879	0.888	0.881	0.872	0.860
Py	0.058	0.059	0.046	0.050	0.04:	0.038	0.046	0.054	0.065
Sp	0.028	0.026	0.035	0.029	0.029	0.034	0.02:	0.029	0.027
Gr	0.045	0.042	0.043	0.053	0.043	0.040	0.043	0.046	0.048
(Ca+Mn)/(Mg+Ca+Mn+Fe)	0.073	0.068	0.078	0.082	0.072	0.074	0.073	0.075	0.075
X	150.98	150.97	165.09	165.33	165.57	165.82	166.55	166.78	166.59
Y	-243.31	-243.37	-210.62	-209.62	-208.40	-207.69	-204.62	-203.61	-202.29
x-axis mm	0.00	0.01	0.00	0.10	0.23	0.30	0.62	0.72	0.85
location	*interior*	*interior*	*rim adj bt*	*nr rm - bt*	*nr bt incl*	*adj bt incl*	*adj fract*	*near fract*	*interior*

TABLE B-1: Quantitative Microprobe Analysis for Garnet Compositions

PC-68A (continued)

	GT1h	GT1i	GT1j	GT1k	GT1l	GT2a	GT2b	GT2c	GT2d	GT2e	GT2f	GT2g	GT2h	GT2i	GT2j	GT2k	GT2l	GT3a
WEIGHT PERCENT OXIDES																		
SiO2	38.307	38.178	38.301	38.493	38.093	38.272	38.374	38.580	38.457	37.548	38.323	37.899	38.318	34.671	38.067	38.166	38.262	38.104
Al2O3	20.635	21.442	21.375	21.893	21.022	21.013	21.308	21.299	21.155	20.951	21.272	21.560	21.143	24.997	21.236	21.027	21.237	21.302
TiO2	0.037	0.000	0.000	0.060	0.017	0.034	0.029	0.043	0.003	0.000	0.023	0.017	0.000	0.055	0.006	0.078	0.000	0.020
Fe2O3	1.370	0.402	0.506	0.097	0.944	0.945	0.575	0.362	0.723	0.700	0.718	0.220	0.824	0.000	0.647	0.731	0.619	0.482
MgO	1.643	1.624	1.698	1.659	1.347	1.223	1.552	1.589	1.615	1.501	1.399	1.347	1.565	1.345	1.651	1.457	1.305	1.363
FeO	38.967	39.934	39.644	40.774	39.869	39.828	39.687	38.714	38.865	39.363	40.150	40.724	39.624	37.628	39.341	39.418	40.130	39.641
MnO	1.203	1.121	1.178	1.119	1.429	1.513	1.106	1.093	1.137	1.225	1.316	1.243	1.284	1.121	1.194	1.253	1.308	1.310
CaO	1.656	1.657	1.619	1.632	1.721	1.700	1.764	1.841	1.966	1.784	1.667	1.632	1.624	1.476	1.978	1.686	1.502	1.920
TOTAL	**103.818**	**104.358**	**104.321**	**105.727**	**104.442**	**104.528**	**104.395**	**103.521**	**103.921**	**103.072**	**104.868**	**104.642**	**104.382**	**101.293**	**104.120**	**103.816**	**104.363**	**104.142**
CATIONS RECALCULATED TO 12 OXYGENS																		
Si	3.014	2.989	2.997	2.977	2.991	3.001	3.001	3.027	3.014	2.983	2.993	2.971	3.001	2.781	2.987	3.004	3.001	2.993
Al	1.913	1.979	1.971	1.996	1.945	1.942	1.964	1.970	1.954	1.962	1.958	1.992	1.951	2.363	1.964	1.951	1.963	1.972
Ti	0.002	0.000	0.000	0.003	0.001	0.002	0.002	0.003	0.000	0.000	0.001	0.001	0.000	0.003	0.000	0.005	0.000	0.001
Fe3+	0.081	0.024	0.02:	0.006	0.056	0.056	0.034	0.021	0.043	0.042	0.042	0.013	0.049	0.000	0.038	0.043	0.037	0.029
Mg	0.193	0.190	0.198	0.191	0.158	0.143	0.181	0.186	0.189	0.178	0.163	0.157	0.183	0.161	0.193	0.171	0.153	0.160
Fe2+	2.564	2.615	2.594	2.637	2.618	2.612	2.596	2.540	2.547	2.616	2.622	2.670	2.595	2.524	2.582	2.595	2.632	2.604
Mn	0.080	0.074	0.078	0.073	0.095	0.100	0.073	0.073	0.076	0.082	0.087	0.083	0.085	0.076	0.079	0.084	0.087	0.087
Ca	0.140	0.139	0.136	0.135	0.145	0.143	0.148	0.155	0.165	0.152	0.139	0.137	0.136	0.127	0.166	0.142	0.126	0.162
TOTAL	**7.987**	**8.00:**	**8.003**	**8.019**	**8.008**	**7.998**	**7.998**	**7.975**	**7.987**	**8.015**	**8.006**	**8.025**	**7.999**	**8.035**	**8.011**	**7.994**	**7.999**	**8.006**
Fe/Fe+Mg	*0.930*	*0.932*	*0.929*	*0.932*	*0.943*	*0.948*	*0.935*	*0.932*	*0.931*	*0.936*	*0.942*	*0.944*	*0.934*	*0.93:*	*0.930*	*0.938*	*0.945*	*0.942*
Alm	0.861	0.866	0.863	0.868	0.868	0.871	0.866	0.860	0.856	0.864	0.871	0.876	0.865	0.874	0.855	0.867	0.878	0.864
Py	0.065	0.063	0.066	0.063	0.052	0.048	0.060	0.063	0.063	0.059	0.054	0.052	0.061	0.056	0.064	0.057	0.051	0.053
Sp	0.027	0.025	0.026	0.024	0.032	0.034	0.024	0.025	0.025	0.027	0.029	0.027	0.028	0.026	0.026	0.028	0.029	0.029
Gr	0.047	0.046	0.045	0.044	0.048	0.048	0.049	0.052	0.056	0.050	0.046	0.045	0.045	0.044	0.055	0.048	0.042	0.054
(Ca+Mn)/(Mg+Ca+Mn+Fe)	0.074	0.071	0.071	0.069	0.07:	0.081	0.074	0.077	0.081	0.077	0.075	0.072	0.074	0.070	0.081	0.076	0.071	0.083
X	167.27	167.51	167.75	167.99	168.23	161.36	162.10	163.71	164.36	165.22	166.36	167.35	168.35	169.35	170.35	171.35	172.35	155.25
Y	-201.44	-200.61	-199.61	-198.75	-197.61	-201.98	-202.31	-202.49	-202.74	-202.99	-203.24	-203.66	-203.75	-204.00	-204.42	-204.95	-204.76	-238.31
x-axis mm	0.96	1.05	1.15	1.24	1.36	0.00	0.08	0.24	0.31	0.40	0.52	0.63	0.73	0.83	0.94	1.05	1.15	0.00
location	*interior*	*interior*	*interior*	*nr rm - qz*	*rim adj qz*	*rim adj bt*	*nr rm - bt*	*±near rim*	*interior*	*interior*	*nr fract*	*interior*	*interior*	*nr fract*	*±near rim*	*nr*	*rm - pl*	*rim adj pl*	*rim adj qz*

TABLE B-1: Quantitative Microprobe Analysis for Garnet Compositions

PC-68A (continued)								*PC-80B*										
	GT3b	**GT3c**	**GT3d**	**GT3e**	**GT3f**	**GT3g**	**GT3h**	**1G1aref**	**1G1bref**	**1G2**	**1G3**	**1G5**	**1G6**	**1G7**	**1G8**	**1G9**	**1G10**	**1G11**
WEIGHT PERCENT OXIDES																		
SiO2	38.694	38.741	36.736	37.433	37.633	38.503	37.980	39.057	38.722	38.453	38.688	39.040	38.815	39.358	38.083	38.066	39.235	38.392
Al2O3	21.146	21.107	22.699	20.790	21.466	21.390	21.322	22.094	21.924	21.968	21.951	21.768	21.808	21.944	21.812	21.878	22.044	22.010
TiO2	0.014	0.060	0.000	0.000	0.000	0.000	0.000	0.092	0.006	0.055	0.022	0.042	0.041	0.004	0.007	0.058	0.040	0.041
Fe2O3	0.721	0.884	0.000	0.945	0.107	0.564	0.294	0.000	0.000	0.000	0.000	0.136	0.000	0.000	0.000	0.000	0.000	
MgO	1.613	1.542	1.595	1.702	1.743	1.677	1.068	2.261	2.356	2.077	1.759	2.315	2.349	2.461	1.781	1.672	2.033	2.031
FeO	38.506	39.511	38.969	39.144	39.092	39.442	40.168	29.962	29.817	30.539	30.767	30.247	29.185	30.270	30.304	29.977	30.901	30.661
MnO	1.169	1.217	1.115	1.143	1.199	1.099	1.578	2.032	1.890	2.001	2.374	1.884	2.127	1.898	2.843	2.538	2.016	1.871
CaO	1.995	1.537	1.759	1.834	2.053	1.851	1.449	7.680	7.457	7.264	7.297	7.451	7.496	7.046	6.251	7.214	6.855	7.454
TOTAL	**103.858**	**104.599**	**102.873**	**102.991**	**103.293**	**104.526**	**103.859**	**103.178**	**102.172**	**102.357**	**102.858**	**102.883**	**101.821**	**102.981**	**101.081**	**101.403**	**103.124**	**102.460**
CATIONS RECALCULATED TO 12 OXYGENS																		
Si	3.028	3.021	2.912	2.977	2.974	3.003	2.997	3.010	3.012	2.998	3.007	3.020	3.025	3.034	3.00:	2.999	3.029	2.992
Al	1.950	1.93:	2.120	1.949	1.999	1.966	1.983	2.007	2.010	2.018	2.011	1.985	2.003	1.994	2.032	2.031	2.006	2.021
Ti	0.001	0.004	0.000	0.000	0.000	0.000	0.000	0.005	0.000	0.003	0.001	0.002	0.002	0.000	0.000	0.003	0.002	0.002
Fe3+	0.043	0.052	0.000	0.057	0.006	0.033	0.018	0.000	0.000	0.000	0.000	0.008	0.000	0.000	0.000	0.000	0.000	0.000
Mg	0.188	0.179	0.188	0.202	0.205	0.195	0.126	0.260	0.273	0.241	0.204	0.267	0.273	0.283	0.210	0.196	0.234	0.236
Fe2+	2.520	2.576	2.583	2.603	2.584	2.573	2.651	1.931	1.93:	1.991	1.000	1.957	1.902	1.952	2.003	1.975	1.995	1.998
Mn	0.078	0.080	0.075	0.077	0.080	0.073	0.105	0.133	0.125	0.132	0.156	0.123	0.140	0.124	0.190	0.169	0.132	0.123
Ca	0.167	0.128	0.149	0.156	0.174	0.155	0.123	0.634	0.622	0.607	0.608	0.618	0.626	0.582	0.529	0.609	0.567	0.622
TOTAL	**7.975**	**7.980**	**8.028**	**8.021**	**8.023**	**7.997**	**8.002**	**7.981**	**7.982**	**7.990**	**7.986**	**7.981**	**7.971**	**7.969**	**7.974**	**7.982**	**7.966**	**7.995**
Fe/Fe+Mg	*0.931*	*0.935*	*0.932*	*0.928*	*0.926*	*0.930*	*0.955*	*0.881*	*0.877*	*0.892*	*0.908*	*0.880*	*0.875*	*0.873*	*0.905*	*0.910*	*0.895*	*0.894*
Alm	0.853	0.869	0.862	0.857	0.849	0.859	0.882	0.653	0.656	0.670	0.674	0.660	0.647	0.664	0.683	0.670	0.681	0.671
Py	0.064	0.061	0.063	0.066	0.068	0.065	0.042	0.088	0.092	0.081	0.069	0.090	0.093	0.096	0.072	0.067	0.07:	0.079
Sp	0.026	0.027	0.025	0.025	0.026	0.024	0.035	0.045	0.042	0.044	0.053	0.042	0.048	0.042	0.065	0.057	0.045	0.041
Gr	0.057	0.043	0.04:	0.051	0.057	0.052	0.041	0.214	0.210	0.204	0.205	0.208	0.213	0.198	0.181	0.206	0.194	0.209
(Ca+Mn)/(Mg+Ca+Mn+Fe)	0.083	0.070	0.075	0.077	0.084	0.076	0.076	0.259	0.252	0.249	0.257	0.250	0.261	0.240	0.245	0.264	0.239	0.250
X	154.74	154.22	153.71	153.20	152.67	152.17	151.65	52.94	53.00	58.65	58.48	50.34	54.17	56.12	59.42	52.65	36.30	
Y	-239.26	-240.21	-241.16	-241.85	-243.05	-244.00	-244.95	59.45	59.46	60.90	63.62	86.68	64.61	60.64	46.52	73.46	57.06	
x-axis mm	0.11	0.22	0.33	0.41	0.54	0.65	0.76											

TABLE B-1: Quantitative Microprobe Analysis for Garnet Compositions

PC-80B (continued)

	1G12	1G13	1GT1a	1GT1b	1GT1c	1GT1d	1GT1e	1GT1f	1GT1g	1GT1h	1GT1i	1GT1j	1GT1k	1GT1l	1GT1m	1GT1n	1GT1o	1GT1p
WEIGHT PERCENT OXIDES																		
SiO2	37.783	38.542	38.248	38.662	38.56:	38.705	38.456	38.743	39.023	38.706	38.481	38.746	38.402	38.123	39.050	38.566	38.318	38.775
Al2O3	21.882	21.532	21.785	21.992	21.594	21.886	21.700	21.666	22.069	21.970	21.753	21.808	21.722	21.563	22.042	23.748	21.676	22.052
TiO2	0.101	0.041	0.003	0.000	0.013	0.062	0.065	0.025	0.000	0.046	0.000	0.023	0.035	0.000	0.056	0.024	0.000	0.072
Fe2O3	0.000	0.000	0.107	0.000	0.000	0.198	0.000	0.000	0.000	0.000	0.000	0.000	0.000	0.000	0.000	0.000		
MgO	1.664	1.674	1.396	1.698	1.550	2.195	1.518	2.410	1.537	1.586	1.756	1.806	1.844	1.435	2.288	1.115	1.157	2.015
FeO	30.401	30.786	30.703	31.011	30.549	30.222	30.401	30.088	30.229	29.664	30.615	30.465	30.356	30.737	29.043	30.313	30.484	28.815
MnO	2.795	2.567	3.210	2.628	2.655	1.991	2.922	1.964	3.001	2.936	2.393	2.257	2.288	3.390	2.102	3.633	3.838	2.443
CaO	6.950	8.000	7.254	7.340	7.413	7.466	7.524	7.416	7.640	7.354	7.193	7.734	7.519	6.567	8.377	6.334	6.520	8.571
TOTAL	**101.576**	**103.142**	**102.599**	**103.331**	**102.451**	**102.527**	**102.586**	**102.510**	**103.499**	**102.262**	**102.191**	**102.839**	**102.166**	**101.815**	**102.958**	**103.733**	**101.993**	**102.743**
CATIONS RECALCULATED TO 12 OXYGENS																		
Si	2.981	2.999	2.995	2.998	3.015	3.008	3.004	3.011	3.014	3.019	3.011	3.010	3.004	3.007	3.011	2.966	3.017	3.002
Al	2.034	1.975	2.010	2.00:	1.990	2.004	1.998	1.984	2.009	2.01:	2.006	1.997	2.003	2.005	2.003	2.153	2.011	2.012
Ti	0.006	0.002	0.000	0.000	0.001	0.004	0.004	0.001	0.000	0.003	0.000	0.001	0.002	0.000	0.003	0.001	0.000	0.004
Fe3+	0.000	0.000	0.000	0.000	0.006	0.000	0.000	0.012	0.000	0.000	0.000	0.000	0.000	0.000	0.000	0.000	0.000	0.000
Mg	0.196	0.194	0.163	0.196	0.181	0.254	0.177	0.279	0.177	0.184	0.205	0.209	0.215	0.169	0.263	0.128	0.136	0.233
Fe2+	2.006	2.004	2.010	2.011	1.997	1.964	1.986	1.955	1.953	1.935	2.003	1.980	1.986	2.028	1.873	1.950	2.007	1.866
Mn	0.187	0.169	0.213	0.173	0.176	0.131	0.193	0.129	0.196	0.194	0.159	0.149	0.152	0.227	0.137	0.237	0.256	0.160
Ca	0.587	0.667	0.609	0.610	0.621	0.622	0.630	0.618	0.632	0.615	0.603	0.644	0.630	0.555	0.692	0.522	0.550	0.711
TOTAL	**7.996**	**8.011**	**7.000**	**7.997**	**7.986**	**7.987**	**7.993**	**7.990**	**7.981**	**7.969**	**7.986**	**7.990**	**7.992**	**7.990**	**7.984**	**7.956**	**7.977**	**7.988**
Fe/Fe+Mg	*0.911*	*0.912*	*0.925*	*0.911*	*0.917*	*0.885*	*0.918*	*0.875*	*0.917*	*0.913*	*0.907*	*0.904*	*0.902*	*0.923*	*0.877*	*0.938*	*0.937*	*0.889*
Alm	0.674	0.660	0.671	0.673	0.671	0.661	0.665	0.656	0.660	0.661	0.675	0.664	0.666	0.681	0.632	0.687	0.681	0.628
Py	0.066	0.064	0.054	0.066	0.061	0.086	0.059	0.094	0.05:	0.063	0.069	0.070	0.072	0.057	0.089	0.045	0.046	0.078
Sp	0.063	0.056	0.071	0.058	0.059	0.044	0.065	0.043	0.066	0.066	0.053	0.04:	0.051	0.076	0.046	0.083	0.087	0.054
Gr	0.197	0.220	0.203	0.204	0.209	0.209	0.211	0.207	0.214	0.210	0.203	0.216	0.211	0.186	0.233	0.184	0.187	0.239
(Ca+Mn)/(Mg+Ca+Mn+Fe)	0.260	0.276	0.274	0.262	0.268	0.253	0.276	0.250	0.280	0.276	0.256	0.266	0.262	0.262	0.280	0.267	0.273	0.293
X	56.77	56.29	55.34	54.87	54.27	53.92	53.44	52.97	52.49	52.02	51.54	51.05	50.59	50.33	49.47	49.17		
Y	44.48	45.88	48.63	50.08	51.46	52.89	54.20	55.69	57.44	58.49	59.89	61.63	62.69	63.90	65.63	66.89		
x-axis mm	0.00	0.15	0.44	0.59	0.74	0.89	1.03	1.18	1.37	1.48	1.63	1.81	1.93	2.05	2.24	2.37		
location	*frag adj hb*	*frag adj hb*	*rim adj hb?±nr rm - hb*		*rim adj bt*	*rim adj ??*	*adj fract*	*interior*	*adj fract*	*adj fract*	*adj fract*	*nr hb incl*	*nr hb incl*	*adj fract*	*adj fract*	*near fract*	*adj fract*	*adj qz incl*

TABLE B-1: Quantitative Microprobe Analysis for Garnet Compositions

PC-80B (continued)

	1GT1q	1GT1r	1GT1s	1GT1t	1GT1u	1GT1v	1GT1w	1GT1x	1GT1y	1GT1z	1GT1aa	1GT1ab	1GT1ac	1GT1ad	1GT1ae	1GT1af	1GT2a	1GT2b
WEIGHT PERCENT OXIDES																		
SiO2	38.554	38.870	38.935	38.683	38.578	38.260	38.787	38.636	38.261	38.352	38.374	38.225	39.076	38.499	38.987	38.585	38.566	38.782
Al2O3	22.008	21.945	21.792	21.871	21.894	21.655	21.849	21.847	21.765	21.521	21.519	21.427	21.950	21.675	21.963	21.749	21.953	21.698
TiO2	0.027	0.080	0.097	0.032	0.045	0.065	0.007	0.052	0.043	0.055	0.072	0.166	0.014	0.013	0.010	0.064	0.014	0.045
Fe2O3	0.000	0.000	0.000	0.000	0.000	0.013	0.000	0.000	0.000	0.000	0.000	0.057	0.000	0.000	0.000	0.000	0.000	0.024
MgO	1.400	2.162	2.180	1.755	2.059	1.46:	1.589	1.906	1.979	1.301	1.156	1.285	2.376	1.553	2.369	1.873	1.412	2.146
FeO	31.072	28.621	28.502	28.909	29.329	31.098	30.893	30.157	30.815	28.872	29.481	30.596	29.655	30.253	30.185	30.066	29.660	30.269
MnO	3.594	2.336	2.314	2.436	2.358	3.069	3.106	1.974	1.850	3.103	3.342	3.546	1.782	3.003	1.736	2.004	3.079	2.067
CaO	6.519	8.579	8.635	8.527	8.596	7.171	6.875	7.844	7.553	8.354	7.818	7.031	8.002	7.442	7.296	7.479	7.276	7.306
TOTAL	**103.174**	**102.593**	**102.455**	**102.213**	**102.859**	**102.801**	**103.106**	**102.416**	**102.266**	**101.558**	**101.762**	**102.333**	**102.855**	**102.438**	**102.546**	**101.820**	**101.960**	**102.337**
CATIONS RECALCULATED TO 12 OXYGENS																		
Si	3.001	3.00:	3.018	3.013	2.992	2.993	3.014	3.008	2.992	3.018	3.01:	3.004	3.017	3.010	3.021	3.019	3.019	3.01:
Al	2.019	2.003	1.990	2.008	2.001	1.997	2.001	2.005	2.006	1.996	1.996	1.985	1.998	1.997	2.006	2.006	2.026	1.991
Ti	0.002	0.005	0.006	0.002	0.003	0.004	0.000	0.003	0.003	0.003	0.004	0.00:	0.001	0.001	0.001	0.004	0.001	0.003
Fe3+	0.000	0.000	0.000	0.000	0.000	0.001	0.000	0.000	0.000	0.000	0.000	0.003	0.000	0.000	0.000	0.000	0.000	0.001
Mg	0.162	0.250	0.252	0.204	0.238	0.171	0.184	0.221	0.231	0.153	0.136	0.151	0.274	0.181	0.274	0.218	0.165	0.249
Fe2+	2.023	1.853	1.847	1.883	1.902	2.035	2.008	1.964	2.015	1.900	1.93:	2.011	1.915	1.978	1.956	1.967	1.942	1.971
Mn	0.237	0.153	0.152	0.161	0.155	0.203	0.204	0.130	0.123	0.207	0.223	0.236	0.117	0.199	0.114	0.133	0.204	0.136
Ca	0.544	0.712	0.717	0.712	0.714	0.601	0.572	0.654	0.633	0.704	0.659	0.592	0.662	0.623	0.606	0.627	0.610	0.610
TOTAL	**7.988**	**7.984**	**7.982**	**7.981**	**8.005**	**8.004**	**7.985**	**7.986**	**8.002**	**7.981**	**7.978**	**7.992**	**7.983**	**7.990**	**7.976**	**7.974**	**7.967**	**7.981**
Fe/Fe+Mg	*0.926*	*0.881*	*0.880*	*0.902*	*0.889*	*0.922*	*0.916*	*0.899*	*0.897*	*0.926*	*0.935*	*0.930*	*0.875*	*0.916*	*0.877*	*0.900*	*0.922*	*0.888*
Alm	0.682	0.624	0.622	0.636	0.632	0.676	0.676	0.661	0.671	0.641	0.656	0.673	0.645	0.663	0.663	0.668	0.665	0.665
Py	0.055	0.084	0.085	0.069	0.079	0.057	0.062	0.075	0.077	0.052	0.046	0.050	0.092	0.061	0.093	0.074	0.056	0.084
Sp	0.07:	0.052	0.051	0.054	0.052	0.068	0.069	0.044	0.041	0.06:	0.075	0.079	0.039	0.067	0.039	0.045	0.06:	0.046
Gr	0.183	0.240	0.242	0.240	0.237	0.200	0.193	0.220	0.211	0.238	0.223	0.198	0.223	0.209	0.205	0.213	0.209	0.206
(Ca+Mn)/(Mg+Ca+Mn+Fe)	0.263	0.291	0.293	0.295	0.289	0.267	0.262	0.264	0.252	0.307	0.298	0.277	0.262	0.276	0.244	0.258	0.279	0.251
X	48.69	48.22	47.74	47.58	46.71	46.20	46.19	45.37	44.42	43.89	43.47	42.72	42.04	41.57	41.09	40.62	51.15	52.60
Y	68.25	69.70	71.00	72.34	73.82	75.39	76.85	78.10	80.90	82.22	83.83	85.04	87.91	89.31	90.81	92.11	52.28	52.39
x-axis mm	2.52	2.67	2.81	2.94	3.11	3.28	3.43	3.57	3.87	4.01	4.18	4.32	4.62	4.76	4.92	5.06	0.00	0.15
location	*adj hb incl*	*interior*	*interior*	*near fract*	*near fract*	*adj fract*	*near fract*	*near fract*	*near fract*	*adj fract*	*adj fract*	*adj fract*	*±near rim*	*adj fract*	*±near rim*	*rim adj qz*	*rim adj ??*	*±near rim*

TABLE B-1: Quantitative Microprobe Analysis for Garnet Compositions

PC-80B (continued)

	1GT2c	1GT2d	1GT2e	1GT2f	1GT2g	1GT2h	2G1	2G2	2G3	2GT1a	2GT1b	2GT1c	2GT1d	2GT1e	2GT1f	2GT1g	2GT1h	2GT1i
WEIGHT PERCENT OXIDES																		
SiO2	38.642	38.505	38.837	38.434	38.910	38.770	38.740	39.181	38.428	39.015	37.903	38.238	39.021	39.056	38.451	38.942	38.634	38.272
Al2O3	21.674	21.573	21.811	21.858	22.175	21.978	21.704	21.747	21.842	21.957	21.643	21.841	21.692	21.564	21.554	21.603	21.566	21.659
TiO2	0.017	0.000	0.039	0.058	0.043	0.000	0.035	0.022	0.049	0.025	0.000	0.000	0.000	0.026	0.017	0.020	0.177	0.424
Fe2O3	0.177	0.152	0.000	0.000	0.000	0.000	0.102	0.095	0.000	0.000	0.000	0.000	0.000	0.190	0.032	0.081	0.000	0.000
MgO	2.347	1.499	1.811	2.060	2.450	1.181	2.185	1.897	2.005	2.222	1.258	1.598	1.284	1.892	1.512	1.361	1.317	1.274
FeO	30.276	31.036	30.828	30.458	30.097	29.736	30.620	30.442	30.194	29.787	30.718	29.854	30.027	28.909	30.387	30.137	30.780	30.452
MnO	1.867	3.329	2.210	2.077	1.796	3.408	1.809	1.882	1.681	1.658	3.219	2.328	3.064	1.876	2.433	2.947	3.074	2.877
CaO	7.494	6.632	7.415	7.417	7.231	7.345	7.383	7.553	8.296	7.784	6.909	7.854	7.488	8.487	7.599	7.412	7.127	7.428
TOTAL	**102.494**	**102.726**	**102.951**	**102.362**	**102.702**	**102.418**	**102.578**	**102.819**	**102.495**	**102.448**	**101.650**	**101.713**	**102.576**	**102.000**	**101.985**	**102.503**	**102.675**	**102.386**
CATIONS RECALCULATED TO 12 OXYGENS																		
Si	3.006	3.011	3.015	2.998	3.009	3.025	3.012	3.035	2.993	3.023	2.997	3.003	3.03:	3.040	3.017	3.037	3.018	2.997
Al	1.987	1.988	1.995	2.009	2.021	2.021	1.989	1.985	2.005	2.005	2.017	2.021	1.992	1.978	1.993	1.986	1.986	1.999
Ti	0.001	0.000	0.002	0.003	0.003	0.000	0.002	0.001	0.003	0.001	0.000	0.000	0.000	0.002	0.001	0.001	0.010	0.025
Fe3+	0.010	0.009	0.000	0.000	0.000	0.000	0.006	0.006	0.000	0.000	0.000	0.000	0.000	0.011	0.002	0.005	0.000	0.000
Mg	0.272	0.175	0.210	0.240	0.282	0.137	0.253	0.219	0.233	0.257	0.148	0.187	0.149	0.220	0.177	0.158	0.153	0.149
Fe2+	1.970	2.02:	2.001	1.987	1.946	1.941	1.991	1.972	1.966	1.930	2.031	1.960	1.956	1.882	1.994	1.966	2.011	1.994
Mn	0.123	0.221	0.145	0.137	0.118	0.225	0.119	0.123	0.111	0.109	0.216	0.155	0.202	0.124	0.162	0.195	0.203	0.191
Ca	0.625	0.556	0.617	0.620	0.599	0.614	0.615	0.627	0.692	0.646	0.585	0.661	0.625	0.708	0.639	0.619	0.597	0.623
TOTAL	**7.994**	**7.990**	**7.985**	**7.994**	**7.978**	**7.964**	**7.988**	**7.968**	**8.002**	**7.972**	**7.994**	**7.987**	**7.964**	**7.964**	**7.984**	**7.967**	**7.979**	**7.978**
Fe/Fe+Mg	*0.879*	*0.921*	*0.905*	*0.892*	*0.873*	*0.934*	*0.887*	*0.900*	*0.894*	*0.883*	*0.932*	*0.913*	*0.929*	*0.896*	*0.919*	*0.925*	*0.929*	*0.931*
Alm	0.659	0.681	0.673	0.666	0.661	0.665	0.668	0.670	0.655	0.656	0.682	0.662	0.667	0.642	0.671	0.669	0.678	0.674
Py	0.091	0.059	0.071	0.080	0.096	0.047	0.085	0.075	0.078	0.087	0.04:	0.063	0.051	0.075	0.059	0.054	0.052	0.050
Sp	0.041	0.074	0.049	0.046	0.03:	0.077	0.040	0.042	0.037	0.037	0.072	0.052	0.069	0.042	0.054	0.066	0.069	0.065
Gr	0.209	0.186	0.207	0.208	0.203	0.211	0.207	0.213	0.231	0.220	0.196	0.223	0.213	0.241	0.215	0.211	0.201	0.211
(Ca+Mn)/(Mg+Ca+Mn+Fe)	0.250	0.260	0.256	0.254	0.243	0.288	0.247	0.255	0.267	0.257	0.269	0.275	0.282	0.284	0.269	0.277	0.270	0.275
X	54.04	55.49	56.94	58.39	59.83	61.28	-91.22	-91.41	-80.33	-67.60	-70.82	-72.66	-74.05	-75.66	-77.27	-78.88	-85.04	-87.11
Y	52.53	52.48	52.71	52.82	53.01	53.03	-108.79	-112.50	-139.46	-125.97	-125.02	-124.96	-124.37	-123.97	-123.74	-123.18	-121.43	-121.37
x-axis mm	0.29	0.44	0.58	0.73	0.87	1.02	0.00	0.34	0.52	0.67	0.84	0.00	1.17	1.81	2.02			
location	*±near rim*	*adj fract*	*nr op incl*	*nr op incl*	*±near rim*	*rim adj hb*	*±near rim*	*nr rm - op*	*±near rim*	*fragment*	*rim adj qz*	*adj fract*	*adj fract*	*near fract*	*adj fract*	*rim adj op*	*rm adj bt? adj op incl*	

TABLE B-1: Quantitative Microprobe Analysis for Garnet Compositions

PC-80B (continued)

	2GT1j	2GT1k	2GT1l	2GT1m	2GT1n	2GT1o	2GT1p	2GT1q	2GT1r	2GT1s	2GT1t	2GT1u	2GT2a	2GT2b	2GT2c	2GT2d	2GT2e	2GT2f
WEIGHT PERCENT OXIDES																		
SiO2	38.912	38.487	38.973	38.711	38.290	39.211	39.220	38.986	38.887	39.061	39.542	39.189	38.833	39.395	38.791	38.711	38.679	38.649
Al2O3	21.489	21.592	21.484	21.640	21.653	21.683	21.698	21.958	22.077	22.116	21.809	21.811	21.595	21.813	21.797	21.569	21.607	21.465
TiO2	0.040	0.052	0.030	0.000	0.019	0.013	0.019	0.098	0.001	0.039	0.117	0.000	0.053	0.000	0.034	0.060	0.000	0.030
Fe2O3	0.193	0.000	0.085	0.000	0.000	0.127	0.212	0.000	0.000	0.000	0.122	0.175	0.007	0.045	0.000	0.023	0.188	0.266
MgO	1.260	1.478	1.288	1.271	1.256	1.775	2.193	1.699	1.647	2.108	2.242	1.624	1.166	1.945	1.226	1.281	1.622	1.410
FeO	30.019	31.080	29.846	30.995	30.312	30.330	29.865	29.768	30.614	29.251	28.999	30.933	29.933	30.192	30.316	30.180	30.708	31.412
MnO	2.925	2.82:	3.110	3.403	3.406	2.041	1.724	2.284	2.913	1.607	1.624	2.300	3.494	2.028	3.296	3.128	2.483	3.097
CaO	7.591	6.833	7.220	6.345	7.029	7.496	7.760	8.165	6.661	8.604	8.528	7.548	7.398	7.435	7.472	7.412	7.409	6.456
TOTAL	**102.429**	**102.352**	**102.036**	**102.365**	**101.965**	**102.676**	**102.691**	**102.958**	**102.800**	**102.786**	**102.983**	**103.580**	**102.479**	**102.853**	**102.932**	**102.364**	**102.696**	**102.785**
CATIONS RECALCULATED TO 12 OXYGENS																		
Si	3.038	3.016	3.050	3.033	3.013	3.042	3.035	3.017	3.021	3.015	3.041	3.025	3.034	3.045	3.01:	3.028	3.016	3.021
Al	1.978	1.994	1.982	1.998	2.008	1.982	1.979	2.003	2.021	2.012	1.976	1.984	1.989	1.987	1.000	1.988	1.985	1.978
Ti	0.002	0.003	0.002	0.000	0.001	0.001	0.001	0.006	0.000	0.002	0.007	0.000	0.003	0.000	0.002	0.004	0.000	0.002
Fe3+	0.011	0.000	0.005	0.000	0.000	0.007	0.012	0.000	0.000	0.000	0.007	0.010	0.000	0.003	0.000	0.001	0.011	0.016
Mg	0.147	0.173	0.150	0.148	0.147	0.205	0.253	0.196	0.191	0.243	0.257	0.187	0.136	0.224	0.142	0.149	0.189	0.164
Fe2+	1.960	2.037	1.954	2.031	1.994	1.968	1.933	1.927	1.989	1.888	1.865	1.997	1.956	1.952	1.974	1.974	2.002	2.054
Mn	0.193	0.188	0.206	0.226	0.227	0.134	0.113	0.150	0.192	0.105	0.106	0.150	0.231	0.133	0.217	0.207	0.164	0.205
Ca	0.635	0.574	0.605	0.533	0.593	0.623	0.643	0.677	0.554	0.712	0.703	0.624	0.619	0.616	0.623	0.621	0.619	0.541
TOTAL	**7.965**	**7.984**	**7.954**	**7.968**	**7.983**	**7.963**	**7.969**	**7.976**	**7.968**	**7.977**	**7.961**	**7.978**	**7.968**	**7.960**	**7.978**	**7.974**	**7.986**	**7.980**
Fe/Fe+Mg	*0.930*	*0.922*	*0.929*	*0.932*	*0.931*	*0.906*	*0.884*	*0.908*	*0.912*	*0.886*	*0.879*	*0.914*	*0.935*	*0.897*	*0.933*	*0.930*	*0.914*	*0.926*
Alm	0.668	0.686	0.670	0.691	0.674	0.672	0.657	0.653	0.680	0.641	0.636	0.675	0.665	0.667	0.668	0.669	0.673	0.693
Py	0.050	0.058	0.052	0.051	0.04:	0.070	0.086	0.067	0.065	0.082	0.088	0.063	0.046	0.077	0.048	0.051	0.063	0.055
Sp	0.066	0.063	0.071	0.077	0.077	0.046	0.038	0.051	0.066	0.036	0.036	0.051	0.079	0.045	0.074	0.070	0.055	0.069
Gr	0.216	0.193	0.208	0.181	0.200	0.213	0.219	0.230	0.190	0.241	0.240	0.211	0.210	0.211	0.211	0.210	0.208	0.182
(Ca+Mn)/(Mg+Ca+Mn+Fe)	0.282	0.256	0.278	0.258	0.277	0.258	0.257	0.280	0.255	0.277	0.276	0.262	0.289	0.256	0.284	0.281	0.263	0.252
X	-88.80	-90.17	-93.39	-95.01	-96.62	-98.23	-101.65	-106.82	-108.08	-109.51	-110.38	-114.35	-85.98	-86.38	-87.23	-87.99	-88.51	-89.06
Y	-121.06	-120.38	-119.78	-119.33	-118.93	-118.79	-118.35	-117.52	-115.78	-115.79	-115.20	-114.39	-105.65	-107.23	-110.63	-113.68	-115.42	-117.15
x-axis mm	2.19	2.34	2.67	2.84	3.00	3.17	3.51	4.03	4.25	4.39	4.50	4.90	0.00	0.16	0.51	0.83	1.01	1.19
location	*rim adj bt*	*adj fract*	*rim adj bt*	*adj fract*	*rim adj bt*	*rim adj qz?*	*near fract*	*nr rm - bt*	*rim adj qz*	*±near rim*	*rim adj op*	*rim adj bt*	*rim adj bt*	*±near rim*	*adj fract*	*rim adj bt*	*near fract*	*adj bt incl*

TABLE B-1: Quantitative Microprobe Analysis for Garnet Compositions

PC-80B (continued)										*PC-86D*								
	2GT2g	**2GT2h**	**2GT2i**	**2GT2j**	**2GT2k**	**2GT2l**	**2GT2m**	**2GT2n**	**2GT2o**	**G1 ref**	**G1 ref**	**G2**	**G3**	**G4**	**G5**	**G6**	**GT1a**	**GT1b**
WEIGHT PERCENT OXIDES																		
SiO2	38.932	38.667	39.185	38.818	38.810	39.098	38.126	39.074	39.153	37.292	38.359	38.074	38.287	38.329	38.288	37.433	36.982	36.477
Al2O3	21.791	21.453	21.992	21.749	21.484	21.886	21.669	22.135	21.731	21.150	21.463	21.357	21.717	21.566	21.574	21.564	20.767	21.250
TiO2	0.016	0.021	0.019	0.040	0.184	0.016	0.023	0.027	0.000	0.000	0.032	0.017	0.029	0.051	0.000	0.020	0.017	0.000
Fe2O3	0.000	0.316	0.000	0.000	0.041	0.000	0.000	0.000	0.162	0.182	0.270	0.097	0.000	0.000	0.083	0.000	0.454	0.000
MgO	1.446	1.274	2.110	1.668	1.543	1.601	1.057	2.051	2.108	2.219	2.337	2.010	1.639	1.090	1.944	1.740	1.801	2.015
FeO	30.729	31.397	29.859	30.615	30.140	30.109	30.643	30.602	30.806	37.339	37.527	36.893	38.530	38.161	38.091	37.756	37.001	37.013
MnO	2.723	3.331	1.768	2.025	2.507	2.509	3.953	1.816	1.634	2.439	2.349	3.123	2.564	3.033	2.598	2.923	3.014	2.710
CaO	7.255	6.504	7.854	7.630	7.493	7.727	6.493	7.532	7.241	1.214	1.261	1.120	1.136	1.459	1.143	1.206	1.240	1.150
TOTAL	**102.892**	**102.963**	**102.787**	**102.545**	**102.202**	**102.946**	**101.964**	**103.237**	**102.835**	**101.835**	**103.598**	**102.691**	**103.902**	**103.689**	**103.721**	**102.642**	**101.276**	**100.615**
CATIONS RECALCULATED TO 12 OXYGENS																		
Si	3.027	3.021	3.028	3.022	3.032	3.029	3.008	3.014	3.032	2.982	3.004	3.011	3.002	3.015	3.003	2.976	2.984	2.957
Al	1.997	1.975	2.003	1.996	1.978	1.998	2.015	2.012	1.983	1.993	1.981	1.991	2.007	1.000	1.994	2.020	1.975	2.031
Ti	0.001	0.001	0.001	0.002	0.011	0.001	0.001	0.002	0.000	0.000	0.002	0.001	0.002	0.003	0.000	0.001	0.001	0.000
Fe3+	0.000	0.019	0.000	0.000	0.002	0.000	0.000	0.000	0.009	0.011	0.016	0.006	0.000	0.000	0.005	0.000	0.028	0.000
Mg	0.168	0.148	0.243	0.194	0.180	0.185	0.124	0.236	0.243	0.264	0.273	0.237	0.192	0.128	0.227	0.206	0.217	0.244
Fe2+	1.998	2.051	1.929	1.993	1.969	1.951	2.022	1.974	1.995	2.497	2.458	2.440	2.526	2.511	2.499	2.510	2.497	2.510
Mn	0.179	0.220	0.116	0.134	0.166	0.165	0.264	0.119	0.107	0.165	0.156	0.209	0.170	0.202	0.173	0.197	0.206	0.186
Ca	0.604	0.544	0.650	0.637	0.627	0.641	0.549	0.622	0.601	0.104	0.106	0.095	0.095	0.123	0.096	0.103	0.107	0.09:
TOTAL	**7.974**	**7.981**	**7.970**	**7.977**	**7.966**	**7.971**	**7.983**	**7.978**	**7.971**	**8.016**	**7.995**	**7.990**	**7.993**	**7.982**	**7.997**	**8.013**	**8.014**	**8.027**
Fe/Fe+Mg	*0.923*	*0.933*	*0.888*	*0.911*	*0.916*	*0.913*	*0.942*	*0.893*	*0.891*	*0.904*	*0.900*	*0.911*	*0.930*	*0.952*	*0.917*	*0.924*	*0.920*	*0.912*
Alm	0.677	0.692	0.657	0.674	0.669	0.663	0.683	0.669	0.677	0.824	0.821	0.818	0.847	0.847	0.834	0.832	0.825	0.826
Py	0.057	0.050	0.083	0.066	0.061	0.063	0.042	0.07:	0.083	0.087	0.091	0.07:	0.064	0.043	0.076	0.068	0.072	0.080
Sp	0.061	0.074	0.039	0.045	0.056	0.056	0.089	0.040	0.036	0.055	0.052	0.070	0.057	0.068	0.058	0.065	0.068	0.061
Gr	0.205	0.184	0.221	0.215	0.213	0.218	0.185	0.211	0.204	0.034	0.035	0.032	0.032	0.042	0.032	0.034	0.035	0.033
(Ca+Mn)/(Mg+Ca+Mn+Fe)	0.266	0.258	0.261	0.260	0.270	0.274	0.275	0.251	0.240	0.089	0.087	0.102	0.089	0.110	0.08:	0.099	0.103	0.094
X	-89.36	-89.89	-90.20	-91.05	-91.57	-92.99	-93.60	-94.87	-95.30	103.40	103.40	48.25	55.35	73.08	92.33	113.24	56.21	58.17
Y	-118.52	-120.37	-121.74	-124.97	-126.55	-131.66	-134.64	-139.52	-141.09	282.69	282.60	280.52	303.03	308.97	301.22	298.97	275.33	275.56
x-axis mm	1.33	1.52	1.66	1.00	2.16	2.69	2.00	3.50	3.67	0.00	0.01						0.00	0.20
location	*rim adj bt*	*rim adj bt*	*±near rim*	*fragment*	*fragment*	*rim adj op*	*fragment*	*fragment*	*fragment*	*interior*	*interior*	*nr rm - bt*	*rim adj bt*	*rim adj bt*	*nr rm - bt*	*nr rm - bt*	*rim adj qz?*	*±near rim*

TABLE B-1: Quantitative Microprobe Analysis for Garnet Compositions

PC-86D (continued)

	GT1c	GT1d	GT1e	GT1f	GT1g	GT1h	GT1i	GT1j	GT1k	GT1l	GT1m	GT1n	GT1o	GT1p	GT1q	GT1r	GT1t	GT1u
WEIGHT PERCENT OXIDES																		
SiO2	37.149	37.509	36.903	37.864	36.971	37.063	37.789	37.142	37.975	38.014	37.314	37.915	37.647	36.996	36.947	37.809	37.566	37.457
Al2O3	20.972	21.448	20.790	21.077	21.488	21.046	21.022	21.039	21.435	21.389	20.988	21.514	21.203	21.217	21.032	21.462	21.154	21.306
TiO2	0.000	0.063	0.000	0.074	0.069	0.052	0.020	0.026	0.040	0.023	0.012	0.023	0.000	0.017	0.029	0.009	0.020	0.000
Fe2O3	0.261	0.000	0.347	0.534	0.000	0.203	0.426	0.290	0.030	0.050	0.172	0.000	0.356	0.001	0.313	0.022	0.256	0.076
MgO	2.049	1.977	1.884	2.053	1.957	1.490	2.221	1.904	1.936	1.738	1.529	1.954	1.935	1.721	2.010	2.297	1.909	1.542
FeO	37.201	38.045	36.980	37.516	37.654	38.417	36.951	37.957	37.562	37.880	37.804	37.846	37.930	38.148	37.817	37.306	37.743	38.397
MnO	2.483	2.605	2.753	2.741	2.497	2.616	2.181	2.620	2.727	2.611	2.499	2.343	2.412	2.691	2.429	2.499	2.582	2.640
CaO	1.238	1.128	1.234	1.190	1.073	1.269	1.388	1.082	1.273	1.210	1.212	1.376	1.379	1.226	1.406	1.310	1.171	1.307
TOTAL	**101.353**	**102.775**	**100.891**	**103.049**	**101.709**	**102.156**	**101.998**	**102.060**	**102.978**	**102.915**	**101.530**	**102.971**	**102.862**	**102.017**	**101.983**	**102.714**	**102.401**	**102.725**
CATIONS RECALCULATED TO 12 OXYGENS																		
Si	2.987	2.977	2.985	2.994	2.964	2.974	3.007	2.975	2.000	3.007	3.000	2.995	2.986	2.968	2.963	2.990	2.991	2.982
Al	1.987	2.006	1.982	1.965	2.030	1.990	1.972	1.986	1.996	1.994	1.989	2.003	1.982	2.006	1.988	2.000	1.985	1.999
Ti	0.000	0.004	0.000	0.004	0.004	0.003	0.001	0.002	0.002	0.001	0.001	0.001	0.000	0.001	0.002	0.001	0.001	0.000
Fe3+	0.016	0.000	0.021	0.032	0.000	0.012	0.026	0.018	0.002	0.003	0.010	0.000	0.021	0.000	0.019	0.001	0.015	0.005
Mg	0.246	0.234	0.227	0.242	0.234	0.178	0.263	0.227	0.228	0.205	0.183	0.230	0.229	0.206	0.240	0.271	0.227	0.183
Fe2+	2.501	2.525	2.502	2.481	2.524	2.578	2.459	2.543	2.481	2.506	2.542	2.500	2.516	2.559	2.536	2.467	2.513	2.557
Mn	0.169	0.175	0.189	0.184	0.170	0.178	0.147	0.178	0.182	0.175	0.170	0.157	0.162	0.183	0.165	0.167	0.174	0.178
Ca	0.107	0.096	0.107	0.101	0.092	0.109	0.118	0.093	0.108	0.103	0.104	0.116	0.117	0.105	0.121	0.111	0.09:	0.112
TOTAL	**8.012**	**8.017**	**8.013**	**8.003**	**8.017**	**8.022**	**7.993**	**8.021**	**7.999**	**7.993**	**7.000**	**8.002**	**8.013**	**8.028**	**8.033**	**8.009**	**8.007**	**8.016**
Fe/Fe+Mg	*0.911*	*0.915*	*0.917*	*0.911*	*0.915*	*0.935*	*0.903*	*0.918*	*0.916*	*0.924*	*0.933*	*0.916*	*0.917*	*0.926*	*0.913*	*0.901*	*0.917*	*0.933*
Alm	0.828	0.833	0.827	0.825	0.836	0.847	0.823	0.836	0.827	0.839	0.847	0.832	0.832	0.838	0.828	0.818	0.834	0.844
Py	0.081	0.077	0.075	0.081	0.077	0.059	0.088	0.075	0.076	0.069	0.061	0.077	0.076	0.067	0.079	0.08:	0.075	0.060
Sp	0.056	0.058	0.062	0.061	0.056	0.058	0.049	0.059	0.061	0.059	0.057	0.052	0.054	0.05:	0.054	0.056	0.058	0.059
Gr	0.035	0.032	0.035	0.034	0.031	0.036	0.03:	0.031	0.036	0.034	0.035	0.039	0.039	0.035	0.03:	0.037	0.033	0.037
(Ca+Mn)/(Mg+Ca+Mn+Fe)	0.091	0.089	0.098	0.095	0.087	0.094	0.089	0.089	0.097	0.093	0.092	0.091	0.092	0.094	0.093	0.092	0.091	0.096
X	60.12	61.22	64.03	64.51	68.50	70.17	71.85	73.81	75.63	77.25	80.08	81.63	83.59	85.77	87.50	89.45	93.26	94.74
Y	275.79	276.22	276.25	276.38	276.70	276.93	277.16	277.39	277.62	277.85	278.14	278.12	278.53	278.91	278.99	279.22	279.56	278.34
x-axis mm	0.39	0.51	0.79	0.84	1.24	1.41	1.58	1.78	1.96	2.13	2.41	2.56	2.77	2.99	3.16	3.36	3.74	3.93
location	*±near rim*	*nr rm - qz*	*nr rm - qz*	*nr rm - qz*	*nr rm - qz*	*adj fract*	*interior*	*±near rim*	*±near rim*	*rim adj qz*	*rim adj qz*	*±near rim*	*±near rim*	*rim adj qz*	*±near rim*	*±near rim*	*±near rim*	*rim adj qz*

TABLE B-1: Quantitative Microprobe Analysis for Garnet Compositions

PC-86D (continued)

	GT1v	GT1w	GT1x	GT1y	GT1z	GT1aa	GT1ab	GT1ac	GT1ad	GT1ae	GT1af	GT1ag	GT1ah	GT1ai	GT1ak	GT1al	GT1am	GT1ao
WEIGHT PERCENT OXIDES																		
SiO2	37.578	36.577	37.192	37.539	37.355	37.46:	36.801	37.402	36.702	36.263	36.814	38.605	37.535	37.645	37.489	36.326	37.984	37.444
Al2O3	21.203	21.009	20.828	21.411	21.336	20.888	21.280	21.652	21.131	20.903	21.466	21.613	21.121	21.137	21.446	21.538	21.104	21.601
TiO2	0.000	0.026	0.000	0.066	0.104	0.000	0.061	0.006	0.086	0.012	0.020	0.035	0.060	0.000	0.078	0.049	0.003	0.000
Fe2O3	0.440	0.134	0.322	0.000	0.033	0.491	0.000	0.000	0.000	0.000	0.000	0.043	0.166	0.150	0.000	0.000	0.449	0.000
MgO	1.984	1.981	1.889	1.868	2.117	1.621	2.184	2.196	1.956	1.826	1.941	2.107	1.837	1.779	1.603	1.858	1.753	1.373
FeO	38.120	37.911	37.319	37.791	37.814	37.810	37.522	37.808	37.310	37.546	37.958	37.759	37.424	37.501	37.895	36.556	37.505	38.226
MnO	2.587	2.473	2.314	2.499	2.660	2.707	2.392	2.479	2.459	2.649	2.639	2.438	2.736	2.566	2.894	2.665	2.984	3.141
CaO	1.265	1.226	1.111	1.277	1.271	1.084	1.282	1.238	1.299	1.193	1.215	1.127	1.216	1.157	1.256	1.147	1.071	1.141
TOTAL	**103.177**	**101.337**	**100.975**	**102.451**	**102.690**	**102.071**	**101.522**	**102.781**	**100.943**	**100.392**	**102.053**	**103.727**	**102.095**	**101.935**	**102.661**	**100.139**	**102.853**	**102.926**
CATIONS RECALCULATED TO 12 OXYGENS																		
Si	2.976	2.955	3.000	2.985	2.968	2.999	2.957	2.964	2.966	2.957	2.949	3.018	2.996	3.007	2.981	2.953	3.00:	2.976
Al	1.979	2.000	1.980	2.007	1.998	1.971	2.015	2.023	2.013	2.009	2.027	1.991	1.987	1.990	2.010	2.063	1.971	2.023
Ti	0.000	0.002	0.000	0.004	0.006	0.000	0.004	0.000	0.005	0.001	0.001	0.002	0.004	0.000	0.005	0.003	0.000	0.000
Fe3+	0.026	0.008	0.01:	0.000	0.002	0.02:	0.000	0.000	0.000	0.000	0.000	0.003	0.00:	0.009	0.000	0.000	0.027	0.000
Mg	0.234	0.239	0.227	0.221	0.251	0.193	0.262	0.259	0.236	0.222	0.232	0.246	0.219	0.212	0.190	0.225	0.207	0.163
Fe2+	2.525	2.561	2.518	2.513	2.513	2.531	2.521	2.506	2.522	2.561	2.543	2.468	2.498	2.505	2.520	2.485	2.485	2.541
Mn	0.174	0.169	0.158	0.168	0.179	0.184	0.163	0.166	0.168	0.183	0.179	0.161	0.185	0.174	0.195	0.183	0.200	0.211
Ca	0.107	0.106	0.096	0.109	0.108	0.093	0.110	0.105	0.112	0.104	0.104	0.094	0.104	0.099	0.107	0.09:	0.091	0.097
TOTAL	**8.021**	**8.03:**	**7.000**	**8.008**	**8.026**	**8.001**	**8.032**	**8.024**	**8.022**	**8.037**	**8.036**	**7.983**	**8.002**	**7.994**	**8.009**	**8.013**	**7.991**	**8.012**
Fe/Fe+Mg	*0.915*	*0.915*	*0.917*	*0.919*	*0.909*	*0.929*	*0.906*	*0.906*	*0.915*	*0.920*	*0.916*	*0.910*	*0.920*	*0.922*	*0.930*	*0.917*	*0.923*	*0.93:*
Alm	0.831	0.833	0.840	0.834	0.824	0.843	0.825	0.825	0.82:	0.834	0.832	0.831	0.831	0.838	0.837	0.82:	0.833	0.844
Py	0.077	0.078	0.076	0.074	0.082	0.065	0.086	0.085	0.078	0.072	0.076	0.083	0.073	0.071	0.063	0.075	0.069	0.054
Sp	0.057	0.055	0.053	0.056	0.059	0.061	0.053	0.055	0.055	0.05:	0.059	0.054	0.062	0.058	0.065	0.061	0.067	0.070
Gr	0.035	0.035	0.032	0.036	0.036	0.031	0.036	0.035	0.037	0.034	0.034	0.032	0.035	0.033	0.036	0.033	0.031	0.032
(Ca+Mn)/(Mg+Ca+Mn+Fe)	0.092	0.08:	0.085	0.092	0.094	0.092	0.089	0.089	0.092	0.094	0.093	0.086	0.096	0.091	0.100	0.095	0.098	0.102
X	98.92	99.58	101.19	102.80	105.10	106.73	109.01	110.96	112.92	114.06	117.38	119.61	120.69	122.70	126.61	128.56	130.85	134.10
Y	280.55	280.63	281.39	280.96	281.05	281.43	281.50	281.74	281.97	282.19	280.75	282.65	282.84	283.11	284.12	283.58	284.19	284.48
x-axis mm	4.40	4.47	4.65	4.81	5.04	5.21	5.44	5.64	5.83	5.95	6.31	6.60	6.71	6.92	7.32	7.52	7.76	8.09
location	*rim adj qz*	*nr rm - qz*	*nr rm - qz*	*±near rim*	*interior*	*adj fract*	*±near rim*	*interior*	*±near rim*	*nr fract*	*nr fract*	*interior*	*near fract*	*near fract*	*adj fract*	*near fract*	*rim adj qz*	***adj fract***

TABLE B-1: Quantitative Microprobe Analysis for Garnet Compositions

PC-86D (continued)

	GT1ap	GT1aq	GT1ar	GT1as	GT1at	GT1au	GT1av	GT1aw	GT1ax	GT2a	GT2b	GT2c	GT2d	GT2e	GT2f	GT2g	GT2h	GT2i
WEIGHT PERCENT OXIDES																		
SiO2	36.494	37.178	37.671	36.970	37.149	36.361	37.155	37.292	37.368	38.156	36.379	37.274	37.868	37.464	37.871	37.693	38.390	37.574
Al2O3	20.661	20.682	21.203	21.192	21.035	21.258	20.994	21.354	21.140	21.585	21.460	21.846	21.186	21.654	21.508	21.121	21.747	21.522
TiO2	0.135	0.049	0.000	0.069	0.035	0.055	0.014	0.000	0.026	0.000	0.000	0.023	0.055	0.046	0.054	0.000	0.014	0.000
Fe2O3	0.292	0.502	0.245	0.000	0.398	0.000	0.011	0.000	0.017	0.000	0.000	0.000	0.148	0.000	0.249	0.636	0.000	0.000
MgO	1.894	1.816	2.060	2.317	1.855	1.969	2.156	1.936	1.688	1.843	2.090	2.133	1.973	2.033	1.895	1.797	1.901	1.916
FeO	36.881	36.466	37.065	36.989	37.679	36.444	36.040	36.255	36.508	37.526	37.802	37.169	37.243	37.845	38.784	38.555	37.921	37.889
MnO	2.921	3.249	2.908	2.649	3.053	3.033	2.967	3.405	3.821	2.573	2.478	2.245	2.488	2.510	2.668	2.569	2.385	2.343
CaO	1.288	1.157	1.231	1.150	1.250	1.191	1.179	1.258	1.110	1.252	1.314	1.217	1.217	1.320	1.249	1.234	1.177	1.357
TOTAL	**100.566**	**101.099**	**102.383**	**101.336**	**102.454**	**100.311**	**100.516**	**101.500**	**101.678**	**102.935**	**101.523**	**101.907**	**102.178**	**102.872**	**104.278**	**103.605**	**103.535**	**102.601**
CATIONS RECALCULATED TO 12 OXYGENS																		
Si	2.968	2.999	2.995	2.970	2.968	2.955	3.001	2.988	2.997	3.00:	2.931	2.969	3.011	2.967	2.971	2.978	3.00:	2.983
Al	1.980	1.966	1.987	2.007	1.981	2.036	1.998	2.016	1.998	2.007	2.038	2.051	1.985	2.021	1.988	1.967	2.009	2.013
Ti	0.008	0.003	0.000	0.004	0.002	0.003	0.001	0.000	0.002	0.000	0.000	0.001	0.003	0.003	0.003	0.000	0.001	0.000
Fe3+	0.018	0.031	0.015	0.000	0.024	0.000	0.001	0.000	0.001	0.000	0.000	0.000	0.009	0.000	0.015	0.038	0.000	0.000
Mg	0.230	0.218	0.244	0.277	0.221	0.239	0.260	0.231	0.202	0.217	0.251	0.253	0.234	0.240	0.222	0.212	0.222	0.227
Fe2+	2.508	2.460	2.464	2.485	2.518	2.477	2.434	2.429	2.448	2.476	2.547	2.476	2.476	2.507	2.544	2.548	2.486	2.515
Mn	0.201	0.222	0.196	0.180	0.207	0.209	0.203	0.231	0.260	0.172	0.169	0.151	0.168	0.168	0.177	0.172	0.158	0.158
Ca	0.112	0.100	0.105	0.099	0.107	0.104	0.102	0.108	0.095	0.106	0.113	0.104	0.104	0.112	0.105	0.104	0.099	0.115
TOTAL	**8.025**	**7.999**	**8.005**	**8.023**	**8.027**	**8.023**	**7.999**	**8.004**	**8.002**	**7.987**	**8.04:**	**8.005**	**7.989**	**8.019**	**8.025**	**8.019**	**7.985**	**8.011**
Fe/Fe+Mg	*0.916*	*0.918*	*0.910*	*0.900*	*0.919*	*0.912*	*0.904*	*0.913*	*0.924*	*0.919*	*0.910*	*0.907*	*0.914*	*0.913*	*0.920*	*0.923*	*0.918*	*0.917*
Alm	0.822	0.820	0.819	0.817	0.825	0.818	0.812	0.810	0.815	0.834	0.827	0.82:	0.831	0.828	0.835	0.839	0.838	0.834
Py	0.075	0.073	0.081	0.091	0.072	0.079	0.087	0.077	0.067	0.073	0.082	0.085	0.078	0.079	0.073	0.06:	0.075	0.075
Sp	0.066	0.074	0.065	0.059	0.068	0.069	0.068	0.077	0.086	0.058	0.055	0.051	0.056	0.056	0.058	0.057	0.053	0.052
Gr	0.037	0.033	0.035	0.033	0.035	0.034	0.034	0.036	0.032	0.036	0.037	0.035	0.035	0.037	0.034	0.034	0.033	0.038
(Ca+Mn)/(Mg+Ca+Mn+Fe)	0.103	0.107	0.09:	0.092	0.103	0.103	0.102	0.113	0.118	0.094	0.092	0.086	0.091	0.093	0.093	0.091	0.087	0.091
X	136.22	138.34	140.30	142.25	144.59	146.96	148.32	149.72	151.84	78.52	79.07	79.62	80.17	80.47	80.71	80.61	82.37	83.48
Y	284.77	284.94	284.83	285.40	285.63	285.85	286.08	286.31	286.54	305.42	303.98	302.59	301.15	298.98	297.61	297.34	293.13	292.89
x-axis mm	8.30	8.51	8.71	8.91	9.15	9.39	9.52	9.67	9.88	0.00	0.15	0.30	0.46	0.68	0.82	0.84	1.30	1.41
location	*near fract*	*±near rim*	*interior*	*interior*	*interior*	*interior*	*±near rim*	*nr rm - pl*	*rim adj pl*	*rim adj qz*	*±near rim*	*±near rim*	*±near rim*	*±near rim*	*nr rm - bt*	*nr rm - bt*	*nr rm - bt*	*nr rm - qz*

TABLE B-1: Quantitative Microprobe Analysis for Garnet Compositions

PC-86D (continued)

	GT2j	GT2k	GT2l	GT2m	GT2n	GT2o	GT2p	GT2q	GT2r	GT2s	GT2t	GT2u	GT2v	GT2w	GT2x	GT2y	GT2z	GT2aa
WEIGHT PERCENT OXIDES																		
SiO2	37.975	36.886	37.867	37.435	37.554	37.335	36.525	37.980	36.699	36.643	37.081	37.298	37.409	38.048	37.207	37.385	37.008	36.993
Al2O3	21.289	21.290	21.563	21.359	21.355	21.269	20.860	21.377	21.241	21.110	21.099	21.325	21.233	21.222	21.032	21.055	21.038	21.494
TiO2	0.000	0.000	0.020	0.000	0.049	0.032	0.000	0.046	0.000	0.000	0.009	0.017	0.046	0.034	0.066	0.000	0.000	0.049
Fe2O3	0.102	0.000	0.000	0.000	0.011	0.000	0.011	0.136	0.000	0.000	0.041	0.137	0.000	0.557	0.152	0.124	0.217	0.000
MgO	1.928	2.109	2.150	2.102	1.972	1.934	1.896	1.93:	2.108	2.009	1.891	1.798	1.943	1.767	1.521	1.972	2.225	2.271
FeO	37.649	37.587	37.555	37.424	37.758	37.905	37.108	37.901	37.448	37.114	37.562	38.375	36.898	38.396	38.019	37.311	36.969	36.244
MnO	2.146	2.409	2.075	2.220	2.432	2.296	2.440	2.479	2.326	2.499	2.483	2.612	2.632	2.744	2.727	2.367	2.733	2.467
CaO	1.262	1.409	1.394	1.364	1.410	1.317	1.242	1.238	1.350	1.348	1.209	1.367	1.127	1.170	1.194	1.113	1.231	1.237
TOTAL	**102.351**	**101.690**	**102.624**	**101.904**	**102.541**	**102.088**	**100.082**	**103.097**	**101.172**	**100.723**	**101.375**	**102.929**	**101.288**	**103.938**	**101.918**	**101.327**	**101.421**	**100.755**
CATIONS RECALCULATED TO 12 OXYGENS																		
Si	3.013	2.960	2.994	2.987	2.984	2.982	2.978	2.999	2.959	2.967	2.983	2.966	3.000	2.992	2.986	3.001	2.974	2.976
Al	1.991	2.014	2.00:	2.008	1.000	2.002	2.004	1.989	2.019	2.015	2.001	1.998	2.007	1.967	1.989	1.992	1.993	2.038
Ti	0.000	0.000	0.001	0.000	0.003	0.002	0.000	0.003	0.000	0.000	0.001	0.001	0.003	0.002	0.004	0.000	0.000	0.003
Fe3+	0.006	0.000	0.000	0.000	0.001	0.000	0.001	0.008	0.000	0.000	0.002	0.008	0.000	0.033	0.009	0.007	0.013	0.000
Mg	0.228	0.252	0.253	0.250	0.234	0.230	0.230	0.228	0.253	0.243	0.227	0.213	0.232	0.207	0.182	0.236	0.267	0.272
Fe2+	2.498	2.522	2.484	2.497	2.509	2.532	2.530	2.503	2.525	2.513	2.527	2.552	2.475	2.525	2.552	2.505	2.485	2.438
Mn	0.144	0.164	0.139	0.150	0.164	0.155	0.168	0.166	0.159	0.171	0.169	0.176	0.179	0.183	0.185	0.161	0.186	0.168
Ca	0.107	0.121	0.118	0.117	0.120	0.113	0.108	0.105	0.117	0.117	0.104	0.116	0.097	0.099	0.103	0.096	0.106	0.107
TOTAL	**7.988**	**8.033**	**7.000**	**8.009**	**8.013**	**8.015**	**8.01:**	**7.000**	**8.032**	**8.026**	**8.015**	**8.030**	**7.993**	**8.007**	**8.011**	**7.999**	**8.023**	**8.002**
Fe/Fe+Mg	*0.916*	*0.909*	*0.907*	*0.909*	*0.915*	*0.917*	*0.917*	*0.916*	*0.909*	*0.912*	*0.918*	*0.923*	*0.914*	*0.924*	*0.933*	*0.914*	*0.903*	*0.900*
Alm	0.839	0.824	0.829	0.829	0.829	0.836	0.833	0.834	0.827	0.826	0.835	0.835	0.82:	0.838	0.844	0.836	0.816	0.817
Py	0.077	0.083	0.085	0.083	0.077	0.076	0.076	0.076	0.083	0.07:	0.075	0.06:	0.078	0.069	0.060	0.079	0.088	0.091
Sp	0.048	0.054	0.046	0.04:	0.054	0.051	0.056	0.055	0.052	0.056	0.056	0.058	0.05:	0.061	0.061	0.054	0.061	0.056
Gr	0.036	0.03:	0.039	0.039	0.03:	0.037	0.036	0.035	0.038	0.038	0.034	0.038	0.033	0.033	0.034	0.032	0.035	0.036
(Ca+Mn)/(Mg+Ca+Mn+Fe)	0.085	0.093	0.086	0.089	0.094	0.089	0.091	0.090	0.090	0.095	0.090	0.096	0.092	0.093	0.095	0.086	0.096	0.092
X	83.47	84.01	84.56	85.11	85.30	86.43	86.76	87.31	87.86	88.41	89.43	89.50	89.73	89.81	91.16	92.28	91.41	92.81
Y	291.69	289.91	288.35	286.70	285.22	283.66	282.10	280.54	278.97	277.41	275.63	275.22	272.72	271.88	269.60	268.03	266.47	264.91
x-axis m	1.53	1.72	1.88	2.06	2.20	2.40	2.56	2.72	2.89	3.05	3.26	3.30	3.56	3.64	3.91	4.10	4.28	4.49
location	*nr rm - qz*	*near rim*	*interior*	*interior*	*±near rim*	*±near rim*	*±near rim*	*±near rim*	*±near rim*	*±near rim*	*nr rm - qz*	*im adj qz*	*nr rm - qz*	*nr rm - qz*	*im adj qz*	*±near rim*	*interior*	*interior*

TABLE B-1: Quantitative Microprobe Analysis for Garnet Compositions

	PC-86D (continued)			*PC-88A*														
	GT2ab	**GT2ac**	**GT2ad**	**G1 ref**	**G1 ref**	**G2**	**G3**	**G4**	**G5**	**G6**	**G7**	**G8**	**GT1a**	**GT1b**	**GT1c**	**GT1d**	**GT1e**	**GT1f**
WEIGHT PERCENT OXIDES																		
SiO2	37.648	36.775	37.383	37.930	38.604	38.461	38.074	38.240	37.408	37.730	37.559	38.128	37.828	37.585	37.936	37.491	37.414	37.820
Al2O3	21.250	21.080	21.396	21.403	21.720	21.46:	21.296	21.166	21.559	21.781	21.203	21.715	21.553	20.756	21.451	21.339	21.573	21.285
TiO2	0.000	0.147	0.006	0.020	0.060	0.026	0.000	0.000	0.040	0.123	0.000	0.000	0.014	0.026	0.000	0.000	0.000	0.014
Fe2O3	0.119	0.000	0.000	0.252	0.118	0.206	0.393	0.586	0.000	0.000	0.200	0.000	0.000	0.576	0.185	0.130	0.000	0.353
MgO	2.270	2.047	1.928	2.646	2.805	1.958	1.999	1.968	1.931	1.765	1.460	1.318	2.112	2.017	2.091	2.328	2.662	2.689
FeO	36.757	36.527	36.480	36.757	36.614	37.451	37.309	37.203	37.301	37.808	37.760	37.898	37.623	36.542	37.559	37.205	36.697	36.640
MnO	2.737	2.757	3.403	1.861	1.796	1.960	1.973	2.098	2.167	2.173	2.383	2.421	1.880	1.891	2.003	1.921	1.666	1.699
CaO	1.226	1.212	1.164	1.959	2.122	1.937	2.108	1.957	1.906	1.981	1.949	1.869	2.031	1.862	1.962	1.902	1.908	2.036
TOTAL	**102.007**	**100.545**	**101.760**	**102.828**	**103.839**	**103.469**	**103.152**	**103.218**	**102.312**	**103.361**	**102.514**	**103.349**	**103.041**	**101.255**	**103.187**	**102.316**	**101.920**	**102.536**
CATIONS RECALCULATED TO 12 OXYGENS																		
Si	2.997	2.976	2.988	2.987	2.000	3.014	2.999	3.009	2.974	2.972	2.991	3.003	2.983	3.013	2.988	2.977	2.972	2.987
Al	1.994	2.011	2.016	1.987	1.989	1.983	1.977	1.963	2.020	2.022	1.990	2.016	2.003	1.961	1.992	1.997	2.01:	1.981
Ti	0.000	0.009	0.000	0.001	0.004	0.002	0.000	0.000	0.002	0.007	0.000	0.000	0.001	0.002	0.000	0.000	0.000	0.001
Fe3+	0.007	0.000	0.000	0.015	0.007	0.012	0.023	0.035	0.000	0.000	0.012	0.000	0.000	0.035	0.011	0.008	0.000	0.021
Mg	0.269	0.247	0.230	0.311	0.325	0.229	0.235	0.231	0.229	0.207	0.173	0.155	0.248	0.241	0.246	0.276	0.315	0.317
Fe2+	2.447	2.472	2.439	2.421	2.379	2.454	2.458	2.449	2.480	2.490	2.515	2.496	2.481	2.449	2.474	2.471	2.438	2.420
Mn	0.185	0.189	0.230	0.124	0.118	0.130	0.132	0.140	0.146	0.145	0.161	0.162	0.126	0.128	0.134	0.129	0.112	0.114
Ca	0.105	0.105	0.09:	0.165	0.177	0.163	0.178	0.165	0.162	0.167	0.166	0.158	0.172	0.160	0.166	0.162	0.162	0.172
TOTAL	**8.003**	**8.009**	**8.003**	**8.011**	**7.999**	**7.987**	**8.001**	**7.992**	**8.014**	**8.010**	**8.008**	**7.989**	**8.014**	**7.988**	**8.010**	**8.020**	**8.019**	**8.012**
Fe/Fe+Mg	*0.901*	*0.909*	*0.914*	*0.886*	*0.880*	*0.915*	*0.913*	*0.914*	*0.916*	*0.923*	*0.936*	*0.942*	*0.909*	*0.910*	*0.910*	*0.900*	*0.885*	*0.884*
Alm	0.814	0.820	0.813	0.801	0.793	0.825	0.819	0.820	0.822	0.827	0.834	0.840	0.820	0.822	0.820	0.813	0.805	0.801
Py	0.08:	0.082	0.077	0.103	0.108	0.077	0.078	0.077	0.076	0.069	0.058	0.052	0.082	0.081	0.081	0.091	0.104	0.105
Sp	0.061	0.063	0.077	0.041	0.039	0.044	0.044	0.047	0.048	0.048	0.053	0.054	0.042	0.043	0.044	0.043	0.037	0.038
Gr	0.035	0.035	0.033	0.055	0.059	0.055	0.059	0.055	0.054	0.056	0.055	0.053	0.057	0.054	0.055	0.053	0.054	0.057
(Ca+Mn)/(Mg+Ca+Mn+Fe)	0.096	0.098	0.110	0.096	0.098	0.098	0.103	0.102	0.102	0.104	0.108	0.107	0.098	0.097	0.099	0.096	0.091	0.095
X	93.36	94.47	94.59	-130.64	-130.70	-124.49	-131.07	-119.14	-129.05	-120.42	-117.63	-119.06	-131.92	-131.45	-131.06	-130.63	-130.20	-129.59
Y	263.35	261.78	260.36	-154.27	-154.28	-124.49	-130.10	-95.16	-131.71	-120.35	-114.87	-122.95	-158.57	-158.16	-157.76	-157.41	-156.68	-156.56
x-axis m	4.66	4.85	4.99	0.00	0.01								0.00	0.06	0.12	0.17	0.26	0.32
location	*±near rim*	*±near rim*	*im adj qz*	*interior*	*interior*	*rim adj pl*	*rim adj pl*	*rim adj pl*	*im adj bt*	*im adj bt*	*im adj bt*	*im adj bt*	*im adj qz*	*nr rm - qz*	*nr rm - qz*	*±near rim*	*interior*	*interior*

TABLE B-1: Quantitative Microprobe Analysis for Garnet Compositions

PC-88A (continued)

	GT1g	GT1h	GT1i	GT1j	GT1k	GT1l	GT1m	GT1n	GT1o	GT1p	GT1q	GT1r	GT1s	GT1t	GT2a	GT2b	GT2c	GT2d
WEIGHT PERCENT OXIDES																		
SiO2	37.966	37.948	37.150	38.012	37.627	37.622	36.848	37.865	37.693	37.440	37.704	37.490	37.257	37.361	37.223	37.752	38.294	38.006
Al2O3	21.237	21.527	21.026	21.133	21.158	21.061	21.241	21.251	21.561	20.847	20.990	21.349	21.102	21.311	21.373	21.697	21.313	21.567
TiO2	0.069	0.078	0.000	0.061	0.038	0.029	0.029	0.000	0.009	0.000	0.023	0.000	0.055	0.000	0.032	0.072	0.043	0.000
Fe2O3	0.401	0.086	0.260	0.582	0.429	0.539	0.000	0.284	0.000	0.684	0.353	0.104	0.238	0.202	0.000	0.000	0.631	0.059
MgO	2.756	2.635	2.684	2.710	2.559	2.616	2.648	2.623	2.569	2.703	2.563	2.494	2.296	1.811	1.686	2.234	2.456	2.249
FeO	36.671	36.942	36.154	36.272	36.801	36.319	36.549	36.102	35.903	35.910	35.852	37.038	36.887	38.253	38.071	37.176	37.355	37.282
MnO	1.697	1.805	1.753	1.768	1.750	1.822	1.781	1.909	1.625	1.872	1.671	1.776	1.897	2.006	1.986	1.958	1.853	1.884
CaO	1.839	2.040	1.921	2.134	2.016	2.153	1.928	2.048	1.965	2.022	1.999	1.898	1.993	1.918	2.002	1.999	1.972	2.104
TOTAL	**102.636**	**103.061**	**100.948**	**102.672**	**102.378**	**102.161**	**101.024**	**102.082**	**101.325**	**101.478**	**101.155**	**102.149**	**101.725**	**102.862**	**102.373**	**102.888**	**103.917**	**103.151**
CATIONS RECALCULATED TO 12 OXYGENS																		
Si	2.993	2.982	2.981	2.995	2.982	2.985	2.960	2.999	2.998	2.989	3.010	2.978	2.977	2.968	2.969	2.977	2.991	2.989
Al	1.973	1.994	1.988	1.963	1.976	1.969	2.011	1.983	2.021	1.961	1.975	1.999	1.987	1.995	2.009	2.016	1.962	1.999
Ti	0.004	0.005	0.000	0.004	0.002	0.002	0.002	0.000	0.001	0.000	0.001	0.000	0.003	0.000	0.002	0.004	0.003	0.000
Fe3+	0.024	0.005	0.016	0.035	0.026	0.032	0.000	0.017	0.000	0.041	0.021	0.006	0.014	0.012	0.000	0.000	0.037	0.003
Mg	0.324	0.309	0.321	0.318	0.302	0.309	0.317	0.310	0.305	0.322	0.305	0.295	0.273	0.214	0.200	0.263	0.286	0.264
Fe2+	2.418	2.428	2.426	2.390	2.439	2.410	2.455	2.391	2.388	2.397	2.394	2.460	2.465	2.541	2.539	2.451	2.440	2.452
Mn	0.113	0.120	0.119	0.118	0.117	0.122	0.121	0.128	0.109	0.127	0.113	0.119	0.128	0.135	0.134	0.131	0.123	0.125
Ca	0.155	0.172	0.165	0.180	0.171	0.183	0.166	0.174	0.167	0.173	0.171	0.162	0.171	0.163	0.171	0.169	0.165	0.177
TOTAL	**8.004**	**8.014**	**8.017**	**8.003**	**8.015**	**8.013**	**8.033**	**8.001**	**7.990**	**8.00:**	**7.990**	**8.01:**	**8.019**	**8.029**	**8.025**	**8.011**	**8.007**	**8.00:**
Fe/Fe+Mg	*0.882*	*0.887*	*0.883*	*0.882*	*0.890*	*0.886*	*0.886*	*0.885*	*0.887*	*0.882*	*0.887*	*0.893*	*0.900*	*0.922*	*0.927*	*0.903*	*0.895*	*0.903*
Alm	0.803	0.802	0.800	0.795	0.805	0.797	0.803	0.796	0.804	0.794	0.803	0.810	0.812	0.832	0.834	0.813	0.810	0.812
Py	0.108	0.102	0.106	0.106	0.09:	0.102	0.104	0.103	0.103	0.107	0.102	0.097	0.090	0.070	0.066	0.087	0.095	0.087
Sp	0.038	0.03:	0.039	0.039	0.039	0.041	0.03:	0.043	0.037	0.042	0.038	0.039	0.042	0.044	0.044	0.043	0.041	0.042
Gr	0.052	0.057	0.055	0.05:	0.057	0.061	0.054	0.058	0.056	0.057	0.057	0.053	0.056	0.054	0.056	0.056	0.055	0.059
(Ca+Mn)/(Mg+Ca+Mn+Fe)	0.089	0.096	0.094	0.099	0.095	0.101	0.094	0.101	0.093	0.099	0.095	0.093	0.098	0.098	0.100	0.099	0.095	0.100
X	-129.34	-128.91	-128.48	-128.05	-127.61	-126.84	-126.58	-126.32	-125.89	-125.63	-125.03	-124.46	-124.17	-123.81	-135.00	-134.38	-133.83	-133.24
Y	-156.21	-155.61	-155.36	-154.96	-154.55	-154.15	-153.75	-153.35	-152.70	-152.37	-152.15	-151.82	-151.25	-150.95	-149.00	-149.22	-149.91	-150.25
x-axis m	0.36	0.44	0.49	0.55	0.61	0.69	0.74	0.79	0.87	0.91	0.97	1.04	1.10	1.15	0.00	0.07	0.15	0.22
location	*interior*	*interior*	*interior*	*interior*	*interior*	*interior*	*interior*	*interior*	*interior*	*interior*	*±near rim*	*nr rm - bt*	*nr rm - bt*	*rim adj bt*	*rim adj bt*	*nr rm - bt*	*±near rim*	*±near rim*

TABLE B-1: Quantitative Microprobe Analysis for Garnet Compositions

PC-88A (continued)

	GT2e	GT2f	GT2g	GT2h	GT2i	GT2j	GT2k	GT2l	GT2m	GT2n	GT2o	GT2p	GT2q	GT2r	GT2s	GT2t	GT3a	GT3b
WEIGHT PERCENT OXIDES																		
SiO2	38.022	37.318	37.749	37.844	37.918	38.051	37.617	36.951	37.563	37.431	37.405	37.710	37.015	37.527	37.490	36.960	37.621	37.224
Al2O3	21.231	21.002	21.307	21.352	21.312	21.692	21.675	21.348	21.344	21.591	21.053	21.180	21.218	21.253	20.791	20.775	21.444	21.380
TiO2	0.000	0.000	0.046	0.078	0.017	0.017	0.000	0.000	0.000	0.000	0.000	0.043	0.066	0.000	0.049	0.000	0.035	0.000
Fe2O3	0.329	0.343	0.447	0.346	0.073	0.000	0.000	0.000	0.000	0.000	0.240	0.483	0.000	0.101	0.628	0.332	0.000	0.023
MgO	1.817	1.404	1.919	2.315	2.411	2.691	2.640	2.498	2.568	2.654	2.473	2.242	1.643	1.907	2.118	1.524	2.297	2.646
FeO	37.425	37.680	38.203	37.505	36.331	36.523	36.477	36.607	36.633	37.166	36.332	37.262	37.199	37.514	36.707	37.174	35.605	37.152
MnO	1.955	2.156	2.066	1.933	1.886	1.898	1.698	1.702	1.591	1.831	1.612	1.920	2.194	1.795	1.821	2.091	1.747	1.709
CaO	1.984	2.129	1.998	2.012	1.926	1.936	1.973	1.772	1.937	1.892	1.997	2.086	1.973	1.968	2.012	1.973	1.943	1.829
TOTAL	**102.763**	**102.032**	**103.735**	**103.385**	**101.874**	**102.808**	**102.080**	**100.878**	**101.636**	**102.565**	**101.112**	**102.926**	**101.308**	**102.065**	**101.616**	**100.829**	**100.692**	**101.963**
CATIONS RECALCULATED TO 12 OXYGENS																		
Si	3.007	2.988	2.972	2.977	3.008	2.990	2.979	2.970	2.990	2.962	2.995	2.980	2.978	2.991	2.998	2.991	3.010	2.964
Al	1.979	1.982	1.977	1.980	1.993	2.009	2.023	2.022	2.002	2.014	1.987	1.973	2.012	1.996	1.959	1.982	2.022	2.007
Ti	0.000	0.000	0.003	0.005	0.001	0.001	0.000	0.000	0.000	0.000	0.000	0.003	0.004	0.000	0.003	0.000	0.002	0.000
Fe3+	0.01:	0.021	0.027	0.021	0.004	0.000	0.000	0.000	0.000	0.000	0.015	0.029	0.000	0.006	0.038	0.020	0.000	0.001
Mg	0.214	0.168	0.225	0.271	0.285	0.315	0.312	0.299	0.305	0.313	0.295	0.264	0.197	0.227	0.252	0.184	0.274	0.314
Fe2+	2.475	2.523	2.515	2.467	2.410	2.400	2.416	2.460	2.439	2.460	2.433	2.463	2.503	2.500	2.455	2.516	2.383	2.474
Mn	0.131	0.146	0.138	0.129	0.127	0.126	0.114	0.116	0.107	0.123	0.109	0.129	0.149	0.121	0.123	0.143	0.118	0.115
Ca	0.168	0.183	0.169	0.170	0.164	0.163	0.167	0.153	0.165	0.160	0.171	0.177	0.170	0.168	0.172	0.171	0.167	0.156
TOTAL	**7.994**	**8.011**	**8.024**	**8.019**	**7.992**	**8.005**	**8.00:**	**8.01:**	**8.009**	**8.031**	**8.005**	**8.016**	**8.013**	**8.008**	**8.001**	**8.008**	**7.976**	**8.032**
Fe/Fe+Mg	*0.920*	*0.938*	*0.918*	*0.901*	*0.894*	*0.884*	*0.886*	*0.892*	*0.889*	*0.887*	*0.892*	*0.903*	*0.927*	*0.917*	*0.907*	*0.932*	*0.897*	*0.887*
Alm	0.828	0.836	0.826	0.812	0.807	0.799	0.803	0.813	0.809	0.805	0.809	0.812	0.829	0.829	0.817	0.835	0.810	0.809
Py	0.072	0.056	0.074	0.089	0.096	0.105	0.104	0.099	0.101	0.102	0.098	0.087	0.065	0.075	0.084	0.061	0.093	0.103
Sp	0.044	0.048	0.045	0.042	0.042	0.042	0.038	0.038	0.036	0.040	0.036	0.042	0.04:	0.040	0.041	0.048	0.040	0.038
Gr	0.056	0.061	0.055	0.056	0.055	0.054	0.056	0.050	0.055	0.053	0.057	0.058	0.056	0.056	0.057	0.057	0.057	0.051
(Ca+Mn)/(Mg+Ca+Mn+Fe)	0.100	0.109	0.101	0.098	0.097	0.096	0.094	0.089	0.090	0.093	0.093	0.101	0.106	0.096	0.099	0.104	0.097	0.089
X	-132.66	-131.94	-131.49	-130.90	-130.31	-129.73	-129.14	-128.56	-127.97	-127.38	-126.80	-126.21	-125.68	-124.89	-124.46	-123.87	-114.65	-113.95
Y	-150.65	-151.23	-151.74	-151.88	-152.45	-152.70	-153.31	-153.52	-153.93	-154.38	-155.00	-155.16	-155.55	-156.07	-156.39	-156.80	-141.62	-140.85
x-axis m	0.29	0.39	0.45	0.51	0.60	0.66	0.74	0.81	0.88	0.95	1.04	1.0:	1.16	1.26	1.31	1.38	0.00	0.10
location	*ear fract*	*ear fract*	*ear fract*	*ear fract*	*interior*	*interior*	*interior*	*interior*	*interior*	*interior*	*interior*	*ear fract*	*adj fract*	*ear fract*	*r rm - qz*	*im adj qz*	*r rm - qz*	*±near rim*

TABLE B-1: Quantitative Microprobe Analysis for Garnet Compositions

PC-88A (continued)

	GT3c	GT3d	GT3e	GT3f	GT3g	GT3h	GT3i	GT3j	GT3k	GT3l	GT3m	GT3n	GT3o	GT4a	GT4b	GT4c	GT4d	GT4e
WEIGHT PERCENT OXIDES																		
SiO2	37.064	38.171	37.928	36.402	37.529	36.812	37.819	36.141	37.672	37.413	37.573	37.703	37.910	36.760	36.58:	37.673	37.648	36.593
Al2O3	21.132	21.347	21.352	21.042	21.643	21.123	21.661	21.347	21.272	21.090	21.655	21.447	21.387	21.042	21.514	21.220	21.647	21.600
TiO2	0.017	0.009	0.009	0.087	0.000	0.006	0.038	0.000	0.000	0.090	0.058	0.041	0.020	0.000	0.000	0.084	0.000	0.000
Fe2O3	0.159	0.353	0.281	0.000	0.000	0.000	0.000	0.000	0.116	0.146	0.000	0.000	0.000	0.000	0.000	0.052	0.000	0.000
MgO	2.548	2.625	2.600	2.58:	2.451	2.490	2.488	2.572	2.598	2.494	2.536	2.366	1.46:	1.683	2.175	2.421	2.498	2.512
FeO	36.807	36.814	36.780	36.166	36.312	35.835	36.343	36.432	36.227	36.008	36.579	36.651	37.361	37.099	37.524	36.445	36.595	37.018
MnO	1.703	1.818	1.868	1.953	1.970	1.877	1.959	1.961	1.773	1.828	1.791	1.926	2.327	2.194	1.928	1.780	1.894	1.988
CaO	1.892	1.758	1.871	1.834	2.014	1.995	2.126	1.963	1.991	2.152	2.282	2.142	1.958	1.857	1.841	1.928	1.939	2.051
TOTAL	**101.322**	**102.895**	**102.689**	**100.074**	**101.919**	**100.138**	**102.434**	**100.416**	**101.649**	**101.221**	**102.474**	**102.276**	**102.433**	**100.635**	**101.572**	**101.603**	**102.221**	**101.762**
CATIONS RECALCULATED TO 12 OXYGENS																		
Si	2.970	3.001	2.991	2.954	2.979	2.977	2.985	2.929	2.996	2.991	2.969	2.987	3.009	2.978	2.938	2.000	2.981	2.928
Al	1.996	1.978	1.985	2.013	2.025	2.013	2.015	2.039	1.994	1.987	2.017	2.002	2.001	2.009	2.036	1.991	2.01:	2.037
Ti	0.001	0.001	0.001	0.005	0.000	0.000	0.002	0.000	0.000	0.005	0.003	0.002	0.001	0.000	0.000	0.005	0.000	0.000
Fe3+	0.00:	0.021	0.017	0.000	0.000	0.000	0.000	0.000	0.007	0.009	0.000	0.000	0.000	0.000	0.000	0.003	0.000	0.000
Mg	0.304	0.308	0.306	0.313	0.290	0.300	0.293	0.311	0.308	0.297	0.299	0.279	0.174	0.203	0.260	0.287	0.295	0.300
Fe2+	2.467	2.421	2.426	2.455	2.411	2.424	2.399	2.469	2.409	2.408	2.417	2.428	2.480	2.514	2.520	2.427	2.423	2.477
Mn	0.116	0.121	0.125	0.134	0.132	0.129	0.131	0.135	0.119	0.124	0.120	0.129	0.156	0.151	0.131	0.120	0.127	0.135
Ca	0.162	0.148	0.158	0.159	0.171	0.173	0.180	0.170	0.170	0.184	0.193	0.182	0.167	0.161	0.158	0.164	0.164	0.176
TOTAL	**8.026**	**7.999**	**8.008**	**8.034**	**8.008**	**8.016**	**8.005**	**8.052**	**8.004**	**8.005**	**8.019**	**8.00:**	**7.989**	**8.017**	**8.044**	**7.998**	**8.00:**	**8.053**
Fe/Fe+Mg	*0.890*	*0.887*	*0.888*	*0.887*	*0.893*	*0.890*	*0.891*	*0.888*	*0.887*	*0.890*	*0.890*	*0.897*	*0.934*	*0.925*	*0.906*	*0.894*	*0.892*	*0.892*
Alm	0.809	0.808	0.805	0.802	0.802	0.801	0.799	0.800	0.801	0.799	0.798	0.804	0.833	0.82:	0.821	0.809	0.805	0.802
Py	0.09:	0.103	0.101	0.102	0.097	0.099	0.098	0.101	0.102	0.099	0.099	0.093	0.058	0.067	0.085	0.096	0.098	0.097
Sp	0.038	0.040	0.041	0.044	0.044	0.043	0.044	0.044	0.03:	0.041	0.03:	0.043	0.053	0.04:	0.043	0.040	0.042	0.044
Gr	0.053	0.049	0.052	0.052	0.057	0.057	0.05:	0.055	0.056	0.061	0.064	0.060	0.056	0.053	0.052	0.055	0.055	0.057
(Ca+Mn)/(Mg+Ca+Mn+Fe)	0.091	0.08:	0.094	0.096	0.101	0.09:	0.104	0.099	0.096	0.102	0.103	0.103	0.108	0.103	0.094	0.095	0.097	0.101
X	-113.06	-112.43	-111.87	-111.18	-110.48	-109.79	-109.10	-108.45	-107.71	-106.77	-106.32	-105.63	-104.94	-123.44	-123.31	-123.35	-123.21	-123.07
Y	-140.08	-139.31	-138.55	-137.61	-137.01	-136.24	-135.47	-134.83	-133.93	-132.96	-132.18	-131.63	-130.86	-129.37	-128.87	-128.38	-127.88	-127.39
x-axis m	0.22	0.32	0.42	0.53	0.62	0.73	0.83	0.92	1.04	1.17	1.26	1.35	1.46	0.00	0.05	0.10	0.15	0.20
location	*±near rim*	*interior*	*interior*	*interior*	*interior*	*interior*	*interior*	*interior*	*interior*	*±near rim*	*±near rim*	*nr rm - bt*	*rim adj bt*	*rim adj bt*	*nr rm - bt*	*nr rm - bt*	*±near rim*	*±near rim*

TABLE B-1: Quantitative Microprobe Analysis for Garnet Compositions

PC-88A (continued)																*PC-93A*		
	GT4f	**GT4g**	**GT4h**	**GT4i**	**GT4j**	**GT5a**	**GT5b**	**GT5c**	**GT5d**	**GT5e**	**GT5f**	**GT5g**	**GT5h**	**GT5i**	**GT5j**	**GT1a**	**GT1b**	**GT1c**
WEIGHT PERCENT OXIDES																		
SiO2	36.832	37.899	37.661	37.536	38.658	37.021	37.199	37.048	37.208	37.239	36.919	37.093	36.004	36.915	37.361	38.277	38.249	38.038
Al2O3	21.692	21.040	21.358	21.037	21.785	20.791	21.010	21.096	21.126	21.070	21.160	21.362	21.177	21.155	21.480	21.047	20.569	20.671
TiO2	0.000	0.055	0.000	0.020	0.069	0.017	0.058	0.052	0.069	0.012	0.017	0.061	0.000	0.038	0.000	0.023	0.000	0.000
Fe2O3	0.000	0.339	0.053	0.309	0.000	0.387	0.107	0.165	0.102	0.321	0.014	0.000	0.000	0.000	0.000	0.631	1.473	0.935
MgO	2.578	2.471	2.462	2.162	1.314	1.735	2.163	2.252	2.335	2.360	2.383	2.305	2.266	2.056	1.686	0.840	1.012	1.075
FeO	36.402	35.803	36.669	36.752	38.521	37.182	36.562	37.144	36.809	36.989	36.880	36.511	36.912	36.860	37.072	26.257	27.434	27.012
MnO	1.775	1.960	1.951	1.878	2.091	1.946	1.917	1.813	1.874	1.722	1.773	1.833	1.945	1.993	2.248	7.831	6.885	7.152
CaO	1.849	1.959	1.852	1.902	1.844	1.936	1.900	1.938	1.888	1.959	1.933	1.937	1.992	1.933	1.817	7.254	7.019	6.449
TOTAL	**101.128**	**101.526**	**102.006**	**101.596**	**104.282**	**101.015**	**100.916**	**101.508**	**101.411**	**101.672**	**101.079**	**101.102**	**100.296**	**100.950**	**101.664**	**102.160**	**102.641**	**101.332**
CATIONS RECALCULATED TO 12 OXYGENS																		
Si	2.951	3.015	2.991	2.998	3.015	2.988	2.992	2.970	2.979	2.977	2.968	2.975	2.930	2.974	2.988	3.019	3.013	3.026
Al	2.048	1.973	1.999	1.980	2.003	1.978	1.991	1.993	1.994	1.985	2.005	2.019	2.031	2.009	2.024	1.957	1.910	1.938
Ti	0.000	0.003	0.000	0.001	0.004	0.001	0.004	0.003	0.004	0.001	0.001	0.004	0.000	0.002	0.000	0.001	0.000	0.000
Fe3+	0.000	0.020	0.003	0.019	0.000	0.023	0.006	0.00:	0.006	0.019	0.001	0.000	0.000	0.000	0.000	0.038	0.087	0.056
Mg	0.308	0.293	0.291	0.257	0.153	0.209	0.259	0.269	0.279	0.281	0.286	0.276	0.275	0.247	0.201	0.099	0.119	0.127
Fe2+	2.439	2.382	2.435	2.455	2.513	2.510	2.459	2.490	2.465	2.473	2.480	2.449	2.512	2.484	2.479	1.732	1.807	1.797
Mn	0.120	0.132	0.131	0.127	0.138	0.133	0.131	0.123	0.127	0.117	0.121	0.125	0.134	0.136	0.152	0.523	0.459	0.482
Ca	0.159	0.167	0.158	0.163	0.154	0.167	0.164	0.166	0.162	0.168	0.167	0.166	0.174	0.167	0.156	0.613	0.592	0.550
TOTAL	**8.025**	**7.985**	**8.008**	**8.001**	**7.979**	**8.00:**	**8.006**	**8.025**	**8.016**	**8.020**	**8.028**	**8.012**	**8.055**	**8.019**	**8.000**	**7.982**	**7.988**	**7.977**
Fe/Fe+Mg	*0.888*	*0.890*	*0.893*	*0.905*	*0.943*	*0.923*	*0.905*	*0.902*	*0.898*	*0.898*	*0.897*	*0.899*	*0.901*	*0.910*	*0.925*	*0.946*	*0.938*	*0.934*
Alm	0.806	0.801	0.808	0.818	0.850	0.831	0.816	0.817	0.813	0.814	0.812	0.812	0.812	0.819	0.82:	0.584	0.607	0.608
Py	0.102	0.099	0.097	0.086	0.052	0.069	0.086	0.088	0.092	0.093	0.094	0.091	0.089	0.081	0.067	0.033	0.03:	0.043
Sp	0.03:	0.044	0.044	0.042	0.047	0.044	0.043	0.040	0.042	0.038	0.03:	0.041	0.043	0.045	0.051	0.176	0.154	0.163
Gr	0.053	0.056	0.052	0.054	0.052	0.056	0.054	0.055	0.053	0.055	0.055	0.055	0.056	0.055	0.052	0.207	0.199	0.186
(Ca+Mn)/(Mg+Ca+Mn+Fe)	0.092	0.101	0.096	0.097	0.099	0.09:	0.098	0.095	0.095	0.094	0.094	0.097	0.099	0.09:	0.103	0.383	0.353	0.349
X	-122.98	-122.89	-122.36	-122.43	-122.32	-131.12	-130.59	-130.06	-129.52	-128.99	-128.46	-127.93	-127.39	-126.86	-126.33	156.52	155.70	154.88
Y	-126.89	-126.40	-125.90	-125.41	-124.91	-110.43	-110.22	-110.16	-110.22	-110.15	-110.08	-110.02	-109.95	-109.88	-109.81	231.97	231.17	230.64
x-axis m	0.25	0.30	0.38	0.43	0.48	0.00	0.06	0.11	0.16	0.22	0.27	0.32	0.38	0.43	0.49	0.00	0.11	0.21
location	*±near rim*	*±near rim*	*nr rm - bt*	*nr rm - bt*	*im adj bt*	*im adj bt*	*nr rm - bt*	*nr rm - bt*	*±near rim*	*±near rim*	*±near rim*	*±near rim*	*nr rm - bt*	*nr rm - bt*	*im adj bt*	*im adj bt*	*nr rm - bt*	*±near rim*

TABLE B-1: Quantitative Microprobe Analysis for Garnet Compositions

PC-93A (continued)

	GT1d	GT1e	GT1f	GT1g	GT1h	GT1i	GT1j	GT1k	GT1l	GT1m	GT1n	GT1o	GT1p	GT1q	GT1r	GT1s	GT1t	GT1u
WEIGHT PERCENT OXIDES																		
SiO2	38.481	36.901	37.922	38.282	37.851	37.802	37.137	38.414	38.392	38.420	38.153	37.744	38.030	37.712	38.182	38.131	38.106	38.127
Al2O3	21.499	22.258	21.288	20.827	20.930	20.778	21.243	21.202	21.104	20.780	21.169	20.917	20.824	20.695	21.176	20.935	20.920	21.018
TiO2	0.000	0.000	0.000	0.000	0.079	0.088	0.053	0.000	0.000	0.003	0.000	0.053	0.000	0.035	0.006	0.000	0.050	0.000
Fe2O3	0.437	0.000	0.093	0.951	0.631	0.783	0.105	0.783	0.764	0.921	0.632	0.786	1.084	1.174	0.612	0.703	0.879	0.550
MgO	0.914	1.037	1.143	0.959	0.820	0.810	0.936	0.731	0.873	0.731	0.978	1.127	1.094	1.071	0.983	0.868	0.882	0.809
FeO	27.670	28.889	29.012	27.643	27.160	27.049	28.978	26.635	27.825	26.226	29.018	29.380	29.517	29.406	28.198	28.577	28.657	27.911
MnO	8.014	6.512	6.433	6.812	7.310	7.278	6.997	7.683	7.161	7.444	6.703	5.891	5.806	5.961	6.077	6.020	6.662	6.696
CaO	6.745	5.766	5.733	6.707	7.118	7.128	6.320	7.883	6.826	7.288	6.272	6.409	6.357	6.488	7.364	6.706	6.564	6.728
TOTAL	**103.760**	**101.363**	**101.624**	**102.181**	**101.899**	**101.716**	**101.769**	**103.331**	**102.945**	**101.813**	**102.925**	**102.307**	**102.712**	**102.542**	**102.598**	**101.93:**	**102.720**	**101.839**
CATIONS RECALCULATED TO 12 OXYGENS																		
Si	2.999	2.941	3.011	3.023	3.002	3.004	2.964	3.003	3.013	3.038	3.001	2.989	2.000	2.986	3.003	3.019	3.004	3.021
Al	1.975	2.091	1.992	1.938	1.957	1.946	1.998	1.953	1.952	1.937	1.962	1.952	1.936	1.931	1.963	1.954	1.944	1.963
Ti	0.000	0.000	0.000	0.000	0.005	0.005	0.003	0.000	0.000	0.000	0.000	0.003	0.000	0.002	0.000	0.000	0.003	0.000
Fe3+	0.026	0.000	0.006	0.057	0.038	0.047	0.006	0.046	0.045	0.055	0.037	0.047	0.064	0.06:	0.036	0.042	0.052	0.033
Mg	0.106	0.123	0.135	0.113	0.097	0.096	0.111	0.085	0.102	0.086	0.115	0.133	0.129	0.126	0.115	0.102	0.104	0.096
Fe2+	1.803	1.926	1.926	1.826	1.802	1.798	1.934	1.741	1.826	1.734	1.909	1.946	1.947	1.947	1.855	1.892	1.889	1.849
Mn	0.529	0.440	0.433	0.456	0.491	0.490	0.473	0.509	0.476	0.499	0.447	0.395	0.388	0.400	0.405	0.404	0.445	0.449
Ca	0.563	0.492	0.488	0.567	0.605	0.607	0.540	0.660	0.574	0.617	0.529	0.544	0.537	0.550	0.621	0.569	0.554	0.571
TOTAL	**8.001**	**8.013**	**7.990**	**7.979**	**7.996**	**7.994**	**8.031**	**7.998**	**7.988**	**7.966**	**7.999**	**8.009**	**8.000**	**8.012**	**7.997**	**7.983**	**7.995**	**7.982**
Fe/Fe+Mg	*0.944*	*0.93:*	*0.934*	*0.942*	*0.949*	*0.949*	*0.946*	*0.953*	*0.947*	*0.953*	*0.943*	*0.936*	*0.938*	*0.939*	*0.941*	*0.949*	*0.948*	*0.951*
Alm	0.601	0.646	0.646	0.616	0.602	0.601	0.632	0.581	0.613	0.591	0.637	0.645	0.649	0.644	0.619	0.638	0.631	0.624
Py	0.035	0.041	0.045	0.038	0.032	0.032	0.036	0.028	0.034	0.029	0.038	0.044	0.043	0.042	0.039	0.035	0.035	0.032
Sp	0.176	0.147	0.145	0.154	0.164	0.164	0.155	0.170	0.160	0.170	0.149	0.131	0.129	0.132	0.135	0.136	0.149	0.152
Gr	0.188	0.165	0.164	0.192	0.202	0.203	0.177	0.220	0.193	0.210	0.176	0.180	0.179	0.182	0.207	0.192	0.185	0.193
(Ca+Mn)/(Mg+Ca+Mn+Fe)	0.364	0.313	0.309	0.345	0.366	0.367	0.331	0.390	0.353	0.380	0.325	0.311	0.308	0.314	0.342	0.328	0.334	0.344
X	152.35	152.27	151.60	150.79	149.97	149.42	148.33	147.21	146.69	145.46	145.05	144.23	143.41	142.60	141.77	140.96	139.65	138.99
Y	229.30	228.63	227.96	227.29	226.62	225.95	225.28	224.30	223.81	223.50	222.60	221.93	221.26	220.59	219.93	219.10	218.11	217.92
x-axis m	0.50	0.57	0.66	0.77	0.87	0.96	1.09	1.24	1.31	1.43	1.53	1.64	1.74	1.85	1.96	2.07	2.24	2.30
location	*nr rm - qz*	*nr rm - qz*	*±near rim*	*nr rm - pl*	*nr rm - pl*	*nr rm - pl*	*nr bt incl*	*dj bt incl*	*nr bt incl*	*nr rm - pl*	*±near rim*	*interior*	*interior*	*interior*	*±near rim*	*±near rim*	*±near rim*	*r rm - qz?*

TABLE B-1: Quantitative Microprobe Analysis for Garnet Compositions

PC-93A (continued)

	GT1v	GT1w	GT1x	GT1y	GT1z	GT1aa	GT1ab	GT1ac	GT1ad	GT1ae	GT1af	GT1ag	GT1ah	GT1ai	GT1aj	GT1ak	GT1al	GT1am
WEIGHT PERCENT OXIDES																		
SiO2	37.668	38.385	37.771	38.177	38.233	38.624	37.254	37.108	36.480	38.172	37.56:	38.191	37.918	37.991	36.965	37.631	38.182	37.790
Al2O3	20.968	21.131	20.838	20.760	21.046	20.614	20.659	20.762	21.073	20.817	20.599	21.089	21.182	21.048	20.618	20.630	21.058	20.777
TiO2	0.000	0.023	0.038	0.000	0.018	0.026	0.026	0.020	0.041	0.000	0.041	0.070	0.018	0.000	0.032	0.047	0.000	0.000
Fe2O3	0.618	0.802	0.921	1.039	1.008	1.397	0.809	0.714	0.112	1.048	1.113	0.678	0.653	0.838	1.056	0.657	0.831	0.987
MgO	0.805	0.794	0.988	1.145	1.130	0.951	0.935	0.800	0.918	0.825	0.815	0.912	0.992	0.987	0.820	0.720	0.912	0.848
FeO	27.498	27.749	28.618	29.235	29.738	28.333	28.425	27.990	29.011	26.685	27.278	28.644	29.572	29.004	28.472	26.872	28.896	27.680
MnO	7.222	7.358	6.424	5.810	5.971	6.443	6.281	7.236	6.400	7.297	7.048	6.765	6.269	6.310	7.096	6.796	6.088	6.167
CaO	7.049	7.067	6.741	6.058	6.424	6.444	6.713	6.746	6.837	7.533	7.346	6.550	6.506	6.767	6.858	7.092	6.970	7.711
TOTAL	**101.828**	**103.309**	**102.339**	**102.224**	**103.568**	**102.832**	**101.102**	**101.376**	**100.872**	**102.377**	**101.810**	**102.899**	**103.110**	**102.945**	**101.917**	**100.445**	**102.937**	**101.960**
CATIONS RECALCULATED TO 12 OXYGENS																		
Si	2.994	3.005	2.991	3.018	2.992	3.034	2.987	2.974	2.942	3.011	2.991	3.003	2.983	2.990	2.957	3.022	3.001	2.997
Al	1.964	1.950	1.945	1.934	1.941	1.908	1.952	1.961	2.003	1.935	1.933	1.955	1.964	1.953	1.944	1.952	1.951	1.942
Ti	0.000	0.001	0.002	0.000	0.001	0.002	0.002	0.001	0.002	0.000	0.002	0.004	0.001	0.000	0.002	0.003	0.000	0.000
Fe3+	0.037	0.047	0.055	0.062	0.059	0.083	0.049	0.043	0.007	0.062	0.067	0.040	0.039	0.04:	0.064	0.03:	0.049	0.059
Mg	0.095	0.093	0.117	0.135	0.132	0.111	0.112	0.096	0.110	0.097	0.097	0.107	0.116	0.116	0.098	0.086	0.107	0.100
Fe2+	1.828	1.817	1.895	1.933	1.946	1.861	1.906	1.876	1.957	1.760	1.816	1.884	1.946	1.909	1.905	1.804	1.899	1.836
Mn	0.486	0.488	0.431	0.389	0.396	0.429	0.427	0.491	0.437	0.488	0.475	0.451	0.418	0.421	0.481	0.462	0.405	0.414
Ca	0.600	0.593	0.572	0.513	0.539	0.542	0.577	0.579	0.591	0.637	0.627	0.552	0.548	0.571	0.588	0.610	0.587	0.655
TOTAL	**8.005**	**7.995**	**8.007**	**7.984**	**8.006**	**7.969**	**8.011**	**8.022**	**8.050**	**7.990**	**8.007**	**7.995**	**8.015**	**8.009**	**8.037**	**7.980**	**7.999**	**8.003**
Fe/Fe+Mg	*0.950*	*0.951*	*0.942*	*0.935*	*0.937*	*0.944*	*0.945*	*0.952*	*0.947*	*0.948*	*0.949*	*0.946*	*0.944*	*0.943*	*0.951*	*0.954*	*0.947*	*0.948*
Alm	0.607	0.608	0.629	0.651	0.646	0.632	0.631	0.617	0.632	0.58:	0.602	0.629	0.643	0.633	0.620	0.609	0.633	0.611
Py	0.032	0.031	0.039	0.045	0.044	0.038	0.037	0.031	0.036	0.033	0.032	0.036	0.038	0.038	0.032	0.029	0.036	0.033
Sp	0.162	0.163	0.143	0.131	0.131	0.146	0.141	0.161	0.141	0.164	0.158	0.151	0.138	0.139	0.157	0.156	0.135	0.138
Gr	0.199	0.198	0.190	0.173	0.179	0.184	0.191	0.190	0.191	0.214	0.208	0.184	0.181	0.189	0.191	0.206	0.196	0.218
(Ca+Mn)/(Mg+Ca+Mn+Fe)	0.361	0.361	0.333	0.304	0.310	0.330	0.332	0.352	0.332	0.377	0.365	0.335	0.319	0.329	0.348	0.362	0.331	0.356
X	138.50	137.68	136.86	136.04	135.22	134.21	132.93	132.48	130.78	129.49	128.34	127.70	126.76	126.21	125.78	123.92	123.45	122.93
Y	217.25	216.58	215.91	215.24	214.57	213.90	212.69	212.56	210.18	209.21	209.80	208.46	207.88	207.21	206.94	205.87	205.20	204.53
x-axis m	2.39	2.49	2.60	2.70	2.81	2.93	3.11	3.15	3.45	3.61	3.74	3.89	3.00	4.08	4.13	4.35	4.43	4.52
location	*r rm - qz?*	*r rm - qz?*	*adj pl incl*	*nr pl incl*	*nr pl incl*	*nr qz incl*	*dj qz incl*	*adj fract*	*im adj qz*	*adj fract*	*adj fract*	*nr rm - qz*	*nr rm - qz*	*nr rm - qz*	*im adj qz*	*im adj qz*	*nr rm - qz*	*nr rm - qz*

TABLE B-1: Quantitative Microprobe Analysis for Garnet Compositions

	PC-93A (continued)								*PC-104E*									
	GT1an	**GT1ao**	**GT1ap**	**GT1aq**	**GT1ar**	**GT1as**	**GT1at**	**GT1au**	**G1**	**GT1a**	**GT1b**	**GT1c**	**GT1d**	**GT1e**	**GT2a**	**GT2b**	**GT2c**	**GT2d**
WEIGHT PERCENT OXIDES																		
SiO2	37.870	37.668	37.483	37.666	38.159	37.699	37.978	38.145	37.734	37.073	38.345	38.124	38.696	37.929	38.364	37.769	37.808	37.522
Al2O3	20.976	20.575	20.644	20.787	20.496	20.774	20.872	20.444	22.179	21.445	21.946	22.033	21.675	21.718	21.439	21.704	21.649	21.622
TiO2	0.012	0.000	0.000	0.000	0.047	0.000	0.000	0.000	0.014	0.032	0.040	0.064	0.023	0.000	0.000	0.000	0.038	0.000
Fe2O3	0.794	1.133	1.012	0.862	1.414	0.958	0.855	1.666	0.000	0.000	0.000	0.000	0.382	0.000	0.229	0.000	0.000	0.000
MgO	0.834	0.859	0.821	0.877	1.020	0.890	1.084	0.956	3.119	2.752	3.237	3.446	3.430	3.009	2.380	2.669	3.022	2.866
FeO	28.499	28.462	28.034	28.203	28.127	27.961	28.861	27.902	36.504	37.728	37.762	37.832	36.974	36.838	37.568	37.966	37.202	37.832
MnO	6.400	6.819	6.754	6.566	5.939	6.459	5.298	6.393	2.639	2.486	2.354	2.078	2.251	2.495	2.571	2.564	2.558	2.584
CaO	7.107	6.327	6.911	6.833	7.031	7.218	7.010	7.212	0.786	0.698	0.809	0.770	0.854	0.742	0.758	0.688	0.806	0.773
TOTAL	**102.492**	**101.843**	**101.659**	**101.794**	**102.233**	**101.959**	**101.958**	**102.718**	**102.975**	**102.214**	**104.493**	**104.347**	**104.285**	**102.731**	**103.309**	**103.360**	**103.083**	**103.199**
CATIONS RECALCULATED TO 12 OXYGENS																		
Si	2.993	3.001	2.991	2.997	3.016	2.994	3.007	3.007	2.960	2.954	2.972	2.958	2.995	2.985	3.012	2.971	2.973	2.958
Al	1.954	1.932	1.941	1.949	1.909	1.944	1.948	1.900	2.051	2.014	2.005	2.015	1.977	2.015	1.984	2.012	2.007	2.009
Ti	0.001	0.000	0.000	0.000	0.003	0.000	0.000	0.000	0.001	0.002	0.002	0.004	0.001	0.000	0.000	0.000	0.002	0.000
Fe3+	0.047	0.068	0.061	0.052	0.084	0.057	0.051	0.099	0.000	0.000	0.000	0.000	0.022	0.000	0.014	0.000	0.000	0.000
Mg	0.098	0.102	0.098	0.104	0.120	0.105	0.128	0.112	0.365	0.327	0.374	0.399	0.396	0.353	0.279	0.313	0.354	0.337
Fe2+	1.883	1.896	1.871	1.876	1.859	1.857	1.911	1.840	2.395	2.514	2.448	2.455	2.393	2.425	2.467	2.498	2.447	2.495
Mn	0.428	0.460	0.456	0.442	0.398	0.434	0.355	0.427	0.175	0.168	0.155	0.137	0.148	0.166	0.171	0.171	0.170	0.173
Ca	0.602	0.540	0.591	0.582	0.595	0.614	0.595	0.609	0.066	0.05:	0.067	0.064	0.071	0.063	0.064	0.058	0.068	0.065
TOTAL	**8.006**	**7.999**	**8.008**	**8.003**	**7.985**	**8.006**	**7.994**	**7.994**	**8.013**	**8.038**	**8.023**	**8.031**	**8.004**	**8.007**	**7.989**	**8.023**	**8.021**	**8.037**
Fe/Fe+Mg	*0.950*	*0.949*	*0.950*	*0.947*	*0.939*	*0.946*	*0.937*	*0.942*	*0.868*	*0.885*	*0.867*	*0.860*	*0.858*	*0.873*	*0.899*	*0.889*	*0.874*	*0.881*
Alm	0.625	0.632	0.620	0.624	0.625	0.617	0.639	0.616	0.798	0.819	0.804	0.804	0.796	0.806	0.828	0.822	0.805	0.813
Py	0.033	0.034	0.032	0.035	0.040	0.035	0.043	0.038	0.122	0.107	0.123	0.131	0.132	0.117	0.094	0.103	0.117	0.110
Sp	0.142	0.153	0.151	0.147	0.134	0.144	0.119	0.143	0.058	0.055	0.051	0.045	0.049	0.055	0.057	0.056	0.056	0.056
Gr	0.200	0.180	0.196	0.194	0.200	0.204	0.199	0.204	0.022	0.019	0.022	0.021	0.023	0.021	0.021	0.019	0.022	0.021
(Ca+Mn)/(Mg+Ca+Mn+Fe)	0.342	0.334	0.347	0.341	0.334	0.348	0.318	0.347	0.080	0.074	0.073	0.066	0.073	0.076	0.079	0.075	0.078	0.078
X	121.68	121.30	120.48	119.66	118.84	118.02	117.15	116.38	179.80	203.21	203.62	204.02	204.41	204.81	205.63	205.93	206.11	206.53
Y	203.51	203.19	202.52	201.85	201.18	200.51	199.84	199.17	358.29	313.66	314.78	315.91	317.03	318.15	320.51	321.53	322.56	323.58
x-axis m	4.68	4.73	4.84	4.94	5.04	5.15	5.26	5.36		0.00	0.12	0.24	0.36	0.48	0.00	0.11	0.21	0.32
location	*nr rm - qz*	*nr rm - bt*	*nr rm - bt*	*nr rm - bt*	*interior*	*±near rim*	*nr rm - bt*	*im adj bt*	*nr rm - qz*	*m adj pl?*	*r rm - pl?*	*±near rim*	*nr rm - qz*	*im adj qz*	*im adj bt*	*nr rm - bt*	*±near rim*	*r bt fract*

TABLE B-1: Quantitative Microprobe Analysis for Garnet Compositions

PC-104E (continued)

	GT2e	GT2f	GT2g	GT2h	GT2i	GT2j	GT2k	GT2l	GT2m	GT2n	GT2o	GT3a	GT3b	GT3c	GT3d	GT3e	GT3f	GT3g
WEIGHT PERCENT OXIDES																		
SiO2	36.946	37.835	37.889	37.642	37.642	38.024	37.989	37.715	38.324	38.224	38.038	37.301	38.776	37.660	38.130	38.414	37.687	37.783
Al2O3	21.276	21.513	21.536	21.560	21.370	21.545	21.419	21.568	21.874	21.790	21.565	21.645	21.704	21.505	21.842	21.540	21.465	21.458
TiO2	0.000	0.035	0.000	0.035	0.026	0.014	0.000	0.020	0.052	0.043	0.055	0.000	0.006	0.029	0.000	0.000	0.000	0.006
Fe2O3	0.122	0.000	0.000	0.000	0.226	0.040	0.092	0.112	0.000	0.000	0.000	0.000	0.330	0.000	0.027	0.223	0.064	0.231
MgO	2.257	2.573	3.031	3.102	3.048	2.597	2.969	2.874	3.070	3.275	2.903	3.411	3.358	3.645	3.613	3.667	3.645	3.620
FeO	38.206	37.382	36.764	36.996	37.199	37.551	36.553	37.959	36.614	36.876	37.118	36.402	37.221	36.390	37.530	36.526	36.644	37.032
MnO	2.789	2.557	2.399	2.382	2.363	2.533	2.471	2.424	2.459	2.212	2.290	2.098	1.932	1.777	1.861	1.650	1.736	1.684
CaO	0.818	0.737	0.751	0.807	0.777	0.798	0.806	0.709	0.742	0.894	0.698	0.774	0.890	0.744	0.758	0.783	0.749	0.775
TOTAL	**102.414**	**102.632**	**102.370**	**102.524**	**102.651**	**103.102**	**102.299**	**103.381**	**103.135**	**103.314**	**102.667**	**101.631**	**104.217**	**101.750**	**103.761**	**102.803**	**101.990**	**102.589**
CATIONS RECALCULATED TO 12 OXYGENS																		
Si	2.952	2.991	2.992	2.974	2.975	2.992	3.001	2.967	2.997	2.987	2.996	2.964	3.002	2.982	2.970	3.005	2.980	2.975
Al	2.003	2.004	2.004	2.007	1.990	1.998	1.994	1.999	2.016	2.007	2.002	2.027	1.980	2.007	2.005	1.986	2.001	1.991
Ti	0.000	0.002	0.000	0.002	0.002	0.001	0.000	0.001	0.003	0.003	0.003	0.000	0.000	0.002	0.000	0.000	0.000	0.000
Fe3+	0.007	0.000	0.000	0.000	0.013	0.002	0.005	0.007	0.000	0.000	0.000	0.000	0.019	0.000	0.002	0.013	0.004	0.014
Mg	0.269	0.303	0.357	0.365	0.359	0.305	0.350	0.337	0.358	0.381	0.341	0.404	0.387	0.430	0.420	0.428	0.430	0.425
Fe2+	2.553	2.471	2.428	2.444	2.459	2.471	2.415	2.497	2.394	2.409	2.445	2.419	2.409	2.410	2.445	2.389	2.423	2.439
Mn	0.189	0.171	0.160	0.159	0.158	0.169	0.165	0.161	0.163	0.146	0.153	0.141	0.127	0.119	0.123	0.109	0.116	0.112
Ca	0.070	0.062	0.064	0.068	0.066	0.067	0.068	0.05:	0.062	0.075	0.059	0.066	0.074	0.063	0.063	0.066	0.064	0.065
TOTAL	**8.043**	**8.005**	**8.006**	**8.021**	**8.022**	**8.006**	**7.999**	**8.029**	**7.992**	**8.008**	**7.999**	**8.022**	**7.999**	**8.013**	**8.027**	**7.996**	**8.018**	**8.022**
Fe/Fe+Mg	*0.905*	*0.891*	*0.872*	*0.870*	*0.873*	*0.890*	*0.874*	*0.881*	*0.870*	*0.863*	*0.878*	*0.857*	*0.861*	*0.848*	*0.854*	*0.848*	*0.849*	*0.852*
Alm	0.829	0.822	0.807	0.805	0.808	0.820	0.805	0.817	0.804	0.800	0.816	0.798	0.804	0.797	0.801	0.799	0.799	0.802
Py	0.087	0.101	0.119	0.120	0.118	0.101	0.117	0.110	0.120	0.127	0.114	0.133	0.129	0.142	0.138	0.143	0.142	0.140
Sp	0.061	0.057	0.053	0.053	0.052	0.056	0.055	0.053	0.055	0.049	0.051	0.047	0.042	0.039	0.040	0.037	0.038	0.037
Gr	0.023	0.021	0.021	0.023	0.022	0.022	0.023	0.01:	0.021	0.025	0.01:	0.022	0.025	0.021	0.021	0.022	0.021	0.021
(Ca+Mn)/(Mg+Ca+Mn+Fe)	0.084	0.078	0.075	0.075	0.074	0.078	0.078	0.072	0.076	0.073	0.071	0.068	0.067	0.060	0.061	0.059	0.059	0.058
X	207.08	206.98	207.43	207.73	208.03	207.93	208.63	208.93	209.16	209.55	209.83	176.83	175.96	174.82	173.76	172.82	171.70	170.81
Y	324.93	325.63	326.89	327.68	328.70	329.61	330.74	331.78	332.80	333.83	334.85	358.68	358.86	359.04	359.22	359.40	359.58	359.77
x-axis m	0.47	0.54	0.67	0.76	0.86	0.95	1.09	1.20	1.30	1.41	1.52	0.00	0.09	0.20	0.31	0.41	0.52	0.61
location	*j bt fract*	*j bt fract*	*interior*	*interior*	*r bt fract*	*r bt fract*	*interior*	*r bt fract*	*±near rim*	*nr rm - pl*	*rim adj pl*	*±near rim*	*±near rim*	*interior*	*interior*	*interior*	*interior*	*interior*

TABLE B-1: Quantitative Microprobe Analysis for Garnet Compositions

PC-104E (continued)

	GT3h	GT3i	GT3j	GT3k	GT3l	GT3m	GT3n	GT3o	GT3p	GT3q	GT3r	GT3s	GT3t	GT3u	GT3v	GT3w	GT3x	GT3y
WEIGHT PERCENT OXIDES																		
SiO2	37.568	37.242	37.431	37.441	37.791	38.888	36.783	38.293	37.412	37.933	37.490	37.970	38.057	38.031	38.347	37.757	37.854	37.636
Al2O3	21.387	21.421	21.257	22.028	21.453	21.853	21.619	21.526	21.373	21.707	21.320	21.589	21.955	21.530	21.360	21.962	21.408	21.547
TiO2	0.023	0.023	0.000	0.000	0.055	0.000	0.000	0.000	0.012	0.032	0.000	0.070	0.000	0.003	0.000	0.020	0.000	0.009
Fe2O3	0.292	0.000	0.224	0.000	0.067	0.173	0.000	0.110	0.031	0.000	0.062	0.187	0.000	0.340	0.322	0.000	0.282	0.085
MgO	3.516	3.523	3.46:	3.413	3.443	3.377	3.067	3.406	3.132	3.495	3.592	3.683	3.682	3.675	3.671	3.613	3.601	3.702
FeO	37.400	36.873	37.038	37.365	37.306	37.678	36.922	37.043	37.481	37.233	36.731	37.495	37.357	37.664	36.229	37.396	37.124	37.290
MnO	1.701	1.661	1.683	1.562	1.504	1.655	1.766	1.476	1.739	1.707	1.436	1.499	1.611	1.280	1.605	1.613	1.578	1.529
CaO	0.748	0.672	0.619	0.723	0.684	0.769	0.686	0.710	0.717	0.740	0.693	0.771	0.710	0.753	0.721	0.648	0.679	0.712
TOTAL	**102.635**	**101.415**	**101.722**	**102.532**	**102.303**	**104.393**	**100.843**	**102.564**	**101.897**	**102.847**	**101.324**	**103.264**	**103.372**	**103.276**	**102.255**	**103.009**	**102.526**	**102.510**
CATIONS RECALCULATED TO 12 OXYGENS																		
Si	2.965	2.967	2.976	2.951	2.983	3.003	2.953	3.007	2.975	2.978	2.984	2.971	2.970	2.975	3.013	2.960	2.982	2.967
Al	1.989	2.012	1.992	2.046	1.996	1.989	2.046	1.992	2.003	2.008	1.000	1.991	2.019	1.985	1.978	2.029	1.987	2.002
Ti	0.001	0.001	0.000	0.000	0.003	0.000	0.000	0.000	0.001	0.002	0.000	0.004	0.000	0.000	0.000	0.001	0.000	0.001
Fe3+	0.017	0.000	0.013	0.000	0.004	0.010	0.000	0.007	0.002	0.000	0.004	0.011	0.000	0.020	0.019	0.000	0.017	0.005
Mg	0.414	0.418	0.411	0.401	0.405	0.389	0.367	0.399	0.371	0.409	0.426	0.430	0.428	0.429	0.430	0.422	0.423	0.435
Fe2+	2.468	2.457	2.463	2.463	2.463	2.434	2.479	2.432	2.492	2.444	2.445	2.453	2.438	2.464	2.381	2.451	2.445	2.458
Mn	0.114	0.112	0.113	0.104	0.101	0.108	0.120	0.098	0.117	0.113	0.097	0.099	0.106	0.085	0.107	0.107	0.105	0.102
Ca	0.063	0.057	0.053	0.061	0.058	0.064	0.059	0.05:	0.061	0.062	0.059	0.065	0.059	0.063	0.061	0.054	0.057	0.060
TOTAL	**8.031**	**8.025**	**8.021**	**8.026**	**8.013**	**7.997**	**8.024**	**7.994**	**8.022**	**8.017**	**8.014**	**8.024**	**8.021**	**8.022**	**7.988**	**8.025**	**8.016**	**8.029**
Fe/Fe+Mg	*0.856*	*0.854*	*0.857*	*0.860*	*0.859*	*0.862*	*0.871*	*0.859*	*0.870*	*0.857*	*0.852*	*0.851*	*0.851*	*0.852*	*0.847*	*0.853*	*0.853*	*0.850*
Alm	0.807	0.807	0.810	0.813	0.814	0.813	0.819	0.814	0.819	0.807	0.808	0.805	0.804	0.810	0.799	0.808	0.807	0.805
Py	0.135	0.137	0.135	0.132	0.134	0.130	0.121	0.133	0.122	0.135	0.141	0.141	0.141	0.141	0.144	0.139	0.140	0.142
Sp	0.037	0.037	0.037	0.034	0.033	0.036	0.03:	0.033	0.039	0.038	0.032	0.033	0.035	0.028	0.036	0.035	0.035	0.033
Gr	0.021	0.019	0.017	0.020	0.019	0.021	0.01:	0.020	0.020	0.021	0.01:	0.021	0.01:	0.021	0.020	0.018	0.019	0.01:
(Ca+Mn)/(Mg+Ca+Mn+Fe)	0.058	0.056	0.055	0.055	0.052	0.057	0.059	0.053	0.059	0.058	0.052	0.054	0.055	0.049	0.056	0.053	0.054	0.053
X	169.81	168.81	168.00	166.80	165.80	164.80	163.80	162.79	161.79	160.79	159.78	158.78	157.78	156.78	155.77	154.77	153.76	152.77
Y	359.95	359.96	360.31	360.49	360.67	360.85	361.01	361.33	361.23	361.58	361.76	361.94	362.12	362.30	362.48	362.66	362.84	363.02
x-axis m	0.71	0.81	0.90	1.02	1.12	1.23	1.33	1.43	1.53	1.64	1.74	1.84	1.95	2.05	2.15	2.25	2.35	2.45
location	*interior*	*interior*	*interior*	*interior*	*interior*	*interior*	*r bt fract*	*interior*	*r bt fract*	*interior*	*interior*	*interior*	*interior*	*interior*	*interior*	*interior*	*interior*	*interior*

TABLE B-1: Quantitative Microprobe Analysis for Garnet Compositions

PC-104E (continued)

	GT3z	GT3aa	GT3ab	GT3ac	GT3ad	GT3ae
WEIGHT PERCENT OXIDES						
SiO2	38.172	38.131	37.512	37.412	37.820	37.463
Al2O3	21.496	21.595	21.597	21.164	21.367	21.137
TiO2	0.061	0.003	0.000	0.000	0.000	0.003
Fe2O3	0.302	0.000	0.000	0.115	0.049	0.156
MgO	3.505	3.422	3.225	3.065	3.011	2.776
FeO	36.890	36.804	37.390	36.595	36.585	36.816
MnO	1.991	1.663	1.857	2.023	2.299	2.318
CaO	0.832	0.723	0.773	0.738	0.756	0.753
TOTAL	**103.249**	**102.341**	**102.354**	**101.112**	**101.887**	**101.422**
CATIONS RECALCULATED TO 12 OXYGENS						
Si	2.985	3.000	2.968	2.992	2.999	2.994
Al	1.981	2.003	2.014	1.995	1.997	1.991
Ti	0.004	0.000	0.000	0.000	0.000	0.000
Fe3+	0.018	0.000	0.000	0.007	0.003	0.009
Mg	0.409	0.401	0.380	0.365	0.356	0.331
Fe2+	2.413	2.422	2.474	2.448	2.426	2.460
Mn	0.132	0.111	0.124	0.137	0.154	0.157
Ca	0.06:	0.061	0.066	0.063	0.064	0.065
TOTAL	**8.011**	**7.998**	**8.026**	**8.007**	**8.001**	**8.006**
Fe/Fe+Mg	*0.855*	*0.858*	*0.867*	*0.870*	*0.872*	*0.882*
Alm	0.798	0.809	0.813	0.812	0.809	0.817
Py	0.135	0.134	0.125	0.121	0.119	0.110
Sp	0.044	0.037	0.041	0.046	0.052	0.052
Gr	0.023	0.020	0.021	0.021	0.021	0.021
(Ca+Mn)/(Mg+Ca+Mn+Fe)	0.067	0.057	0.062	0.067	0.073	0.074
X	151.53	150.76	149.55	148.43	147.75	146.75
Y	363.20	363.39	363.57	364.10	363.93	364.11
x-axis m	2.58	2.66	2.78	2.91	2.98	3.08
location	*interior*	*interior*	*±near rim*	*nr rm - bt*	*nr rm - bt*	*im adj bt*

PC-104F

	GT1a	GT1b	GT1c	GT1d	GT1e	GT1f	GT1g	GT1h	GT1i	GT1j	GT1k	GT1l
WEIGHT PERCENT OXIDES												
SiO2	38.242	38.302	38.240	37.710	37.949	38.304	37.521	37.755	38.029	38.770	37.888	38.106
Al2O3	21.656	22.041	21.674	21.982	21.832	21.750	21.266	21.783	21.846	22.018	21.657	21.815
TiO2	0.043	0.000	0.046	0.032	0.003	0.000	0.023	0.069	0.000	0.000	0.000	0.000
Fe2O3	0.000	0.000	0.179	0.000	0.000	0.151	0.000	0.000	0.000	0.000	0.000	0.000
MgO	2.451	2.979	3.150	3.286	3.259	3.230	3.006	3.317	3.254	3.358	3.403	3.441
FeO	37.695	38.239	37.971	37.614	38.013	37.864	36.717	37.483	38.004	38.059	37.330	37.384
MnO	2.213	2.020	1.804	1.745	1.800	1.659	1.694	1.715	1.592	1.493	1.658	1.309
CaO	0.905	0.954	0.860	0.906	0.959	0.983	0.965	0.865	0.917	0.824	0.915	0.875
TOTAL	**103.205**	**104.535**	**103.924**	**103.275**	**103.815**	**103.941**	**101.192**	**102.987**	**103.642**	**104.522**	**102.851**	**102.930**
CATIONS RECALCULATED TO 12 OXYGENS												
Si	3.002	2.971	2.980	2.955	2.963	2.981	2.995	2.965	2.970	2.993	2.977	2.984
Al	2.004	2.015	1.991	2.030	2.009	1.995	2.001	2.016	2.011	2.003	2.005	2.014
Ti	0.003	0.000	0.003	0.002	0.000	0.000	0.001	0.004	0.000	0.000	0.000	0.000
Fe3+	0.000	0.000	0.011	0.000	0.000	0.009	0.000	0.000	0.000	0.000	0.000	0.000
Mg	0.287	0.344	0.366	0.384	0.379	0.375	0.358	0.388	0.379	0.386	0.399	0.402
Fe2+	2.475	2.480	2.475	2.465	2.482	2.465	2.451	2.462	2.482	2.457	2.453	2.449
Mn	0.147	0.133	0.119	0.116	0.119	0.109	0.115	0.114	0.105	0.098	0.110	0.087
Ca	0.076	0.079	0.072	0.076	0.080	0.082	0.083	0.073	0.077	0.068	0.077	0.073
TOTAL	**7.993**	**8.022**	**8.016**	**8.028**	**8.033**	**8.017**	**8.003**	**8.023**	**8.024**	**8.005**	**8.021**	**8.009**
Fe/Fe+Mg	*0.896*	*0.878*	*0.871*	*0.865*	*0.867*	*0.868*	*0.873*	*0.864*	*0.868*	*0.864*	*0.860*	*0.859*
Alm	0.829	0.817	0.816	0.811	0.811	0.813	0.815	0.811	0.816	0.816	0.807	0.813
Py	0.096	0.113	0.121	0.126	0.124	0.124	0.119	0.128	0.124	0.128	0.131	0.133
Sp	0.049	0.044	0.039	0.038	0.039	0.036	0.038	0.038	0.035	0.032	0.036	0.029
Gr	0.026	0.026	0.024	0.025	0.026	0.027	0.028	0.024	0.025	0.023	0.025	0.024
(Ca+Mn)/(Mg+Ca+Mn+Fe)	0.075	0.06:	0.063	0.063	0.065	0.063	0.066	0.062	0.05:	0.055	0.062	0.053
X	103.33	103.65	103.98	104.30	104.53	104.95	105.59	105.92	106.56	106.89	107.21	107.13
Y	-230.53	-231.52	-232.52	-233.61	-234.29	-235.50	-237.48	-238.48	-240.46	-241.46	-242.45	-243.45
x-axis m	0.00	0.10	0.21	0.32	0.39	0.52	0.73	0.84	1.04	1.15	1.25	1.35
location	*im adj bt*	*nr rm - bt*	*±near rim*	*interior*	*interior*	*interior*	*nr fract*	*interior*	*interior*	*interior*	*interior*	*interior*

TABLE B-1: Quantitative Microprobe Analysis for Garnet Compositions

PC-104F (continued)

	GT1m	GT1n	GT1o	GT1p	GT1q	GT2a	GT2b	GT2c	GT2d	GT2e	GT2f	GT2g	GT2h	GT2i	GT2j	GT2k	GT2l	GT2m
WEIGHT PERCENT OXIDES																		
SiO2	38.391	38.108	38.720	37.977	38.200	38.523	37.980	38.458	37.577	38.080	38.243	38.086	38.658	38.780	38.635	38.852	37.863	37.690
Al2O3	21.734	21.660	21.866	21.605	21.665	21.817	21.661	21.943	21.883	21.720	22.009	21.670	21.395	22.124	21.490	21.779	22.165	21.806
TiO2	0.006	0.000	0.000	0.015	0.000	0.000	0.000	0.003	0.015	0.026	0.023	0.000	0.000	0.000	0.000	0.003	0.000	0.000
Fe2O3	0.003	0.072	0.000	0.000	0.111	0.000	0.080	0.030	0.000	0.050	0.000	0.000	0.663	0.009	0.616	0.575	0.000	0.000
MgO	3.373	3.480	3.212	3.338	3.124	3.092	3.270	3.287	3.394	3.449	3.456	3.474	3.416	3.382	3.382	3.243	3.136	3.211
FeO	37.229	37.145	37.190	37.071	37.587	37.252	37.529	38.125	37.133	37.592	37.436	36.997	36.917	38.128	37.234	38.385	37.678	37.832
MnO	1.535	1.574	1.659	1.672	1.846	1.918	1.975	1.764	1.606	1.605	1.867	1.625	1.794	1.835	1.742	1.781	1.739	1.738
CaO	0.945	0.985	0.802	0.807	0.930	0.905	0.797	0.860	1.004	0.885	0.975	0.938	0.934	0.918	1.010	0.946	0.850	0.928
TOTAL	**103.216**	**103.024**	**103.449**	**102.485**	**103.463**	**103.507**	**103.292**	**104.46:**	**102.612**	**103.407**	**104.009**	**102.790**	**103.777**	**105.176**	**104.109**	**105.564**	**103.431**	**103.205**
CATIONS RECALCULATED TO 12 OXYGENS																		
Si	2.997	2.984	3.012	2.990	2.987	3.002	2.976	2.978	2.959	2.976	2.970	2.987	3.005	2.980	2.997	2.983	2.960	2.960
Al	1.000	1.999	2.005	2.005	1.996	2.004	2.001	2.003	2.031	2.001	2.015	2.003	1.960	2.004	1.965	1.970	2.043	2.018
Ti	0.000	0.000	0.000	0.001	0.000	0.000	0.000	0.000	0.001	0.002	0.001	0.000	0.000	0.000	0.000	0.000	0.000	0.000
Fe3+	0.000	0.004	0.000	0.000	0.007	0.000	0.005	0.002	0.000	0.003	0.000	0.000	0.039	0.001	0.036	0.033	0.000	0.000
Mg	0.393	0.406	0.373	0.392	0.364	0.359	0.382	0.379	0.398	0.402	0.400	0.406	0.396	0.387	0.391	0.371	0.366	0.376
Fe2+	2.431	2.433	2.420	2.441	2.458	2.428	2.459	2.469	2.445	2.457	2.431	2.427	2.400	2.450	2.415	2.464	2.464	2.484
Mn	0.102	0.104	0.109	0.111	0.122	0.127	0.131	0.116	0.107	0.106	0.123	0.108	0.118	0.119	0.114	0.116	0.115	0.116
Ca	0.079	0.083	0.067	0.068	0.078	0.076	0.067	0.071	0.085	0.074	0.081	0.079	0.078	0.076	0.084	0.078	0.071	0.078
TOTAL	**8.002**	**8.014**	**7.985**	**8.007**	**8.012**	**7.996**	**8.021**	**8.019**	**8.025**	**8.021**	**8.021**	**8.011**	**7.996**	**8.018**	**8.003**	**8.015**	**8.018**	**8.032**
Fe/Fe+Mg	*0.861*	*0.857*	*0.867*	*0.862*	*0.871*	*0.871*	*0.866*	*0.867*	*0.860*	*0.859*	*0.859*	*0.857*	*0.858*	*0.863*	*0.861*	*0.869*	*0.871*	*0.869*
Alm	0.809	0.804	0.815	0.810	0.813	0.812	0.809	0.813	0.806	0.808	0.801	0.804	0.802	0.808	0.804	0.814	0.817	0.814
Py	0.131	0.134	0.125	0.130	0.120	0.120	0.126	0.125	0.131	0.132	0.132	0.135	0.132	0.128	0.130	0.123	0.121	0.123
Sp	0.034	0.035	0.037	0.037	0.041	0.042	0.043	0.038	0.035	0.035	0.041	0.036	0.03:	0.039	0.038	0.038	0.038	0.038
Gr	0.026	0.027	0.023	0.023	0.026	0.025	0.022	0.023	0.028	0.024	0.027	0.026	0.026	0.025	0.028	0.026	0.024	0.026
(Ca+Mn)/(Mg+Ca+Mn+Fe)	0.060	0.062	0.059	0.05:	0.066	0.068	0.065	0.062	0.063	0.059	0.067	0.062	0.066	0.064	0.066	0.064	0.062	0.063
X	108.23	108.50	108.83	109.15	109.47	68.28	68.47	68.65	68.84	69.02	69.21	69.40	69.58	69.77	69.95	70.14	70.33	70.51
Y	-245.66	-246.43	-247.42	-248.18	-249.41	-309.91	-308.90	-307.90	-306.89	-305.89	-304.88	-303.88	-302.87	-301.87	-300.62	-299.86	-298.63	-297.85
x-axis m	1.60	1.68	1.79	1.87	1.00	0.00	0.10	0.20	0.31	0.41	0.51	0.61	0.72	0.82	0.94	1.02	1.15	1.23
location	*interior*	*interior*	*±near rim*	*±near rim*	*r rm - qz*	*im adj qz*	*r rm - qz*	*±near rim*	*±near rim*	*interior*	*interior*	*interior*	*interior*	*interior*	*±near rim*	*r rm - qz*	*r rm - qz*	*r rm - qz*

TABLE B-1: Quantitative Microprobe Analysis for Garnet Compositions

PC-104F (continued)				*PC-107F*													
	GT2n	**GT2o**	**GT2p**	**GR1**	**GC2**	**GC3**	**G4**	**G4ref**	**2G1**	**3G1**	**3G2**	**3G3**	**GT1a**	**GT1b**	**GT1c**	**GT1d**	**GT1e**	**GT1f**
WEIGHT PERCENT OXIDES																		
SiO2	38.024	38.028	38.141	38.072	38.029	38.755	38.246	38.121	38.197	38.526	38.428	37.322	38.783	38.174	37.817	38.002	38.881	37.877
Al2O3	21.861	21.682	21.648	21.694	21.604	21.405	21.796	21.637	21.325	21.484	21.437	21.492	21.306	21.599	21.562	21.562	21.537	21.577
TiO2	0.084	0.000	0.000	0.009	0.000	0.070	0.040	0.026	0.075	0.006	0.017	0.092	0.036	0.013	0.078	0.030	0.000	0.037
Fe2O3	0.000	0.040	0.011	0.000	0.086	0.489	0.000	0.223	0.615	0.148	0.000	0.205	0.583	0.045				
MgO	3.080	3.005	3.115	1.664	2.041	1.833	1.951	2.124	1.836	1.697	2.163	1.567	1.439	2.132	2.184	2.225	2.172	2.155
FeO	37.426	37.835	37.382	30.117	30.500	30.294	30.205	30.954	30.721	31.036	30.899	30.402	29.643	30.740	30.879	30.576	30.305	30.798
MnO	1.876	1.82:	1.847	3.500	2.681	3.011	2.875	2.814	3.369	4.094	2.730	4.174	4.002	2.546	2.475	2.748	2.653	2.610
CaO	0.876	0.983	0.891	7.305	7.214	7.065	6.937	7.004	6.747	7.218	6.994	6.950	7.181	7.014	6.908	7.047	7.239	6.925
TOTAL	**103.227**	**103.403**	**103.035**	**102.361**	**102.155**	**102.922**	**102.050**	**102.903**	**102.270**	**104.061**	**102.668**	**101.999**	**103.005**	**102.366**	**101.903**	**102.395**	**103.370**	**102.024**
CATIONS RECALCULATED TO 12 OXYGENS																		
Si	2.978	2.980	2.992	2.987	2.985	3.016	2.997	2.976	3.001	2.988	3.001	2.956	3.022	2.989	2.977	2.977	3.009	2.978
Al	2.018	2.002	2.001	2.006	1.998	1.963	2.013	1.991	1.975	1.964	1.973	2.006	1.957	1.993	2.000	1.991	1.964	1.000
Ti	0.005	0.000	0.000	0.001	0.000	0.004	0.002	0.002	0.004	0.000	0.001	0.005	0.002	0.001	0.005	0.002	0.000	0.002
Fe3+	0.000	0.002	0.001	0.000	0.005	0.029	0.000	0.013	0.000	0.000	0.000	0.000	0.036	0.009	0.000	0.012	0.034	0.003
Mg	0.360	0.351	0.364	0.195	0.239	0.213	0.228	0.247	0.215	0.196	0.252	0.185	0.167	0.249	0.256	0.260	0.251	0.253
Fe2+	2.451	2.479	2.452	1.976	2.002	1.972	1.980	2.021	2.019	2.013	2.018	2.014	1.932	2.013	2.033	2.003	1.961	2.025
Mn	0.124	0.121	0.123	0.233	0.178	0.198	0.191	0.186	0.224	0.269	0.181	0.280	0.264	0.169	0.165	0.182	0.174	0.174
Ca	0.074	0.083	0.075	0.614	0.607	0.589	0.582	0.586	0.568	0.600	0.585	0.58:	0.600	0.588	0.583	0.592	0.600	0.583
TOTAL	**8.009**	**8.018**	**8.007**	**8.00:**	**8.014**	**7.984**	**7.994**	**8.021**	**8.007**	**8.02:**	**8.011**	**8.036**	**7.979**	**8.00:**	**8.018**	**8.019**	**7.992**	**8.018**
Fe/Fe+Mg	*0.872*	*0.876*	*0.871*	*0.910*	*0.893*	*0.903*	*0.897*	*0.891*	*0.904*	*0.911*	*0.889*	*0.916*	*0.920*	*0.890*	*0.888*	*0.885*	*0.887*	*0.889*
Alm	0.815	0.817	0.814	0.655	0.662	0.663	0.664	0.665	0.667	0.654	0.665	0.656	0.652	0.667	0.669	0.660	0.657	0.667
Py	0.120	0.116	0.121	0.065	0.079	0.072	0.077	0.081	0.071	0.064	0.083	0.060	0.056	0.082	0.084	0.086	0.084	0.083
Sp	0.041	0.040	0.041	0.077	0.059	0.067	0.064	0.061	0.074	0.087	0.059	0.091	0.089	0.056	0.054	0.060	0.058	0.057
Gr	0.024	0.027	0.025	0.204	0.201	0.198	0.195	0.193	0.188	0.195	0.193	0.192	0.202	0.195	0.192	0.195	0.201	0.192
(Ca+Mn)/(Mg+Ca+Mn+Fe)	0.066	0.067	0.066	0.281	0.259	0.265	0.259	0.254	0.262	0.282	0.252	0.283	0.292	0.251	0.246	0.255	0.259	0.250
X	70.70	70.88	71.07	-196.16	-195.52	-194.96	-191.92	-191.92	-195.52	-194.96	-191.92	-191.92	-193.55	-193.54	-193.55	-193.58	-193.55	-193.55
Y	-296.84	-295.84	-294.83	-108.46	-110.63	-109.56	-111.72	-111.72	-110.63	-109.56	-111.72	-111.72	-108.74	-109.42	-110.20	-110.92	-111.65	-112.38
x-axis m	1.33	1.43	1.53		0.00	0.12							0.00	0.07	0.15	0.22	0.29	0.36

TABLE B-1: Quantitative Microprobe Analysis for Garnet Compositions

PC-107F (continued)

	GT1g	GT1h	GT1i	GT1j	GT1k	GT1l	GT1m	GT1n	GT1o	GT1p	GT1q	GT2a	GT2b	GT2c	GT2d	GT3a	GT3b	GT3c
WEIGHT PERCENT OXIDES																		
SiO2	38.445	38.383	38.190	38.847	38.912	38.770	38.121	38.385	39.194	37.916	38.285	38.200	38.031	38.120	38.484	38.477	38.060	38.793
Al2O3	21.539	21.378	21.308	21.575	21.275	21.230	21.293	21.422	21.469	21.415	21.524	21.619	21.768	21.453	21.378	21.441	21.347	21.449
TiO2	0.047	0.067	0.061	0.081	0.063	0.030	0.051	0.001	0.000	0.077	0.057	0.098	0.028	0.084	0.091	0.076	0.050	0.036
Fe2O3	0.313	0.481	0.512	0.268	0.643	0.715	0.375	0.315	0.641	0.351	0.134	0.081	0.000	0.188	0.393	0.352	0.313	0.506
MgO	2.176	2.013	2.192	2.108	2.010	1.773	2.057	2.051	2.006	2.056	1.631	1.615	2.063	1.627	1.616	1.485	2.042	2.037
FeO	30.345	30.569	30.189	30.260	30.020	29.633	30.105	30.308	29.975	30.752	29.847	30.245	30.882	30.307	29.778	30.175	30.225	30.256
MnO	2.748	2.734	2.723	2.744	2.769	3.356	2.643	2.529	2.630	2.610	3.324	3.873	2.682	3.461	3.449	3.441	2.681	2.862
CaO	7.072	7.056	7.115	6.956	6.957	7.195	7.137	7.024	7.352	7.255	7.505	7.151	6.997	7.133	7.432	7.405	7.136	7.003
TOTAL	**102.685**	**102.681**	**102.290**	**102.839**	**102.649**	**102.702**	**101.782**	**102.035**	**103.267**	**102.432**	**102.307**	**102.882**	**102.451**	**102.373**	**102.621**	**102.852**	**101.854**	**102.942**
CATIONS RECALCULATED TO 12 OXYGENS																		
Si	2.997	2.998	2.992	3.018	3.029	3.023	2.999	3.009	3.02:	2.974	3.001	2.986	2.978	2.993	3.008	3.005	2.994	3.015
Al	1.979	1.968	1.968	1.975	1.952	1.951	1.975	1.979	1.956	1.980	1.988	1.992	2.009	1.985	1.969	1.973	1.979	1.965
Ti	0.003	0.004	0.004	0.005	0.004	0.002	0.003	0.000	0.000	0.005	0.003	0.006	0.002	0.005	0.005	0.004	0.003	0.002
Fe3+	0.018	0.028	0.030	0.016	0.038	0.042	0.022	0.019	0.037	0.021	0.008	0.005	0.000	0.011	0.023	0.021	0.019	0.02:
Mg	0.253	0.234	0.256	0.244	0.233	0.206	0.241	0.240	0.231	0.240	0.191	0.188	0.241	0.190	0.188	0.173	0.240	0.236
Fe2+	1.978	1.997	1.978	1.966	1.954	1.932	1.981	1.987	1.938	2.018	1.956	1.977	2.022	1.990	1.946	1.971	1.989	1.967
Mn	0.181	0.181	0.181	0.181	0.183	0.222	0.176	0.168	0.172	0.173	0.221	0.256	0.178	0.230	0.228	0.228	0.179	0.188
Ca	0.591	0.58:	0.597	0.579	0.580	0.601	0.602	0.58:	0.609	0.610	0.630	0.599	0.587	0.600	0.622	0.620	0.602	0.583
TOTAL	**8.001**	**8.000**	**8.005**	**7.982**	**7.973**	**7.979**	**7.999**	**7.992**	**7.973**	**8.021**	**7.998**	**8.00:**	**8.016**	**8.004**	**7.991**	**7.994**	**8.004**	**7.986**
Fe/Fe+Mg	*0.887*	*0.895*	*0.885*	*0.890*	*0.893*	*0.904*	*0.891*	*0.892*	*0.893*	*0.894*	*0.911*	*0.913*	*0.894*	*0.913*	*0.912*	*0.919*	*0.893*	*0.893*
Alm	0.659	0.665	0.657	0.662	0.662	0.653	0.660	0.666	0.657	0.663	0.653	0.655	0.668	0.661	0.652	0.659	0.661	0.661
Py	0.084	0.078	0.085	0.082	0.079	0.06:	0.080	0.080	0.078	0.079	0.064	0.062	0.07:	0.063	0.063	0.058	0.07:	0.079
Sp	0.060	0.060	0.060	0.061	0.062	0.075	0.059	0.056	0.058	0.057	0.074	0.085	0.059	0.077	0.077	0.076	0.059	0.063
Gr	0.197	0.197	0.198	0.195	0.197	0.203	0.201	0.198	0.206	0.201	0.210	0.198	0.194	0.199	0.208	0.207	0.200	0.196
(Ca+Mn)/(Mg+Ca+Mn+Fe)	0.257	0.257	0.258	0.256	0.259	0.278	0.259	0.254	0.265	0.258	0.284	0.283	0.253	0.276	0.285	0.283	0.259	0.259
X	-193.55	-193.55	-193.55	-193.55	-193.55	-193.55	-193.55	-193.55	-193.55	-193.60	-193.55	-189.14	-189.14	-189.14	-189.14	-198.87	-195.83	-192.78
Y	-113.11	-113.83	-114.56	-115.29	-115.94	-116.74	-117.47	-118.29	-118.93	-119.47	-120.38	-116.80	-118.50	-120.19	-121.89	-111.17	-111.21	-111.25
x-axis m	0.44	0.51	0.58	0.66	0.72	0.80	0.87	0.96	1.02	1.07	1.16	0.00	0.17	0.34	0.51	0.00	0.30	0.61
location	*±near rim*	*nr rm - pl*	*±near rim*	*±near rim*	*nr rm - qz*	*nr rm - qz*	*nr rm - qz*	*±near rim*	*nr rm - pl*	*nr rm - pl*	*rim adj pl*	*adj qz?*	*±near rim*	*ar fract*	*adj qz?*	*adj qz?*	*±near rim*	*ar fract*

TABLE B-1: Quantitative Microprobe Analysis for Garnet Compositions

PC-107F (continued)

	GT3d	GT4a	GT4b	GT4c	GT4d	GT5a	GT5b	GT5c	GT5d	GT5e	GT5f	GT6a	GT6b	GT6c	GT6d	GT6e	GT6f
WEIGHT PERCENT OXIDES																	
SiO2	37.897	39.840	37.820	38.651	37.885	38.890	38.071	38.088	37.952	37.758	38.798	37.819	38.793	38.779	38.533	38.116	38.246
Al2O3	21.395	21.326	21.322	21.557	21.222	21.428	21.426	21.440	21.467	21.435	21.350	21.558	21.595	21.246	21.379	21.176	21.811
TiO2	0.016	0.031	0.043	0.067	0.037	0.026	0.019	0.000	0.011	0.000	0.006	0.050	0.019	0.028	0.037	0.011	0.053
Fe2O3	0.194	0.646	0.407	0.271	0.294	0.478	0.266	0.327	0.237	0.180	0.766	0.163	0.393	0.813	0.619	0.699	0.000
MgO	1.722	1.425	1.964	1.952	1.606	1.661	2.065	2.177	2.170	2.125	1.526	1.724	2.023	1.997	1.753	2.107	1.451
FeO	29.504	28.849	30.529	30.363	29.810	29.749	30.411	30.526	30.552	30.686	30.434	30.695	30.287	30.377	30.346	30.221	30.366
MnO	4.033	3.672	2.896	3.035	3.780	3.566	2.744	2.728	2.796	2.622	3.639	3.169	2.762	2.840	3.527	2.711	4.101
CaO	7.062	7.218	7.162	6.960	6.883	7.127	6.991	6.880	6.866	6.896	7.113	7.430	7.284	6.958	7.057	7.142	6.987
TOTAL	**101.823**	**103.007**	**102.143**	**102.856**	**101.517**	**102.925**	**101.993**	**102.166**	**102.051**	**101.702**	**103.632**	**102.608**	**103.156**	**103.038**	**103.251**	**102.183**	**103.015**
CATIONS RECALCULATED TO 12 OXYGENS																	
Si	2.990	3.079	2.977	3.009	2.999	3.025	2.992	2.989	2.983	2.980	3.011	2.968	3.009	3.016	2.000	2.993	2.987
Al	1.990	1.943	1.978	1.978	1.980	1.965	1.985	1.983	1.989	1.994	1.953	1.994	1.974	1.947	1.961	1.960	2.008
Ti	0.001	0.002	0.003	0.004	0.002	0.002	0.001	0.000	0.001	0.000	0.000	0.003	0.001	0.002	0.002	0.001	0.003
Fe3+	0.012	0.038	0.024	0.016	0.018	0.028	0.016	0.019	0.014	0.011	0.045	0.00:	0.023	0.048	0.036	0.041	0.000
Mg	0.203	0.164	0.230	0.227	0.190	0.193	0.242	0.255	0.254	0.250	0.177	0.202	0.234	0.231	0.203	0.247	0.169
Fe2+	1.947	1.865	2.00:	1.977	1.974	1.935	1.999	2.003	2.009	2.025	1.975	2.015	1.964	1.975	1.976	1.984	1.983
Mn	0.270	0.240	0.193	0.200	0.253	0.235	0.183	0.181	0.186	0.175	0.239	0.211	0.181	0.187	0.233	0.180	0.271
Ca	0.597	0.598	0.604	0.581	0.584	0.594	0.589	0.579	0.578	0.583	0.591	0.625	0.605	0.580	0.589	0.601	0.585
TOTAL	**8.008**	**7.929**	**8.019**	**7.990**	**7.000**	**7.977**	**8.006**	**8.00:**	**8.014**	**8.018**	**7.990**	**8.027**	**7.992**	**7.986**	**7.999**	**8.006**	**8.006**
Fe/Fe+Mg	*0.906*	*0.919*	*0.897*	*0.897*	*0.912*	*0.909*	*0.892*	*0.887*	*0.888*	*0.890*	*0.918*	*0.909*	*0.894*	*0.895*	*0.907*	*0.889*	*0.922*
Alm	0.646	0.650	0.662	0.662	0.658	0.655	0.664	0.664	0.663	0.668	0.662	0.660	0.658	0.664	0.658	0.659	0.659
Py	0.067	0.057	0.076	0.076	0.063	0.065	0.080	0.084	0.084	0.082	0.059	0.066	0.078	0.078	0.068	0.082	0.056
Sp	0.089	0.084	0.064	0.067	0.085	0.07:	0.061	0.060	0.062	0.058	0.080	0.069	0.061	0.063	0.078	0.05:	0.090
Gr	0.198	0.208	0.199	0.195	0.195	0.201	0.195	0.192	0.191	0.192	0.198	0.205	0.203	0.195	0.196	0.199	0.194
(Ca+Mn)/(Mg+Ca+Mn+Fe)	0.287	0.292	0.262	0.262	0.279	0.280	0.256	0.252	0.253	0.250	0.279	0.274	0.264	0.258	0.274	0.259	0.285
X	-189.74	-197.46	-195.74	-193.87	-192.07	-195.86	-195.07	-194.28	-193.58	-192.71	-191.92	-197.28	-194.94	-192.68	-190.44	-188.13	-185.79
Y	-111.29	-113.60	-113.77	-114.13	-114.32	-114.96	-114.92	-114.87	-114.83	-114.78	-114.74	-117.93	-117.98	-117.93	-117.93	-117.93	-117.93
x-axis m	0.91	0.00	0.17	0.36	0.54	0.00	0.08	0.16	0.23	0.32	0.39	0.00	0.23	0.46	0.68	0.92	1.15

TABLE B-1: Quantitative Microprobe Analysis for Garnet Compositions

PC-108C

	G1	G1a	GT1a	GT1b	GT1c	GT1d	GT1e	GT1f	GT1g	GT1h	GT1i	GT1j	GT1k	GT1l	GT1m	GT1n	GT2a	GT2b
WEIGHT PERCENT OXIDES																		
SiO2	39.070	38.788	38.036	38.58:	38.442	37.873	37.747	38.565	38.553	38.766	38.585	38.047	38.501	38.227	38.485	38.032	38.789	38.808
Al2O3	21.730	21.685	21.310	21.453	21.587	21.612	21.648	21.695	21.350	21.448	21.374	21.547	21.897	21.822	21.613	21.558	21.576	21.579
TiO2	0.043	0.000	0.072	0.078	0.000	0.020	0.020	0.000	0.009	0.026	0.000	0.000	0.046	0.000	0.026	0.000	0.055	0.009
Fe2O3	0.332	0.393	0.442	0.443	0.000	0.000	0.000	0.106	0.589	0.509	0.535	0.212	0.000	0.000	0.203	0.062	0.374	0.601
MgO	3.197	3.092	2.550	2.643	2.530	2.990	3.125	3.161	3.166	2.908	2.958	2.578	2.498	2.983	2.758	2.153	2.473	2.692
FeO	35.423	35.552	35.284	35.299	34.996	34.996	35.812	35.403	35.415	35.526	34.950	35.530	35.793	35.314	35.606	35.261	35.475	35.831
MnO	3.416	3.695	4.585	4.327	4.108	3.870	3.328	3.252	3.196	3.315	3.847	4.359	4.293	3.834	3.927	5.086	4.573	4.268
CaO	1.239	1.211	1.191	1.228	1.171	1.222	1.220	1.221	1.157	1.328	1.214	1.276	1.233	1.205	1.151	1.238	1.158	1.187
TOTAL	**104.450**	**104.416**	**103.46:**	**104.061**	**102.834**	**102.583**	**102.900**	**103.403**	**103.435**	**103.826**	**103.463**	**103.549**	**104.261**	**103.385**	**103.769**	**103.390**	**104.473**	**104.975**
CATIONS RECALCULATED TO 12 OXYGENS																		
Si	3.013	3.001	2.987	3.004	3.019	2.984	2.970	3.005	3.008	3.014	3.011	2.983	2.992	2.987	3.001	2.991	3.009	2.998
Al	1.975	1.977	1.972	1.968	1.998	2.007	2.007	1.993	1.963	1.965	1.966	1.991	2.006	2.00:	1.986	1.998	1.973	1.965
Ti	0.002	0.000	0.004	0.005	0.000	0.001	0.001	0.000	0.001	0.002	0.000	0.000	0.003	0.000	0.002	0.000	0.003	0.001
Fe3+	0.019	0.023	0.026	0.026	0.000	0.000	0.000	0.006	0.035	0.02:	0.031	0.013	0.000	0.000	0.012	0.004	0.022	0.035
Mg	0.368	0.357	0.299	0.307	0.296	0.351	0.367	0.367	0.368	0.337	0.344	0.301	0.289	0.348	0.321	0.252	0.286	0.310
Fe2+	2.285	2.300	2.317	2.298	2.298	2.306	2.356	2.307	2.311	2.310	2.281	2.330	2.326	2.308	2.322	2.319	2.301	2.315
Mn	0.223	0.242	0.305	0.285	0.273	0.258	0.222	0.215	0.211	0.218	0.254	0.289	0.283	0.254	0.259	0.339	0.300	0.279
Ca	0.102	0.100	0.100	0.102	0.099	0.103	0.103	0.102	0.097	0.111	0.102	0.107	0.103	0.101	0.096	0.104	0.096	0.098
TOTAL	**7.987**	**7.999**	**8.00:**	**7.995**	**7.982**	**8.011**	**8.026**	**7.995**	**7.993**	**7.987**	**7.990**	**8.015**	**8.002**	**8.008**	**7.999**	**8.008**	**7.991**	**8.001**
Fe/Fe+Mg	*0.861*	*0.866*	*0.886*	*0.882*	*0.886*	*0.868*	*0.865*	*0.863*	*0.863*	*0.873*	*0.869*	*0.885*	*0.889*	*0.869*	*0.879*	*0.902*	*0.889*	*0.882*
Alm	0.767	0.767	0.767	0.768	0.775	0.764	0.773	0.771	0.774	0.776	0.765	0.769	0.775	0.767	0.774	0.769	0.771	0.771
Py	0.123	0.119	0.099	0.102	0.09:	0.116	0.120	0.123	0.123	0.113	0.115	0.09:	0.096	0.115	0.107	0.084	0.096	0.103
Sp	0.075	0.081	0.101	0.095	0.092	0.086	0.073	0.072	0.071	0.073	0.085	0.096	0.094	0.084	0.087	0.112	0.101	0.093
Gr	0.034	0.034	0.033	0.034	0.033	0.034	0.034	0.034	0.032	0.037	0.034	0.035	0.034	0.034	0.032	0.035	0.032	0.033
(Ca+Mn)/(Mg+Ca+Mn+Fe)	0.109	0.114	0.134	0.130	0.125	0.120	0.107	0.106	0.103	0.111	0.119	0.131	0.128	0.118	0.119	0.147	0.133	0.126
X	154.02	154.21	149.93	150.82	151.57	153.22	154.17	155.41	156.51	157.61	158.71	159.80	160.90	162.00	163.09	164.18	155.67	155.68
Y	128.67	128.57	128.13	128.09	128.05	128.00	127.96	127.92	127.88	127.86	127.79	127.75	127.71	127.66	127.62	127.58	135.54	134.53
x-axis m	0.00	0.02	0.00	0.09	0.16	0.33	0.42	0.55	0.66	0.77	0.88	0.99	1.0:	1.21	1.32	1.43	0.00	0.10
location	*interior*	*interior*	*m adj pl?*	*nr rm - pl*	*adj fract*	*±nr fract*	*interior*	*interior*	*interior*	*nr fract*	*±nr fract*	*ear fract*	*ear fract*	*±near rim*	*nr rm - bt*	*m adj bt?*	*m adj pl?*	*nr rm - pl*

TABLE B-1: Quantitative Microprobe Analysis for Garnet Compositions

PC-108C (continued)

	GT2c	GT2d	GT2e	GT2f	GT2g	GT2h	GT2i	GT2j	GT2k	GT2l	GT2m	GT2n	GT2o	GT2p	GT3a	GT3b	GT3c	GT3d
WEIGHT PERCENT OXIDES																		
SiO2	38.439	38.601	39.008	38.711	38.810	38.388	38.592	39.051	38.820	37.848	37.597	38.235	38.689	38.767	37.945	38.180	38.413	39.256
Al2O3	21.604	21.612	21.556	21.898	21.507	21.787	21.240	21.729	21.670	21.504	21.400	21.666	21.645	21.255	21.682	21.507	21.621	21.931
TiO2	0.000	0.003	0.000	0.055	0.000	0.052	0.000	0.000	0.026	0.000	0.014	0.017	0.063	0.000	0.063	0.000	0.000	0.000
Fe2O3	0.241	0.269	0.565	0.134	0.569	0.090	0.655	0.398	0.293	0.253	0.161	0.042	0.414	0.600	0.000	0.372	0.242	0.207
MgO	2.900	3.039	3.007	3.151	3.209	3.275	3.187	3.296	3.225	3.183	2.960	2.872	2.718	2.356	2.421	2.601	2.485	2.765
FeO	35.636	35.256	35.559	36.210	35.667	35.794	35.007	35.524	35.304	35.814	35.637	35.662	36.000	34.682	35.102	34.953	35.305	35.735
MnO	3.763	3.681	3.520	3.369	3.086	3.440	3.148	3.189	3.375	3.285	3.513	3.852	4.202	4.665	4.840	4.979	4.790	4.145
CaO	1.101	1.208	1.196	1.219	1.206	1.155	1.207	1.262	1.238	1.193	1.191	1.062	1.123	1.189	1.220	1.284	1.206	1.153
TOTAL	**103.684**	**103.669**	**104.411**	**104.747**	**104.054**	**103.981**	**103.036**	**104.449**	**103.951**	**103.080**	**102.473**	**103.408**	**104.854**	**103.514**	**103.273**	**103.876**	**104.062**	**105.192**
CATIONS RECALCULATED TO 12 OXYGENS																		
Si	2.998	3.005	3.015	2.987	3.009	2.983	3.018	3.011	3.009	2.973	2.974	2.992	2.993	3.030	2.982	2.985	2.995	3.015
Al	1.986	1.983	1.964	1.992	1.965	1.995	1.957	1.974	1.979	1.991	1.995	1.998	1.973	1.958	2.008	1.982	1.987	1.985
Ti	0.000	0.000	0.000	0.003	0.000	0.003	0.000	0.000	0.002	0.000	0.001	0.001	0.004	0.000	0.004	0.000	0.000	0.000
Fe3+	0.014	0.016	0.033	0.008	0.033	0.005	0.039	0.023	0.017	0.015	0.00:	0.002	0.024	0.035	0.000	0.022	0.014	0.012
Mg	0.337	0.353	0.347	0.362	0.371	0.379	0.372	0.379	0.373	0.373	0.349	0.335	0.313	0.275	0.284	0.303	0.289	0.317
Fe2+	2.325	2.295	2.299	2.337	2.312	2.326	2.289	2.291	2.288	2.353	2.358	2.334	2.329	2.267	2.307	2.285	2.302	2.295
Mn	0.249	0.243	0.230	0.220	0.203	0.226	0.209	0.208	0.222	0.219	0.235	0.255	0.275	0.309	0.322	0.330	0.316	0.270
Ca	0.092	0.101	0.099	0.101	0.100	0.096	0.101	0.104	0.103	0.100	0.101	0.089	0.093	0.09:	0.103	0.108	0.101	0.095
TOTAL	**8.001**	**7.995**	**7.986**	**8.00:**	**7.992**	**8.014**	**7.984**	**7.990**	**7.992**	**8.024**	**8.023**	**8.007**	**8.005**	**7.973**	**8.00:**	**8.014**	**8.004**	**7.987**
Fe/Fe+Mg	*0.873*	*0.867*	*0.869*	*0.866*	*0.862*	*0.860*	*0.860*	*0.858*	*0.860*	*0.863*	*0.871*	*0.874*	*0.881*	*0.892*	*0.891*	*0.883*	*0.889*	*0.879*
Alm	0.774	0.767	0.773	0.774	0.774	0.768	0.771	0.768	0.767	0.773	0.775	0.775	0.774	0.768	0.765	0.755	0.765	0.771
Py	0.112	0.118	0.116	0.120	0.124	0.125	0.125	0.127	0.125	0.122	0.115	0.111	0.104	0.093	0.094	0.100	0.096	0.106
Sp	0.083	0.081	0.078	0.073	0.068	0.075	0.070	0.06:	0.074	0.072	0.077	0.085	0.091	0.105	0.107	0.109	0.105	0.091
Gr	0.031	0.034	0.033	0.033	0.034	0.032	0.034	0.035	0.034	0.033	0.033	0.02:	0.031	0.034	0.034	0.036	0.034	0.032
(Ca+Mn)/(Mg+Ca+Mn+Fe)	0.113	0.115	0.111	0.106	0.101	0.107	0.104	0.105	0.109	0.105	0.111	0.114	0.122	0.138	0.141	0.145	0.139	0.122
X	155.68	155.69	155.69	155.70	155.71	155.71	155.72	155.72	155.73	155.74	155.74	155.64	155.75	155.76	176.98	175.97	174.97	173.96
Y	133.51	132.50	131.48	130.47	129.45	128.44	127.42	126.41	125.39	124.38	123.09	122.35	121.33	120.32	258.76	258.77	258.78	258.79
x-axis m	0.20	0.30	0.41	0.51	0.61	0.71	0.81	0.91	1.02	1.12	1.25	1.32	1.42	1.52	0.00	0.10	0.20	0.30

TABLE B-1: Quantitative Microprobe Analysis for Garnet Compositions

PC-108C (continued)

	GT3e	GT3f	GT3g	GT3h	GT3i	GT3j	GT3k	GT3l	GT3m	GT3n	GT3o	GT3p	GT3q	GT3r	GT3s	GT3t	GT3u	GT3v
WEIGHT PERCENT OXIDES																		
SiO2	38.901	38.776	38.779	38.937	38.784	38.958	38.660	39.081	38.933	38.937	38.893	38.631	39.079	39.053	39.244	38.904	38.990	39.136
Al2O3	21.703	21.312	21.390	21.603	21.986	22.154	21.700	21.755	22.034	21.700	21.793	22.138	21.881	21.680	21.756	21.801	21.543	21.857
TiO2	0.000	0.046	0.006	0.017	0.000	0.000	0.017	0.000	0.067	0.000	0.017	0.000	0.009	0.000	0.000	0.020	0.009	0.000
Fe2O3	0.360	0.757	0.621	0.551	0.000	0.000	0.205	0.556	0.000	0.471	0.306	0.003	0.228	0.343	0.46:	0.366	0.605	0.312
MgO	2.942	3.180	3.355	3.256	2.520	3.351	3.566	3.713	3.787	3.900	3.886	4.008	3.964	3.842	3.860	3.835	3.733	3.639
FeO	35.808	35.509	34.723	36.100	36.547	36.155	35.656	35.986	35.518	35.608	35.794	36.320	35.535	35.406	35.428	36.040	35.251	36.063
MnO	3.669	3.295	3.399	3.041	3.215	2.814	2.534	2.505	2.412	2.304	2.187	2.345	2.344	2.085	2.372	2.272	2.535	2.379
CaO	1.128	1.083	1.256	1.034	1.212	1.090	1.201	1.252	1.205	1.224	1.226	1.229	1.129	1.188	1.259	1.185	1.284	1.168
TOTAL	**104.511**	**103.958**	**103.529**	**104.539**	**104.264**	**104.522**	**103.539**	**104.848**	**103.956**	**104.144**	**104.102**	**104.674**	**104.169**	**103.597**	**104.389**	**104.423**	**103.950**	**104.554**
CATIONS RECALCULATED TO 12 OXYGENS																		
Si	3.007	3.011	3.015	3.006	3.007	2.999	3.003	2.000	3.002	3.002	2.000	2.971	3.007	3.01:	3.015	2.996	3.012	3.008
Al	1.977	1.950	1.960	1.966	2.009	2.010	1.986	1.968	2.003	1.972	1.981	2.006	1.985	1.976	1.970	1.978	1.962	1.980
Ti	0.000	0.003	0.000	0.001	0.000	0.000	0.001	0.000	0.004	0.000	0.001	0.000	0.001	0.000	0.000	0.001	0.001	0.000
Fe3+	0.021	0.044	0.036	0.032	0.000	0.000	0.012	0.032	0.000	0.027	0.018	0.000	0.013	0.020	0.027	0.021	0.035	0.018
Mg	0.339	0.368	0.389	0.375	0.291	0.385	0.413	0.425	0.435	0.448	0.447	0.459	0.455	0.443	0.442	0.440	0.430	0.417
Fe2+	2.315	2.306	2.258	2.331	2.370	2.328	2.316	2.310	2.291	2.296	2.309	2.336	2.287	2.289	2.276	2.321	2.277	2.318
Mn	0.240	0.217	0.224	0.199	0.211	0.184	0.167	0.163	0.158	0.150	0.143	0.153	0.153	0.137	0.154	0.148	0.166	0.155
Ca	0.093	0.090	0.105	0.086	0.101	0.08:	0.09:	0.103	0.09:	0.101	0.101	0.101	0.093	0.098	0.104	0.098	0.106	0.096
TOTAL	**7.993**	**7.989**	**7.987**	**7.994**	**7.989**	**7.996**	**7.997**	**8.000**	**7.992**	**7.998**	**7.000**	**8.026**	**7.993**	**7.983**	**7.987**	**8.003**	**7.989**	**7.993**
Fe/Fe+Mg	*0.872*	*0.862*	*0.853*	*0.861*	*0.891*	*0.858*	*0.849*	*0.845*	*0.840*	*0.837*	*0.838*	*0.836*	*0.834*	*0.838*	*0.837*	*0.841*	*0.841*	*0.848*
Alm	0.775	0.774	0.759	0.780	0.797	0.780	0.773	0.770	0.768	0.766	0.770	0.766	0.765	0.772	0.765	0.772	0.764	0.776
Py	0.113	0.123	0.131	0.125	0.098	0.129	0.138	0.142	0.146	0.150	0.149	0.151	0.152	0.149	0.149	0.146	0.144	0.140
Sp	0.080	0.073	0.075	0.067	0.071	0.062	0.056	0.054	0.053	0.050	0.048	0.050	0.051	0.046	0.052	0.049	0.056	0.052
Gr	0.031	0.030	0.035	0.029	0.034	0.030	0.033	0.034	0.033	0.034	0.034	0.033	0.031	0.033	0.035	0.033	0.036	0.032
(Ca+Mn)/(Mg+Ca+Mn+Fe)	0.112	0.103	0.110	0.095	0.105	0.092	0.089	0.089	0.086	0.084	0.081	0.083	0.082	0.079	0.087	0.082	0.091	0.084
X	172.96	171.95	170.95	169.94	168.94	167.93	166.84	165.92	164.91	163.82	162.90	161.90	160.89	159.89	158.88	157.88	156.87	155.63
Y	258.80	258.81	258.82	258.83	258.83	258.84	258.85	258.86	258.87	258.98	258.89	258.90	258.91	258.92	258.94	258.94	258.95	258.96
x-axis m	0.40	0.50	0.60	0.70	0.80	0.91	1.01	1.11	1.21	1.32	1.41	1.51	1.61	1.71	1.81	1.91	2.01	2.14
location	*±near rim*	*interior*	*interior*	*interior*	*adj fract*	*interior*	*interior*	*interior*	*interior*	*interior*	*interior*	*interior*	*interior*	*interior*	*interior*	*interior*	*interior*	*interior*

TABLE B-1: Quantitative Microprobe Analysis for Garnet Compositions

	PC-108C (continued)								*PC-109A*										
	GT3w	**GT3x**	**GT3y**	**GT3z**	**GT3aa**	**GT3ab**	**GT3ac**	**GT3ad**	**GT1a**	**GT1b**	**GT1c**	**GT1d**	**GT1e**	**GT2a**	**GT2b**	**GT2d**	**GT2e**	**GT2f**	**GT2g**
WEIGHT PERCENT OXIDES																			
SiO2	38.744	38.229	38.297	38.874	38.748	38.960	38.699	38.284	38.382	39.373	38.341	39.012	38.226	38.695	38.784	38.729	38.348	38.191	38.319
Al2O3	21.604	21.56:	21.733	21.808	21.538	21.780	21.838	21.366	21.239	23.054	21.474	21.773	21.626	22.073	21.931	21.769	21.720	21.540	21.486
TiO2	0.000	0.029	0.064	0.000	0.000	0.000	0.055	0.000	0.000	0.003	0.014	0.000	0.038	0.078	0.000	0.101	0.014	0.061	0.040
Fe2O3	0.458	0.412	0.144	0.266	0.360	0.411	0.000	0.403	0.682	0.000	0.430	0.286	0.160	0.000	0.000	0.187	0.223	0.081	0.304
MgO	3.415	2.546	3.084	3.209	2.834	2.778	2.596	2.318	2.517	2.588	2.639	2.657	2.686	3.102	2.968	2.023	2.349	2.050	2.729
FeO	35.898	36.945	36.258	35.752	35.444	36.080	35.019	35.173	36.335	36.369	36.797	36.289	36.672	36.476	36.382	37.788	37.312	37.673	36.239
MnO	2.743	3.648	3.237	3.525	3.567	4.044	4.351	4.698	3.260	3.039	3.089	3.280	3.193	2.715	2.927	3.446	3.405	2.971	3.250
CaO	1.161	1.165	1.262	1.089	1.243	1.155	1.213	1.232	1.262	1.221	1.181	1.426	1.221	1.223	1.215	1.263	1.301	1.132	1.212
TOTAL	**104.023**	**104.544**	**104.079**	**104.523**	**103.734**	**105.208**	**103.771**	**103.474**	**103.677**	**105.647**	**103.965**	**104.723**	**103.822**	**104.362**	**104.207**	**105.31**	**104.67**	**103.70**	**103.58**
CATIONS RECALCULATED TO 12 OXYGENS																			
Si	3.002	2.976	2.979	3.001	3.016	2.000	3.011	3.003	3.004	2.997	2.993	3.012	2.986	2.991	3.003	2.995	2.981	2.997	2.997
Al	1.973	1.979	1.992	1.984	1.975	1.976	2.003	1.975	1.959	2.068	1.975	1.981	1.991	2.011	2.001	1.984	1.990	1.992	1.980
Ti	0.000	0.002	0.004	0.000	0.000	0.000	0.003	0.000	0.000	0.000	0.001	0.000	0.002	0.005	0.000	0.006	0.001	0.004	0.002
Fe3+	0.027	0.024	0.008	0.016	0.021	0.024	0.000	0.024	0.040	0.000	0.025	0.017	0.009	0.000	0.000	0.011	0.013	0.005	0.018
Mg	0.394	0.296	0.358	0.369	0.329	0.319	0.301	0.271	0.294	0.294	0.307	0.306	0.313	0.357	0.343	0.233	0.272	0.240	0.318
Fe2+	2.326	2.406	2.358	2.308	2.307	2.323	2.279	2.308	2.378	2.315	2.402	2.343	2.396	2.358	2.356	2.444	2.426	2.472	2.370
Mn	0.180	0.241	0.213	0.231	0.235	0.264	0.287	0.312	0.216	0.196	0.204	0.214	0.211	0.178	0.192	0.226	0.224	0.197	0.215
Ca	0.096	0.097	0.105	0.090	0.104	0.095	0.101	0.104	0.106	0.09:	0.099	0.118	0.102	0.101	0.101	0.105	0.108	0.095	0.102
TOTAL	**7.998**	**8.020**	**8.017**	**7.999**	**7.986**	**8.000**	**7.984**	**7.997**	**7.997**	**7.969**	**8.006**	**7.990**	**8.011**	**7.000**	**7.996**	**8.002**	**8.016**	**8.001**	**8.002**
Fe/Fe+Mg	*0.855*	*0.891*	*0.868*	*0.862*	*0.875*	*0.879*	*0.883*	*0.895*	*0.890*	*0.887*	*0.887*	*0.885*	*0.885*	*0.868*	*0.873*	*0.913*	*0.899*	*0.912*	*0.882*
Alm	0.776	0.792	0.777	0.770	0.776	0.774	0.768	0.771	0.794	0.797	0.797	0.786	0.793	0.787	0.788	0.813	0.800	0.823	0.789
Py	0.132	0.097	0.118	0.123	0.111	0.106	0.101	0.091	0.098	0.101	0.102	0.103	0.104	0.119	0.115	0.078	0.08:	0.07:	0.106
Sp	0.060	0.079	0.070	0.077	0.079	0.088	0.097	0.104	0.072	0.068	0.068	0.072	0.06:	0.059	0.064	0.075	0.074	0.066	0.072
Gr	0.032	0.032	0.035	0.030	0.035	0.032	0.034	0.035	0.035	0.034	0.033	0.03:	0.034	0.034	0.034	0.035	0.036	0.032	0.034
(Ca+Mn)/(Mg+Ca+Mn+Fe)	0.092	0.111	0.105	0.107	0.114	0.120	0.131	0.139	0.108	0.102	0.101	0.112	0.104	0.093	0.098	0.110	0.110	0.097	0.105
X	154.86	153.85	152.85	151.85	150.84	149.87	148.72	147.82	-92.72	-93.39	-94.07	-94.74	-95.41	-91.95	-92.94	-95.27	-95.92	-96.90	-97.89
Y	258.96	258.97	258.98	258.99	259.00	258.59	259.02	259.03	283.58	284.29	284.81	285.30	285.88	279.17	279.19	279.15	279.26	279.29	279.31
x-axis m	2.21	2.31	2.41	2.51	2.62	2.72	2.84	2.93	0.00	0.0:	0.18	0.27	0.35	0.00	0.0:	0.33	0.40	0.50	0.60
location	*interior*	*adj fract*	*ar fract*	*interior*	*±near rim*	*±near rim*	*near rim*	*m adj pl?*	*rim adj pl*	*nr rm - pl*	*nr rm*	*nr rm - bt*	*im adj bt*	*rim adj pl*	*nr rm - pl*	*adj fract*	*adj fract*	*adj fract*	*rm adj pl*

TABLE B-1: Quantitative Microprobe Analysis for Garnet Compositions

	PC-110A												*PC-111A*							
	GT1a	**GT1b**	**GT1c**	**GT1d**	**GT1e**	**GT1f**	**GT1g**	**GT2a**	**GT2b**	**GT2c**	**GT2d**	**GT2e**	**GT1a**	**GT1b**	**GT1c**	**GT1d**	**GT1e**	**GT1f**	**GT2a**	**GT2b**
WEIGHT PERCENT OXIDES																				
SiO2	38.307	38.687	38.441	38.475	38.523	38.453	38.614	38.077	38.434	38.555	38.603	38.000	38.112	38.327	37.386	37.254	38.604	38.215	37.573	37.877
Al2O3	21.496	21.469	21.555	21.474	21.557	21.468	21.566	21.247	21.317	21.349	21.299	21.179	21.447	21.525	21.662	21.595	21.913	21.603	21.420	21.749
TiO2	0.072	0.055	0.000	0.043	0.032	0.009	0.009	0.032	0.038	0.029	0.000	0.000	0.093	0.023	0.081	0.041	0.000	0.000	0.000	0.058
Fe2O3	0.041	0.573	0.220	0.441	0.254	0.314	0.494	0.469	0.502	0.377	0.648	0.595	0.187	0.332	0.000	0.000	0.000	0.299	0.251	0.125
MgO	2.026	2.137	2.115	1.982	2.047	1.929	1.734	1.699	1.987	1.919	2.015	1.247	2.46:	2.878	2.912	2.711	2.698	2.679	3.129	3.179
FeO	35.380	36.226	35.734	36.042	35.563	35.345	35.919	35.435	35.621	35.293	35.317	36.719	37.633	37.447	38.086	37.495	37.841	37.907	37.212	37.948
MnO	3.687	3.420	3.488	3.631	3.800	3.965	4.201	4.128	3.431	3.717	3.680	4.061	1.469	1.302	1.255	1.241	1.438	1.418	1.153	1.191
CaO	2.074	2.112	2.125	2.215	2.177	2.230	2.419	2.346	2.332	2.164	2.346	2.073	1.820	1.745	1.854	1.688	1.617	1.817	1.835	1.822
TOTAL	**103.08**	**104.68**	**103.68**	**104.30**	**103.95**	**103.71**	**104.96**	**103.43**	**103.66**	**103.40**	**103.91**	**103.874**	**103.231**	**103.579**	**103.236**	**102.025**	**104.111**	**103.938**	**102.573**	**103.949**
CATIONS RECALCULATED TO 12 OXYGENS																				
Si	3.00:	3.001	3.005	2.998	3.005	3.008	2.995	2.997	3.008	3.021	3.013	2.993	2.992	2.992	2.943	2.960	2.997	2.982	2.966	2.954
Al	1.991	1.963	1.986	1.972	1.982	1.979	1.972	1.971	1.966	1.971	1.959	1.966	1.985	1.981	2.00:	2.023	2.005	1.987	1.993	1.999
Ti	0.004	0.003	0.000	0.003	0.002	0.001	0.001	0.002	0.002	0.002	0.000	0.000	0.005	0.001	0.005	0.002	0.000	0.000	0.000	0.003
Fe3+	0.002	0.033	0.013	0.026	0.015	0.019	0.029	0.028	0.02:	0.022	0.038	0.035	0.011	0.01:	0.000	0.000	0.000	0.018	0.015	0.007
Mg	0.237	0.247	0.246	0.230	0.238	0.225	0.201	0.199	0.232	0.224	0.234	0.146	0.289	0.335	0.342	0.321	0.312	0.312	0.368	0.370
Fe2+	2.325	2.350	2.336	2.348	2.320	2.312	2.330	2.332	2.331	2.312	2.305	2.419	2.471	2.445	2.507	2.492	2.457	2.473	2.456	2.475
Mn	0.245	0.225	0.231	0.240	0.251	0.263	0.276	0.275	0.227	0.247	0.243	0.271	0.098	0.086	0.084	0.084	0.095	0.094	0.077	0.079
Ca	0.175	0.176	0.178	0.185	0.182	0.187	0.201	0.198	0.196	0.182	0.196	0.175	0.153	0.146	0.156	0.144	0.135	0.152	0.155	0.152
TOTAL	**7.989**	**7.998**	**7.995**	**8.001**	**7.995**	**7.993**	**8.004**	**8.002**	**7.992**	**7.981**	**7.989**	**8.006**	**8.004**	**8.006**	**8.047**	**8.026**	**8.000**	**8.016**	**8.030**	**8.039**
Fe/Fe+Mg	*0.907*	*0.905*	*0.905*	*0.911*	*0.907*	*0.911*	*0.921*	*0.921*	*0.910*	*0.912*	*0.908*	*0.943*	*0.895*	*0.880*	*0.880*	*0.886*	*0.887*	*0.888*	*0.870*	*0.870*
Alm	0.780	0.784	0.781	0.782	0.776	0.774	0.775	0.776	0.781	0.780	0.774	0.803	0.821	0.812	0.812	0.820	0.819	0.816	0.804	0.805
Py	0.07:	0.082	0.082	0.077	0.07:	0.075	0.067	0.066	0.078	0.076	0.079	0.049	0.096	0.111	0.111	0.106	0.104	0.103	0.120	0.120
Sp	0.082	0.075	0.077	0.07:	0.084	0.088	0.092	0.092	0.076	0.083	0.082	0.090	0.032	0.029	0.027	0.028	0.032	0.031	0.025	0.026
Gr	0.059	0.059	0.059	0.062	0.061	0.063	0.067	0.066	0.066	0.061	0.066	0.058	0.051	0.049	0.051	0.047	0.045	0.050	0.051	0.04:
(Ca+Mn)/(Mg+Ca+Mn+Fe)	0.141	0.134	0.137	0.141	0.145	0.151	0.159	0.157	0.142	0.144	0.148	0.148	0.083	0.077	0.078	0.075	0.076	0.081	0.076	0.075
X	-170.47	-169.61	-168.51	-167.42	-166.32	-165.23	-164.17	-132.71	-131.53	-130.12	-128.82	-127.72	-158.49	-157.47	-156.45	-155.42	-154.59	-153.38	-149.57	-148.56
Y	208.81	209.04	209.28	209.51	209.74	209.98	210.21	235.18	236.56	237.95	239.33	240.71	-190.74	-190.38	-190.02	-189.66	-189.20	-188.99	-187.63	-187.27
x-axis m	0.00	0.09	0.20	0.31	0.43	0.54	0.65	0.00	0.18	0.38	0.57	0.75	0.00	0.11	0.22	0.33	0.42	0.54	0.00	0.11
location	*im adj qz*	*r rm - qz*	*±near rim*	*r rm - qz*	*nr rm - pl*	*r rm - qz*	*im adj qz*	*rim adj bt*	*r rm - qz*	*r rm - qz*	*r rm - qz*	*m adj pl?*	*rm adj bt*	*nr rm - bt*	*±near rim*	*±near rim*	*nr rm - bt*	*rm adj bt*	*rm adj qz*	*r rm - qz*

TABLE B-1: Quantitative Microprobe Analysis for Garnet Compositions

PC-111A (continued)

	GT2c	GT2d	GT2e	GT2f	GT2g	GT2h	GT2i	GT2j	GT2k	GT2l	GT2m	GT2n	GT2o	GT2p	GT3a	GT3b	GT3c	GT3d
WEIGHT PERCENT OXIDES																		
SiO2	38.044	38.088	37.758	38.063	36.843	37.143	37.346	37.505	38.341	37.356	37.663	37.742	37.625	37.964	38.561	38.110	38.178	37.540
Al2O3	21.423	21.767	21.265	21.434	21.176	21.325	21.001	21.170	21.264	21.209	21.334	21.451	21.650	21.555	21.271	21.439	21.377	21.584
TiO2	0.012	0.035	0.000	0.000	0.020	0.049	0.000	0.029	0.000	0.009	0.023	0.006	0.000	0.000	0.032	0.020	0.035	0.000
Fe2O3	0.333	0.000	0.519	0.434	0.205	0.000	0.727	0.439	0.486	0.396	0.306	0.280	0.000	0.170	0.811	0.353	0.546	0.061
MgO	3.182	2.847	2.574	2.421	2.786	2.977	3.142	3.176	2.871	3.012	2.703	2.924	3.033	2.640	2.719	2.730	2.828	2.710
FeO	36.920	37.998	38.091	38.487	37.544	36.737	37.007	36.810	37.218	37.473	38.050	37.669	37.497	37.912	37.647	37.667	37.601	38.116
MnO	1.044	1.274	1.166	1.306	1.095	1.119	0.953	1.089	1.079	1.229	1.147	1.196	1.174	1.253	1.335	1.222	1.188	1.195
CaO	1.843	1.502	1.794	1.679	1.923	1.834	1.969	1.82:	1.514	1.569	1.578	1.748	1.589	1.799	1.758	1.801	1.910	1.852
TOTAL	**102.801**	**103.511**	**103.167**	**103.824**	**101.592**	**101.184**	**102.145**	**102.048**	**102.773**	**102.253**	**102.804**	**103.016**	**102.568**	**103.293**	**104.134**	**103.342**	**103.663**	**103.058**
CATIONS RECALCULATED TO 12 OXYGENS																		
Si	2.987	2.979	2.975	2.981	2.949	2.969	2.964	2.973	3.012	2.964	2.975	2.970	2.968	2.980	3.000	2.987	2.984	2.959
Al	1.982	2.007	1.975	1.979	1.998	2.009	1.965	1.978	1.969	1.984	1.986	1.990	2.013	1.994	1.950	1.981	1.969	2.005
Ti	0.001	0.002	0.000	0.000	0.001	0.003	0.000	0.002	0.000	0.001	0.001	0.000	0.000	0.000	0.002	0.001	0.002	0.000
Fe3+	0.01:	0.000	0.031	0.026	0.012	0.000	0.043	0.026	0.029	0.024	0.018	0.017	0.000	0.010	0.048	0.021	0.032	0.004
Mg	0.372	0.332	0.302	0.283	0.332	0.355	0.372	0.375	0.336	0.356	0.318	0.343	0.357	0.309	0.315	0.319	0.330	0.318
Fe2+	2.424	2.486	2.510	2.521	2.513	2.456	2.456	2.440	2.445	2.487	2.513	2.479	2.474	2.489	2.449	2.469	2.458	2.513
Mn	0.069	0.084	0.078	0.087	0.074	0.076	0.064	0.073	0.072	0.083	0.077	0.07:	0.079	0.083	0.088	0.081	0.079	0.07:
Ca	0.155	0.126	0.151	0.141	0.165	0.157	0.167	0.155	0.127	0.133	0.134	0.147	0.134	0.151	0.147	0.151	0.160	0.156
TOTAL	**8.011**	**8.016**	**8.022**	**8.017**	**8.045**	**8.024**	**8.032**	**8.023**	**7.990**	**8.031**	**8.022**	**8.026**	**8.025**	**8.017**	**7.999**	**8.011**	**8.013**	**8.036**
Fe/Fe+Mg	*0.867*	*0.882*	*0.892*	*0.899*	*0.883*	*0.874*	*0.869*	*0.867*	*0.879*	*0.875*	*0.888*	*0.878*	*0.874*	*0.890*	*0.886*	*0.886*	*0.882*	*0.888*
Alm	0.802	0.821	0.825	0.832	0.815	0.807	0.803	0.802	0.820	0.813	0.826	0.813	0.813	0.821	0.817	0.817	0.812	0.819
Py	0.123	0.110	0.099	0.093	0.108	0.117	0.122	0.123	0.113	0.116	0.105	0.112	0.117	0.102	0.105	0.106	0.109	0.104
Sp	0.023	0.028	0.026	0.029	0.024	0.025	0.021	0.024	0.024	0.027	0.025	0.026	0.026	0.028	0.029	0.027	0.026	0.026
Gr	0.051	0.042	0.04:	0.046	0.054	0.052	0.055	0.051	0.043	0.044	0.044	0.048	0.044	0.04:	0.049	0.050	0.053	0.051
(Ca+Mn)/(Mg+Ca+Mn+Fe)	0.074	0.06:	0.075	0.075	0.078	0.077	0.076	0.075	0.067	0.071	0.069	0.075	0.06:	0.077	0.078	0.077	0.079	0.077
X	-147.54	-146.53	-143.49	-142.62	-141.46	-140.45	-139.43	-138.42	-137.41	-136.39	-135.47	-134.37	-133.44	-132.34	-128.71	-127.73	-126.97	-125.78
Y	-186.92	-186.56	-185.30	-185.07	-184.52	-184.43	-184.08	-183.72	-183.36	-183.01	-182.91	-182.30	-181.94	-181.59	-180.56	-180.20	-180.00	-179.48
x-axis m	0.22	0.32	0.65	0.74	0.87	0.97	1.08	1.19	1.29	1.40	1.49	1.62	1.72	1.83	0.00	0.10	0.18	0.31
location	*r rm - pl?*	*j bt fract*	*dj qz incl*	*dj qz incl*	*j bt fract*	*r bt fract*	*interior*	*interior*	*r bt fract*	*j bt fract*	*j bt fract*	*r bt fract*	*nr rm - bt*	*rm adj bt*	*rm adj qz*	*nr rm - qz*	*nr rm - qz*	*nr rm - qz*

TABLE B-1: Quantitative Microprobe Analysis for Garnet Compositions

PC-111A (continued)

	GT3e	GT3f	GT3g	GT3h	GT3i	GT3j	GT3k	GT3l	GT3m	GT3n	GT3o	GT4a	GT4b	GT4c	GT4d	GT4e	GT4f	GT4g
WEIGHT PERCENT OXIDES																		
SiO2	37.971	37.411	37.56:	37.392	37.882	38.46:	38.322	38.165	37.706	38.009	38.005	37.020	37.921	37.554	37.795	37.517	37.774	37.477
Al2O3	21.422	21.123	21.431	21.230	21.529	21.671	21.502	21.252	21.782	21.428	21.561	21.105	21.234	21.354	21.410	21.512	21.299	21.230
TiO2	0.038	0.000	0.038	0.043	0.000	0.093	0.055	0.000	0.081	0.009	0.041	0.000	0.041	0.000	0.026	0.043	0.035	0.035
Fe2O3	0.070	0.431	0.263	0.247	0.000	0.280	0.279	0.754	0.000	0.422	0.094	0.207	0.613	0.169	0.332	0.000	0.182	0.431
MgO	2.535	2.388	2.489	2.329	2.56:	2.534	2.729	2.617	2.854	2.832	2.646	2.716	2.592	2.764	2.885	2.326	1.991	2.574
FeO	37.315	37.708	38.381	38.260	37.899	38.378	37.668	38.027	37.994	37.594	37.523	37.366	38.090	37.066	37.143	38.222	38.833	37.852
MnO	1.287	1.355	1.313	1.262	1.184	1.329	1.189	1.323	1.267	1.251	1.443	1.157	1.338	1.131	1.214	1.266	1.312	1.352
CaO	1.811	1.870	1.831	1.671	1.584	1.862	1.754	1.732	1.884	1.872	1.853	1.672	1.661	2.104	2.168	1.892	1.369	1.867
TOTAL	**102.449**	**102.286**	**103.316**	**102.434**	**102.648**	**104.617**	**103.498**	**103.870**	**103.568**	**103.417**	**103.166**	**101.243**	**103.490**	**102.142**	**102.973**	**102.778**	**102.795**	**102.818**
CATIONS RECALCULATED TO 12 OXYGENS																		
Si	2.998	2.975	2.961	2.972	2.990	2.984	2.996	2.985	2.954	2.979	2.984	2.968	2.979	2.977	2.973	2.969	2.992	2.965
Al	1.994	1.980	1.991	1.989	2.003	1.981	1.981	1.959	2.011	1.979	1.995	1.995	1.966	1.995	1.985	2.006	1.989	1.980
Ti	0.002	0.000	0.002	0.003	0.000	0.005	0.003	0.000	0.005	0.001	0.002	0.000	0.002	0.000	0.002	0.003	0.002	0.002
Fe3+	0.004	0.026	0.016	0.015	0.000	0.016	0.016	0.044	0.000	0.025	0.006	0.013	0.036	0.010	0.01:	0.000	0.011	0.026
Mg	0.298	0.283	0.292	0.276	0.302	0.293	0.318	0.305	0.333	0.331	0.310	0.325	0.304	0.327	0.338	0.274	0.235	0.304
Fe2+	2.464	2.508	2.530	2.543	2.501	2.490	2.462	2.487	2.489	2.464	2.464	2.506	2.502	2.457	2.443	2.529	2.573	2.505
Mn	0.086	0.091	0.088	0.085	0.079	0.087	0.079	0.088	0.084	0.083	0.096	0.079	0.089	0.076	0.081	0.085	0.088	0.091
Ca	0.153	0.159	0.155	0.142	0.134	0.155	0.147	0.145	0.158	0.157	0.156	0.144	0.140	0.179	0.183	0.160	0.116	0.158
TOTAL	**8.000**	**8.022**	**8.034**	**8.024**	**8.009**	**8.012**	**8.002**	**8.013**	**8.035**	**8.019**	**8.013**	**8.028**	**8.018**	**8.021**	**8.024**	**8.026**	**8.006**	**8.02:**
Fe/Fe+Mg	*0.892*	*0.899*	*0.896*	*0.902*	*0.892*	*0.895*	*0.886*	*0.891*	*0.882*	*0.882*	*0.888*	*0.885*	*0.892*	*0.883*	*0.878*	*0.902*	*0.916*	*0.892*
Alm	0.821	0.825	0.826	0.835	0.829	0.823	0.819	0.822	0.812	0.812	0.814	0.821	0.825	0.809	0.802	0.82:	0.854	0.819
Py	0.099	0.093	0.095	0.091	0.100	0.097	0.106	0.101	0.109	0.109	0.102	0.106	0.100	0.107	0.111	0.090	0.078	0.099
Sp	0.029	0.030	0.029	0.028	0.026	0.029	0.026	0.029	0.027	0.027	0.032	0.026	0.029	0.025	0.027	0.028	0.029	0.02:
Gr	0.051	0.052	0.051	0.047	0.044	0.051	0.049	0.048	0.052	0.052	0.052	0.047	0.046	0.059	0.060	0.053	0.039	0.052
(Ca+Mn)/(Mg+Ca+Mn+Fe)	0.07:	0.082	0.079	0.075	0.071	0.080	0.075	0.077	0.079	0.079	0.083	0.073	0.075	0.084	0.087	0.080	0.068	0.081
X	-124.81	-123.83	-122.85	-121.81	-120.90	-119.93	-118.95	-117.98	-117.00	-116.03	-115.05	-130.36	-129.83	-129.31	-128.79	-128.49	-127.64	-126.68
Y	-179.12	-178.48	-178.39	-178.03	-177.67	-177.31	-176.95	-176.59	-176.23	-175.65	-175.51	-171.43	-170.47	-169.63	-168.73	-167.88	-166.68	-165.96
x-axis m	0.42	0.53	0.63	0.74	0.84	0.94	1.05	1.15	1.26	1.37	1.47	0.00	0.11	0.21	0.31	0.40	0.55	0.67
location	*nr fract*	*adj fract*	*dj bt incl*	*dj bt incl*	*nr bt incl*	*adj fract*	*nr bt incl*	*±near rim*	*±near rim*	*nr rm - bt*	*im adj bt*	*im adj qz*	*adj fract*	*nr fract*	*±near rim*	*dj bt incl*	*adj fract*	*nr fract*

TABLE B-1: Quantitative Microprobe Analysis for Garnet Compositions

PC-111A (continued)							*PC-113/4a*											
	GT4h	**GT4i**	**GT4j**	**GT4k**	**GT4l**	**GT4m**	**1T**	**2T**	**3T**	**4T**	**5T**	**6T**	**7T**	**8T**	**9T**	**10T**	**11T**	**12T**
WEIGHT PERCENT OXIDES																		
SiO2	37.730	37.501	38.158	38.038	37.993	38.226	35.528	37.067	36.272	37.497	37.136	37.564	37.333	36.114	36.453	36.668	36.952	37.123
Al2O3	21.433	21.292	21.46:	21.276	21.568	21.575	22.384	22.421	22.610	22.177	21.883	22.282	21.924	22.331	22.778	22.846	22.611	22.554
TiO2	0.000	0.009	0.009	0.006	0.000	0.014	0.052	0.031	0.002	0.000	0.000	0.056	0.000	0.038	0.059	0.000	0.000	0.012
Fe2O3	0.160	0.475	0.462	0.644	0.378	0.393	0.004	0.000	0.092	0.107	0.074	0.018	0.000	0.007	0.000	0.004	0.000	0.011
MgO	2.575	2.296	2.460	2.993	2.732	2.462	2.890	3.861	3.964	4.045	4.075	4.219	4.285	4.362	4.385	4.274	4.405	4.416
FeO	37.956	38.932	38.273	37.358	38.062	38.165	37.387	38.907	37.444	37.521	37.040	37.310	37.350	36.751	36.670	36.840	36.841	36.000
MnO	1.182	1.502	1.310	1.233	1.467	1.632	1.435	1.027	1.109	1.111	1.108	0.882	0.993	0.996	0.943	0.810	0.987	0.928
CaO	1.708	1.511	1.900	1.777	1.843	1.872	1.067	1.090	1.076	1.070	1.164	1.091	1.073	1.218	0.957	1.117	1.097	1.140
TOTAL	**102.744**	**103.518**	**104.042**	**103.325**	**104.043**	**104.339**	**100.747**	**104.404**	**102.568**	**103.528**	**102.480**	**103.423**	**102.959**	**101.817**	**102.244**	**102.559**	**102.892**	**103.183**
CATIONS RECALCULATED TO 12 OXYGENS																		
Si	2.980	2.959	2.981	2.982	2.967	2.978	2.868	2.886	2.865	2.925	2.926	2.926	2.927	2.867	2.872	2.880	2.893	2.899
Al	1.995	1.980	1.977	1.966	1.985	1.981	2.130	2.057	2.105	2.039	2.032	2.046	2.026	2.089	2.115	2.115	2.087	2.076
Ti	0.000	0.001	0.001	0.000	0.000	0.001	0.003	0.002	0.000	0.000	0.000	0.003	0.000	0.002	0.003	0.000	0.000	0.001
Fe3+	0.00:	0.028	0.027	0.038	0.022	0.023	0.000	0.000	0.005	0.006	0.004	0.001	0.000	0.000	0.000	0.000	0.000	0.001
Mg	0.303	0.270	0.286	0.350	0.318	0.286	0.348	0.448	0.467	0.46:	0.479	0.490	0.501	0.516	0.515	0.500	0.514	0.514
Fe2+	2.507	2.569	2.500	2.449	2.486	2.486	2.524	2.533	2.473	2.448	2.441	2.431	2.449	2.440	2.416	2.420	2.412	2.416
Mn	0.079	0.100	0.087	0.082	0.097	0.108	0.098	0.068	0.074	0.073	0.074	0.058	0.066	0.067	0.063	0.054	0.065	0.061
Ca	0.145	0.128	0.159	0.149	0.154	0.156	0.092	0.091	0.091	0.08:	0.098	0.091	0.090	0.104	0.081	0.094	0.092	0.095
TOTAL	**8.018**	**8.036**	**8.017**	**8.016**	**8.029**	**8.019**	**8.064**	**8.084**	**8.080**	**8.052**	**8.055**	**8.047**	**8.05:**	**8.086**	**8.067**	**8.063**	**8.064**	**8.063**
Fe/Fe+Mg	*0.892*	*0.905*	*0.897*	*0.875*	*0.887*	*0.897*	*0.879*	*0.850*	*0.841*	*0.839*	*0.836*	*0.832*	*0.82:*	*0.825*	*0.824*	*0.829*	*0.824*	*0.825*
Alm	0.826	0.838	0.825	0.808	0.814	0.819	0.824	0.807	0.796	0.794	0.789	0.792	0.788	0.780	0.786	0.789	0.782	0.783
Py	0.09:	0.088	0.095	0.115	0.104	0.094	0.114	0.143	0.150	0.153	0.155	0.160	0.161	0.165	0.168	0.163	0.167	0.167
Sp	0.026	0.033	0.029	0.027	0.032	0.036	0.032	0.022	0.024	0.024	0.024	0.019	0.021	0.021	0.021	0.018	0.021	0.01:
Gr	0.048	0.042	0.052	0.049	0.051	0.052	0.030	0.029	0.029	0.029	0.032	0.02:	0.029	0.033	0.026	0.031	0.02:	0.031
(Ca+Mn)/(Mg+Ca+Mn+Fe)	0.074	0.074	0.081	0.076	0.082	0.087	0.062	0.051	0.053	0.053	0.056	0.049	0.050	0.055	0.047	0.048	0.051	0.051
X	-126.70	-126.18	-126.12	-125.13	-124.61	-124.09	-85.69	-85.11	-84.75	-84.43	-84.12	-83.80	-83.47	-83.17	-82.86	-82.54	-82.20	-82.01
Y	-165.14	-164.24	-163.37	-162.44	-161.54	-160.64	-292.93	-290.37	-289.09	-287.75	-286.54	-285.16	-283.96	-282.70	-281.42	-280.29	-278.88	-277.46
x-axis m	0.75	0.86	0.94	1.08	1.18	1.29	0.00	0.26	0.40	0.53	0.66	0.80	0.92	1.05	1.19	1.30	1.45	1.59
location	*±nr fract*	*adj fract*	*adj fract*	*nr qz incl*	*nr rm - bt*	*rm adj bt*	*im adj bt*	*±near rim*	*±near rim*	*interior*	*interior*	*interior*	*interior*	*interior*	*interior*	*interior*	*interior*	*interior*

TABLE B-1: Quantitative Microprobe Analysis for Garnet Compositions

PC-113A/4a (continued)

	13T	14T	15T	16T	17T	18T	19T	20T	21T	22T	23T	24T	1	1a	2	2a	3	3a
WEIGHT PERCENT OXIDES																		
SiO2	37.376	36.679	37.242	36.924	36.987	36.333	36.342	36.188	36.426	36.198	36.410	36.807	35.678	35.676	36.756	36.121	36.895	36.563
Al2O3	22.413	22.526	22.372	22.469	22.711	22.393	22.309	22.234	22.197	22.120	22.489	22.058	22.186	21.765	22.230	21.901	22.049	22.480
TiO2	0.000	0.035	0.000	0.005	0.031	0.000	0.052	0.042	0.000	0.000	0.026	0.045	0.000	0.000	0.016	0.021	0.000	0.031
Fe2O3	0.007	0.000	0.015	0.011	0.059	0.000	0.000	0.011	0.000	0.063	0.011	0.000	0.048	0.041	0.000	0.085	0.022	0.033
MgO	4.253	4.251	4.059	3.989	3.897	3.939	4.037	3.858	3.665	3.705	3.640	3.583	2.890	3.260	2.892	3.159	2.780	3.349
FeO	37.136	37.284	37.573	36.687	38.021	37.484	37.971	36.439	37.036	37.985	38.030	37.242	37.454	37.484	38.684	37.743	38.978	38.123
MnO	0.862	0.878	0.963	0.983	0.978	1.010	1.219	1.095	1.147	1.209	1.247	1.267	1.359	1.295	1.335	1.336	1.335	1.058
CaO	1.154	1.05:	1.086	1.073	1.089	1.032	0.983	1.036	0.991	1.093	0.928	1.024	1.070	1.086	1.071	1.054	1.127	1.080
TOTAL	**103.203**	**102.714**	**103.310**	**102.141**	**103.773**	**102.191**	**102.913**	**100.904**	**101.462**	**102.373**	**102.782**	**102.026**	**100.686**	**100.607**	**102.984**	**101.418**	**103.187**	**102.717**
CATIONS RECALCULATED TO 12 OXYGENS																		
Si	2.917	2.884	2.911	2.911	2.885	2.879	2.868	2.895	2.903	2.876	2.876	2.919	2.882	2.886	2.906	2.897	2.915	2.889
Al	2.062	2.087	2.061	2.088	2.088	2.091	2.075	2.096	2.085	2.071	2.094	2.061	2.112	2.075	2.071	2.070	2.053	2.093
Ti	0.000	0.002	0.000	0.000	0.002	0.000	0.003	0.003	0.000	0.000	0.002	0.003	0.000	0.000	0.001	0.001	0.000	0.002
Fe3+	0.000	0.000	0.001	0.001	0.003	0.000	0.000	0.001	0.000	0.004	0.001	0.000	0.003	0.002	0.000	0.005	0.001	0.002
Mg	0.495	0.498	0.473	0.469	0.453	0.465	0.475	0.460	0.435	0.439	0.429	0.424	0.348	0.393	0.341	0.378	0.327	0.394
Fe2+	2.424	2.451	2.456	2.419	2.480	2.484	2.506	2.438	2.469	2.524	2.512	2.46:	2.530	2.536	2.558	2.532	2.576	2.519
Mn	0.057	0.059	0.064	0.066	0.065	0.068	0.082	0.074	0.077	0.081	0.083	0.085	0.093	0.089	0.089	0.091	0.089	0.071
Ca	0.097	0.089	0.091	0.091	0.091	0.088	0.083	0.089	0.085	0.093	0.079	0.087	0.093	0.094	0.091	0.091	0.095	0.091
TOTAL	**8.052**	**8.071**	**8.058**	**8.044**	**8.067**	**8.075**	**8.092**	**8.055**	**8.054**	**8.087**	**8.075**	**8.048**	**8.061**	**8.075**	**8.057**	**8.064**	**8.058**	**8.062**
Fe/Fe+Mg	*0.82:*	*0.831*	*0.839*	*0.838*	*0.845*	*0.842*	*0.841*	*0.841*	*0.850*	*0.852*	*0.854*	*0.854*	*0.879*	*0.866*	*0.882*	*0.870*	*0.887*	*0.865*
Alm	0.789	0.791	0.796	0.795	0.803	0.800	0.797	0.796	0.805	0.805	0.810	0.806	0.826	0.815	0.831	0.819	0.834	0.819
Py	0.161	0.161	0.153	0.154	0.147	0.150	0.151	0.150	0.142	0.140	0.138	0.138	0.114	0.126	0.111	0.122	0.106	0.128
Sp	0.019	0.019	0.021	0.022	0.021	0.022	0.026	0.024	0.025	0.026	0.027	0.028	0.030	0.029	0.029	0.029	0.029	0.023
Gr	0.031	0.029	0.029	0.02:	0.029	0.028	0.026	0.029	0.028	0.02:	0.025	0.028	0.030	0.030	0.029	0.029	0.031	0.02:
(Ca+Mn)/(Mg+Ca+Mn+Fe)	0.050	0.048	0.050	0.051	0.050	0.050	0.052	0.053	0.053	0.056	0.052	0.056	0.061	0.059	0.059	0.059	0.05:	0.053
X	-81.60	-81.28	-80.93	-80.66	-80.77	-80.03	-79.71	-79.40	-79.08	-78.77	-78.45	-78.14	-83.18	-83.14	-69.56	-69.69	-67.98	-68.32
Y	-276.31	-275.03	-273.74	-272.48	-271.20	-269.92	-268.64	-267.36	-266.08	-264.81	-263.53	-262.25	-294.10	-293.76	-285.17	-285.06	-275.20	-275.51
x-axis m	1.71	1.85	1.98	2.11	2.24	2.38	2.52	2.65	2.78	2.91	3.04	3.17	0.00	0.03	0.00	0.02	0.00	0.05
location	*interior*	*interior*	*interior*	*interior*	*interior*	*interior*	*interior*	*interior*	*±near rim*	*±near rim*	*±near rim*	*im adj qz*	*rim adj bt*	*nr rm - bt*	*rim adj bt*	*rim adj bt*	*rim adj bt*	*nr rm - bt*

TABLE B-1: Quantitative Microprobe Analysis for Garnet Compositions

PC-113A/4a (continued)

													113B	*PC-113C*				
	4	**5**	**6**	**7**	**7a**	**8**	**8a**	**9**	**9a**	**10**	**11**	**12**	**G1**	**GR1**	**GR2**	**GR3**	**GR4**	**GR5**
WEIGHT PERCENT OXIDES																		
SiO2	36.728	36.834	37.490	36.436	36.948	36.784	36.969	36.471	36.540	36.936	36.869	37.491	37.384	38.723	38.246	38.378	38.131	38.215
Al2O3	22.389	22.215	21.987	21.979	21.843	22.315	22.355	22.071	22.411	22.033	22.658	22.410	22.489	21.833	21.964	21.832	21.862	22.219
TiO2	0.000	0.047	0.000	0.000	0.000	0.014	0.000	0.000	0.017	0.028	0.021	0.08:	0.027	0.023	0.000	0.001	0.000	0.000
Fe2O3	0.000	0.004	0.000	0.000	0.081	0.000	0.082	0.019	0.015	0.022	0.02:	0.000						
MgO	3.772	4.431	4.278	3.753	4.023	3.729	3.981	3.287	3.566	3.863	4.355	4.158	4.049	3.355	3.028	3.592	3.247	3.559
FeO	37.035	37.098	37.327	37.037	37.523	36.800	37.396	37.394	38.322	37.597	36.535	37.097	36.796	35.823	36.916	36.977	36.723	36.206
MnO	0.910	0.791	0.787	0.995	0.995	0.820	1.097	1.008	1.051	0.886	0.902	0.780	1.108	1.278	1.266	1.360	1.310	1.332
CaO	1.041	1.173	1.220	1.015	1.103	1.000	1.069	1.028	1.073	1.07:	1.033	1.194	0.994	0.995	1.002	0.883	1.070	0.965
TOTAL	**101.876**	**102.593**	**103.090**	**101.215**	**102.517**	**101.463**	**102.950**	**101.277**	**102.994**	**102.445**	**102.404**	**103.220**	**102.847**	**102.030**	**102.422**	**103.023**	**102.343**	**102.496**
CATIONS RECALCULATED TO 12 OXYGENS																		
Si	2.909	2.897	2.932	2.910	2.917	2.921	2.903	2.916	2.882	2.916	2.896	2.923	2.925	3.033	3.003	2.996	2.996	2.988
Al	2.08:	2.059	2.027	2.069	2.032	2.088	2.069	2.07:	2.083	2.050	2.098	2.059	2.074	2.016	2.032	2.009	2.025	2.048
Ti	0.000	0.003	0.000	0.000	0.000	0.001	0.000	0.000	0.001	0.002	0.001	0.005	0.002	0.001	0.000	0.000	0.000	0.000
Fe3+	0.000	0.000	0.000	0.000	0.005	0.000	0.005	0.001	0.001	0.001	0.002	0.000						
Mg	0.445	0.520	0.499	0.447	0.473	0.441	0.466	0.392	0.419	0.455	0.510	0.483	0.472	0.392	0.354	0.418	0.380	0.415
Fe2+	2.453	2.440	2.442	2.474	2.477	2.444	2.455	2.500	2.528	2.482	2.400	2.419	2.408	2.347	2.424	2.414	2.413	2.368
Mn	0.061	0.053	0.052	0.067	0.067	0.055	0.073	0.068	0.070	0.059	0.060	0.052	0.073	0.085	0.084	0.08:	0.087	0.088
Ca	0.088	0.099	0.102	0.087	0.093	0.085	0.08:	0.088	0.091	0.091	0.087	0.09:	0.083	0.084	0.084	0.074	0.090	0.081
TOTAL	**8.046**	**8.071**	**8.054**	**8.055**	**8.065**	**8.035**	**8.061**	**8.044**	**8.075**	**8.057**	**8.053**	**8.042**	**8.037**	**7.957**	**7.981**	**7.000**	**7.992**	**7.988**
Fe/Fe+Mg	*0.846*	*0.824*	*0.82:*	*0.847*	*0.840*	*0.847*	*0.840*	*0.865*	*0.858*	*0.845*	*0.825*	*0.833*	*0.836*	*0.857*	*0.872*	*0.852*	*0.864*	*0.851*
Alm	0.805	0.784	0.789	0.805	0.796	0.808	0.796	0.820	0.813	0.804	0.785	0.792	0.793	0.807	0.823	0.806	0.812	0.802
Py	0.146	0.167	0.161	0.145	0.152	0.146	0.151	0.129	0.135	0.147	0.167	0.158	0.156	0.135	0.120	0.140	0.128	0.141
Sp	0.020	0.017	0.017	0.022	0.021	0.018	0.024	0.022	0.023	0.019	0.01:	0.017	0.024	0.029	0.029	0.030	0.029	0.02:
Gr	0.029	0.032	0.033	0.028	0.030	0.028	0.029	0.029	0.029	0.02:	0.028	0.033	0.027	0.029	0.029	0.025	0.030	0.027
(Ca+Mn)/(Mg+Ca+Mn+Fe)	0.049	0.049	0.04:	0.050	0.051	0.046	0.053	0.051	0.052	0.049	0.048	0.04:	0.052	0.058	0.057	0.055	0.05:	0.057
X	-70.92	-77.17	-78.95	-89.36	-89.03	-89.79	-89.52	-86.88	-86.90	-88.13	-84.10	-76.27	78.38	-72.74	-64.91	-47.89	-63.16	-49.53
Y	-276.61	-277.36	-282.29	-278.30	-278.30	-285.22	-285.54	-275.51	-275.77	-288.10	-285.99	-281.97	351.18	369.68	379.75	360.93	350.29	349.76
x-axis mm				0.00	0.03	0.00	0.04	0.00	0.03									
location	*±near rim*	*interior*	*interior*	*rim adj pl*	*nr rm - pl*	*im adj qz*	*r rm - qz*	*rim adj bt*	*nr rm - bt*	*±near rim*	*interior*	*interior*	*rim adj pl*	*rim adj pl*	*rim adj pl*	*rim adj bt*	*ragment*	*rag adj pl*

TABLE B-1: Quantitative Microprobe Analysis for Garnet Compositions

PC-113C (continued)

	GC1	GC2	GC3	GC4	G5	GT1a	GT1b	GT1c	GT1d	GT1e	GT1f	GT1g	GT2a	GT2b	GT2c	GT2d	GT2e	GT2f
WEIGHT PERCENT OXIDES																		
SiO2	39.208	38.359	39.093	38.777	38.657	38.999	38.779	39.059	38.931	39.172	39.173	38.743	38.559	39.243	36.312	38.543	38.814	38.468
Al2O3	22.334	21.693	22.158	22.168	22.043	22.079	22.079	22.260	22.154	22.215	22.276	22.154	22.164	22.055	22.247	21.875	22.077	22.042
TiO2	0.010	0.000	0.000	0.000	0.018	0.000	0.000	0.000	0.040	0.061	0.048	0.000	0.015	0.000	0.030	0.045	0.063	0.039
Fe2O3																		
MgO	4.034	3.981	3.878	3.874	3.530	3.510	3.723	3.777	3.770	3.792	3.695	3.573	3.632	3.732	3.788	3.859	3.897	4.047
FeO	35.772	36.46:	36.282	36.386	36.539	35.938	36.617	36.411	35.802	36.196	36.142	36.325	36.601	36.581	36.312	36.127	36.896	36.063
MnO	0.950	0.977	1.156	1.023	1.211	1.234	1.038	1.138	1.066	1.048	1.107	1.175	1.218	1.212	1.237	1.085	1.025	0.931
CaO	1.047	1.066	1.058	1.090	0.950	1.044	1.096	1.003	1.092	1.091	1.130	0.982	0.915	0.876	0.989	1.057	1.094	1.056
TOTAL	**103.355**	**102.546**	**103.625**	**103.318**	**102.948**	**102.804**	**103.332**	**103.648**	**102.855**	**103.575**	**103.571**	**102.952**	**103.104**	**103.699**	**100.915**	**102.591**	**103.866**	**102.646**
CATIONS RECALCULATED TO 12 OXYGENS																		
Si	3.020	2.999	3.015	3.002	3.009	3.029	3.006	3.013	3.019	3.019	3.01:	3.011	2.998	3.027	2.903	3.006	2.996	2.996
Al	2.028	1.999	2.014	2.023	2.022	2.021	2.017	2.023	2.025	2.018	2.024	2.029	2.031	2.005	2.096	2.011	2.008	2.023
Ti	0.001	0.000	0.000	0.000	0.001	0.000	0.000	0.000	0.002	0.004	0.003	0.000	0.001	0.000	0.002	0.003	0.004	0.002
Fe3+																		
Mg	0.463	0.464	0.446	0.447	0.410	0.406	0.430	0.434	0.436	0.436	0.425	0.414	0.421	0.429	0.451	0.449	0.448	0.46:
Fe2+	2.305	2.385	2.340	2.356	2.378	2.335	2.374	2.348	2.322	2.333	2.330	2.361	2.380	2.359	2.427	2.357	2.382	2.349
Mn	0.062	0.065	0.076	0.067	0.07:	0.081	0.068	0.074	0.070	0.068	0.072	0.077	0.080	0.079	0.084	0.072	0.067	0.061
Ca	0.086	0.089	0.087	0.090	0.079	0.087	0.091	0.083	0.091	0.090	0.093	0.082	0.076	0.072	0.085	0.088	0.091	0.088
TOTAL	**7.965**	**8.001**	**7.978**	**7.986**	**7.979**	**7.960**	**7.986**	**7.976**	**7.966**	**7.968**	**7.966**	**7.974**	**7.986**	**7.971**	**8.048**	**7.985**	**7.996**	**7.990**
Fe/Fe+Mg	*0.833*	*0.837*	*0.840*	*0.840*	*0.853*	*0.852*	*0.847*	*0.844*	*0.842*	*0.843*	*0.846*	*0.851*	*0.850*	*0.846*	*0.843*	*0.840*	*0.842*	*0.833*
Alm	0.790	0.794	0.794	0.796	0.807	0.803	0.801	0.799	0.796	0.797	0.798	0.805	0.805	0.803	0.797	0.795	0.797	0.791
Py	0.159	0.155	0.151	0.151	0.139	0.140	0.145	0.148	0.149	0.149	0.145	0.141	0.142	0.146	0.148	0.151	0.150	0.158
Sp	0.021	0.021	0.026	0.023	0.027	0.028	0.023	0.025	0.024	0.023	0.025	0.026	0.027	0.027	0.028	0.024	0.022	0.021
Gr	0.02:	0.02:	0.02:	0.031	0.027	0.02:	0.031	0.028	0.031	0.031	0.032	0.028	0.026	0.025	0.028	0.02:	0.030	0.02:
(Ca+Mn)/(Mg+Ca+Mn+Fe)	0.051	0.051	0.055	0.053	0.054	0.058	0.054	0.054	0.055	0.054	0.057	0.054	0.053	0.052	0.055	0.054	0.053	0.050
X	-63.85	-62.25	-56.37	-59.37	-48.87	-71.22	-68.69	-66.16	-63.42	-60.98	-58.57	-56.13	-71.43	-70.28	-68.95	-67.71	-66.47	-65.24
Y	364.88	368.30	363.31	357.13	359.52	366.40	364.27	362.15	359.73	357.58	355.77	353.87	373.21	372.02	371.01	369.92	368.82	367.72
x-axis mm						0.00	0.33	0.66	1.03	1.35	1.65	1.96	0.00	0.17	0.33	0.50	0.66	0.83
location	*interior*	*interior*	*interior*	*interior*	*nr rm - bt*	*rim adj bt*	*±near rim*	*interior*	*interior*	*interior*	*±near rim*	*im adj qz*	*rim adj pl*	*nr rm - pl*	*interior*	*interior*	*interior*	*interior*

TABLE B-1: Quantitative Microprobe Analysis for Garnet Compositions

PC-113C (continued)

	GT2g	GT2h	GT2i	GT2j	GT2k	GT2l	GT2m	GT2n	GT2o	GT2p	GT2q	GT2r	GT2s	GT3a	GT3b	GT3c	GT3d	GT3e
WEIGHT PERCENT OXIDES																		
SiO2	38.790	38.973	39.401	38.839	38.981	38.476	38.764	39.064	38.491	38.718	38.624	38.482	38.662	38.811	38.800	36.423	39.115	38.103
Al2O3	22.213	22.196	22.241	22.042	22.145	22.031	22.288	22.085	22.145	22.327	22.043	21.947	22.085	21.966	22.104	22.116	22.150	21.814
TiO2	0.000	0.000	0.000	0.000	0.031	0.000	0.000	0.000	0.000	0.023	0.068	0.014	0.000	0.021	0.000	0.000	0.018	0.000
Fe2O3																		
MgO	3.989	4.115	4.007	4.087	4.004	4.005	4.022	3.886	3.907	3.845	3.723	3.543	3.119	3.472	3.758	3.827	3.875	3.976
FeO	36.378	35.841	36.008	36.115	35.861	36.386	36.216	36.342	36.084	36.448	36.425	36.701	37.040	36.808	36.557	36.423	35.956	36.552
MnO	1.086	0.954	1.120	0.964	1.075	1.052	0.968	1.026	1.016	1.149	1.133	1.196	1.446	1.269	1.189	1.116	1.032	1.166
CaO	1.045	1.088	1.054	1.082	1.120	1.177	1.119	0.989	1.039	0.994	1.060	1.034	0.969	0.864	0.963	1.074	1.041	1.073
TOTAL	**103.501**	**103.167**	**103.831**	**103.129**	**103.217**	**103.127**	**103.377**	**103.392**	**102.682**	**103.504**	**103.076**	**102.917**	**103.321**	**103.211**	**103.371**	**100.979**	**103.187**	**102.684**
CATIONS RECALCULATED TO 12 OXYGENS																		
Si	2.998	3.012	3.025	3.009	3.014	2.989	2.997	3.019	2.997	2.994	3.001	3.001	3.008	3.016	3.006	2.910	3.023	2.981
Al	2.023	2.022	2.013	2.012	2.018	2.017	2.031	2.011	2.032	2.035	2.019	2.017	2.025	2.012	2.018	2.082	2.018	2.011
Ti	0.000	0.000	0.000	0.000	0.002	0.000	0.000	0.000	0.000	0.001	0.004	0.001	0.000	0.001	0.000	0.000	0.001	0.000
Fe3+																		
Mg	0.460	0.474	0.459	0.472	0.461	0.464	0.464	0.448	0.454	0.443	0.431	0.412	0.362	0.402	0.434	0.456	0.447	0.464
Fe2+	2.351	2.317	2.312	2.340	2.318	2.364	2.341	2.349	2.350	2.357	2.367	2.394	2.410	2.392	2.369	2.433	2.324	2.391
Mn	0.071	0.063	0.073	0.063	0.070	0.069	0.063	0.067	0.067	0.075	0.075	0.079	0.095	0.084	0.078	0.076	0.068	0.077
Ca	0.087	0.090	0.087	0.08:	0.093	0.098	0.093	0.082	0.087	0.082	0.088	0.086	0.081	0.072	0.07:	0.092	0.086	0.08:
TOTAL	**7.990**	**7.977**	**7.968**	**7.985**	**7.976**	**8.002**	**7.988**	**7.976**	**7.987**	**7.988**	**7.985**	**7.990**	**7.980**	**7.978**	**7.985**	**8.049**	**7.967**	**8.014**
Fe/Fe+Mg	*0.836*	*0.82:*	*0.834*	*0.832*	*0.834*	*0.836*	*0.835*	*0.840*	*0.838*	*0.842*	*0.846*	*0.853*	*0.869*	*0.856*	*0.845*	*0.842*	*0.839*	*0.838*
Alm	0.792	0.787	0.789	0.789	0.788	0.789	0.791	0.797	0.795	0.797	0.799	0.806	0.818	0.811	0.800	0.796	0.795	0.791
Py	0.155	0.161	0.157	0.159	0.157	0.155	0.157	0.152	0.153	0.150	0.146	0.139	0.123	0.136	0.147	0.149	0.153	0.153
Sp	0.024	0.021	0.025	0.021	0.024	0.023	0.021	0.023	0.023	0.025	0.025	0.027	0.032	0.028	0.026	0.025	0.023	0.026
Gr	0.029	0.031	0.02:	0.030	0.032	0.033	0.031	0.028	0.029	0.028	0.02:	0.029	0.027	0.024	0.027	0.030	0.029	0.02:
(Ca+Mn)/(Mg+Ca+Mn+Fe)	0.053	0.052	0.054	0.052	0.055	0.056	0.053	0.051	0.052	0.053	0.055	0.056	0.05:	0.053	0.053	0.055	0.053	0.055
X	-63.99	-62.76	-61.44	-60.28	-59.04	-57.47	-56.56	-55.32	-54.09	-52.69	-51.61	-50.31	-49.13	-68.75	-66.23	-63.71	-61.19	-58.67
Y	366.49	365.72	364.43	363.34	362.24	360.87	360.05	358.95	357.85	356.64	355.66	354.46	353.47	376.55	374.24	371.86	369.63	367.32
x-axis m	1.00	1.15	1.33	1.49	1.66	1.87	1.99	2.15	2.32	2.51	2.65	2.83	2.98	0.00	0.34	0.69	1.03	1.37
location	*interior*	*interior*	*interior*	*interior*	*interior*	*interior*	*interior*	*interior*	*interior*	*interior*	*±near rim*	*nr rm - bt*	*im adj bt*	*rim adj pl*	*±near rim*	*interior*	*interior*	*interior*

TABLE B-1: Quantitative Microprobe Analysis for Garnet Compositions

PC-113C (continued)

	GT3f	GT3g	GT3h	GT3i	GT4a	GT4b	GT4c	GT4d	GT4e	GT4f	GT4g	GT4h	GT4i	GT4j	GT4k	GT4l	GT5a	GT5b
WEIGHT PERCENT OXIDES																		
SiO2	39.369	38.866	38.638	38.579	39.010	38.545	39.205	38.563	38.621	38.900	38.453	38.855	38.488	38.572	38.678	38.318	38.747	37.925
Al2O3	22.311	22.105	21.962	21.977	22.039	22.080	22.445	22.049	22.259	22.029	22.002	22.361	22.313	22.036	22.261	21.709	22.056	22.115
TiO2	0.072	0.000	0.017	0.000	0.000	0.013	0.000	0.000	0.000	0.000	0.000	0.049	0.007	0.030	0.028	0.000	0.035	0.000
Fe2O3																		
MgO	3.851	3.897	3.869	3.021	3.147	3.224	3.674	3.805	3.828	4.083	4.028	3.924	3.816	3.434	3.454	3.309	2.982	3.828
FeO	36.175	36.653	36.258	36.740	37.280	36.679	36.017	36.097	36.235	36.251	36.108	36.050	36.721	37.165	36.654	36.780	37.575	36.576
MnO	1.113	0.950	1.095	1.295	1.356	1.368	1.191	1.149	1.071	1.034	0.998	1.013	1.119	1.175	1.283	1.348	1.296	1.253
CaO	1.064	1.112	1.042	0.979	1.009	1.006	1.009	1.022	1.050	1.025	1.018	1.050	1.054	1.116	0.987	1.009	0.901	1.011
TOTAL	**103.955**	**103.583**	**102.881**	**102.591**	**103.841**	**102.915**	**103.541**	**102.685**	**103.064**	**103.322**	**102.607**	**103.302**	**103.518**	**103.528**	**103.345**	**102.473**	**103.592**	**102.708**
CATIONS RECALCULATED TO 12 OXYGENS																		
Si	3.021	3.004	3.006	3.018	3.019	3.006	3.020	3.004	2.997	3.009	2.998	3.002	2.981	2.995	3.000	3.007	3.010	2.967
Al	2.018	2.014	2.014	2.026	2.00:	2.02:	2.038	2.025	2.036	2.008	2.021	2.036	2.037	2.017	2.035	2.008	2.019	2.039
Ti	0.004	0.000	0.001	0.000	0.000	0.001	0.000	0.000	0.000	0.000	0.000	0.003	0.000	0.002	0.002	0.000	0.002	0.000
Fe3+																		
Mg	0.441	0.449	0.449	0.352	0.363	0.375	0.422	0.442	0.443	0.471	0.468	0.452	0.441	0.398	0.399	0.387	0.345	0.446
Fe2+	2.322	2.369	2.359	2.404	2.412	2.392	2.320	2.352	2.352	2.345	2.354	2.330	2.379	2.413	2.378	2.414	2.441	2.393
Mn	0.072	0.062	0.072	0.086	0.089	0.090	0.078	0.076	0.070	0.068	0.066	0.066	0.073	0.077	0.084	0.08:	0.085	0.083
Ca	0.088	0.092	0.087	0.082	0.084	0.084	0.083	0.085	0.087	0.085	0.085	0.087	0.088	0.093	0.082	0.085	0.075	0.085
TOTAL	**7.966**	**7.989**	**7.987**	**7.969**	**7.976**	**7.978**	**7.961**	**7.984**	**7.985**	**7.987**	**7.992**	**7.977**	**7.000**	**7.995**	**7.981**	**7.989**	**7.978**	**8.013**
Fe/Fe+Mg	*0.841*	*0.841*	*0.840*	*0.872*	*0.869*	*0.865*	*0.846*	*0.842*	*0.842*	*0.833*	*0.834*	*0.837*	*0.844*	*0.859*	*0.856*	*0.862*	*0.876*	*0.843*
Alm	0.795	0.797	0.795	0.822	0.818	0.813	0.799	0.796	0.797	0.790	0.792	0.794	0.798	0.810	0.808	0.811	0.828	0.796
Py	0.151	0.151	0.151	0.120	0.123	0.127	0.145	0.150	0.150	0.159	0.157	0.154	0.148	0.133	0.136	0.130	0.117	0.148
Sp	0.025	0.021	0.024	0.029	0.030	0.031	0.027	0.026	0.024	0.023	0.022	0.023	0.025	0.026	0.029	0.030	0.029	0.028
Gr	0.02:	0.031	0.029	0.028	0.028	0.029	0.029	0.029	0.02:	0.029	0.029	0.02:	0.029	0.031	0.028	0.029	0.026	0.028
(Ca+Mn)/(Mg+Ca+Mn+Fe)	0.055	0.052	0.054	0.057	0.059	0.059	0.056	0.055	0.053	0.051	0.051	0.052	0.054	0.057	0.057	0.059	0.054	0.056
X	-56.14	-53.62	-51.10	-48.58	-57.74	-59.06	-60.37	-61.41	-62.63	-63.76	-64.82	-66.31	-67.53	-68.95	-70.08	-71.21	-55.33	-56.40
Y	365.01	362.71	360.40	358.10	376.65	374.87	373.20	371.70	370.05	368.24	366.66	365.09	363.44	361.55	360.14	358.49	369.66	368.23
x-axis m	1.71	2.05	2.39	2.73	0.00	0.22	0.43	0.62	0.82	1.04	1.23	1.44	1.65	1.88	2.06	2.26	0.00	0.18
location	*interior*	*interior*	*±near rim*	*im adj bt*	*±adj bt*	*rm ± - bt*	*±near rim*	*±near rim*	*interior*	*interior*	*interior*	*interior*	*±near rim*	*±near rim*	*rm ± - bt*	*±adj bt*	*im adj bt*	*±near rim*

TABLE B-1: Quantitative Microprobe Analysis for Garnet Compositions

	PC-113C (continued)													*PC-113E*				
	GT5c	**GT5d**	**GT5e**	**GT5f**	**GT5g**	**GT5h**	**GT5i**	**GT5j**	**GT6a**	**GT6b**	**GT6c**	**GT6d**	**GT6e**	**GR1**	**GC2**	**GC3**	**GC4a**	**GC4b**
WEIGHT PERCENT OXIDES																		
SiO2	38.724	38.518	38.131	38.419	38.802	38.46:	38.552	37.929	38.542	38.701	38.652	38.682	37.834	37.541	38.700	38.204	39.026	39.112
Al2O3	21.880	22.121	21.984	21.808	22.081	22.290	22.266	21.993	22.165	22.106	21.917	22.145	21.895	21.828	22.289	21.934	22.296	22.169
TiO2	0.000	0.000	0.000	0.000	0.000	0.020	0.004	0.000	0.044	0.000	0.000	0.000	0.000	0.020	0.000	0.000	0.000	0.046
Fe2O3	0.000	0.000	0.000	0.000	0.000													
MgO	3.986	3.960	4.092	4.141	4.032	3.931	3.693	3.206	3.381	3.993	3.943	3.820	3.101	3.959	4.775	4.807	4.108	4.095
FeO	36.276	36.176	35.991	36.422	36.122	36.438	36.988	37.303	36.588	36.648	35.924	36.362	36.886	35.980	35.048	34.867	35.932	35.399
MnO	1.028	1.103	0.975	1.010	0.993	1.065	1.160	1.443	1.331	1.083	1.008	1.187	1.368	1.091	0.915	0.902	1.003	1.063
CaO	1.083	1.084	1.111	1.036	1.066	1.113	1.046	1.134	1.029	1.115	1.107	1.133	1.098	0.816	1.107	1.093	0.884	0.846
TOTAL	**102.977**	**102.962**	**102.284**	**102.836**	**103.096**	**103.327**	**103.709**	**103.008**	**103.080**	**103.646**	**102.551**	**103.329**	**102.182**	**101.235**	**102.834**	**101.807**	**103.249**	**102.730**
CATIONS RECALCULATED TO 12 OXYGENS																		
Si	3.009	2.994	2.984	2.994	3.007	2.982	2.984	2.972	2.999	2.992	3.012	2.998	2.983	2.974	2.992	2.988	3.013	3.028
Al	2.004	2.026	2.028	2.003	2.017	2.036	2.032	2.031	2.033	2.015	2.013	2.023	2.035	2.038	2.031	2.022	2.029	2.023
Ti	0.000	0.000	0.000	0.000	0.000	0.001	0.000	0.000	0.003	0.000	0.000	0.000	0.000	0.001	0.000	0.000	0.000	0.003
Fe3+	0.000	0.000	0.000	0.000	0.000													
Mg	0.462	0.459	0.477	0.481	0.466	0.454	0.426	0.374	0.392	0.460	0.458	0.441	0.365	0.468	0.550	0.560	0.473	0.473
Fe2+	2.357	2.351	2.355	2.374	2.341	2.362	2.395	2.444	2.381	2.370	2.341	2.357	2.432	2.383	2.266	2.280	2.320	2.292
Mn	0.068	0.073	0.065	0.067	0.065	0.06:	0.076	0.096	0.088	0.071	0.067	0.078	0.091	0.073	0.05:	0.05:	0.066	0.06:
Ca	0.090	0.090	0.093	0.087	0.089	0.092	0.087	0.095	0.086	0.092	0.092	0.094	0.093	0.069	0.092	0.092	0.073	0.070
TOTAL	**7.989**	**7.993**	**8.002**	**8.005**	**7.985**	**7.999**	**7.000**	**8.013**	**7.982**	**8.000**	**7.982**	**7.991**	**7.999**	**8.006**	**7.992**	**8.001**	**7.973**	**7.958**
Fe/Fe+Mg	*0.836*	*0.837*	*0.831*	*0.831*	*0.834*	*0.839*	*0.849*	*0.867*	*0.859*	*0.837*	*0.836*	*0.842*	*0.870*	*0.836*	*0.805*	*0.803*	*0.831*	*0.829*
Alm	0.792	0.791	0.788	0.789	0.791	0.793	0.803	0.812	0.808	0.792	0.791	0.793	0.816	0.796	0.763	0.762	0.791	0.789
Py	0.155	0.154	0.160	0.160	0.157	0.153	0.143	0.124	0.133	0.154	0.155	0.149	0.122	0.156	0.185	0.187	0.161	0.163
Sp	0.023	0.024	0.022	0.022	0.022	0.023	0.026	0.032	0.02:	0.024	0.023	0.026	0.031	0.025	0.020	0.020	0.022	0.024
Gr	0.030	0.030	0.031	0.029	0.02:	0.031	0.029	0.032	0.029	0.031	0.031	0.032	0.031	0.023	0.031	0.031	0.025	0.024
(Ca+Mn)/(Mg+Ca+Mn+Fe)	0.053	0.055	0.053	0.051	0.052	0.055	0.055	0.063	0.059	0.055	0.054	0.058	0.062	0.048	0.051	0.051	0.047	0.048
X	-57.47	-58.54	-59.61	-60.78	-61.73	-62.82	-63.90	-64.97	-51.69	-53.97	-56.25	-58.53	-60.81	24.42	48.07	37.43	45.87	45.87
Y	366.80	365.37	363.94	362.38	361.22	359.64	358.21	356.78	366.04	362.79	359.55	356.30	353.05	-318.34	-310.16	-327.34	-324.98	-324.98
x-axis m	0.36	0.54	0.71	0.91	1.06	1.25	1.43	1.61	0.00	0.40	0.79	1.19	1.59					
location	*interior*	*interior*	*interior*	*interior*	*interior*	*interior*	*rm ± - bt*	*±adj bt*	*±adj bt*	*interior*	*interior*	*near rim*	*m ±adj pl*	*im adj qz*	*interior*	*interior*	*dj bt incl*	*dj bt incl*

TABLE B-1: Quantitative Microprobe Analysis for Garnet Compositions

PC-113E (continued)

	GC5	GC6	GC7	GT1a	GT1b	GT1c	GT1d	GT1e	GT1f	GT1g	GT1h	GT1i	GT2a	GT2b	GT2c	GT2d	GT2e	GT2f
WEIGHT PERCENT OXIDES																		
SiO2	39.038	37.856	38.057	38.057	37.544	37.365	38.213	38.400	38.319	37.797	38.401	38.591	37.672	38.231	38.165	38.874	38.393	38.301
Al2O3	22.074	21.977	21.852	21.925	21.873	21.728	21.745	22.084	22.005	22.058	22.021	22.190	21.969	21.971	21.778	21.936	21.904	22.026
TiO2	0.000	0.036	0.069	0.000	0.013	0.020	0.022	0.028	0.031	0.020	0.018	0.042	0.000	0.000	0.017	0.000	0.042	0.001
Fe2O3	0.000	0.000	0.000	0.000	0.000	0.000	0.000	0.000	0.000	0.000	0.000	0.000	0.000	0.000	0.000	0.000	0.000	0.000
MgO	4.205	4.346	3.592	3.598	4.100	4.198	4.311	4.448	4.696	4.680	4.759	4.574	4.746	4.755	4.713	4.707	4.640	4.380
FeO	35.317	36.022	36.300	36.299	35.944	36.251	35.824	34.965	35.043	35.551	35.278	35.442	35.095	35.447	35.194	34.977	35.359	35.665
MnO	0.996	0.953	1.165	1.255	1.033	1.136	1.067	0.93:	0.977	0.991	0.968	0.985	0.923	0.916	0.920	0.933	0.93:	1.026
CaO	1.031	0.953	0.925	1.021	1.038	1.046	1.010	1.118	1.068	1.115	1.111	0.934	1.052	1.126	1.084	0.906	1.111	1.102
TOTAL	**102.661**	**102.143**	**101.960**	**102.155**	**101.545**	**101.744**	**102.192**	**101.983**	**102.139**	**102.212**	**102.556**	**102.758**	**101.457**	**102.446**	**101.871**	**102.333**	**102.389**	**102.501**
CATIONS RECALCULATED TO 12 OXYGENS																		
Si	3.025	2.968	2.994	2.990	2.965	2.953	2.992	2.997	2.989	2.957	2.985	2.992	2.964	2.979	2.988	3.018	2.991	2.986
Al	2.016	2.031	2.026	2.030	2.036	2.024	2.006	2.031	2.023	2.034	2.018	2.028	2.037	2.018	2.00:	2.007	2.011	2.023
Ti	0.000	0.002	0.004	0.000	0.001	0.001	0.001	0.002	0.002	0.001	0.001	0.002	0.000	0.000	0.001	0.000	0.002	0.000
Fe3+	0.000	0.000	0.000	0.000	0.000	0.000	0.000	0.000	0.000	0.000	0.000	0.000	0.000	0.000	0.000	0.000	0.000	0.000
Mg	0.486	0.508	0.421	0.421	0.483	0.495	0.503	0.518	0.546	0.546	0.552	0.529	0.557	0.552	0.550	0.545	0.539	0.509
Fe2+	2.289	2.362	2.388	2.385	2.374	2.396	2.346	2.282	2.286	2.326	2.293	2.298	2.309	2.310	2.305	2.271	2.303	2.325
Mn	0.065	0.063	0.078	0.084	0.069	0.076	0.071	0.062	0.065	0.066	0.064	0.065	0.062	0.060	0.061	0.061	0.062	0.068
Ca	0.086	0.080	0.078	0.086	0.088	0.089	0.085	0.094	0.089	0.094	0.093	0.078	0.089	0.094	0.091	0.075	0.093	0.092
TOTAL	**7.967**	**8.014**	**7.989**	**7.995**	**8.016**	**8.034**	**8.004**	**7.986**	**7.998**	**8.024**	**8.005**	**7.991**	**8.017**	**8.013**	**8.006**	**7.978**	**8.001**	**8.003**
Fe/Fe+Mg	*0.825*	*0.823*	*0.850*	*0.850*	*0.831*	*0.829*	*0.823*	*0.815*	*0.807*	*0.810*	*0.806*	*0.813*	*0.806*	*0.807*	*0.807*	*0.807*	*0.810*	*0.820*
Alm	0.782	0.784	0.805	0.801	0.788	0.784	0.781	0.772	0.766	0.767	0.764	0.774	0.766	0.766	0.766	0.769	0.769	0.777
Py	0.166	0.169	0.142	0.142	0.160	0.162	0.167	0.175	0.183	0.180	0.184	0.178	0.185	0.183	0.183	0.185	0.180	0.170
Sp	0.022	0.021	0.026	0.028	0.023	0.025	0.024	0.021	0.022	0.022	0.021	0.022	0.020	0.020	0.020	0.021	0.021	0.023
Gr	0.029	0.027	0.026	0.029	0.029	0.029	0.028	0.032	0.02:	0.031	0.031	0.026	0.029	0.031	0.030	0.026	0.031	0.031
(Ca+Mn)/(Mg+Ca+Mn+Fe)	0.052	0.048	0.053	0.057	0.052	0.054	0.052	0.053	0.052	0.053	0.052	0.048	0.04:	0.051	0.051	0.046	0.052	0.053
X	57.76	51.66	52.78	41.19	40.60	40.01	39.41	38.82	38.18	37.64	37.04	36.45	34.84	34.33	33.77	33.21	32.65	32.08
Y	-319.33	-336.54	-337.17	-285.18	-288.35	-291.69	-294.94	-298.36	-301.44	-304.70	-307.95	-311.15	-318.17	-321.37	-324.69	-328.00	-331.31	-334.62
x-axis mm				0.00	0.32	0.66	0.99	1.34	1.65	1.98	2.31	2.64	0.00	0.32	0.66	0.00	1.33	1.67
location	*interior*	*dj bt incl*	*rm-bt incl*	*m adj sil?*	*±near rim*	*±near rim*	*interior*	*interior*	*interior*	*interior*	*interior*	*"rim" - qz*	*"rim" - qz*	*interior*	*interior*	*interior*	*interior*	*interior*

TABLE B-1: Quantitative Microprobe Analysis for Garnet Compositions

PC-113E (continued)

	GT2g	GT2h	GT2i	GT3a	GT3b	GT3c	GT3d	GT3e	GT3f	GT3g	GT3h	GT3i	GT3j	GT3k	GT3l	GT3m	GT3n	GT3o
WEIGHT PERCENT OXIDES																		
SiO2	38.552	38.578	38.193	38.599	37.635	38.059	38.219	38.281	38.46:	38.086	37.664	38.459	38.681	38.640	38.708	38.553	38.326	38.968
Al2O3	21.980	22.044	21.751	22.081	21.562	21.740	21.792	21.880	22.044	21.886	21.910	21.775	22.211	21.979	22.321	22.253	22.018	22.069
TiO2	0.015	0.000	0.018	0.004	0.024	0.000	0.000	0.000	0.000	0.008	0.000	0.000	0.000	0.022	0.014	0.013	0.007	0.015
Fe2O3	0.000	0.000	0.000	0.000	0.000	0.000	0.000	0.000	0.000	0.000	0.000	0.000	0.000	0.000	0.000	0.000	0.000	0.000
MgO	4.130	3.82:	3.626	3.380	3.802	3.911	3.941	3.797	3.903	3.742	3.597	3.911	4.069	4.211	4.144	4.194	4.333	4.334
FeO	35.471	35.993	36.308	36.379	36.072	35.472	35.759	35.691	35.963	36.569	36.546	35.960	35.682	35.511	35.220	35.298	35.173	35.248
MnO	1.036	1.226	1.274	1.292	1.176	1.079	1.154	1.151	1.078	1.163	1.277	1.116	1.000	1.009	1.063	0.998	0.954	1.047
CaO	1.111	1.048	1.045	0.822	0.999	1.077	1.012	1.102	1.073	1.112	0.833	1.123	1.085	1.101	1.094	1.104	1.041	0.971
TOTAL	**102.295**	**102.719**	**102.215**	**102.557**	**101.270**	**101.338**	**101.877**	**101.902**	**102.531**	**102.566**	**101.827**	**102.344**	**102.728**	**102.473**	**102.564**	**102.413**	**101.852**	**102.652**
CATIONS RECALCULATED TO 12 OXYGENS																		
Si	3.007	3.004	2.999	3.014	2.984	3.002	3.001	3.004	3.000	2.983	2.974	3.007	3.004	3.007	3.004	2.999	2.998	3.020
Al	2.020	2.023	2.013	2.032	2.015	2.021	2.017	2.024	2.026	2.020	2.039	2.007	2.033	2.016	2.042	2.040	2.030	2.016
Ti	0.001	0.000	0.001	0.000	0.001	0.000	0.000	0.000	0.000	0.000	0.000	0.000	0.000	0.001	0.001	0.001	0.000	0.001
Fe3+	0.000	0.000	0.000	0.000	0.000	0.000	0.000	0.000	0.000	0.000	0.000	0.000	0.000	0.000	0.000	0.000	0.000	0.000
Mg	0.480	0.445	0.424	0.393	0.449	0.460	0.461	0.444	0.454	0.437	0.423	0.456	0.471	0.489	0.480	0.486	0.505	0.501
Fe2+	2.313	2.344	2.384	2.376	2.392	2.340	2.348	2.342	2.346	2.395	2.413	2.352	2.317	2.311	2.286	2.296	2.301	2.285
Mn	0.068	0.081	0.085	0.086	0.079	0.072	0.077	0.077	0.071	0.077	0.085	0.074	0.066	0.067	0.06:	0.066	0.063	0.069
Ca	0.093	0.087	0.088	0.069	0.085	0.091	0.085	0.093	0.08:	0.093	0.071	0.094	0.090	0.092	0.091	0.092	0.087	0.081
TOTAL	**7.982**	**7.984**	**7.994**	**7.970**	**8.007**	**7.987**	**7.990**	**7.984**	**7.987**	**8.006**	**8.006**	**7.989**	**7.980**	**7.983**	**7.974**	**7.980**	**7.986**	**7.971**
Fe/Fe+Mg	*0.828*	*0.841*	*0.849*	*0.858*	*0.842*	*0.836*	*0.836*	*0.841*	*0.838*	*0.846*	*0.851*	*0.838*	*0.831*	*0.826*	*0.827*	*0.825*	*0.820*	*0.820*
Alm	0.783	0.793	0.800	0.813	0.796	0.790	0.790	0.792	0.792	0.798	0.806	0.790	0.787	0.781	0.781	0.781	0.778	0.778
Py	0.162	0.150	0.142	0.135	0.150	0.155	0.155	0.150	0.153	0.146	0.141	0.153	0.160	0.165	0.164	0.165	0.171	0.171
Sp	0.023	0.027	0.028	0.029	0.026	0.024	0.026	0.026	0.024	0.026	0.029	0.025	0.022	0.023	0.024	0.022	0.021	0.023
Gr	0.031	0.02:	0.029	0.023	0.028	0.031	0.029	0.031	0.030	0.031	0.023	0.032	0.031	0.031	0.031	0.031	0.029	0.028
(Ca+Mn)/(Mg+Ca+Mn+Fe)	0.055	0.057	0.058	0.053	0.055	0.055	0.055	0.057	0.054	0.057	0.052	0.057	0.053	0.054	0.055	0.054	0.051	0.051
X	31.52	30.88	30.40	51.91	51.60	51.38	51.12	50.85	50.59	50.32	50.06	49.79	49.44	49.16	49.00	48.73	48.47	48.20
Y	-337.94	-341.34	-344.56	-277.69	-279.27	-280.63	-282.10	-283.36	-285.04	-286.62	-287.81	-289.46	-290.86	-292.62	-293.87	-295.34	-296.81	-298.38
x-axis m	2.00	2.35	2.68	0.00	0.16	0.30	0.45	0.58	0.75	0.91	1.03	1.20	1.34	1.52	1.64	1.79	1.94	2.10
location	*±near rim*	*rm - hole*	*m - hole*	*m adj bt*	*nr rm - bt*	*±near rim*	*±near rim*	*±near rim*	*±near rim*	*adj fract*	*adj fract*	*interior*	*interior*	*interior*	*interior*	*interior*	*interior*	*interior*

TABLE B-1: Quantitative Microprobe Analysis for Garnet Compositions

PC-113E (continued)

	GT3p	GT3q	GT3r	GT3s	GT3t	GT3u	GT3v	GT3w	GT3x	GT3y	GT3z	GT3aa	GT3ab	GT3ac	GT3ad	GT3ae	GT3af	GT3ag
WEIGHT PERCENT OXIDES																		
SiO2	38.58:	39.090	38.635	38.661	38.713	38.275	39.354	38.301	38.358	39.185	38.801	37.546	38.647	37.795	38.585	38.967	38.546	37.442
Al2O3	22.125	21.964	21.892	22.147	22.159	22.059	22.018	21.998	22.082	22.015	22.175	21.818	22.225	21.765	22.173	22.234	22.167	21.529
TiO2	0.000	0.000	0.000	0.025	0.011	0.010	0.013	0.018	0.000	0.000	0.004	0.000	0.027	0.045	0.000	0.008	0.014	0.000
Fe2O3	0.000	0.000	0.103	0.000	0.000	0.000	0.000	0.000	0.000	0.000	0.000	0.000	0.000	0.000	0.000	0.000	0.000	0.000
MgO	4.553	4.622	4.845	4.760	4.848	4.930	4.753	4.868	4.835	4.735	4.696	4.648	4.452	4.449	4.360	4.388	4.342	4.457
FeO	35.199	35.045	35.614	34.267	35.010	35.259	34.345	34.845	34.084	35.089	34.666	35.200	34.785	35.496	35.408	35.317	35.328	35.159
MnO	1.090	0.925	0.982	0.816	0.914	0.900	0.888	0.891	0.983	0.803	0.895	1.034	1.026	1.016	1.034	0.989	0.906	0.984
CaO	1.120	0.976	1.085	1.145	1.115	1.204	1.199	1.073	1.119	1.214	1.121	1.112	1.093	1.143	1.098	1.085	1.092	1.127
TOTAL	**102.677**	**102.622**	**103.156**	**101.821**	**102.770**	**102.637**	**102.56:**	**101.994**	**101.461**	**103.041**	**102.358**	**101.358**	**102.255**	**101.709**	**102.658**	**102.988**	**102.395**	**100.698**
CATIONS RECALCULATED TO 12 OXYGENS																		
Si	2.995	3.026	2.989	3.009	2.995	2.974	3.037	2.988	2.999	3.021	3.009	2.962	3.004	2.973	2.996	3.010	2.999	2.975
Al	2.023	2.004	1.996	2.032	2.021	2.01:	2.003	2.023	2.035	2.000	2.027	2.029	2.036	2.018	2.029	2.024	2.032	2.016
Ti	0.000	0.000	0.000	0.001	0.001	0.001	0.001	0.001	0.000	0.000	0.000	0.000	0.002	0.003	0.000	0.000	0.001	0.000
Fe3+	0.000	0.000	0.006	0.000	0.000	0.000	0.000	0.000	0.000	0.000	0.000	0.000	0.000	0.000	0.000	0.000	0.000	0.000
Mg	0.527	0.533	0.559	0.552	0.559	0.571	0.547	0.566	0.563	0.544	0.543	0.547	0.516	0.522	0.505	0.505	0.504	0.528
Fe2+	2.284	2.268	2.305	2.230	2.265	2.291	2.217	2.273	2.228	2.262	2.248	2.323	2.261	2.335	2.299	2.282	2.298	2.336
Mn	0.072	0.061	0.064	0.054	0.05:	0.059	0.058	0.059	0.065	0.052	0.059	0.069	0.068	0.068	0.068	0.065	0.05:	0.066
Ca	0.093	0.081	0.090	0.096	0.092	0.100	0.099	0.08:	0.094	0.100	0.093	0.094	0.091	0.096	0.091	0.08:	0.091	0.096
TOTAL	**7.994**	**7.973**	**8.009**	**7.974**	**7.994**	**8.016**	**7.961**	**7.000**	**7.984**	**7.979**	**7.978**	**8.023**	**7.977**	**8.015**	**7.989**	**7.977**	**7.984**	**8.017**
Fe/Fe+Mg	*0.813*	*0.810*	*0.805*	*0.802*	*0.802*	*0.800*	*0.802*	*0.801*	*0.798*	*0.806*	*0.805*	*0.809*	*0.814*	*0.817*	*0.820*	*0.819*	*0.820*	*0.816*
Alm	0.768	0.771	0.764	0.761	0.761	0.758	0.759	0.761	0.755	0.764	0.764	0.766	0.770	0.773	0.776	0.776	0.778	0.772
Py	0.177	0.181	0.185	0.188	0.188	0.189	0.187	0.189	0.191	0.184	0.184	0.180	0.176	0.173	0.170	0.172	0.171	0.174
Sp	0.024	0.021	0.021	0.018	0.020	0.01:	0.01:	0.01:	0.022	0.018	0.020	0.023	0.023	0.022	0.023	0.022	0.020	0.022
Gr	0.031	0.028	0.02:	0.033	0.031	0.033	0.034	0.030	0.032	0.034	0.032	0.031	0.031	0.032	0.031	0.031	0.031	0.032
(Ca+Mn)/(Mg+Ca+Mn+Fe)	0.055	0.048	0.051	0.051	0.051	0.053	0.054	0.04:	0.054	0.052	0.052	0.054	0.054	0.054	0.054	0.053	0.051	0.054
X	47.94	47.67	47.41	46.95	46.79	46.62	46.35	46.09	45.82	45.56	45.29	45.03	44.76	44.50	44.23	43.97	43.70	43.44
Y	-299.75	-301.22	-302.69	-304.16	-305.88	-307.10	-308.57	-310.04	-311.51	-312.99	-314.70	-315.93	-317.40	-318.98	-320.34	-321.81	-323.36	-324.75
x-axis m	2.24	2.39	2.54	2.70	2.87	2.99	3.14	3.29	3.44	3.59	3.76	3.89	4.04	4.20	4.34	4.49	4.64	4.78
location	*interior*	*interior*	*interior*	*interior*	*interior*	*interior*	*interior*	*interior*	*interior*	*interior*	*interior*	*interior*	*interior*	*interior*	*interior*	*interior*	*interior*	*interior*

TABLE B-1: Quantitative Microprobe Analysis for Garnet Compositions

PC-113E (continued)

	GT3ah	GT3ai	GT3aj	GT3ak	GT3al	GT3am	GT3an	GT3ao	GT3ap	GT3aq	GT3ar	GT3as	GT3at	GT3au	GT4a	GT4b	GT4c	GT4d
WEIGHT PERCENT OXIDES																		
SiO2	38.831	38.331	38.034	38.363	38.265	38.626	38.511	38.951	38.849	37.893	37.503	38.449	37.589	37.528	38.886	38.232	38.174	38.058
Al2O3	22.052	21.816	22.035	21.891	22.126	22.221	21.771	22.245	22.238	21.701	21.693	22.038	21.517	21.833	22.180	21.863	21.928	22.084
TiO2	0.045	0.023	0.000	0.000	0.000	0.000	0.000	0.044	0.024	0.027	0.032	0.022	0.013	0.000	0.000	0.000	0.007	0.076
Fe2O3	0.000	0.000	0.000	0.000	0.000	0.000	0.000	0.000	0.000	0.000	0.000	0.000	0.000	0.000	0.000	0.000	0.000	0.000
MgO	4.377	4.610	4.597	4.664	4.687	4.713	4.579	4.487	4.461	4.255	4.084	3.926	3.714	3.211	2.953	3.906	3.996	4.141
FeO	34.808	34.706	35.011	34.799	34.777	34.412	33.824	34.510	34.624	35.048	35.883	35.513	35.995	36.518	35.837	35.123	36.258	35.836
MnO	0.873	0.849	0.842	0.917	0.941	0.901	0.856	0.947	0.945	1.021	1.128	1.121	1.168	1.271	1.362	1.103	1.028	1.069
CaO	1.157	1.110	1.116	1.199	1.048	1.118	1.183	1.038	1.062	0.999	1.025	1.057	1.035	0.968	0.999	1.036	1.041	1.161
TOTAL	**102.143**	**101.445**	**101.635**	**101.833**	**101.844**	**101.991**	**100.724**	**102.222**	**102.203**	**100.944**	**101.348**	**102.126**	**101.031**	**101.329**	**102.217**	**101.263**	**102.432**	**102.425**
CATIONS RECALCULATED TO 12 OXYGENS																		
Si	3.019	3.005	2.982	2.998	2.989	3.004	3.028	3.020	3.016	2.996	2.969	3.005	2.988	2.981	3.038	3.011	2.986	2.974
Al	2.021	2.016	2.036	2.016	2.037	2.037	2.018	2.033	2.034	2.022	2.024	2.030	2.016	2.044	2.043	2.029	2.022	2.034
Ti	0.003	0.001	0.000	0.000	0.000	0.000	0.000	0.003	0.001	0.002	0.002	0.001	0.001	0.000	0.000	0.000	0.000	0.004
Fe3+	0.000	0.000	0.000	0.000	0.000	0.000	0.000	0.000	0.000	0.000	0.000	0.000	0.000	0.000	0.000	0.000	0.000	0.000
Mg	0.507	0.539	0.537	0.543	0.546	0.546	0.537	0.519	0.516	0.502	0.482	0.457	0.440	0.380	0.344	0.459	0.466	0.482
Fe2+	2.263	2.275	2.295	2.274	2.272	2.238	2.224	2.238	2.248	2.317	2.376	2.321	2.393	2.425	2.342	2.314	2.372	2.342
Mn	0.058	0.056	0.056	0.061	0.062	0.059	0.057	0.062	0.062	0.068	0.076	0.074	0.079	0.086	0.090	0.074	0.068	0.071
Ca	0.096	0.093	0.094	0.100	0.088	0.093	0.09:	0.086	0.088	0.085	0.087	0.089	0.088	0.082	0.084	0.087	0.087	0.097
TOTAL	**7.968**	**7.986**	**8.000**	**7.994**	**7.993**	**7.978**	**7.963**	**7.961**	**7.966**	**7.991**	**8.017**	**7.978**	**8.004**	**7.998**	**7.93:**	**7.974**	**8.002**	**8.005**
Fe/Fe+Mg	*0.817*	*0.809*	*0.810*	*0.807*	*0.806*	*0.804*	*0.806*	*0.812*	*0.813*	*0.822*	*0.831*	*0.835*	*0.845*	*0.864*	*0.872*	*0.835*	*0.836*	*0.829*
Alm	0.774	0.768	0.770	0.764	0.766	0.762	0.762	0.770	0.771	0.780	0.787	0.789	0.798	0.816	0.819	0.789	0.792	0.783
Py	0.173	0.182	0.180	0.182	0.184	0.186	0.184	0.179	0.177	0.169	0.160	0.156	0.147	0.128	0.120	0.156	0.156	0.161
Sp	0.01:	0.019	0.019	0.020	0.021	0.020	0.01:	0.021	0.021	0.023	0.025	0.025	0.026	0.029	0.032	0.025	0.023	0.024
Gr	0.033	0.032	0.031	0.034	0.02:	0.032	0.034	0.02:	0.030	0.029	0.029	0.030	0.029	0.028	0.029	0.02:	0.029	0.033
(Ca+Mn)/(Mg+Ca+Mn+Fe)	0.053	0.051	0.050	0.054	0.051	0.052	0.054	0.051	0.052	0.052	0.054	0.055	0.056	0.057	0.061	0.055	0.052	0.056
X	43.17	42.91	42.64	42.60	41.92	41.85	41.58	41.32	41.05	40.79	40.53	40.17	40.00	39.73	57.32	56.77	56.23	55.75
Y	-326.12	-327.69	-329.51	-330.63	-332.10	-333.34	-335.05	-336.52	-337.99	-339.46	-341.08	-342.40	-343.87	-345.34	-282.99	-286.15	-289.27	-292.40
x-axis m	4.92	5.08	5.27	5.38	5.54	5.67	5.84	5.99	6.14	6.29	6.45	6.59	6.74	6.88	0.00	0.32	0.64	0.95
location	*interior*	*interior*	*interior*	*interior*	*interior*	*interior*	*interior*	*interior*	*±near rim*	*±near rim*	*±near rim*	*±near rim*	*r rm-hole*	*adj hole*	*rim adj bt*	*±near rim*	*±near rim*	*±near rim*

TABLE B-1: Quantitative Microprobe Analysis for Garnet Compositions

PC-113E (continued)

	GT4e	GT4f	GT4g	GT4h	GT4i	GT4j	GT4k	GT4l	GT4m	GT4n	GT4o	GT4p	GT4q	GT4r	GT4s	GT4t	GT5a	GT5b
WEIGHT PERCENT OXIDES																		
SiO2	38.511	38.823	38.913	38.464	38.762	38.925	37.973	38.288	36.429	38.813	39.014	38.215	38.725	39.038	37.762	38.041	37.902	38.199
Al2O3	22.323	22.215	22.300	22.130	22.350	22.532	21.874	21.819	21.477	22.296	22.377	21.606	21.864	22.051	21.845	21.644	21.899	21.692
TiO2	0.006	0.038	0.000	0.000	0.034	0.001	0.008	0.000	0.003	0.014	0.000	0.000	0.021	0.003	0.018	0.000	0.021	0.015
Fe2O3	0.000	0.000	0.000	0.000	0.000	0.000	0.000	0.000	0.000	0.000	0.000	0.000	0.000	0.000	0.000	0.000	0.000	0.000
MgO	4.272	4.438	4.588	4.707	4.732	4.772	4.628	4.487	4.378	4.315	4.145	4.065	4.439	4.461	4.203	3.073	3.812	4.108
FeO	35.764	35.753	34.492	34.372	34.506	34.420	35.336	35.432	36.438	35.122	35.133	35.468	34.992	34.884	35.451	36.427	36.128	35.962
MnO	1.015	0.945	0.907	0.942	0.958	0.929	0.962	0.903	1.037	0.987	1.004	1.100	0.907	0.872	1.107	1.291	1.181	1.067
CaO	1.087	1.106	1.129	1.076	1.072	1.091	1.083	1.104	1.090	1.056	1.070	1.096	1.096	1.099	1.099	0.987	1.028	1.065
TOTAL	**102.978**	**103.318**	**102.329**	**101.691**	**102.414**	**102.670**	**101.864**	**102.033**	**100.852**	**102.603**	**102.743**	**101.550**	**102.044**	**102.408**	**101.485**	**101.463**	**101.971**	**102.108**
CATIONS RECALCULATED TO 12 OXYGENS																		
Si	2.985	2.996	3.014	3.002	3.002	3.003	2.977	2.995	2.917	3.008	3.018	3.008	3.018	3.026	2.977	3.012	2.982	2.996
Al	2.03:	2.021	2.036	2.036	2.03:	2.049	2.021	2.011	2.027	2.037	2.03:	2.004	2.008	2.015	2.02:	2.020	2.030	2.005
Ti	0.000	0.002	0.000	0.000	0.002	0.000	0.000	0.000	0.000	0.001	0.000	0.000	0.001	0.000	0.001	0.000	0.001	0.001
Fe3+	0.000	0.000	0.000	0.000	0.000	0.000	0.000	0.000	0.000	0.000	0.000	0.000	0.000	0.000	0.000	0.000	0.000	0.000
Mg	0.494	0.511	0.530	0.548	0.546	0.549	0.541	0.523	0.523	0.499	0.478	0.477	0.516	0.516	0.494	0.363	0.447	0.480
Fe2+	2.319	2.308	2.234	2.243	2.235	2.221	2.317	2.318	2.440	2.276	2.273	2.335	2.281	2.261	2.338	2.412	2.377	2.359
Mn	0.067	0.062	0.059	0.062	0.063	0.061	0.064	0.05:	0.070	0.065	0.066	0.073	0.05:	0.057	0.074	0.087	0.079	0.071
Ca	0.090	0.092	0.094	0.090	0.089	0.090	0.091	0.093	0.094	0.088	0.089	0.092	0.092	0.091	0.093	0.084	0.087	0.08:
TOTAL	**7.994**	**7.991**	**7.968**	**7.980**	**7.976**	**7.972**	**8.012**	**7.999**	**8.06:**	**7.973**	**7.962**	**7.990**	**7.976**	**7.966**	**8.007**	**7.978**	**8.002**	**8.001**
Fe/Fe+Mg	*0.824*	*0.819*	*0.808*	*0.804*	*0.804*	*0.802*	*0.811*	*0.816*	*0.824*	*0.820*	*0.826*	*0.82:*	*0.816*	*0.814*	*0.826*	*0.869*	*0.842*	*0.831*
Alm	0.781	0.777	0.766	0.762	0.762	0.760	0.769	0.774	0.780	0.778	0.782	0.784	0.774	0.773	0.780	0.819	0.795	0.786
Py	0.166	0.172	0.182	0.186	0.186	0.188	0.180	0.175	0.167	0.170	0.165	0.160	0.175	0.176	0.165	0.123	0.150	0.160
Sp	0.022	0.021	0.020	0.021	0.021	0.021	0.021	0.020	0.023	0.022	0.023	0.025	0.020	0.01:	0.025	0.029	0.026	0.024
Gr	0.030	0.031	0.032	0.031	0.030	0.031	0.030	0.031	0.02:	0.030	0.031	0.031	0.031	0.031	0.031	0.028	0.029	0.02:
(Ca+Mn)/(Mg+Ca+Mn+Fe)	0.053	0.052	0.053	0.052	0.052	0.052	0.051	0.051	0.052	0.052	0.053	0.056	0.051	0.051	0.056	0.058	0.055	0.054
X	55.13	54.58	54.03	53.49	52.94	52.39	51.84	51.29	50.75	50.02	49.65	48.92	48.55	48.01	47.36	46.91	29.84	33.14
Y	-295.52	-298.65	-301.77	-304.90	-308.03	-311.22	-314.28	-317.77	-320.53	-323.82	-326.94	-330.30	-333.03	-336.16	-339.28	-342.41	-293.52	-293.80
x-axis m	1.27	1.59	1.91	2.22	2.54	2.87	3.18	3.53	3.81	4.15	4.46	4.81	5.08	5.40	5.72	6.03	0.00	0.33
location	*interior*	*interior*	*interior*	*interior*	*interior*	*interior*	*interior*	*interior*	*interior*	*interior*	*interior*	*interior*	*interior*	*interior*	*±near rim*	*im adj bt*	*m adj sil?*	*±near rim*

TABLE B-1: Quantitative Microprobe Analysis for Garnet Compositions

PC-113E (continued)

	GT5c	GT5d	GT5e	GT5f	GT5g	GT5h	GT5i	GT5j	GT5k	GT5l	GT6a	GT6b	GT6c	GT6d	GT6e	GT6f	GT6g	GT6h
WEIGHT PERCENT OXIDES																		
SiO2	38.557	38.252	38.297	38.813	38.606	38.705	38.158	38.650	38.357	38.323	38.123	38.330	38.319	38.509	38.711	38.738	38.391	38.679
Al2O3	22.062	22.003	22.020	22.159	22.004	22.236	21.842	21.823	21.917	21.946	21.746	21.968	21.741	21.929	22.105	21.797	21.775	21.988
TiO2	0.000	0.000	0.034	0.013	0.006	0.000	0.000	0.003	0.022	0.000	0.067	0.000	0.030	0.021	0.000	0.000	0.013	0.000
Fe2O3	0.000	0.000	0.000	0.000	0.000	0.000	0.000	0.000	0.000	0.000	0.000	0.000	0.000	0.000	0.000	0.000	0.000	0.000
MgO	4.254	4.247	4.121	4.089	4.236	4.122	4.219	4.187	3.984	2.958	3.615	4.108	4.295	4.425	4.431	4.556	4.624	4.670
FeO	35.438	35.507	35.041	35.172	35.255	35.452	35.631	35.553	35.224	37.327	36.101	35.256	35.157	35.037	34.783	34.282	34.995	35.294
MnO	1.114	1.051	0.961	1.010	1.028	1.024	1.125	1.042	1.121	1.393	1.214	1.083	1.131	0.904	1.011	0.891	0.923	0.943
CaO	1.085	1.097	1.084	1.069	1.153	1.095	1.047	1.075	1.037	0.957	1.004	1.022	1.064	1.025	1.088	1.076	1.119	1.078
TOTAL	**102.510**	**102.157**	**101.558**	**102.325**	**102.288**	**102.634**	**102.022**	**102.333**	**101.662**	**102.904**	**101.870**	**101.767**	**101.737**	**101.850**	**102.129**	**101.340**	**101.840**	**102.652**
CATIONS RECALCULATED TO 12 OXYGENS																		
Si	3.001	2.991	3.004	3.018	3.008	3.005	2.991	3.014	3.009	3.000	3.000	3.004	3.005	3.009	3.012	3.031	3.002	3.001
Al	2.023	2.027	2.036	2.031	2.020	2.035	2.018	2.006	2.027	2.025	2.017	2.029	2.009	2.019	2.027	2.00:	2.007	2.011
Ti	0.000	0.000	0.002	0.001	0.000	0.000	0.000	0.000	0.001	0.000	0.004	0.000	0.002	0.001	0.000	0.000	0.001	0.000
Fe3+	0.000	0.000	0.000	0.000	0.000	0.000	0.000	0.000	0.000	0.000	0.000	0.000	0.000	0.000	0.000	0.000	0.000	0.000
Mg	0.494	0.495	0.482	0.474	0.492	0.477	0.493	0.487	0.466	0.345	0.424	0.480	0.502	0.515	0.514	0.531	0.539	0.540
Fe2+	2.306	2.321	2.298	2.287	2.297	2.302	2.336	2.318	2.311	2.444	2.376	2.311	2.306	2.289	2.263	2.243	2.289	2.290
Mn	0.073	0.06:	0.064	0.067	0.068	0.067	0.075	0.069	0.075	0.092	0.081	0.072	0.075	0.05:	0.067	0.059	0.061	0.062
Ca	0.091	0.092	0.091	0.089	0.096	0.091	0.088	0.08:	0.087	0.080	0.085	0.086	0.089	0.086	0.091	0.090	0.094	0.08:
TOTAL	**7.988**	**7.996**	**7.976**	**7.966**	**7.982**	**7.977**	**8.000**	**7.983**	**7.976**	**7.987**	**7.987**	**7.981**	**7.989**	**7.980**	**7.974**	**7.964**	**7.993**	**7.994**
Fe/Fe+Mg	*0.824*	*0.824*	*0.827*	*0.828*	*0.824*	*0.828*	*0.826*	*0.826*	*0.832*	*0.876*	*0.849*	*0.828*	*0.821*	*0.816*	*0.815*	*0.808*	*0.809*	*0.809*
Alm	0.778	0.780	0.783	0.784	0.778	0.784	0.781	0.782	0.786	0.825	0.801	0.784	0.776	0.776	0.771	0.767	0.767	0.768
Py	0.167	0.166	0.164	0.163	0.167	0.162	0.165	0.164	0.159	0.117	0.143	0.163	0.169	0.175	0.175	0.182	0.181	0.181
Sp	0.025	0.023	0.022	0.023	0.023	0.023	0.025	0.023	0.025	0.031	0.027	0.024	0.025	0.020	0.023	0.020	0.021	0.021
Gr	0.031	0.031	0.031	0.031	0.033	0.031	0.029	0.030	0.02:	0.027	0.029	0.029	0.030	0.029	0.031	0.031	0.031	0.030
(Ca+Mn)/(Mg+Ca+Mn+Fe)	0.055	0.054	0.053	0.053	0.056	0.054	0.054	0.054	0.055	0.058	0.056	0.054	0.055	0.049	0.054	0.051	0.052	0.051
X	36.43	39.73	43.03	46.33	49.62	52.92	56.22	59.79	62.49	66.11	27.68	29.19	30.94	32.20	33.71	35.21	36.72	38.22
Y	-294.07	-294.35	-294.62	-294.90	-295.42	-295.53	-295.81	-295.97	-296.14	-296.55	-301.77	-301.95	-302.20	-302.75	-302.86	-303.12	-303.34	-303.74
x-axis m	0.66	0.99	1.32	1.65	1.99	2.32	2.65	3.01	3.28	3.64	0.00	0.15	0.33	0.47	0.62	0.77	0.92	1.08
location	*interior*	*interior*	*interior*	*interior*	*interior*	*interior*	*interior*	*interior*	*±near rim*	*im adj bt*	*im adj qz*	*nr rm - qz*	*±near rim*	*interior*	*interior*	*interior*	*interior*	*interior*

TABLE B-1: Quantitative Microprobe Analysis for Garnet Compositions

PC-113E (continued)

	GT6i	GT6j	GT6k	GT6l	GT6m	GT6n	GT6o	GT6p	GT6q	GT6r	GT6s	GT6t	GT6u	GT6v	GT6w	GT6x	GT6y	GT6z
WEIGHT PERCENT OXIDES																		
SiO2	38.987	39.497	38.693	39.161	38.93:	39.127	39.251	38.976	38.870	38.680	39.129	38.554	39.092	38.810	38.267	38.670	38.58:	38.499
Al2O3	21.967	22.136	21.981	22.267	22.125	22.081	22.064	22.355	22.127	22.267	22.096	21.815	22.008	22.328	22.099	22.081	22.037	22.083
TiO2	0.030	0.024	0.044	0.063	0.000	0.021	0.000	0.000	0.003	0.000	0.000	0.024	0.037	0.000	0.059	0.008	0.024	0.015
Fe2O3	0.000	0.000	0.000	0.000	0.000	0.000	0.000	0.000	0.000	0.000	0.000	0.000	0.000	0.000	0.000	0.000	0.000	0.000
MgO	4.566	4.571	4.670	4.644	4.710	4.611	4.660	4.632	4.724	4.651	4.556	4.702	4.495	4.562	4.431	4.327	4.201	4.066
FeO	34.337	34.262	34.453	34.289	34.905	34.009	34.400	33.423	34.572	34.492	34.708	34.971	34.201	34.785	35.194	35.710	35.557	35.905
MnO	0.853	0.854	0.873	0.941	0.966	0.893	0.814	0.832	0.974	0.902	0.961	0.955	0.875	0.865	0.970	0.969	1.021	1.075
CaO	1.066	1.104	1.138	1.121	1.169	1.080	1.116	1.121	1.142	1.156	1.046	1.189	1.111	1.086	1.057	1.096	1.110	1.078
TOTAL	**101.806**	**102.448**	**101.852**	**102.486**	**102.815**	**101.822**	**102.305**	**101.339**	**102.412**	**102.148**	**102.496**	**102.210**	**101.819**	**102.436**	**102.077**	**102.861**	**102.540**	**102.721**
CATIONS RECALCULATED TO 12 OXYGENS																		
Si	3.033	3.047	3.014	3.024	3.009	3.038	3.037	3.033	3.012	3.004	3.028	3.003	3.039	3.007	2.988	2.000	3.003	2.996
Al	2.014	2.013	2.018	2.027	2.015	2.021	2.012	2.04:	2.021	2.038	2.015	2.003	2.016	2.039	2.034	2.019	2.021	2.025
Ti	0.002	0.001	0.003	0.004	0.000	0.001	0.000	0.000	0.000	0.000	0.000	0.001	0.002	0.000	0.003	0.000	0.001	0.001
Fe3+	0.000	0.000	0.000	0.000	0.000	0.000	0.000	0.000	0.000	0.000	0.000	0.000	0.000	0.000	0.000	0.000	0.000	0.000
Mg	0.530	0.526	0.542	0.535	0.543	0.534	0.537	0.537	0.546	0.539	0.526	0.546	0.521	0.527	0.516	0.500	0.487	0.472
Fe2+	2.234	2.211	2.244	2.215	2.256	2.208	2.226	2.175	2.240	2.240	2.246	2.278	2.223	2.254	2.298	2.317	2.314	2.337
Mn	0.056	0.056	0.058	0.062	0.063	0.059	0.053	0.055	0.064	0.059	0.063	0.063	0.058	0.057	0.064	0.064	0.067	0.071
Ca	0.089	0.091	0.095	0.093	0.097	0.08:	0.093	0.093	0.095	0.096	0.087	0.099	0.093	0.090	0.088	0.091	0.093	0.08:
TOTAL	**7.958**	**7.945**	**7.974**	**7.959**	**7.983**	**7.950**	**7.957**	**7.943**	**7.978**	**7.977**	**7.964**	**7.994**	**7.951**	**7.974**	**7.992**	**7.991**	**7.986**	**7.991**
Fe/Fe+Mg	*0.808*	*0.808*	*0.805*	*0.806*	*0.806*	*0.805*	*0.805*	*0.802*	*0.804*	*0.806*	*0.810*	*0.807*	*0.810*	*0.811*	*0.817*	*0.822*	*0.826*	*0.832*
Alm	0.768	0.767	0.764	0.763	0.762	0.764	0.765	0.760	0.761	0.763	0.769	0.763	0.768	0.770	0.775	0.780	0.781	0.787
Py	0.182	0.182	0.185	0.184	0.183	0.185	0.185	0.188	0.185	0.184	0.180	0.183	0.180	0.180	0.174	0.168	0.165	0.159
Sp	0.019	0.019	0.01:	0.021	0.021	0.020	0.018	0.019	0.022	0.020	0.022	0.021	0.01:	0.019	0.022	0.021	0.023	0.024
Gr	0.031	0.032	0.032	0.032	0.033	0.031	0.032	0.033	0.032	0.033	0.02:	0.033	0.032	0.031	0.02:	0.031	0.031	0.030
(Ca+Mn)/(Mg+Ca+Mn+Fe)	0.04:	0.051	0.052	0.053	0.054	0.051	0.050	0.052	0.054	0.053	0.051	0.054	0.052	0.050	0.051	0.052	0.054	0.054
X	39.89	41.24	42.74	44.25	45.76	47.26	48.77	50.27	51.78	53.29	54.79	56.30	57.81	59.31	60.82	62.51	63.83	65.34
Y	-303.76	-304.21	-304.48	-304.75	-304.92	-305.29	-305.56	-305.68	-305.92	-306.37	-306.64	-306.91	-307.19	-307.46	-307.73	-307.88	-308.27	-308.35
x-axis m	1.24	1.39	1.54	1.69	1.84	1.00	2.15	2.30	2.46	2.61	2.77	2.92	3.07	3.23	3.38	3.55	3.69	3.84
location	*interior*	*interior*	*interior*	*interior*	*interior*	*interior*	*interior*	*interior*	*interior*	*interior*	*interior*	*interior*	*interior*	*interior*	*interior*	*interior*	*±near rim*	*±near rim*

TABLE B-1: Quantitative Microprobe Analysis for Garnet Compositions

PC-113E (continued)

	GT6aa	GT6ab	GT7a	GT7b	GT7c	GT7d	GT7e	GT7f	GT7g	GT7h	GT7i	GT7j	GT7k	GT7l	GT8a	GT8b	GT8c	GT8d
WEIGHT PERCENT OXIDES																		
SiO2	37.965	38.732	36.314	38.604	38.244	38.714	38.370	39.275	39.025	38.267	38.652	38.208	38.215	37.274	38.307	38.443	38.374	38.181
Al2O3	21.685	22.243	20.820	21.520	21.806	22.251	22.017	22.269	22.136	21.792	21.871	21.881	21.828	21.471	21.717	21.387	21.761	21.573
TiO2	0.052	0.007	0.018	0.045	0.000	0.025	0.018	0.025	0.015	0.010	0.046	0.006	0.031	0.057	0.014	0.000	0.055	0.035
Fe2O3	0.000	0.000	0.157	0.052	0.000	0.000	0.000	0.000	0.000	0.057	0.000	0.000	0.000	0.000	0.160	0.679	0.255	0.409
MgO	3.827	3.151	2.941	4.138	4.501	4.550	4.659	4.628	4.652	4.634	4.274	4.005	3.281	2.979	3.759	3.822	3.845	3.845
FeO	36.565	39.799	37.139	35.346	35.287	34.757	34.583	33.707	34.643	35.955	34.913	35.450	35.984	37.685	37.367	36.864	37.647	37.437
MnO	1.055	1.342	1.324	1.001	1.028	0.965	0.900	0.935	0.942	1.002	0.93:	0.927	1.136	1.451	1.050	1.171	1.036	1.020
CaO	1.033	1.001	1.056	1.055	1.129	1.159	1.117	1.132	1.055	1.037	0.987	0.955	0.917	0.919	1.055	1.109	1.096	1.126
TOTAL	**102.182**	**106.275**	**99.769**	**101.761**	**101.995**	**102.421**	**101.664**	**101.971**	**102.468**	**102.754**	**101.683**	**101.432**	**101.392**	**101.836**	**103.429**	**103.475**	**104.069**	**103.626**
CATIONS RECALCULATED TO 12 OXYGENS																		
Si	2.985	2.961	2.958	3.026	2.993	3.003	2.999	3.03:	3.021	2.980	3.022	3.006	3.017	2.967	2.983	2.992	2.974	2.973
Al	2.009	2.004	1.999	1.988	2.011	2.034	2.028	2.031	2.019	2.000	2.016	2.029	2.031	2.014	1.993	1.962	1.987	1.980
Ti	0.003	0.000	0.001	0.003	0.000	0.001	0.001	0.001	0.001	0.001	0.003	0.000	0.002	0.003	0.001	0.000	0.003	0.002
Fe3+	0.000	0.000	0.00:	0.003	0.000	0.000	0.000	0.000	0.000	0.003	0.000	0.000	0.000	0.000	0.009	0.03:	0.015	0.024
Mg	0.449	0.359	0.357	0.484	0.525	0.526	0.543	0.534	0.537	0.538	0.498	0.46:	0.386	0.353	0.436	0.443	0.444	0.446
Fe2+	2.404	2.544	2.530	2.317	2.309	2.255	2.261	2.182	2.242	2.342	2.283	2.332	2.376	2.509	2.434	2.400	2.440	2.438
Mn	0.070	0.087	0.091	0.067	0.068	0.063	0.05:	0.061	0.062	0.066	0.062	0.062	0.076	0.098	0.069	0.077	0.068	0.067
Ca	0.087	0.082	0.092	0.089	0.095	0.096	0.094	0.094	0.088	0.087	0.083	0.081	0.078	0.078	0.088	0.093	0.091	0.094
TOTAL	**8.007**	**8.037**	**8.037**	**7.976**	**8.001**	**7.979**	**7.985**	**7.943**	**7.969**	**8.017**	**7.967**	**7.979**	**7.966**	**8.023**	**8.014**	**8.007**	**8.022**	**8.023**
Fe/Fe+Mg	*0.843*	*0.876*	*0.876*	*0.827*	*0.815*	*0.811*	*0.806*	*0.803*	*0.807*	*0.813*	*0.821*	*0.832*	*0.860*	*0.876*	*0.848*	*0.844*	*0.846*	*0.845*
Alm	0.799	0.828	0.824	0.784	0.770	0.767	0.765	0.760	0.766	0.772	0.780	0.792	0.815	0.826	0.804	0.796	0.802	0.801
Py	0.149	0.117	0.116	0.164	0.175	0.179	0.184	0.186	0.183	0.177	0.170	0.160	0.132	0.116	0.144	0.147	0.146	0.147
Sp	0.023	0.028	0.02:	0.023	0.023	0.022	0.020	0.021	0.021	0.022	0.021	0.021	0.026	0.032	0.023	0.026	0.022	0.022
Gr	0.029	0.027	0.030	0.030	0.032	0.033	0.032	0.033	0.02:	0.029	0.028	0.027	0.027	0.026	0.029	0.031	0.02:	0.031
(Ca+Mn)/(Mg+Ca+Mn+Fe)	0.052	0.055	0.05:	0.053	0.054	0.054	0.052	0.054	0.051	0.050	0.04:	0.048	0.053	0.058	0.052	0.056	0.052	0.053
X	66.84	68.35	25.39	28.44	31.48	34.59	37.58	40.63	43.67	46.72	49.77	52.82	56.26	58.91	78.11	77.18	76.24	75.31
Y	-308.81	-309.08	-330.21	-330.63	-331.04	-331.46	-331.88	-332.29	-332.71	-333.13	-333.54	-333.54	-334.37	-334.79	-361.88	-361.88	-361.88	-361.88
x-axis m	3.99	4.15	0.00	0.31	0.61	0.93	1.23	1.54	1.85	2.15	2.46	2.77	3.12	3.39	0.00	0.09	0.19	0.28
location	*nr rm - bt*	*im adj bt*	*im adj bt*	*±near rim*	*interior*	*interior*	*interior*	*interior*	*interior*	*interior*	*interior*	*±near rim*	*nr rm - bt*	*im adj bt*	*m adj sil?*	*±near rim*	*interior*	*interior*

TABLE B-1: Quantitative Microprobe Analysis for Garnet Compositions

PC-113E (continued)

	GT8e	GT8f	GT8g	GT8h	GT8i	GT8j	GT8k	GT8l	GT8m	GT8n	GT8o	GT8p	GT8q	GT8r	GT8s	GT8t	GT8u	GT8v
WEIGHT PERCENT OXIDES																		
SiO2	38.228	37.885	38.502	37.852	37.973	38.122	38.534	38.235	38.575	38.117	38.694	38.327	39.469	38.117	38.596	38.271	38.174	37.711
Al2O3	21.690	21.611	21.609	21.403	21.820	21.872	21.538	21.905	21.736	21.774	21.879	21.792	21.938	21.304	21.717	21.925	21.773	22.276
TiO2	0.000	0.032	0.075	0.081	0.000	0.000	0.035	0.066	0.026	0.000	0.061	0.014	0.000	0.012	0.000	0.026	0.029	0.000
Fe2O3	0.348	0.180	0.488	0.302	0.003	0.000	0.58:	0.000	0.409	0.141	0.261	0.165	0.446	0.763	0.417	0.188	0.044	0.000
MgO	3.831	3.782	3.879	3.844	3.906	3.903	4.077	3.970	3.992	3.871	3.937	3.858	3.914	3.948	4.036	4.012	3.779	3.797
FeO	37.551	37.310	37.395	36.880	37.340	37.010	36.922	36.806	37.808	37.653	37.450	37.431	37.414	36.958	37.030	37.850	37.336	37.258
MnO	1.084	1.145	1.093	0.952	1.094	1.166	1.145	1.030	1.104	0.980	1.192	1.125	1.113	1.149	1.216	1.073	1.094	1.018
CaO	1.133	1.114	1.114	1.224	1.127	1.097	1.031	1.052	0.705	1.026	1.113	1.046	0.969	1.111	1.039	1.111	1.110	1.013
TOTAL	**103.865**	**103.059**	**104.155**	**102.538**	**103.263**	**103.170**	**103.872**	**103.064**	**104.355**	**103.562**	**104.587**	**103.758**	**105.263**	**103.362**	**104.051**	**104.456**	**103.339**	**103.073**
CATIONS RECALCULATED TO 12 OXYGENS																		
Si	2.970	2.967	2.980	2.975	2.965	2.974	2.985	2.979	2.980	2.969	2.979	2.977	3.010	2.975	2.985	2.957	2.976	2.947
Al	1.986	1.995	1.971	1.982	2.008	2.011	1.967	2.012	1.979	1.999	1.986	1.995	1.972	1.960	1.979	1.997	2.001	2.052
Ti	0.000	0.002	0.004	0.005	0.000	0.000	0.002	0.004	0.002	0.000	0.004	0.001	0.000	0.001	0.000	0.002	0.002	0.000
Fe3+	0.020	0.011	0.028	0.018	0.000	0.000	0.034	0.000	0.024	0.008	0.015	0.00:	0.026	0.045	0.024	0.011	0.003	0.000
Mg	0.444	0.442	0.448	0.450	0.455	0.454	0.471	0.461	0.460	0.449	0.452	0.447	0.445	0.459	0.465	0.462	0.439	0.442
Fe2+	2.440	2.444	2.420	2.424	2.438	2.414	2.392	2.399	2.443	2.452	2.412	2.431	2.387	2.413	2.395	2.446	2.434	2.435
Mn	0.071	0.076	0.072	0.063	0.072	0.077	0.075	0.068	0.072	0.065	0.078	0.074	0.072	0.076	0.07:	0.070	0.072	0.067
Ca	0.094	0.094	0.092	0.103	0.094	0.092	0.086	0.088	0.058	0.086	0.092	0.087	0.079	0.093	0.086	0.092	0.093	0.085
TOTAL	**8.026**	**8.029**	**8.016**	**8.020**	**8.032**	**8.021**	**8.012**	**8.011**	**8.017**	**8.028**	**8.017**	**8.021**	**7.991**	**8.022**	**8.014**	**8.037**	**8.020**	**8.028**
Fe/Fe+Mg	*0.846*	*0.847*	*0.844*	*0.843*	*0.843*	*0.842*	*0.836*	*0.839*	*0.842*	*0.845*	*0.842*	*0.845*	*0.843*	*0.840*	*0.837*	*0.841*	*0.847*	*0.846*
Alm	0.800	0.800	0.798	0.797	0.797	0.795	0.791	0.795	0.805	0.804	0.795	0.800	0.800	0.793	0.791	0.797	0.801	0.804
Py	0.146	0.145	0.148	0.148	0.149	0.149	0.156	0.153	0.152	0.147	0.149	0.147	0.149	0.151	0.154	0.151	0.145	0.146
Sp	0.023	0.025	0.024	0.021	0.024	0.025	0.025	0.023	0.024	0.021	0.026	0.024	0.024	0.025	0.026	0.023	0.024	0.022
Gr	0.031	0.031	0.031	0.034	0.031	0.030	0.028	0.029	0.019	0.028	0.030	0.029	0.027	0.031	0.029	0.030	0.031	0.028
(Ca+Mn)/(Mg+Ca+Mn+Fe)	0.054	0.056	0.054	0.055	0.055	0.056	0.053	0.052	0.043	0.049	0.056	0.053	0.051	0.056	0.055	0.053	0.054	0.050
X	74.38	73.45	72.51	71.58	70.65	69.71	68.78	67.85	66.92	65.98	65.05	64.12	63.18	62.25	61.32	60.38	59.45	58.52
Y	-361.88	-361.88	-361.88	-361.88	-361.88	-361.88	-361.88	-361.88	-361.88	-361.83	-362.07	-361.88	-361.94	-361.88	-361.88	-361.88	-361.88	-361.88
x-axis m	0.37	0.47	0.56	0.65	0.75	0.84	0.93	1.03	1.12	1.21	1.31	1.40	1.50	1.59	1.68	1.78	1.87	1.96
location	*interior*	*interior*	*interior*	*interior*	*interior*	*interior*	*interior*	*interior*	*interior*	*interior*	*interior*	*interior*	*interior*	*interior*	*interior*	*interior*	*interior*	*interior*

TABLE B-1: Quantitative Microprobe Analysis for Garnet Compositions

	PC-113E (continued)			*PC-116/3a*														
	GT8w	**GT8x**	**GT8y**	**1**	**1a**	**2**	**2a**	**3**	**4**	**5**	**6**	**7**	**8**	**9**	**10**	**11**	**12**	**13**
WEIGHT PERCENT OXIDES																		
SiO2	37.935	38.593	37.773	37.176	37.139	36.990	37.153	36.996	36.888	36.893	37.054	37.297	37.489	37.061	36.792	36.934	36.927	36.941
Al2O3	21.937	21.515	21.58:	22.284	21.917	21.904	22.175	22.197	22.496	22.270	22.161	22.091	21.984	22.212	22.375	21.962	22.322	22.253
TiO2	0.000	0.000	0.000	0.078	0.005	0.000	0.000	0.000	0.012	0.00:	0.073	0.017	0.000	0.040	0.000	0.000	0.000	0.088
Fe2O3	0.000	0.533	0.308															
MgO	3.822	3.689	3.051	3.758	3.680	3.148	3.192	3.268	4.365	4.520	4.566	4.581	4.610	4.464	4.643	4.560	4.651	4.503
FeO	37.928	36.797	38.975	36.816	36.05:	37.073	36.655	37.027	35.616	35.121	34.894	35.159	34.954	34.557	35.205	35.420	35.522	35.440
MnO	1.073	1.322	1.209	1.971	1.935	2.210	2.151	2.076	1.650	1.598	1.641	1.632	1.710	1.646	1.603	1.661	1.557	1.612
CaO	1.141	1.206	1.019	0.856	0.917	0.857	0.894	0.866	0.759	0.822	0.828	0.812	0.804	0.791	0.778	0.747	0.859	0.778
TOTAL	**103.836**	**103.655**	**103.925**	**102.939**	**101.652**	**102.183**	**102.220**	**102.430**	**101.786**	**101.234**	**101.216**	**101.588**	**101.550**	**100.770**	**101.395**	**101.283**	**101.838**	**101.616**
CATIONS RECALCULATED TO 12 OXYGENS																		
Si	2.952	2.997	2.956	2.919	2.946	2.936	2.939	2.925	2.911	2.922	2.932	2.941	2.955	2.93:	2.911	2.929	2.912	2.918
Al	2.012	1.969	1.992	2.062	2.049	2.049	2.067	2.069	2.092	2.079	2.067	2.053	2.042	2.077	2.086	2.053	2.074	2.072
Ti	0.000	0.000	0.000	0.005	0.000	0.000	0.000	0.000	0.001	0.001	0.004	0.001	0.000	0.002	0.000	0.000	0.000	0.005
Fe3+	0.000	0.031	0.018															
Mg	0.443	0.427	0.356	0.440	0.435	0.373	0.376	0.385	0.514	0.534	0.539	0.539	0.542	0.528	0.548	0.539	0.547	0.530
Fe2+	2.468	2.390	2.551	2.417	2.392	2.461	2.425	2.449	2.350	2.326	2.309	2.319	2.304	2.293	2.329	2.349	2.342	2.341
Mn	0.071	0.087	0.080	0.131	0.130	0.149	0.144	0.139	0.110	0.107	0.110	0.109	0.114	0.111	0.107	0.112	0.104	0.108
Ca	0.095	0.100	0.086	0.072	0.078	0.073	0.076	0.073	0.064	0.06:	0.070	0.069	0.068	0.067	0.066	0.063	0.073	0.066
TOTAL	**8.042**	**8.002**	**8.039**	**8.046**	**8.02:**	**8.03:**	**8.027**	**8.040**	**8.042**	**8.038**	**8.031**	**8.031**	**8.024**	**8.019**	**8.046**	**8.045**	**8.051**	**8.041**
Fe/Fe+Mg	*0.848*	*0.848*	*0.878*	*0.846*	*0.846*	*0.869*	*0.866*	*0.864*	*0.821*	*0.813*	*0.811*	*0.812*	*0.810*	*0.813*	*0.810*	*0.813*	*0.811*	*0.815*
Alm	0.802	0.795	0.82:	0.790	0.788	0.806	0.803	0.804	0.774	0.766	0.763	0.764	0.761	0.765	0.764	0.767	0.764	0.769
Py	0.144	0.142	0.116	0.144	0.143	0.122	0.125	0.126	0.169	0.176	0.178	0.177	0.179	0.176	0.180	0.176	0.178	0.174
Sp	0.023	0.029	0.026	0.043	0.043	0.049	0.048	0.046	0.036	0.035	0.036	0.036	0.038	0.037	0.035	0.036	0.034	0.035
Gr	0.031	0.033	0.028	0.023	0.026	0.024	0.025	0.024	0.021	0.023	0.023	0.023	0.022	0.022	0.022	0.021	0.024	0.022
(Ca+Mn)/(Mg+Ca+Mn+Fe)	0.054	0.062	0.054	0.066	0.069	0.073	0.073	0.06:	0.057	0.058	0.059	0.059	0.060	0.059	0.057	0.057	0.058	0.057
X	57.59	56.65	55.72	-57.17	-57.37	-64.08	-63.96	-65.72	-65.67	-65.58	-65.71	-65.39	-66.15	-66.99	-66.99	-66.26	-67.40	-67.26
Y	-361.88	-361.88	-361.88	127.65	127.65	122.44	122.54	122.62	125.66	129.14	132.03	136.71	139.54	143.83	148.50	152.57	155.03	158.17
x-axis m	2.06	2.15	2.24	0.00	0.02	0.00	0.02	0.00	0.30	0.65	0.94	1.41	1.70	2.14	2.61	3.02	3.29	3.61
location	*interior*	*±near rim*	*im adj bt*	*im adj qz*	*nr rm - qz*	*im adj bt*	*nr rm - bt*	*im adj bt*	*±near rim*	*interior*	*interior*	*interior*	*interior*	*interior*	*interior*	*interior*	*interior*	*±near rim*

TABLE B-1: Quantitative Microprobe Analysis for Garnet Compositions

PC-116/3a continued				*PC-119A*														
	14	**15**	**15a**	**GR1**	**GR2**	**GR3**	**G8**	**G9**	**GC4**	**GC5**	**GC6**	**GC7**	**G10ref**	**GT1a**	**GT1b**	**GT1c**	**GT1d**	**GT1e**
WEIGHT PERCENT OXIDES																		
SiO2	38.024	36.982	37.087	38.422	38.181	38.041	38.386	37.619	38.576	39.019	38.272	38.446	39.458	37.414	37.817	38.689	38.372	38.490
Al2O3	21.820	22.277	22.267	22.358	21.789	22.097	21.887	21.583	22.212	22.111	22.394	22.250	22.180	21.898	21.660	22.057	21.815	22.138
TiO2	0.014	0.000	0.052	0.000	0.007	0.028	0.004	0.018	0.000	0.000	0.000	0.018	0.049	0.000	0.018	0.000	0.017	0.000
Fe2O3	0.000	0.000	0.000	0.000	0.000	0.000	0.000	0.000	0.000	0.071	0.000	0.000	0.000	0.213	0.000			
MgO	3.851	3.387	3.413	3.690	3.202	2.674	2.989	3.096	4.647	4.685	4.927	4.900	4.952	4.024	4.093	4.457	4.482	4.215
FeO	35.663	36.122	35.968	35.975	36.371	36.720	36.030	36.221	34.468	34.569	34.318	34.738	35.039	35.634	35.093	35.492	35.487	35.425
MnO	2.003	2.368	2.203	2.069	2.478	2.429	2.688	2.702	1.718	1.623	1.659	1.669	1.509	2.091	2.083	1.872	1.902	1.960
CaO	0.825	0.838	0.880	1.075	1.126	0.984	0.998	1.150	1.109	1.194	1.206	1.205	1.190	1.148	1.116	1.134	1.223	1.228
TOTAL	**102.200**	**101.973**	**101.870**	**103.589**	**103.154**	**102.973**	**102.982**	**102.389**	**102.730**	**103.201**	**102.776**	**103.226**	**104.448**	**102.209**	**101.880**	**103.701**	**103.511**	**103.456**
CATIONS RECALCULATED TO 12 OXYGENS																		
Si	2.986	2.929	2.936	2.977	2.987	2.984	3.003	2.973	2.990	3.008	2.965	2.970	3.006	2.947	2.978	2.986	2.973	2.980
Al	2.01:	2.07:	2.077	2.042	2.009	2.043	2.018	2.010	2.029	2.009	2.045	2.026	1.991	2.033	2.011	2.006	1.992	2.01:
Ti	0.001	0.000	0.003	0.000	0.000	0.002	0.000	0.001	0.000	0.000	0.000	0.001	0.003	0.000	0.001	0.000	0.001	0.000
Fe3+	0.000	0.000	0.000	0.000	0.000	0.000	0.000	0.000	0.000	0.004	0.000	0.000	0.000	0.012	0.000			
Mg	0.451	0.400	0.403	0.426	0.373	0.313	0.349	0.365	0.537	0.538	0.569	0.564	0.562	0.473	0.481	0.513	0.518	0.486
Fe2+	2.342	2.393	2.381	2.331	2.380	2.409	2.357	2.394	2.234	2.228	2.224	2.245	2.232	2.347	2.311	2.291	2.300	2.294
Mn	0.133	0.159	0.148	0.136	0.164	0.161	0.178	0.181	0.113	0.106	0.109	0.109	0.097	0.140	0.139	0.122	0.125	0.129
Ca	0.069	0.071	0.075	0.089	0.094	0.083	0.084	0.097	0.092	0.099	0.100	0.09:	0.097	0.097	0.094	0.094	0.102	0.102
TOTAL	**8.003**	**8.031**	**8.022**	**8.002**	**8.008**	**7.993**	**7.988**	**8.021**	**7.995**	**7.988**	**8.012**	**8.016**	**7.993**	**8.036**	**8.015**	**8.011**	**8.023**	**8.010**
Fe/Fe+Mg	*0.839*	*0.857*	*0.855*	*0.845*	*0.864*	*0.885*	*0.871*	*0.868*	*0.806*	*0.805*	*0.796*	*0.799*	*0.799*	*0.832*	*0.828*	*0.817*	*0.816*	*0.825*
Alm	0.782	0.792	0.792	0.782	0.790	0.812	0.794	0.788	0.751	0.750	0.741	0.744	0.747	0.768	0.764	0.759	0.756	0.762
Py	0.151	0.132	0.134	0.143	0.124	0.105	0.117	0.120	0.180	0.181	0.190	0.187	0.188	0.155	0.159	0.170	0.170	0.162
Sp	0.044	0.053	0.049	0.046	0.055	0.054	0.060	0.05:	0.038	0.036	0.036	0.036	0.033	0.046	0.046	0.041	0.041	0.043
Gr	0.023	0.023	0.025	0.02:	0.031	0.028	0.028	0.032	0.031	0.033	0.033	0.033	0.033	0.032	0.031	0.031	0.033	0.034
(Ca+Mn)/(Mg+Ca+Mn+Fe)	0.068	0.076	0.074	0.076	0.086	0.082	0.088	0.092	0.069	0.069	0.06:	0.069	0.065	0.077	0.077	0.072	0.074	0.077
X	-69.21	-52.16	-52.50	99.04	105.87	101.55	107.14	109.41	82.45	83.65	89.46	95.02	89.63	80.37	80.37	80.37	80.37	80.24
Y	161.23	153.45	153.43	358.31	334.90	334.12	369.13	362.49	346.97	352.68	353.03	346.36	351.01	359.40	355.63	351.50	348.10	344.11
x-axis m	3.97	0.00	0.03											0.00	0.38	0.79	1.13	1.53
location	*adj qz?*	*im adj bt*	*nr rm - bt*	*im adj bt*	*ag adj bt*	*im adj bt*	*ragment*	*im adj bt*	*interior*	*interior*	*interior*	*interior*	*interior*	*rm - sil?*	*rm - hole*	*interior*	*interior*	*±near rim*

TABLE B-1: Quantitative Microprobe Analysis for Garnet Compositions

PC-119A (continued)

	GT1f	GT1g	GT2a	GT2b	GT2c	GT2d	GT2e	GT2f	GT2g	GT2h	GT2i	GT2j	GT2k	GT2l	GT2m	GT2n	GT2o	GT2p
WEIGHT PERCENT OXIDES																		
SiO2	38.797	37.649	37.787	37.910	37.684	38.592	38.107	38.583	37.878	37.948	38.000	37.899	39.136	38.174	38.729	38.580	38.520	38.252
Al2O3	22.037	21.723	21.902	21.473	21.622	22.036	21.929	22.139	21.805	21.884	21.945	21.805	22.382	21.907	22.065	22.356	22.269	22.004
TiO2	0.000	0.032	0.053	0.000	0.024	0.011	0.000	0.000	0.000	0.001	0.033	0.042	0.024	0.000	0.027	0.003	0.057	0.000
Fe2O3	0.000	0.000	0.000	0.000	0.000	0.000	0.000	0.000	0.000	0.000	0.000	0.000	0.000	0.000	0.000	0.000	0.000	0.000
MgO	3.899	3.334	3.180	3.099	3.551	3.815	3.965	3.883	4.283	4.56:	4.685	4.772	4.788	4.789	4.912	4.806	4.786	4.782
FeO	35.321	36.212	36.417	36.270	36.335	35.809	35.526	35.112	35.000	35.430	34.607	34.805	34.734	34.624	34.766	34.345	35.141	34.704
MnO	2.115	2.298	2.294	2.228	2.122	2.199	2.192	1.831	1.778	1.700	1.775	1.654	1.601	1.631	1.56:	1.608	1.564	1.662
CaO	1.144	1.083	1.088	1.082	1.187	1.080	1.037	1.001	1.112	1.084	1.057	1.103	1.173	1.181	1.156	1.130	1.158	1.116
TOTAL	**103.313**	**102.331**	**102.721**	**102.062**	**102.525**	**103.542**	**102.756**	**102.549**	**101.856**	**102.617**	**102.102**	**102.080**	**103.838**	**102.306**	**103.225**	**102.828**	**103.495**	**102.520**
CATIONS RECALCULATED TO 12 OXYGENS																		
Si	3.005	2.970	2.970	2.997	2.968	2.991	2.978	3.005	2.978	2.964	2.972	2.968	2.998	2.978	2.989	2.984	2.971	2.978
Al	2.012	2.01:	2.029	2.001	2.007	2.013	2.01:	2.032	2.020	2.015	2.023	2.013	2.020	2.014	2.007	2.038	2.024	2.019
Ti	0.000	0.002	0.003	0.000	0.001	0.001	0.000	0.000	0.000	0.000	0.002	0.002	0.001	0.000	0.002	0.000	0.003	0.000
Fe3+	0.000	0.000	0.000	0.000	0.000	0.000	0.000	0.000	0.000	0.000	0.000	0.000	0.000	0.000	0.000	0.000	0.000	0.000
Mg	0.450	0.392	0.373	0.365	0.417	0.441	0.462	0.451	0.502	0.532	0.546	0.557	0.547	0.557	0.565	0.554	0.550	0.555
Fe2+	2.288	2.389	2.394	2.398	2.393	2.321	2.322	2.287	2.301	2.314	2.264	2.280	2.225	2.259	2.244	2.222	2.267	2.259
Mn	0.139	0.154	0.153	0.149	0.142	0.144	0.145	0.121	0.118	0.112	0.118	0.110	0.104	0.108	0.103	0.105	0.102	0.110
Ca	0.095	0.092	0.092	0.092	0.100	0.08:	0.087	0.084	0.094	0.091	0.089	0.093	0.096	0.099	0.096	0.094	0.096	0.093
TOTAL	**7.989**	**8.018**	**8.013**	**8.002**	**8.028**	**8.001**	**8.013**	**7.979**	**8.012**	**8.029**	**8.014**	**8.023**	**7.991**	**8.015**	**8.006**	**7.997**	**8.014**	**8.013**
Fe/Fe+Mg	*0.836*	*0.859*	*0.865*	*0.868*	*0.852*	*0.840*	*0.834*	*0.835*	*0.821*	*0.813*	*0.806*	*0.804*	*0.803*	*0.802*	*0.799*	*0.800*	*0.805*	*0.803*
Alm	0.770	0.789	0.795	0.798	0.784	0.775	0.770	0.777	0.763	0.759	0.751	0.750	0.749	0.747	0.746	0.747	0.752	0.749
Py	0.151	0.130	0.124	0.122	0.137	0.147	0.153	0.153	0.166	0.174	0.181	0.183	0.184	0.184	0.188	0.186	0.183	0.184
Sp	0.047	0.051	0.051	0.04:	0.046	0.048	0.048	0.041	0.039	0.037	0.039	0.036	0.035	0.036	0.034	0.035	0.034	0.036
Gr	0.032	0.030	0.030	0.031	0.033	0.02:	0.029	0.028	0.031	0.02:	0.029	0.031	0.032	0.033	0.032	0.032	0.032	0.031
(Ca+Mn)/(Mg+Ca+Mn+Fe)	0.079	0.081	0.081	0.080	0.079	0.078	0.077	0.069	0.070	0.067	0.068	0.067	0.067	0.068	0.066	0.067	0.066	0.067
X	80.37	80.37	87.46	87.42	87.32	87.22	87.06	87.05	86.85	86.75	86.65	86.55	86.45	86.35	86.25	86.15	86.05	85.95
Y	340.31	336.80	370.09	368.49	367.07	364.88	363.58	361.42	359.97	358.31	356.62	354.94	353.09	351.58	350.07	347.98	346.53	344.54
x-axis m	1.91	2.26	0.00	0.16	0.30	0.52	0.65	0.87	1.02	1.18	1.35	1.52	1.70	1.86	2.01	2.22	2.36	2.56
location	*rm - hole*	*im adj bt*	*m adj bt?*	*nr rm - bt*	*nr rm - bt*	*nr rm-sil?*	*nr rm-sil?*	*nr rm-sil?*	*±near rim*	*interior*	*interior*	*interior*	*interior*	*interior*	*interior*	*interior*	*interior*	*interior*

TABLE B-1: Quantitative Microprobe Analysis for Garnet Compositions

PC-119A (continued)

	GT2q	GT2r	GT2s	GT2t	GT2u	GT2v	GT2w	GT3a	GT3b	GT3c	GT3d	GT3e	GT3f	GT3g	GT3h	GT3i	GT3j	GT4a
WEIGHT PERCENT OXIDES																		
SiO2	38.870	38.575	39.116	38.761	38.766	38.881	38.376	38.736	38.360	38.193	38.503	38.124	38.934	38.868	39.026	38.155	38.274	38.176
Al2O3	22.251	22.298	22.284	22.048	22.204	22.137	22.038	21.841	21.909	21.950	22.062	21.981	22.297	22.131	22.044	21.961	21.801	21.803
TiO2	0.024	0.008	0.024	0.004	0.013	0.000	0.000	0.000	0.061	0.000	0.000	0.011	0.020	0.000	0.000	0.004	0.000	0.034
Fe2O3	0.000	0.000	0.000	0.000	0.000	0.000	0.000	0.000	0.000	0.000	0.000	0.000	0.000	0.000	0.020	0.000	0.055	0.000
MgO	4.732	4.637	4.448	4.326	4.208	3.983	3.951	3.126	3.989	4.525	4.874	4.860	4.925	4.816	4.694	3.926	3.986	3.767
FeO	34.768	34.868	35.734	35.533	35.672	35.096	35.172	36.537	35.698	35.171	34.517	34.553	34.367	34.791	35.127	35.855	36.148	35.350
MnO	1.740	1.608	1.672	1.741	1.800	1.943	2.142	2.160	1.918	1.686	1.683	1.534	1.537	1.427	1.588	1.827	1.873	2.131
CaO	1.186	1.126	1.147	1.080	1.126	1.103	1.085	1.046	1.108	1.110	1.094	1.182	1.100	1.143	1.162	1.098	1.095	1.083
TOTAL	**103.571**	**103.120**	**104.425**	**103.493**	**103.789**	**103.143**	**102.764**	**103.446**	**103.043**	**102.635**	**102.733**	**102.245**	**103.180**	**103.176**	**103.661**	**102.826**	**103.232**	**102.344**
CATIONS RECALCULATED TO 12 OXYGENS																		
Si	2.990	2.982	2.993	2.995	2.989	3.00:	2.990	3.014	2.986	2.977	2.986	2.974	2.997	2.998	3.002	2.979	2.981	2.992
Al	2.017	2.032	2.00:	2.008	2.018	2.01:	2.024	2.003	2.010	2.016	2.016	2.021	2.023	2.012	1.998	2.021	2.001	2.014
Ti	0.001	0.000	0.001	0.000	0.001	0.000	0.000	0.000	0.004	0.000	0.000	0.001	0.001	0.000	0.000	0.000	0.000	0.002
Fe3+	0.000	0.000	0.000	0.000	0.000	0.000	0.000	0.000	0.000	0.000	0.000	0.000	0.000	0.000	0.001	0.000	0.003	0.000
Mg	0.543	0.534	0.507	0.498	0.484	0.460	0.459	0.363	0.463	0.526	0.563	0.565	0.565	0.554	0.538	0.457	0.463	0.440
Fe2+	2.237	2.254	2.287	2.296	2.300	2.272	2.292	2.377	2.324	2.292	2.239	2.254	2.213	2.244	2.260	2.341	2.354	2.317
Mn	0.113	0.105	0.108	0.114	0.118	0.127	0.141	0.142	0.126	0.111	0.111	0.101	0.100	0.093	0.103	0.121	0.124	0.141
Ca	0.098	0.093	0.094	0.089	0.093	0.092	0.091	0.087	0.092	0.093	0.091	0.099	0.091	0.095	0.096	0.092	0.091	0.091
TOTAL	**7.000**	**8.002**	**8.001**	**8.001**	**8.002**	**7.980**	**7.998**	**7.985**	**8.005**	**8.015**	**8.006**	**8.015**	**7.990**	**7.996**	**7.998**	**8.011**	**8.017**	**7.998**
Fe/Fe+Mg	*0.805*	*0.808*	*0.818*	*0.822*	*0.826*	*0.832*	*0.833*	*0.868*	*0.834*	*0.813*	*0.799*	*0.800*	*0.797*	*0.802*	*0.808*	*0.837*	*0.836*	*0.840*
Alm	0.748	0.755	0.763	0.766	0.768	0.770	0.768	0.801	0.773	0.759	0.745	0.747	0.745	0.752	0.754	0.778	0.776	0.775
Py	0.181	0.179	0.169	0.166	0.162	0.156	0.154	0.122	0.154	0.174	0.188	0.187	0.190	0.185	0.180	0.152	0.153	0.147
Sp	0.038	0.035	0.036	0.038	0.039	0.043	0.047	0.048	0.042	0.037	0.037	0.034	0.034	0.031	0.035	0.040	0.041	0.047
Gr	0.033	0.031	0.031	0.02:	0.031	0.031	0.030	0.029	0.031	0.031	0.030	0.033	0.031	0.032	0.032	0.031	0.030	0.030
(Ca+Mn)/(Mg+Ca+Mn+Fe)	0.071	0.067	0.068	0.068	0.070	0.074	0.078	0.077	0.073	0.068	0.067	0.066	0.064	0.063	0.067	0.071	0.071	0.078
X	85.85	85.74	85.74	85.54	85.44	85.55	85.24	92.01	91.91	91.81	91.72	91.62	91.52	91.42	91.33	91.23	91.13	79.20
Y	343.16	341.63	339.79	338.11	336.43	334.83	333.06	365.61	362.19	357.98	354.91	351.26	347.53	343.64	340.50	336.41	333.32	356.86
x-axis m	2.70	2.85	3.04	3.21	3.37	3.53	3.71	0.00	0.34	0.76	1.07	1.44	1.81	2.20	2.51	2.92	3.23	0.00
location	*interior*	*interior*	*interior*	*±near rim*	*±near rim*	*r rm - qz*	*±near rim*	*rim adj bt*	*±near rim*	*interior*	*interior*	*interior*	*interior*	*interior*	*interior*	*±near rim*	*±near rim*	*rm - hole*

TABLE B-1: Quantitative Microprobe Analysis for Garnet Compositions

PC-119A (continued)

	GT4b	GT4c	GT4d	GT4e	GT4f	GT4g	GT4h	GT5a	GT5b	GT5c	GT5d	GT5e	GT5f	GT5g	GT5h	GT5i	GT5j	GT5k
WEIGHT PERCENT OXIDES																		
SiO2	38.105	38.011	38.391	38.606	38.924	38.963	38.160	38.270	37.988	39.137	38.779	39.175	39.157	39.363	38.835	38.113	39.072	38.119
Al2O3	21.706	21.862	21.919	21.865	22.432	21.937	22.090	21.818	21.672	22.209	22.287	22.032	22.397	21.990	22.050	21.982	22.345	22.051
TiO2	0.007	0.000	0.006	0.000	0.016	0.000	0.037	0.001	0.013	0.004	0.033	0.042	0.034	0.000	0.000	0.000	0.000	0.000
Fe2O3	0.082	0.000	0.011	0.070	0.000	0.000	0.000	0.000	0.000	0.000	0.000	0.000	0.000	0.049	0.000	0.000	0.000	0.000
MgO	4.458	4.712	4.745	4.673	3.920	3.556	3.326	3.883	4.247	4.367	4.532	4.684	4.784	4.788	4.828	4.921	4.827	4.906
FeO	35.322	34.965	35.209	35.035	35.503	35.333	35.529	34.713	35.312	34.980	34.896	34.478	34.562	34.279	34.503	34.472	34.335	34.786
MnO	1.712	1.766	1.755	1.701	1.873	2.118	2.268	2.138	1.841	1.726	1.747	1.674	1.591	1.599	1.707	1.576	1.580	1.563
CaO	1.127	1.062	1.066	1.077	1.092	1.094	1.039	1.086	1.127	1.137	1.183	1.102	1.229	1.249	1.177	1.166	1.154	1.148
TOTAL	**102.519**	**102.378**	**103.102**	**103.027**	**103.760**	**103.001**	**102.449**	**101.909**	**102.200**	**103.560**	**103.457**	**103.187**	**103.754**	**103.317**	**103.100**	**102.230**	**103.313**	**102.573**
CATIONS RECALCULATED TO 12 OXYGENS																		
Si	2.978	2.970	2.978	2.993	2.998	3.026	2.990	3.003	2.981	3.011	2.989	3.018	2.999	3.025	2.999	2.973	3.003	2.967
Al	1.000	2.013	2.004	1.998	2.036	2.008	2.040	2.018	2.004	2.014	2.025	2.000	2.022	1.992	2.007	2.021	2.024	2.023
Ti	0.000	0.000	0.000	0.000	0.001	0.000	0.002	0.000	0.001	0.000	0.002	0.002	0.002	0.000	0.000	0.000	0.000	0.000
Fe3+	0.005	0.000	0.001	0.004	0.000	0.000	0.000	0.000	0.000	0.000	0.000	0.000	0.000	0.003	0.000	0.000	0.000	0.000
Mg	0.519	0.549	0.549	0.540	0.450	0.412	0.389	0.454	0.497	0.501	0.521	0.538	0.546	0.549	0.556	0.572	0.553	0.569
Fe2+	2.309	2.285	2.284	2.271	2.287	2.295	2.328	2.278	2.317	2.250	2.249	2.221	2.214	2.203	2.228	2.249	2.207	2.264
Mn	0.113	0.117	0.115	0.112	0.122	0.139	0.151	0.142	0.122	0.112	0.114	0.109	0.103	0.104	0.112	0.104	0.103	0.103
Ca	0.094	0.089	0.089	0.08:	0.090	0.091	0.087	0.091	0.095	0.094	0.098	0.091	0.101	0.103	0.097	0.098	0.095	0.096
TOTAL	**8.019**	**8.023**	**8.019**	**8.007**	**7.983**	**7.970**	**7.987**	**7.988**	**8.017**	**7.982**	**7.997**	**7.980**	**7.988**	**7.978**	**7.998**	**8.017**	**7.985**	**8.022**
Fe/Fe+Mg	*0.816*	*0.806*	*0.806*	*0.808*	*0.836*	*0.848*	*0.857*	*0.834*	*0.823*	*0.818*	*0.812*	*0.805*	*0.802*	*0.801*	*0.800*	*0.797*	*0.800*	*0.799*
Alm	0.760	0.752	0.752	0.754	0.775	0.781	0.788	0.768	0.764	0.761	0.754	0.751	0.747	0.745	0.744	0.744	0.746	0.747
Py	0.171	0.181	0.181	0.179	0.153	0.140	0.132	0.153	0.164	0.169	0.175	0.182	0.184	0.185	0.186	0.189	0.187	0.188
Sp	0.037	0.039	0.038	0.037	0.041	0.047	0.051	0.048	0.040	0.038	0.038	0.037	0.035	0.035	0.037	0.034	0.035	0.034
Gr	0.031	0.029	0.029	0.02:	0.031	0.031	0.029	0.031	0.031	0.032	0.033	0.031	0.034	0.035	0.033	0.032	0.032	0.032
(Ca+Mn)/(Mg+Ca+Mn+Fe)	0.068	0.068	0.067	0.067	0.072	0.078	0.081	0.079	0.072	0.06:	0.071	0.068	0.069	0.06:	0.06:	0.067	0.067	0.066
X	82.46	85.97	89.11	92.09	98.99	102.04	105.24	77.09	78.81	80.10	81.42	83.11	84.62	86.13	87.64	89.15	90.85	91.82
Y	356.87	356.90	356.88	356.88	356.68	357.06	356.90	350.81	350.74	350.66	350.66	350.52	350.44	350.37	350.49	350.22	350.04	350.08
x-axis m	0.33	0.68	0.99	1.29	1.98	2.29	2.61	0.00	0.17	0.30	0.43	0.60	0.75	0.91	1.06	1.21	1.38	1.48
location	*±near rim*	*interior*	*interior*	*interior*	*±near rim*	*±near rim*	*im adj bt*	*adj hole*	*r rm-hole*	*±near rim*	*interior*	*interior*	*interior*	*interior*	*interior*	*interior*	*interior*	*interior*

TABLE B-1: Quantitative Microprobe Analysis for Garnet Compositions

PC-119A (continued)

	GT5l	GT5m	GT5n	GT5o	GT5p	GT5q	GT5r	GT5s	GT5t	GT6a	GT6b	GT6c	GT6d	GT6e	GT6f	GT6g	GT6h	GT6i
WEIGHT PERCENT OXIDES																		
SiO2	38.878	38.948	38.060	38.072	38.604	37.854	38.214	38.070	38.008	37.861	37.493	38.605	38.804	38.887	38.255	39.483	38.640	38.541
Al2O3	22.122	22.053	21.756	21.812	22.010	21.509	21.785	21.797	22.078	21.560	21.842	22.011	21.886	22.173	21.812	22.611	22.357	22.101
TiO2	0.016	0.028	0.031	0.035	0.041	0.047	0.006	0.025	0.013	0.000	0.000	0.021	0.000	0.000	0.000	0.000	0.000	0.004
Fe2O3	0.000	0.000	0.038	0.000	0.000	0.158	0.000	0.000	0.000	0.000	0.000	0.000	0.065	0.000	0.000	0.000	0.000	0.000
MgO	4.879	4.680	4.567	4.545	4.341	4.367	4.121	3.751	3.803	3.183	4.133	4.418	4.566	4.775	4.989	4.735	4.806	4.513
FeO	34.944	34.731	35.493	35.070	34.721	35.144	35.505	35.633	35.372	35.960	35.052	34.855	35.008	34.669	34.406	34.607	34.863	34.476
MnO	1.504	1.601	1.631	1.759	1.781	1.825	1.926	2.155	2.068	2.205	2.085	1.729	1.607	1.513	1.666	1.629	1.664	1.801
CaO	1.199	1.168	1.072	1.131	1.144	1.131	1.148	1.165	1.058	1.130	1.190	1.163	1.197	1.130	1.147	1.137	1.192	1.106
TOTAL	**103.542**	**103.209**	**102.648**	**102.424**	**102.642**	**102.035**	**102.705**	**102.596**	**102.400**	**101.899**	**101.795**	**102.802**	**103.133**	**103.147**	**102.275**	**104.202**	**103.522**	**102.542**
CATIONS RECALCULATED TO 12 OXYGENS																		
Si	2.992	3.005	2.972	2.975	2.000	2.976	2.985	2.982	2.977	2.994	2.958	2.997	3.002	2.999	2.982	3.008	2.976	2.995
Al	2.006	2.005	2.002	2.009	2.016	1.993	2.005	2.013	2.038	2.00:	2.031	2.014	1.996	2.016	2.004	2.02:	2.029	2.024
Ti	0.001	0.002	0.002	0.002	0.002	0.003	0.000	0.001	0.001	0.000	0.000	0.001	0.000	0.000	0.000	0.000	0.000	0.000
Fe3+	0.000	0.000	0.002	0.000	0.000	0.009	0.000	0.000	0.000	0.000	0.000	0.000	0.004	0.000	0.000	0.000	0.000	0.000
Mg	0.560	0.538	0.532	0.529	0.503	0.512	0.480	0.438	0.444	0.375	0.486	0.511	0.527	0.549	0.580	0.538	0.552	0.523
Fe2+	2.249	2.241	2.318	2.292	2.256	2.311	2.319	2.335	2.317	2.378	2.312	2.263	2.265	2.236	2.243	2.205	2.245	2.240
Mn	0.098	0.105	0.108	0.116	0.117	0.122	0.127	0.143	0.137	0.148	0.139	0.114	0.105	0.099	0.110	0.105	0.109	0.119
Ca	0.099	0.097	0.08:	0.095	0.095	0.095	0.096	0.098	0.089	0.096	0.101	0.097	0.099	0.093	0.096	0.093	0.098	0.092
TOTAL	**8.004**	**7.991**	**8.024**	**8.018**	**7.990**	**8.020**	**8.013**	**8.00:**	**8.003**	**8.001**	**8.027**	**7.995**	**7.998**	**7.993**	**8.016**	**7.978**	**8.009**	**7.993**
Fe/Fe+Mg	*0.801*	*0.806*	*0.813*	*0.812*	*0.818*	*0.819*	*0.829*	*0.842*	*0.839*	*0.864*	*0.826*	*0.816*	*0.811*	*0.803*	*0.795*	*0.804*	*0.803*	*0.811*
Alm	0.748	0.752	0.761	0.756	0.759	0.760	0.767	0.775	0.776	0.794	0.761	0.758	0.756	0.751	0.741	0.750	0.747	0.753
Py	0.186	0.181	0.174	0.175	0.169	0.168	0.159	0.145	0.149	0.125	0.160	0.171	0.176	0.184	0.191	0.183	0.184	0.176
Sp	0.033	0.035	0.035	0.038	0.039	0.040	0.042	0.048	0.046	0.049	0.046	0.038	0.035	0.033	0.036	0.036	0.036	0.03:
Gr	0.033	0.032	0.029	0.031	0.032	0.031	0.032	0.033	0.02:	0.032	0.033	0.032	0.033	0.031	0.032	0.032	0.033	0.031
(Ca+Mn)/(Mg+Ca+Mn+Fe)	0.066	0.068	0.065	0.06:	0.072	0.071	0.074	0.07:	0.076	0.081	0.079	0.071	0.068	0.065	0.068	0.067	0.069	0.071
X	93.67	94.66	96.37	97.67	99.48	101.70	102.72	104.23	105.74	77.86	80.81	83.90	87.48	90.14	92.24	96.27	98.56	102.41
Y	350.01	349.93	349.86	349.79	349.60	349.63	349.57	349.49	349.42	342.61	342.51	342.41	342.31	342.21	342.10	342.00	342.05	341.80
x-axis m	1.66	1.76	1.93	2.06	2.25	2.47	2.57	2.72	2.87	0.00	0.30	0.60	0.96	1.23	1.44	1.84	2.07	2.46
location	*interior*	*interior*	*interior*	*interior*	*±near rim*	*nr rm - sil*	*nr rm - sil*	*nr rm - sil*	*m adj qz?*	*m adj sil?*	*±near rim*	*interior*	*interior*	*interior*	*interior*	*interior*	*interior*	*interior*

TABLE B-1: Quantitative Microprobe Analysis for Garnet Compositions

PC-119A continued			*PC-128/10a*														
	GT6j	**GT6k**	**1T**	**2T**	**3T**	**4T**	**5T**	**7T**	**8T**	**9T**	**10T**	**11T**	**12T**	**14T**	**15T**	**16T**	**17T**	**18T**
WEIGHT PERCENT OXIDES																		
SiO2	37.982	38.46:	37.05:	37.149	37.495	37.490	37.834	37.482	37.654	37.405	37.272	37.343	37.679	37.151	37.236	37.290	37.451	37.193
Al2O3	21.834	21.849	22.041	22.164	21.893	21.743	22.362	22.491	22.291	22.207	22.026	22.147	22.330	22.240	22.363	22.555	21.805	21.999
TiO2	0.006	0.000	0.016	0.021	0.012	0.047	0.000	0.005	0.066	0.052	0.00:	0.000	0.012	0.000	0.000	0.031	0.047	0.029
Fe2O3	0.000	0.000																
MgO	4.176	3.838	2.554	3.008	3.417	4.006	4.597	4.911	5.05:	4.968	4.924	4.810	4.845	5.029	5.262	4.778	4.750	4.862
FeO	35.277	35.172	36.327	36.608	36.768	35.859	35.035	34.492	35.919	34.706	34.136	35.031	34.968	34.553	35.492	35.190	34.190	34.200
MnO	1.860	2.204	2.875	2.199	1.497	1.178	0.915	1.070	0.967	0.861	0.864	0.932	1.027	0.952	0.779	0.954	0.978	1.132
CaO	1.098	1.099	1.354	1.484	1.497	1.752	1.839	1.876	1.750	1.806	1.883	1.810	1.954	1.719	1.835	1.886	1.883	1.748
TOTAL	**102.233**	**102.632**	**102.228**	**102.634**	**102.578**	**102.075**	**102.582**	**102.326**	**103.705**	**102.006**	**101.115**	**102.073**	**102.814**	**101.645**	**102.967**	**102.685**	**101.104**	**101.162**
CATIONS RECALCULATED TO 12 OXYGENS																		
Si	2.978	3.003	2.942	2.932	2.952	2.953	2.946	2.924	2.913	2.929	2.93:	2.928	2.931	2.920	2.899	2.908	2.956	2.936
Al	2.018	2.00:	2.062	2.061	2.031	2.019	2.052	2.068	2.033	2.04:	2.048	2.047	2.047	2.060	2.052	2.073	2.028	2.047
Ti	0.000	0.000	0.001	0.001	0.001	0.003	0.000	0.000	0.004	0.003	0.001	0.000	0.001	0.000	0.000	0.002	0.003	0.002
Fe3+	0.000	0.000																
Mg	0.488	0.447	0.302	0.354	0.401	0.46:	0.534	0.571	0.584	0.580	0.579	0.562	0.562	0.589	0.611	0.555	0.559	0.572
Fe2+	2.313	2.296	2.411	2.416	2.421	2.363	2.282	2.250	2.324	2.273	2.252	2.297	2.275	2.271	2.310	2.295	2.257	2.258
Mn	0.124	0.146	0.193	0.147	0.09:	0.079	0.060	0.071	0.063	0.057	0.058	0.062	0.068	0.063	0.051	0.063	0.065	0.076
Ca	0.092	0.092	0.115	0.126	0.126	0.148	0.153	0.157	0.145	0.152	0.159	0.152	0.163	0.145	0.153	0.158	0.159	0.148
TOTAL	**8.013**	**7.992**	**8.027**	**8.037**	**8.032**	**8.034**	**8.028**	**8.042**	**8.066**	**8.043**	**8.036**	**8.048**	**8.045**	**8.04:**	**8.076**	**8.054**	**8.027**	**8.039**
Fe/Fe+Mg	*0.826*	*0.837*	*0.889*	*0.872*	*0.858*	*0.834*	*0.810*	*0.798*	*0.799*	*0.797*	*0.795*	*0.803*	*0.802*	*0.794*	*0.791*	*0.805*	*0.801*	*0.798*
Alm	0.767	0.770	0.798	0.794	0.794	0.772	0.753	0.738	0.746	0.742	0.739	0.747	0.742	0.740	0.739	0.747	0.742	0.739
Py	0.162	0.150	0.100	0.116	0.132	0.154	0.176	0.187	0.187	0.189	0.190	0.183	0.183	0.192	0.195	0.181	0.184	0.187
Sp	0.041	0.049	0.064	0.048	0.033	0.026	0.01:	0.023	0.020	0.019	0.019	0.020	0.022	0.021	0.016	0.021	0.021	0.025
Gr	0.031	0.031	0.038	0.041	0.041	0.048	0.051	0.051	0.046	0.04:	0.052	0.04:	0.053	0.047	0.049	0.051	0.052	0.048
(Ca+Mn)/(Mg+Ca+Mn+Fe)																		
	0.072	0.07:	0.102	0.08:	0.074	0.074	0.071	0.075	0.067	0.068	0.071	0.06:	0.075	0.068	0.065	0.072	0.074	0.073
X	105.36	108.52	115.45	114.99	114.54	114.09	113.63	112.73	112.27	111.82	111.37	110.91	110.46	109.55	109.10	108.65	108.19	107.74
Y	341.70	341.60	96.13	96.85	97.57	98.28	99.00	100.44	101.16	101.88	102.59	103.31	104.03	105.47	106.19	106.90	107.62	108.34
x-axis m	2.75	3.07	0.00	0.09	0.17	0.25	0.34	0.51	0.60	0.68	0.76	0.85	0.93	1.10	1.19	1.27	1.36	1.44
location	*±near rim*	*im adj qz*	*im adj bt*	*nr rm - bt*	*nr rm - bt*	*±near rim*	*±near rim*	*interior*	*interior*	*interior*	*interior*	*interior*	*interior*	*interior*	*interior*	*interior*	*interior*	*interior*

TABLE B-1: Quantitative Microprobe Analysis for Garnet Compositions

PC-128/10a continued

	22T	23T	24T	25T	1	1a	2	3	3a	4	4a	5	5a	6	6a	7	8	9
WEIGHT PERCENT OXIDES																		
SiO2	37.025	36.718	36.725	36.550	36.599	36.492	37.139	36.669	37.004	37.364	36.717	36.478	36.630	36.975	36.913	37.115	37.150	37.119
Al2O3	22.136	22.044	21.436	21.554	22.388	22.302	22.375	21.429	22.185	22.384	22.108	22.136	22.288	21.488	21.468	22.187	22.226	22.174
TiO2	0.024	0.012	0.031	0.009	0.000	0.045	0.061	0.000	0.000	0.049	0.031	0.019	0.061	0.000	0.002	0.000	0.000	0.00:
Fe2O3																		
MgO	4.143	3.849	3.295	2.663	2.668	2.760	3.454	2.266	3.100	2.220	2.539	2.757	3.010	2.568	2.849	4.452	4.819	4.810
FeO	35.755	36.323	36.436	35.748	36.018	35.994	36.521	35.483	36.543	37.515	36.919	35.790	36.039	36.317	36.893	34.627	34.493	34.765
MnO	1.135	1.229	1.884	3.115	2.756	2.973	1.281	2.93:	1.851	3.146	2.571	2.533	1.781	2.510	2.346	0.948	0.900	0.863
CaO	1.693	1.644	1.471	1.515	1.416	1.402	1.445	1.452	1.395	1.270	1.394	1.537	1.634	1.245	1.450	1.713	1.969	1.722
TOTAL	**101.910**	**101.820**	**101.278**	**101.155**	**101.845**	**101.967**	**102.278**	**100.237**	**102.078**	**103.947**	**102.280**	**101.250**	**101.444**	**101.105**	**101.922**	**101.044**	**101.557**	**101.464**
CATIONS RECALCULATED TO 12 OXYGENS																		
Si	2.922	2.911	2.939	2.937	2.914	2.906	2.927	2.967	2.932	2.929	2.920	2.919	2.918	2.966	2.945	2.936	2.923	2.925
Al	2.059	2.060	2.022	2.041	2.101	2.093	2.079	2.043	2.071	2.068	2.072	2.088	2.093	2.032	2.018	2.069	2.061	2.059
Ti	0.001	0.001	0.002	0.001	0.000	0.003	0.004	0.000	0.000	0.003	0.002	0.001	0.004	0.000	0.000	0.000	0.000	0.001
Fe3+																		
Mg	0.487	0.455	0.393	0.319	0.317	0.328	0.406	0.273	0.366	0.259	0.301	0.329	0.357	0.307	0.339	0.525	0.565	0.565
Fe2+	2.360	2.409	2.439	2.402	2.398	2.397	2.407	2.401	2.421	2.459	2.455	2.395	2.401	2.436	2.461	2.291	2.270	2.291
Mn	0.076	0.083	0.128	0.212	0.186	0.201	0.086	0.201	0.124	0.209	0.173	0.172	0.120	0.171	0.159	0.064	0.060	0.058
Ca	0.143	0.140	0.126	0.130	0.121	0.120	0.122	0.126	0.118	0.107	0.119	0.132	0.139	0.107	0.124	0.145	0.166	0.145
TOTAL	**8.048**	**8.058**	**8.048**	**8.042**	**8.036**	**8.045**	**8.02:**	**8.012**	**8.033**	**8.034**	**8.042**	**8.036**	**8.032**	**8.018**	**8.046**	**8.029**	**8.046**	**8.044**
Fe/Fe+Mg	*0.829*	*0.841*	*0.861*	*0.883*	*0.883*	*0.880*	*0.856*	*0.898*	*0.869*	*0.905*	*0.891*	*0.879*	*0.870*	*0.888*	*0.879*	*0.814*	*0.801*	*0.802*
Alm	0.770	0.781	0.790	0.784	0.794	0.787	0.797	0.800	0.799	0.810	0.805	0.791	0.796	0.806	0.798	0.757	0.742	0.749
Py	0.159	0.147	0.127	0.104	0.105	0.108	0.134	0.091	0.121	0.086	0.099	0.109	0.118	0.102	0.110	0.174	0.185	0.185
Sp	0.025	0.027	0.041	0.069	0.062	0.066	0.028	0.067	0.041	0.069	0.057	0.057	0.03:	0.057	0.051	0.021	0.01:	0.019
Gr	0.047	0.045	0.041	0.043	0.040	0.039	0.040	0.042	0.039	0.035	0.039	0.044	0.046	0.035	0.040	0.048	0.054	0.048
(Ca+Mn)/(Mg+Ca+Mn+Fe)	0.071	0.072	0.082	0.112	0.101	0.105	0.069	0.109	0.080	0.104	0.096	0.100	0.086	0.092	0.092	0.069	0.074	0.066
X	105.93	105.47	105.02	104.57	109.02	108.97	107.91	108.53	108.52	112.33	112.07	117.90	116.90	114.38	113.58	111.58	109.87	108.81
Y	111.21	111.93	112.65	113.37	93.67	93.65	95.44	113.32	112.80	111.90	111.85	103.54	103.54	95.53	95.85	98.02	100.71	103.40
x-axis m	1.78	1.87	1.95	2.04	0.00	0.01		0.00	0.05	0.00	0.03	0.00	0.10	0.00	0.09			
location	*±near rim*	*±near rim*	*nr rm - bt*	*im adj bt*	*im adj bt*	*im adj bt*	*nr rm - bt*	*m adj ms*	*r rm - ms*	*m adj ms*	*m adj ms*	*m adj ms*	*r rm - ms*	*m adj ms*	*r rm - ms*	*±near rim*	*interior*	*interior*

TABLE B-1: Quantitative Microprobe Analysis for Garnet Compositions

PC-128/10a continued				*PC-128/10c*														
	10	**11**	**11a**	**1T**	**2T**	**3T**	**4T**	**5T**	**6T**	**7T**	**8T**	**9T**	**10T**	**11T**	**1**	**1a**	**2**	**2a**
WEIGHT PERCENT OXIDES																		
SiO2	37.195	36.635	36.950	37.043	37.703	36.691	36.839	36.408	36.527	36.247	36.984	36.514	36.532	36.565	36.611	36.857	36.881	36.666
Al2O3	22.147	21.793	21.516	21.863	22.364	22.397	22.608	22.804	22.636	22.412	22.454	22.401	22.529	22.514	22.646	22.231	22.334	22.016
TiO2	0.000	0.000	0.000	0.000	0.101	0.000	0.000	0.042	0.012	0.012	0.042	0.000	0.000	0.068	0.058	0.000	0.000	0.005
Fe2O3																		
MgO	4.474	2.622	2.748	3.326	3.473	4.078	4.489	4.403	4.228	5.048	4.016	3.858	3.573	3.05:	3.594	3.530	3.558	3.594
FeO	35.232	36.229	36.660	35.001	35.643	35.280	35.024	35.363	35.515	33.398	35.705	34.787	34.925	34.511	34.632	34.412	35.022	35.746
MnO	1.057	2.956	2.448	3.139	2.939	2.612	2.481	2.335	2.245	2.296	2.933	2.915	3.966	4.342	3.641	3.531	2.752	2.858
CaO	1.842	1.747	1.732	1.304	1.275	1.370	1.309	1.332	1.376	1.354	1.358	1.236	1.324	1.445	1.343	1.431	1.356	1.270
TOTAL	**101.948**	**101.983**	**102.055**	**101.677**	**103.498**	**102.426**	**102.750**	**102.688**	**102.539**	**100.767**	**103.492**	**101.710**	**102.850**	**102.506**	**102.525**	**101.992**	**101.903**	**102.155**
CATIONS RECALCULATED TO 12 OXYGENS																		
Si	2.926	2.923	2.944	2.943	2.939	2.892	2.887	2.860	2.875	2.881	2.891	2.897	2.880	2.893	2.887	2.918	2.919	2.908
Al	2.053	2.04:	2.020	2.048	2.055	2.081	2.088	2.112	2.09:	2.099	2.069	2.094	2.093	2.099	2.105	2.074	2.083	2.058
Ti	0.000	0.000	0.000	0.000	0.006	0.000	0.000	0.003	0.001	0.001	0.002	0.000	0.000	0.004	0.003	0.000	0.000	0.000
Fe3+																		
Mg	0.525	0.312	0.326	0.394	0.404	0.479	0.524	0.516	0.496	0.598	0.468	0.456	0.420	0.361	0.422	0.417	0.420	0.425
Fe2+	2.318	2.418	2.443	2.326	2.324	2.326	2.295	2.323	2.338	2.220	2.334	2.308	2.303	2.283	2.284	2.278	2.318	2.371
Mn	0.070	0.200	0.165	0.211	0.194	0.174	0.165	0.155	0.150	0.155	0.194	0.196	0.265	0.291	0.243	0.237	0.185	0.192
Ca	0.155	0.149	0.148	0.111	0.106	0.116	0.110	0.112	0.116	0.115	0.114	0.105	0.112	0.122	0.113	0.121	0.115	0.108
TOTAL	**8.047**	**8.052**	**8.046**	**8.033**	**8.028**	**8.068**	**8.069**	**8.081**	**8.075**	**8.069**	**8.072**	**8.056**	**8.073**	**8.054**	**8.058**	**8.045**	**8.03:**	**8.063**
Fe/Fe+Mg	*0.815*	*0.886*	*0.882*	*0.855*	*0.852*	*0.829*	*0.814*	*0.818*	*0.825*	*0.788*	*0.833*	*0.835*	*0.846*	*0.864*	*0.844*	*0.845*	*0.847*	*0.848*
Alm	0.755	0.785	0.793	0.765	0.767	0.751	0.742	0.748	0.754	0.719	0.751	0.753	0.743	0.747	0.746	0.746	0.763	0.766
Py	0.171	0.101	0.106	0.130	0.133	0.155	0.169	0.166	0.160	0.194	0.150	0.149	0.135	0.118	0.138	0.136	0.138	0.137
Sp	0.023	0.065	0.054	0.069	0.064	0.056	0.053	0.050	0.048	0.050	0.062	0.064	0.086	0.095	0.079	0.078	0.061	0.062
Gr	0.051	0.049	0.048	0.037	0.035	0.037	0.036	0.036	0.037	0.037	0.037	0.034	0.036	0.040	0.037	0.03:	0.038	0.035
(Ca+Mn)/(Mg+Ca+Mn+Fe)																		
	0.074	0.113	0.102	0.106	0.099	0.094	0.089	0.086	0.086	0.087	0.099	0.098	0.122	0.135	0.116	0.117	0.099	0.097
X	105.51	102.12	102.40	98.58	103.06	107.08	113.73	116.34	119.39	121.76	125.05	129.46	132.99	134.31	114.24	114.24	110.86	110.79
Y	103.40	106.91	106.91	-216.24	-215.84	-214.31	-210.55	-205.52	-201.67	-200.15	-196.77	-194.34	-192.70	-192.70	-226.66	-226.35	-205.68	-205.46
x-axis mm		0.00	0.03	0.00	0.45	0.88	1.64	2.21	2.70	2.98	3.45	3.96	4.35	4.48	0.00	0.03	0.00	0.02
location	*nr fract*	*m adj ms*	*m adj ms*	*rim - crd?*	*frag nr bt*	*nr fract*	*nr fract*	*nr fract*	*nr fract*	*interior*	*r bt fract*	*fragment*	*fragment*	*rm - crd?*	*m adj crd*	*m adj crd*	*nr rm - cd*	*j bt fract*

TABLE B-1: Quantitative Microprobe Analysis for Garnet Compositions

PC-128/10c continued

	3	3a	4	5	6	7	8	9	10	grt1	grt1a	grt1b	grt1c	grt2	grt2a	grt2b	GT1a	GT1b
WEIGHT PERCENT OXIDES																		
SiO2	36.678	36.810	37.052	37.169	36.498	36.921	36.916	37.267	36.566	37.254	37.669	37.691	37.939	38.347	38.066	37.507	38.797	38.614
Al2O3	22.370	22.357	22.345	22.500	22.173	22.630	22.402	22.508	22.287	21.975	22.334	22.252	22.342	22.599	22.168	21.990	21.992	21.671
TiO2	0.059	0.016	0.019	0.028	0.000	0.061	0.000	0.054	0.009	0.000	0.018	0.000	0.042	0.008	0.021	0.001	0.055	0.000
Fe2O3	0.104	0.068																
MgO	3.276	3.520	4.135	5.348	4.546	4.513	5.033	4.807	4.085	3.292	3.670	3.860	3.877	3.126	3.665	3.663	3.206	3.348
FeO	34.024	34.666	34.181	33.746	33.638	34.703	34.106	34.700	34.769	35.829	35.820	36.326	35.628	35.225	35.282	34.981	38.077	36.652
MnO	3.051	3.186	2.313	1.999	2.097	2.229	2.026	1.950	2.407	3.193	3.302	3.348	3.138	3.749	3.595	3.422	1.642	1.587
CaO	1.334	1.296	1.308	1.288	1.241	1.300	1.288	1.367	1.344	1.315	1.283	1.328	1.233	1.348	1.275	1.323	1.219	1.096
TOTAL	**100.790**	**101.851**	**101.353**	**102.078**	**100.194**	**102.357**	**101.771**	**102.654**	**101.466**	**102.858**	**104.096**	**104.805**	**104.199**	**104.402**	**104.072**	**102.887**	**105.092**	**103.036**
CATIONS RECALCULATED TO 12 OXYGENS																		
Si	2.928	2.916	2.930	2.907	2.916	2.896	2.904	2.909	2.902	2.935	2.927	2.916	2.937	2.961	2.952	2.943	2.985	3.013
Al	2.104	2.087	2.083	2.074	2.088	2.092	2.077	2.071	2.085	2.040	2.045	2.029	2.039	2.057	2.026	2.034	1.994	1.993
Ti	0.004	0.001	0.001	0.002	0.000	0.004	0.000	0.003	0.001	0.000	0.001	0.000	0.002	0.000	0.001	0.000	0.003	0.000
Fe3+	0.006	0.004																
Mg	0.390	0.416	0.487	0.624	0.541	0.528	0.58:	0.559	0.483	0.387	0.425	0.445	0.447	0.360	0.424	0.429	0.368	0.389
Fe2+	2.271	2.296	2.261	2.207	2.247	2.277	2.244	2.266	2.308	2.360	2.327	2.350	2.307	2.275	2.288	2.296	2.450	2.392
Mn	0.206	0.214	0.155	0.132	0.142	0.148	0.135	0.129	0.162	0.213	0.217	0.219	0.206	0.245	0.236	0.227	0.107	0.105
Ca	0.114	0.110	0.111	0.108	0.106	0.109	0.109	0.114	0.114	0.111	0.107	0.110	0.102	0.112	0.106	0.111	0.100	0.092
TOTAL	**8.017**	**8.03:**	**8.028**	**8.054**	**8.040**	**8.054**	**8.058**	**8.052**	**8.055**	**8.045**	**8.04:**	**8.06:**	**8.041**	**8.00:**	**8.034**	**8.03:**	**8.012**	**7.988**
Fe/Fe+Mg	*0.854*	*0.847*	*0.823*	*0.780*	*0.806*	*0.812*	*0.792*	*0.802*	*0.827*	*0.859*	*0.846*	*0.841*	*0.838*	*0.863*	*0.844*	*0.843*	*0.869*	*0.860*
Alm	0.762	0.756	0.750	0.719	0.740	0.744	0.729	0.738	0.752	0.769	0.756	0.752	0.753	0.760	0.749	0.750	0.810	0.803
Py	0.131	0.137	0.162	0.203	0.178	0.172	0.192	0.182	0.158	0.126	0.138	0.142	0.146	0.120	0.139	0.140	0.122	0.131
Sp	0.069	0.070	0.051	0.043	0.047	0.048	0.044	0.042	0.053	0.069	0.071	0.070	0.067	0.082	0.077	0.074	0.035	0.035
Gr	0.038	0.036	0.037	0.035	0.035	0.036	0.035	0.037	0.037	0.036	0.035	0.035	0.033	0.037	0.035	0.036	0.033	0.031
(Ca+Mn)/(Mg+Ca+Mn+Fe)	0.107	0.107	0.088	0.078	0.082	0.084	0.079	0.079	0.090	0.106	0.105	0.105	0.101	0.119	0.112	0.111	0.069	0.066
X	102.58	102.67	104.64	114.41	118.77	112.30	118.30	123.20	127.47	96.26	96.84	97.44	98.19	135.16	134.64	134.04	-160.47	-159.57
Y	-198.21	-198.43	-205.48	-221.64	-209.62	-201.05	-199.06	-201.84	-192.86	-218.95	-218.78	-218.50	-218.31	-207.38	-207.54	-207.54	-333.86	-333.30
x-axis m	0.00	0.02								0.00	0.06	0.13	0.20	0.00	0.05	0.11	0.00	0.11
location	*adj crd?*	*r rm-crd?*	*nr fract*	*interior*	*nr fract*	*nr fract*	*interior*	*interior*	*agnrfract*	*m adj crd*	*r rm - crd*	*r rm - crd*	*nr rm - cd*	*m adj crd*	*r rm - crd*	*r rm - crd*	*rim - hole*	*rm - hole*

PC-133A

TABLE B-1: Quantitative Microprobe Analysis for Garnet Compositions

PC-133A continued

	GT1c	GT1d	GT1e	GT1f	GT1g	GT1h	GT1i	GT1j	GT1k	GT1l	GT1m	GT1n	GT1o	GT1p	GT1q	GT1r	GT2a	GT2b
WEIGHT PERCENT OXIDES																		
SiO2	38.927	38.476	39.429	38.521	39.145	39.261	38.493	39.586	38.654	38.807	39.292	38.663	37.275	38.800	37.682	38.527	37.868	38.776
Al2O3	22.121	21.949	21.409	21.593	21.805	21.589	21.941	21.771	22.203	21.766	21.711	21.315	21.882	21.584	20.631	21.569	21.701	21.486
TiO2	0.078	0.000	0.000	0.000	0.093	0.020	0.017	0.046	0.000	0.000	0.000	0.035	0.041	0.023	0.000	0.020	0.000	0.029
Fe2O3	0.000	0.000	0.826	0.509	0.368	0.543	0.132	0.767	0.000	0.357	0.455	0.772	0.000	0.410	0.870	0.446	0.099	0.651
MgO	3.157	3.386	3.416	3.456	3.469	3.621	3.670	3.445	3.532	3.553	3.688	3.677	3.441	3.644	3.398	3.432	3.231	3.523
FeO	37.420	37.449	36.395	37.354	37.065	35.997	37.293	36.899	37.242	36.643	36.063	35.971	36.529	36.192	35.128	36.856	37.447	36.447
MnO	1.659	1.655	1.549	1.491	1.410	1.350	1.322	1.635	1.461	1.509	1.292	1.443	1.434	1.291	1.361	1.563	1.687	1.466
CaO	1.193	1.269	1.204	1.232	1.519	1.585	1.533	1.726	1.679	1.625	1.634	1.620	1.713	1.587	1.525	1.424	1.421	1.639
TOTAL	**104.555**	**104.184**	**104.228**	**104.156**	**104.874**	**103.966**	**104.401**	**105.875**	**104.771**	**104.260**	**104.135**	**103.496**	**102.315**	**103.531**	**100.595**	**103.837**	**103.454**	**104.017**
CATIONS RECALCULATED TO 12 OXYGENS																		
Si	2.999	2.981	3.038	2.987	3.004	3.026	2.973	3.00:	2.973	2.996	3.023	3.004	2.942	3.009	3.014	2.992	2.964	3.001
Al	2.009	2.004	1.944	1.973	1.972	1.961	1.997	1.951	2.013	1.980	1.969	1.952	2.036	1.973	1.945	1.974	2.002	1.960
Ti	0.005	0.000	0.000	0.000	0.005	0.001	0.001	0.003	0.000	0.000	0.000	0.002	0.002	0.001	0.000	0.001	0.000	0.002
Fe3+	0.000	0.000	0.048	0.02:	0.021	0.032	0.008	0.044	0.000	0.021	0.026	0.045	0.000	0.024	0.052	0.026	0.006	0.038
Mg	0.363	0.391	0.392	0.399	0.397	0.416	0.423	0.390	0.405	0.409	0.423	0.426	0.405	0.421	0.405	0.397	0.377	0.406
Fe2+	2.411	2.426	2.345	2.422	2.379	2.321	2.409	2.346	2.396	2.365	2.320	2.337	2.411	2.347	2.349	2.394	2.451	2.359
Mn	0.108	0.109	0.101	0.098	0.092	0.088	0.087	0.105	0.095	0.099	0.084	0.095	0.096	0.085	0.092	0.103	0.112	0.096
Ca	0.099	0.105	0.099	0.102	0.125	0.131	0.127	0.141	0.138	0.134	0.135	0.135	0.145	0.132	0.131	0.118	0.119	0.136
TOTAL	**7.992**	**8.017**	**7.967**	**8.012**	**7.994**	**7.976**	**8.024**	**7.990**	**8.020**	**8.004**	**7.980**	**7.996**	**8.037**	**7.992**	**7.988**	**8.006**	**8.032**	**7.998**
Fe/Fe+Mg	*0.869*	*0.861*	*0.857*	*0.858*	*0.857*	*0.848*	*0.851*	*0.857*	*0.855*	*0.853*	*0.846*	*0.846*	*0.856*	*0.848*	*0.853*	*0.858*	*0.867*	*0.853*
Alm	0.809	0.800	0.798	0.802	0.795	0.785	0.791	0.787	0.790	0.787	0.783	0.781	0.789	0.786	0.789	0.795	0.801	0.787
Py	0.122	0.129	0.134	0.132	0.133	0.141	0.139	0.131	0.133	0.136	0.143	0.142	0.132	0.141	0.136	0.132	0.123	0.136
Sp	0.036	0.036	0.034	0.032	0.031	0.02:	0.028	0.035	0.031	0.033	0.028	0.032	0.031	0.028	0.031	0.034	0.037	0.032
Gr	0.033	0.035	0.034	0.034	0.042	0.044	0.042	0.047	0.046	0.045	0.046	0.045	0.047	0.044	0.044	0.039	0.039	0.045
(Ca+Mn)/(Mg+Ca+Mn+Fe)	0.069	0.071	0.068	0.066	0.072	0.074	0.070	0.082	0.077	0.078	0.074	0.077	0.079	0.073	0.075	0.074	0.076	0.077
X	-158.67	-158.03	-156.50	-155.97	-155.07	-154.16	-153.27	-151.65	-151.29	-150.43	-149.66	-148.76	-147.66	-146.96	-146.06	-145.16	-141.02	-140.30
Y	-332.85	-331.81	-331.96	-331.07	-330.51	-329.95	-329.84	-328.46	-328.05	-327.50	-327.16	-326.60	-326.04	-325.48	-324.93	-324.37	-327.58	-326.84
x-axis m	0.21	0.33	0.48	0.59	0.69	0.80	0.89	1.10	1.16	1.26	1.34	1.45	1.57	1.66	1.77	1.87	0.00	0.10
location	*±near rim*	*±near rim*	*interior*	*interior*	*interior*	*interior*	*interior*	*interior*	*interior*	*interior*	*interior*	*interior*	*interior*	*interior*	*r rm adj ?*	*rim adj ?*	*im adj bt*	*nr rm - bt*

TABLE B-1: Quantitative Microprobe Analysis for Garnet Compositions

PC-133A continued

	GT2c	GT2d	GT2e	GT2f	GT2g	GT2h	GT2i	GT2j	GT2k	GT2l	GT2m	GT2n	GT2o	GT2p	GT2q	GT2r	GT2s	GT2t
WEIGHT PERCENT OXIDES																		
SiO2	39.406	38.790	39.542	39.103	38.985	39.185	39.090	38.931	39.546	39.109	39.105	39.281	39.055	39.420	39.366	39.005	39.334	38.861
Al2O3	21.952	21.549	21.772	21.987	22.052	22.151	21.815	21.780	21.949	22.173	22.078	21.878	21.905	21.849	21.592	21.785	21.691	21.739
TiO2	0.035	0.000	0.003	0.003	0.000	0.000	0.000	0.000	0.000	0.017	0.029	0.000	0.026	0.038	0.000	0.038	0.000	0.000
Fe2O3	0.338	0.541	0.776	0.190	0.000	0.000	0.350	0.220	0.406	0.000	0.098	0.304	0.404	0.594	0.899	0.422	0.684	0.387
MgO	3.620	3.686	3.836	3.808	3.811	3.810	3.722	3.897	4.070	3.807	4.303	4.497	4.593	4.633	4.606	4.645	4.508	4.209
FeO	36.643	36.286	36.333	36.46:	36.339	36.713	36.668	36.071	36.253	36.674	36.476	35.697	35.897	35.904	35.537	35.557	35.673	36.044
MnO	1.528	1.236	1.511	1.282	1.402	1.300	1.351	1.460	1.372	1.382	1.395	1.155	1.250	1.198	1.273	1.162	1.228	1.311
CaO	1.604	1.620	1.691	1.691	1.421	1.345	1.375	1.270	1.335	1.238	1.066	1.144	1.344	1.225	1.255	1.319	1.223	1.257
TOTAL	**105.126**	**103.708**	**105.464**	**104.534**	**104.010**	**104.504**	**104.371**	**103.629**	**104.931**	**104.400**	**104.550**	**103.956**	**104.474**	**104.861**	**104.528**	**103.933**	**104.341**	**103.808**
CATIONS RECALCULATED TO 12 OXYGENS																		
Si	3.00:	3.005	3.00:	3.001	3.004	3.005	3.007	3.010	3.016	3.003	2.996	3.015	2.991	3.004	3.010	2.998	3.012	2.000
Al	1.976	1.967	1.953	1.989	2.003	2.002	1.978	1.985	1.973	2.007	1.993	1.979	1.977	1.963	1.946	1.974	1.958	1.978
Ti	0.002	0.000	0.000	0.000	0.000	0.000	0.000	0.000	0.000	0.001	0.002	0.000	0.002	0.002	0.000	0.002	0.000	0.000
Fe3+	0.019	0.032	0.044	0.011	0.000	0.000	0.020	0.013	0.023	0.000	0.006	0.018	0.023	0.034	0.052	0.024	0.039	0.023
Mg	0.412	0.426	0.435	0.436	0.438	0.436	0.427	0.449	0.463	0.436	0.491	0.515	0.524	0.526	0.525	0.532	0.515	0.484
Fe2+	2.341	2.351	2.313	2.341	2.342	2.355	2.359	2.333	2.312	2.355	2.337	2.291	2.299	2.288	2.273	2.286	2.285	2.327
Mn	0.099	0.081	0.097	0.083	0.092	0.085	0.088	0.096	0.089	0.08:	0.091	0.075	0.081	0.077	0.083	0.076	0.07:	0.086
Ca	0.131	0.134	0.138	0.139	0.117	0.111	0.113	0.105	0.109	0.102	0.088	0.094	0.110	0.100	0.103	0.109	0.100	0.104
TOTAL	**7.990**	**7.996**	**7.991**	**7.999**	**7.995**	**7.993**	**7.993**	**7.991**	**7.986**	**7.993**	**8.003**	**7.987**	**8.007**	**7.995**	**7.991**	**8.001**	**7.989**	**8.000**
Fe/Fe+Mg	*0.850*	*0.847*	*0.842*	*0.843*	*0.842*	*0.844*	*0.847*	*0.839*	*0.833*	*0.844*	*0.826*	*0.817*	*0.814*	*0.813*	*0.812*	*0.811*	*0.816*	*0.828*
Alm	0.785	0.786	0.775	0.781	0.784	0.789	0.790	0.782	0.778	0.790	0.777	0.770	0.763	0.765	0.762	0.761	0.767	0.775
Py	0.138	0.142	0.146	0.145	0.146	0.146	0.143	0.151	0.156	0.146	0.163	0.173	0.174	0.176	0.176	0.177	0.173	0.161
Sp	0.033	0.027	0.033	0.028	0.031	0.028	0.029	0.032	0.02:	0.030	0.030	0.025	0.027	0.026	0.028	0.025	0.027	0.029
Gr	0.044	0.045	0.046	0.046	0.039	0.037	0.038	0.035	0.037	0.034	0.029	0.032	0.037	0.033	0.035	0.036	0.034	0.035
(Ca+Mn)/(Mg+Ca+Mn+Fe)	0.077	0.072	0.079	0.074	0.06:	0.065	0.067	0.067	0.067	0.064	0.059	0.057	0.064	0.059	0.062	0.061	0.060	0.063
X	-139.58	-138.87	-138.15	-137.43	-136.64	-136.00	-135.29	-134.57	-133.85	-133.32	-132.42	-131.70	-130.99	-130.27	-129.57	-128.84	-128.12	-127.41
Y	-326.10	-325.37	-324.63	-323.89	-323.07	-322.42	-321.68	-320.94	-320.20	-319.57	-318.73	-317.99	-317.25	-316.52	-315.66	-315.04	-314.30	-313.39
x-axis m	0.21	0.31	0.41	0.51	0.63	0.72	0.82	0.93	1.03	1.11	1.23	1.34	1.44	1.54	1.65	1.75	1.85	1.97
location	*±near rim*	*interior*	*interior*	*interior*	*interior*	*interior*	*interior*	*interior*	*interior*	*interior*	*interior*	*interior*	*interior*	*interior*	*interior*	*interior*	*interior*	*±near rim*

TABLE B-1: Quantitative Microprobe Analysis for Garnet Compositions

PC-133A continued

PC-134D

	GT2u	GT2v	GT3a	GT3b	GT3c	GT3d	GT3e	GT3f	GT3g	GT3h	GT3i	GT3j	GT1a	GT1b	GT1c	GT1d	GT1e	GT1f
WEIGHT PERCENT OXIDES																		
SiO2	38.437	38.760	38.560	38.809	38.954	39.081	38.934	39.373	39.56:	39.075	39.109	37.285	38.693	38.411	39.319	38.905	36.789	38.672
Al2O3	22.079	21.844	21.704	22.121	22.087	21.569	21.363	21.623	21.880	21.808	21.262	21.724	21.731	21.874	21.535	22.007	21.925	21.763
TiO2	0.000	0.000	0.000	0.000	0.014	0.064	0.000	0.044	0.000	0.046	0.000	0.014	0.000	0.000	0.006	0.009	0.009	0.023
Fe2O3	0.000	0.361	0.122	0.000	0.035	0.656	0.947	0.597	0.581	0.412	0.780	0.000	0.239	0.101	0.771	0.081	0.000	0.223
MgO	4.158	3.839	3.227	3.395	3.584	3.749	3.952	3.974	3.936	3.875	3.642	3.494	2.882	3.802	4.178	4.273	4.545	4.432
FeO	35.924	37.411	36.800	37.048	37.007	35.914	36.005	35.507	36.266	36.656	35.838	37.042	37.069	36.465	35.271	35.785	35.870	35.199
MnO	1.369	1.254	1.885	1.765	1.624	1.462	1.189	1.348	1.417	1.301	1.386	1.698	2.618	2.081	1.897	1.837	1.917	1.828
CaO	1.213	1.136	1.187	1.265	1.480	1.816	1.615	1.649	1.593	1.435	1.172	1.068	1.088	1.149	1.163	1.172	1.152	1.159
TOTAL	**103.180**	**104.605**	**103.485**	**104.403**	**104.785**	**104.311**	**104.005**	**104.115**	**105.243**	**104.608**	**103.189**	**102.325**	**104.320**	**103.883**	**104.140**	**104.069**	**102.207**	**103.299**
CATIONS RECALCULATED TO 12 OXYGENS																		
Si	2.983	2.985	3.003	2.993	2.991	3.007	3.006	3.024	3.013	2.000	3.037	2.948	3.000	2.978	3.021	2.994	2.905	2.995
Al	2.01:	1.982	1.992	2.010	1.999	1.956	1.944	1.957	1.964	1.973	1.946	2.024	1.986	1.999	1.950	1.996	2.040	1.987
Ti	0.000	0.000	0.000	0.000	0.001	0.004	0.000	0.003	0.000	0.003	0.000	0.001	0.000	0.000	0.000	0.001	0.001	0.001
Fe3+	0.000	0.021	0.007	0.000	0.002	0.038	0.055	0.035	0.033	0.024	0.046	0.000	0.014	0.006	0.045	0.005	0.000	0.013
Mg	0.481	0.441	0.375	0.390	0.410	0.430	0.455	0.455	0.447	0.443	0.422	0.412	0.333	0.439	0.479	0.490	0.535	0.512
Fe2+	2.332	2.409	2.397	2.389	2.377	2.311	2.324	2.281	2.310	2.353	2.328	2.449	2.404	2.365	2.267	2.303	2.369	2.280
Mn	0.090	0.082	0.124	0.115	0.106	0.095	0.078	0.088	0.091	0.085	0.091	0.114	0.172	0.137	0.123	0.120	0.128	0.120
Ca	0.101	0.094	0.099	0.105	0.122	0.150	0.134	0.136	0.130	0.118	0.098	0.091	0.090	0.096	0.096	0.097	0.098	0.096
TOTAL	**8.007**	**8.014**	**7.997**	**8.002**	**8.007**	**7.992**	**7.995**	**7.977**	**7.988**	**7.999**	**7.967**	**8.039**	**7.000**	**8.019**	**7.981**	**8.005**	**8.075**	**8.004**
Fe/Fe+Mg	*0.829*	*0.845*	*0.865*	*0.860*	*0.853*	*0.843*	*0.836*	*0.834*	*0.838*	*0.841*	*0.847*	*0.856*	*0.878*	*0.843*	*0.826*	*0.825*	*0.816*	*0.817*
Alm	0.776	0.796	0.800	0.797	0.788	0.774	0.777	0.771	0.776	0.785	0.792	0.799	0.801	0.779	0.765	0.765	0.757	0.758
Py	0.160	0.146	0.125	0.130	0.136	0.144	0.152	0.154	0.150	0.148	0.144	0.134	0.111	0.145	0.161	0.163	0.171	0.170
Sp	0.030	0.027	0.042	0.038	0.035	0.032	0.026	0.02:	0.031	0.028	0.031	0.037	0.057	0.045	0.042	0.03:	0.041	0.03:
Gr	0.034	0.031	0.033	0.035	0.040	0.050	0.045	0.046	0.044	0.039	0.033	0.029	0.030	0.031	0.032	0.032	0.031	0.032
(Ca+Mn)/(Mg+Ca+Mn+Fe)	0.064	0.058	0.075	0.073	0.075	0.082	0.071	0.076	0.074	0.068	0.064	0.067	0.088	0.077	0.074	0.072	0.072	0.072
X	-126.93	-126.06	-155.84	-156.75	-157.67	-158.58	-159.49	-160.41	-161.32	-162.23	-163.15	-164.06	102.85	102.08	101.30	100.53	99.58	98.98
Y	-313.04	-312.09	-80.20	-80.60	-81.00	-81.40	-81.81	-82.10	-82.61	-83.01	-83.42	-83.82	-298.28	-297.63	-296.98	-296.33	-295.50	-295.03
x-axis m	2.03	2.16	0.00	0.0:	0.20	0.30	0.40	0.50	0.60	0.70	0.80	0.90	0.00	0.10	0.20	0.30	0.43	0.51
location	*r rim - qz*	*im adj qz*	*m adj bt?*	*r rm - bt?*	*±near rim*	*±near rim*	*interior*	*interior*	*±near rim*	*±near rim*	*nr rm - qz*	*im adj qz*	*im adj bt*	*nr rm - bt*	*±near rim*	*interior*	*interior*	*interior*

TABLE B-1: Quantitative Microprobe Analysis for Garnet Compositions

PC-134D continued

	GT1g	GT1h	GT1i	GT1j	GT1k	GT1l	GT1m	GT1n	GT1o	GT1p	GT1q	GT1r	GT1s	GT1t	GT1u	GT1v	GT1w	GT1x
WEIGHT PERCENT OXIDES																		
SiO2	38.572	38.641	37.841	39.300	37.242	39.161	37.741	38.802	38.742	38.626	39.286	38.862	38.930	38.774	38.770	38.609	38.796	38.482
Al2O3	21.932	21.496	21.849	21.779	21.436	21.974	21.485	21.648	21.348	21.779	22.048	21.942	21.46:	21.585	22.037	21.910	21.579	21.718
TiO2	0.032	0.076	0.000	0.006	0.020	0.017	0.012	0.006	0.006	0.000	0.017	0.000	0.052	0.000	0.012	0.000	0.000	0.000
Fe2O3	0.225	0.422	0.000	0.572	0.000	0.072	0.428	0.613	0.706	0.189	0.140	0.173	0.549	0.592	0.000	0.329	0.547	0.464
MgO	4.433	4.203	4.198	4.061	3.645	3.594	3.633	3.141	3.096	3.397	3.754	3.746	3.919	4.131	4.025	4.015	3.866	3.916
FeO	36.092	35.110	36.016	35.797	35.716	36.109	36.466	36.857	36.243	36.400	36.244	36.308	34.965	35.268	35.531	36.248	35.627	35.979
MnO	1.853	1.957	1.999	2.131	2.118	2.269	2.388	2.750	2.687	2.383	2.318	2.308	2.368	2.340	2.409	2.408	2.371	2.561
CaO	1.113	1.123	1.167	1.134	1.126	1.173	1.198	1.215	1.068	1.197	1.079	1.125	1.169	1.167	1.178	1.180	1.092	1.174
TOTAL	**104.252**	**103.028**	**103.070**	**104.780**	**101.303**	**104.369**	**103.351**	**105.032**	**103.896**	**103.971**	**104.886**	**104.464**	**103.422**	**103.857**	**103.962**	**104.699**	**103.878**	**104.294**
CATIONS RECALCULATED TO 12 OXYGENS																		
Si	2.971	3.004	2.956	3.008	2.965	3.012	2.957	2.990	3.012	2.995	3.007	2.993	3.017	2.997	2.991	2.971	3.002	2.975
Al	1.991	1.969	2.011	1.965	2.012	1.992	1.984	1.966	1.956	1.990	1.989	1.992	1.961	1.966	2.004	1.987	1.968	1.979
Ti	0.002	0.004	0.000	0.000	0.001	0.001	0.001	0.000	0.000	0.000	0.001	0.000	0.003	0.000	0.001	0.000	0.000	0.000
Fe3+	0.013	0.025	0.000	0.033	0.000	0.004	0.025	0.036	0.041	0.011	0.008	0.010	0.032	0.034	0.000	0.019	0.032	0.027
Mg	0.509	0.487	0.489	0.463	0.433	0.412	0.424	0.361	0.359	0.393	0.428	0.430	0.453	0.476	0.463	0.461	0.446	0.451
Fe2+	2.325	2.283	2.353	2.292	2.378	2.323	2.389	2.375	2.356	2.360	2.320	2.338	2.266	2.280	2.293	2.333	2.305	2.326
Mn	0.121	0.129	0.132	0.138	0.143	0.148	0.158	0.180	0.177	0.156	0.150	0.151	0.155	0.153	0.157	0.157	0.155	0.168
Ca	0.092	0.094	0.098	0.093	0.096	0.097	0.101	0.100	0.089	0.099	0.089	0.093	0.097	0.097	0.097	0.097	0.091	0.097
TOTAL	**8.025**	**7.995**	**8.039**	**7.993**	**8.028**	**7.989**	**8.038**	**8.008**	**7.990**	**8.005**	**7.993**	**8.006**	**7.984**	**8.003**	**8.006**	**8.026**	**7.998**	**8.023**
Fe/Fe+Mg	*0.820*	*0.824*	*0.828*	*0.832*	*0.846*	*0.849*	*0.849*	*0.868*	*0.868*	*0.857*	*0.844*	*0.845*	*0.833*	*0.827*	*0.832*	*0.835*	*0.838*	*0.838*
Alm	0.763	0.763	0.766	0.767	0.780	0.780	0.778	0.788	0.790	0.784	0.777	0.776	0.763	0.758	0.762	0.765	0.769	0.765
Py	0.167	0.163	0.159	0.155	0.142	0.138	0.138	0.120	0.120	0.130	0.143	0.143	0.152	0.158	0.154	0.151	0.149	0.148
Sp	0.03:	0.043	0.043	0.046	0.047	0.04:	0.052	0.059	0.059	0.052	0.050	0.050	0.052	0.051	0.052	0.052	0.052	0.055
Gr	0.030	0.031	0.032	0.031	0.032	0.032	0.033	0.033	0.02:	0.033	0.02:	0.031	0.033	0.032	0.032	0.032	0.030	0.032
(Ca+Mn)/(Mg+Ca+Mn+Fe)	0.06:	0.074	0.075	0.077	0.078	0.082	0.084	0.093	0.089	0.085	0.07:	0.081	0.085	0.083	0.085	0.083	0.082	0.087
X	98.21	97.44	96.67	95.89	95.12	94.35	93.57	92.80	91.50	91.25	90.48	89.71	88.76	88.16	87.39	86.61	85.84	85.07
Y	-294.38	-293.73	-293.08	-292.43	-291.78	-291.13	-290.48	-289.83	-289.17	-288.52	-287.87	-287.30	-286.57	-285.92	-285.27	-284.62	-283.97	-283.32
x-axis m	0.61	0.71	0.81	0.91	1.01	1.11	1.21	1.31	1.46	1.53	1.63	1.73	1.84	1.93	2.03	2.14	2.24	2.34
location	*interior*	*interior*	*interior*	*interior*	*±near rim*	*±near rim*	*±near rim*	*adj fract*	*adj fract*	*nr fract*	*±nr fract*	*±nr fract*	*interior*	*interior*	*interior*	*interior*	*interior*	*interior*

TABLE B-1: Garnet Compositions

PC-134D continued

	GT1y	GT1z	GT1aa	GTab	GTac	GTad
WEIGHT PERCENT OXIDES						
SiO2	39.015	38.333	39.043	39.035	38.478	38.481
Al2O3	21.654	21.657	21.576	21.375	21.560	21.751
TiO2	0.000	0.000	0.000	0.020	0.075	0.000
Fe2O3	0.566	0.324	0.638	0.785	0.542	0.000
MgO	3.704	3.720	3.618	3.517	3.283	2.673
FeO	35.559	35.754	35.416	35.191	36.475	36.287
MnO	2.635	2.607	2.796	2.807	2.936	2.972
CaO	1.245	1.231	1.217	1.222	1.178	1.195
TOTAL	**104.378**	**103.626**	**104.304**	**103.952**	**104.527**	**103.359**
CATIONS RECALCULATED TO 12 OXYGENS						
Si	3.005	2.981	3.010	3.01:	2.980	3.007
Al	1.966	1.985	1.961	1.949	1.968	2.003
Ti	0.000	0.000	0.000	0.001	0.004	0.000
Fe3+	0.033	0.019	0.037	0.046	0.032	0.000
Mg	0.425	0.431	0.416	0.406	0.379	0.311
Fe2+	2.291	2.326	2.284	2.276	2.362	2.372
Mn	0.172	0.172	0.183	0.184	0.193	0.197
Ca	0.103	0.103	0.101	0.101	0.098	0.100
TOTAL	**7.995**	**8.017**	**7.991**	**7.982**	**8.016**	**7.991**
Fe/Fe+Mg	*0.843*	*0.844*	*0.846*	*0.849*	*0.862*	*0.884*
Alm	0.766	0.767	0.766	0.767	0.779	0.796
Py	0.142	0.142	0.139	0.137	0.125	0.105
Sp	0.058	0.057	0.061	0.062	0.064	0.066
Gr	0.034	0.034	0.034	0.034	0.032	0.034
(Ca+Mn)/(Mg+Ca+Mn+Fe)						
	0.092	0.091	0.095	0.096	0.096	0.09:
X	84.30	83.52	82.75	81.98	81.13	80.43
Y	-282.67	-282.02	-281.37	-280.72	-280.06	-279.41
x-axis m	2.44	2.54	2.64	2.74	2.85	2.94
location	*±near rim*	*±near rim*	*±near rim*	*±near rim*	*nr rm - bt*	*im adj bt*

TABLE B-2: Quantitative Microprobe Analysis for Biotite Compositions

	PC-19D																*PC-50E*			
	M6	**B1**	**B2**	**B4a**	**B4b**	**B4c**	**B5**	**B6**	**B7**	**B8a**	**B8b**	**B8c**	**B9**	**B10**	**B11**	**B12**	**B1b**	**B3**	**B11**	**BT2c**
WEIGHT PERCENT OXIDES				*right side matrix*		*left side matrix*														
SiO2	35.108	34.624	33.885	35.056	34.954	35.770	34.690	35.216	34.914	35.499	35.431	34.507	34.814	34.445	34.866	34.829	36.970	37.067	36.541	36.848
Al2O3	17.793	18.055	18.119	17.741	17.067	17.873	18.222	18.028	17.970	18.062	18.085	17.932	17.986	18.171	18.490	18.436	16.442	17.082	16.627	16.678
TiO2	3.016	3.287	2.169	2.465	2.382	2.612	2.145	1.910	2.815	1.627	1.731	2.288	2.804	2.339	2.810	3.409	2.122	2.052	1.686	1.674
MgO	5.019	4.989	5.701	5.311	5.327	5.479	5.583	5.296	5.304	5.755	5.577	5.308	4.784	5.074	4.618	4.698	10.606	10.592	11.390	11.270
FeO	27.819	27.412	28.771	27.757	28.079	26.682	28.141	27.882	27.893	27.343	27.119	28.555	28.660	28.197	27.733	27.210	20.504	19.659	19.824	19.339
MnO	0.244	0.335	0.225	0.373	0.230	0.261	0.398	0.176	0.255	0.354	0.217	0.296	0.208	0.309	0.269	0.242	0.194	0.100	0.058	0.105
CaO	0.052	0.074	0.157	0.009	0.121	0.027	0.031	0.038	0.018	0.000	0.079	0.034	0.054	0.034	0.016	0.018	0.100	0.140	0.401	0.080
Na2O	0.106	0.137	0.070	0.086	0.151	0.148	0.071	0.079	0.106	0.117	0.049	0.116	0.158	0.035	0.113	0.086	0.367	0.308	0.271	0.312
K2O	9.619	8.980	8.460	9.332	9.106	9.257	9.155	9.019	8.922	9.279	8.961	8.939	9.531	9.160	9.585	9.509	8.857	8.869	8.896	9.087
Cr2O3	0.000	0.014	0.000	0.000	0.007	0.016	0.053	0.000	0.002	0.035	0.000	0.019	0.018	0.000	0.051	0.018	0.045	0.067	0.063	0.118
Cl	0.049	0.060	0.049	0.077	0.052	0.052	0.029	0.043	0.063	0.052	0.066	0.060	0.040	0.037	0.032	0.034	0.165	0.162	0.130	0.188
F	0.145	0.106	0.150	0.076	0.190	0.000	0.200	0.000	0.000	0.128	0.090	0.080	0.000	0.024	0.022	0.091	0.155	0.224	0.132	0.158
TOTAL	*98.970*	*98.073*	*97.756*	*98.283*	*97.666*	*98.177*	*98.718*	*97.687*	*98.262*	*98.251*	*97.405*	*98.134*	*99.057*	*97.825*	*98.605*	*98.580*	*96.527*	*96.322*	*96.019*	*95.857*
-O = Cl	-0.011	-0.014	-0.011	-0.017	-0.012	-0.012	-0.007	-0.00:	-0.014	-0.012	-0.015	-0.014	-0.009	-0.008	-0.007	-0.008	-0.037	-0.037	-0.029	-0.042
-O = F	-0.061	-0.045	-0.063	-0.032	-0.080	0.000	-0.084	0.000	0.000	-0.054	-0.038	-0.034	0.000	-0.010	-0.009	-0.038	-0.065	-0.094	-0.056	-0.067
TOTAL	**98.898**	**98.015**	**97.682**	**98.234**	**97.574**	**98.165**	**98.627**	**97.677**	**98.248**	**98.185**	**97.352**	**98.087**	**99.048**	**97.807**	**98.589**	**98.534**	**96.425**	**96.191**	**95.934**	**95.748**
CATIONS RECALCULATED TO 22 OXYGENS																				
Si	5.384	5.337	5.270	5.405	5.439	5.46:	5.336	5.440	5.368	5.454	5.471	5.343	5.347	5.342	5.355	5.338	5.58:	5.588	5.542	5.587
Al	3.216	3.280	3.321	3.224	3.130	3.221	3.304	3.282	3.256	3.270	3.292	3.273	3.256	3.321	3.347	3.330	2.930	3.035	2.972	2.981
Ti	0.348	0.381	0.254	0.286	0.279	0.300	0.248	0.222	0.326	0.188	0.201	0.266	0.324	0.273	0.325	0.393	0.241	0.233	0.192	0.191
Mg	1.147	1.147	1.322	1.221	1.236	1.249	1.280	1.220	1.216	1.318	1.284	1.225	1.095	1.173	1.057	1.074	2.391	2.381	2.575	2.548
Fe	3.568	3.534	3.742	3.579	3.654	3.412	3.620	3.602	3.586	3.513	3.502	3.698	3.681	3.657	3.562	3.488	2.593	2.479	2.514	2.452
Mn	0.032	0.044	0.02:	0.049	0.030	0.034	0.052	0.023	0.033	0.046	0.028	0.039	0.027	0.041	0.035	0.031	0.025	0.013	0.007	0.014
Ca	0.009	0.012	0.026	0.001	0.020	0.004	0.005	0.006	0.003	0.000	0.013	0.006	0.009	0.006	0.003	0.003	0.016	0.023	0.065	0.013
Na	0.032	0.041	0.021	0.026	0.046	0.044	0.021	0.024	0.032	0.035	0.015	0.035	0.047	0.011	0.034	0.026	0.108	0.090	0.07:	0.092
K	1.882	1.766	1.679	1.836	1.808	1.806	1.797	1.777	1.750	1.819	1.765	1.766	1.868	1.812	1.878	1.859	1.709	1.706	1.721	1.758
Cr	0.000	0.002	0.000	0.000	0.001	0.002	0.006	0.000	0.000	0.004	0.000	0.002	0.002	0.000	0.006	0.002	0.005	0.008	0.008	0.014
TOTAL	**15.617**	**15.544**	**15.665**	**15.627**	**15.643**	**15.543**	**15.669**	**15.597**	**15.569**	**15.647**	**15.572**	**15.653**	**15.657**	**15.636**	**15.600**	**15.545**	**15.608**	**15.555**	**15.677**	**15.649**
Fe/Fe+Mg	*0.757*	*0.755*	*0.739*	*0.746*	*0.747*	*0.732*	*0.739*	*0.747*	*0.747*	*0.727*	*0.732*	*0.751*	*0.771*	*0.757*	*0.771*	*0.765*	*0.520*	*0.510*	*0.494*	*0.490*
Mg/6	0.191	0.191	0.220	0.203	0.206	0.208	0.213	0.203	0.203	0.220	0.214	0.204	0.183	0.196	0.176	0.179	0.398	0.397	0.429	0.425
Fe/6	0.595	0.589	0.624	0.597	0.609	0.569	0.603	0.600	0.598	0.586	0.584	0.616	0.614	0.610	0.594	0.581	0.432	0.413	0.419	0.409
Ti/6	0.058	0.064	0.042	0.048	0.046	0.050	0.041	0.037	0.054	0.031	0.034	0.044	0.054	0.046	0.054	0.066	0.040	0.039	0.032	0.032
Alvi/6	0.100	0.103	0.099	0.105	0.095	0.115	0.107	0.120	0.104	0.121	0.127	0.103	0.101	0.111	0.117	0.111	0.087	0.104	0.086	0.095
(Alvi+Ti)/(Alvi+Ti+Fe+Mg)	0.167	0.176	0.143	0.160	0.148	0.175	0.153	0.164	0.165	0.159	0.168	0.152	0.163	0.162	0.182	0.189	0.133	0.150	0.122	0.132
Na+K	1.913	1.807	1.700	1.861	1.853	1.850	1.818	1.801	1.782	1.854	1.780	1.801	1.915	1.823	1.912	1.885	1.816	1.796	1.801	1.850
Na/K	*0.017*	*0.023*	*0.013*	*0.014*	*0.025*	*0.024*	*0.012*	*0.013*	*0.018*	*0.019*	*0.008*	*0.01:*	*0.025*	*0.006*	*0.018*	*0.014*	*0.063*	*0.053*	*0.046*	*0.052*
X	-209.19	-61.13	-61.13	-47.49	-47.64	-47.90	-45.64	-55.93	-52.02	-52.02	-51.28	-50.22	-220.52	-213.27	-215.62	-157.26	-61.65	-76.67	-111.21	-130.34
Y	357.95	272.84	272.84	360.00	361.53	363.10	352.96	247.05	245.91	236.43	236.07	235.54	352.12	355.24	358.54	371.59	239.49	249.58	98.21	120.10
x-axis (mm)				0.00	0.15	0.31				0.00	0.08	0.20								
location	*near gt*	*adj gt*	*adj gt*	*matrix*	*matrix*	*matrix*	*matrix*	*matrix*	*matrix*	*matrix*	*matrix*	*matrix*	*matrix*	*matrix*	*matrix*	*leuco*	*matrix*	*matrix*	*adj gt*	*adj gt*

TABLE B-2: Quantitative Microprobe Analysis for Biotite Compositions

	PC-66A						***PC-68A***												***PC-80B***	
	B1	**B3b**	**B4a**	**B4b**	**B4c**	**B7**	**B1**	**B2**	**B3**	**B4**	**B5b**	**B5c**	**B5d**	**B6**	**B7**	**B8**	**B9**	**B10**	**1B5**	**1B6**
WEIGHT PERCENT OXIDES																				
SiO2	34.810	35.249	35.403	35.390	35.388	35.435	35.105	34.869	34.550	34.026	34.917	34.494	34.754	34.881	35.156	34.667	34.628	34.335	35.736	36.606
Al2O3	18.080	17.150	16.920	16.768	16.525	17.378	18.649	19.591	19.202	19.036	18.826	19.167	19.322	19.009	19.389	19.043	19.681	19.051	16.917	17.114
TiO2	1.023	2.300	2.173	2.264	2.302	2.390	2.110	2.398	2.408	2.361	2.211	2.150	1.977	2.270	2.243	2.517	2.418	2.274	2.302	2.280
MgO	4.082	4.527	4.908	4.654	4.800	4.710	5.299	5.288	5.031	4.911	5.021	5.271	5.320	5.646	5.561	5.082	5.498	5.502	8.350	8.681
FeO	29.991	27.904	28.280	28.585	28.635	28.719	27.787	26.621	27.293	28.112	26.622	27.069	26.089	26.790	26.033	26.937	27.290	26.755	23.299	22.308
MnO	0.344	0.217	0.378	0.312	0.290	0.427	0.016	0.044	0.016	0.066	0.027	0.055	0.116	0.000	0.116	0.011	0.071	0.000	0.079	0.065
CaO	0.007	0.085	0.083	0.090	0.083	0.013	0.043	0.005	0.022	0.025	0.002	0.052	0.043	0.007	0.023	0.000	0.000	0.013	0.021	0.040
Na2O	0.034	0.036	0.075	0.065	0.082	0.132	0.190	0.179	0.207	0.157	0.239	0.248	0.113	0.197	0.283	0.235	0.232	0.233	0.138	0.138
K2O	8.911	9.152	9.048	9.227	9.351	9.386	9.216	9.310	9.091	8.886	8.893	9.080	9.013	8.655	9.001	9.019	8.857	8.771	8.851	8.820
Cr2O3	0.037	0.030	0.021	0.000	0.026	0.033	0.011	0.000	0.083	0.000	0.009	0.000	0.000	0.000	0.055	0.005	0.000	0.048	0.000	0.016
Cl	0.020	0.000	0.069	0.037	0.034	0.066	0.086	0.035	0.049	0.075	0.095	0.049	0.066	0.000	0.012	0.009	0.023	0.049	0.014	0.001
F	0.115	0.186	0.169	0.290	0.194	0.188	0.202	0.171	0.049	0.109	0.034	0.147	0.201	0.079	0.179	0.153	0.130	0.120	0.114	0.324
TOTAL	*97.454*	*96.836*	*97.527*	*97.682*	*97.710*	*98.877*	*98.714*	*98.511*	*98.001*	*97.764*	*96.896*	*97.782*	*97.014*	*97.534*	*98.051*	*97.678*	*98.828*	*97.151*	*95.821*	*96.393*
-O = Cl	-0.005	0.000	-0.016	-0.008	-0.008	-0.015	-0.019	-0.008	-0.011	-0.017	-0.021	-0.011	-0.015	0.000	-0.003	-0.002	-0.005	-0.011	-0.003	-0.000
-O = F	-0.048	-0.078	-0.071	-0.122	-0.082	-0.079	-0.085	-0.072	-0.021	-0.046	-0.014	-0.062	-0.085	-0.033	-0.075	-0.064	-0.055	-0.051	-0.048	-0.136
TOTAL	**97.401**	**96.758**	**97.440**	**97.552**	**97.621**	**98.783**	**98.610**	**98.431**	**97.969**	**97.701**	**96.860**	**97.709**	**96.914**	**97.501**	**97.973**	**97.612**	**98.768**	**97.089**	**95.770**	**96.256**
CATIONS RECALCULATED TO 22 OXYGENS																				
Si	5.457	5.518	5.515	5.523	5.523	5.461	5.377	5.317	5.311	5.272	5.405	5.317	5.370	5.354	5.363	5.338	5.267	5.311	5.512	5.578
Al	3.340	3.164	3.106	3.084	3.03:	3.156	3.367	3.521	3.479	3.476	3.434	3.482	3.518	3.439	3.486	3.456	3.528	3.473	3.075	3.074
Ti	0.121	0.271	0.255	0.266	0.270	0.277	0.243	0.275	0.278	0.275	0.257	0.249	0.230	0.262	0.257	0.292	0.277	0.265	0.267	0.261
Mg	0.954	1.056	1.140	1.083	1.117	1.082	1.210	1.202	1.153	1.134	1.159	1.211	1.225	1.292	1.265	1.166	1.247	1.269	1.920	1.972
Fe	3.932	3.653	3.684	3.730	3.737	3.701	3.559	3.395	3.508	3.643	3.446	3.489	3.371	3.439	3.321	3.468	3.471	3.461	3.005	2.843
Mn	0.046	0.029	0.04:	0.041	0.038	0.056	0.002	0.006	0.002	0.009	0.004	0.007	0.015	0.000	0.015	0.001	0.009	0.000	0.010	0.008
Ca	0.001	0.014	0.014	0.015	0.014	0.002	0.007	0.001	0.004	0.004	0.000	0.009	0.007	0.001	0.004	0.000	0.000	0.002	0.003	0.007
Na	0.010	0.011	0.023	0.01:	0.025	0.039	0.056	0.053	0.062	0.047	0.072	0.074	0.034	0.059	0.084	0.070	0.068	0.06:	0.041	0.041
K	1.782	1.828	1.798	1.837	1.862	1.845	1.801	1.811	1.783	1.756	1.756	1.785	1.776	1.695	1.752	1.772	1.719	1.731	1.741	1.715
Cr	0.005	0.004	0.003	0.000	0.003	0.004	0.001	0.000	0.010	0.000	0.001	0.000	0.000	0.000	0.007	0.001	0.000	0.006	0.000	0.002
TOTAL	**15.647**	**15.547**	**15.586**	**15.598**	**15.629**	**15.624**	**15.624**	**15.580**	**15.589**	**15.617**	**15.534**	**15.623**	**15.547**	**15.541**	**15.552**	**15.564**	**15.586**	**15.586**	**15.575**	**15.500**
Fe/Fe+Mg	*0.805*	*0.776*	*0.764*	*0.775*	*0.770*	*0.774*	*0.746*	*0.739*	*0.753*	*0.763*	*0.748*	*0.742*	*0.733*	*0.727*	*0.724*	*0.748*	*0.736*	*0.732*	*0.610*	*0.58:*
Mg/6	0.159	0.176	0.190	0.180	0.186	0.180	0.202	0.200	0.192	0.189	0.193	0.202	0.204	0.215	0.211	0.194	0.208	0.211	0.320	0.329
Fe/6	0.655	0.609	0.614	0.622	0.623	0.617	0.593	0.566	0.585	0.607	0.574	0.582	0.562	0.573	0.553	0.578	0.579	0.577	0.501	0.474
Ti/6	0.020	0.045	0.042	0.044	0.045	0.046	0.041	0.046	0.046	0.046	0.043	0.042	0.038	0.044	0.043	0.049	0.046	0.044	0.044	0.044
Alvi/6	0.133	0.114	0.104	0.101	0.094	0.103	0.124	0.140	0.132	0.125	0.140	0.133	0.148	0.132	0.141	0.132	0.133	0.131	0.098	0.109
(Alvi+Ti)/(Alvi+Ti+Fe+Mg)	0.158	0.168	0.154	0.153	0.146	0.158	0.171	0.195	0.186	0.176	0.192	0.182	0.196	0.182	0.194	0.190	0.185	0.181	0.148	0.159
Na+K	1.792	1.839	1.821	1.857	1.887	1.885	1.857	1.864	1.844	1.804	1.828	1.859	1.810	1.753	1.835	1.842	1.787	1.801	1.783	1.755
Na/K	*0.006*	*0.006*	*0.013*	*0.011*	*0.013*	*0.021*	*0.031*	*0.029*	*0.035*	*0.027*	*0.041*	*0.042*	*0.019*	*0.035*	*0.048*	*0.03:*	*0.03:*	*0.040*	*0.024*	*0.024*
X	-158.81	-176.16	-176.50	-175.76	-174.94	-73.44	164.64	153.56	159.58	168.73	82.46	82.83	83.06	76.30	64.86	61.61	49.67	45.63	41.82	41.64
Y	-343.48	-84.82	-69.24	-68.66	-67.73	-330.73	-211.46	-196.76	-239.22	-243.06	-82.02	-80.92	-79.82	-79.43	-72.97	-71.01	-321.83	-330.91	93.45	94.40
x-axis (mm)			0.00	0.09	0.22						0.00	0.12	0.23							
location	*adj gt*	*matrix*	*matrix*	*matrix*	*matrix*	*matrix*	*adj gt*	*near gt*	*near gt*	*±near gt*	*±near gt*	*±near gt*	*±near gt*	*matrix*	*matrix*	*matrix*	*matrix*	*matrix*	*±adj gt*	*near gt*

TABLE B-2: Quantitative Microprobe Analysis for Biotite Compositions

PC-80B continued					*PC-83A*					*PC-84C*						*PC-86D*			
	2B1	**2B2**	**mB3**	**mB5**	**bt2**	**bt4**	**bt5**	**bt7**	**bt7a**	**bt1**	**bt2**	**bt3**	**bt4**	**bt5**	**bt 6**	**B3**	**B7**	**BT1d**	**BT1e**
WEIGHT PERCENT OXIDES																			
SiO2	36.569	35.795	36.076	35.827	34.611	34.300	34.649	34.122	34.393	34.322	33.877	34.455	34.316	34.420	34.226	35.398	34.928	34.793	34.810
Al2O3	17.103	16.739	17.180	17.119	19.182	19.247	19.555	19.392	19.438	19.852	19.513	20.488	20.319	20.157	19.460	20.872	18.535	18.324	18.804
TiO2	2.466	2.288	2.312	2.298	2.566	2.346	2.314	2.605	2.599	2.576	2.404	2.633	2.847	2.465	2.949	0.421	3.373	3.311	3.299
MgO	8.757	8.584	8.581	7.966	7.412	7.591	7.767	7.517	7.702	7.233	7.291	7.607	7.329	7.359	7.258	8.490	6.563	6.210	6.365
FeO	22.486	23.160	23.925	23.763	21.978	22.483	22.022	22.204	22.303	21.915	22.694	21.086	21.727	22.201	22.364	21.090	23.921	24.922	23.488
MnO	0.147	0.091	0.140	0.036	0.248	0.150	0.184	0.225	0.170	0.214	0.300	0.153	0.223	0.303	0.248	0.000	0.055	0.016	0.116
CaO	0.053	0.080	0.007	0.016	0.024	0.040	0.013	0.020	0.011	0.000	0.000	0.049	0.029	0.000	0.031	0.057	0.125	0.067	0.079
Na2O	0.083	0.144	0.027	0.151	0.201	0.172	0.225	0.335	0.297	0.219	0.258	0.158	0.279	0.152	0.040	0.132	0.177	0.112	0.049
K2O	8.936	8.806	8.964	8.831	9.499	9.401	9.172	9.516	9.148	9.582	9.402	9.476	9.878	9.574	9.753	9.501	9.114	8.889	9.220
Cr2O3	0.032	0.032	0.059	0.000	0.000	0.095	0.032	0.026	0.000	0.012	0.025	0.060	0.000	0.058	0.081	0.000	0.037	0.005	0.000
Cl	0.020	0.011	0.042	0.006	0.097	0.108	0.148	0.105	0.085	0.077	0.043	0.054	0.054	0.085	0.071	0.032	0.034	0.020	0.037
F	0.156	0.271	0.245	0.178	0.305	0.334	0.185	0.233	0.349	0.084	0.274	0.118	0.242	0.144	0.172	0.123	0.100	0.071	0.100
TOTAL	*96.808*	*96.001*	*97.558*	*96.191*	*96.123*	*96.267*	*96.266*	*96.300*	*96.495*	*96.086*	*96.081*	*96.337*	*97.243*	*96.918*	*96.653*	*96.116*	*96.962*	*96.740*	*96.367*
-O = Cl	-0.005	-0.002	-0.009	-0.001	-0.022	-0.024	-0.033	-0.024	-0.019	-0.017	-0.00:	-0.012	-0.012	-0.019	-0.016	-0.007	-0.008	-0.005	-0.008
-O = F	-0.066	-0.114	-0.103	-0.075	-0.128	-0.141	-0.078	-0.098	-0.147	-0.035	-0.115	-0.04:	-0.102	-0.061	-0.072	-0.052	-0.042	-0.02:	-0.042
TOTAL	**96.738**	**95.884**	**97.445**	**96.115**	**95.973**	**96.102**	**96.155**	**96.178**	**96.329**	**96.033**	**95.956**	**96.275**	**97.129**	**96.838**	**96.565**	**96.057**	**96.912**	**96.706**	**96.317**
CATIONS RECALCULATED TO 22 OXYGENS																			
Si	5.551	5.517	5.483	5.514	5.328	5.287	5.308	5.255	5.274	5.271	5.239	5.245	5.217	5.248	5.250	5.376	5.348	5.355	5.353
Al	3.059	3.041	3.078	3.105	3.480	3.497	3.530	3.520	3.513	3.593	3.557	3.676	3.640	3.622	3.518	3.736	3.344	3.324	3.408
Ti	0.282	0.265	0.264	0.266	0.297	0.272	0.267	0.302	0.300	0.298	0.280	0.302	0.326	0.283	0.340	0.048	0.388	0.383	0.382
Mg	1.981	1.972	1.944	1.828	1.701	1.744	1.774	1.726	1.761	1.656	1.681	1.726	1.661	1.673	1.660	1.922	1.498	1.425	1.459
Fe	2.854	2.985	3.041	3.058	2.829	2.898	2.821	2.860	2.860	2.815	2.935	2.684	2.762	2.831	2.869	2.678	3.063	3.208	3.021
Mn	0.019	0.012	0.018	0.005	0.032	0.01:	0.024	0.029	0.022	0.028	0.039	0.01:	0.029	0.039	0.032	0.000	0.007	0.002	0.015
Ca	0.009	0.013	0.001	0.003	0.004	0.007	0.002	0.003	0.002	0.000	0.000	0.008	0.005	0.000	0.005	0.009	0.021	0.011	0.013
Na	0.024	0.043	0.008	0.045	0.060	0.051	0.067	0.100	0.088	0.065	0.077	0.047	0.082	0.045	0.012	0.039	0.053	0.033	0.015
K	1.730	1.731	1.738	1.734	1.865	1.849	1.792	1.870	1.790	1.877	1.855	1.840	1.916	1.862	1.909	1.841	1.780	1.745	1.809
Cr	0.004	0.004	0.007	0.000	0.000	0.012	0.004	0.003	0.000	0.001	0.003	0.007	0.000	0.007	0.00:	0.000	0.004	0.001	0.000
TOTAL	**15.514**	**15.583**	**15.583**	**15.557**	**15.597**	**15.637**	**15.588**	**15.667**	**15.609**	**15.605**	**15.667**	**15.555**	**15.637**	**15.609**	**15.606**	**15.648**	**15.506**	**15.488**	**15.473**
Fe/Fe+Mg	*0.58:*	*0.602*	*0.610*	*0.626*	*0.625*	*0.624*	*0.614*	*0.624*	*0.619*	*0.630*	*0.636*	*0.609*	*0.624*	*0.629*	*0.634*	*0.582*	*0.672*	*0.692*	*0.674*
Mg/6	0.330	0.329	0.324	0.305	0.283	0.291	0.296	0.288	0.293	0.276	0.280	0.288	0.277	0.279	0.277	0.320	0.250	0.237	0.243
Fe/6	0.476	0.498	0.507	0.510	0.472	0.483	0.46:	0.477	0.477	0.469	0.489	0.447	0.460	0.472	0.478	0.446	0.510	0.535	0.503
Ti/6	0.047	0.044	0.044	0.044	0.04:	0.045	0.044	0.050	0.050	0.04:	0.047	0.050	0.054	0.047	0.057	0.008	0.065	0.064	0.064
Alvi/6	0.102	0.093	0.094	0.103	0.135	0.131	0.140	0.129	0.131	0.144	0.133	0.154	0.143	0.145	0.128	0.185	0.115	0.113	0.127
(Alvi+Ti)/(Alvi+Ti+Fe+Mg)	0.156	0.142	0.142	0.153	0.196	0.185	0.194	0.190	0.190	0.206	0.189	0.217	0.211	0.204	0.197	0.201	0.192	0.187	0.203
Na+K	1.755	1.774	1.746	1.779	1.925	1.900	1.859	1.970	1.878	1.943	1.932	1.887	1.998	1.907	1.921	1.880	1.833	1.779	1.823
Na/K	*0.014*	*0.025*	*0.005*	*0.026*	*0.032*	*0.028*	*0.037*	*0.054*	*0.049*	*0.035*	*0.042*	*0.025*	*0.043*	*0.024*	*0.006*	*0.021*	*0.029*	*0.019*	*0.008*
X	-118.50	-108.92	-118.50	-108.92	-107.27	-38.56	-39.06	-30.91	-38.66	80.99	62.30	68.88	68.91	68.60	156.19	73.34	194.72	85.29	86.29
Y	-113.34	-104.44	-113.34	-104.44	-249.12	-295.77	-291.61	-305.08	-304.86	-105.42	-231.89	-243.80	245.51	-252.25	-277.42	308.54	319.39	315.39	315.62
x-axis (mm)								0.00	0.78									0.00	0.10
location	*j hb, nr gt*	*nr gt*	*matrix*	*matrix*	*primary*	*cross*	*primary*	*primary*	*primary*	*primary*	*primary*	*primary*	*cross*	*cross*	*primary*	*adj gt*	*matrix*	*near gt*	*near gt*

TABLE B-2: Quantitative Microprobe Analysis for Biotite Compositions

PC-86D continued | ***PC-88A***

	BT1f	BT2a	BT2b	BT2c	BT2d	BT2h	BT4b	BT4c	BT5a	BT5b	BT5c	BT6a	BT6b	BT6c	BT6d	BT6e	BT6f	B8	B11	B12
WEIGHT PERCENT OXIDES																				
SiO2	34.290	35.090	35.074	35.056	34.919	34.917	34.46:	34.518	34.499	34.452	34.564	34.971	35.230	34.592	35.196	34.336	35.017	35.129	35.315	36.198
Al2O3	18.401	18.666	18.483	18.740	18.366	18.913	18.382	18.814	18.517	18.417	18.355	18.953	19.191	18.856	18.925	18.937	18.226	19.747	19.614	22.275
TiO2	3.174	2.848	3.467	3.526	3.420	3.164	3.189	3.368	3.308	3.213	3.268	3.444	3.576	3.576	3.646	3.360	3.344	0.016	0.080	0.042
MgO	6.538	6.817	6.273	6.297	6.386	6.527	6.039	6.211	6.307	6.095	5.729	6.310	6.385	6.314	6.526	6.174	6.432	9.995	8.037	8.767
FeO	24.593	23.818	24.297	24.327	23.859	23.701	24.560	24.149	24.716	24.659	25.015	22.808	22.927	23.871	24.143	23.993	24.154	21.800	23.482	19.320
MnO	0.044	0.077	0.129	0.005	0.099	0.085	0.060	0.217	0.000	0.044	0.049	0.000	0.000	0.000	0.055	0.014	0.036	0.000	0.050	0.053
CaO	0.058	0.059	0.043	0.047	0.052	0.027	0.049	0.022	0.054	0.002	0.025	0.070	0.011	0.074	0.070	0.067	0.088	0.086	0.079	0.034
Na2O	0.088	0.098	0.092	0.047	0.025	0.103	0.118	0.124	0.082	0.097	0.023	0.131	0.100	0.081	0.089	0.119	0.074	0.235	0.251	0.064
K2O	8.882	9.100	9.274	9.268	9.168	9.259	8.919	9.46:	8.798	9.162	9.374	9.295	9.272	9.321	9.505	8.904	9.204	8.684	9.356	10.015
Cr2O3	0.018	0.030	0.062	0.009	0.000	0.000	0.069	0.000	0.036	0.000	0.025	0.038	0.048	0.050	0.034	0.002	0.091	0.000	0.009	0.005
Cl	0.014	0.034	0.043	0.032	0.029	0.037	0.000	0.032	0.023	0.052	0.020	0.046	0.017	0.077	0.083	0.052	0.049	0.026	0.009	0.000
F	0.372	0.134	0.155	0.180	0.196	0.030	0.159	0.036	0.178	0.072	0.151	0.248	0.053	0.001	0.030	0.101	0.090	0.081	0.266	0.205
TOTAL	*96.472*	*96.771*	*97.392*	*97.534*	*96.519*	*96.763*	*96.014*	*96.961*	*96.518*	*96.265*	*96.598*	*96.314*	*96.810*	*96.813*	*98.302*	*96.059*	*96.805*	*95.799*	*96.548*	*96.978*
-O = Cl	-0.003	-0.008	-0.00:	-0.007	-0.007	-0.008	0.000	-0.007	-0.005	-0.012	-0.005	-0.010	-0.004	-0.017	-0.019	-0.012	-0.011	-0.006	-0.002	0.000
-O = F	-0.157	-0.056	-0.065	-0.076	-0.083	-0.013	-0.067	-0.015	-0.075	-0.030	-0.064	-0.104	-0.022	-0.000	-0.013	-0.043	-0.038	-0.034	-0.112	-0.086
TOTAL	**96.312**	**96.707**	**97.317**	**97.451**	**96.430**	**96.742**	**95.947**	**96.939**	**96.438**	**96.223**	**96.530**	**96.199**	**96.784**	**96.795**	**98.271**	**96.005**	**96.756**	**95.759**	**96.434**	**96.892**
CATIONS RECALCULATED TO 22 OXYGENS																				
Si	5.310	5.376	5.361	5.345	5.375	5.346	5.349	5.304	5.323	5.338	5.353	5.369	5.362	5.306	5.319	5.306	5.378	5.360	5.418	5.395
Al	3.358	3.370	3.329	3.367	3.332	3.413	3.362	3.407	3.368	3.363	3.350	3.430	3.443	3.409	3.371	3.449	3.299	3.551	3.547	3.913
Ti	0.370	0.328	0.399	0.404	0.396	0.364	0.372	0.389	0.384	0.374	0.381	0.398	0.409	0.413	0.414	0.391	0.386	0.002	0.009	0.005
Mg	1.509	1.557	1.429	1.431	1.465	1.490	1.397	1.423	1.451	1.408	1.323	1.444	1.449	1.444	1.46:	1.422	1.473	2.274	1.838	1.948
Fe	3.185	3.051	3.106	3.102	3.071	3.035	3.187	3.103	3.189	3.195	3.240	2.929	2.918	3.062	3.052	3.101	3.102	2.782	3.013	2.408
Mn	0.006	0.00:	0.017	0.001	0.013	0.011	0.008	0.028	0.000	0.006	0.006	0.000	0.000	0.000	0.007	0.002	0.005	0.000	0.007	0.007
Ca	0.00:	0.00:	0.007	0.008	0.009	0.004	0.008	0.004	0.009	0.000	0.004	0.012	0.002	0.012	0.011	0.011	0.015	0.014	0.013	0.005
Na	0.026	0.029	0.027	0.014	0.007	0.031	0.036	0.037	0.025	0.029	0.007	0.039	0.029	0.024	0.026	0.036	0.022	0.06:	0.075	0.019
K	1.755	1.778	1.808	1.803	1.800	1.809	1.766	1.856	1.732	1.811	1.852	1.821	1.800	1.824	1.833	1.755	1.803	1.690	1.831	1.904
Cr	0.002	0.004	0.007	0.001	0.000	0.000	0.008	0.000	0.004	0.000	0.003	0.005	0.006	0.006	0.004	0.000	0.011	0.000	0.001	0.001
TOTAL	**15.531**	**15.513**	**15.490**	**15.475**	**15.468**	**15.503**	**15.494**	**15.550**	**15.485**	**15.526**	**15.519**	**15.446**	**15.419**	**15.498**	**15.508**	**15.474**	**15.493**	**15.742**	**15.752**	**15.605**
Fe/Fe+Mg	*0.678*	*0.662*	*0.685*	*0.684*	*0.677*	*0.671*	*0.695*	*0.686*	*0.687*	*0.694*	*0.710*	*0.670*	*0.668*	*0.680*	*0.675*	*0.686*	*0.678*	*0.550*	*0.621*	*0.553*
Mg/6	0.252	0.259	0.238	0.239	0.244	0.248	0.233	0.237	0.242	0.235	0.220	0.241	0.241	0.241	0.245	0.237	0.245	0.379	0.306	0.325
Fe/6	0.531	0.509	0.518	0.517	0.512	0.506	0.531	0.517	0.532	0.533	0.540	0.488	0.486	0.510	0.509	0.517	0.517	0.464	0.502	0.401
Ti/6	0.062	0.055	0.066	0.067	0.066	0.061	0.062	0.065	0.064	0.062	0.064	0.066	0.068	0.069	0.069	0.065	0.064	0.000	0.002	0.001
Alvi/6	0.111	0.124	0.115	0.119	0.118	0.127	0.119	0.118	0.115	0.117	0.117	0.133	0.134	0.119	0.115	0.126	0.113	0.152	0.161	0.218
(Alvi+Ti)/(Alvi+Ti+Fe+Mg)	0.181	0.189	0.194	0.198	0.195	0.199	0.191	0.195	0.188	0.189	0.192	0.215	0.218	0.200	0.196	0.202	0.189	0.153	0.167	0.232
Na+K	1.781	1.808	1.836	1.816	1.808	1.839	1.801	1.893	1.756	1.840	1.859	1.860	1.82:	1.848	1.859	1.791	1.825	1.760	1.906	1.923
Na/K	*0.015*	*0.016*	*0.015*	*0.008*	*0.004*	*0.017*	*0.020*	*0.01:*	*0.014*	*0.016*	*0.004*	*0.021*	*0.016*	*0.013*	*0.014*	*0.020*	*0.012*	*0.041*	*0.041*	*0.00:*
X	87.28	59.32	60.22	61.12	62.02	65.62	113.50	112.08	77.14	76.29	75.44	191.16	192.29	193.42	194.54	195.67	196.80	-128.82	-110.04	-111.90
Y	315.37	331.00	331.23	331.34	331.69	332.61	259.28	259.20	228.29	228.28	228.27	317.88	317.65	317.43	317.20	316.98	316.75	-131.98	-96.83	-133.15
x-axis (m	0.20	0.00	0.09	0.18	0.28	0.65	0.00	0.14	0.00	0.09	0.17	0.00	0.12	0.23	0.34	0.46	0.58			
location	*near gt*	*±near gt*	*±near gt*	*±near gt*	*±near gt*	*±near gt*	*near gt*	*near gt*	*±near gt*	*±near gt*	*±near gt*	*matrix*	*matrix*	*matrix*	*matrix*	*matrix*	*matrix*	*adj gt*	*near gt*	*fracture*

TABLE B-2: Quantitative Microprobe Analysis for Biotite Compositions

PC-88A continued

	B13	B14	B16	B17	BT1a	BT1d	BT3b	BT3c	BT3d	BT3e	BT4a	BT4b	BT4c	BT4d	BT4e	BT4f	BT4g	BT4h	BT5a	BT5b
WEIGHT PERCENT OXIDES																				
SiO2	35.339	35.204	35.341	35.254	35.526	35.369	35.106	34.596	35.303	35.774	34.995	35.254	35.062	35.019	35.114	35.215	35.280	36.403	35.347	35.212
Al2O3	18.098	18.587	18.410	18.551	19.367	20.091	18.431	18.181	17.974	19.001	18.669	18.224	18.320	18.376	18.136	18.943	19.629	18.951	18.596	18.464
TiO2	3.810	3.769	3.463	3.709	0.058	0.066	3.400	3.663	3.614	3.086	2.888	3.638	3.517	3.492	3.718	3.586	3.400	3.529	3.424	3.660
MgO	6.392	6.547	6.607	6.394	9.125	8.699	6.216	6.332	6.194	5.905	7.005	6.414	6.448	6.375	6.239	6.077	5.981	5.761	6.437	6.054
FeO	24.749	24.472	23.572	23.489	23.058	22.307	23.816	24.245	24.560	23.411	23.608	23.721	23.949	24.330	24.591	23.744	22.748	22.159	23.566	23.566
MnO	0.066	0.060	0.107	0.044	0.014	0.019	0.019	0.058	0.000	0.044	0.028	0.085	0.028	0.063	0.049	0.077	0.069	0.110	0.077	0.080
CaO	0.065	0.022	0.013	0.034	0.140	0.061	0.076	0.038	0.031	0.032	0.092	0.018	0.000	0.013	0.018	0.034	0.009	0.916	0.007	0.043
Na2O	0.102	0.065	0.104	0.025	0.250	0.161	0.082	0.182	0.034	0.012	0.135	0.145	0.064	0.130	0.096	0.144	0.045	0.550	0.071	0.108
K2O	9.451	9.444	9.816	9.867	8.658	8.843	8.999	9.618	9.294	9.247	9.200	9.424	9.715	9.360	9.405	9.184	9.456	8.195	9.835	9.536
Cr2O3	0.018	0.030	0.041	0.027	0.000	0.007	0.000	0.100	0.000	0.027	0.071	0.018	0.000	0.052	0.052	0.007	0.089	0.022	0.021	0.086
Cl	0.000	0.023	0.020	0.017	0.029	0.029	0.026	0.009	0.026	0.032	0.009	0.000	0.032	0.006	0.014	0.011	0.032	0.060	0.003	0.054
F	0.212	0.091	0.164	0.097	0.413	0.456	0.132	0.114	0.070	0.000	0.092	0.163	0.166	0.085	0.122	0.098	0.185	0.031	0.088	0.216
TOTAL	*98.302*	*98.314*	*97.658*	*97.508*	*96.638*	*96.108*	*96.303*	*97.136*	*97.100*	*96.571*	*96.792*	*97.104*	*97.301*	*97.301*	*97.554*	*97.120*	*96.923*	*96.687*	*97.472*	*97.079*
-O = Cl	0.000	-0.005	-0.005	-0.004	-0.007	-0.007	-0.006	-0.002	-0.006	-0.007	-0.002	0.000	-0.007	-0.001	-0.003	-0.002	-0.007	-0.014	-0.001	-0.012
-O = F	-0.089	-0.038	-0.069	-0.041	-0.174	-0.192	-0.056	-0.048	-0.029	0.000	-0.039	-0.069	-0.06:	-0.036	-0.051	-0.041	-0.078	-0.013	-0.037	-0.091
TOTAL	**98.213**	**98.270**	**97.584**	**97.463**	**96.458**	**95.909**	**96.242**	**97.086**	**97.065**	**96.564**	**96.751**	**97.035**	**97.224**	**97.264**	**97.499**	**97.076**	**96.838**	**96.660**	**97.434**	**96.976**
CATIONS RECALCULATED TO 22 OXYGENS																				
Si	5.365	5.328	5.380	5.368	5.420	5.409	5.401	5.320	5.409	5.459	5.356	5.391	5.367	5.356	5.366	5.368	5.369	5.501	5.383	5.391
Al	3.238	3.315	3.303	3.329	3.483	3.621	3.342	3.295	3.246	3.417	3.368	3.285	3.305	3.312	3.266	3.403	3.521	3.375	3.338	3.331
Ti	0.435	0.429	0.397	0.425	0.007	0.008	0.393	0.424	0.417	0.354	0.333	0.418	0.405	0.402	0.427	0.411	0.389	0.401	0.392	0.421
Mg	1.447	1.477	1.499	1.451	2.076	1.983	1.426	1.451	1.415	1.343	1.598	1.462	1.471	1.453	1.421	1.381	1.357	1.298	1.461	1.382
Fe	3.142	3.097	3.001	2.991	2.942	2.853	3.064	3.118	3.147	2.987	3.022	3.034	3.066	3.112	3.143	3.027	2.895	2.800	3.001	3.017
Mn	0.008	0.008	0.014	0.006	0.002	0.002	0.002	0.008	0.000	0.006	0.004	0.011	0.004	0.008	0.006	0.00:	0.009	0.014	0.00:	0.010
Ca	0.011	0.004	0.002	0.006	0.023	0.00:	0.013	0.006	0.005	0.005	0.015	0.003	0.000	0.002	0.003	0.006	0.001	0.148	0.001	0.007
Na	0.030	0.019	0.031	0.007	0.074	0.048	0.025	0.054	0.010	0.004	0.040	0.043	0.019	0.039	0.028	0.043	0.013	0.161	0.021	0.032
K	1.831	1.823	1.906	1.917	1.685	1.725	1.766	1.887	1.817	1.800	1.796	1.839	1.897	1.826	1.834	1.786	1.836	1.580	1.911	1.862
Cr	0.002	0.004	0.005	0.003	0.000	0.001	0.000	0.012	0.000	0.003	0.009	0.002	0.000	0.006	0.006	0.001	0.011	0.003	0.003	0.010
TOTAL	**15.510**	**15.505**	**15.538**	**15.503**	**15.711**	**15.659**	**15.431**	**15.574**	**15.465**	**15.379**	**15.541**	**15.488**	**15.534**	**15.516**	**15.501**	**15.434**	**15.401**	**15.280**	**15.521**	**15.464**
Fe/Fe+Mg	*0.685*	*0.677*	*0.667*	*0.673*	*0.586*	*0.58:*	*0.682*	*0.682*	*0.690*	*0.690*	*0.654*	*0.675*	*0.676*	*0.682*	*0.689*	*0.687*	*0.681*	*0.683*	*0.673*	*0.686*
Mg/6	0.241	0.246	0.250	0.242	0.346	0.331	0.238	0.242	0.236	0.224	0.266	0.244	0.245	0.242	0.237	0.230	0.226	0.216	0.244	0.230
Fe/6	0.524	0.516	0.500	0.499	0.490	0.475	0.511	0.520	0.524	0.498	0.504	0.506	0.511	0.519	0.524	0.504	0.483	0.467	0.500	0.503
Ti/6	0.073	0.072	0.066	0.071	0.001	0.001	0.066	0.071	0.069	0.059	0.055	0.06:	0.068	0.067	0.071	0.069	0.065	0.067	0.065	0.070
Alvi/6	0.101	0.107	0.114	0.116	0.151	0.172	0.124	0.102	0.109	0.146	0.121	0.113	0.112	0.111	0.105	0.128	0.148	0.146	0.120	0.120
(Alvi+Ti)/(Alvi+Ti+Fe+Mg)	0.185	0.190	0.193	0.202	0.153	0.177	0.202	0.185	0.190	0.221	0.186	0.196	0.192	0.190	0.188	0.211	0.231	0.238	0.200	0.206
Na+K	1.861	1.843	1.937	1.924	1.759	1.773	1.791	1.941	1.827	1.804	1.837	1.882	1.916	1.865	1.862	1.828	1.849	1.741	1.932	1.894
Na/K	*0.016*	*0.011*	*0.016*	*0.004*	*0.044*	*0.028*	*0.014*	*0.029*	*0.006*	*0.002*	*0.022*	*0.023*	*0.010*	*0.021*	*0.016*	*0.024*	*0.007*	*0.102*	*0.011*	*0.017*
X	-90.81	-172.28	-188.12	-176.33	-118.92	-117.44	-88.62	-88.69	-88.76	-88.83	-76.42	-76.53	-76.65	-76.76	-76.88	-76.99	-77.11	-77.22	-78.77	-78.83
Y	-118.76	-304.26	-299.32	-323.41	-122.78	-121.32	-97.41	-96.65	-95.88	-95.11	-126.19	-127.42	-128.66	-129.89	-131.12	-132.35	-133.59	-134.82	-123.18	-121.52
x-axis (mm)					0.00	0.21	0.00	0.08	0.15	0.23	0.00	0.12	0.25	0.37	0.50	0.62	0.74	0.87	0.00	0.17
location	*leuco*	*hst mtrx*	*hst mtrx*	*hst mtrx*	*adj gt*	*adj gt*	*leuco*	*leuco*	*leuco*	*leuco*	*hst±nr gt*	*hst±nr gt*	*hst±nr gt*	*hst±nr gt*	*hst±nr gt*	*hst±nr gt*	*hst±nr gt*	*hst±nr gt*	*hst±nr gt*	*hst±nr gt*

TABLE B-2: Quantitative Microprobe Analysis for Biotite Compositions

PC-88A continued

PC-93A

	BT5c	BT5e	BT5f	BT6a	BT6b	BT6c	BT7b	BT7c	BT8a	BT8c	BT8e	B1	B2	B3	B4a	B4b	B4c	B5	B6	B7
WEIGHT PERCENT OXIDES																				
SiO2	34.935	34.527	35.057	35.202	35.448	35.156	34.863	34.709	35.335	35.506	35.233	35.131	35.936	35.547	36.252	36.073	36.111	35.993	35.588	36.241
Al2O3	18.222	18.604	18.553	19.343	19.406	18.556	18.390	18.086	18.913	18.429	18.553	18.040	18.127	17.282	17.045	17.159	16.738	16.861	16.811	16.871
TiO2	3.234	3.065	2.551	4.145	3.781	3.388	3.623	3.418	3.425	3.529	3.610	0.646	0.837	2.149	3.167	3.246	3.074	2.526	2.858	3.030
MgO	6.318	6.467	6.737	6.528	6.438	6.394	6.207	6.312	6.648	6.072	6.205	5.401	5.705	5.827	6.005	6.217	6.310	6.199	6.391	6.235
FeO	24.604	25.037	24.358	22.816	23.111	24.029	23.612	24.008	22.662	23.843	23.320	28.170	27.092	26.326	25.489	25.950	25.872	26.211	26.279	26.135
MnO	0.044	0.102	0.058	0.072	0.000	0.052	0.058	0.080	0.055	0.143	0.006	0.291	0.481	0.223	0.209	0.328	0.286	0.198	0.242	0.239
CaO	0.036	0.186	0.049	0.036	0.034	0.013	0.025	0.027	0.032	0.063	0.036	0.041	0.041	0.000	0.038	0.041	0.016	0.045	0.000	0.009
Na2O	0.128	0.082	0.117	0.020	0.077	0.032	0.107	0.142	0.052	0.000	0.111	0.158	0.035	0.069	0.004	0.107	0.168	0.064	0.063	0.050
K2O	8.838	9.062	8.872	9.789	9.730	9.302	9.530	9.378	9.345	9.447	9.390	9.088	9.114	8.909	9.673	9.332	9.479	9.392	9.293	9.394
Cr2O3	0.103	0.000	0.009	0.000	0.032	0.014	0.041	0.000	0.048	0.002	0.014	0.000	0.028	0.000	0.057	0.030	0.012	0.000	0.051	0.053
Cl	0.000	0.000	0.017	0.034	0.000	0.000	0.043	0.000	0.014	0.014	0.017	0.009	0.000	0.000	0.026	0.014	0.003	0.037	0.023	0.003
F	0.101	0.163	0.130	0.113	0.210	0.166	0.075	0.137	0.218	0.139	0.000	0.098	0.066	0.182	0.076	0.170	0.220	0.245	0.302	0.326
TOTAL	*96.563*	*97.295*	*96.508*	*98.098*	*98.267*	*97.102*	*96.574*	*96.297*	*96.747*	*97.187*	*96.495*	*97.073*	*97.462*	*96.514*	*98.041*	*98.667*	*98.289*	*97.771*	*97.901*	*98.586*
-O = Cl	0.000	0.000	-0.004	-0.008	0.000	0.000	-0.00:	0.000	-0.003	-0.003	-0.004	-0.002	0.000	0.000	-0.006	-0.003	-0.001	-0.008	-0.005	-0.001
-O = F	-0.043	-0.069	-0.055	-0.048	-0.088	-0.06:	-0.032	-0.058	-0.092	-0.059	0.000	-0.041	-0.028	-0.077	-0.032	-0.072	-0.093	-0.103	-0.127	-0.137
TOTAL	**96.520**	**97.226**	**96.449**	**98.043**	**98.179**	**97.032**	**96.533**	**96.239**	**96.652**	**97.125**	**96.491**	**97.02:**	**97.434**	**96.437**	**98.003**	**98.592**	**98.196**	**97.659**	**97.769**	**98.448**
CATIONS RECALCULATED TO 22 OXYGENS																				
Si	5.378	5.302	5.392	5.304	5.335	5.376	5.364	5.368	5.388	5.420	5.398	5.482	5.541	5.526	5.534	5.483	5.518	5.536	5.477	5.524
Al	3.306	3.367	3.363	3.435	3.442	3.344	3.335	3.297	3.399	3.316	3.350	3.318	3.294	3.166	3.066	3.074	3.015	3.057	3.049	3.031
Ti	0.374	0.354	0.295	0.46:	0.428	0.390	0.419	0.398	0.393	0.405	0.416	0.076	0.097	0.251	0.364	0.371	0.353	0.292	0.331	0.347
Mg	1.450	1.480	1.545	1.466	1.445	1.457	1.424	1.455	1.511	1.382	1.417	1.256	1.311	1.350	1.366	1.409	1.438	1.421	1.466	1.417
Fe	3.168	3.215	3.133	2.875	2.909	3.073	3.038	3.105	2.890	3.044	2.988	3.676	3.494	3.423	3.254	3.298	3.306	3.372	3.382	3.331
Mn	0.006	0.013	0.008	0.009	0.000	0.007	0.008	0.011	0.007	0.019	0.001	0.039	0.063	0.029	0.027	0.042	0.037	0.026	0.032	0.031
Ca	0.006	0.031	0.008	0.006	0.005	0.002	0.004	0.004	0.005	0.010	0.006	0.007	0.007	0.000	0.006	0.007	0.003	0.007	0.000	0.001
Na	0.038	0.024	0.035	0.006	0.023	0.009	0.032	0.043	0.015	0.000	0.033	0.048	0.011	0.021	0.001	0.032	0.04:	0.019	0.019	0.015
K	1.736	1.775	1.741	1.882	1.868	1.815	1.870	1.850	1.818	1.840	1.835	1.809	1.793	1.767	1.884	1.809	1.848	1.843	1.824	1.827
Cr	0.013	0.000	0.001	0.000	0.004	0.002	0.005	0.000	0.006	0.000	0.002	0.000	0.003	0.000	0.007	0.004	0.001	0.000	0.006	0.006
TOTAL	**15.475**	**15.561**	**15.519**	**15.452**	**15.459**	**15.474**	**15.498**	**15.532**	**15.433**	**15.436**	**15.445**	**15.711**	**15.614**	**15.533**	**15.509**	**15.528**	**15.569**	**15.574**	**15.586**	**15.531**
Fe/Fe+Mg	*0.686*	*0.685*	*0.670*	*0.662*	*0.668*	*0.678*	*0.681*	*0.681*	*0.657*	*0.688*	*0.678*	*0.745*	*0.727*	*0.717*	*0.704*	*0.701*	*0.697*	*0.703*	*0.698*	*0.702*
Mg/6	0.242	0.247	0.257	0.244	0.241	0.243	0.237	0.243	0.252	0.230	0.236	0.209	0.219	0.225	0.228	0.235	0.240	0.237	0.244	0.236
Fe/6	0.528	0.536	0.522	0.479	0.485	0.512	0.506	0.518	0.482	0.507	0.498	0.613	0.582	0.56:	0.542	0.550	0.551	0.562	0.564	0.555
Ti/6	0.062	0.059	0.049	0.078	0.071	0.065	0.06:	0.066	0.066	0.068	0.069	0.013	0.016	0.042	0.061	0.062	0.059	0.049	0.055	0.058
Alvi/6	0.114	0.111	0.126	0.123	0.130	0.120	0.116	0.111	0.131	0.123	0.125	0.133	0.139	0.115	0.100	0.093	0.089	0.099	0.088	0.093
(Alvi+Ti)/(Alvi+Ti+Fe+Mg)	0.187	0.179	0.183	0.218	0.217	0.197	0.200	0.189	0.211	0.205	0.209	0.151	0.163	0.165	0.173	0.165	0.157	0.156	0.150	0.160
Na+K	1.774	1.800	1.776	1.887	1.891	1.824	1.902	1.893	1.833	1.840	1.868	1.857	1.803	1.788	1.885	1.841	1.898	1.862	1.843	1.841
Na/K	*0.022*	*0.014*	*0.020*	*0.003*	*0.012*	*0.005*	*0.017*	*0.023*	*0.008*	*0.000*	*0.018*	*0.026*	*0.006*	*0.012*	*0.001*	*0.017*	*0.027*	*0.010*	*0.010*	*0.008*
X	-78.88	-78.99	-79.05	-93.56	-93.56	-93.56	-175.87	-175.88	-183.14	-182.83	-182.72	147.47	157.14	178.81	152.52	149.91	146.56	118.47	114.27	144.87
Y	-119.85	-116.52	-114.86	-159.58	-158.19	-156.80	-305.97	-307.11	-312.13	-309.66	-307.18	220.84	231.58	225.13	142.25	143.26	144.72	146.17	156.98	282.94
x-axis (m	0.33	0.67	0.83	0.00	0.14	0.28	0.00	0.11	0.00	0.25	0.50				0.00	0.28	0.65			
location	*hst±nr gt*	*hst±nr gt*	*hst±nr gt*	*leuco*	*leuco*	*leuco*	*hst mtrx*	*hst mtrx*	*hst mtrx*	*hst mtrx*	*hst mtrx*	*adj gt*	*adj gt*	*adj gt*	*matrix*	*matrix*	*matrix*	*matrix*	*matrix*	*matrix*

TABLE B-2: Quantitative Microprobe Analysis for Biotite Compositions

	PC-93A continued			***PC-104E***														***PC-104F***		
	B8	**B9**	**B10**	**B1a**	**B2b**	**BT2a**	**BT2b**	**BT2c**	**BT2d**	**BT2e**	**BT3a**	**BT3b**	**BT3c**	**BT4b**	**Bt1**	**Bt6**	**Bt7**	**B1**	**B2a**	**B3**
WEIGHT PERCENT OXIDES																				
SiO2	35.565	36.083	35.898	35.287	35.458	35.690	36.191	35.544	35.091	34.542	35.739	35.403	35.308	34.930	34.652	34.636	34.513	35.967	36.279	35.884
Al2O3	17.090	16.995	17.048	20.223	20.045	19.052	19.176	18.654	18.059	17.408	18.711	18.337	18.371	18.716	19.144	19.100	19.684	19.893	19.313	18.834
TiO2	2.821	3.057	2.733	1.370	2.376	3.476	3.687	3.548	3.522	3.134	3.754	3.780	3.730	3.575	2.808	2.625	2.46:	2.440	2.896	2.970
MgO	6.552	5.948	5.894	9.208	7.821	7.895	8.128	8.195	8.168	8.931	7.919	8.166	8.083	7.721	8.482	8.397	8.250	7.975	8.105	7.824
FeO	26.032	26.195	25.836	20.576	21.330	21.483	20.927	21.313	22.370	23.036	21.572	21.977	21.374	21.245	21.035	21.437	21.268	22.403	22.699	22.697
MnO	0.215	0.209	0.151	0.086	0.000	0.000	0.117	0.033	0.089	0.031	0.145	0.000	0.039	0.039	0.095	0.145	0.000	0.114	0.064	0.080
CaO	0.020	0.047	0.007	0.050	0.057	0.068	0.034	0.066	0.014	0.020	0.030	0.016	0.025	0.055	0.069	0.064	0.051	0.057	0.000	0.000
Na2O	0.133	0.131	0.053	0.159	0.182	0.070	0.119	0.237	0.211	0.080	0.185	0.051	0.116	0.199	0.112	0.050	0.212	0.154	0.201	0.167
K2O	9.278	9.311	9.453	8.888	9.727	9.310	9.292	9.568	9.405	9.302	9.537	9.296	9.466	9.118	9.272	9.162	9.448	9.038	9.483	8.929
Cr2O3	0.000	0.000	0.000	0.038	0.065	0.045	0.149	0.049	0.106	0.079	0.138	0.080	0.123	0.033	0.019	0.065	0.004	0.076	0.088	0.045
Cl	0.029	0.006	0.029	0.026	0.003	0.009	0.012	0.017	0.000	0.009	0.009	0.032	0.029	0.032	0.054	0.006	0.029	0.006	0.012	0.000
F	0.221	0.160	0.255	0.192	0.316	0.199	0.082	0.144	0.102	0.137	0.225	0.144	0.040	0.202	0.146	0.319	0.288	0.247	0.116	0.128
TOTAL	*97.956*	*98.142*	*97.357*	*96.103*	*97.380*	*97.297*	*97.914*	*97.368*	*97.137*	*96.709*	*97.964*	*97.282*	*96.704*	*95.865*	*95.888*	*96.006*	*96.217*	*98.370*	*99.256*	*97.558*
-O = Cl	-0.007	-0.001	-0.007	-0.006	-0.001	-0.002	-0.003	-0.004	0.000	-0.002	-0.002	-0.007	-0.007	-0.007	-0.012	-0.001	-0.007	-0.001	-0.003	0.000
-O = F	-0.093	-0.067	-0.107	-0.081	-0.133	-0.084	-0.035	-0.061	-0.043	-0.058	-0.095	-0.061	-0.017	-0.085	-0.062	-0.134	-0.121	-0.104	-0.049	-0.054
TOTAL	**97.856**	**98.073**	**97.243**	**96.016**	**97.246**	**97.211**	**97.877**	**97.304**	**97.094**	**96.649**	**97.867**	**97.214**	**96.681**	**95.773**	**95.814**	**95.870**	**96.089**	**98.265**	**99.204**	**97.504**
CATIONS RECALCULATED TO 22 OXYGENS																				
Si	5.457	5.517	5.536	5.342	5.345	5.372	5.387	5.358	5.335	5.303	5.362	5.351	5.358	5.346	5.301	5.307	5.276	5.362	5.374	5.401
Al	3.091	3.063	3.099	3.608	3.561	3.380	3.364	3.314	3.236	3.150	3.309	3.267	3.285	3.376	3.452	3.449	3.546	3.496	3.372	3.341
Ti	0.326	0.352	0.317	0.156	0.269	0.394	0.413	0.402	0.403	0.362	0.424	0.430	0.426	0.412	0.323	0.303	0.284	0.274	0.323	0.336
Mg	1.499	1.356	1.355	2.078	1.758	1.772	1.804	1.842	1.851	2.044	1.771	1.840	1.828	1.762	1.934	1.918	1.880	1.773	1.790	1.756
Fe	3.341	3.350	3.332	2.605	2.689	2.704	2.605	2.687	2.844	2.958	2.707	2.778	2.712	2.719	2.691	2.747	2.719	2.793	2.812	2.857
Mn	0.028	0.027	0.01:	0.011	0.000	0.000	0.015	0.004	0.012	0.004	0.018	0.000	0.005	0.005	0.012	0.019	0.000	0.014	0.008	0.010
Ca	0.003	0.008	0.001	0.008	0.009	0.011	0.005	0.011	0.002	0.003	0.005	0.003	0.004	0.009	0.011	0.011	0.008	0.009	0.000	0.000
Na	0.03:	0.039	0.016	0.047	0.053	0.020	0.034	0.069	0.062	0.024	0.054	0.015	0.034	0.059	0.033	0.015	0.063	0.044	0.058	0.049
K	1.816	1.816	1.860	1.717	1.871	1.788	1.764	1.840	1.824	1.822	1.825	1.792	1.832	1.780	1.810	1.791	1.843	1.719	1.792	1.715
Cr	0.000	0.000	0.000	0.005	0.008	0.005	0.018	0.006	0.013	0.00:	0.016	0.00:	0.015	0.004	0.002	0.008	0.000	0.009	0.010	0.005
TOTAL	**15.600**	**15.527**	**15.535**	**15.577**	**15.563**	**15.446**	**15.409**	**15.534**	**15.581**	**15.678**	**15.491**	**15.485**	**15.500**	**15.472**	**15.56:**	**15.565**	**15.619**	**15.493**	**15.537**	**15.471**
Fe/Fe+Mg	*0.690*	*0.712*	*0.711*	*0.556*	*0.605*	*0.604*	*0.591*	*0.593*	*0.606*	*0.591*	*0.604*	*0.602*	*0.597*	*0.607*	*0.582*	*0.589*	*0.591*	*0.612*	*0.611*	*0.619*
Mg/6	0.250	0.226	0.226	0.346	0.293	0.295	0.301	0.307	0.309	0.341	0.295	0.307	0.305	0.294	0.322	0.320	0.313	0.295	0.298	0.293
Fe/6	0.557	0.558	0.555	0.434	0.448	0.451	0.434	0.448	0.474	0.493	0.451	0.463	0.452	0.453	0.449	0.458	0.453	0.466	0.469	0.476
Ti/6	0.054	0.059	0.053	0.026	0.045	0.066	0.069	0.067	0.067	0.060	0.071	0.072	0.071	0.069	0.054	0.050	0.047	0.046	0.054	0.056
Alvi/6	0.091	0.097	0.106	0.158	0.151	0.125	0.125	0.112	0.095	0.075	0.112	0.103	0.107	0.120	0.125	0.126	0.137	0.143	0.124	0.124
(Alvi+Ti)/(Alvi+Ti+Fe+Mg)	0.153	0.165	0.169	0.191	0.209	0.204	0.209	0.192	0.172	0.140	0.196	0.185	0.191	0.202	0.189	0.185	0.194	0.199	0.188	0.190
Na+K	1.856	1.855	1.876	1.763	1.924	1.808	1.799	1.909	1.886	1.846	1.879	1.807	1.867	1.839	1.843	1.806	1.905	1.764	1.850	1.763
Na/K	*0.022*	*0.021*	*0.009*	*0.027*	*0.028*	*0.011*	*0.01:*	*0.038*	*0.034*	*0.013*	*0.029*	*0.008*	*0.019*	*0.033*	*0.018*	*0.008*	*0.034*	*0.026*	*0.032*	*0.028*
X	124.46	137.63	162.21	210.96	211.00	60.22	60.31	60.40	60.49	60.58	48.92	50.02	51.05	46.19	-86.11	-129.00	-124.77	185.30	169.71	173.11
Y	284.13	294.33	276.90	315.05	304.39	330.00	333.23	336.47	339.70	342.93	348.30	347.95	347.61	346.42	-67.92	-220.98	-224.20	-69.68	-66.63	-62.87
x-axis (mm)						0.00	0.32	0.65	0.97	1.29	0.00	0.12	0.22							
location	*matrix*	*matrix*	*matrix*	*adj gt*	*near gt*	*matrix*	*matrix*	*matrix*	*matrix*	*matrix*	*matrix*	*matrix*	*matrix*	*matrix*	*corona*	*corona*	*corona*	*matrix*	*matrix*	*matrix*

TABLE B-2: Quantitative Microprobe Analysis for Biotite Compositions

PC-104F continued						*PC-107F*													
	BT1c	**BT2a**	**BT2b**	**BT2c**	**BT3b**	**B1**	**B2**	**B5**	**B6**	**B8**	**B9**	**B10**	**B13**	**BT1a**	**BT1b**	**BT2b**	**BT2c**	**BT3d**	**BT4a**	**BT4b**
WEIGHT PERCENT OXIDES																				
SiO2	34.986	36.594	35.255	35.409	35.387	34.509	34.641	35.219	34.474	34.784	34.442	34.771	35.360	35.107	34.737	35.462	35.220	35.550	35.313	35.370
Al2O3	20.324	19.412	18.497	18.833	18.892	16.592	16.127	15.985	15.82:	15.749	15.623	15.906	15.694	15.945	15.573	15.709	15.815	15.824	16.279	16.141
TiO2	1.912	2.307	2.377	2.479	2.237	4.278	4.369	4.006	4.126	4.026	4.182	3.991	4.103	3.510	3.798	3.514	3.664	4.313	3.918	3.688
MgO	8.150	7.588	8.013	7.902	8.203	6.515	6.548	7.158	6.948	7.132	6.847	6.667	7.001	7.076	6.879	7.079	7.086	6.800	6.917	7.037
FeO	21.609	21.432	23.043	23.040	22.723	24.551	25.035	25.155	25.543	26.086	26.350	26.412	25.415	26.047	26.306	25.601	26.152	25.369	25.050	25.128
MnO	0.056	0.042	0.081	0.083	0.006	0.051	0.094	0.062	0.112	0.123	0.158	0.086	0.146	0.103	0.054	0.085	0.047	0.093	0.020	0.092
CaO	0.128	0.034	0.020	0.020	0.057	0.015	0.025	0.023	0.027	0.041	0.042	0.025	0.039	0.049	0.035	0.010	0.035	0.017	0.045	0.032
Na2O	0.143	0.079	0.071	0.181	0.179	0.125	0.011	0.088	0.083	0.171	0.067	0.179	0.089	0.110	0.090	0.093	0.085	0.020	0.158	0.101
K2O	8.817	9.261	9.332	8.977	9.070	9.293	9.482	8.893	8.937	8.811	8.677	9.023	8.998	8.926	8.901	8.950	8.941	8.959	9.014	9.023
Cr2O3	0.000	0.027	0.000	0.016	0.068	0.014	0.000	0.046	0.000	0.000	0.038	0.018	0.011	0.026	0.000	0.007	0.007	0.021	0.000	0.000
Cl	0.032	0.020	0.012	0.044	0.000	0.017	0.000	0.021	0.000	0.006	0.026	0.012	0.038	0.000	0.010	0.000	0.000	0.000	0.007	0.000
F	0.253	0.107	0.204	0.215	0.242	0.264	0.099	0.066	0.085	0.142	0.119	0.050	0.078	0.419	0.188	0.223	0.053	0.132	0.170	0.077
TOTAL	*96.410*	*96.903*	*96.905*	*97.199*	*97.064*	*96.224*	*96.431*	*96.722*	*96.165*	*97.071*	*96.571*	*97.140*	*96.972*	*97.318*	*96.571*	*96.733*	*97.105*	*97.098*	*96.891*	*96.689*
-O = Cl	-0.007	-0.005	-0.003	-0.00:	0.000	-0.004	0.000	-0.005	0.000	-0.001	-0.006	-0.003	-0.009	0.000	-0.002	0.000	0.000	0.000	-0.002	0.000
-O = F	-0.107	-0.045	-0.086	-0.091	-0.102	-0.111	-0.042	-0.028	-0.036	-0.05:	-0.050	-0.021	-0.033	-0.176	-0.079	-0.094	-0.022	-0.056	-0.072	-0.032
TOTAL	**96.296**	**96.853**	**96.816**	**97.099**	**96.962**	**96.109**	**96.389**	**96.689**	**96.129**	**97.00:**	**96.515**	**97.116**	**96.931**	**97.142**	**96.490**	**96.639**	**97.083**	**97.042**	**96.818**	**96.657**
CATIONS RECALCULATED TO 22 OXYGENS																				
Si	5.310	5.503	5.382	5.376	5.374	5.378	5.396	5.444	5.388	5.395	5.379	5.397	5.466	5.440	5.427	5.501	5.448	5.478	5.451	5.469
Al	3.636	3.440	3.328	3.370	3.381	3.048	2.961	2.912	2.916	2.879	2.876	2.910	2.859	2.912	2.867	2.872	2.883	2.874	2.961	2.941
Ti	0.218	0.261	0.273	0.283	0.256	0.502	0.512	0.466	0.485	0.46:	0.491	0.466	0.477	0.409	0.446	0.410	0.426	0.500	0.455	0.429
Mg	1.844	1.701	1.824	1.789	1.857	1.514	1.521	1.650	1.619	1.649	1.594	1.543	1.613	1.634	1.602	1.637	1.634	1.562	1.592	1.622
Fe	2.743	2.695	2.942	2.925	2.886	3.200	3.261	3.252	3.339	3.383	3.442	3.428	3.285	3.375	3.437	3.321	3.383	3.269	3.234	3.249
Mn	0.007	0.005	0.011	0.011	0.001	0.007	0.012	0.008	0.015	0.016	0.021	0.011	0.019	0.014	0.007	0.011	0.006	0.012	0.003	0.012
Ca	0.021	0.005	0.003	0.003	0.009	0.003	0.004	0.004	0.005	0.007	0.007	0.004	0.006	0.008	0.006	0.002	0.006	0.003	0.007	0.005
Na	0.042	0.023	0.021	0.053	0.053	0.038	0.003	0.026	0.025	0.051	0.020	0.054	0.027	0.033	0.027	0.028	0.026	0.006	0.047	0.030
K	1.707	1.777	1.817	1.739	1.757	1.848	1.884	1.754	1.782	1.743	1.729	1.787	1.774	1.764	1.774	1.771	1.764	1.761	1.775	1.780
Cr	0.000	0.003	0.000	0.002	0.008	0.002	0.000	0.006	0.000	0.000	0.005	0.002	0.001	0.003	0.000	0.001	0.001	0.003	0.000	0.000
TOTAL	**15.528**	**15.414**	**15.600**	**15.551**	**15.581**	**15.538**	**15.555**	**15.521**	**15.573**	**15.593**	**15.564**	**15.602**	**15.528**	**15.592**	**15.594**	**15.553**	**15.578**	**15.468**	**15.525**	**15.537**
Fe/Fe+Mg	*0.598*	*0.613*	*0.617*	*0.621*	*0.608*	*0.679*	*0.682*	*0.663*	*0.673*	*0.672*	*0.683*	*0.690*	*0.671*	*0.674*	*0.682*	*0.670*	*0.674*	*0.677*	*0.670*	*0.667*
Mg/6	0.307	0.284	0.304	0.298	0.309	0.252	0.253	0.275	0.270	0.275	0.266	0.257	0.269	0.272	0.267	0.273	0.272	0.260	0.265	0.270
Fe/6	0.457	0.449	0.490	0.488	0.481	0.533	0.544	0.542	0.556	0.564	0.574	0.571	0.548	0.563	0.573	0.553	0.564	0.545	0.539	0.542
Ti/6	0.036	0.044	0.046	0.047	0.043	0.084	0.085	0.078	0.081	0.078	0.082	0.078	0.07:	0.068	0.074	0.068	0.071	0.083	0.076	0.072
Alvi/6	0.158	0.157	0.118	0.124	0.126	0.071	0.059	0.059	0.051	0.046	0.043	0.051	0.054	0.059	0.049	0.062	0.055	0.059	0.069	0.068
(Alvi+Ti)/(Alvi+Ti+Fe+Mg)																				
	0.202	0.215	0.171	0.179	0.176	0.164	0.154	0.144	0.137	0.129	0.129	0.134	0.141	0.132	0.128	0.136	0.131	0.150	0.152	0.147
Na+K	1.749	1.800	1.838	1.792	1.810	1.886	1.888	1.780	1.807	1.795	1.749	1.840	1.801	1.797	1.801	1.799	1.790	1.767	1.822	1.810
Na/K	*0.025*	*0.013*	*0.012*	*0.031*	*0.030*	*0.020*	*0.002*	*0.015*	*0.014*	*0.029*	*0.012*	*0.030*	*0.015*	*0.019*	*0.015*	*0.016*	*0.014*	*0.003*	*0.027*	*0.017*
X	62.74	183.67	184.95	186.22	201.31	-198.61	-198.59	-201.57	-202.59	-189.19	-169.12	-171.13	-146.98	-195.16	-195.97	-195.55	-194.89	-202.60	-198.60	-199.95
Y	-298.47	-73.56	-72.68	-71.81	-69.20	-117.54	-113.96	-111.24	-111.24	-113.42	-123.91	-124.37	-132.53	-106.75	-106.34	-106.39	-105.80	-115.79	-115.30	-115.07
x-axis (mm)		0.00	0.16	0.31										0.00	0.09	0.00	0.09		0.00	0.14
location	*adj gt*	*matrix*	*matrix*	*matrix*	*matrix*	*near gt*	*near gt*	*near gt*	*near gt*	*near gt*	*±near gt*	*±near gt*	*±near gt*	*near gt*	*near gt*	*near gt*	*near gt*	*near gt*	*near gt*	*near gt*

TABLE B-2: Quantitative Microprobe Analysis for Biotite Compositions

	PC-107F continued				*PC-108C*														
	BT4c	**BT4d**	**BT4e**	**BT4f**	**BT1a**	**BT1b**	**BT1c**	**BT1d**	**BT2a**	**BT2b**	**BT2c**	**BT3a**	**BT3b**	**BT3c**	**BT3d**	**BT4b**	**BT4c**	**BT4d**	**BT5a**	**BT5b**
WEIGHT PERCENT OXIDES																				
SiO2	35.311	35.385	34.670	34.352	35.246	35.443	35.193	35.56:	34.954	35.647	35.669	35.527	35.401	35.595	36.148	35.571	35.737	35.915	35.622	35.340
Al2O3	15.752	15.650	15.861	15.898	19.493	18.577	18.534	18.645	18.153	18.706	18.860	18.226	18.075	18.231	18.543	18.225	18.126	17.966	18.343	18.102
TiO2	3.972	4.087	4.089	3.82:	3.597	3.793	3.872	3.640	3.223	3.220	3.273	3.754	3.851	3.751	3.749	3.665	3.896	3.838	3.843	3.746
MgO	6.938	6.849	6.928	6.794	7.339	7.287	7.255	7.132	7.46:	7.584	7.689	7.568	7.259	7.580	7.596	7.324	7.381	7.848	7.468	7.371
FeO	25.514	25.730	25.807	25.516	21.173	22.694	23.155	22.426	23.161	23.273	23.056	23.931	23.204	22.903	22.847	23.414	23.732	23.689	22.625	23.751
MnO	0.150	0.108	0.101	0.184	0.064	0.083	0.111	0.014	0.089	0.127	0.097	0.066	0.133	0.210	0.200	0.169	0.069	0.078	0.222	0.083
CaO	0.009	0.043	0.018	0.044	0.175	0.079	0.109	0.054	0.041	0.041	0.063	0.000	0.029	0.002	0.000	0.005	0.027	0.011	0.197	0.054
Na2O	0.000	0.128	0.025	0.101	0.114	0.052	0.156	0.200	0.041	0.047	0.145	0.122	0.145	0.115	0.064	0.067	0.097	0.089	0.003	0.115
K2O	9.171	9.009	9.002	9.159	9.007	9.138	9.449	8.928	9.56:	9.384	9.539	9.331	9.155	9.062	9.615	9.616	9.339	9.400	9.049	9.205
Cr2O3	0.000	0.001	0.056	0.018	0.076	0.076	0.000	0.000	0.014	0.043	0.079	0.081	0.088	0.067	0.070	0.057	0.000	0.000	0.020	0.036
Cl	0.004	0.025	0.014	0.000	0.318	0.338	0.381	0.359	0.291	0.390	0.306	0.357	0.320	0.355	0.277	0.326	0.369	0.231	0.343	0.332
F	0.176	0.137	0.078	0.160	0.225	0.319	0.296	0.143	0.464	0.370	0.292	0.226	0.304	0.255	0.475	0.385	0.252	0.237	0.568	0.337
TOTAL	*96.997*	*97.152*	*96.649*	*96.056*	*96.827*	*97.879*	*98.511*	*97.111*	*97.471*	*98.832*	*99.068*	*99.189*	*97.964*	*98.126*	*99.584*	*98.824*	*99.025*	*99.302*	*98.303*	*98.472*
-O = Cl	-0.001	-0.006	-0.003	0.000	-0.072	-0.076	-0.086	-0.081	-0.066	-0.088	-0.069	-0.081	-0.072	-0.080	-0.063	-0.074	-0.083	-0.052	-0.077	-0.075
-O = F	-0.074	-0.058	-0.033	-0.067	-0.095	-0.134	-0.125	-0.060	-0.195	-0.156	-0.123	-0.095	-0.128	-0.107	-0.200	-0.162	-0.106	-0.09:	-0.239	-0.142
TOTAL	**96.922**	**97.089**	**96.613**	**95.989**	**96.661**	**97.668**	**98.300**	**96.970**	**97.210**	**98.588**	**98.876**	**99.013**	**97.764**	**97.939**	**99.321**	**98.588**	**98.836**	**99.150**	**97.986**	**98.255**
CATIONS RECALCULATED TO 22 OXYGENS																				
Si	5.466	5.46:	5.395	5.390	5.340	5.363	5.320	5.400	5.354	5.364	5.345	5.337	5.371	5.376	5.388	5.368	5.371	5.374	5.379	5.350
Al	2.874	2.851	2.909	2.93:	3.481	3.313	3.302	3.336	3.277	3.317	3.331	3.227	3.232	3.245	3.258	3.241	3.211	3.168	3.264	3.230
Ti	0.463	0.475	0.479	0.452	0.410	0.432	0.440	0.416	0.371	0.364	0.369	0.424	0.439	0.426	0.420	0.416	0.440	0.432	0.436	0.427
Mg	1.601	1.578	1.607	1.589	1.658	1.644	1.635	1.614	1.706	1.701	1.718	1.695	1.642	1.707	1.688	1.648	1.654	1.751	1.681	1.664
Fe	3.303	3.326	3.358	3.348	2.683	2.872	2.927	2.847	2.967	2.929	2.889	3.007	2.944	2.893	2.848	2.955	2.983	2.964	2.857	3.007
Mn	0.01:	0.014	0.013	0.025	0.008	0.011	0.014	0.002	0.012	0.016	0.012	0.008	0.017	0.027	0.025	0.022	0.009	0.00:	0.028	0.011
Ca	0.001	0.007	0.003	0.007	0.028	0.013	0.018	0.009	0.007	0.007	0.010	0.000	0.005	0.000	0.000	0.001	0.004	0.002	0.032	0.009
Na	0.000	0.038	0.008	0.031	0.034	0.015	0.046	0.059	0.012	0.014	0.042	0.036	0.043	0.034	0.019	0.01:	0.028	0.026	0.001	0.034
K	1.811	1.777	1.787	1.833	1.741	1.764	1.822	1.729	1.870	1.801	1.824	1.788	1.772	1.746	1.828	1.851	1.791	1.794	1.743	1.778
Cr	0.000	0.000	0.007	0.002	0.009	0.009	0.000	0.000	0.002	0.005	0.009	0.00:	0.011	0.008	0.008	0.007	0.000	0.000	0.002	0.004
TOTAL	**15.540**	**15.537**	**15.566**	**15.618**	**15.392**	**15.434**	**15.523**	**15.411**	**15.577**	**15.518**	**15.549**	**15.532**	**15.476**	**15.461**	**15.482**	**15.528**	**15.492**	**15.520**	**15.424**	**15.512**
Fe/Fe+Mg	*0.674*	*0.678*	*0.676*	*0.678*	*0.618*	*0.636*	*0.642*	*0.638*	*0.635*	*0.633*	*0.627*	*0.639*	*0.642*	*0.629*	*0.628*	*0.642*	*0.643*	*0.629*	*0.630*	*0.644*
Mg/6	0.267	0.263	0.268	0.265	0.276	0.274	0.272	0.269	0.284	0.284	0.286	0.282	0.274	0.284	0.281	0.275	0.276	0.292	0.280	0.277
Fe/6	0.551	0.554	0.560	0.558	0.447	0.479	0.488	0.475	0.494	0.488	0.482	0.501	0.491	0.482	0.475	0.492	0.497	0.494	0.476	0.501
Ti/6	0.077	0.079	0.07:	0.075	0.068	0.072	0.073	0.069	0.062	0.061	0.062	0.071	0.073	0.071	0.070	0.069	0.073	0.072	0.073	0.071
Alvi/6	0.057	0.054	0.051	0.055	0.137	0.113	0.104	0.123	0.105	0.114	0.113	0.094	0.101	0.103	0.108	0.102	0.097	0.090	0.107	0.097
(Alvi+Ti)/(Alvi+Ti+Fe+Mg)	0.141	0.140	0.136	0.137	0.221	0.197	0.189	0.205	0.177	0.184	0.185	0.174	0.185	0.185	0.190	0.182	0.181	0.171	0.192	0.177
Na+K	1.811	1.815	1.795	1.864	1.774	1.779	1.868	1.788	1.882	1.815	1.866	1.824	1.815	1.780	1.847	1.871	1.819	1.820	1.744	1.812
Na/K	*0.000*	*0.022*	*0.004*	*0.017*	*0.019*	*0.009*	*0.025*	*0.034*	*0.007*	*0.008*	*0.023*	*0.01:*	*0.024*	*0.019*	*0.010*	*0.011*	*0.016*	*0.014*	*0.001*	*0.019*
X	-201.34	-202.66	-204.01	-205.37	148.52	151.76	155.00	158.24	147.16	144.39	141.62	112.10	113.76	115.35	116.98	101.27	99.09	96.91	67.51	68.43
Y	-114.95	-114.72	-114.53	-114.33	116.11	116.11	116.11	116.11	256.42	256.10	255.78	345.15	344.47	343.80	343.13	343.88	344.39	344.89	167.69	167.23
x-axis (m	0.28	0.41	0.55	0.68	0.00	0.32	0.65	0.97	0.00	0.28	0.56	0.00	0.18	0.35	0.53	0.00	0.22	0.45	0.00	0.10
location	*near gt*	*near gt*	*near gt*	*near gt*	*near gt*	*by corona*	*by corona*	*by corona*	*by corona*	*by corona*	*by corona*	*matrix*	*matrix*	*matrix*	*matrix*	*matrix*	*matrix*	*matrix*	*matrix*	*matrix*

TABLE B-2: Quantitative Microprobe Analysis for Biotite Compositions

PC-108C continued												*PC-109A*							*PC-110A*	
	BT5c	**BT6a**	**BT6b**	**BT6c**	**Bt1**	**Bt1b**	**Bt5**	**Bt6**	**Bt7**	**Bt11**	**Bt12**	**B2**	**B3a**	**B3b**	**B4a**	**B5**	**BT1b**	**BT1c**	**B1**	**B2a**
WEIGHT PERCENT OXIDES																				
SiO2	35.219	35.306	35.300	34.411	34.520	34.46:	34.262	33.993	34.779	34.711	34.893	35.955	35.887	35.880	35.701	35.467	35.409	35.690	35.807	35.279
Al2O3	18.244	18.472	18.467	18.233	18.323	18.596	18.077	17.851	19.510	18.811	18.935	18.043	18.272	17.979	18.149	18.298	17.792	18.274	18.026	17.647
TiO2	3.740	2.826	4.006	3.811	3.865	4.020	3.321	3.232	2.332	3.104	2.776	3.075	2.970	2.982	2.930	3.107	3.144	2.837	3.783	3.795
MgO	7.230	7.607	7.336	7.164	7.153	7.262	7.427	7.476	8.520	8.139	8.125	8.834	9.166	8.942	8.405	8.958	8.757	8.658	7.384	7.409
FeO	23.002	23.264	23.003	22.639	21.755	21.360	22.601	22.864	20.690	20.794	21.627	22.073	21.424	21.974	21.469	21.129	22.606	21.676	23.983	23.287
MnO	0.130	0.191	0.094	0.097	0.156	0.092	0.089	0.141	0.148	0.000	0.184	0.120	0.072	0.056	0.006	0.067	0.017	0.000	0.091	0.130
CaO	0.061	0.034	0.000	0.020	0.093	0.020	0.097	0.055	0.038	0.035	0.080	0.116	0.036	0.066	0.000	0.000	0.034	0.127	0.000	0.036
Na2O	0.027	0.034	0.097	0.172	0.071	0.054	0.162	0.139	0.112	0.000	0.053	0.127	0.071	0.074	0.000	0.055	0.043	0.104	0.105	0.093
K2O	9.601	9.511	9.339	9.129	9.430	9.595	9.254	9.695	9.509	9.795	9.739	9.257	9.444	9.400	9.216	9.516	9.140	9.137	9.396	9.237
Cr2O3	0.000	0.000	0.072	0.014	0.000	0.049	0.072	0.086	0.016	0.034	0.081	0.024	0.024	0.000	0.000	0.018	0.034	0.000	0.014	0.000
Cl	0.306	0.329	0.415	0.320	0.354	0.357	0.340	0.368	0.345	0.225	0.324	0.081	0.116	0.107	0.174	0.133	0.119	0.087	0.020	0.063
F	0.392	0.306	0.335	0.120	0.380	0.252	0.358	0.150	0.291	0.305	0.181	0.277	0.375	0.208	0.264	0.281	0.261	0.381	0.036	0.152
TOTAL	*97.952*	*97.880*	*98.464*	*96.130*	*96.100*	*96.127*	*96.060*	*96.050*	*96.290*	*95.953*	*96.998*	*97.982*	*97.857*	*97.668*	*96.314*	*97.029*	*97.356*	*96.971*	*98.645*	*97.128*
-O = Cl	-0.069	-0.074	-0.094	-0.072	-0.07:	-0.081	-0.077	-0.083	-0.078	-0.051	-0.073	-0.018	-0.026	-0.024	-0.039	-0.030	-0.027	-0.01:	-0.005	-0.014
-O = F	-0.165	-0.129	-0.141	-0.051	-0.160	-0.106	-0.151	-0.063	-0.123	-0.128	-0.076	-0.117	-0.158	-0.088	-0.111	-0.118	-0.110	-0.160	-0.015	-0.064
TOTAL	**97.718**	**97.677**	**98.229**	**96.007**	**95.860**	**95.93:**	**95.833**	**95.904**	**96.08:**	**95.774**	**96.849**	**97.847**	**97.673**	**97.556**	**96.164**	**96.881**	**97.219**	**96.791**	**98.625**	**97.04:**
CATIONS RECALCULATED TO 22 OXYGENS																				
Si	5.356	5.371	5.331	5.312	5.332	5.307	5.317	5.294	5.316	5.333	5.322	5.405	5.395	5.409	5.444	5.374	5.375	5.413	5.380	5.386
Al	3.270	3.312	3.287	3.317	3.336	3.375	3.306	3.276	3.515	3.406	3.404	3.197	3.237	3.195	3.262	3.268	3.183	3.267	3.192	3.175
Ti	0.428	0.323	0.455	0.443	0.449	0.466	0.388	0.379	0.268	0.359	0.318	0.348	0.336	0.338	0.336	0.354	0.359	0.324	0.428	0.436
Mg	1.639	1.725	1.652	1.649	1.647	1.667	1.718	1.736	1.942	1.864	1.847	1.980	2.054	2.00:	1.911	2.024	1.982	1.958	1.654	1.686
Fe	2.926	2.960	2.905	2.923	2.810	2.750	2.933	2.978	2.645	2.672	2.759	2.775	2.693	2.771	2.738	2.678	2.870	2.749	3.014	2.973
Mn	0.017	0.025	0.012	0.013	0.020	0.012	0.012	0.019	0.019	0.000	0.024	0.015	0.009	0.007	0.001	0.009	0.002	0.000	0.012	0.017
Ca	0.00:	0.006	0.000	0.003	0.015	0.003	0.016	0.009	0.006	0.006	0.013	0.019	0.006	0.011	0.000	0.000	0.006	0.021	0.000	0.006
Na	0.008	0.010	0.028	0.052	0.021	0.016	0.049	0.042	0.033	0.000	0.016	0.037	0.021	0.022	0.000	0.016	0.013	0.031	0.031	0.028
K	1.863	1.846	1.799	1.798	1.858	1.885	1.832	1.926	1.854	1.920	1.895	1.775	1.811	1.808	1.793	1.840	1.770	1.768	1.801	1.799
Cr	0.000	0.000	0.009	0.002	0.000	0.006	0.009	0.011	0.002	0.004	0.00:	0.003	0.003	0.000	0.000	0.002	0.004	0.000	0.002	0.000
TOTAL	**15.516**	**15.577**	**15.479**	**15.510**	**15.490**	**15.487**	**15.579**	**15.668**	**15.601**	**15.563**	**15.608**	**15.554**	**15.565**	**15.56:**	**15.485**	**15.564**	**15.564**	**15.529**	**15.512**	**15.504**
Fe/Fe+Mg	*0.641*	*0.632*	*0.638*	*0.639*	*0.630*	*0.623*	*0.631*	*0.632*	*0.577*	*0.589*	*0.599*	*0.584*	*0.567*	*0.580*	*0.589*	*0.56:*	*0.592*	*0.584*	*0.646*	*0.638*
Mg/6	0.273	0.288	0.275	0.275	0.275	0.278	0.286	0.289	0.324	0.311	0.308	0.330	0.342	0.335	0.318	0.337	0.330	0.326	0.276	0.281
Fe/6	0.488	0.493	0.484	0.487	0.468	0.458	0.489	0.496	0.441	0.445	0.460	0.463	0.449	0.462	0.456	0.446	0.478	0.458	0.502	0.495
Ti/6	0.071	0.054	0.076	0.074	0.075	0.078	0.065	0.063	0.045	0.05:	0.053	0.058	0.056	0.056	0.056	0.059	0.05:	0.054	0.071	0.073
Alvi/6	0.104	0.114	0.103	0.105	0.111	0.114	0.104	0.095	0.139	0.123	0.121	0.100	0.105	0.101	0.118	0.107	0.093	0.113	0.095	0.093
(Alvi+Ti)/(Alvi+Ti+Fe+Mg)	0.188	0.177	0.191	0.190	0.200	0.206	0.178	0.168	0.193	0.195	0.185	0.166	0.169	0.165	0.183	0.175	0.159	0.176	0.176	0.176
Na+K	1.871	1.856	1.828	1.849	1.880	1.901	1.881	1.968	1.888	1.920	1.911	1.812	1.832	1.82:	1.793	1.856	1.783	1.798	1.832	1.826
Na/K	*0.004*	*0.005*	*0.016*	*0.029*	*0.011*	*0.009*	*0.027*	*0.022*	*0.018*	*0.000*	*0.008*	*0.021*	*0.011*	*0.012*	*0.000*	*0.009*	*0.007*	*0.017*	*0.017*	*0.015*
X	69.34	69.25	73.53	77.80	-152.20	-152.34	-146.71	-147.21	-147.62	-154.99	-155.64	-104.12	-104.12	-104.08	-84.35	-81.04	-91.63	-90.88	-79.01	-81.14
Y	166.77	160.92	161.18	161.44	367.33	367.22	352.48	353.74	224.87	63.12	64.08	331.14	332.39	333.03	328.81	328.51	275.46	275.72	122.81	138.10
x-axis (m	0.20	0.00	0.43	0.86	0.00	0.02							0.00	0.06			0.00	0.08		0.00
location	*matrix*	*matrix*	*matrix*	*matrix*	*corona1*	*corona1*	*corona1*	*corona1*	*corona 2*	*corona 2*	*corona 2*	*matrix*	*matrix*	*matrix*	*matrix*	*matrix*	*adj. gt*	*adj. gt*	*matrix*	*matrix*

TABLE B-2: Quantitative Microprobe Analysis for Biotite Compositions

PC-110A continued

PC-111A

	B2b	B3a	B3b	BT1a	BT1b	BT1c	BT1d	BT2a	BT2b	BT2c	BT3a	BT3b	BT3c	BT4a	BT4b	BT4c	BT5b	B1b	B2a	B2b
WEIGHT PERCENT OXIDES																				
SiO2	35.251	35.146	35.364	35.118	35.708	35.674	35.931	36.056	35.522	35.305	36.102	35.814	35.981	35.684	36.362	35.692	35.701	36.004	34.364	35.299
Al2O3	17.628	17.417	17.738	18.002	17.987	18.136	17.975	18.906	18.798	18.609	18.119	18.316	18.335	17.667	17.977	18.331	18.359	19.378	18.829	19.281
TiO2	3.600	3.371	3.573	2.690	3.367	3.173	3.203	2.232	2.205	2.050	3.669	3.725	3.588	3.697	3.645	3.760	3.812	4.028	3.336	3.553
MgO	7.412	7.447	7.106	7.450	6.829	7.087	6.724	7.100	7.106	6.880	7.481	7.219	7.461	7.509	7.525	7.125	7.231	7.266	7.175	7.164
FeO	24.209	24.518	24.165	25.416	25.547	24.372	24.736	24.232	24.148	24.203	22.739	22.805	23.132	23.561	23.876	23.174	23.856	22.723	22.596	22.473
MnO	0.135	0.171	0.094	0.052	0.119	0.138	0.088	0.224	0.108	0.036	0.138	0.183	0.119	0.116	0.064	0.136	0.222	0.000	0.072	0.000
CaO	0.000	0.118	0.000	0.063	0.014	0.000	0.014	0.000	0.038	0.052	0.000	0.041	0.036	0.023	0.005	0.043	0.029	0.016	0.048	0.102
Na2O	0.067	0.134	0.097	0.160	0.092	0.173	0.157	0.064	0.141	0.088	0.093	0.008	0.114	0.042	0.061	0.099	0.058	0.139	0.018	0.109
K2O	9.154	9.417	9.388	8.834	9.438	9.170	9.556	9.391	9.421	9.009	9.337	9.912	9.808	9.629	9.213	9.294	9.449	9.321	9.137	9.162
Cr2O3	0.029	0.057	0.000	0.000	0.027	0.048	0.000	0.038	0.000	0.020	0.004	0.000	0.000	0.061	0.063	0.022	0.000	0.011	0.043	0.000
Cl	0.026	0.081	0.000	0.017	0.006	0.014	0.000	0.029	0.014	0.020	0.012	0.000	0.035	0.023	0.000	0.000	0.000	0.017	0.026	0.012
F	0.166	0.220	0.231	0.081	0.119	0.231	0.146	0.184	0.296	0.089	0.174	0.161	0.254	0.164	0.100	0.243	0.141	0.133	0.289	0.328
TOTAL	*97.677*	*98.097*	*97.756*	*97.883*	*99.253*	*98.216*	*98.530*	*98.456*	*97.797*	*96.361*	*97.868*	*98.184*	*98.863*	*98.176*	*98.891*	*97.919*	*98.858*	*99.036*	*95.933*	*97.483*
-O = Cl	-0.006	-0.018	0.000	-0.004	-0.001	-0.003	0.000	-0.007	-0.003	-0.005	-0.003	0.000	-0.008	-0.005	0.000	0.000	0.000	-0.004	-0.006	-0.003
-O = F	-0.06:	-0.093	-0.097	-0.034	-0.050	-0.097	-0.062	-0.078	-0.125	-0.038	-0.073	-0.068	-0.107	-0.069	-0.042	-0.102	-0.059	-0.056	-0.122	-0.138
TOTAL	**97.601**	**97.986**	**97.659**	**97.845**	**99.202**	**98.116**	**98.469**	**98.372**	**97.669**	**96.319**	**97.792**	**98.116**	**98.748**	**98.102**	**98.849**	**97.817**	**98.799**	**98.976**	**95.805**	**97.342**
CATIONS RECALCULATED TO 22 OXYGENS																				
Si	5.370	5.361	5.387	5.351	5.378	5.401	5.433	5.432	5.402	5.430	5.437	5.398	5.394	5.398	5.433	5.391	5.357	5.342	5.300	5.335
Al	3.165	3.131	3.184	3.233	3.193	3.236	3.203	3.357	3.369	3.373	3.216	3.253	3.240	3.150	3.166	3.263	3.247	3.389	3.423	3.434
Ti	0.412	0.387	0.409	0.308	0.381	0.361	0.364	0.253	0.252	0.237	0.416	0.422	0.405	0.421	0.410	0.427	0.430	0.450	0.387	0.404
Mg	1.683	1.693	1.614	1.692	1.533	1.599	1.516	1.595	1.611	1.578	1.679	1.622	1.667	1.693	1.676	1.604	1.617	1.607	1.650	1.614
Fe	3.084	3.127	3.078	3.239	3.218	3.086	3.128	3.053	3.071	3.113	2.864	2.874	2.900	2.981	2.983	2.927	2.993	2.820	2.915	2.840
Mn	0.017	0.022	0.012	0.007	0.015	0.018	0.011	0.029	0.014	0.005	0.018	0.023	0.015	0.015	0.008	0.017	0.028	0.000	0.009	0.000
Ca	0.000	0.019	0.000	0.010	0.002	0.000	0.002	0.000	0.006	0.009	0.000	0.007	0.006	0.004	0.001	0.007	0.005	0.003	0.008	0.017
Na	0.01:	0.03:	0.029	0.047	0.027	0.051	0.046	0.019	0.042	0.026	0.027	0.002	0.033	0.012	0.018	0.029	0.017	0.040	0.005	0.032
K	1.779	1.832	1.824	1.717	1.813	1.771	1.843	1.805	1.828	1.768	1.794	1.906	1.876	1.858	1.756	1.791	1.809	1.764	1.798	1.767
Cr	0.003	0.007	0.000	0.000	0.003	0.006	0.000	0.005	0.000	0.002	0.000	0.000	0.000	0.007	0.007	0.003	0.000	0.001	0.005	0.000
TOTAL	**15.533**	**15.620**	**15.538**	**15.606**	**15.563**	**15.528**	**15.546**	**15.546**	**15.596**	**15.542**	**15.450**	**15.508**	**15.536**	**15.538**	**15.458**	**15.459**	**15.503**	**15.415**	**15.500**	**15.443**
Fe/Fe+Mg	*0.647*	*0.649*	*0.656*	*0.657*	*0.677*	*0.659*	*0.674*	*0.657*	*0.656*	*0.664*	*0.630*	*0.639*	*0.635*	*0.638*	*0.640*	*0.646*	*0.649*	*0.637*	*0.639*	*0.638*
Mg/6	0.281	0.282	0.269	0.282	0.256	0.267	0.253	0.266	0.269	0.263	0.280	0.270	0.278	0.282	0.279	0.267	0.270	0.268	0.275	0.269
Fe/6	0.514	0.521	0.513	0.540	0.536	0.514	0.521	0.509	0.512	0.519	0.477	0.479	0.483	0.497	0.497	0.488	0.499	0.46:	0.486	0.473
Ti/6	0.069	0.065	0.068	0.051	0.064	0.060	0.061	0.042	0.042	0.03:	0.069	0.070	0.067	0.070	0.068	0.071	0.072	0.075	0.065	0.067
Alvi/6	0.089	0.082	0.095	0.097	0.095	0.106	0.106	0.131	0.129	0.134	0.109	0.108	0.106	0.091	0.09:	0.109	0.101	0.122	0.121	0.128
(Alvi+Ti)/(Alvi+Ti+Fe+Mg)	0.166	0.154	0.173	0.153	0.167	0.176	0.177	0.183	0.179	0.182	0.190	0.193	0.185	0.172	0.178	0.193	0.183	0.211	0.196	0.208
Na+K	1.799	1.872	1.853	1.765	1.840	1.822	1.889	1.824	1.869	1.794	1.821	1.908	1.909	1.870	1.774	1.820	1.826	1.804	1.803	1.798
Na/K	*0.011*	*0.022*	*0.016*	*0.028*	*0.015*	*0.029*	*0.025*	*0.010*	*0.023*	*0.015*	*0.015*	*0.001*	*0.018*	*0.007*	*0.010*	*0.016*	*0.009*	*0.023*	*0.003*	*0.018*
X	-80.52	-83.69	-83.32	-167.07	-166.91	-166.75	-166.59	-133.36	-132.81	-132.25	-58.98	-58.74	-58.51	-60.79	-60.35	-59.91	-76.17	-114.09	-193.61	-193.95
Y	136.96	112.52	114.42	205.21	202.26	199.30	196.35	233.35	233.71	234.07	231.29	232.75	234.20	219.59	217.99	216.38	116.72	-175.40	-39.37	-41.15
x-axis (m	0.13	0.00	0.19	0.00	0.30	0.59	0.89	0.00	0.07	0.13	0.00	0.15	0.29	0.00	0.17	0.33	0.00		0.00	0.18
location	*matrix*	*matrix*	*matrix*	*adj. gt*	*adj. gt*	*±adj. gt*	*±adj. gt*	*±adj. gt*	*adj. gt*	*adj. gt*	*matrix*	*matrix*	*matrix*	*matrix*	*matrix*	*matrix*	*matrix*	*adj gt*	*matrix*	*matrix*

TABLE B-2: Quantitative Microprobe Analysis for Biotite Compositions

	PC-111A continued										*PC-113C*									
	B3b	**B4b**	**BT1a**	**BT1b**	**BT1c**	**BT1d**	**BT1e**	**BT2a**	**BT2c**	**BT2d**	**B1**	**B2**	**B3**	**B4**	**B5**	**B6**	**B7**	**B8**	**B9**	**B10**
WEIGHT PERCENT OXIDES																				
SiO2	35.629	35.799	35.475	35.382	35.675	35.528	35.811	35.617	35.475	35.387	35.615	36.577	36.048	35.693	36.011	35.961	35.519	35.463	35.131	35.561
Al2O3	19.492	18.936	18.943	19.837	18.789	19.147	18.866	18.440	19.191	19.169	18.893	20.030	19.487	18.874	19.146	18.822	18.906	18.624	18.642	18.486
TiO2	3.510	3.489	3.670	3.154	3.338	3.721	3.533	3.457	3.567	3.580	3.032	1.998	3.430	3.135	3.207	3.599	3.513	3.344	3.255	3.364
MgO	6.923	6.913	6.987	7.110	7.217	7.122	7.043	7.181	6.956	7.265	9.295	10.850	8.863	9.045	9.416	8.988	9.325	8.820	8.873	8.829
FeO	22.730	23.083	21.932	22.014	22.785	22.800	22.807	22.448	22.625	22.597	19.978	18.866	20.689	20.647	20.146	20.616	20.720	20.901	20.660	20.528
MnO	0.000	0.033	0.014	0.156	0.100	0.000	0.033	0.000	0.111	0.044	0.000	0.010	0.009	0.004	0.000	0.066	0.000	0.010	0.000	0.019
CaO	0.048	0.027	0.000	0.045	0.016	0.016	0.000	0.041	0.050	0.052	0.049	0.001	0.014	0.024	0.008	0.024	0.024	0.017	0.023	0.028
Na2O	0.109	0.114	0.100	0.025	0.070	0.110	0.122	0.095	0.121	0.020	0.130	0.064	0.133	0.104	0.035	0.153	0.129	0.133	0.157	0.110
K2O	9.493	9.403	9.308	9.386	9.324	9.513	9.611	9.551	9.379	9.503	9.469	9.561	9.352	9.558	9.484	9.714	9.757	9.680	9.683	9.604
Cr2O3	0.045	0.000	0.065	0.033	0.087	0.029	0.060	0.000	0.000	0.090	0.000	0.030	0.053	0.000	0.095	0.084	0.041	0.028	0.074	0.076
Cl	0.009	0.000	0.000	0.003	0.029	0.000	0.035	0.041	0.000	0.026	0.000	0.000	0.007	0.003	0.008	0.000	0.001	0.013	0.010	0.022
F	0.325	0.300	0.246	0.047	0.298	0.204	0.310	0.226	0.250	0.262	0.339	0.361	0.285	0.345	0.328	0.244	0.311	0.052	0.241	0.271
TOTAL	*98.313*	*98.097*	*96.740*	*97.192*	*97.728*	*98.190*	*98.231*	*97.097*	*97.725*	*97.995*	*96.800*	*98.348*	*98.370*	*97.432*	*97.884*	*98.271*	*98.246*	*97.085*	*96.749*	*96.898*
-O = Cl	-0.002	0.000	0.000	-0.001	-0.007	0.000	-0.008	-0.009	0.000	-0.006	0.000	0.000	-0.002	-0.001	-0.002	0.000	-0.000	-0.003	-0.002	-0.005
-O = F	-0.137	-0.126	-0.104	-0.01:	-0.125	-0.086	-0.131	-0.095	-0.105	-0.110	-0.143	-0.152	-0.120	-0.145	-0.138	-0.103	-0.131	-0.022	-0.101	-0.114
TOTAL	**98.174**	**97.971**	**96.636**	**97.172**	**97.596**	**98.104**	**98.093**	**96.993**	**97.620**	**97.879**	**96.657**	**98.196**	**98.248**	**97.286**	**97.744**	**98.168**	**98.115**	**97.060**	**96.645**	**96.779**
CATIONS RECALCULATED TO 22 OXYGENS																				
Si	5.347	5.391	5.388	5.338	5.390	5.338	5.388	5.414	5.354	5.330	5.368	5.374	5.344	5.362	5.361	5.354	5.301	5.348	5.328	5.375
Al	3.448	3.361	3.391	3.527	3.345	3.391	3.346	3.303	3.413	3.403	3.356	3.469	3.405	3.342	3.359	3.302	3.326	3.310	3.332	3.293
Ti	0.396	0.395	0.419	0.358	0.379	0.421	0.400	0.395	0.405	0.406	0.344	0.221	0.382	0.354	0.359	0.403	0.394	0.379	0.371	0.382
Mg	1.549	1.552	1.582	1.599	1.625	1.595	1.580	1.627	1.565	1.631	2.088	2.377	1.959	2.026	2.08:	1.995	2.075	1.983	2.006	1.989
Fe	2.853	2.907	2.786	2.778	2.879	2.865	2.870	2.853	2.855	2.846	2.518	2.318	2.565	2.594	2.508	2.567	2.586	2.636	2.620	2.595
Mn	0.000	0.004	0.002	0.01:	0.013	0.000	0.004	0.000	0.014	0.006	0.000	0.001	0.001	0.001	0.000	0.008	0.000	0.001	0.000	0.002
Ca	0.008	0.004	0.000	0.007	0.003	0.003	0.000	0.007	0.008	0.008	0.008	0.000	0.002	0.004	0.001	0.004	0.004	0.003	0.004	0.005
Na	0.032	0.033	0.029	0.007	0.021	0.032	0.036	0.028	0.035	0.006	0.038	0.018	0.038	0.030	0.010	0.044	0.037	0.039	0.046	0.032
K	1.817	1.806	1.804	1.807	1.797	1.824	1.845	1.852	1.806	1.826	1.821	1.792	1.769	1.832	1.801	1.845	1.858	1.862	1.873	1.852
Cr	0.005	0.000	0.008	0.004	0.010	0.003	0.007	0.000	0.000	0.011	0.000	0.003	0.006	0.000	0.011	0.00:	0.005	0.003	0.009	0.009
TOTAL	**15.455**	**15.454**	**15.409**	**15.445**	**15.462**	**15.472**	**15.476**	**15.479**	**15.455**	**15.473**	**15.540**	**15.574**	**15.471**	**15.544**	**15.501**	**15.532**	**15.586**	**15.566**	**15.58:**	**15.534**
Fe/Fe+Mg	*0.648*	*0.652*	*0.638*	*0.635*	*0.639*	*0.642*	*0.645*	*0.637*	*0.646*	*0.636*	*0.547*	*0.494*	*0.567*	*0.562*	*0.546*	*0.563*	*0.555*	*0.571*	*0.566*	*0.566*
Mg/6	0.258	0.259	0.264	0.267	0.271	0.266	0.263	0.271	0.261	0.272	0.348	0.396	0.326	0.338	0.348	0.332	0.346	0.331	0.334	0.332
Fe/6	0.475	0.484	0.464	0.463	0.480	0.478	0.478	0.476	0.476	0.474	0.420	0.386	0.427	0.432	0.418	0.428	0.431	0.439	0.437	0.432
Ti/6	0.066	0.066	0.06:	0.05:	0.063	0.070	0.067	0.066	0.068	0.068	0.057	0.037	0.064	0.059	0.05:	0.067	0.066	0.063	0.062	0.064
Alvi/6	0.132	0.125	0.130	0.144	0.123	0.122	0.122	0.119	0.128	0.122	0.121	0.140	0.125	0.117	0.120	0.109	0.105	0.110	0.110	0.111
(Alvi+Ti)/(Alvi+Ti+Fe+Mg)	0.213	0.205	0.215	0.218	0.198	0.205	0.203	0.199	0.210	0.203	0.188	0.185	0.200	0.186	0.190	0.188	0.180	0.184	0.182	0.186
Na+K	1.849	1.840	1.833	1.814	1.818	1.856	1.880	1.880	1.841	1.832	1.859	1.810	1.807	1.862	1.811	1.889	1.895	1.901	1.920	1.884
Na/K	*0.018*	*0.018*	*0.016*	*0.004*	*0.011*	*0.018*	*0.019*	*0.015*	*0.01:*	*0.003*	*0.021*	*0.010*	*0.022*	*0.017*	*0.006*	*0.024*	*0.020*	*0.021*	*0.025*	*0.017*
X	-181.25	-126.81	-197.93	-198.24	-198.56	-198.87	-199.19	-116.63	-117.90	-118.53	-71.10	-55.37	-52.24	-51.68	-47.30	-45.94	-49.25	-49.25	-71.64	-73.19
Y	-60.96	-63.09	-65.79	-67.50	-69.79	-71.80	-73.80	-62.49	-58.81	-56.97	367.86	370.06	369.07	367.20	361.07	358.77	352.63	351.63	357.91	357.47
x-axis (mm)			0.00	0.17	0.41	0.61	0.81	0.00	0.39	0.58										
location	*matrix*	*matrix*	*matrix*	*matrix*	*matrix*	*matrix*	*matrix*	*matrix*	*matrix*	*matrix*	*adj gt*	*adj gt*	*±adj gt*	*±adj gt*	*adj gt*	*±adj gt*	*adj gt*	*±adj gt*	*±adj gt*	*±adj gt*

TABLE B-2: Quantitative Microprobe Analysis for Biotite Compositions

PC-113C continued

	B11	B13	B14	B15	BT1a	BT1b	BT1c	BT1d	BT1e	BT1f	BT1g	BT1h	BT1i	BT1j	BT2a	BT2b	BT2c	BT2d	BT2e	BT3b
WEIGHT PERCENT OXIDES																				
SiO2	34.836	34.897	34.945	34.752	35.628	35.564	34.899	35.191	36.079	35.459	35.596	35.414	35.729	35.169	35.219	35.665	36.048	35.680	35.911	35.024
Al2O3	18.557	18.638	18.499	18.667	18.546	18.479	18.597	18.464	18.498	18.628	18.560	18.597	18.485	18.845	19.162	18.658	18.748	18.608	18.742	18.412
TiO2	4.102	3.836	3.814	3.854	3.153	3.537	3.413	3.567	3.633	3.704	3.640	3.623	3.732	3.546	3.651	3.635	3.551	3.492	3.526	3.460
MgO	8.664	8.540	8.650	8.617	9.275	8.562	8.068	8.523	8.596	8.599	8.410	8.555	8.265	8.795	8.257	8.742	8.740	8.573	8.636	8.504
FeO	20.033	20.919	20.832	21.428	20.916	21.211	22.871	21.509	21.747	21.189	20.762	21.140	21.018	20.324	20.080	20.845	21.289	21.109	20.855	20.841
MnO	0.094	0.010	0.023	0.053	0.037	0.055	0.004	0.076	0.000	0.014	0.000	0.065	0.029	0.000	0.092	0.026	0.000	0.058	0.043	0.017
CaO	0.021	0.021	0.008	0.000	0.055	0.023	0.048	0.029	0.061	0.018	0.030	0.038	0.028	0.016	0.016	0.037	0.005	0.015	0.046	0.045
Na2O	0.085	0.121	0.166	0.129	0.112	0.188	0.192	0.115	0.150	0.104	0.124	0.117	0.125	0.133	0.181	0.099	0.219	0.145	0.085	0.086
K2O	9.526	9.316	9.424	9.745	9.375	9.526	9.209	9.463	9.441	9.376	9.519	9.518	9.516	9.836	9.316	9.526	9.244	9.537	9.745	9.614
Cr2O3	0.064	0.005	0.048	0.027	0.052	0.064	0.041	0.033	0.061	0.056	0.090	0.080	0.021	0.040	0.044	0.056	0.031	0.039	0.090	0.047
Cl	0.004	0.000	0.000	0.000	0.000	0.011	0.021	0.006	0.008	0.000	0.000	0.015	0.020	0.013	0.017	0.000	0.006	0.000	0.017	0.014
F	0.292	0.271	0.223	0.273	0.287	0.249	0.258	0.248	0.211	0.361	0.349	0.356	0.237	0.191	0.320	0.315	0.291	0.259	0.301	0.266
TOTAL	*96.278*	*96.574*	*96.632*	*97.545*	*97.436*	*97.469*	*97.621*	*97.224*	*98.485*	*97.508*	*97.080*	*97.518*	*97.205*	*96.908*	*96.355*	*97.604*	*98.172*	*97.515*	*97.997*	*96.330*
-O = Cl	-0.001	0.000	0.000	0.000	0.000	-0.002	-0.005	-0.001	-0.002	0.000	0.000	-0.003	-0.005	-0.003	-0.004	0.000	-0.001	0.000	-0.004	-0.003
-O = F	-0.123	-0.114	-0.094	-0.115	-0.121	-0.105	-0.109	-0.104	-0.089	-0.152	-0.147	-0.150	-0.09:	-0.080	-0.135	-0.133	-0.123	-0.109	-0.127	-0.112
TOTAL	**96.154**	**96.460**	**96.538**	**97.430**	**97.315**	**97.362**	**97.508**	**97.118**	**98.394**	**97.356**	**96.933**	**97.365**	**97.101**	**96.825**	**96.216**	**97.471**	**98.048**	**97.406**	**97.866**	**96.215**
CATIONS RECALCULATED TO 22 OXYGENS																				
Si	5.298	5.301	5.305	5.255	5.356	5.358	5.290	5.326	5.376	5.338	5.374	5.338	5.387	5.315	5.337	5.354	5.374	5.366	5.372	5.342
Al	3.326	3.337	3.310	3.327	3.286	3.281	3.323	3.293	3.249	3.305	3.303	3.304	3.285	3.357	3.422	3.301	3.294	3.298	3.304	3.310
Ti	0.469	0.438	0.436	0.438	0.357	0.401	0.389	0.406	0.407	0.419	0.413	0.411	0.423	0.403	0.416	0.410	0.398	0.395	0.397	0.397
Mg	1.964	1.934	1.958	1.943	2.079	1.923	1.823	1.923	1.910	1.930	1.893	1.922	1.858	1.982	1.865	1.956	1.942	1.922	1.926	1.934
Fe	2.548	2.657	2.645	2.710	2.630	2.672	2.899	2.722	2.710	2.668	2.622	2.665	2.650	2.569	2.545	2.617	2.654	2.655	2.609	2.658
Mn	0.012	0.001	0.003	0.007	0.005	0.007	0.001	0.00:	0.000	0.002	0.000	0.008	0.004	0.000	0.012	0.003	0.000	0.007	0.005	0.002
Ca	0.003	0.003	0.001	0.000	0.009	0.004	0.008	0.005	0.00:	0.003	0.005	0.006	0.005	0.003	0.003	0.006	0.001	0.002	0.007	0.007
Na	0.025	0.036	0.049	0.038	0.033	0.055	0.056	0.034	0.043	0.030	0.036	0.034	0.037	0.039	0.053	0.029	0.063	0.042	0.025	0.025
K	1.848	1.805	1.825	1.880	1.798	1.831	1.781	1.827	1.795	1.801	1.834	1.82:	1.82:	1.896	1.801	1.824	1.758	1.82:	1.860	1.871
Cr	0.008	0.001	0.006	0.003	0.006	0.008	0.005	0.004	0.007	0.007	0.011	0.00:	0.003	0.005	0.005	0.007	0.004	0.005	0.011	0.006
TOTAL	**15.502**	**15.513**	**15.538**	**15.600**	**15.557**	**15.540**	**15.575**	**15.550**	**15.507**	**15.502**	**15.490**	**15.527**	**15.480**	**15.568**	**15.460**	**15.508**	**15.489**	**15.523**	**15.516**	**15.552**
Fe/Fe+Mg	*0.565*	*0.579*	*0.575*	*0.582*	*0.559*	*0.582*	*0.614*	*0.586*	*0.587*	*0.580*	*0.581*	*0.581*	*0.588*	*0.565*	*0.577*	*0.572*	*0.577*	*0.580*	*0.575*	*0.579*
Mg/6	0.327	0.322	0.326	0.324	0.346	0.320	0.304	0.320	0.318	0.322	0.315	0.320	0.310	0.330	0.311	0.326	0.324	0.320	0.321	0.322
Fe/6	0.425	0.443	0.441	0.452	0.438	0.445	0.483	0.454	0.452	0.445	0.437	0.444	0.442	0.428	0.424	0.436	0.442	0.443	0.435	0.443
Ti/6	0.078	0.073	0.073	0.073	0.059	0.067	0.065	0.068	0.068	0.06:	0.069	0.069	0.071	0.067	0.069	0.068	0.066	0.066	0.066	0.066
Alvi/6	0.104	0.106	0.103	0.097	0.107	0.107	0.102	0.103	0.104	0.107	0.113	0.107	0.112	0.112	0.127	0.109	0.111	0.111	0.113	0.109
(Alvi+Ti)/(Alvi+Ti+Fe+Mg)	0.195	0.190	0.186	0.180	0.175	0.185	0.175	0.181	0.183	0.188	0.195	0.187	0.195	0.191	0.210	0.189	0.188	0.188	0.191	0.186
Na+K	1.873	1.841	1.874	1.918	1.831	1.886	1.837	1.861	1.838	1.831	1.870	1.864	1.867	1.935	1.854	1.853	1.821	1.872	1.884	1.896
Na/K	*0.014*	*0.01:*	*0.027*	*0.020*	*0.018*	*0.030*	*0.032*	*0.019*	*0.024*	*0.017*	*0.01:*	*0.019*	*0.020*	*0.021*	*0.029*	*0.016*	*0.036*	*0.023*	*0.013*	*0.014*
X	-65.52	-48.60	-85.51	-89.63	-68.14	-67.73	-67.65	-67.28	-66.98	-66.79	-66.41	-66.13	-65.84	-65.55	-67.71	-67.04	-66.38	-65.78	-65.04	-53.04
Y	356.71	279.69	275.46	275.46	357.96	357.00	356.05	355.09	353.98	353.18	352.29	351.27	350.32	349.36	353.24	353.45	353.67	353.88	354.09	382.05
x-axis (mm)					0.00	0.10	0.20	0.30	0.42	0.50	0.60	0.70	0.80	0.90	0.00	0.07	0.14	0.20	0.28	0.00
location	*±adj gt*	*kfs incln*	*matrix*	*matrix*	*±adj gt*	*±adj gt*	*near gt*	*near gt*	*near gt*	*near gt*	*near gt*	*near gt*	*near gt*	*near gt*	*±adj gt*	*±adj gt*	*±adj gt*	*±adj gt*	*±adj gt*	*near gt*

TABLE B-2: Quantitative Microprobe Analysis for Biotite Compositions

PC-113C continued

	BT3c	BT3d	BT3e	BT3f	BT3g	BT3h	BT3i	BT3j	BT4a	BT4b	BT4c	BT4d	BT4e	BT5a	BT5b	BT5c	BT5d	BT5e	Bt2a	Bt3
WEIGHT PERCENT OXIDES																				
SiO2	35.522	34.904	35.543	35.311	35.335	35.619	35.181	35.303	35.361	35.446	35.657	35.438	35.464	35.524	35.533	35.960	35.853	35.578	35.141	34.789
Al2O3	19.163	18.667	18.706	18.820	18.744	18.786	18.582	19.243	18.513	18.662	18.696	18.850	19.000	19.277	18.905	18.873	18.909	18.82:	18.550	18.485
TiO2	3.585	3.608	3.588	3.756	3.652	3.752	3.790	3.702	3.652	3.809	3.642	3.796	3.710	2.792	3.270	3.391	3.466	3.397	3.688	3.748
MgO	8.324	8.557	8.499	8.602	8.565	8.374	8.546	8.170	8.754	8.597	8.679	8.496	8.637	9.997	9.192	8.812	8.807	8.933	8.880	8.612
FeO	20.363	20.891	20.970	20.656	20.976	20.58:	20.985	20.251	20.494	20.437	20.800	20.468	20.043	19.373	20.082	20.160	20.184	20.483	20.309	20.533
MnO	0.062	0.091	0.052	0.000	0.022	0.000	0.000	0.035	0.096	0.065	0.128	0.066	0.019	0.009	0.004	0.000	0.069	0.000	0.033	0.000
CaO	0.023	0.040	0.012	0.008	0.018	0.000	0.009	0.008	0.025	0.038	0.038	0.022	0.000	0.073	0.043	0.037	0.043	0.052	0.000	0.000
Na2O	0.064	0.086	0.111	0.119	0.094	0.119	0.088	0.062	0.084	0.101	0.158	0.122	0.161	0.115	0.087	0.120	0.162	0.159	0.091	0.146
K2O	9.377	9.676	9.686	9.564	9.587	9.547	9.584	9.597	9.650	9.654	9.776	9.729	9.650	9.527	9.428	9.611	9.494	9.864	9.433	9.643
Cr2O3	0.038	0.008	0.023	0.059	0.074	0.064	0.055	0.055	0.029	0.052	0.055	0.035	0.091	0.012	0.101	0.042	0.076	0.047	0.058	0.065
Cl	0.000	0.001	0.000	0.000	0.015	0.010	0.001	0.000	0.014	0.007	0.025	0.027	0.014	0.008	0.001	0.004	0.014	0.001	0.003	0.000
F	0.252	0.208	0.331	0.227	0.250	0.383	0.171	0.196	0.292	0.279	0.175	0.240	0.314	0.336	0.347	0.316	0.264	0.344	0.222	0.367
TOTAL	*96.773*	*96.737*	*97.521*	*97.122*	*97.332*	*97.244*	*96.992*	*96.622*	*96.964*	*97.147*	*97.829*	*97.289*	*97.103*	*97.043*	*96.993*	*97.326*	*97.341*	*97.688*	*96.408*	*96.388*
-O = Cl	0.000	-0.000	0.000	0.000	-0.003	-0.002	-0.000	0.000	-0.003	-0.002	-0.006	-0.006	-0.003	-0.002	-0.000	-0.001	-0.003	-0.000	-0.001	0.000
-O = F	-0.106	-0.088	-0.139	-0.096	-0.105	-0.161	-0.072	-0.083	-0.123	-0.117	-0.074	-0.101	-0.132	-0.141	-0.146	-0.133	-0.111	-0.145	-0.094	-0.155
TOTAL	**96.667**	**96.649**	**97.382**	**97.026**	**97.223**	**97.081**	**96.920**	**96.539**	**96.838**	**97.028**	**97.750**	**97.182**	**96.968**	**96.900**	**96.847**	**97.192**	**97.227**	**97.543**	**96.314**	**96.233**
CATIONS RECALCULATED TO 22 OXYGENS																				
Si	5.356	5.301	5.351	5.323	5.327	5.364	5.320	5.334	5.346	5.344	5.344	5.335	5.338	5.327	5.348	5.392	5.374	5.341	5.330	5.305
Al	3.405	3.341	3.319	3.344	3.330	3.334	3.312	3.427	3.299	3.316	3.303	3.344	3.370	3.407	3.353	3.335	3.341	3.331	3.316	3.322
Ti	0.407	0.412	0.406	0.426	0.414	0.425	0.431	0.421	0.415	0.432	0.411	0.430	0.420	0.315	0.370	0.382	0.391	0.384	0.421	0.430
Mg	1.871	1.937	1.907	1.933	1.925	1.880	1.927	1.840	1.973	1.932	1.939	1.907	1.938	2.235	2.062	1.970	1.968	1.999	2.008	1.958
Fe	2.567	2.654	2.640	2.604	2.644	2.593	2.654	2.559	2.591	2.577	2.607	2.577	2.523	2.429	2.528	2.528	2.530	2.571	2.576	2.618
Mn	0.008	0.012	0.007	0.000	0.003	0.000	0.000	0.004	0.012	0.008	0.016	0.008	0.002	0.001	0.001	0.000	0.009	0.000	0.004	0.000
Ca	0.004	0.007	0.002	0.001	0.003	0.000	0.001	0.001	0.004	0.006	0.006	0.004	0.000	0.012	0.007	0.006	0.007	0.008	0.000	0.000
Na	0.019	0.025	0.032	0.035	0.028	0.035	0.026	0.018	0.025	0.029	0.046	0.036	0.047	0.033	0.025	0.035	0.047	0.046	0.027	0.043
K	1.804	1.875	1.860	1.839	1.844	1.834	1.849	1.850	1.861	1.857	1.869	1.868	1.853	1.822	1.810	1.839	1.816	1.889	1.825	1.876
Cr	0.005	0.001	0.003	0.007	0.009	0.008	0.007	0.007	0.003	0.006	0.007	0.004	0.011	0.001	0.012	0.005	0.009	0.006	0.007	0.008
TOTAL	**15.444**	**15.565**	**15.528**	**15.513**	**15.525**	**15.474**	**15.527**	**15.462**	**15.530**	**15.507**	**15.548**	**15.513**	**15.502**	**15.582**	**15.517**	**15.492**	**15.491**	**15.575**	**15.514**	**15.560**
Fe/Fe+Mg	*0.578*	*0.578*	*0.581*	*0.574*	*0.579*	*0.580*	*0.579*	*0.582*	*0.568*	*0.571*	*0.573*	*0.575*	*0.566*	*0.521*	*0.551*	*0.562*	*0.562*	*0.563*	*0.562*	*0.572*
Mg/6	0.312	0.323	0.318	0.322	0.321	0.313	0.321	0.307	0.329	0.322	0.323	0.318	0.323	0.372	0.344	0.328	0.328	0.333	0.335	0.326
Fe/6	0.428	0.442	0.440	0.434	0.441	0.432	0.442	0.427	0.432	0.429	0.435	0.429	0.420	0.405	0.421	0.421	0.422	0.429	0.429	0.436
Ti/6	0.068	0.069	0.068	0.071	0.069	0.071	0.072	0.070	0.069	0.072	0.068	0.072	0.070	0.053	0.062	0.064	0.065	0.064	0.070	0.072
Alvi/6	0.127	0.107	0.112	0.111	0.109	0.116	0.105	0.127	0.108	0.110	0.108	0.113	0.118	0.122	0.117	0.121	0.119	0.112	0.108	0.104
(Alvi+Ti)/(Alvi+Ti+Fe+Mg)	0.208	0.187	0.191	0.194	0.190	0.201	0.188	0.212	0.189	0.195	0.189	0.198	0.202	0.184	0.189	0.198	0.197	0.188	0.189	0.188
Na+K	1.822	1.900	1.893	1.874	1.871	1.869	1.875	1.868	1.886	1.886	1.915	1.904	1.900	1.856	1.836	1.873	1.863	1.935	1.852	1.919
Na/K	*0.010*	*0.014*	*0.017*	*0.019*	*0.015*	*0.019*	*0.014*	*0.00:*	*0.013*	*0.016*	*0.025*	*0.019*	*0.025*	*0.018*	*0.014*	*0.019*	*0.026*	*0.025*	*0.015*	*0.023*
X	-52.42	-51.72	-51.16	-50.40	-49.74	-49.01	-48.41	-47.75	-50.57	-49.93	-49.29	-48.41	-48.00	-72.35	-72.57	-72.79	-73.01	-73.18	-126.21	-136.14
Y	380.83	379.73	378.63	377.52	376.25	375.32	374.22	373.12	374.51	375.00	375.48	375.96	376.44	365.50	365.65	365.81	365.97	366.13	359.15	386.53
x-axis (m	0.14	0.27	0.39	0.53	0.67	0.79	0.91	1.04	0.00	0.08	0.16	0.26	0.32	0.00	0.03	0.05	0.08	0.10		0.00
location	*near gt*	*near gt*	*near gt*	*near gt*	*near gt*	*near gt*	*near gt*	*near gt*	*near gt*	*near gt*	*near gt*	*near gt*	*near gt*	*adj gt*	*±adj gt*	*±adj gt*	*±adj gt*	*±adj gt*	*matrix*	*matrix*

TABLE B-2: Quantitative Microprobe Analysis for Biotite Compositions

PC-113C continued

	Bt3a	Bt4	Bt4a	Bt5	Bt5a	Bt6	Bt7	Bt7a	Bt7b
WEIGHT PERCENT OXIDES									
SiO2	34.489	34.836	35.022	34.507	34.978	34.905	34.628	34.650	34.511
Al2O3	19.047	18.492	18.543	18.202	18.289	18.179	18.550	18.345	18.445
TiO2	3.721	3.895	3.842	3.758	3.850	4.347	3.920	3.770	3.822
MgO	8.372	8.638	8.558	8.505	8.278	8.615	8.58:	8.658	8.921
FeO	20.492	21.058	21.182	21.170	21.840	20.875	20.767	21.157	21.065
MnO	0.000	0.150	0.056	0.028	0.036	0.000	0.078	0.084	0.033
CaO	0.016	0.038	0.000	0.011	0.000	0.000	0.000	0.000	0.018
Na2O	0.064	0.062	0.169	0.095	0.039	0.016	0.173	0.135	0.177
K2O	9.565	9.376	9.638	9.771	9.653	9.46:	9.415	9.717	9.834
Cr2O3	0.044	0.067	0.079	0.048	0.086	0.060	0.101	0.012	0.019
Cl	0.006	0.000	0.000	0.000	0.009	0.000	0.003	0.000	0.009
F	0.250	0.343	0.150	0.273	0.165	0.373	0.166	0.359	0.218
TOTAL	*96.066*	*96.955*	*97.239*	*96.368*	*97.223*	*96.840*	*96.391*	*96.887*	*97.072*
-O = Cl	-0.001	0.000	0.000	0.000	-0.002	0.000	-0.001	0.000	-0.002
-O = F	-0.105	-0.144	-0.063	-0.115	-0.06:	-0.157	-0.06:	-0.151	-0.092
TOTAL	**95.959**	**96.811**	**97.176**	**96.253**	**97.151**	**96.683**	**96.320**	**96.736**	**96.978**
CATIONS RECALCULATED TO 22 OXYGENS									
Si	5.266	5.286	5.294	5.285	5.307	5.299	5.273	5.278	5.243
Al	3.427	3.307	3.304	3.286	3.270	3.253	3.329	3.294	3.303
Ti	0.427	0.445	0.437	0.433	0.439	0.496	0.449	0.432	0.437
Mg	1.905	1.954	1.929	1.942	1.872	1.950	1.950	1.966	2.020
Fe	2.616	2.672	2.678	2.711	2.771	2.650	2.645	2.695	2.676
Mn	0.000	0.019	0.007	0.004	0.005	0.000	0.010	0.011	0.004
Ca	0.003	0.006	0.000	0.002	0.000	0.000	0.000	0.000	0.003
Na	0.019	0.018	0.04:	0.028	0.012	0.005	0.051	0.03:	0.052
K	1.863	1.815	1.859	1.909	1.868	1.834	1.829	1.888	1.906
Cr	0.005	0.008	0.009	0.006	0.010	0.007	0.012	0.001	0.002
TOTAL	**15.532**	**15.529**	**15.566**	**15.605**	**15.554**	**15.494**	**15.548**	**15.606**	**15.647**
Fe/Fe+Mg	*0.579*	*0.578*	*0.581*	*0.583*	*0.597*	*0.576*	*0.576*	*0.578*	*0.56:*
Mg/6	0.318	0.326	0.321	0.324	0.312	0.325	0.325	0.328	0.337
Fe/6	0.436	0.445	0.446	0.452	0.462	0.442	0.441	0.449	0.446
Ti/6	0.071	0.074	0.073	0.072	0.073	0.083	0.075	0.072	0.073
Alvi/6	0.115	0.099	0.09:	0.095	0.096	0.092	0.100	0.095	0.091
(Alvi+Ti)/(Alvi+Ti+Fe+Mg)	0.199	0.183	0.183	0.177	0.180	0.186	0.186	0.177	0.173
Na+K	1.882	1.833	1.908	1.937	1.880	1.839	1.880	1.928	1.958
Na/K	*0.010*	*0.010*	*0.027*	*0.015*	*0.006*	*0.003*	*0.028*	*0.021*	*0.027*
X	-136.72	-145.97	-147.00	-80.15	-79.33	-80.33	-102.62	-103.31	-104.09
Y	386.53	401.90	401.45	156.19	156.59	152.15	154.31	153.29	152.19
x-axis (m	0.06	0.00	0.11	0.00	0.09		0.00	0.12	0.26
location	*matrix*	*matrix*	*matrix*	*kfs incln*	*kfs incln*	*kfs incln*	*matrix*	*matrix*	*matrix*

PC-113E

	B1	B2	B3	B4	B5	B6	B7	B8	B9	B10
WEIGHT PERCENT OXIDES										
SiO2	34.398	34.804	34.910	35.236	41.028	34.960	35.235	36.007	36.512	34.592
Al2O3	19.514	19.120	19.486	19.663	17.307	19.362	18.482	19.668	20.856	18.796
TiO2	3.738	3.777	3.381	3.444	3.242	3.781	3.785	2.738	1.828	4.543
MgO	10.694	10.583	10.953	10.894	9.113	10.140	9.118	13.693	12.600	9.638
FeO	20.209	20.319	20.456	19.720	19.458	21.023	22.289	17.275	17.616	21.591
MnO	0.085	0.021	0.088	0.055	0.017	0.000	0.067	0.013	0.028	0.052
CaO	0.024	0.131	0.127	0.039	0.082	0.000	0.084	0.047	0.021	0.012
Na2O	0.216	0.485	0.268	0.206	0.239	0.219	0.219	0.236	0.234	0.154
K2O	10.790	10.354	9.872	10.360	9.231	10.174	10.410	9.892	9.984	10.405
Cr2O3	0.065	0.091	0.083	0.000	0.011	0.038	0.027	0.041	0.031	0.056
Cl	0.018	0.000	0.000	0.015	0.017	0.021	0.000	0.027	0.012	0.000
F	0.436	0.377	0.452	0.489	0.392	0.272	0.388	0.442	0.484	0.278
TOTAL	*100.187*	*100.062*	*100.076*	*100.121*	*100.137*	*99.990*	*100.104*	*100.079*	*100.206*	*100.117*
-O = Cl	-0.004	0.000	0.000	-0.003	-0.004	-0.005	0.000	-0.006	-0.003	0.000
-O = F	-0.184	-0.159	-0.190	-0.206	-0.165	-0.115	-0.163	-0.186	-0.204	-0.117
TOTAL	**99.999**	**99.903**	**99.886**	**99.912**	**99.968**	**99.871**	**99.941**	**99.887**	**99.999**	**99.000**
CATIONS RECALCULATED TO 22 OXYGENS										
Si	5.078	5.132	5.132	5.166	5.876	5.152	5.234	5.197	5.256	5.122
Al	3.395	3.323	3.376	3.398	2.921	3.363	3.236	3.346	3.538	3.280
Ti	0.415	0.419	0.374	0.380	0.349	0.419	0.423	0.297	0.198	0.506
Mg	2.353	2.326	2.400	2.381	1.946	2.228	2.019	2.947	2.704	2.127
Fe	2.495	2.506	2.515	2.418	2.330	2.591	2.769	2.085	2.121	2.674
Mn	0.011	0.003	0.011	0.007	0.002	0.000	0.008	0.002	0.003	0.007
Ca	0.004	0.021	0.020	0.006	0.013	0.000	0.013	0.007	0.003	0.002
Na	0.062	0.139	0.076	0.059	0.066	0.063	0.063	0.066	0.065	0.044
K	2.032	1.948	1.851	1.938	1.686	1.913	1.973	1.822	1.833	1.965
Cr	0.008	0.011	0.00:	0.000	0.001	0.004	0.003	0.005	0.004	0.007
TOTAL	**15.853**	**15.826**	**15.765**	**15.753**	**15.190**	**15.733**	**15.742**	**15.774**	**15.725**	**15.734**
Fe/Fe+Mg	*0.515*	*0.519*	*0.512*	*0.504*	*0.545*	*0.538*	*0.578*	*0.414*	*0.440*	*0.557*
Mg/6	0.392	0.388	0.400	0.397	0.324	0.371	0.337	0.491	0.451	0.355
Fe/6	0.416	0.418	0.419	0.403	0.388	0.432	0.461	0.348	0.353	0.446
Ti/6	0.069	0.06:	0.062	0.063	0.058	0.06:	0.071	0.04:	0.033	0.084
Alvi/6	0.079	0.076	0.085	0.094	0.133	0.086	0.078	0.091	0.132	0.067
(Alvi+Ti)/(Alvi+Ti+Fe+Mg)	0.155	0.153	0.152	0.164	0.211	0.162	0.157	0.143	0.171	0.159
Na+K	2.094	2.086	1.928	1.996	1.753	1.975	2.036	1.888	1.899	2.00:
Na/K	*0.030*	*0.071*	*0.041*	*0.030*	*0.039*	*0.033*	*0.032*	*0.036*	*0.036*	*0.023*
X	51.74	57.27	66.49	68.86	59.34	47.18	25.05	46.62	52.10	80.84
Y	-277.00	-282.18	-296.82	-309.21	-335.00	-343.01	-329.94	-325.13	-336.96	-281.13
x-axis (m										
location	*adj gt*	*adj gt*	*adj gt*	*adj gt*	*adj gt*	*adj gt*	*adj gt*	*gt incln*	*gt incln*	*near gt*

TABLE B-2: Quantitative Microprobe Analysis for Biotite Compositions

PC-113E continued

	B11	B12	B13	B14	BT1c	BT1d	BT1e	BT1f	BT1g	BT1h	BT1i	BT1j	BT1k	BT2a	BT2b	BT2c	BT2d	BT2e	BT3a
WEIGHT PERCENT OXIDES																			
SiO2	34.639	35.634	35.542	35.809	35.555	35.042	34.870	34.480	34.674	34.811	34.765	34.586	34.575	34.891	34.036	34.917	34.350	34.625	35.017
Al2O3	18.935	18.481	18.235	18.221	20.029	19.253	19.068	19.016	18.985	19.600	19.350	19.149	19.062	19.223	18.861	19.127	18.955	19.264	19.844
TiO2	4.146	3.633	3.829	3.924	4.594	4.347	4.151	4.313	4.364	4.201	4.198	4.388	4.452	4.395	4.489	4.216	4.550	4.305	3.515
MgO	9.677	8.418	8.758	8.788	8.813	9.285	9.533	9.663	9.568	9.553	9.663	9.682	9.699	9.024	9.645	9.252	9.515	9.507	9.997
FeO	21.925	21.479	21.019	21.085	20.153	20.739	21.786	21.640	21.119	21.237	21.366	20.997	21.872	21.690	21.82:	21.473	21.362	21.374	20.500
MnO	0.016	0.023	0.023	0.042	0.000	0.036	0.000	0.000	0.019	0.000	0.000	0.089	0.019	0.000	0.081	0.000	0.087	0.030	0.000
CaO	0.011	0.000	0.030	0.030	0.026	0.000	0.039	0.000	0.000	0.012	0.011	0.017	0.029	0.013	0.026	0.043	0.021	0.020	0.044
Na2O	0.184	0.148	0.181	0.148	0.185	0.174	0.147	0.205	0.177	0.191	0.143	0.213	0.199	0.159	0.177	0.176	0.157	0.262	0.166
K2O	10.021	9.401	9.595	9.298	10.259	10.843	10.020	10.215	10.736	10.063	10.069	10.507	9.728	10.314	10.494	10.369	10.630	10.157	10.588
Cr2O3	0.094	0.032	0.034	0.060	0.042	0.054	0.045	0.099	0.029	0.048	0.031	0.053	0.108	0.060	0.029	0.044	0.099	0.072	0.034
Cl	0.002	0.024	0.021	0.021	0.013	0.014	0.017	0.005	0.040	0.016	0.000	0.009	0.015	0.005	0.016	0.019	0.003	0.016	0.001
F	0.304	0.286	0.237	0.222	0.316	0.243	0.271	0.362	0.257	0.364	0.334	0.390	0.291	0.332	0.343	0.292	0.347	0.321	0.360
TOTAL	*99.954*	*97.559*	*97.504*	*97.648*	*99.985*	*100.030*	*99.947*	*99.998*	*99.968*	*100.096*	*99.930*	*100.080*	*100.049*	*100.106*	*100.027*	*99.928*	*100.076*	*99.953*	*100.066*
-O = Cl	-0.000	-0.005	-0.005	-0.005	-0.003	-0.003	-0.004	-0.001	-0.009	-0.004	0.000	-0.002	-0.003	-0.001	-0.004	-0.004	-0.001	-0.004	-0.000
-O = F	-0.128	-0.120	-0.09:	-0.094	-0.133	-0.102	-0.114	-0.152	-0.108	-0.153	-0.141	-0.164	-0.123	-0.140	-0.144	-0.123	-0.146	-0.135	-0.152
TOTAL	**99.826**	**97.433**	**97.399**	**97.550**	**99.849**	**99.925**	**99.829**	**99.844**	**99.851**	**99.939**	**99.789**	**99.914**	**99.923**	**99.965**	**99.879**	**99.801**	**99.929**	**99.814**	**99.914**
CATIONS RECALCULATED TO 22 OXYGENS																			
Si	5.133	5.365	5.352	5.371	5.207	5.173	5.157	5.112	5.138	5.131	5.135	5.118	5.109	5.159	5.066	5.169	5.098	5.123	5.155
Al	3.307	3.280	3.236	3.221	3.457	3.350	3.324	3.322	3.315	3.405	3.369	3.339	3.320	3.350	3.309	3.337	3.315	3.359	3.443
Ti	0.462	0.411	0.434	0.443	0.506	0.483	0.462	0.481	0.486	0.466	0.466	0.488	0.495	0.489	0.503	0.469	0.508	0.479	0.389
Mg	2.138	1.889	1.966	1.965	1.924	2.043	2.102	2.136	2.114	2.099	2.128	2.136	2.137	1.989	2.140	2.042	2.105	2.097	2.194
Fe	2.717	2.705	2.647	2.645	2.468	2.560	2.695	2.683	2.617	2.618	2.639	2.598	2.703	2.682	2.717	2.658	2.651	2.645	2.524
Mn	0.002	0.003	0.003	0.005	0.000	0.005	0.000	0.000	0.002	0.000	0.000	0.011	0.002	0.000	0.010	0.000	0.011	0.004	0.000
Ca	0.002	0.000	0.005	0.005	0.004	0.000	0.006	0.000	0.000	0.002	0.002	0.003	0.005	0.002	0.004	0.007	0.003	0.003	0.007
Na	0.053	0.043	0.053	0.043	0.053	0.04:	0.042	0.059	0.051	0.055	0.041	0.061	0.057	0.046	0.051	0.051	0.045	0.075	0.047
K	1.894	1.806	1.843	1.779	1.917	2.042	1.891	1.932	2.029	1.892	1.897	1.983	1.834	1.946	1.993	1.958	2.012	1.917	1.988
Cr	0.011	0.004	0.004	0.007	0.005	0.006	0.005	0.012	0.003	0.006	0.004	0.006	0.013	0.007	0.003	0.005	0.012	0.008	0.004
TOTAL	**15.719**	**15.506**	**15.542**	**15.484**	**15.541**	**15.712**	**15.683**	**15.736**	**15.756**	**15.672**	**15.681**	**15.744**	**15.675**	**15.669**	**15.797**	**15.695**	**15.760**	**15.710**	**15.751**
Fe/Fe+Mg	*0.560*	*0.589*	*0.574*	*0.574*	*0.562*	*0.556*	*0.562*	*0.557*	*0.553*	*0.555*	*0.554*	*0.549*	*0.559*	*0.574*	*0.559*	*0.566*	*0.557*	*0.558*	*0.535*
Mg/6	0.356	0.315	0.328	0.327	0.321	0.341	0.350	0.356	0.352	0.350	0.355	0.356	0.356	0.332	0.357	0.340	0.351	0.349	0.366
Fe/6	0.453	0.451	0.441	0.441	0.411	0.427	0.449	0.447	0.436	0.436	0.440	0.433	0.451	0.447	0.453	0.443	0.442	0.441	0.421
Ti/6	0.077	0.069	0.072	0.074	0.084	0.081	0.077	0.080	0.081	0.078	0.078	0.081	0.083	0.082	0.084	0.078	0.085	0.07:	0.065
Alvi/6	0.073	0.107	0.098	0.099	0.111	0.087	0.080	0.072	0.076	0.089	0.084	0.076	0.072	0.085	0.063	0.084	0.069	0.080	0.09:
(Alvi+Ti)/(Alvi+Ti+Fe+Mg)	0.157	0.187	0.181	0.183	0.210	0.179	0.164	0.160	0.166	0.175	0.169	0.166	0.160	0.176	0.153	0.172	0.162	0.169	0.173
Na+K	1.947	1.849	1.896	1.822	1.969	2.092	1.933	1.991	2.080	1.947	1.938	2.044	1.891	1.991	2.044	2.009	2.058	1.992	2.036
Na/K	*0.028*	*0.024*	*0.029*	*0.024*	*0.027*	*0.024*	*0.022*	*0.031*	*0.025*	*0.029*	*0.022*	*0.031*	*0.031*	*0.023*	*0.026*	*0.026*	*0.022*	*0.039*	*0.024*
X	81.47	113.45	131.33	128.64	73.65	74.09	74.45	74.82	75.18	75.55	75.86	76.04	76.65	72.08	73.24	74.40	75.56	76.72	67.93
Y	-347.87	-358.59	-356.94	-298.37	-287.99	-289.61	-291.23	-292.84	-294.46	-295.95	-297.60	-299.31	-300.93	-291.94	-291.81	-291.68	-291.40	-291.42	-330.92
x-axis (mm)					0.00	0.17	0.33	0.50	0.66	0.82	0.99	1.16	1.33	0.00	0.12	0.23	0.35	0.47	0.00
location	*near gt*	*matrix*	*matrix*	*matrix*	*near gt*	*near gt*	*near gt*	*near gt*	*near gt*	*near gt*	*near gt*	*near gt*	*near gt*	*near gt*	*near gt*	*near gt*	*near gt*	*near gt*	*adj gt*

TABLE B-2: Quantitative Microprobe Analysis for Biotite Compositions

PC-113E continued

	BT3b	BT3c	BT3d	BT3e	BT3f	BT3g	BT3h	BT4b	BT5b	BT5c	BT5d	BT6a	BT6b	BT6c	BT6d	BT7a	BT7b	BT7c	BT7d
WEIGHT PERCENT OXIDES																			
SiO2	35.325	35.359	35.154	34.633	34.683	34.454	34.640	35.989	35.943	35.290	35.407	34.784	36.292	36.053	35.597	35.027	35.558	35.357	35.765
Al2O3	19.768	19.322	19.230	19.309	19.449	19.599	19.531	18.379	18.214	18.285	18.301	18.008	18.750	17.906	18.228	18.542	18.755	18.234	18.582
TiO2	3.384	3.326	3.485	3.473	3.443	3.689	3.712	4.096	3.825	3.967	4.000	3.661	3.488	3.762	3.822	3.521	3.610	3.571	3.390
MgO	10.248	10.084	9.796	10.257	10.263	10.164	9.932	8.515	8.696	8.834	8.596	8.800	8.338	8.613	8.462	8.691	8.745	8.931	8.719
FeO	20.396	21.061	21.753	21.226	21.270	20.597	21.117	21.405	21.221	21.325	20.945	21.888	20.746	21.737	21.682	21.292	21.263	21.172	21.770
MnO	0.000	0.000	0.024	0.096	0.021	0.018	0.043	0.068	0.000	0.052	0.046	0.058	0.047	0.116	0.000	0.083	0.000	0.000	0.017
CaO	0.060	0.054	0.056	0.008	0.001	0.045	0.025	0.021	0.014	0.002	0.023	0.056	0.041	0.043	0.047	0.054	0.000	0.000	0.036
Na2O	0.247	0.240	0.187	0.236	0.274	0.274	0.300	0.120	0.198	0.224	0.179	0.079	0.204	0.224	0.150	0.198	0.232	0.156	0.208
K2O	10.195	10.160	9.913	10.312	10.164	10.774	10.306	9.388	9.293	9.510	9.383	9.438	9.314	9.554	9.457	9.662	9.375	9.637	9.128
Cr2O3	0.089	0.059	0.031	0.039	0.071	0.026	0.052	0.039	0.000	0.052	0.000	0.065	0.022	0.070	0.057	0.047	0.137	0.108	0.057
Cl	0.001	0.008	0.019	0.016	0.006	0.008	0.000	0.014	0.001	0.000	0.022	0.032	0.003	0.003	0.000	0.000	0.000	0.000	0.006
F	0.295	0.385	0.337	0.401	0.296	0.316	0.359	0.258	0.311	0.238	0.263	0.261	0.156	0.087	0.395	0.266	0.188	0.299	0.342
TOTAL	*100.008*	*100.058*	*99.985*	*100.006*	*99.941*	*99.964*	*100.017*	*98.292*	*97.716*	*97.779*	*97.165*	*97.130*	*97.401*	*98.168*	*97.897*	*97.383*	*97.863*	*97.465*	*98.020*
-O = Cl	-0.000	-0.002	-0.004	-0.004	-0.001	-0.002	0.000	-0.003	-0.000	0.000	-0.005	-0.007	-0.001	-0.001	0.000	0.000	0.000	0.000	-0.001
-O = F	-0.124	-0.162	-0.142	-0.169	-0.125	-0.133	-0.151	-0.109	-0.131	-0.100	-0.111	-0.110	-0.066	-0.037	-0.166	-0.112	-0.079	-0.126	-0.144
TOTAL	**99.884**	**99.894**	**99.839**	**99.834**	**99.815**	**99.829**	**99.866**	**98.180**	**97.585**	**97.679**	**97.049**	**97.013**	**97.335**	**98.131**	**97.731**	**97.271**	**97.784**	**97.339**	**97.875**
CATIONS RECALCULATED TO 22 OXYGENS																			
Si	5.183	5.208	5.192	5.127	5.126	5.097	5.120	5.369	5.391	5.308	5.345	5.293	5.432	5.399	5.359	5.299	5.326	5.336	5.359
Al	3.419	3.354	3.347	3.369	3.387	3.417	3.402	3.232	3.220	3.241	3.256	3.230	3.308	3.161	3.234	3.306	3.311	3.243	3.281
Ti	0.373	0.368	0.387	0.387	0.383	0.410	0.413	0.460	0.432	0.449	0.454	0.419	0.393	0.424	0.433	0.401	0.407	0.405	0.382
Mg	2.242	2.214	2.157	2.264	2.261	2.242	2.188	1.894	1.944	1.981	1.934	1.996	1.860	1.923	1.899	1.960	1.953	2.009	1.948
Fe	2.503	2.594	2.687	2.628	2.629	2.548	2.610	2.671	2.662	2.682	2.644	2.785	2.597	2.722	2.730	2.694	2.663	2.672	2.728
Mn	0.000	0.000	0.003	0.012	0.003	0.002	0.005	0.009	0.000	0.007	0.006	0.007	0.006	0.015	0.000	0.011	0.000	0.000	0.002
Ca	0.009	0.009	0.009	0.001	0.000	0.007	0.004	0.003	0.002	0.000	0.004	0.009	0.007	0.007	0.008	0.009	0.000	0.000	0.006
Na	0.070	0.069	0.054	0.068	0.079	0.079	0.086	0.035	0.058	0.065	0.052	0.023	0.059	0.065	0.044	0.058	0.067	0.046	0.060
K	1.908	1.909	1.868	1.947	1.916	2.033	1.943	1.787	1.778	1.825	1.807	1.832	1.778	1.825	1.816	1.865	1.791	1.856	1.745
Cr	0.010	0.007	0.004	0.005	0.008	0.003	0.006	0.005	0.000	0.006	0.000	0.004	0.000	0.000	0.000	0.006	0.016	0.013	0.007
TOTAL	**15.718**	**15.732**	**15.706**	**15.807**	**15.791**	**15.838**	**15.778**	**15.464**	**15.486**	**15.565**	**15.503**	**15.599**	**15.440**	**15.542**	**15.522**	**15.606**	**15.534**	**15.581**	**15.518**
Fe/Fe+Mg	*0.528*	*0.540*	*0.555*	*0.537*	*0.538*	*0.532*	*0.544*	*0.585*	*0.578*	*0.575*	*0.578*	*0.583*	*0.583*	*0.586*	*0.58:*	*0.579*	*0.577*	*0.571*	*0.583*
Mg/6	0.374	0.369	0.359	0.377	0.377	0.374	0.365	0.316	0.324	0.330	0.322	0.333	0.310	0.320	0.316	0.327	0.325	0.335	0.325
Fe/6	0.417	0.432	0.448	0.438	0.438	0.425	0.435	0.445	0.444	0.447	0.441	0.464	0.433	0.454	0.455	0.449	0.444	0.445	0.455
Ti/6	0.062	0.061	0.065	0.065	0.064	0.068	0.069	0.077	0.072	0.075	0.076	0.06:	0.065	0.071	0.072	0.067	0.068	0.068	0.064
Alvi/6	0.100	0.094	0.08:	0.083	0.086	0.086	0.087	0.100	0.102	0.092	0.100	0.087	0.123	0.093	0.099	0.101	0.106	0.097	0.107
(Alvi+Ti)/(Alvi+Ti+Fe+Mg)																			
	0.171	0.162	0.161	0.153	0.155	0.162	0.163	0.189	0.184	0.176	0.187	0.165	0.203	0.175	0.181	0.178	0.184	0.174	0.179
Na+K	1.979	1.978	1.921	2.015	1.995	2.112	2.029	1.822	1.836	1.890	1.859	1.855	1.838	1.890	1.860	1.923	1.859	1.901	1.805
Na/K	*0.037*	*0.036*	*0.029*	*0.035*	*0.041*	*0.039*	*0.044*	*0.019*	*0.032*	*0.036*	*0.029*	*0.013*	*0.033*	*0.036*	*0.024*	*0.031*	*0.038*	*0.025*	*0.035*
X	66.45	64.97	63.49	62.00	60.52	59.04	57.84	113.71	118.71	118.35	118.11	80.40	80.94	81.48	82.02	66.08	65.87	65.67	65.46
Y	-331.94	-332.96	-333.99	-335.01	-336.18	-337.23	-338.31	-332.75	-351.80	-353.73	-355.53	-54.13	-53.05	-51.96	-50.88	-31.53	-30.25	-28.97	-27.70
x-axis (m	0.18	0.36	0.54	0.72	0.91	1.09	1.25		0.00	0.20	0.38	0.00	0.12	0.24	0.36	0.00	0.13	0.26	0.39
location	*adj gt*	*adj gt*	*adj gt*	*adj gt*	*adj gt*	*adj gt*	*adj gt*	*matrix*	*matrix*	*matrix*	*matrix*	*near gt*	*near gt*	*near gt*	*near gt*	*matrix*	*matrix*	*matrix*	*matrix*

TABLE B-2: Quantitative Microprobe Analysis for Biotite Compositions

	PC-113E (continued)					*PC-113/4a*													*PC-116/3a*	
	BT7e	**BT8a**	**BT8b**	**BT8c**	**BT8e**	**1**	**1a**	**2**	**2a**	**2***	**3**	**3a**	**3b**	**4**	**4a**	**5**	**5a**	**6**	**1**	**1a**
WEIGHT PERCENT OXIDES																				
SiO2	35.443	35.485	35.314	35.356	35.275	34.160	34.145	35.195	34.554	35.065	34.157	35.063	34.628	35.147	35.223	34.434	34.739	34.677	35.039	34.706
Al2O3	18.143	18.268	18.174	18.452	18.325	18.872	18.715	18.689	18.608	19.198	18.392	19.007	18.595	19.492	19.302	18.343	18.669	18.490	19.300	19.068
TiO2	3.325	3.884	3.773	3.942	3.982	3.892	3.767	2.722	3.04:	3.200	1.896	2.740	3.353	1.978	2.123	3.755	3.655	3.926	2.256	2.265
MgO	8.742	8.419	8.476	8.957	8.541	8.742	9.055	9.620	9.205	9.052	9.256	8.879	8.926	11.076	10.368	8.871	8.704	8.760	10.563	10.502
FeO	21.328	21.532	21.506	21.564	21.300	20.994	20.950	21.012	21.198	21.102	22.997	22.240	21.952	19.512	19.328	21.061	21.445	21.637	18.916	19.811
MnO	0.094	0.116	0.000	0.077	0.000	0.058	0.040	0.084	0.040	0.000	0.015	0.109	0.000	0.047	0.069	0.135	0.000	0.058	0.000	0.022
CaO	0.009	0.000	0.007	0.043	0.020	0.016	0.059	0.059	0.013	0.000	0.039	0.036	0.000	0.000	0.000	0.01:	0.029	0.033	0.029	0.049
Na2O	0.244	0.120	0.083	0.180	0.242	0.132	0.042	0.132	0.105	0.074	0.069	0.134	0.074	0.198	0.110	0.094	0.170	0.000	0.009	0.031
K2O	9.348	9.259	9.523	9.446	9.517	9.666	9.882	9.417	9.397	9.387	9.040	9.572	9.267	9.875	9.862	9.701	9.503	9.720	9.607	9.485
Cr2O3	0.045	0.043	0.108	0.005	0.070	0.095	0.134	0.022	0.032	0.038	0.000	0.000	0.089	0.064	0.058	0.111	0.067	0.035	0.000	0.042
Cl	0.000	0.020	0.023	0.000	0.012															
F	0.448	0.314	0.193	0.380	0.263	0.243	0.177	0.428	0.220	0.328	0.210	0.300	0.344	0.375	0.496	0.332	0.128	0.212	0.560	0.183
TOTAL	*97.169*	*97.460*	*97.180*	*98.402*	*97.547*	*96.871*	*96.965*	*97.378*	*96.422*	*97.444*	*96.071*	*98.07:*	*97.228*	*97.765*	*96.939*	*96.857*	*97.109*	*97.546*	*96.281*	*96.165*
-O = Cl	0.000	-0.005	-0.005	0.000	-0.003	0.000	0.000	0.000	0.000	0.000	0.000	0.000	0.000	0.000	0.000	0.000	0.000	0.000	0.000	0.000
-O = F	-0.189	-0.132	-0.081	-0.160	-0.111	-0.102	-0.075	-0.180	-0.093	-0.138	-0.088	-0.126	-0.145	-0.158	-0.209	-0.140	-0.054	-0.089	-0.236	-0.077
TOTAL	**96.980**	**97.323**	**97.094**	**98.242**	**97.434**	**96.769**	**96.890**	**97.198**	**96.329**	**97.306**	**95.983**	**97.953**	**97.083**	**97.607**	**96.729**	**96.717**	**97.056**	**97.457**	**96.045**	**96.088**
CATIONS RECALCULATED TO 22 OXYGENS																				
Si	5.371	5.353	5.345	5.293	5.319	5.197	5.193	5.313	5.271	5.279	5.270	5.282	5.257	5.254	5.311	5.249	5.263	5.246	5.304	5.267
Al	3.240	3.248	3.242	3.255	3.257	3.384	3.355	3.325	3.345	3.406	3.344	3.374	3.327	3.434	3.430	3.295	3.333	3.297	3.443	3.411
Ti	0.379	0.441	0.430	0.444	0.452	0.445	0.431	0.309	0.350	0.362	0.220	0.310	0.383	0.222	0.241	0.431	0.416	0.447	0.257	0.259
Mg	1.975	1.893	1.913	1.999	1.920	1.983	2.053	2.165	2.093	2.032	2.129	1.994	2.020	2.468	2.331	2.016	1.966	1.975	2.384	2.376
Fe	2.703	2.716	2.722	2.700	2.686	2.671	2.664	2.653	2.704	2.657	2.967	2.802	2.787	2.439	2.437	2.685	2.717	2.737	2.395	2.515
Mn	0.012	0.015	0.000	0.00:	0.000	0.007	0.005	0.011	0.005	0.000	0.002	0.014	0.000	0.006	0.009	0.017	0.000	0.007	0.000	0.003
Ca	0.001	0.000	0.001	0.007	0.003	0.003	0.00:	0.009	0.002	0.000	0.006	0.006	0.000	0.000	0.000	0.003	0.005	0.005	0.005	0.008
Na	0.072	0.035	0.024	0.052	0.071	0.039	0.012	0.039	0.031	0.021	0.021	0.039	0.022	0.057	0.032	0.028	0.04:	0.000	0.003	0.009
K	1.807	1.782	1.839	1.804	1.831	1.876	1.917	1.814	1.829	1.803	1.779	1.839	1.795	1.883	1.897	1.887	1.836	1.876	1.855	1.836
Cr	0.005	0.005	0.013	0.001	0.008	0.012	0.016	0.003	0.004	0.005	0.000	0.000	0.011	0.008	0.007	0.013	0.008	0.004	0.000	0.005
TOTAL	**15.566**	**15.488**	**15.529**	**15.564**	**15.547**	**15.617**	**15.656**	**15.640**	**15.635**	**15.565**	**15.738**	**15.660**	**15.600**	**15.773**	**15.694**	**15.624**	**15.594**	**15.595**	**15.646**	**15.689**
Fe/Fe+Mg	*0.578*	*0.589*	*0.587*	*0.575*	*0.583*	*0.574*	*0.565*	*0.551*	*0.564*	*0.567*	*0.582*	*0.584*	*0.580*	*0.497*	*0.511*	*0.571*	*0.580*	*0.581*	*0.501*	*0.514*
Mg/6	0.329	0.316	0.319	0.333	0.320	0.330	0.342	0.361	0.349	0.339	0.355	0.332	0.337	0.411	0.388	0.336	0.328	0.329	0.397	0.396
Fe/6	0.450	0.453	0.454	0.450	0.448	0.445	0.444	0.442	0.451	0.443	0.495	0.467	0.464	0.407	0.406	0.447	0.453	0.456	0.399	0.419
Ti/6	0.063	0.074	0.072	0.074	0.075	0.074	0.072	0.052	0.058	0.060	0.037	0.052	0.064	0.037	0.040	0.072	0.069	0.075	0.043	0.043
Alvi/6	0.102	0.100	0.098	0.091	0.096	0.097	0.091	0.106	0.103	0.114	0.102	0.109	0.097	0.115	0.123	0.091	0.099	0.090	0.125	0.113
(Alvi+Ti)/(Alvi+Ti+Fe+Mg)	0.175	0.184	0.180	0.174	0.182	0.181	0.172	0.164	0.168	0.183	0.141	0.168	0.167	0.157	0.171	0.172	0.178	0.173	0.174	0.161
Na+K	1.879	1.817	1.863	1.856	1.902	1.915	1.930	1.852	1.860	1.824	1.800	1.879	1.816	1.941	1.929	1.914	1.886	1.876	1.858	1.846
Na/K	*0.03:*	*0.01:*	*0.013*	*0.029*	*0.039*	*0.021*	*0.006*	*0.021*	*0.017*	*0.012*	*0.012*	*0.021*	*0.012*	*0.031*	*0.017*	*0.015*	*0.027*	*0.000*	*0.001*	*0.005*
X	65.26	93.79	94.58	95.37	96.95															
Y	-26.42	-145.52	-144.95	-144.39	-143.27															
x-axis (m	0.52	0.00	0.0:	0.19	0.39															
location	*matrix*	*matrix*	*matrix*	*matrix*	*matrix*	*±adj gt*	*±adj gt*	*adj gt*	*±adj gt*	*±adj gt*	*adj gt*	*±adj gt*	*±adj gt*	*adj gt*	*adj gt*	*matrix*	*matrix*	*matrix*	*adj gt*	*adj gt*

TABLE B-2: Quantitative Microprobe Analysis for Biotite Compositions

PC-116/3a (continued)										*PC-119A*										
	2	**2a**	**3a**	**4a**	**5**	**5a**	**bt1**	**bt2**	**bt3**	**B1**	**B3**	**B5**	**B6**	**B7**	**B10**	**B11**	**B12**	**B13**	**BT1a**	**BT1b**
WEIGHT PERCENT OXIDES																				
SiO2	34.742	34.832	34.900	34.623	34.947	35.031	35.008	35.218	34.765	35.095	35.756	35.459	35.777	35.862	35.389	35.748	35.991	35.771	36.508	36.089
Al2O3	18.960	19.221	18.793	19.185	18.985	18.803	19.327	18.970	19.073	18.966	19.775	19.280	19.634	19.105	20.015	18.637	18.511	18.551	19.858	19.581
TiO2	2.687	2.476	3.439	3.413	3.166	3.416	2.757	2.849	3.561	2.082	1.999	2.221	1.270	2.689	1.881	3.423	3.592	3.693	1.294	1.320
MgO	9.753	9.817	9.056	9.020	9.153	8.973	9.747	9.535	8.860	10.199	9.713	9.457	10.411	9.625	11.019	8.669	8.947	8.189	10.536	10.565
FeO	19.840	19.885	20.949	20.354	20.680	20.471	20.005	19.724	20.204	20.053	19.758	20.641	19.147	20.354	20.387	21.060	20.435	20.461	18.212	18.850
MnO	0.033	0.088	0.069	0.000	0.000	0.066	0.000	0.123	0.039	0.035	0.013	0.066	0.000	0.108	0.098	0.007	0.048	0.078	0.039	0.000
CaO	0.052	0.023	0.000	0.00:	0.000	0.000	0.036	0.038	0.042	0.012	0.000	0.000	0.013	0.000	0.058	0.027	0.014	0.034	0.031	0.014
Na2O	0.169	0.115	0.052	0.174	0.031	0.096	0.073	0.193	0.131	0.062	0.124	0.135	0.141	0.143	0.040	0.143	0.147	0.053	0.118	0.143
K2O	9.448	9.695	9.756	9.811	9.712	9.820	9.873	9.564	9.368	9.313	9.730	9.654	9.662	9.580	10.707	9.358	9.568	9.504	9.466	9.584
Cr2O3	0.000	0.074	0.048	0.070	0.086	0.077	0.000	0.046	0.058	0.042	0.009	0.036	0.026	0.044	0.050	0.067	0.013	0.020	0.022	0.000
Cl	0.034	0.034	0.048	0.015	0.006	0.006	0.013	0.004	0.004	0.000	0.006	0.021	0.000	0.000						
F	0.296	0.240	0.389	0.415	0.324	0.359	0.325	0.369	0.385	0.158	0.305	0.291	0.256	0.396	0.334	0.231	0.330	0.264	0.484	0.301
TOTAL	*95.981*	*96.466*	*97.450*	*97.077*	*97.083*	*97.112*	*97.185*	*96.663*	*96.534*	*96.032*	*97.188*	*97.246*	*96.350*	*97.910*	*99.982*	*97.370*	*97.602*	*96.639*	*96.568*	*96.447*
-O = Cl	0.000	0.000	0.000	0.000	0.000	0.000	-0.008	-0.008	-0.011	-0.003	-0.001	-0.001	-0.003	-0.001	-0.001	0.000	-0.001	-0.005	0.000	0.000
-O = F	-0.125	-0.101	-0.164	-0.175	-0.136	-0.151	-0.137	-0.155	-0.162	-0.067	-0.128	-0.123	-0.108	-0.167	-0.141	-0.097	-0.139	-0.111	-0.204	-0.127
TOTAL	**95.856**	**96.365**	**97.286**	**96.902**	**96.946**	**96.961**	**97.041**	**96.500**	**96.361**	**95.962**	**97.058**	**97.122**	**96.239**	**97.742**	**99.840**	**97.273**	**97.462**	**96.523**	**96.364**	**96.320**
CATIONS RECALCULATED TO 22 OXYGENS																				
Si	5.291	5.281	5.273	5.243	5.285	5.299	5.275	5.327	5.276	5.328	5.357	5.340	5.389	5.356	5.206	5.374	5.392	5.410	5.454	5.417
Al	3.403	3.434	3.346	3.424	3.383	3.352	3.432	3.382	3.412	3.393	3.492	3.422	3.486	3.363	3.46:	3.302	3.268	3.307	3.497	3.464
Ti	0.308	0.282	0.391	0.389	0.360	0.389	0.312	0.324	0.407	0.238	0.225	0.252	0.144	0.302	0.208	0.387	0.405	0.420	0.145	0.149
Mg	2.214	2.219	2.03:	2.036	2.063	2.023	2.190	2.150	2.005	2.308	2.170	2.123	2.338	2.143	2.417	1.943	1.998	1.846	2.347	2.364
Fe	2.527	2.521	2.647	2.578	2.615	2.58:	2.521	2.495	2.564	2.546	2.476	2.599	2.412	2.542	2.508	2.648	2.560	2.588	2.276	2.366
Mn	0.004	0.011	0.009	0.000	0.000	0.008	0.000	0.016	0.005	0.005	0.002	0.008	0.000	0.014	0.012	0.001	0.006	0.00:	0.005	0.000
Ca	0.009	0.004	0.000	0.002	0.000	0.000	0.006	0.006	0.007	0.002	0.000	0.000	0.002	0.000	0.009	0.004	0.002	0.006	0.005	0.002
Na	0.04:	0.034	0.015	0.051	0.009	0.028	0.021	0.057	0.039	0.018	0.036	0.039	0.041	0.041	0.011	0.042	0.043	0.016	0.034	0.042
K	1.836	1.875	1.881	1.895	1.874	1.895	1.898	1.845	1.814	1.804	1.860	1.855	1.857	1.825	2.00:	1.795	1.829	1.834	1.804	1.835
Cr	0.000	0.009	0.006	0.008	0.010	0.009	0.000	0.005	0.007	0.005	0.001	0.004	0.003	0.005	0.006	0.008	0.002	0.002	0.003	0.000
TOTAL	**15.642**	**15.670**	**15.608**	**15.626**	**15.600**	**15.593**	**15.656**	**15.607**	**15.534**	**15.646**	**15.619**	**15.643**	**15.672**	**15.591**	**15.858**	**15.502**	**15.504**	**15.439**	**15.56:**	**15.640**
Fe/Fe+Mg	*0.533*	*0.532*	*0.565*	*0.559*	*0.559*	*0.561*	*0.535*	*0.537*	*0.561*	*0.524*	*0.533*	*0.550*	*0.508*	*0.543*	*0.509*	*0.577*	*0.562*	*0.584*	*0.492*	*0.500*
Mg/6	0.369	0.370	0.340	0.339	0.344	0.337	0.365	0.358	0.334	0.385	0.362	0.354	0.390	0.357	0.403	0.324	0.333	0.308	0.391	0.394
Fe/6	0.421	0.420	0.441	0.430	0.436	0.432	0.420	0.416	0.427	0.424	0.413	0.433	0.402	0.424	0.418	0.441	0.427	0.431	0.379	0.394
Ti/6	0.051	0.047	0.065	0.065	0.060	0.065	0.052	0.054	0.068	0.03:	0.038	0.042	0.024	0.050	0.035	0.065	0.068	0.070	0.024	0.025
Alvi/6	0.116	0.119	0.103	0.111	0.111	0.109	0.118	0.118	0.115	0.120	0.142	0.127	0.146	0.120	0.113	0.113	0.110	0.120	0.159	0.147
(Alvi+Ti)/(Alvi+Ti+Fe+Mg)	0.175	0.174	0.177	0.186	0.180	0.184	0.178	0.182	0.193	0.165	0.188	0.177	0.177	0.179	0.152	0.188	0.189	0.204	0.192	0.179
Na+K	1.886	1.909	1.896	1.946	1.883	1.923	1.919	1.902	1.852	1.822	1.896	1.894	1.898	1.867	2.021	1.836	1.871	1.849	1.838	1.877
Na/K	*0.027*	*0.018*	*0.008*	*0.027*	*0.005*	*0.015*	*0.011*	*0.031*	*0.021*	*0.010*	*0.019*	*0.021*	*0.022*	*0.023*	*0.006*	*0.023*	*0.023*	*0.008*	*0.019*	*0.023*
X							-128.80	-124.66	-104.94	77.77	105.79	108.72	106.17	109.77	80.58	135.39	146.95	156.40	96.90	97.70
Y							320.34	326.68	316.73	355.91	368.71	362.41	357.19	340.29	335.27	350.25	354.82	339.82	362.20	361.27
x-axis (mm)																			0.00	0.12
location	*adj gt*	*adj gt*	*±matrix*	*±matrix*	*±matrix*	*±matrix*	*adj gt*	*adj gt*	*±adj gt*	*±adj gt*	*±adj gt*	*adj gt*	*adj gt*	*±adj gt*	*adj gt*	*matrix*	*matrix*	*matrix*	*±adj gt*	*±adj gt*

TABLE B-2: Quantitative Microprobe Analysis for Biotite Compositions

	PC-119 (continued)														*PC-128/10a*				
	BT1c	**BT1d**	**BT1e**	**BT1f**	**BT2b**	**BT3f**	**BT3g**	**BT4b**	**BT4c**	**BT4d**	**BT4e**	**BT5a**	**BT5b**	**BT5c**	**1a**	**7**	**7a**	**8**	**8a**
WEIGHT PERCENT OXIDESlow total																			
SiO2	35.567	35.540	35.693	35.379	35.207	35.392	35.699	35.518	35.662	35.501	35.405	35.077	35.902	35.500	34.547	34.657	35.286	34.952	35.126
Al2O3	19.421	19.313	19.687	19.627	19.714	19.293	19.605	18.909	18.515	18.806	19.401	18.639	18.720	19.087	20.298	19.604	19.431	18.995	19.134
TiO2	1.331	1.308	1.357	1.356	1.328	1.767	1.891	2.957	2.924	3.226	2.861	3.006	3.088	3.069	0.996	3.012	3.247	3.801	3.730
MgO	10.465	10.577	10.582	10.473	10.505	9.565	9.572	8.236	8.700	8.414	8.983	8.648	8.574	8.889	8.842	8.209	8.596	8.294	8.583
FeO	19.463	19.781	18.418	18.533	18.947	19.736	19.330	21.080	21.633	21.348	20.936	21.249	21.324	20.681	20.092	20.294	21.286	20.828	20.128
MnO	0.082	0.000	0.070	0.000	0.028	0.090	0.058	0.110	0.142	0.068	0.119	0.125	0.036	0.101	0.022	0.047	0.000	0.149	0.076
CaO	0.030	0.088	0.170	0.035	0.035	0.010	0.037	0.031	0.016	0.000	0.025	0.036	0.000	0.022	0.085	0.007	0.000	0.000	0.036
Na2O	0.138	0.128	0.164	0.135	0.056	0.095	0.048	0.049	0.100	0.077	0.081	0.050	0.147	0.062	0.047	0.122	0.259	0.142	0.188
K2O	9.273	9.462	9.722	9.926	9.620	9.914	9.674	9.371	9.671	9.477	9.564	9.403	9.714	9.715	9.720	9.783	10.011	9.788	9.780
Cr2O3	0.000	0.052	0.035	0.018	0.055	0.073	0.036	0.059	0.099	0.087	0.100	0.000	0.028	0.012	0.000	0.019	0.016	0.07:	0.07:
Cl	0.000	0.025	0.027	0.000	0.018	0.004	0.014	0.010	0.000	0.006	0.000	0.000	0.000	0.001					
F	0.424	0.417	0.346	0.517	0.432	0.423	0.389	0.193	0.244	0.266	0.240	0.282	0.312	0.181	0.348	0.211	0.160	0.106	0.063
TOTAL	*96.194*	*96.691*	*96.271*	*95.999*	*95.945*	*96.362*	*96.353*	*96.523*	*97.706*	*97.276*	*97.715*	*96.515*	*97.845*	*97.320*	*94.995*	*95.964*	*98.292*	*97.136*	*96.922*
-O = Cl	0.000	-0.006	-0.006	0.000	-0.004	-0.001	-0.003	-0.002	0.000	-0.001	0.000	0.000	0.000	-0.000	0.000	0.000	0.000	0.000	0.000
-O = F	-0.179	-0.176	-0.146	-0.218	-0.182	-0.178	-0.164	-0.081	-0.103	-0.112	-0.101	-0.119	-0.131	-0.076	-0.147	-0.089	-0.067	-0.045	-0.026
TOTAL	**96.016**	**96.510**	**96.119**	**95.781**	**95.759**	**96.183**	**96.186**	**96.439**	**97.603**	**97.163**	**97.614**	**96.396**	**97.714**	**97.244**	**94.849**	**95.875**	**98.225**	**97.091**	**96.896**
CATIONS RECALCULATED TO 22 OXYGENS																			
Si	5.378	5.362	5.376	5.363	5.339	5.373	5.391	5.387	5.372	5.358	5.308	5.341	5.389	5.339	5.322	5.290	5.278	5.282	5.295
Al	3.461	3.434	3.495	3.507	3.523	3.452	3.489	3.380	3.287	3.345	3.428	3.345	3.312	3.383	3.685	3.527	3.426	3.383	3.400
Ti	0.151	0.148	0.154	0.155	0.151	0.202	0.215	0.337	0.331	0.366	0.323	0.344	0.349	0.347	0.115	0.346	0.365	0.432	0.423
Mg	2.359	2.379	2.376	2.367	2.375	2.165	2.155	1.862	1.954	1.893	2.008	1.963	1.919	1.993	2.031	1.868	1.917	1.868	1.929
Fe	2.461	2.496	2.320	2.349	2.403	2.506	2.441	2.674	2.725	2.694	2.625	2.706	2.677	2.601	2.588	2.58:	2.663	2.632	2.538
Mn	0.011	0.000	0.009	0.000	0.004	0.012	0.007	0.014	0.018	0.009	0.015	0.016	0.005	0.013	0.003	0.006	0.000	0.019	0.00:
Ca	0.005	0.014	0.027	0.006	0.006	0.002	0.006	0.005	0.003	0.000	0.004	0.006	0.000	0.004	0.014	0.001	0.000	0.000	0.006
Na	0.041	0.037	0.048	0.03:	0.017	0.028	0.014	0.014	0.029	0.023	0.023	0.015	0.043	0.018	0.014	0.036	0.075	0.042	0.055
K	1.789	1.821	1.868	1.920	1.861	1.920	1.864	1.813	1.859	1.825	1.829	1.827	1.860	1.864	1.910	1.905	1.910	1.887	1.881
Cr	0.000	0.006	0.004	0.002	0.007	0.009	0.004	0.007	0.012	0.010	0.012	0.000	0.003	0.001	0.000	0.002	0.002	0.00:	0.00:
TOTAL	**15.655**	**15.699**	**15.678**	**15.708**	**15.684**	**15.668**	**15.586**	**15.495**	**15.591**	**15.522**	**15.576**	**15.563**	**15.556**	**15.563**	**15.682**	**15.56:**	**15.636**	**15.554**	**15.545**
Fe/Fe+Mg	*0.511*	*0.512*	*0.494*	*0.498*	*0.503*	*0.537*	*0.531*	*0.589*	*0.582*	*0.587*	*0.567*	*0.580*	*0.582*	*0.566*	*0.560*	*0.581*	*0.581*	*0.585*	*0.568*
Mg/6	0.393	0.396	0.396	0.394	0.396	0.361	0.359	0.310	0.326	0.315	0.335	0.327	0.320	0.332	0.338	0.311	0.319	0.311	0.321
Fe/6	0.410	0.416	0.387	0.392	0.400	0.418	0.407	0.446	0.454	0.449	0.438	0.451	0.446	0.434	0.431	0.432	0.444	0.439	0.423
Ti/6	0.025	0.025	0.026	0.026	0.025	0.034	0.036	0.056	0.055	0.061	0.054	0.057	0.058	0.058	0.019	0.058	0.061	0.072	0.071
Alvi/6	0.140	0.133	0.145	0.145	0.144	0.138	0.147	0.128	0.110	0.117	0.123	0.114	0.117	0.120	0.168	0.136	0.117	0.111	0.116
(Alvi+Ti)/(Alvi+Ti+Fe+Mg)	0.170	0.162	0.179	0.178	0.175	0.180	0.192	0.196	0.175	0.189	0.186	0.181	0.186	0.189	0.195	0.207	0.189	0.196	0.200
Na+K	1.829	1.859	1.916	1.959	1.877	1.948	1.878	1.828	1.888	1.847	1.853	1.841	1.903	1.882	1.924	1.941	1.985	1.929	1.936
Na/K	*0.023*	*0.021*	*0.026*	*0.021*	*0.009*	*0.015*	*0.008*	*0.008*	*0.016*	*0.012*	*0.013*	*0.008*	*0.023*	*0.00:*	*0.007*	*0.019*	*0.039*	*0.022*	*0.029*
X	98.50	99.30	100.10	100.90	99.88	108.55	108.40	104.09	103.64	102.99	102.65	102.84	103.54	104.61					
Y	360.41	359.39	358.34	357.55	359.11	349.78	348.61	326.61	325.36	324.10	322.87	325.63	325.07	324.68					
x-axis (m	0.24	0.37	0.50	0.61	0.00	0.12	0.00	0.13	0.27	0.40	0.00	0.09	0.20						
location	*adj gt*	*adj gt*	*adj gt*	*adj gt*	*adj gt*	*±adj gt*	*±adj gt*	*near gt*	*near gt*	*near gt*	*near gt*	*near gt*	*near gt*	*near gt*	*±adj gt*	*matrix*	*matrix*	*matrix*	*matrix*

TABLE B-2: Quantitative Microprobe Analysis for Biotite Compositions

	PC-128/10b										***PC-128/10c***									
	bt1	**bt2**	**bt3a**	**bt4**	**bt5**	**bt6**	**bt7**	**bt8**	**bt9**	**bt10**	**1**	**1a**	**2a**	**3**	**4**	**4a**	**5**	**5a**	**6**	**6a**
WEIGHT PERCENT OXIDES																				
SiO2	37.252	37.006	36.795	36.300	36.478	36.653	36.564	35.447	36.438	36.984	35.706	35.656	35.984	35.962	34.945	35.169	35.383	35.272	35.831	35.131
Al2O3	20.411	20.264	19.892	19.650	20.238	20.223	20.034	19.070	20.197	20.936	19.309	19.446	20.357	19.822	18.966	18.817	18.756	18.535	19.019	18.690
TiO2	1.509	1.593	2.156	2.502	1.197	1.597	1.920	2.419	1.889	0.020	2.668	2.356	0.166	1.686	2.836	2.936	2.813	2.696	2.689	2.647
MgO	12.732	13.001	12.496	12.094	13.610	13.040	12.200	11.836	11.605	14.803	11.376	11.212	14.257	11.494	11.337	11.097	11.864	11.823	11.500	11.801
FeO	14.517	15.047	15.824	15.688	14.660	14.680	15.630	16.334	16.069	13.541	18.762	17.688	15.729	18.077	18.313	18.248	17.857	18.327	18.923	18.291
MnO	0.000	0.127	0.093	0.166	0.133	0.158	0.104	0.056	0.110	0.088	0.108	0.184	0.047	0.004	0.094	0.148	0.098	0.101	0.097	0.126
CaO	0.014	0.038	0.000	0.052	0.045	0.056	0.043	0.018	0.036	0.038	0.019	0.000	0.075	0.101	0.003	0.000	0.000	0.039	0.007	0.003
Na2O	0.231	0.235	0.224	0.245	0.191	0.307	0.174	0.177	0.233	0.175	0.217	0.186	0.034	0.259	0.296	0.137	0.198	0.214	0.194	0.013
K2O	9.554	9.088	9.512	9.273	9.463	9.662	9.451	9.244	9.553	9.215	9.067	8.93:	9.182	9.271	9.127	9.161	9.137	8.991	9.03:	9.373
Cr2O3	0.000	0.000	0.041	0.000	0.000	0.000	0.101	0.007	0.000	0.018	0.050	0.089	0.054	0.06:	0.000	0.013	0.051	0.000	0.000	0.029
Cl	0.017	0.000	0.029	0.003	0.012	0.000	0.026	0.011	0.000	0.009										
F	0.385	0.428	0.333	0.265	0.440	0.292	0.245	0.321	0.236	0.607	0.303	0.296	0.451	0.372	0.246	0.03:	0.408	0.362	0.363	0.254
TOTAL	*96.622*	*96.827*	*97.395*	*96.238*	*96.467*	*96.668*	*96.492*	*94.93:*	*96.366*	*96.434*	*97.585*	*96.052*	*96.336*	*97.117*	*96.164*	*95.765*	*96.564*	*96.360*	*97.662*	*96.357*
-O = Cl	-0.004	0.000	-0.007	-0.001	-0.003	0.000	-0.006	-0.002	0.000	-0.002	0.000	0.000	0.000	0.000	0.000	0.000	0.000	0.000	0.000	0.000
-O = F	-0.162	-0.180	-0.140	-0.112	-0.185	-0.123	-0.103	-0.135	-0.099	-0.256	-0.128	-0.125	-0.190	-0.157	-0.104	-0.017	-0.172	-0.152	-0.153	-0.107
TOTAL	**96.456**	**96.647**	**97.248**	**96.126**	**96.279**	**96.545**	**96.383**	**94.802**	**96.267**	**96.176**	**97.458**	**95.927**	**96.146**	**96.960**	**96.05:**	**95.748**	**96.392**	**96.208**	**97.509**	**96.250**
CATIONS RECALCULATED TO 22 OXYGENS																				
Si	5.452	5.414	5.387	5.374	5.369	5.382	5.394	5.353	5.394	5.403	5.294	5.340	5.324	5.342	5.262	5.302	5.298	5.301	5.314	5.283
Al	3.521	3.494	3.432	3.429	3.511	3.500	3.483	3.394	3.524	3.605	3.374	3.433	3.550	3.46:	3.366	3.343	3.310	3.283	3.324	3.312
Ti	0.166	0.175	0.237	0.279	0.133	0.176	0.213	0.275	0.210	0.002	0.298	0.265	0.019	0.188	0.321	0.333	0.317	0.305	0.300	0.299
Mg	2.778	2.836	2.727	2.669	2.986	2.854	2.683	2.664	2.561	3.224	2.515	2.503	3.145	2.545	2.545	2.494	2.648	2.649	2.542	2.645
Fe	1.777	1.841	1.937	1.942	1.805	1.803	1.928	2.063	1.989	1.654	2.326	2.216	1.946	2.245	2.306	2.301	2.236	2.303	2.347	2.300
Mn	0.000	0.016	0.012	0.021	0.017	0.01:	0.013	0.007	0.014	0.011	0.014	0.023	0.006	0.000	0.012	0.019	0.012	0.013	0.012	0.016
Ca	0.002	0.006	0.000	0.008	0.007	0.009	0.007	0.003	0.006	0.006	0.003	0.000	0.012	0.016	0.001	0.000	0.000	0.006	0.001	0.001
Na	0.066	0.067	0.064	0.070	0.055	0.087	0.04:	0.052	0.067	0.04:	0.063	0.054	0.00:	0.075	0.086	0.040	0.057	0.062	0.056	0.004
K	1.784	1.696	1.777	1.751	1.777	1.810	1.779	1.781	1.804	1.717	1.715	1.708	1.733	1.757	1.753	1.762	1.745	1.724	1.710	1.798
Cr	0.000	0.000	0.005	0.000	0.000	0.000	0.012	0.001	0.000	0.002	0.006	0.011	0.006	0.008	0.000	0.002	0.006	0.000	0.000	0.003
TOTAL	**15.546**	**15.545**	**15.577**	**15.544**	**15.659**	**15.641**	**15.560**	**15.592**	**15.569**	**15.675**	**15.607**	**15.554**	**15.751**	**15.647**	**15.653**	**15.594**	**15.629**	**15.646**	**15.607**	**15.661**
Fe/Fe+Mg	*0.390*	*0.394*	*0.415*	*0.421*	*0.377*	*0.387*	*0.418*	*0.436*	*0.437*	*0.339*	*0.481*	*0.469*	*0.382*	*0.469*	*0.475*	*0.480*	*0.458*	*0.465*	*0.480*	*0.465*
Mg/6	0.463	0.473	0.455	0.445	0.498	0.476	0.447	0.444	0.427	0.537	0.419	0.417	0.524	0.424	0.424	0.416	0.441	0.441	0.424	0.441
Fe/6	0.296	0.307	0.323	0.324	0.301	0.300	0.321	0.344	0.332	0.276	0.388	0.369	0.324	0.374	0.384	0.383	0.373	0.384	0.391	0.383
Ti/6	0.028	0.029	0.03:	0.046	0.022	0.029	0.036	0.046	0.035	0.000	0.04:	0.044	0.003	0.031	0.054	0.056	0.053	0.051	0.050	0.04:
Alvi/6	0.162	0.151	0.136	0.134	0.147	0.147	0.146	0.124	0.153	0.168	0.111	0.129	0.146	0.135	0.105	0.107	0.101	0.097	0.106	0.099
(Alvi+Ti)/(Alvi+Ti+Fe+Mg)	0.200	0.188	0.185	0.190	0.174	0.185	0.191	0.178	0.199	0.172	0.166	0.180	0.149	0.173	0.164	0.169	0.159	0.152	0.161	0.153
Na+K	1.849	1.763	1.840	1.822	1.831	1.897	1.828	1.833	1.871	1.767	1.777	1.762	1.743	1.831	1.840	1.802	1.803	1.786	1.766	1.802
Na/K	*0.037*	*0.039*	*0.036*	*0.040*	*0.031*	*0.048*	*0.028*	*0.029*	*0.037*	*0.029*	*0.036*	*0.032*	*0.006*	*0.042*	*0.049*	*0.023*	*0.033*	*0.036*	*0.033*	*0.002*
X	172.27	174.04	169.29	186.31	38.88	32.58	81.21	90.80	90.80	80.90										
Y	352.41	358.13	375.00	361.70	316.22	323.28	344.76	381.75	381.75	200.11										
x-axis (mm)																				
location	*adj crd*	*adj crd*	*near crd*	*near crd*	*adj crd*	*adj crd*	*±matrix*	*matrix*	*matrix*	*psdmrph*	*±adj crd*	*adj crd*	*fracture*	*±adj gt*	*adj crd*	*adj crd*	*near gt*	*near gt*	*near gt*	*near gt*

TABLE B-2: Quantitative Microprobe Analysis for Biotite Compositions

PC-128/10c (continued)							*PC-131/2*				*PC-133A*									
	bt11	**bt12**	**bt13**	**bt14**	**bt15**	**bt16**	**bt1**	**bt2**	**bt3**	**bt4**	**B1a**	**B1b**	**B2a**	**B2b**	**BT1a**	**BT1b**	**BT1c**	**BT1d**	**BT2a**	**BT2b**
WEIGHT PERCENT OXIDES																				
SiO2	36.147	36.736	36.340	36.396	36.391	36.444	34.82:	34.557	35.182	34.602	35.068	35.669	36.386	35.842	35.750	35.821	35.951	36.037	35.512	35.850
Al2O3	19.226	18.883	19.272	19.142	19.240	19.510	18.869	18.507	19.181	18.943	18.929	18.658	19.361	19.229	19.050	18.692	18.431	18.887	18.684	18.636
TiO2	2.549	3.020	3.022	3.155	3.146	3.321	3.346	3.372	3.163	3.384	3.534	3.606	3.905	3.927	3.460	3.497	3.573	3.739	3.788	3.675
MgO	10.933	11.921	12.220	11.583	11.572	11.462	8.208	7.811	8.341	7.867	8.703	8.757	8.548	8.597	9.161	8.720	9.001	9.009	8.368	8.678
FeO	19.390	17.730	17.312	17.864	17.982	16.967	21.758	22.025	21.718	21.946	20.980	20.711	20.749	20.625	20.994	21.395	20.959	21.554	20.719	21.067
MnO	0.051	0.203	0.095	0.044	0.048	0.110	0.301	0.184	0.270	0.323	0.022	0.000	0.089	0.103	0.006	0.000	0.028	0.047	0.008	0.000
CaO	0.000	0.004	0.025	0.003	0.024	0.013	0.038	0.002	0.036	0.038	0.080	0.005	0.030	0.000	0.025	0.027	0.048	0.036	0.052	0.007
Na2O	0.193	0.124	0.131	0.119	0.104	0.087	0.165	0.196	0.145	0.137	0.059	0.096	0.002	0.059	0.088	0.145	0.112	0.133	0.066	0.068
K2O	8.518	8.981	9.137	9.169	9.183	9.240	9.458	9.361	9.832	9.432	9.616	9.711	9.503	9.386	9.205	9.514	9.128	9.299	9.076	9.461
Cr2O3	0.073	0.007	0.000	0.029	0.000	0.043	0.000	0.000	0.000	0.000	0.044	0.000	0.024	0.087	0.044	0.040	0.022	0.000	0.051	0.029
Cl	0.011	0.006	0.005	0.012	0.000	0.003	0.000	0.009	0.000	0.000	0.000	0.006	0.012	0.009	0.035	0.000	0.046	0.006	0.000	0.000
F	0.390	0.406	0.441	0.270	0.316	0.411	0.160	0.311	0.348	0.173	0.107	0.244	0.140	0.192	0.369	0.269	0.241	0.299	0.120	0.134
TOTAL	*97.481*	*98.021*	*98.000*	*97.786*	*98.006*	*97.611*	*97.133*	*96.335*	*98.216*	*96.845*	*97.142*	*97.463*	*98.749*	*98.056*	*98.187*	*98.120*	*97.540*	*99.046*	*96.444*	*97.605*
-O = Cl	-0.002	-0.001	-0.001	-0.003	0.000	-0.001	0.000	-0.002	0.000	0.000	0.000	-0.001	-0.003	-0.002	-0.008	0.000	-0.010	-0.001	0.000	0.000
-O = F	-0.164	-0.171	-0.186	-0.114	-0.133	-0.173	-0.067	-0.131	-0.147	-0.073	-0.045	-0.103	-0.059	-0.081	-0.155	-0.113	-0.101	-0.126	-0.051	-0.056
TOTAL	**97.314**	**97.849**	**97.813**	**97.670**	**97.873**	**97.437**	**97.066**	**96.202**	**98.06:**	**96.772**	**97.097**	**97.359**	**98.687**	**97.973**	**98.024**	**98.007**	**97.428**	**98.919**	**96.393**	**97.549**
CATIONS RECALCULATED TO 22 OXYGENS																				
Si	5.359	5.387	5.328	5.351	5.343	5.353	5.286	5.306	5.290	5.274	5.292	5.360	5.366	5.332	5.327	5.356	5.386	5.332	5.368	5.370
Al	3.360	3.263	3.330	3.317	3.329	3.377	3.375	3.349	3.399	3.403	3.367	3.304	3.365	3.371	3.346	3.294	3.255	3.294	3.329	3.290
Ti	0.284	0.333	0.333	0.349	0.347	0.367	0.382	0.389	0.358	0.388	0.401	0.408	0.433	0.439	0.388	0.393	0.403	0.416	0.431	0.414
Mg	2.417	2.606	2.671	2.539	2.533	2.510	1.857	1.788	1.870	1.788	1.958	1.962	1.879	1.907	2.035	1.944	2.010	1.987	1.886	1.938
Fe	2.404	2.174	2.123	2.197	2.208	2.084	2.761	2.828	2.731	2.798	2.648	2.603	2.559	2.566	2.616	2.675	2.626	2.667	2.619	2.639
Mn	0.006	0.025	0.012	0.005	0.006	0.014	0.039	0.024	0.034	0.042	0.003	0.000	0.011	0.013	0.001	0.000	0.004	0.006	0.001	0.000
Ca	0.000	0.001	0.004	0.000	0.004	0.002	0.006	0.000	0.006	0.006	0.013	0.001	0.005	0.000	0.004	0.004	0.008	0.006	0.008	0.001
Na	0.056	0.035	0.037	0.034	0.02:	0.025	0.049	0.058	0.042	0.041	0.017	0.028	0.001	0.017	0.025	0.042	0.033	0.038	0.019	0.01:
K	1.611	1.680	1.709	1.720	1.720	1.731	1.831	1.834	1.886	1.834	1.851	1.861	1.788	1.781	1.750	1.815	1.745	1.755	1.750	1.808
Cr	0.009	0.001	0.000	0.003	0.000	0.005	0.000	0.000	0.000	0.000	0.005	0.000	0.003	0.010	0.005	0.005	0.003	0.000	0.006	0.003
TOTAL	**15.506**	**15.506**	**15.547**	**15.516**	**15.520**	**15.467**	**15.585**	**15.576**	**15.617**	**15.573**	**15.555**	**15.526**	**15.411**	**15.437**	**15.497**	**15.529**	**15.471**	**15.502**	**15.418**	**15.483**
Fe/Fe+Mg	*0.499*	*0.455*	*0.443*	*0.464*	*0.466*	*0.454*	*0.598*	*0.613*	*0.594*	*0.610*	*0.575*	*0.56:*	*0.577*	*0.574*	*0.562*	*0.579*	*0.566*	*0.573*	*0.581*	*0.577*
Mg/6	0.403	0.434	0.445	0.423	0.422	0.418	0.309	0.298	0.312	0.298	0.326	0.327	0.313	0.318	0.339	0.324	0.335	0.331	0.314	0.323
Fe/6	0.401	0.362	0.354	0.366	0.368	0.347	0.460	0.471	0.455	0.466	0.441	0.434	0.427	0.428	0.436	0.446	0.438	0.445	0.437	0.440
Ti/6	0.047	0.056	0.056	0.058	0.058	0.061	0.064	0.065	0.05:	0.065	0.067	0.068	0.072	0.073	0.065	0.066	0.067	0.069	0.072	0.069
Alvi/6	0.120	0.108	0.110	0.111	0.112	0.122	0.110	0.109	0.115	0.113	0.110	0.111	0.122	0.117	0.112	0.108	0.107	0.104	0.116	0.110
(Alvi+Ti)/(Alvi+Ti+Fe+Mg)	0.172	0.171	0.171	0.177	0.177	0.193	0.184	0.184	0.185	0.189	0.187	0.190	0.208	0.204	0.186	0.184	0.184	0.183	0.200	0.190
Na+K	1.667	1.715	1.746	1.754	1.750	1.756	1.880	1.892	1.928	1.875	1.869	1.889	1.789	1.798	1.775	1.857	1.777	1.793	1.770	1.828
Na/K	*0.034*	*0.021*	*0.022*	*0.01:*	*0.017*	*0.014*	*0.027*	*0.032*	*0.022*	*0.022*	*0.009*	*0.015*	*0.000*	*0.00:*	*0.015*	*0.023*	*0.019*	*0.022*	*0.011*	*0.011*
X			80.13	130.47	125.47	151.04	143.69	131.07	84.76	62.21	-164.39	-164.88	-80.74	-80.96	-140.83	-141.99	-143.14	-144.30	-80.16	-79.34
Y			-285.82	-366.03	-373.00	-369.61	243.45	246.43	92.89	70.45	-86.01	-87.01	-62.63	-61.26	-315.07	-314.30	-313.98	-313.43	-52.22	-49.40
x-axis (mm)											0.00	0.11	0.00	0.14	0.00	0.14	0.26	0.39	0.00	0.29
location	*adj crd*	*±matrix*	*±matrix*	*matrix*	*matrix*	*matrix*					*adj gt*	*±adj gt*	*matrix*	*matrix*	*adj gt*	*±adj gt*	*±adj gt*	*±adj gt*	*matrix*	*matrix*

TABLE B-2: Quantitative Microprobe Analysis for Biotite Compositions

	PC-133A (continued)						***PC-134D***													
	BT2c	**BT3a**	**BT3b**	**BT3c**	**BT3d**	**BT4c**	**B2**	**B3**	**BT1c**	**BT1d**	**BT1e**	**BT2a**	**BT2b**	**BT2c**	**BT2d**	**BT3a**	**BT3b**	**BT3c**	**BT3d**	**BT4c**
WEIGHT PERCENT OXIDES																				
SiO2	35.102	35.242	35.509	35.834	35.960	35.340	36.239	36.625	35.783	35.540	35.424	35.555	36.159	36.129	35.712	35.912	35.271	35.390	35.702	35.272
Al2O3	18.739	18.517	18.816	18.698	18.657	20.016	20.320	20.422	18.878	18.852	19.055	19.361	19.018	19.042	18.975	19.158	19.394	19.077	19.286	18.979
TiO2	3.792	3.943	3.904	3.850	3.776	3.710	0.947	0.452	2.802	2.913	2.886	2.902	2.911	3.034	2.979	2.970	3.054	2.931	2.837	2.815
MgO	8.377	8.407	8.640	8.554	8.488	8.224	9.895	10.508	7.770	8.231	8.174	8.237	8.277	8.420	8.346	8.168	8.414	8.273	8.262	8.083
FeO	21.079	21.007	20.662	20.824	21.010	20.140	19.732	18.286	21.907	22.029	22.004	21.754	21.721	21.483	22.323	21.162	20.673	20.768	20.669	21.205
MnO	0.042	0.072	0.014	0.053	0.106	0.000	0.020	0.048	0.047	0.117	0.000	0.092	0.064	0.058	0.092	0.092	0.053	0.100	0.039	0.000
CaO	0.039	0.084	0.009	0.039	0.045	0.000	0.025	0.011	0.052	0.104	0.070	0.000	0.045	0.045	0.016	0.052	0.018	0.046	0.055	0.020
Na2O	0.175	0.025	0.000	0.059	0.050	0.054	0.025	0.221	0.160	0.206	0.167	0.123	0.256	0.148	0.133	0.095	0.124	0.175	0.127	0.222
K2O	9.312	9.345	9.455	9.147	9.065	9.210	9.356	10.033	9.088	9.090	9.269	9.361	9.382	9.438	9.305	9.472	9.465	9.506	9.424	9.103
Cr2O3	0.049	0.018	0.020	0.111	0.060	0.035	0.096	0.018	0.049	0.114	0.051	0.123	0.080	0.076	0.074	0.034	0.005	0.000	0.054	0.067
Cl	0.032	0.006	0.009	0.006	0.000	0.020	0.000	0.000	0.029	0.041	0.017	0.003	0.026	0.072	0.006	0.000	0.035	0.009	0.000	0.032
F	0.152	0.254	0.133	0.158	0.122	0.209	0.107	0.403	0.191	0.243	0.194	0.200	0.208	0.232	0.215	0.195	0.315	0.347	0.314	0.180
TOTAL	*96.890*	*96.920*	*97.171*	*97.333*	*97.339*	*96.958*	*96.762*	*97.027*	*96.756*	*97.480*	*97.311*	*97.711*	*98.147*	*98.177*	*98.176*	*97.310*	*96.821*	*96.622*	*96.769*	*95.978*
-O = Cl	-0.007	-0.001	-0.002	-0.001	0.000	-0.005	0.000	0.000	-0.007	-0.009	-0.004	-0.001	-0.006	-0.016	-0.001	0.000	-0.008	-0.002	0.000	-0.007
-O = F	-0.064	-0.107	-0.056	-0.067	-0.051	-0.088	-0.045	-0.170	-0.080	-0.102	-0.082	-0.084	-0.088	-0.098	-0.091	-0.082	-0.133	-0.146	-0.132	-0.076
TOTAL	**96.819**	**96.812**	**97.113**	**97.265**	**97.288**	**96.865**	**96.717**	**96.857**	**96.669**	**97.368**	**97.225**	**97.626**	**98.054**	**98.063**	**98.084**	**97.228**	**96.680**	**96.474**	**96.637**	**95.895**
CATIONS RECALCULATED TO 22 OXYGENS																				
Si	5.311	5.332	5.336	5.371	5.387	5.299	5.415	5.456	5.423	5.362	5.350	5.340	5.402	5.394	5.352	5.399	5.334	5.370	5.392	5.380
Al	3.342	3.302	3.333	3.303	3.294	3.537	3.579	3.586	3.372	3.352	3.392	3.427	3.349	3.351	3.351	3.394	3.457	3.412	3.433	3.412
Ti	0.432	0.449	0.441	0.434	0.426	0.418	0.106	0.051	0.319	0.331	0.328	0.328	0.327	0.341	0.336	0.336	0.347	0.335	0.322	0.323
Mg	1.890	1.896	1.936	1.911	1.896	1.838	2.204	2.334	1.755	1.851	1.840	1.844	1.843	1.874	1.864	1.831	1.897	1.871	1.860	1.838
Fe	2.667	2.658	2.597	2.610	2.632	2.526	2.466	2.278	2.777	2.779	2.779	2.732	2.714	2.682	2.798	2.661	2.614	2.635	2.611	2.705
Mn	0.005	0.009	0.002	0.007	0.014	0.000	0.003	0.006	0.006	0.015	0.000	0.012	0.008	0.007	0.012	0.012	0.007	0.013	0.005	0.000
Ca	0.006	0.014	0.001	0.006	0.007	0.000	0.004	0.002	0.008	0.017	0.011	0.000	0.007	0.007	0.003	0.008	0.003	0.007	0.009	0.003
Na	0.051	0.007	0.000	0.017	0.015	0.016	0.007	0.064	0.047	0.060	0.049	0.036	0.074	0.043	0.039	0.028	0.036	0.052	0.037	0.066
K	1.797	1.804	1.813	1.749	1.733	1.762	1.784	1.907	1.757	1.749	1.786	1.793	1.788	1.798	1.779	1.817	1.826	1.840	1.816	1.771
Cr	0.006	0.002	0.002	0.013	0.007	0.004	0.011	0.002	0.006	0.014	0.006	0.015	0.009	0.009	0.009	0.004	0.001	0.000	0.006	0.008
TOTAL	**15.508**	**15.473**	**15.461**	**15.421**	**15.410**	**15.400**	**15.579**	**15.685**	**15.471**	**15.530**	**15.541**	**15.526**	**15.523**	**15.506**	**15.541**	**15.488**	**15.521**	**15.535**	**15.492**	**15.506**
Fe/Fe+Mg	*0.585*	*0.584*	*0.573*	*0.577*	*0.581*	*0.579*	*0.528*	*0.494*	*0.613*	*0.600*	*0.602*	*0.597*	*0.595*	*0.589*	*0.600*	*0.592*	*0.580*	*0.585*	*0.584*	*0.595*
Mg/6	0.315	0.316	0.323	0.319	0.316	0.306	0.367	0.389	0.293	0.309	0.307	0.307	0.307	0.312	0.311	0.305	0.316	0.312	0.310	0.306
Fe/6	0.445	0.443	0.433	0.435	0.439	0.421	0.411	0.380	0.463	0.463	0.463	0.455	0.452	0.447	0.466	0.443	0.436	0.439	0.435	0.451
Ti/6	0.072	0.075	0.074	0.072	0.071	0.06:	0.018	0.008	0.053	0.055	0.055	0.055	0.055	0.057	0.056	0.056	0.058	0.056	0.054	0.054
Alvi/6	0.109	0.106	0.112	0.112	0.114	0.139	0.166	0.174	0.132	0.119	0.124	0.128	0.125	0.124	0.117	0.132	0.132	0.130	0.138	0.132
(Alvi+Ti)/(Alvi+Ti+Fe+Mg)	0.192	0.192	0.197	0.197	0.196	0.223	0.191	0.192	0.197	0.184	0.188	0.193	0.191	0.192	0.182	0.201	0.201	0.199	0.204	0.197
Na+K	1.849	1.811	1.813	1.766	1.747	1.778	1.791	1.971	1.804	1.810	1.835	1.829	1.862	1.840	1.818	1.844	1.862	1.892	1.853	1.837
Na/K	*0.029*	*0.004*	*0.000*	*0.00:*	*0.008*	*0.009*	*0.004*	*0.034*	*0.027*	*0.034*	*0.027*	*0.020*	*0.042*	*0.024*	*0.022*	*0.015*	*0.01:*	*0.028*	*0.021*	*0.037*
X	-78.52	-90.31	-90.22	-90.12	-90.03	-123.66	77.32	99.00	172.18	174.58	176.99	154.07	155.16	156.26	157.35	156.98	156.75	156.52	156.29	161.15
Y	-46.57	-45.60	-47.40	-49.21	-51.01	-119.49	-277.76	-261.17	-308.84	-308.20	-307.56	-192.81	-187.93	-183.06	-178.18	-95.34	-93.12	-91.02	-88.67	-104.64
x-axis (m	0.59	0.00	0.18	0.36	0.54				0.00	0.25	0.50	0.00	0.50	0.00	1.50	0.00	0.22	0.43	0.67	
location	*matrix*	*matrix*	*matrix*	*matrix*	*matrix*	*matrix*	*±adj gt*	*±adj gt*	*±matrix*	*±matrix*	*±matrix*	*±matrix*	*±matrix*	*±matrix*	*±matrix*	*±matrix*	*±matrix*	*±matrix*	*±matrix*	*±matrix*

TABLE B-2: Biotite Compositions

PC-134D (continued)				*PC-134D-2 Matrix Biotite*			
	BT5a	**BT5b**	**BT5c**	**bt1**	**bt1a**	**bt3**	**bt4**
WEIGHT PERCENT OXIDES							
SiO2	36.032	35.781	36.120	34.379	34.508	34.988	34.926
Al2O3	19.488	19.163	19.142	19.132	19.120	18.840	18.789
TiO2	2.869	2.973	3.079	3.278	3.229	3.151	3.228
MgO	8.169	8.215	8.132	8.308	8.372	8.219	8.449
FeO	21.218	21.150	21.401	21.209	21.030	21.903	21.291
MnO	0.122	0.117	0.039	0.098	0.098	0.162	0.064
CaO	0.039	0.055	0.066	0.022	0.000	0.029	0.000
Na2O	0.210	0.135	0.173	0.191	0.177	0.163	0.208
K2O	9.152	9.113	9.510	9.679	9.823	9.627	9.356
Cr2O3	0.045	0.116	0.000	0.041	0.021	0.074	0.039
Cl	0.000	0.000	0.003	0.020	0.000	0.006	0.009
F	0.246	0.197	0.172	0.290	0.108	0.166	0.055
TOTAL	*97.58:*	*97.015*	*97.837*	*96.647*	*96.486*	*97.328*	*96.414*
-O = Cl	0.000	0.000	-0.001	-0.005	0.000	-0.001	-0.002
-O = F	-0.104	-0.083	-0.072	-0.122	-0.046	-0.06:	-0.023
TOTAL	**97.486**	**96.932**	**97.764**	**96.520**	**96.441**	**97.257**	**96.389**
CATIONS RECALCULATED TO 22 OXYGENS							
Si	5.393	5.389	5.403	5.247	5.262	5.303	5.314
Al	3.438	3.401	3.375	3.441	3.436	3.366	3.369
Ti	0.323	0.337	0.346	0.376	0.370	0.359	0.369
Mg	1.823	1.844	1.813	1.890	1.903	1.857	1.916
Fe	2.656	2.664	2.677	2.707	2.682	2.776	2.709
Mn	0.016	0.015	0.005	0.013	0.013	0.021	0.008
Ca	0.006	0.009	0.011	0.004	0.000	0.005	0.000
Na	0.061	0.039	0.050	0.057	0.052	0.048	0.061
K	1.747	1.751	1.815	1.885	1.911	1.862	1.816
Cr	0.005	0.014	0.000	0.005	0.003	0.009	0.005
TOTAL	**15.467**	**15.462**	**15.496**	**15.624**	**15.630**	**15.605**	**15.568**
Fe/Fe+Mg	*0.593*	*0.591*	*0.596*	*0.589*	*0.585*	*0.599*	*0.586*
Mg/6	0.304	0.307	0.302	0.315	0.317	0.310	0.319
Fe/6	0.443	0.444	0.446	0.451	0.447	0.463	0.452
Ti/6	0.054	0.056	0.058	0.063	0.062	0.05:	0.062
Alvi/6	0.138	0.132	0.130	0.115	0.116	0.111	0.114
(Alvi+Ti)/(Alvi+Ti+Fe+Mg)	0.205	0.200	0.200	0.188	0.189	0.182	0.185
Na+K	1.808	1.790	1.865	1.941	1.963	1.909	1.877
Na/K	*0.035*	*0.023*	*0.028*	*0.030*	*0.027*	*0.026*	*0.034*
X	166.24	168.23	170.22	40.17	45.85	59.46	68.30
Y	-113.97	-111.91	-109.84	-168.19	-167.61	-166.99	-173.16
x-axis (m	0.00	0.29	0.57	0.00	0.57		
location	*±matrix*	*±matrix*	*±matrix*	*gt-free thin section adjacent to PC-134D*			

TABLE B-3: Quantitative Microprobe Analysis for Cordierite Compositions

PC-128/10b

	CT1	CT1a	CT1b	CT1c	CT1d	CT1e	CT1f	CT1g	CT1h	CT1i	CT1j	CT1k	C2	C3	C4	C5	C6	C7	C8
WEIGHT PERCENT OXIDES																			
SiO2	49.384	49.548	48.282	48.218	49.201	48.820	49.539	49.82:	49.618	49.373	49.494	50.364	49.552	49.564	49.464	48.711	49.024	49.335	48.164
Al2O3	33.742	33.694	33.437	33.161	33.311	33.712	33.644	33.658	33.633	33.818	33.755	33.703	33.492	33.816	33.385	33.406	33.623	33.768	33.058
TiO2	0.016	0.000	0.000	0.027	0.002	0.006	0.000	0.000	0.000	0.000	0.018	0.000	0.000	0.000	0.000	0.043	0.029	0.031	0.000
MgO	9.56:	9.615	9.206	9.477	9.460	9.56:	9.531	9.506	9.556	9.788	9.814	9.617	9.642	9.849	9.380	9.600	9.547	9.622	9.905
FeO	6.059	6.292	6.418	6.246	6.371	6.408	6.379	6.269	6.436	6.665	6.392	6.056	5.969	6.261	6.387	6.150	5.915	6.045	5.869
MnO	0.317	0.262	0.262	0.265	0.256	0.196	0.276	0.242	0.305	0.268	0.348	0.320	0.202	0.302	0.285	0.305	0.248	0.323	0.305
CaO	0.048	0.039	0.025	0.011	0.052	0.016	0.030	0.020	0.020	0.007	0.000	0.036	0.041	0.000	0.045	0.000	0.025	0.039	0.034
Na2O	0.251	0.260	0.218	0.268	0.289	0.282	0.253	0.245	0.216	0.278	0.317	0.226	0.218	0.332	0.177	0.288	0.283	0.301	0.283
Cr2O3	0.000	0.004	0.000	0.056	0.000	0.000	0.091	0.069	0.019	0.000	0.000	0.000	0.000	0.017	0.048	0.019	0.043	0.000	0.037
TOTAL	**99.387**	**99.714**	**97.848**	**97.729**	**98.942**	**99.010**	**99.743**	**99.839**	**99.803**	**100.197**	**100.138**	**100.322**	**99.116**	**100.141**	**99.171**	**98.522**	**98.737**	**99.464**	**97.655**
Cl	*0.009*	*0.024*	*0.009*	*0.000*	*0.000*	*0.000*	*0.000*	*0.000*	*0.000*	*0.003*	*0.000*	*0.012*	*0.021*	*0.000*	*0.000*	*0.000*	*0.000*	*0.021*	*0.000*
F	*0.119*	*0.000*	*0.000*	*0.039*	*0.008*	*0.000*	*0.000*	*0.000*	*0.000*	*0.016*	*0.006*	*0.019*	*0.041*	*0.000*	*0.117*	*0.003*	*0.075*	*0.018*	*0.111*
CATIONS RECALCULATED TO 18 OXYGENS																			
Si	4.984	4.989	4.960	4.959	4.996	4.956	4.989	5.007	4.994	4.959	4.970	5.02:	5.008	4.972	5.008	4.966	4.978	4.977	4.952
Al	4.014	3.998	4.048	4.01:	3.986	4.033	3.994	3.986	3.990	4.003	3.995	3.967	3.989	3.998	3.984	4.014	4.024	4.015	4.006
Ti	0.001	0.000	0.000	0.002	0.000	0.000	0.000	0.000	0.000	0.000	0.001	0.000	0.000	0.000	0.000	0.003	0.002	0.002	0.000
Mg	1.440	1.443	1.410	1.453	1.432	1.448	1.431	1.424	1.434	1.466	1.469	1.432	1.453	1.473	1.416	1.459	1.445	1.447	1.518
Fe	0.511	0.530	0.551	0.537	0.541	0.544	0.537	0.527	0.542	0.560	0.537	0.506	0.504	0.525	0.541	0.524	0.502	0.510	0.505
Mn	0.027	0.022	0.023	0.023	0.022	0.017	0.023	0.021	0.026	0.023	0.02:	0.027	0.017	0.026	0.024	0.026	0.021	0.028	0.027
Ca	0.005	0.004	0.003	0.001	0.006	0.002	0.003	0.002	0.002	0.001	0.000	0.004	0.004	0.000	0.005	0.000	0.003	0.004	0.004
Na	0.049	0.051	0.043	0.053	0.057	0.056	0.049	0.048	0.042	0.054	0.062	0.044	0.043	0.065	0.035	0.057	0.056	0.059	0.056
Cr	0.000	0.000	0.000	0.005	0.000	0.000	0.007	0.005	0.002	0.000	0.000	0.000	0.000	0.001	0.004	0.002	0.003	0.000	0.003
TOTAL	**11.032**	**11.038**	**11.038**	**11.053**	**11.03:**	**11.055**	**11.035**	**11.021**	**11.031**	**11.066**	**11.063**	**11.009**	**11.019**	**11.060**	**11.016**	**11.051**	**11.034**	**11.042**	**11.071**
Fe/Fe+Mg	*0.262*	*0.269*	*0.281*	*0.270*	*0.274*	*0.273*	*0.273*	*0.270*	*0.274*	*0.276*	*0.268*	*0.261*	*0.258*	*0.263*	*0.276*	*0.264*	*0.258*	*0.261*	*0.249*
X	163.91	164.14	164.41	164.50	165.00	165.19	165.74	166.03	165.90	166.31	166.42	167.25	167.64	167.57	163.22	161.83	169.71	171.59	36.14
Y	357.41	356.83	355.57	354.94	354.35	353.71	352.72	350.73	350.75	349.87	349.03	347.83	348.97	353.96	350.83	349.72	353.91	354.63	321.89
x-axis mm	0.00	0.06	0.19	0.25	0.33	0.40	0.51	0.71	0.73	0.82	0.91	1.05							0.00
location	*rim - qz*	*near rim*	*'spike'*	*interior*	*interior*	*interior*	*interior*	*interior*	*interior*	*'spike'*	*near rim*	*rim - qz*	*near rim*	*interior*	*interior*	*rim - qz*	*adj fract*	*near rim*	*interior*

TABLE B-3: Quantitative Microprobe Analysis for Cordierite Compositions

PC-128/10b (continued)					*PC-128 /10c*														
	C8a	**C8b**	**C8c**	**C8d**	**crd1**	**crd1a**	**crd1b**	**crd1c**	**crd1d**	**crd1e**	**crd1f**	**crd1g**	**crd1h**	**crd5**	**crd5a**	**crd5b**	**crd6**	**crd6a**	**crd6b**
WEIGHT PERCENT OXIDES																			
SiO2	48.555	48.895	48.893	48.997	48.500	49.386	49.389	49.197	49.018	49.452	49.424	49.618	49.124	49.234	48.923	49.038	49.489	49.290	49.608
Al2O3	33.099	33.151	33.527	33.239	33.705	33.693	33.416	33.332	32.995	33.534	33.385	33.451	33.591	33.892	33.692	33.546	33.265	33.461	33.027
TiO2	0.000	0.014	0.000	0.084	0.019	0.000	0.000	0.009	0.008	0.012	0.000	0.023	0.017	0.000	0.023	0.000	0.000	0.009	0.012
MgO	9.371	9.757	9.564	9.754	9.096	9.081	8.961	9.103	9.091	9.005	8.950	9.067	9.164	9.153	8.962	9.003	9.116	9.066	8.865
FeO	6.321	6.094	6.158	5.964	8.117	8.100	8.149	7.954	8.352	8.452	8.191	8.071	7.877	8.057	7.774	7.962	7.961	8.092	8.136
MnO	0.204	0.268	0.297	0.357	0.182	0.227	0.186	0.196	0.186	0.207	0.241	0.174	0.283	0.200	0.196	0.249	0.264	0.238	0.201
CaO	0.020	0.034	0.043	0.027	0.013	0.028	0.020	0.010	0.031	0.018	0.025	0.021	0.009	0.005	0.000	0.006	0.013	0.003	0.000
Na2O	0.255	0.306	0.307	0.336	0.103	0.138	0.076	0.098	0.139	0.138	0.109	0.125	0.149	0.135	0.122	0.152	0.089	0.105	0.133
Cr2O3	0.000	0.000	0.048	0.056	0.005	0.000	0.000	0.012	0.000	0.000	0.002	0.000	0.006	0.010	0.000	0.000	0.023	0.000	0.067
TOTAL	**97.825**	**98.519**	**98.837**	**98.814**	**99.740**	**100.653**	**100.197**	**99.911**	**99.820**	**100.818**	**100.327**	**100.550**	**100.220**	**100.686**	**99.692**	**99.956**	**100.220**	**100.264**	**100.049**
Cl	*0.015*	*0.000*	*0.009*	*0.000*	*0.011*	*0.019*	*0.004*	*0.012*	*0.008*	*0.004*	*0.000*	*0.000*	*0.008*	*0.007*	*0.000*	*0.000*	*0.000*	*0.011*	*0.000*
F	*0.000*	*0.000*	*0.047*	*0.000*	*0.018*	*0.001*	*0.000*	*0.000*	*0.072*	*0.043*	*0.000*	*0.030*	*0.075*	*0.000*	*0.018*	*0.000*	*0.000*	*0.040*	*0.016*
CATIONS RECALCULATED TO 18 OXYGENS																			
Si	4.985	4.983	4.969	4.979	4.926	4.966	4.987	4.979	4.978	4.972	4.987	4.991	4.959	4.949	4.959	4.964	4.994	4.975	5.016
Al	4.005	3.982	4.016	3.981	4.034	3.993	3.976	3.976	3.949	3.974	3.970	3.965	3.997	4.015	4.025	4.002	3.956	3.980	3.936
Ti	0.000	0.001	0.000	0.006	0.001	0.000	0.000	0.001	0.001	0.001	0.000	0.002	0.001	0.000	0.002	0.000	0.000	0.001	0.001
Mg	1.434	1.482	1.449	1.478	1.377	1.361	1.349	1.374	1.376	1.350	1.346	1.359	1.379	1.371	1.354	1.359	1.371	1.364	1.336
Fe	0.543	0.519	0.523	0.507	0.689	0.681	0.688	0.673	0.709	0.711	0.691	0.679	0.665	0.677	0.659	0.674	0.672	0.683	0.688
Mn	0.018	0.023	0.026	0.031	0.016	0.019	0.016	0.017	0.016	0.018	0.021	0.015	0.024	0.017	0.017	0.021	0.023	0.020	0.017
Ca	0.002	0.004	0.005	0.003	0.001	0.003	0.002	0.001	0.003	0.002	0.003	0.002	0.001	0.001	0.000	0.001	0.001	0.000	0.000
Na	0.051	0.061	0.061	0.066	0.020	0.027	0.015	0.019	0.027	0.027	0.021	0.024	0.029	0.026	0.024	0.02:	0.017	0.021	0.026
Cr	0.000	0.000	0.004	0.005	0.000	0.000	0.000	0.001	0.000	0.000	0.000	0.000	0.000	0.001	0.000	0.000	0.002	0.000	0.005
TOTAL	**11.038**	**11.055**	**11.052**	**11.055**	**11.066**	**11.051**	**11.033**	**11.041**	**11.060**	**11.054**	**11.039**	**11.037**	**11.056**	**11.057**	**11.039**	**11.050**	**11.036**	**11.044**	**11.026**
Fe/Fe+Mg	*0.275*	*0.259*	*0.265*	*0.255*	*0.334*	*0.334*	*0.338*	*0.329*	*0.340*	*0.345*	*0.339*	*0.333*	*0.325*	*0.331*	*0.327*	*0.332*	*0.329*	*0.334*	*0.340*
					cordierite adjacent garnet									*cordierite ±adjacent garnet*			*cordierite ±adjacent garnet*		
X	37.93	39.60	40.43	40.89	95.94	95.50	94.90	94.14	94.28	94.44	94.72	95.03	95.27	139.20	141.46	142.23	151.71	148.83	154.45
Y	321.48	320.61	319.59	318.90	-218.46	-218.67	-219.26	-219.71	-221.26	-222.00	-222.58	-222.99	-223.68	-208.22	-208.57	-211.90	-201.73	-201.18	-199.97
x-axis mm	0.18	0.37	0.50	0.59	0.00	0.05	0.13	0.22	0.38	0.45	0.52	0.57	0.64	0.00	0.23	0.57	0.00	0.29	0.87
location	*interior*	*interior*	*interior*	*near rim*	*rim - gt*	*near rim*	*interior*	*interior*	*interior*	*interior*	*interior*	*near rim*	*rim - bt*	*nr rim?*	*nr rim?*	*±rim*	*interior?*	*interior*	*interior?*

TABLE B-3: Cordierite Compositions

PC-128/10c (continued)

	crd7	crd7a	crd8	crd8a	crd8b
WEIGHT PERCENT OXIDES					
SiO2	49.987	49.164	48.422	48.901	49.048
Al2O3	33.701	33.694	33.846	33.126	33.762
TiO2	0.005	0.004	0.000	0.015	0.027
MgO	9.573	9.520	9.717	9.413	9.655
FeO	7.319	7.466	7.131	7.150	7.232
MnO	0.190	0.117	0.187	0.146	0.194
CaO	0.000	0.024	0.025	0.012	0.026
Na2O	0.105	0.097	0.107	0.068	0.148
Cr2O3	0.013	0.000	0.000	0.000	0.000
TOTAL	**100.893**	**100.086**	**99.435**	**98.831**	**100.092**
Cl	*0.010*	*0.006*	*0.031*	*0.000*	*0.011*
F	*0.000*	*0.047*	*0.000*	*0.000*	*0.037*
CATIONS RECALCULATED TO 18 OXYGENS					
Si	4.992	4.956	4.913	4.984	4.943
Al	3.967	4.003	4.047	3.979	4.010
Ti	0.000	0.000	0.000	0.001	0.002
Mg	1.425	1.431	1.46:	1.430	1.451
Fe	0.611	0.629	0.605	0.609	0.610
Mn	0.016	0.00:	0.016	0.013	0.017
Ca	0.000	0.003	0.003	0.001	0.003
Na	0.020	0.019	0.021	0.013	0.029
Cr	0.001	0.000	0.000	0.000	0.000
TOTAL	**11.034**	**11.051**	**11.074**	**11.032**	**11.064**
Fe/Fe+Mg	*0.300*	*0.306*	*0.292*	*0.299*	*0.296*
	crd-sil mat in matr		*matrix*		
X	37.50	34.46	103.49	102.32	103.73
Y	-356.69	-353.62	-68.90	-69.89	-71.99
x-axis mm			0.00	0.15	0.41
location	*nr rim?*	*nr rim?*	*mtrx int*	*mtrx int*	*mtrx int*

TABLE B-4: Quantitative Microprobe Analysis for Plagioclase Compositions

PC-19D

	P1a	**P1b**	**P1c**	**P1d**	**P2a**	**P2b**	**P2c**	**P3a**	**P3b**	**P3c**	**P4a**	**P4b**	**P4c**	**P4d**	**P5**	**P6a**	**P6b**	**PT1a**
WEIGHT PERCENT OXIDES																		
SiO2	61.713	62.100	62.062	62.175	61.789	61.968	61.653	61.703	62.402	61.513	61.174	62.447	61.666	62.064	62.050	61.661	61.794	61.014
Al2O3	25.296	24.968	24.935	24.701	24.948	25.060	24.646	24.360	24.813	24.468	24.778	24.800	24.689	24.813	24.593	25.131	24.710	24.694
FeO	0.240	0.122	0.000	0.096	0.142	0.022	0.147	0.039	0.123	0.018	0.000	0.068	0.054	0.078	0.053	0.162	0.127	0.036
CaO	5.729	5.517	5.435	5.526	5.750	5.368	5.447	5.769	5.484	5.816	6.062	5.297	5.546	5.606	5.629	6.049	5.808	5.574
Na2O	8.862	8.813	8.827	8.939	8.603	8.682	8.56:	8.885	9.041	8.761	8.690	8.806	8.725	8.960	8.841	8.585	8.731	8.787
K2O	0.030	0.098	0.052	0.059	0.105	0.151	0.036	0.109	0.098	0.100	0.082	0.121	0.096	0.075	0.087	0.125	0.032	0.107
TOTAL	**101.870**	**101.618**	**101.311**	**101.496**	**101.337**	**101.251**	**100.499**	**100.865**	**101.961**	**100.676**	**100.786**	**101.539**	**100.776**	**101.596**	**101.253**	**101.713**	**101.202**	**100.212**
CATIONS RECALCULATED TO 8 OXYGENS																		
Si	2.696	2.715	2.719	2.722	2.711	2.716	2.722	2.722	2.721	2.718	2.702	2.729	2.718	2.716	2.723	2.699	2.715	2.708
Al	1.303	1.287	1.287	1.275	1.290	1.295	1.283	1.266	1.275	1.274	1.290	1.277	1.283	1.280	1.272	1.296	1.280	1.292
Fe	0.009	0.004	0.000	0.004	0.005	0.001	0.005	0.001	0.004	0.001	0.000	0.002	0.002	0.003	0.002	0.006	0.005	0.001
Ca	0.268	0.258	0.255	0.259	0.270	0.252	0.258	0.273	0.256	0.275	0.287	0.248	0.262	0.263	0.265	0.284	0.273	0.265
Na	0.751	0.747	0.750	0.759	0.732	0.738	0.734	0.760	0.764	0.750	0.744	0.746	0.746	0.760	0.752	0.729	0.744	0.756
K	0.002	0.005	0.003	0.003	0.006	0.008	0.002	0.006	0.005	0.006	0.005	0.007	0.005	0.004	0.005	0.007	0.002	0.006
TOTAL	**5.029**	**5.018**	**5.014**	**5.022**	**5.013**	**5.00:**	**5.004**	**5.028**	**5.026**	**5.023**	**5.028**	**5.009**	**5.016**	**5.026**	**5.019**	**5.021**	**5.018**	**5.028**
An	0.263	0.256	0.253	0.254	0.268	0.253	0.259	0.263	0.250	0.267	0.277	0.248	0.259	0.256	0.259	0.278	0.268	0.258
Ab	0.736	0.739	0.744	0.743	0.726	0.739	0.739	0.732	0.745	0.728	0.719	0.745	0.736	0.740	0.736	0.715	0.730	0.736
Or	0.002	0.005	0.003	0.003	0.006	0.008	0.002	0.006	0.005	0.005	0.004	0.007	0.005	0.004	0.005	0.007	0.002	0.006
X	-45.35	-45.04	-44.81	-44.65	-53.91	-53.56	-53.16	-51.06	-50.49	-49.88	-214.91	-214.39	-213.84	-213.50	-54.54	-54.32	-55.11	-133.90
Y	362.29	362.93	363.47	363.92	356.84	356.32	355.43	252.17	252.26	252.47	363.75	364.26	365.06	365.81	160.17	157.63	157.92	364.89
x-axis mm	0.00	0.07	0.13	0.18	0.00	0.06	0.16	0.00	0.06	0.12	0.00	0.07	0.17	0.25		0.00	0.08	0.00
location	*mtrx rim*	*mtrx int*	*mtrx int*	*mtrx rim*	*mtrx rim*	*mtrx int*	*mtrx rim*	*mtrx rim*	*mtrx int*	*mtrx rim*	*mtrx rim*	*mtrx int*	*mtrx int*	*mtrx rim*	*adj int*	*adj rim*	*adj int*	*leuco rim*

TABLE B-4: Quantitative Microprobe Analysis for Plagioclase Compositions

	PC-19D (continued)								*PC-50E*									
	PT1b	**PT1c**	**PT1d**	**PT1f**	**PT1g**	**PT1h**	**PT1i**	**PT1j**	**P1**	**P5**	**P6**	**P7**	**P8**	**P9**	**P17**	**P18**	**P19**	**P19c**
WEIGHT PERCENT OXIDES																		
SiO2	61.265	61.909	61.519	62.579	61.096	61.361	61.311	59.026	59.250	59.348	59.651	59.831	59.073	59.589	60.098	59.633	59.292	59.573
Al2O3	24.454	25.159	24.693	24.550	24.380	24.804	24.911	24.242	25.982	25.607	25.200	25.639	25.850	25.758	25.759	25.252	25.714	25.493
FeO	0.035	0.061	0.107	0.123	0.000	0.028	0.119	0.135	0.137	0.091	0.092	0.062	0.079	0.124	0.133	0.062	0.176	0.017
CaO	5.455	5.726	5.671	5.392	5.840	5.534	5.852	8.142	8.063	7.837	7.535	7.575	8.075	8.128	7.580	7.771	7.724	7.466
Na2O	8.980	8.906	8.911	8.908	9.010	8.729	8.819	8.372	7.186	7.359	7.517	7.541	7.298	6.947	7.863	7.398	7.393	7.484
K2O	0.141	0.114	0.082	0.114	0.125	0.080	0.118	0.296	0.078	0.045	0.018	0.038	0.043	0.055	0.059	0.040	0.079	0.074
TOTAL	**100.330**	**101.875**	**100.983**	**101.666**	**100.451**	**100.536**	**101.130**	**100.213**	**100.696**	**100.287**	**100.013**	**100.686**	**100.418**	**100.601**	**101.492**	**100.156**	**100.378**	**100.107**
CATIONS RECALCULATED TO 8 OXYGENS																		
Si	2.716	2.704	2.711	2.733	2.710	2.712	2.700	2.652	2.630	2.644	2.661	2.652	2.630	2.644	2.647	2.658	2.640	2.655
Al	1.278	1.295	1.282	1.264	1.274	1.292	1.293	1.284	1.359	1.344	1.325	1.339	1.357	1.347	1.337	1.327	1.349	1.339
Fe	0.001	0.002	0.004	0.004	0.000	0.001	0.004	0.005	0.005	0.003	0.003	0.002	0.003	0.005	0.005	0.002	0.007	0.001
Ca	0.259	0.268	0.268	0.252	0.278	0.262	0.276	0.392	0.384	0.374	0.360	0.360	0.385	0.386	0.358	0.371	0.368	0.356
Na	0.772	0.754	0.761	0.754	0.775	0.748	0.753	0.729	0.619	0.636	0.650	0.648	0.630	0.598	0.671	0.639	0.638	0.647
K	0.008	0.006	0.005	0.006	0.007	0.005	0.007	0.017	0.004	0.003	0.001	0.002	0.002	0.003	0.003	0.002	0.004	0.004
TOTAL	**5.035**	**5.029**	**5.031**	**5.015**	**5.044**	**5.019**	**5.033**	**5.079**	**5.001**	**5.003**	**5.002**	**5.004**	**5.008**	**4.983**	**5.022**	**4.000**	**5.007**	**5.001**
An	0.249	0.261	0.259	0.249	0.262	0.258	0.267	0.344	0.381	0.370	0.356	0.356	0.379	0.391	0.346	0.366	0.364	0.354
Ab	0.743	0.733	0.737	0.745	0.731	0.737	0.727	0.641	0.615	0.628	0.643	0.642	0.619	0.605	0.650	0.631	0.631	0.642
Or	0.008	0.006	0.004	0.006	0.007	0.004	0.006	0.015	0.004	0.003	0.001	0.002	0.002	0.003	0.003	0.002	0.004	0.004
X	-136.41	-138.92	-141.42	-146.44	-148.95	-151.45	-153.96	-156.47	-125.87	-113.51	-112.70	-109.20	-114.74	-124.11	-110.31	-129.86	-48.74	-48.93
Y	365.49	366.09	366.70	367.90	368.50	369.10	369.71	370.31	88.66	91.49	97.74	99.88	105.19	109.15	104.71	87.38	260.68	260.17
x-axis mm	0.26	0.52	0.77	1.29	1.55	1.80	2.06										0.00	0.06
location	*leuco int*	*leuco int*	*leuco int*	*leuco int*	*leuco int*	*leuco int*	*leuco ±rm*	*diff. plag*	*incl*	*incl*	*incl*	*adj / incl*	*incl*	*incl*	*adjacent*	*adjacent*	*mtrx rim*	*mtrx int*

TABLE B-4: Quantitative Microprobe Analysis for Plagioclase Compositions

PC-50E (continued)																	*PC-66A*	
	P21a	**P21b**	**P22b**	**P22e**	**P23**	**PT1a**	**PT1d**	**PT1e**	**PT1f**	**PT1i**	**PT3c**	**PT3d**	**PT4b**	**PT4c**	**PT4e**	**PT5d**	**P1b**	**P2a**
WEIGHT PERCENT OXIDES																		
SiO2	59.589	60.282	60.392	59.640	60.676	60.287	60.139	59.998	60.083	59.881	59.472	59.591	59.811	60.051	60.069	59.502	60.265	62.267
Al2O3	25.406	25.467	25.371	25.368	25.495	25.216	25.291	25.423	25.205	25.519	25.321	25.426	25.033	25.205	25.437	25.054	25.533	24.864
FeO	0.041	0.058	0.022	0.132	0.000	0.176	0.097	0.050	0.029	0.090	0.130	0.142	0.054	0.070	0.067	0.112	0.056	0.134
CaO	7.948	7.844	7.133	7.693	7.745	7.456	7.507	7.518	7.586	7.909	7.966	7.546	7.787	7.494	7.787	7.762	6.821	5.704
Na2O	7.328	7.388	7.932	7.838	7.322	7.509	7.483	7.480	7.686	7.475	7.325	7.412	7.824	7.629	7.194	7.689	8.158	8.602
K2O	0.026	0.037	0.088	0.028	0.053	0.183	0.050	0.063	0.027	0.044	0.033	0.059	0.033	0.123	0.045	0.014	0.086	0.077
TOTAL	**100.338**	**101.076**	**100.938**	**100.699**	**101.291**	**100.827**	**100.567**	**100.532**	**100.616**	**100.918**	**100.247**	**100.176**	**100.542**	**100.572**	**100.599**	**100.133**	**100.919**	**101.648**
CATIONS RECALCULATED TO 8 OXYGENS																		
Si	2.652	2.661	2.669	2.649	2.669	2.669	2.667	2.662	2.665	2.651	2.651	2.655	2.660	2.666	2.662	2.657	2.664	2.721
Al	1.333	1.325	1.321	1.328	1.322	1.316	1.322	1.329	1.318	1.332	1.330	1.335	1.312	1.319	1.329	1.318	1.330	1.280
Fe	0.002	0.002	0.001	0.005	0.000	0.007	0.004	0.002	0.001	0.003	0.005	0.005	0.002	0.003	0.002	0.004	0.002	0.005
Ca	0.379	0.371	0.338	0.366	0.365	0.354	0.357	0.357	0.361	0.375	0.380	0.360	0.371	0.356	0.370	0.371	0.323	0.267
Na	0.632	0.632	0.680	0.675	0.625	0.645	0.643	0.643	0.661	0.642	0.633	0.640	0.675	0.657	0.618	0.666	0.699	0.729
K	0.001	0.002	0.005	0.002	0.003	0.010	0.003	0.004	0.002	0.002	0.002	0.003	0.002	0.007	0.003	0.001	0.005	0.004
TOTAL	**4.999**	**4.994**	**5.013**	**5.025**	**4.984**	**5.000**	**4.995**	**4.997**	**5.007**	**5.005**	**5.001**	**4.999**	**5.022**	**5.007**	**4.984**	**5.017**	**5.023**	**5.006**
An	0.374	0.369	0.330	0.351	0.368	0.351	0.356	0.356	0.352	0.368	0.375	0.359	0.354	0.349	0.373	0.358	0.315	0.267
Ab	0.624	0.629	0.665	0.647	0.629	0.639	0.642	0.641	0.646	0.629	0.623	0.638	0.644	0.644	0.624	0.641	0.681	0.729
Or	0.001	0.002	0.005	0.002	0.003	0.010	0.003	0.004	0.001	0.002	0.002	0.003	0.002	0.007	0.003	0.001	0.005	0.004
X	-61.62	-61.92	-67.94	-66.43	-60.42	-131.78	-132.11	-132.22	-132.33	-132.67	-116.67	-115.96	-98.93	-98.44	-97.46	-97.78	-142.08	-120.35
Y	248.33	247.91	244.52	246.23	232.00	115.68	114.21	113.72	113.22	111.75	116.45	116.94	116.98	116.38	115.17	116.93	-339.14	-319.50
x-axis mm	0.00	0.05	0.08	0.33		0.00	0.15	0.20	0.25	0.40	0.17	0.26	0.08	0.15	0.31			0.00
location	*mtrx rim*	*mtrx int*	*mtrx int*	*mtrx rim*	*mtrx int*	*rm nr grt*	*int nr grt*	*int nr grt*	*int nr grt*	*int nr grt*	*incl. int*	*incl. int*	*int nr grt*	*int nr grt*	*int nr grt*	*rm nr grt*	*int nr grt*	*mtrx rim*

TABLE B-4: Quantitative Microprobe Analysis for Plagioclase Compositions

	PC-66A (continued)						*PC-68A*											
	P2b	**P3a**	**P3b**	**P3c**	**P3d**	**P4b**	**P1a**	**P1b**	**P1c**	**P2a**	**P2b**	**P2c**	**P3a**	**P3b**	**P4a**	**P4b**	**P4c**	**P5a**
WEIGHT PERCENT OXIDES																		
SiO2	60.734	60.594	60.561	61.032	59.884	60.416	60.028	60.398	60.151	60.009	60.270	59.885	59.559	60.193	60.401	60.103	59.891	60.275
Al2O3	25.898	25.997	25.505	25.477	25.665	25.370	26.090	25.514	25.569	25.806	25.490	26.097	25.993	25.866	25.726	25.689	26.209	25.835
FeO	0.014	0.195	0.160	0.000	0.636	0.296	0.060	0.058	0.039	0.146	0.000	0.094	0.160	0.000	0.014	0.072	0.167	0.100
CaO	6.595	6.643	6.797	6.687	6.58:	6.667	7.020	6.802	7.296	7.096	6.482	7.208	6.991	6.890	7.061	7.184	7.238	6.914
Na2O	7.977	8.223	7.932	8.218	8.019	7.715	7.788	8.065	8.028	8.111	7.960	7.960	8.039	8.107	8.150	7.788	7.550	7.943
K2O	0.105	0.104	0.093	0.105	0.279	0.220	0.055	0.048	0.095	0.073	0.036	0.016	0.025	0.041	0.080	0.177	0.045	0.066
TOTAL	**101.323**	**101.756**	**101.048**	**101.519**	**101.073**	**100.684**	**101.041**	**100.885**	**101.178**	**101.241**	**100.238**	**101.260**	**100.767**	**101.097**	**101.432**	**101.013**	**101.100**	**101.133**
CATIONS RECALCULATED TO 8 OXYGENS																		
Si	2.668	2.657	2.671	2.678	2.651	2.675	2.648	2.668	2.656	2.648	2.674	2.641	2.640	2.655	2.658	2.656	2.642	2.657
Al	1.341	1.343	1.326	1.318	1.339	1.324	1.357	1.328	1.330	1.342	1.333	1.356	1.358	1.345	1.334	1.338	1.363	1.342
Fe	0.001	0.007	0.006	0.000	0.023	0.011	0.002	0.002	0.001	0.005	0.000	0.003	0.006	0.000	0.001	0.003	0.006	0.004
Ca	0.310	0.312	0.321	0.314	0.313	0.316	0.332	0.322	0.345	0.336	0.308	0.341	0.332	0.326	0.333	0.340	0.342	0.327
Na	0.679	0.699	0.678	0.699	0.688	0.662	0.666	0.691	0.687	0.694	0.685	0.681	0.691	0.693	0.695	0.667	0.646	0.679
K	0.006	0.006	0.005	0.006	0.016	0.012	0.003	0.003	0.005	0.004	0.002	0.001	0.001	0.002	0.004	0.00:	0.003	0.004
TOTAL	**5.005**	**5.024**	**5.008**	**5.015**	**5.031**	**5.001**	**5.008**	**5.014**	**5.025**	**5.02:**	**5.003**	**5.022**	**5.028**	**5.021**	**5.025**	**5.014**	**5.001**	**5.013**
An	0.312	0.307	0.320	0.308	0.307	0.319	0.331	0.317	0.333	0.325	0.310	0.333	0.324	0.319	0.322	0.334	0.345	0.324
Ab	0.682	0.687	0.675	0.686	0.677	0.668	0.665	0.680	0.662	0.671	0.688	0.666	0.674	0.679	0.673	0.656	0.652	0.673
Or	0.006	0.006	0.005	0.006	0.016	0.013	0.003	0.003	0.005	0.004	0.002	0.001	0.001	0.002	0.004	0.00:	0.003	0.004
X	-119.98	-164.48	-164.48	-164.55	-165.45	-152.01	72.93	72.46	71.32	75.71	74.36	72.30	68.52	68.52	60.63	58.86	57.27	142.83
Y	-318.49	-87.46	-86.86	-86.06	-85.08	-92.38	-80.64	-79.63	-79.40	-73.21	-72.86	-73.13	-83.59	-84.57	-300.62	-300.68	-300.68	-341.36
x-axis mm	0.11	0.00	0.06	0.14	0.27		0.00	0.11	0.23	0.00	0.14	0.35	0.00	0.0:	0.00	0.18	0.34	0.00
location	*mtrx int*	*mtrx rim*	*mtrx int*	*mtrx rim*	*mtrx int*	*mtrx ±int*	*mtrx rim*	*mtrx int*	*mtrx rim*	*mtrx rim*	*mtrx int*	*mtrx rim*	*mtrx rim*	*mtrx int*	*rm ±nr gt*	*int ±nr gt*	*rm ±nr gt*	*leuco ±rm*

TABLE B-4: Quantitative Microprobe Analysis for Plagioclase Compositions

PC-68A (continued)												*PC-80B*						
	P5b	**P5c**	**P5d**	**P5e**	**P5f**	**F1**	**F2**	**F2a**	**F2b**	**F3**	**6a**	**P1**	**P2**	**P4**	**P5**	**P6**	**P7**	**P8**
WEIGHT PERCENT OXIDES																		
SiO2	61.215	60.889	61.727	62.322	59.917	60.300	59.834	60.829	61.439	60.439	44.819	44.703	45.058	45.217	45.373	45.177	44.935	45.100
Al2O3	25.247	25.536	25.160	24.584	25.731	26.213	25.685	25.183	25.330	26.019	35.348	35.733	35.567	36.472	36.297	36.277	36.093	36.067
FeO	0.000	0.000	0.109	0.174	0.044	0.275	0.207	0.118	0.316	0.107	0.159	0.224	0.213	0.056	0.063	0.080	0.066	0.056
CaO	6.253	6.712	6.266	5.384	6.854	7.216	7.058	6.689	6.588	7.083	19.820	19.738	18.757	19.762	20.020	19.253	19.314	19.862
Na2O	8.535	7.971	8.331	8.952	7.976	8.166	7.856	8.333	8.161	7.863	0.499	0.641	0.745	0.569	0.558	0.497	0.543	0.486
K2O	0.036	0.041	0.086	0.059	0.080	0.064	0.039	0.043	0.027	0.016	0.000	0.026	0.346	0.039	0.000	0.024	0.009	0.000
TOTAL	**101.286**	**101.149**	**101.679**	**101.475**	**100.602**	**102.234**	**100.679**	**101.195**	**101.861**	**101.527**	**100.645**	**101.065**	**100.686**	**102.115**	**102.311**	**101.308**	**100.960**	**101.571**
CATIONS RECALCULATED TO 8 OXYGENS																		
Si	2.690	2.678	2.700	2.728	2.656	2.638	2.653	2.680	2.687	2.654	2.061	2.049	2.069	2.047	2.051	2.057	2.055	2.053
Al	1.307	1.324	1.297	1.268	1.344	1.352	1.342	1.308	1.306	1.347	1.916	1.930	1.925	1.946	1.934	1.947	1.945	1.935
Fe	0.000	0.000	0.004	0.006	0.002	0.010	0.008	0.004	0.012	0.004	0.006	0.009	0.008	0.002	0.002	0.003	0.003	0.002
Ca	0.294	0.316	0.294	0.253	0.326	0.338	0.335	0.316	0.309	0.333	0.976	0.969	0.923	0.959	0.970	0.939	0.946	0.969
Na	0.727	0.680	0.707	0.760	0.685	0.693	0.675	0.712	0.692	0.669	0.044	0.057	0.066	0.04:	0.049	0.044	0.048	0.043
K	0.002	0.002	0.005	0.003	0.005	0.004	0.002	0.002	0.002	0.001	0.000	0.002	0.020	0.002	0.000	0.001	0.001	0.000
TOTAL	**5.021**	**5.001**	**5.007**	**5.019**	**5.017**	**5.034**	**5.015**	**5.023**	**5.007**	**5.008**	**5.004**	**5.015**	**5.012**	**5.006**	**5.006**	**4.992**	**4.997**	**5.001**
An	0.288	0.317	0.292	0.249	0.321	0.327	0.331	0.307	0.308	0.332	0.956	0.943	0.914	0.948	0.952	0.954	0.951	0.958
Ab	0.710	0.681	0.703	0.748	0.675	0.670	0.667	0.691	0.690	0.667	0.044	0.055	0.066	0.049	0.048	0.045	0.048	0.042
Or	0.002	0.002	0.005	0.003	0.004	0.003	0.002	0.002	0.002	0.001	0.000	0.001	0.020	0.002	0.000	0.001	0.001	0.000
X	138.72	132.24	129.14	124.91	116.19	172.99	171.95	171.11	171.36	181.80								
Y	-342.86	-345.37	-346.48	-347.46	-348.10	262.12	255.36	254.40	253.31	282.37								
x-axis mm	0.44	1.13	1.46	1.90	2.77		0.00	0.13	0.24									
location	*leuco int*	*leuco int*	*leuco int*	*leuco int*	*leuco rm*	*adjacent*	*rm nr gt*	*int nr gt*	*rm nr gt*	*adjacent*	*matrix*	*near grt*	*near grt*	*mtrx rim*	*mtrx int*	*mtrx rim*	*mtrx int*	*mtrx int*

TABLE B-4: Quantitative Microprobe Analysis for Plagioclase Compositions

	PC-84C		*PC-86D*															
	f1	**f2**	**P2**	**P3**	**PT1a**	**PT1b**	**PT1e**	**PT2a**	**PT2b**	**PT2c**	**PT2d**	**PT2e**	**PT2f**	**PT2h**	**PT3a**	**PT3d**	**PT3f**	**PT4b**
WEIGHT PERCENT OXIDES																		
SiO2	64.186	64.228	61.615	61.903	62.312	62.154	62.331	62.924	62.586	62.736	63.015	62.586	62.698	62.783	62.031	63.322	62.339	63.177
Al2O3	23.130	23.077	24.203	24.437	23.346	23.733	23.665	24.800	24.135	23.923	24.035	23.375	23.749	24.247	23.893	23.585	24.031	23.826
FeO	0.166	0.000	0.105	0.129	0.047	0.057	0.124	0.075	0.000	0.025	0.097	0.000	0.011	0.129	0.184	0.053	0.089	0.000
CaO	3.819	4.258	6.004	6.146	5.616	5.476	5.384	5.846	5.737	5.758	5.434	5.422	5.399	5.575	5.537	5.069	5.577	5.333
Na2O	9.858	9.624	8.558	8.643	8.809	8.687	8.694	8.510	8.673	8.768	8.535	9.071	8.866	8.632	8.508	9.078	8.534	8.610
K2O	0.073	0.032	0.114	0.093	0.174	0.294	0.268	0.099	0.241	0.251	0.384	0.311	0.195	0.150	0.191	0.133	0.241	0.221
TOTAL	**101.232**	**101.219**	**100.599**	**101.351**	**100.304**	**100.401**	**100.466**	**102.254**	**101.372**	**101.461**	**101.500**	**100.765**	**100.918**	**101.516**	**100.344**	**101.240**	**100.811**	**101.167**
CATIONS RECALCULATED TO 8 OXYGENS																		
Si	2.804	2.805	2.725	2.719	2.760	2.750	2.755	2.731	2.743	2.748	2.756	2.762	2.758	2.745	2.745	2.773	2.746	2.767
Al	1.191	1.188	1.261	1.265	1.219	1.238	1.233	1.269	1.247	1.235	1.239	1.216	1.231	1.249	1.246	1.217	1.247	1.230
Fe	0.006	0.000	0.004	0.005	0.002	0.002	0.005	0.003	0.000	0.001	0.004	0.000	0.000	0.005	0.007	0.002	0.003	0.000
Ca	0.179	0.199	0.284	0.289	0.267	0.260	0.255	0.272	0.269	0.270	0.255	0.256	0.254	0.261	0.263	0.238	0.263	0.250
Na	0.835	0.815	0.734	0.736	0.757	0.745	0.745	0.716	0.737	0.745	0.724	0.776	0.756	0.732	0.730	0.771	0.729	0.731
K	0.004	0.002	0.006	0.005	0.00:	0.017	0.015	0.005	0.014	0.014	0.021	0.018	0.011	0.008	0.011	0.007	0.014	0.012
TOTAL	**5.01:**	**5.009**	**5.015**	**5.019**	**5.014**	**5.012**	**5.008**	**4.996**	**5.009**	**5.014**	**4.998**	**5.027**	**5.010**	**5.000**	**5.002**	**5.008**	**5.002**	**4.990**
An	0.176	0.196	0.278	0.281	0.258	0.254	0.251	0.274	0.264	0.263	0.255	0.244	0.249	0.261	0.262	0.234	0.262	0.252
Ab	0.820	0.802	0.716	0.714	0.732	0.730	0.734	0.721	0.723	0.724	0.724	0.739	0.740	0.731	0.728	0.759	0.725	0.736
Or	0.004	0.002	0.006	0.005	0.00:	0.016	0.015	0.006	0.013	0.014	0.021	0.017	0.011	0.008	0.011	0.007	0.014	0.012
X	68.85	71.36	94.94	65.51	57.43	56.42	53.32	55.22	55.15	55.07	55.00	54.93	54.86	54.71	130.76	132.67	133.54	127.38
Y	-124.94	-109.36	257.31	259.99	313.81	314.17	315.26	317.62	316.80	315.99	315.17	314.36	313.54	311.91	338.00	340.58	342.30	297.18
x-axis mm					0.00	0.11	0.44	0.00	0.08	0.16	0.25	0.33	0.41	0.57	0.00	0.32	0.52	0.10
location			*adjacent*	*adjacent*	*rm nr grt*	*int nr grt*	*int nr grt*	*rm nr grt*	*int nr grt*	*int nr grt*	*int nr grt*	*int nr grt*	*int nr grt*	*rm nr grt*	*rm ±nr gt*	*int ±near*	*rm ±nr gt*	*int nr grt*

TABLE B-4: Quantitative Microprobe Analysis for Plagioclase Compositions

	PC-86D (continued)													*PC-88A*				
	PT4c	**PT4d**	**PT4e**	**PT4f**	**PT6b**	**PT6d**	**PT6e**	**PT7a**	**PT7c**	**PT7d**	**PT7e**	**PT8a**	**PT8b**	**P1**	**P4**	**P5**	**P6**	**P7**
WEIGHT PERCENT OXIDES																		
SiO2	62.266	62.653	62.667	62.116	62.664	62.196	62.236	62.094	62.768	62.751	63.070	62.215	62.592	60.461	61.028	60.814	60.534	60.351
Al2O3	23.703	23.448	23.918	24.376	24.103	24.130	23.741	24.249	23.721	23.563	23.755	23.950	23.665	25.138	25.006	25.514	25.238	25.439
FeO	0.083	0.050	0.012	0.036	0.019	0.027	0.039	0.045	0.001	0.115	0.078	0.188	0.000	0.080	0.137	0.124	0.018	0.051
CaO	5.228	5.411	5.492	5.874	5.529	5.552	5.593	5.694	5.245	5.498	5.495	5.774	5.400	6.985	6.977	7.243	7.448	7.244
Na2O	8.976	8.656	8.518	8.715	8.566	8.348	8.676	8.666	8.820	8.373	8.937	8.653	8.334	7.896	7.710	7.428	7.440	7.754
K2O	0.227	0.181	0.238	0.092	0.217	0.208	0.156	0.162	0.280	0.282	0.196	0.095	0.114	0.164	0.096	0.218	0.173	0.104
TOTAL	**100.483**	**100.399**	**100.845**	**101.209**	**101.098**	**100.461**	**100.441**	**100.910**	**100.835**	**100.582**	**101.531**	**100.875**	**100.105**	**100.724**	**100.954**	**101.341**	**100.851**	**100.943**
CATIONS RECALCULATED TO 8 OXYGENS																		
Si	2.753	2.768	2.756	2.728	2.750	2.745	2.751	2.734	2.762	2.767	2.759	2.741	2.767	2.677	2.692	2.674	2.675	2.667
Al	1.235	1.221	1.240	1.262	1.246	1.255	1.237	1.258	1.230	1.224	1.225	1.244	1.233	1.312	1.300	1.322	1.315	1.325
Fe	0.003	0.002	0.000	0.001	0.001	0.001	0.001	0.002	0.000	0.004	0.003	0.007	0.000	0.003	0.005	0.005	0.001	0.002
Ca	0.248	0.256	0.259	0.276	0.260	0.263	0.265	0.269	0.247	0.260	0.258	0.273	0.256	0.331	0.330	0.341	0.353	0.343
Na	0.769	0.741	0.726	0.742	0.729	0.714	0.744	0.740	0.752	0.716	0.758	0.739	0.714	0.678	0.659	0.633	0.638	0.664
K	0.013	0.010	0.013	0.005	0.012	0.012	0.009	0.009	0.016	0.016	0.011	0.005	0.006	0.009	0.005	0.012	0.00:	0.006
TOTAL	**5.021**	**4.998**	**4.994**	**5.015**	**4.998**	**4.990**	**5.007**	**5.011**	**5.007**	**4.987**	**5.013**	**5.009**	**4.977**	**5.011**	**4.991**	**4.988**	**4.991**	**5.006**
An	0.240	0.254	0.259	0.270	0.260	0.266	0.260	0.264	0.244	0.262	0.251	0.268	0.262	0.325	0.332	0.346	0.353	0.339
Ab	0.747	0.736	0.727	0.725	0.728	0.723	0.731	0.727	0.741	0.722	0.738	0.727	0.731	0.666	0.663	0.642	0.638	0.656
Or	0.012	0.010	0.013	0.005	0.012	0.012	0.009	0.009	0.016	0.016	0.011	0.005	0.007	0.009	0.005	0.012	0.00:	0.006
X	127.08	126.77	126.46	126.16	213.81	216.27	217.40	213.59	215.14	215.92	216.69	194.17	193.85	-122.72	-119.63	-93.84	-84.38	-85.05
Y	298.11	299.04	299.97	300.90	318.58	318.81	318.87	303.59	303.09	302.84	302.59	306.89	305.83	-158.45	-94.96	-144.03	-153.22	-158.50
x-axis mm	0.20	0.29	0.39	0.49	0.09	0.34	0.45	0.00	0.16	0.24	0.33	0.00	0.11					
location	*int nr grt*	*int nr grt*	*int nr grt*	*rm nr grt*	*int mtrx*	*int mtrx*	*int mtrx*	*rim mtrx*	*int mtrx*	*int mtrx*	*rim mtrx*	*rim mtrx*	*int mtrx*	*int ±adj gt* leucosome	*int adj gt* leucosome	*int±nr gt* leucosome	*interior* leuco/host	*interior* leuco/host

TABLE B-4: Quantitative Microprobe Analysis for Plagioclase Compositions

PC-88A (continued)

	P8	P9	P10	PT1a	PT2d	PT3c	PT4a	PT4b	PT4d	PT5a	PT5b	PT5f	PT5j	PT6c	PT6d	PT6e	PT7a	PT7c
WEIGHT PERCENT OXIDES																		
SiO2	60.705	61.152	60.416	59.632	59.666	60.311	59.883	59.752	61.240	60.362	60.599	60.285	60.507	60.370	60.872	60.832	60.534	60.120
Al2O3	25.499	25.696	25.017	26.749	25.428	24.865	25.399	25.509	25.108	24.951	24.999	25.519	25.056	24.652	24.569	24.874	25.278	25.092
FeO	0.110	0.088	0.074	0.170	0.115	0.132	0.085	0.000	0.050	0.020	0.027	0.018	0.157	0.003	0.004	0.046	0.136	0.094
CaO	7.195	6.975	7.151	7.990	7.739	6.990	7.565	7.764	7.124	7.209	7.157	7.683	7.091	6.985	7.151	7.096	6.999	7.185
Na2O	7.757	7.896	7.571	7.439	7.154	7.815	7.821	7.267	7.402	7.441	7.850	7.495	7.689	7.878	7.881	7.542	7.759	7.697
K2O	0.185	0.178	0.275	0.083	0.168	0.085	0.101	0.190	0.089	0.188	0.189	0.228	0.200	0.279	0.235	0.138	0.158	0.261
TOTAL	**101.451**	**101.985**	**100.504**	**102.063**	**100.270**	**100.198**	**100.854**	**100.482**	**101.013**	**100.171**	**100.821**	**101.228**	**100.700**	**100.167**	**100.712**	**100.528**	**100.864**	**100.449**
CATIONS RECALCULATED TO 8 OXYGENS																		
Si	2.669	2.673	2.681	2.614	2.656	2.683	2.654	2.654	2.695	2.684	2.681	2.660	2.680	2.689	2.696	2.693	2.676	2.672
Al	1.322	1.324	1.308	1.382	1.334	1.304	1.327	1.336	1.302	1.308	1.304	1.327	1.308	1.294	1.282	1.298	1.317	1.314
Fe	0.004	0.003	0.003	0.006	0.004	0.005	0.003	0.000	0.002	0.001	0.001	0.001	0.006	0.000	0.000	0.002	0.005	0.003
Ca	0.339	0.327	0.340	0.375	0.369	0.333	0.359	0.370	0.336	0.343	0.339	0.363	0.337	0.333	0.339	0.337	0.331	0.342
Na	0.661	0.669	0.651	0.632	0.617	0.674	0.672	0.626	0.632	0.642	0.673	0.641	0.660	0.680	0.677	0.647	0.665	0.663
K	0.010	0.00:	0.016	0.005	0.00:	0.005	0.006	0.011	0.005	0.011	0.011	0.013	0.011	0.016	0.013	0.008	0.009	0.015
TOTAL	**5.006**	**5.005**	**4.999**	**5.014**	**4.990**	**5.004**	**5.021**	**4.996**	**4.972**	**4.988**	**5.009**	**5.004**	**5.002**	**5.012**	**5.008**	**4.985**	**5.003**	**5.00:**
An	0.335	0.325	0.338	0.371	0.371	0.329	0.346	0.367	0.345	0.345	0.332	0.357	0.334	0.324	0.330	0.339	0.330	0.335
Ab	0.654	0.665	0.647	0.625	0.620	0.666	0.648	0.622	0.649	0.644	0.658	0.630	0.655	0.661	0.657	0.653	0.661	0.650
Or	0.010	0.00:	0.016	0.005	0.00:	0.005	0.006	0.011	0.005	0.011	0.010	0.013	0.011	0.015	0.013	0.008	0.009	0.015
X	-165.29	-168.05	-177.26	-139.71	-137.49	-122.74	-138.27	-137.69	-136.54	-103.25	-102.57	-99.87	-97.17	-84.76	-85.10	-85.50	-181.80	-181.85
Y	-323.21	-333.99	-338.07	-147.46	-160.19	-155.43	-97.92	-96.90	-94.85	-129.79	-129.14	-126.57	-124.01	-149.45	-148.36	-147.26	-307.16	-308.71
x-axis mm							0.00	0.12	0.35	0.00	0.09	0.47	0.84	0.22	0.34	0.45	0.00	0.16
	interior	*interior*	*interior*	*rm±nr gt*	*int±nr gt*	*int adj gt*	*rm±nr gt*	*int±nr gt*	*rm±nr gt*	*rm±adj gt*	*int±adj gt*	*int±adj gt*	*rm±adj gt*	*interior*	*interior*	*interior*	*rim*	*interior*
location	host	host	host	leucosome	leucosome	leucosome	leucosome	leucosome	leucosome	leucosome	leucosome	leucosome	leucosome	host	host	host	host	host

TABLE B-4: Quantitative Microprobe Analysis for Plagioclase Compositions

PC-88A (continued)			*PC-93A*															
	PT8a	**PT8c**	**P1a**	**P1b**	**P1c**	**P2a**	**P2b**	**P2c**	**P2d**	**P3**	**P4**	**P5a**	**P5b**	**P6a**	**P6b**	**P7a**	**P7b**	**P7c**
WEIGHT PERCENT OXIDES																		
SiO2	60.045	60.129	58.627	58.568	58.329	58.179	59.075	58.966	58.218	58.957	58.871	59.093	58.519	58.564	58.730	58.076	58.599	58.057
Al2O3	25.158	25.621	26.964	26.773	26.611	26.932	26.744	26.681	26.921	26.898	26.803	26.401	26.979	27.229	26.833	27.128	26.708	26.413
FeO	0.046	0.010	0.044	0.164	0.086	0.054	0.113	0.186	0.089	0.001	0.000	0.107	0.043	0.107	0.007	0.109	0.074	0.181
CaO	7.142	7.440	8.173	8.029	7.868	8.154	8.068	7.869	8.564	8.041	7.965	7.721	8.050	8.295	8.041	8.260	7.975	8.015
Na2O	8.010	7.306	7.104	7.506	7.357	7.341	7.544	7.430	6.952	7.238	7.293	7.225	7.288	7.056	7.163	6.964	7.296	7.241
K2O	0.123	0.208	0.068	0.140	0.097	0.084	0.084	0.127	0.091	0.181	0.143	0.070	0.088	0.156	0.161	0.045	0.127	0.127
TOTAL	**100.524**	**100.714**	**100.980**	**101.180**	**100.348**	**100.744**	**101.628**	**101.259**	**100.835**	**101.316**	**101.075**	**100.617**	**100.967**	**101.407**	**100.935**	**100.582**	**100.779**	**100.034**
CATIONS RECALCULATED TO 8 OXYGENS																		
Si	2.667	2.661	2.596	2.595	2.601	2.587	2.603	2.607	2.586	2.603	2.605	2.622	2.593	2.586	2.602	2.584	2.602	2.600
Al	1.317	1.337	1.407	1.398	1.399	1.411	1.389	1.390	1.410	1.400	1.398	1.381	1.409	1.417	1.401	1.422	1.398	1.394
Fe	0.002	0.000	0.002	0.006	0.003	0.002	0.004	0.007	0.003	0.000	0.000	0.004	0.002	0.004	0.000	0.004	0.003	0.007
Ca	0.340	0.353	0.388	0.381	0.376	0.388	0.381	0.373	0.408	0.380	0.378	0.367	0.382	0.392	0.382	0.394	0.379	0.385
Na	0.690	0.627	0.610	0.645	0.636	0.633	0.645	0.637	0.599	0.620	0.626	0.622	0.626	0.604	0.615	0.601	0.628	0.629
K	0.007	0.012	0.004	0.008	0.006	0.005	0.005	0.007	0.005	0.010	0.008	0.004	0.005	0.009	0.009	0.003	0.007	0.007
TOTAL	**5.023**	**4.990**	**5.007**	**5.033**	**5.020**	**5.026**	**5.027**	**5.020**	**5.011**	**5.012**	**5.013**	**4.000**	**5.018**	**5.012**	**5.00:**	**5.007**	**5.017**	**5.021**
An	0.328	0.356	0.387	0.369	0.369	0.379	0.370	0.367	0.403	0.377	0.373	0.370	0.377	0.390	0.379	0.395	0.374	0.377
Ab	0.665	0.632	0.609	0.624	0.625	0.617	0.626	0.626	0.592	0.613	0.619	0.626	0.618	0.601	0.612	0.603	0.619	0.616
Or	0.007	0.012	0.004	0.008	0.005	0.005	0.005	0.007	0.005	0.010	0.008	0.004	0.005	0.009	0.009	0.003	0.007	0.007
X	-181.99	-181.63	143.27	142.76	143.39	142.39	141.13	140.14	138.30	121.08	134.62	146.62	147.38	151.92	152.12	130.48	128.36	126.77
Y	-317.55	-319.34	277.90	278.70	280.68	276.15	275.74	275.18	274.37	283.27	292.36	291.47	292.11	145.25	146.18	149.78	149.89	149.12
x-axis mm	0.00	0.18	0.00	0.0:	0.30	0.00	0.13	0.25	0.45			0.00	0.0:	0.00	0.0:	0.00	0.21	0.39
	rim	*interior*																
location	host	host	*mtrx rim*	*mtrx int*	*mtrx ±int*	*mtrx rim*	*mtrx int*	*mtrx int*	*mtrx rim*	*mtrx int*	*mtrx int*	*mtrx int*	*mtrx rim*	*mtrx rim*	*mtrx int*	*mtrx rim*	*mtrx int*	*mtrx rim*

TABLE B-4: Quantitative Microprobe Analysis for Plagioclase Compositions

PC-93A (continued)					*PC-104E*													
	P8a	**P8b**	**P9a**	**P9b**	**P1a**	**P1b**	**P2a**	**P2b**	**PT1a**	**PT1b**	**PT1c**	**PT1d**	**PT1e**	**PT2a**	**PT2b**	**PT2c**	**F1**	**F2**
WEIGHT PERCENT OXIDES																		
SiO2	58.465	58.908	58.826	58.675	64.051	63.806	63.383	63.593	63.267	63.403	63.369	63.342	64.154	63.608	63.391	63.679	64.047	63.045
Al2O3	26.999	26.296	26.866	26.408	22.919	23.189	23.817	23.385	23.592	23.836	24.027	23.872	22.988	23.728	23.469	23.573	23.585	23.398
FeO	0.136	0.103	0.027	0.128	0.188	0.145	0.066	0.000	0.055	0.068	0.102	0.135	0.125	0.000	0.049	0.072	0.237	0.185
CaO	8.130	7.958	8.178	7.946	4.242	4.384	4.575	4.219	4.181	4.522	4.475	4.445	3.700	4.46:	4.424	4.290	4.449	4.764
Na2O	7.061	7.319	7.273	7.249	9.525	9.526	9.486	9.544	9.613	9.390	9.797	9.270	9.543	9.814	8.877	9.260	9.843	9.133
K2O	0.197	0.165	0.052	0.084	0.108	0.128	0.101	0.096	0.103	0.197	0.146	0.124	0.069	0.183	0.270	0.185	0.062	0.112
TOTAL	**100.988**	**100.749**	**101.222**	**100.490**	**101.033**	**101.178**	**101.428**	**100.837**	**100.811**	**101.416**	**101.916**	**101.188**	**100.579**	**101.803**	**100.480**	**101.059**	**102.223**	**100.637**
CATIONS RECALCULATED TO 8 OXYGENS																		
Si	2.592	2.616	2.600	2.612	2.806	2.793	2.770	2.790	2.779	2.771	2.760	2.772	2.815	2.772	2.789	2.787	2.780	2.777
Al	1.411	1.377	1.399	1.385	1.183	1.196	1.227	1.209	1.221	1.228	1.233	1.231	1.189	1.219	1.217	1.216	1.206	1.215
Fe	0.005	0.004	0.001	0.005	0.007	0.005	0.002	0.000	0.002	0.002	0.004	0.005	0.005	0.000	0.002	0.003	0.009	0.007
Ca	0.386	0.379	0.387	0.379	0.199	0.206	0.214	0.198	0.197	0.212	0.209	0.208	0.174	0.209	0.209	0.201	0.207	0.225
Na	0.607	0.630	0.623	0.626	0.809	0.809	0.804	0.812	0.819	0.796	0.827	0.786	0.812	0.829	0.757	0.786	0.828	0.780
K	0.011	0.009	0.003	0.005	0.006	0.007	0.006	0.005	0.006	0.011	0.008	0.007	0.004	0.010	0.015	0.010	0.003	0.006
TOTAL	**5.012**	**5.015**	**5.014**	**5.011**	**5.010**	**5.016**	**5.022**	**5.014**	**5.023**	**5.019**	**5.041**	**5.009**	**4.998**	**5.039**	**4.989**	**5.003**	**5.033**	**5.009**
An	0.385	0.372	0.382	0.375	0.196	0.201	0.209	0.195	0.193	0.208	0.200	0.208	0.176	0.199	0.213	0.202	0.199	0.222
Ab	0.604	0.619	0.615	0.620	0.798	0.792	0.785	0.799	0.802	0.781	0.792	0.785	0.820	0.791	0.772	0.788	0.797	0.771
Or	0.011	0.009	0.003	0.005	0.006	0.007	0.005	0.005	0.006	0.011	0.008	0.007	0.004	0.00:	0.015	0.010	0.003	0.006
X	144.55	143.69	133.85	133.84	63.13	63.97	66.83	67.84	63.97	63.79	63.62	63.44	63.26	62.05	62.87	63.68	-86.20	-86.44
Y	161.20	160.44	247.56	249.48	339.10	338.39	358.39	357.70	336.79	335.18	333.58	331.97	330.36	322.55	322.25	321.95	-65.60	-66.93
x-axis mm	0.00	0.11	0.00	0.19	0.00	0.11	0.00	0.12	0.00	0.16	0.32	0.48	0.65	0.00	0.09	0.17		
location	*mtrx rim*	*mtrx int*	*rm nr grt*	*int nr grt*	*rim mtrx*	*int mtrx*	*rim mtrx*	*int mtrx*	*rim mtrx*	*int mtrx*	*int mtrx*	*int mtrx*	*rim mtrx*	*rim mtrx*	*int mtrx*	*rim mtrx*	*gt corona*	*gt corona*

TABLE B-4: Quantitative Microprobe Analysis for Plagioclase Compositions

PC-104E (continued)						*PC-104F*												*PC-107F*	
	F3	**F3a**	**F3b**	**F6**	**F7**	**P1a**	**P1b**	**P1c**	**P3a**	**P3b**	**PT1a**	**PT1b**	**PT1c**	**PT2a**	**PT2b**	**PT2c**	**PT2d**	**P1**	**P2**
WEIGHT PERCENT OXIDES																			
SiO2	63.252	63.984	63.620	62.188	62.364	62.664	62.094	62.904	63.046	63.162	62.853	62.671	63.369	63.010	63.923	63.223	63.325	55.641	53.769
Al2O3	23.635	23.736	22.703	23.704	23.382	24.543	24.348	23.785	24.281	24.690	24.035	24.010	23.972	23.492	23.596	24.149	23.627	27.373	29.091
FeO	0.028	0.187	0.105	0.207	0.167	0.000	0.053	0.077	0.206	0.037	0.131	0.125	0.165	0.101	0.170	0.115	0.214	0.197	0.261
CaO	4.184	4.096	4.129	4.829	4.231	4.957	4.811	4.639	4.927	4.880	4.910	4.823	4.743	4.345	4.193	4.917	4.614	9.835	12.035
Na2O	9.358	9.615	9.596	9.146	9.805	9.099	9.003	9.112	9.289	9.169	9.371	9.026	9.550	9.308	9.301	8.884	9.603	6.248	4.860
K2O	0.073	0.089	0.107	0.043	0.089	0.204	0.153	0.130	0.094	0.165	0.176	0.272	0.078	0.131	0.211	0.242	0.126	0.104	0.070
TOTAL	**100.530**	**101.707**	**100.260**	**100.117**	**100.038**	**101.467**	**100.462**	**100.647**	**101.843**	**102.103**	**101.476**	**100.927**	**101.877**	**100.387**	**101.394**	**101.530**	**101.509**	**99.398**	**100.086**
CATIONS RECALCULATED TO 8 OXYGENS																			
Si	2.782	2.784	2.808	2.756	2.767	2.740	2.741	2.768	2.748	2.743	2.751	2.755	2.761	2.779	2.789	2.760	2.769	2.522	2.432
Al	1.225	1.217	1.181	1.238	1.223	1.265	1.267	1.233	1.247	1.264	1.240	1.244	1.231	1.221	1.213	1.242	1.218	1.462	1.551
Fe	0.001	0.007	0.004	0.008	0.006	0.000	0.002	0.003	0.008	0.001	0.005	0.005	0.006	0.004	0.006	0.004	0.008	0.007	0.00:
Ca	0.197	0.191	0.195	0.229	0.201	0.232	0.228	0.219	0.230	0.227	0.230	0.227	0.221	0.205	0.196	0.230	0.216	0.478	0.583
Na	0.798	0.811	0.821	0.786	0.844	0.771	0.770	0.777	0.785	0.772	0.795	0.769	0.807	0.796	0.787	0.752	0.814	0.549	0.426
K	0.004	0.005	0.006	0.002	0.005	0.011	0.009	0.007	0.005	0.009	0.00:	0.015	0.004	0.007	0.012	0.014	0.007	0.006	0.004
TOTAL	**5.007**	**5.015**	**5.015**	**5.019**	**5.046**	**5.019**	**5.016**	**5.008**	**5.023**	**5.016**	**5.031**	**5.015**	**5.02:**	**5.012**	**5.003**	**5.002**	**5.032**	**5.024**	**5.007**
An	0.197	0.190	0.191	0.225	0.192	0.229	0.226	0.218	0.226	0.225	0.222	0.225	0.214	0.204	0.197	0.231	0.208	0.462	0.575
Ab	0.799	0.805	0.803	0.772	0.804	0.760	0.765	0.775	0.769	0.766	0.768	0.760	0.781	0.789	0.791	0.755	0.785	0.532	0.421
Or	0.004	0.005	0.006	0.002	0.005	0.011	0.009	0.007	0.005	0.009	0.009	0.015	0.004	0.007	0.012	0.014	0.007	0.006	0.004
X	-80.75	-81.31	-82.39	-128.69	-131.46	122.18	123.13	124.69	186.28	185.41	160.58	159.46	158.34	195.80	196.63	197.46	198.29	-199.48	-191.46
Y	-85.86	-86.62	-88.40	-221.07	-223.82	-245.86	-246.65	-247.49	-70.58	-71.05	-55.57	-55.19	-54.80	-58.30	-57.74	-57.18	-56.63	-110.96	-111.40
x-axis mm						0.00	0.12	0.30	0.00	0.0:	0.00	0.12	0.24	0.00	0.10	0.20	0.30		
location	*rm adj gt*	*int adj gt*	*rm adj gt*	*gt corona*	*gt corona*	*rm adj gt*	*int adj gt*	*int adj gt*	*rim mtrx*	*int mtrx*	*rim mtrx*	*int mtrx*	*rim mtrx*	*rim mtrx*	*int mtrx*	*int mtrx*	*rim mtrx*	*rm nr gt*	*inclusion*

TABLE B-4: Quantitative Microprobe Analysis for Plagioclase Compositions

PC-107F continued															*PC-108C*				
	P4	**P8**	**P12**	**2P1**	**2P2**	**3P1**	**3P2**	**PT1c**	**PT1d**	**PT2c**	**PT2d**	**PT3a**	**PT3c**	**PT3d**	**P1a**	**P1b**	**P2a**	**P2b**	**P3a**
WEIGHT PERCENT OXIDES																			
SiO2	54.595	53.818	57.361	59.011	57.282	58.701	57.153	56.944	57.508	57.776	56.673	57.009	57.244	54.842	61.492	61.778	61.990	61.429	61.537
Al2O3	28.702	29.032	26.859	27.285	27.793	27.420	27.315	26.671	26.766	26.721	27.034	27.070	26.568	28.384	25.529	25.241	25.706	25.305	25.384
FeO	0.255	0.302	0.118	0.028	0.228	0.298	0.000	0.062	0.060	0.121	0.650	0.331	0.059	0.261	0.105	0.000	0.057	0.072	0.162
CaO	11.036	12.295	9.325	8.822	9.079	8.817	8.773	8.929	9.230	8.727	9.535	9.392	9.008	11.319	6.456	6.068	6.086	6.252	6.427
Na2O	5.099	4.701	6.400	6.873	6.678	6.962	7.174	6.509	6.488	6.514	6.031	5.987	6.395	5.247	8.306	8.371	8.576	8.329	8.397
K2O	0.240	0.055	0.122	0.118	0.038	0.089	0.134	0.159	0.095	0.116	0.155	0.296	0.110	0.061	0.123	0.246	0.068	0.303	0.080
TOTAL	**99.927**	**100.203**	**100.185**	**102.137**	**101.098**	**102.287**	**100.549**	**99.274**	**100.147**	**99.975**	**100.078**	**100.085**	**99.384**	**100.114**	**102.011**	**101.704**	**102.483**	**101.690**	**101.987**
CATIONS RECALCULATED TO 8 OXYGENS																			
Si	2.467	2.433	2.56:	2.587	2.544	2.575	2.554	2.573	2.576	2.587	2.549	2.559	2.581	2.474	2.684	2.701	2.690	2.691	2.688
Al	1.528	1.547	1.418	1.410	1.455	1.418	1.438	1.420	1.413	1.410	1.433	1.432	1.412	1.509	1.314	1.301	1.315	1.306	1.307
Fe	0.00:	0.011	0.004	0.001	0.008	0.011	0.000	0.002	0.002	0.005	0.025	0.012	0.002	0.00:	0.004	0.000	0.002	0.003	0.006
Ca	0.534	0.595	0.448	0.414	0.432	0.414	0.420	0.432	0.443	0.419	0.460	0.452	0.435	0.547	0.302	0.284	0.283	0.293	0.301
Na	0.447	0.412	0.556	0.584	0.575	0.592	0.622	0.56:	0.563	0.566	0.526	0.521	0.559	0.459	0.703	0.710	0.722	0.707	0.711
K	0.014	0.003	0.007	0.007	0.002	0.005	0.008	0.009	0.005	0.007	0.009	0.017	0.006	0.004	0.007	0.014	0.004	0.017	0.004
TOTAL	**4.999**	**5.002**	**5.003**	**5.003**	**5.017**	**5.015**	**5.042**	**5.007**	**5.002**	**4.993**	**5.001**	**4.994**	**4.996**	**5.003**	**5.014**	**5.00:**	**5.015**	**5.018**	**5.017**
An	0.537	0.589	0.443	0.412	0.428	0.410	0.400	0.427	0.438	0.423	0.462	0.456	0.435	0.542	0.298	0.282	0.281	0.288	0.296
Ab	0.449	0.408	0.550	0.581	0.56:	0.585	0.592	0.564	0.557	0.571	0.529	0.526	0.559	0.455	0.695	0.704	0.716	0.695	0.700
Or	0.014	0.003	0.007	0.007	0.002	0.005	0.007	0.009	0.005	0.007	0.009	0.017	0.006	0.003	0.007	0.014	0.004	0.017	0.004
X	-189.57	-197.49	-178.07	-191.46	-189.57	-197.49	-178.07	-202.78	-203.19	-196.73	-197.20	-194.83	-194.53	-194.38	106.00	105.71	92.92	91.41	116.44
Y	-110.52	-113.36	-111.11	-111.40	-110.52	-113.36	-111.11	-105.68	-106.09	-104.98	-104.70	-106.82	-107.71	-108.15	342.68	339.61	331.00	327.24	335.09
x-axis mm				0.00	0.21			0.12	0.17	0.11	0.16	0.00	0.09	0.14	0.00	0.31	0.00	0.41	0.00
location	*adjacent*	*adjacent*	*mtrx ±int*	*rm ±mtrx*	*int ±mtrx*	*int nr gt*	*int ±mtrx*	*int ±mtrx*	*rm ±mtrx*	*int ±mtrx*	*rm ±mtrx*	*rm nr gt*	*int nr gt*	*rm adj gt*	*rim mtrx*	*int mtrx*	*rim mtrx*	*int mtrx*	*rim mtrx*

TABLE B-4: Quantitative Microprobe Analysis for Plagioclase Compositions

PC-108C (continued)																	*PC-109A*	
	P3b	**P4a**	**P4b**	**P4c**	**P4d**	**P5a**	**P5b**	**P7**	**P8**	**F1**	**F2**	**F3**	**F4**	**F5**	**F6**	**F13**	**P1a**	**P1b**
WEIGHT PERCENT OXIDES																		
SiO2	61.482	61.516	61.794	61.420	61.531	61.438	61.792	61.852	60.118	61.253	60.522	59.915	60.164	59.796	60.440	59.82:	61.727	61.499
Al2O3	25.505	25.383	25.106	25.269	26.026	25.158	25.418	24.814	25.698	25.202	25.368	25.527	25.357	25.440	25.114	24.914	24.880	24.436
FeO	0.023	0.064	0.018	0.000	0.031	0.139	0.103	0.176	0.287	0.193	0.077	0.222	0.123	0.160	0.151	0.175	0.100	0.000
CaO	6.293	6.259	6.072	6.142	6.513	6.226	6.216	6.311	6.884	6.423	6.747	6.765	6.679	6.544	6.487	6.386	5.873	5.808
Na2O	8.821	8.362	8.410	8.462	8.409	8.433	8.428	8.554	8.145	8.369	8.055	8.070	8.247	8.249	8.364	8.154	8.564	8.147
K2O	0.164	0.187	0.182	0.207	0.200	0.118	0.248	0.134	0.150	0.100	0.077	0.055	0.018	0.125	0.141	0.120	0.148	0.201
TOTAL	**102.288**	**101.771**	**101.582**	**101.500**	**102.710**	**101.512**	**102.205**	**101.841**	**101.282**	**101.540**	**100.846**	**100.554**	**100.588**	**100.314**	**100.697**	**99.579**	**101.292**	**100.091**
CATIONS RECALCULATED TO 8 OXYGENS																		
Si	2.681	2.691	2.705	2.693	2.670	2.695	2.693	2.706	2.653	2.688	2.674	2.659	2.668	2.661	2.678	2.679	2.710	2.727
Al	1.311	1.309	1.295	1.306	1.331	1.301	1.305	1.279	1.337	1.304	1.321	1.335	1.325	1.334	1.311	1.315	1.287	1.277
Fe	0.001	0.002	0.001	0.000	0.001	0.005	0.004	0.006	0.011	0.007	0.003	0.008	0.005	0.006	0.006	0.007	0.004	0.000
Ca	0.294	0.293	0.285	0.289	0.303	0.293	0.290	0.296	0.326	0.302	0.319	0.322	0.317	0.312	0.308	0.306	0.276	0.276
Na	0.746	0.709	0.714	0.719	0.707	0.717	0.712	0.726	0.697	0.712	0.690	0.694	0.709	0.712	0.719	0.708	0.729	0.700
K	0.009	0.010	0.010	0.012	0.011	0.007	0.014	0.007	0.008	0.006	0.004	0.003	0.001	0.007	0.008	0.007	0.008	0.011
TOTAL	**5.041**	**5.015**	**5.009**	**5.019**	**5.024**	**5.017**	**5.018**	**5.021**	**5.031**	**5.019**	**5.012**	**5.022**	**5.025**	**5.032**	**5.029**	**5.021**	**5.015**	**4.991**
An	0.280	0.290	0.282	0.283	0.296	0.288	0.286	0.288	0.316	0.296	0.315	0.316	0.309	0.303	0.298	0.300	0.273	0.279
Ab	0.711	0.700	0.708	0.706	0.693	0.706	0.701	0.705	0.676	0.698	0.681	0.681	0.690	0.690	0.695	0.693	0.719	0.709
Or	0.009	0.010	0.010	0.011	0.011	0.007	0.014	0.007	0.008	0.005	0.004	0.003	0.001	0.007	0.008	0.007	0.008	0.012
X	119.56	65.11	64.36	63.81	63.30	66.36	65.90	167.99	168.84	-155.03	-154.18	-152.63	-147.31	-146.18	-147.49	-154.49	-99.79	-99.59
Y	333.36	173.17	170.66	167.36	164.94	154.78	153.14	259.66	265.33	367.07	366.72	367.00	353.31	352.59	225.24	65.49	326.40	327.75
x-axis mm	0.36	0.00	0.26	0.60	0.84	0.00	0.17										0.00	0.14
location	*int mtrx*	*mtrx nr rm*	*int mtrx*	*int mtrx*	*rim mtrx*	*rim mtrx*	*int mtrx*	*incl?*	*gt corona*	*gt corona*	*gt corona*	*gt corona*	*gt corona*	*gt corona*	*gt corona*	*gt corona*	*rim mtrx*	*int mtrx*

TABLE B-4: Quantitative Microprobe Analysis for Plagioclase Compositions

PC-109A (continued)												*PC-110A*						
	P1c	**P1d**	**P2**	**P3a**	**P3b**	**PT1a**	**PT1b**	**PT1d**	**PT2a**	**PT2b**	**PT2c**	**P1**	**P2a**	**P2b**	**P3a**	**P3b**	**P4a**	**P4b**
WEIGHT PERCENT OXIDES																		
SiO2	61.319	62.375	61.738	62.321	62.502	60.345	59.714	61.995	62.344	62.020	61.817	60.032	59.771	60.287	60.408	60.052	59.446	60.032
Al2O3	25.249	25.338	25.300	24.994	24.816	25.503	25.905	24.410	24.443	24.425	24.715	26.166	25.849	25.778	26.489	25.420	25.979	25.729
FeO	0.076	0.000	0.038	0.047	0.107	0.136	0.074	0.054	0.115	0.203	0.130	0.065	0.068	0.047	0.030	0.010	0.074	0.007
CaO	6.086	5.535	5.953	5.382	5.592	6.634	6.731	5.421	5.434	5.439	5.333	7.228	7.047	7.056	7.303	7.056	7.351	7.118
Na2O	8.179	8.776	8.393	8.976	8.809	8.399	7.867	8.555	8.641	8.514	8.840	7.955	7.606	7.742	8.100	7.711	7.783	8.017
K2O	0.176	0.137	0.210	0.171	0.096	0.116	0.189	0.135	0.091	0.121	0.064	0.084	0.279	0.091	0.098	0.173	0.095	0.127
TOTAL	**101.085**	**102.161**	**101.632**	**101.891**	**101.922**	**101.133**	**100.480**	**100.56:**	**101.068**	**100.722**	**100.899**	**101.530**	**100.620**	**101.001**	**102.428**	**100.422**	**100.728**	**101.030**
CATIONS RECALCULATED TO 8 OXYGENS																		
Si	2.697	2.711	2.701	2.718	2.724	2.664	2.650	2.734	2.737	2.733	2.721	2.640	2.651	2.660	2.635	2.666	2.637	2.653
Al	1.309	1.298	1.304	1.285	1.275	1.327	1.355	1.269	1.265	1.268	1.282	1.356	1.351	1.341	1.362	1.330	1.358	1.340
Fe	0.003	0.000	0.001	0.002	0.004	0.005	0.003	0.002	0.004	0.007	0.005	0.002	0.003	0.002	0.001	0.000	0.003	0.000
Ca	0.287	0.258	0.279	0.251	0.261	0.314	0.320	0.256	0.256	0.257	0.251	0.341	0.335	0.334	0.341	0.336	0.349	0.337
Na	0.697	0.740	0.712	0.759	0.744	0.719	0.677	0.732	0.735	0.727	0.754	0.678	0.654	0.662	0.685	0.664	0.669	0.687
K	0.00:	0.008	0.012	0.00:	0.005	0.007	0.011	0.008	0.005	0.007	0.004	0.005	0.016	0.005	0.005	0.00:	0.005	0.007
TOTAL	**5.002**	**5.014**	**5.009**	**5.024**	**5.014**	**5.035**	**5.016**	**5.001**	**5.001**	**4.000**	**5.017**	**5.023**	**5.009**	**5.003**	**5.029**	**5.006**	**5.022**	**5.024**
An	0.288	0.257	0.278	0.247	0.258	0.302	0.318	0.257	0.257	0.259	0.249	0.333	0.333	0.333	0.331	0.333	0.341	0.327
Ab	0.702	0.736	0.710	0.744	0.736	0.692	0.672	0.735	0.738	0.734	0.747	0.663	0.651	0.662	0.664	0.658	0.654	0.666
Or	0.00:	0.008	0.012	0.009	0.005	0.006	0.011	0.008	0.005	0.007	0.004	0.005	0.016	0.005	0.005	0.00:	0.005	0.007
X	-98.78	-99.18	-105.14	-121.51	-120.00	-91.91	-90.56	-87.85	-103.75	-103.20	-102.65	-161.62	-155.02	-153.77	-74.87	-73.39	-67.32	-65.90
Y	328.97	329.90	327.98	348.17	348.19	280.36	281.48	283.70	334.78	335.47	336.16	198.52	222.59	225.22	254.21	254.24	212.52	212.16
x-axis mm	0.28	0.38		0.00	0.15	0.00	0.18	0.35	0.00	0.09	0.18		0.00	0.29	0.00	0.15	0.00	0.15
location	*int mtrx*	*rim mtrx*	*int mtrx*	*rim mtrx*	*int mtrx*	*rm adj gt*	*int adj gt*	*int nr gt*	*rim mtrx*	*int mtrx*	*rim mtrx*	*int nr gt*	*rm nr gt*	*int nr gt*	*rim mtrx*	*int mtrx*	*rim mtrx*	*int mtrx*

TABLE B-4: Quantitative Microprobe Analysis for Plagioclase Compositions

	PC-110A (continued)													*PC-111A*				
	P5a	**P5b**	**P6a**	**P6b**	**P6c**	**P6d**	**F1**	**F2**	**F3**	**F3a**	**F3b**	**F3c**	**F4**	**P1a**	**P1b**	**P2a**	**P2b**	**P3a**
WEIGHT PERCENT OXIDES																		
SiO2	59.918	59.678	59.700	59.790	60.199	60.094	58.634	57.583	60.378	60.185	60.018	60.416	59.457	58.995	59.801	58.772	59.451	59.727
Al2O3	26.114	25.656	25.934	25.429	25.162	26.182	26.258	27.063	25.721	25.826	25.468	25.756	26.083	26.503	26.342	26.543	26.217	26.531
FeO	0.220	0.073	0.181	0.002	0.077	0.029	0.150	0.143	0.028	0.029	0.116	0.143	0.125	0.228	0.028	0.086	0.129	0.214
CaO	7.095	7.074	7.018	6.971	6.798	7.081	8.029	8.403	7.179	7.342	7.059	7.189	7.311	7.991	7.336	7.633	7.485	7.825
Na2O	7.760	7.818	7.851	7.735	7.828	7.833	7.517	7.345	7.923	8.011	7.785	7.847	8.016	7.327	7.789	7.401	7.578	7.448
K2O	0.123	0.159	0.141	0.123	0.123	0.104	0.093	0.063	0.100	0.141	0.145	0.116	0.136	0.163	0.216	0.324	0.297	0.161
TOTAL	**101.230**	**100.458**	**100.825**	**100.050**	**100.187**	**101.323**	**100.681**	**100.600**	**101.329**	**101.534**	**100.591**	**101.467**	**101.128**	**101.207**	**101.512**	**100.759**	**101.157**	**101.906**
CATIONS RECALCULATED TO 8 OXYGENS																		
Si	2.643	2.652	2.644	2.664	2.677	2.645	2.609	2.569	2.659	2.649	2.662	2.658	2.631	2.610	2.632	2.611	2.629	2.622
Al	1.357	1.344	1.354	1.335	1.319	1.358	1.377	1.423	1.335	1.340	1.331	1.335	1.360	1.382	1.367	1.390	1.366	1.373
Fe	0.008	0.003	0.007	0.000	0.003	0.001	0.006	0.005	0.001	0.001	0.004	0.005	0.005	0.008	0.001	0.003	0.005	0.008
Ca	0.335	0.337	0.333	0.333	0.324	0.334	0.383	0.402	0.339	0.346	0.335	0.339	0.347	0.379	0.346	0.363	0.355	0.368
Na	0.664	0.674	0.674	0.668	0.675	0.669	0.649	0.635	0.676	0.684	0.670	0.669	0.688	0.629	0.665	0.637	0.650	0.634
K	0.007	0.009	0.008	0.007	0.007	0.006	0.005	0.004	0.006	0.008	0.008	0.007	0.008	0.009	0.012	0.018	0.017	0.009
TOTAL	**5.014**	**5.018**	**5.020**	**5.006**	**5.005**	**5.013**	**5.029**	**5.039**	**5.015**	**5.027**	**5.011**	**5.013**	**5.037**	**5.018**	**5.023**	**5.023**	**5.021**	**5.013**
An	0.333	0.330	0.328	0.330	0.322	0.331	0.369	0.386	0.332	0.334	0.331	0.334	0.333	0.373	0.338	0.356	0.347	0.364
Ab	0.660	0.661	0.664	0.663	0.671	0.663	0.626	0.611	0.663	0.659	0.661	0.660	0.660	0.618	0.650	0.625	0.636	0.627
Or	0.007	0.009	0.008	0.007	0.007	0.006	0.005	0.003	0.005	0.008	0.008	0.006	0.007	0.009	0.012	0.018	0.016	0.009
X	-77.46:	-77.860	-70.700	-70.82:	-71.080	-71.13	166.960	168.690	116.620	117.130	116.950	116.860	142.63	-180.250	-179.56:	-183.660	-184.110	-189.890
Y	131.140	129.340	128.130	126.050	123.860	122.20	-174.860	-182.720	-201.640	-202.530	-203.110	-204.730	-193.04	-56.600	-57.56:	-70.000	-71.110	-72.260
x-axis mm	0.00	0.18	0.00	0.21	0.43	0.59			0.00	0.10	0.16	0.33		0.00	0.12	0.00	0.12	0.00
location	*rim mtrx*	*int mtrx*	*rim mtrx*	*int mtrx*	*int mtrx*	*rim mtrx*	*gt corona*	*gt corona*	*adj gt rm*	*adj gt int*	*adj gt int*	*adj gt rm*	*adj gt int*	*rim mtrx*	*int mtrx*	*rim mtrx*	*int mtrx*	*rim mtrx*

TABLE B-4: Quantitative Microprobe Analysis for Plagioclase Compositions

PC-111A (continued)

	P3b	P4a	P4b	PT1a	PT1b	PT1d	PT1e	PT2a	PT2b	PT2c	PT2d	PT3a	PT3b	PT3c	PT4a	PT4b	PT4c	PT4d
WEIGHT PERCENT OXIDES																		
SiO2	59.841	59.378	59.527	59.188	59.658	59.425	58.954	59.631	59.792	59.409	59.256	59.931	60.202	59.655	59.240	59.686	59.760	59.462
Al2O3	26.541	26.409	26.033	26.461	26.137	25.505	25.775	26.289	26.207	26.707	26.703	27.077	26.165	26.563	26.542	25.794	26.262	26.232
FeO	0.066	0.002	0.000	0.063	0.058	0.056	0.140	0.038	0.097	0.000	0.195	0.224	0.099	0.080	0.001	0.099	0.101	0.239
CaO	7.699	7.919	7.671	7.800	7.562	7.440	7.815	7.921	7.623	7.521	7.518	7.738	7.399	7.674	8.020	7.491	7.365	7.820
Na2O	7.375	7.411	7.510	7.439	7.058	7.567	7.522	7.477	7.163	7.473	7.469	7.659	7.345	7.644	7.315	7.354	7.772	7.308
K2O	0.305	0.172	0.191	0.209	0.191	0.257	0.089	0.168	0.277	0.159	0.155	0.198	0.207	0.157	0.143	0.257	0.214	0.109
TOTAL	**101.827**	**101.291**	**100.932**	**101.160**	**100.664**	**100.250**	**100.295**	**101.524**	**101.159**	**101.269**	**101.296**	**102.827**	**101.417**	**101.773**	**101.261**	**100.681**	**101.474**	**101.170**
CATIONS RECALCULATED TO 8 OXYGENS																		
Si	2.627	2.621	2.635	2.617	2.642	2.649	2.630	2.627	2.639	2.619	2.615	2.609	2.647	2.621	2.616	2.647	2.633	2.628
Al	1.373	1.374	1.358	1.379	1.364	1.340	1.355	1.365	1.363	1.388	1.389	1.389	1.356	1.376	1.381	1.348	1.364	1.366
Fe	0.002	0.000	0.000	0.002	0.002	0.002	0.005	0.001	0.004	0.000	0.007	0.008	0.004	0.003	0.000	0.004	0.004	0.009
Ca	0.362	0.375	0.364	0.370	0.359	0.355	0.374	0.374	0.360	0.355	0.355	0.361	0.349	0.361	0.379	0.356	0.348	0.370
Na	0.628	0.634	0.645	0.638	0.606	0.654	0.651	0.639	0.613	0.639	0.639	0.646	0.626	0.651	0.626	0.632	0.664	0.626
K	0.017	0.00:	0.011	0.012	0.011	0.015	0.005	0.009	0.016	0.009	0.009	0.011	0.012	0.009	0.008	0.015	0.012	0.006
TOTAL	**5.009**	**5.014**	**5.013**	**5.018**	**4.984**	**5.015**	**5.020**	**5.015**	**4.994**	**5.011**	**5.014**	**5.025**	**4.994**	**5.021**	**5.011**	**5.002**	**5.023**	**5.005**
An	0.360	0.368	0.357	0.363	0.368	0.347	0.363	0.366	0.364	0.354	0.354	0.354	0.353	0.354	0.374	0.355	0.340	0.369
Ab	0.623	0.623	0.632	0.626	0.621	0.639	0.632	0.625	0.620	0.637	0.637	0.635	0.635	0.638	0.618	0.631	0.649	0.625
Or	0.017	0.00:	0.011	0.012	0.011	0.014	0.005	0.009	0.016	0.009	0.009	0.011	0.012	0.009	0.008	0.015	0.012	0.006
X	-189.860	-116.350	-116.350	-112.640	-112.300	-111.610	-111.27	-183.17	-183.56	-183.95	-184.34	-131.58	-132.80	-134.020	-115.850	-114.500	-113.140	-111.790
Y	-74.050	-56.700	-55.010	-176.820	-178.760	-182.640	-184.58	-35.03	-35.75	-36.47	-37.19	-61.47	-61.50	-61.530	-62.56:	-63.580	-65.010	-65.580
x-axis mm	0.18	0.00	0.17	0.00	0.20	21.40	21.60	0.00	0.08	0.16	0.25	0.00	0.12	0.24	0.00	0.17	0.37	0.51
location	*int mtrx*	*rim mtrx*	*int mtrx*	*rm adj gt*	*int adj gt*	*int adj gt*	*rm adj gt*	*rim mtrx*	*int mtrx*	*int mtrx*	*rim mtrx*	*rim mtrx*	*int mtrx*	*rim mtrx*	*rim mtrx*	*int mtrx*	*int mtrx*	*rim mtrx*

TABLE B-4: Quantitative Microprobe Analysis for Plagioclase Compositions

	PC-113/4a									*PC-113C*								
	4	**f1**	**f1a**	**f1b**	**f1c**	**f2**	**f2a**	**f3**	**f3a**	**P2**	**P3**	**P4**	**P5**	**P6**	**P7**	**P9**	**P10**	**P11**
WEIGHT PERCENT OXIDES																		
SiO2	60.898	64.471	63.480	64.154	64.326	63.801	62.976	64.141	62.714	62.435	62.291	62.783	61.632	62.416	62.021	62.649	62.964	62.542
Al2O3	24.650	24.183	24.055	24.310	23.581	24.243	24.481	23.890	24.888	23.534	23.755	23.878	23.992	23.665	23.631	24.005	23.794	23.413
FeO	0.009	0.231	0.000	0.023	0.082	0.098	0.036	0.000	0.048	0.000	0.014	0.147	0.033	0.302	0.126	0.071	0.200	0.216
CaO	5.633	4.715	5.099	5.002	4.879	5.109	5.854	4.769	5.894	4.946	4.837	4.918	5.204	4.778	4.895	5.216	5.053	4.901
Na2O	8.467	9.206	9.139	8.956	9.376	8.691	8.521	9.089	8.507	8.705	8.813	8.766	8.756	8.827	8.838	8.531	8.587	8.807
K2O	0.220	0.114	0.201	0.249	0.110	0.148	0.201	0.153	0.239	0.144	0.113	0.088	0.153	0.063	0.111	0.120	0.126	0.071
TOTAL	**99.877**	**102.920**	**101.974**	**102.694**	**102.354**	**102.090**	**102.069**	**102.042**	**102.290**	**99.764**	**99.823**	**100.580**	**99.770**	**100.051**	**99.622**	**100.592**	**100.724**	**99.950**
CATIONS RECALCULATED TO 8 OXYGENS																		
Si	2.710	2.774	2.761	2.767	2.785	2.766	2.739	2.781	2.724	2.770	2.763	2.764	2.741	2.764	2.759	2.758	2.768	2.772
Al	1.293	1.226	1.233	1.236	1.203	1.239	1.255	1.221	1.274	1.231	1.242	1.239	1.258	1.235	1.239	1.245	1.233	1.223
Fe	0.000	0.008	0.000	0.001	0.003	0.004	0.001	0.000	0.002	0.000	0.001	0.005	0.001	0.011	0.005	0.003	0.007	0.008
Ca	0.269	0.217	0.238	0.231	0.226	0.237	0.273	0.222	0.274	0.235	0.230	0.232	0.248	0.227	0.233	0.246	0.238	0.233
Na	0.731	0.768	0.771	0.749	0.787	0.731	0.719	0.764	0.716	0.749	0.758	0.748	0.755	0.758	0.762	0.728	0.732	0.757
K	0.013	0.006	0.011	0.014	0.006	0.008	0.011	0.008	0.013	0.008	0.006	0.005	0.009	0.004	0.006	0.007	0.007	0.004
TOTAL	**5.015**	**5.000**	**5.013**	**4.997**	**5.010**	**4.984**	**4.998**	**4.995**	**5.004**	**4.993**	**4.999**	**4.993**	**5.012**	**4.999**	**5.005**	**4.987**	**4.985**	**4.997**
An	0.266	0.219	0.233	0.233	0.222	0.243	0.272	0.223	0.273	0.237	0.231	0.235	0.245	0.229	0.233	0.251	0.244	0.234
Ab	0.722	0.774	0.756	0.754	0.772	0.748	0.717	0.769	0.714	0.755	0.762	0.760	0.746	0.767	0.761	0.742	0.749	0.762
Or	0.012	0.006	0.011	0.014	0.006	0.008	0.011	0.009	0.013	0.008	0.006	0.005	0.009	0.004	0.006	0.007	0.007	0.004
X	118.59	120.40	121.87	123.01	128.39	129.28	144.09	143.41	-73.74	-70.12	-69.11	-69.36	-67.80	-68.22	-49.08	-49.48	-66.36	
Y	152.79	152.40	152.44	152.31	156.25	156.18	169.49	170.81	368.04	375.04	374.25	378.06	377.63	380.24	366.07	350.44	357.76	
x-axis mm	0.00	0.19	0.33	0.45	0.00	0.09	0.00	0.15										
location	*±near grt*	*rim mtrx*	*int mtrx*	*int mtrx*	*rim mtrx*	*rim mtrx*	*int mtrx*	*rim mtrx*	*int mtrx*	*±adj gt*	*±adj gt*	*adj gt*	*±adj gt*	*adj gt*	*±adj gt*	*adj gt*	*adj gt*	*adj grt*

TABLE B-4: Quantitative Microprobe Analysis for Plagioclase Compositions

PC-113C (continued) | *PC-113E*

	P12	**PT1b**	**PT1d**	**PT1e**	**PT1f**	**PT2a**	**PT2b**	**PT2c**	**PT2d**	**F1**	**F1a**	**F1b**	**F1c**	**F5**	**F5a**	**F5b**	**P1**	**P2**
WEIGHT PERCENT OXIDES																		
SiO2	61.495	62.388	61.543	61.874	63.841	63.020	61.882	61.686	62.107	61.546	61.498	62.015	62.612	63.118	61.512	61.871	62.402	61.932
Al2O3	23.975	23.868	24.160	24.167	23.536	23.856	24.349	24.176	24.166	24.335	23.963	24.428	24.033	24.287	24.044	24.019	23.877	24.195
FeO	0.308	0.037	0.029	0.000	0.149	0.096	0.000	0.000	0.125	0.000	0.035	0.084	0.005	0.091	0.133	0.000	0.000	0.000
CaO	5.805	4.946	5.691	5.274	4.436	4.920	5.578	5.735	5.266	5.323	5.712	5.468	4.907	5.406	5.58:	5.752	5.782	5.902
Na2O	8.455	8.527	8.251	8.585	9.109	8.711	8.359	8.297	8.600	9.024	8.599	8.623	9.104	9.194	8.515	8.430	8.413	8.690
K2O	0.076	0.244	0.175	0.156	0.073	0.114	0.226	0.205	0.095	0.162	0.246	0.253	0.112	0.121	0.212	0.173	0.185	0.160
TOTAL	**100.114**	**100.010**	**99.849**	**100.056**	**101.144**	**100.717**	**100.394**	**100.099**	**100.359**	**100.390**	**100.053**	**100.871**	**100.773**	**102.217**	**100.006**	**100.245**	**100.659**	**100.879**
CATIONS RECALCULATED TO 8 OXYGENS																		
Si	2.732	2.762	2.735	2.742	2.790	2.769	2.735	2.735	2.744	2.725	2.733	2.731	2.754	2.744	2.734	2.740	2.751	2.730
Al	1.255	1.245	1.265	1.262	1.212	1.235	1.268	1.263	1.258	1.270	1.255	1.268	1.246	1.244	1.259	1.254	1.240	1.257
Fe	0.011	0.001	0.001	0.000	0.005	0.004	0.000	0.000	0.005	0.000	0.001	0.003	0.000	0.003	0.005	0.000	0.000	0.000
Ca	0.276	0.235	0.271	0.250	0.208	0.232	0.264	0.272	0.249	0.253	0.272	0.258	0.231	0.252	0.266	0.273	0.273	0.279
Na	0.728	0.732	0.711	0.738	0.772	0.742	0.716	0.713	0.737	0.775	0.741	0.736	0.776	0.775	0.734	0.724	0.719	0.743
K	0.004	0.014	0.00:	0.009	0.004	0.006	0.013	0.012	0.005	0.009	0.014	0.014	0.006	0.007	0.012	0.00:	0.010	0.009
TOTAL	**5.007**	**4.989**	**4.993**	**5.000**	**4.992**	**4.988**	**4.996**	**4.996**	**4.998**	**5.032**	**5.017**	**5.010**	**5.014**	**5.025**	**5.00:**	**5.000**	**4.994**	**5.017**
An	0.274	0.239	0.273	0.251	0.211	0.236	0.266	0.273	0.251	0.244	0.265	0.256	0.228	0.244	0.263	0.271	0.272	0.271
Ab	0.722	0.747	0.717	0.740	0.785	0.757	0.721	0.715	0.743	0.748	0.722	0.730	0.766	0.750	0.725	0.719	0.717	0.721
Or	0.004	0.014	0.010	0.009	0.004	0.007	0.013	0.012	0.005	0.009	0.014	0.014	0.006	0.006	0.012	0.00:	0.010	0.009
X	-71.96	-45.81	-44.62	-44.03	-43.44	-44.32	-44.71	-45.10	-45.50	-144.68	-145.31	-146.10	-147.08	-74.32	-74.51	-74.91	85.89	85.49
Y	358.82	379.44	378.39	377.86	377.34	379.21	378.60	377.99	377.38	357.36	356.54	355.24	353.70	151.62	150.73	149.56	-46.24	-45.11
x-axis mm		0.08	0.24	0.32	0.40	0.00	0.07	0.14	0.22	0.00	0.10	0.26	0.44	0.00	0.09	0.21		
location	*adj gt*	*int nr grt*	*int nr grt*	*int nr grt*	*rm nr grt*	*rm nr grt*	*int nr grt*	*int nr grt*	*rm nr grt*	*rim mtrx*	*int mtrx*	*int mtrx*	*rim mtrx*	*rim mtrx*	*int mtrx*	*int? mtrx*	*int ±nr gt*	*int ±nr gt*

TABLE B-4: Quantitative Microprobe Analysis for Plagioclase Compositions

PC-113E (continued)																	*PC-116/3a*	
	P3	**P5**	**P6**	**P7**	**P8**	**P9**	**P11**	**P12**	**PT1b**	**PT1d**	**PT1e**	**f1**	**f1a**	**f2**	**f2a**	**f3**	**3**	**6**
WEIGHT PERCENT OXIDES																		
SiO2	63.178	63.005	63.844	62.698	63.004	62.556	62.276	61.805	62.631	61.673	62.391	62.268	62.500	62.409	63.044	63.001	62.039	62.299
Al2O3	23.613	23.368	22.996	23.678	23.564	23.880	24.318	23.493	23.215	23.612	23.496	23.931	23.985	23.599	23.532	24.453	23.805	23.442
FeO	0.020	0.130	0.159	0.061	0.000	0.096	0.088	0.080	0.093	0.103	0.003	0.500	0.145	0.292	0.092	0.233	0.000	0.000
CaO	4.910	4.893	4.660	4.976	5.361	5.515	5.353	5.559	5.084	5.423	5.380	4.822	4.908	4.919	4.562	4.947	4.761	4.721
Na2O	8.842	8.920	9.475	9.035	8.882	8.926	8.651	8.658	8.998	8.668	8.934	9.417	8.742	8.928	9.189	9.480	9.019	8.971
K2O	0.215	0.164	0.089	0.101	0.193	0.170	0.202	0.110	0.164	0.227	0.234	0.110	0.112	0.016	0.039	0.069	0.096	0.057
TOTAL	**100.778**	**100.480**	**101.223**	**100.549**	**101.004**	**101.143**	**100.888**	**99.705**	**100.185**	**99.706**	**100.438**	**101.048**	**100.392**	**100.163**	**100.458**	**102.183**	**99.721**	**99.490**
CATIONS RECALCULATED TO 8 OXYGENS																		
Si	2.776	2.778	2.795	2.764	2.767	2.749	2.739	2.753	2.774	2.748	2.759	2.743	2.757	2.763	2.777	2.740	2.756	2.771
Al	1.223	1.214	1.187	1.230	1.220	1.237	1.261	1.233	1.212	1.240	1.225	1.242	1.247	1.231	1.222	1.253	1.246	1.229
Fe	0.001	0.005	0.006	0.002	0.000	0.004	0.003	0.003	0.003	0.004	0.000	0.018	0.005	0.011	0.003	0.008	0.000	0.000
Ca	0.231	0.231	0.219	0.235	0.252	0.260	0.252	0.265	0.241	0.259	0.255	0.228	0.232	0.233	0.215	0.231	0.227	0.225
Na	0.753	0.763	0.804	0.772	0.756	0.760	0.738	0.748	0.773	0.749	0.766	0.804	0.748	0.766	0.785	0.799	0.777	0.774
K	0.012	0.009	0.005	0.006	0.011	0.00:	0.011	0.006	0.009	0.013	0.013	0.006	0.006	0.001	0.002	0.004	0.005	0.003
TOTAL	**4.996**	**5.000**	**5.016**	**5.00:**	**5.006**	**5.018**	**5.005**	**5.008**	**5.012**	**5.013**	**5.018**	**5.041**	**4.996**	**5.005**	**5.005**	**5.035**	**5.012**	**5.003**
An	0.232	0.230	0.213	0.232	0.247	0.252	0.252	0.260	0.236	0.254	0.247	0.219	0.235	0.233	0.215	0.223	0.225	0.225
Ab	0.756	0.760	0.782	0.762	0.742	0.739	0.737	0.734	0.755	0.734	0.741	0.775	0.758	0.766	0.783	0.773	0.770	0.772
Or	0.012	0.009	0.005	0.006	0.011	0.009	0.011	0.006	0.009	0.013	0.013	0.006	0.006	0.001	0.002	0.004	0.005	0.003
X	87.68	81.15	78.33	78.24	78.76	79.70	77.87	85.25	80.30	79.75	79.48	-213.18	-212.98	-217.87	-218.45	-204.55	-48.320	-95.690
Y	-42.22	-63.44	-64.92	-121.65	-119.80	-119.34	-108.94	-106.29	-125.98	-124.61	-124.13	111.80	112.31	109.68	111.38	109.75	199.220	124.150
x-axis mm									0.07	0.22	0.28	0.00	0.06	0.00	0.18			
location	*int ±nr gt*	*int nr grt*	*rim nr grt*	*±rm mtrx*	*int mtrx*	*int mtrx*	*int mtrx*	*int mtrx*	*±int mtrx*	*int mtrx*	*rim mtrx*	*rm adj gt*	*int adj gt*	*rm adj gt*	*±rm adj gt*	*±rm adj gt*	*nr grt*	*nr grt*

TABLE B-4: Quantitative Microprobe Analysis for Plagioclase Compositions

PC-116/3a (continued)

PC-119A

	f2a	**f2c**	**f4**	**f4a**	**f4b**	**f4c**	**f5**	**f5a**	**P1**	**P2**	**P6**	**P8**	**PT1b**	**PT1c**	**PT1d**	**PT1f**	**mP1**	**mP2**
WEIGHT PERCENT OXIDES																		
SiO2	61.474	61.274	62.285	62.274	63.124	62.995	63.628	63.157	60.713	60.276	61.112	61.308	62.337	62.409	62.724	61.635	61.763	61.189
Al2O3	23.622	23.635	23.831	23.857	23.713	23.543	23.562	23.947	24.494	24.712	24.363	24.561	24.498	24.691	24.885	24.675	25.169	25.103
FeO	0.000	0.013	0.001	0.085	0.000	0.286	0.000	0.031	0.162	0.273	0.151	0.028	0.162	0.123	0.070	0.190	0.007	0.063
CaO	4.783	5.128	4.745	4.792	4.493	4.523	4.309	4.786	5.928	6.124	5.667	5.952	5.304	5.593	5.657	5.750	6.358	6.310
Na2O	9.509	9.211	9.355	9.229	9.415	9.518	9.407	9.162	8.458	8.140	8.726	8.445	8.524	8.495	8.443	8.441	8.483	8.353
K2O	0.194	0.221	0.222	0.331	0.288	0.078	0.112	0.146	0.078	0.121	0.090	0.114	0.308	0.306	0.200	0.272	0.218	0.175
TOTAL	**99.582**	**99.482**	**100.439**	**100.568**	**101.033**	**100.943**	**101.018**	**101.229**	**99.833**	**99.646**	**100.109**	**100.408**	**101.133**	**101.617**	**101.979**	**100.963**	**101.998**	**101.193**
CATIONS RECALCULATED TO 8 OXYGENS																		
Si	2.745	2.740	2.753	2.751	2.770	2.769	2.786	2.764	2.706	2.694	2.716	2.714	2.736	2.728	2.729	2.716	2.697	2.693
Al	1.243	1.246	1.241	1.242	1.226	1.220	1.216	1.235	1.287	1.302	1.276	1.282	1.267	1.272	1.276	1.281	1.295	1.302
Fe	0.000	0.000	0.000	0.003	0.000	0.011	0.000	0.001	0.006	0.010	0.006	0.001	0.006	0.005	0.003	0.007	0.000	0.002
Ca	0.229	0.246	0.225	0.227	0.211	0.213	0.202	0.224	0.283	0.293	0.270	0.282	0.249	0.262	0.264	0.271	0.297	0.298
Na	0.823	0.799	0.802	0.791	0.801	0.811	0.799	0.778	0.731	0.705	0.752	0.725	0.725	0.720	0.712	0.721	0.718	0.713
K	0.011	0.013	0.013	0.019	0.016	0.004	0.006	0.008	0.004	0.007	0.005	0.006	0.017	0.017	0.011	0.015	0.012	0.00:
TOTAL	**5.051**	**5.043**	**5.033**	**5.032**	**5.025**	**5.029**	**5.009**	**5.011**	**5.018**	**5.011**	**5.025**	**5.011**	**5.002**	**5.004**	**4.995**	**5.012**	**5.021**	**5.017**
An	0.215	0.232	0.216	0.219	0.205	0.207	0.201	0.222	0.278	0.292	0.263	0.279	0.251	0.262	0.267	0.269	0.289	0.292
Ab	0.774	0.756	0.772	0.763	0.779	0.789	0.793	0.770	0.718	0.701	0.732	0.715	0.731	0.721	0.722	0.715	0.699	0.699
Or	0.010	0.012	0.012	0.018	0.016	0.004	0.006	0.008	0.004	0.007	0.005	0.006	0.017	0.017	0.011	0.015	0.012	0.00:
X	-49.180	-48.890	-58.35	-58.26	-58.05	-57.91	-70.36	-70.36	106.55	109.79	114.65	115.12						
Y	211.860	215.630	82.81	81.74	80.90	79.94	85.88	86.41	369.00	360.71	327.28	346.90						
x-axis mm	0.13	0.51	0.00	0.11	0.19	0.29	0.00	0.05										
location	*int nr gt*	*int nr gt*	*rim mtrx*	*int mtrx*	*nr fract?*	*rim mtrx*	*rim mtrx*	*int mtrx*	*adjacent*	*adjacent*	*rim nr grt*	*rim nr grt*	*int nr grt*	*int nr grt*	*int nr grt*	*int nr grt*	*±rm mtrx*	*±rm mtrx*

TABLE B-4: Quantitative Microprobe Analysis for Plagioclase Compositions

PC-119A (continued)								*PC-128/10a*		*PC-128/10c*									
	mP3	**mP4**	**mP5**	**mP6**	**mP7**	**mP8**	**mP9**	**2**	**3**	**2a**	**3**	**3a**	**pl1**	**pl1a**	**pl1b**	**pl2**	**pl2a**	**pl3**	**pl3a**
WEIGHT PERCENT OXIDES																			
SiO2	62.389	62.115	61.348	62.073	61.938	61.944	61.729	59.396	59.654	59.018	58.951	58.355	58.851	59.653	59.226	58.813	59.952	59.746	59.683
Al2O3	25.338	24.565	25.174	25.193	25.357	25.363	24.917	25.512	25.499	25.792	25.819	25.659	26.581	26.248	26.627	26.484	25.799	25.920	26.017
FeO	0.102	0.014	0.018	0.095	0.000	0.182	0.070	0.000	0.047	0.000	0.000	0.192	0.238	0.062	0.176	0.166	0.090	0.106	0.058
CaO	6.124	5.867	6.213	6.082	5.876	6.202	5.894	6.943	7.236	7.521	7.454	7.647	7.901	7.278	7.707	7.713	7.212	7.594	7.349
Na2O	8.542	8.516	8.359	8.393	8.187	8.564	8.185	7.649	7.633	7.291	7.418	7.56:	7.205	7.521	7.331	7.316	7.593	7.296	7.383
K2O	0.195	0.193	0.186	0.225	0.215	0.218	0.150	0.166	0.128	0.022	0.077	0.087	0.112	0.203	0.113	0.144	0.225	0.103	0.238
TOTAL	**102.690**	**101.270**	**101.298**	**102.061**	**101.573**	**102.473**	**100.945**	**99.666**	**100.197**	**99.644**	**99.719**	**99.510**	**100.888**	**100.965**	**101.180**	**100.636**	**100.871**	**100.765**	**100.728**
CATIONS RECALCULATED TO 8 OXYGENS																			
Si	2.703	2.725	2.695	2.705	2.707	2.694	2.715	2.657	2.656	2.641	2.638	2.625	2.610	2.637	2.616	2.613	2.652	2.645	2.644
Al	1.294	1.270	1.303	1.294	1.306	1.300	1.291	1.345	1.338	1.360	1.362	1.361	1.389	1.367	1.386	1.387	1.345	1.353	1.358
Fe	0.004	0.001	0.001	0.003	0.000	0.007	0.003	0.000	0.002	0.000	0.000	0.007	0.009	0.002	0.007	0.006	0.003	0.004	0.002
Ca	0.284	0.276	0.292	0.284	0.275	0.289	0.278	0.333	0.345	0.361	0.357	0.369	0.375	0.345	0.365	0.367	0.342	0.360	0.349
Na	0.718	0.724	0.712	0.709	0.694	0.722	0.698	0.663	0.659	0.633	0.644	0.660	0.619	0.645	0.628	0.630	0.651	0.626	0.634
K	0.011	0.011	0.010	0.013	0.012	0.012	0.008	0.009	0.007	0.001	0.004	0.005	0.006	0.011	0.006	0.008	0.013	0.006	0.014
TOTAL	**5.014**	**5.007**	**5.014**	**5.009**	**4.993**	**5.023**	**4.993**	**5.007**	**5.008**	**4.996**	**5.005**	**5.027**	**5.009**	**5.007**	**5.008**	**5.012**	**5.007**	**4.994**	**5.001**
An	0.281	0.273	0.288	0.282	0.281	0.282	0.282	0.331	0.341	0.363	0.355	0.357	0.375	0.344	0.365	0.365	0.340	0.363	0.350
Ab	0.709	0.717	0.702	0.705	0.707	0.706	0.709	0.660	0.652	0.636	0.640	0.639	0.619	0.644	0.628	0.627	0.648	0.631	0.636
Or	0.011	0.011	0.010	0.012	0.012	0.012	0.009	0.009	0.007	0.001	0.004	0.005	0.006	0.011	0.006	0.008	0.013	0.006	0.014
X													60.230	58.220	55.93:	154.310	154.310	155.160	153.800
Y													-303.370	-300.610	-297.020	-371.620	-372.740	-366.050	-365.350
x-axis mm													0.00	0.34	0.77	0.00	0.11	0.00	0.15
location	*int mtrx*	*int mtrx*	*rim mtrx*	*rim mtrx*	*±rm mtrx*	*int mtrx*	*int mtrx*	*±mtrx*	*±mtrx*	*±mtrx*	*±mtrx*	*±mtrx*	*rm mtrx*	*int mtrx*	*rm mtrx*	*rm mtrx*	*int mtrx*	*rm mtrx*	*int mtrx*

TABLE B-4: Quantitative Microprobe Analysis for Plagioclase Compositions

PC-128/10c (cont'd)			*131/2*	*PC-133A*														
	pl3b	**pl3c**	**f6**	**P1**	**P2a**	**P2b**	**P3a**	**P3b**	**P3c**	**P3d**	**P4a**	**P4b**	**P5a**	**P5b**	**P6a**	**P6b**	**P6c**	**P6d**
WEIGHT PERCENT OXIDES																		
SiO2	59.598	59.457	62.255	62.392	62.622	62.496	62.200	62.155	61.850	62.555	62.241	62.450	61.405	63.161	62.016	62.756	62.764	62.390
Al2O3	25.875	26.344	23.596	24.883	24.415	24.518	24.459	24.524	24.371	24.297	24.631	24.056	24.742	24.022	24.670	24.024	24.100	24.655
FeO	0.042	0.083	0.000	0.169	0.169	0.064	0.101	0.054	0.081	0.113	0.159	0.087	0.160	0.086	0.103	0.057	0.127	0.180
CaO	7.322	7.800	4.575	5.584	5.641	5.386	5.669	5.572	5.006	5.113	5.296	5.224	5.496	4.944	5.482	5.063	4.996	5.860
Na2O	7.260	7.022	9.487	8.626	8.747	8.744	8.608	8.544	8.988	8.773	8.839	8.615	8.473	8.707	8.646	8.872	8.997	8.328
K2O	0.272	0.107	0.192	0.164	0.266	0.278	0.233	0.285	0.301	0.267	0.237	0.267	0.298	0.343	0.171	0.299	0.269	0.189
TOTAL	**100.369**	**100.813**	**100.105**	**101.818**	**101.860**	**101.486**	**101.270**	**101.134**	**100.597**	**101.118**	**101.403**	**100.699**	**100.574**	**101.263**	**101.088**	**101.071**	**101.253**	**101.602**
CATIONS RECALCULATED TO 8 OXYGENS																		
Si	2.648	2.631	2.760	2.722	2.734	2.735	2.730	2.730	2.732	2.745	2.728	2.751	2.714	2.764	2.725	2.755	2.752	2.728
Al	1.355	1.374	1.233	1.279	1.256	1.265	1.265	1.269	1.269	1.257	1.272	1.249	1.289	1.239	1.277	1.243	1.245	1.270
Fe	0.002	0.003	0.000	0.006	0.006	0.002	0.004	0.002	0.003	0.004	0.006	0.003	0.006	0.003	0.004	0.002	0.005	0.007
Ca	0.349	0.370	0.217	0.261	0.264	0.253	0.267	0.262	0.237	0.240	0.249	0.247	0.260	0.232	0.258	0.238	0.235	0.274
Na	0.625	0.602	0.815	0.730	0.740	0.742	0.732	0.728	0.770	0.746	0.751	0.736	0.726	0.739	0.736	0.755	0.765	0.706
K	0.015	0.006	0.011	0.009	0.015	0.016	0.013	0.016	0.017	0.015	0.013	0.015	0.017	0.019	0.00:	0.017	0.015	0.011
TOTAL	**4.995**	**4.986**	**5.037**	**5.008**	**5.016**	**5.012**	**5.011**	**5.007**	**5.027**	**5.007**	**5.019**	**5.000**	**5.013**	**4.996**	**5.00:**	**5.00:**	**5.016**	**4.995**
An	0.352	0.378	0.208	0.261	0.259	0.250	0.263	0.261	0.231	0.240	0.245	0.247	0.259	0.234	0.257	0.236	0.231	0.277
Ab	0.632	0.616	0.781	0.730	0.727	0.735	0.724	0.723	0.752	0.745	0.741	0.738	0.724	0.746	0.733	0.748	0.754	0.712
Or	0.016	0.006	0.010	0.009	0.015	0.015	0.013	0.016	0.017	0.015	0.013	0.015	0.017	0.019	0.00:	0.017	0.015	0.011
X	151.290	148.920	59.36	-147.01	-169.07	-168.63	-90.26	-90.07	-90.07	-89.04	-76.96	-76.96	-106.56	-104.77	-116.12	-114.42	-112.74	-111.26
Y	-362.460	-360.140	71.32	-334.39	-100.86	-102.72	-46.38	-44.51	-41.45	-38.69	-68.65	-70.03	-127.48	-127.96	-96.92	-96.56	-95.90	-95.72
x-axis mm	0.54	0.87			0.00	0.19	0.00	0.19	0.49	0.79	0.00	0.14	0.00	0.19	0.00	0.17	0.35	0.50
location	*int mtrx*	*rm mtrx*	*rm adj gt*	*rm nr gt*	*int nr gt*	*rim mtrx*	*int mtrx*	*int mtrx*	*rim mtrx*	*rim mtrx*	*int mtrx*	*rim mtrx*	*int mtrx*	*rim mtrx*	*int mtrx*	*int mtrx*	*rim mtrx*	

TABLE B-4: Quantitative Microprobe Analysis for Plagioclase Compositions

PC-134D

	P1	P2	P3	P4	P5a	P5b	P5c	P6	P7a	P7b	P7c	P7d	P7e	P8a	P8b	P8c	P9b
WEIGHT PERCENT OXIDES																	
SiO2	61.966	61.979	62.232	62.239	61.695	61.791	62.206	62.022	62.610	61.963	62.038	61.811	61.410	61.890	61.412	61.404	61.661
Al2O3	25.186	25.060	24.663	24.992	24.744	24.889	24.999	25.076	24.776	25.163	25.260	25.020	25.079	25.301	25.066	24.888	25.003
FeO	0.071	0.134	0.045	0.099	0.070	0.018	0.092	0.035	0.130	0.045	0.041	0.091	0.191	0.259	0.073	0.242	0.186
CaO	5.586	6.011	5.842	5.802	5.513	5.797	5.728	5.905	5.536	5.880	5.677	5.754	5.939	5.861	6.033	5.595	5.922
Na2O	8.491	8.474	8.802	8.600	8.778	8.721	8.848	8.741	8.640	8.727	8.724	8.797	8.586	8.497	8.462	8.502	8.724
K2O	0.118	0.130	0.162	0.141	0.141	0.205	0.121	0.159	0.144	0.221	0.221	0.187	0.198	0.200	0.171	0.107	0.118
TOTAL	**101.418**	**101.788**	**101.746**	**101.873**	**100.941**	**101.421**	**101.994**	**101.938**	**101.836**	**101.999**	**101.961**	**101.660**	**101.403**	**102.008**	**101.217**	**100.738**	**101.614**
CATIONS RECALCULATED TO 8 OXYGENS																	
Si	2.712	2.708	2.721	2.715	2.716	2.710	2.712	2.707	2.729	2.704	2.705	2.706	2.697	2.700	2.700	2.709	2.702
Al	1.299	1.290	1.271	1.285	1.284	1.287	1.285	1.290	1.273	1.294	1.298	1.291	1.298	1.301	1.299	1.294	1.291
Fe	0.003	0.005	0.002	0.004	0.003	0.001	0.003	0.001	0.005	0.002	0.002	0.003	0.007	0.009	0.003	0.009	0.007
Ca	0.262	0.281	0.274	0.271	0.260	0.272	0.268	0.276	0.259	0.275	0.265	0.270	0.280	0.274	0.284	0.265	0.278
Na	0.720	0.718	0.746	0.727	0.749	0.742	0.748	0.740	0.730	0.738	0.738	0.747	0.731	0.719	0.721	0.727	0.741
K	0.007	0.007	0.009	0.008	0.008	0.012	0.007	0.009	0.008	0.012	0.012	0.010	0.011	0.011	0.00:	0.006	0.007
TOTAL	**5.002**	**5.00:**	**5.022**	**5.010**	**5.020**	**5.023**	**5.023**	**5.023**	**5.004**	**5.025**	**5.020**	**5.027**	**5.025**	**5.014**	**5.016**	**5.010**	**5.026**
An	0.265	0.280	0.266	0.269	0.256	0.266	0.262	0.269	0.259	0.268	0.261	0.263	0.274	0.273	0.280	0.265	0.271
Ab	0.728	0.713	0.725	0.723	0.737	0.723	0.732	0.722	0.733	0.720	0.727	0.727	0.716	0.716	0.711	0.729	0.723
Or	0.007	0.007	0.009	0.008	0.008	0.011	0.007	0.009	0.008	0.012	0.012	0.010	0.011	0.011	0.009	0.006	0.006
X	85.11	87.72	99.05	99.81	162.81	164.01	166.45	159.65	153.63	153.73	154.66	155.03	155.39	154.56	153.30	151.98	155.58
Y	-299.23	-297.43	-260.75	-256.25	-326.66	-329.17	-332.09	-323.96	-203.51	-202.04	-199.77	-198.05	-196.77	-183.06	-182.82	-183.16	-99.14
x-axis mm					0.00	0.28	0.66		0.00	0.15	0.39	0.57	0.70	0.00	0.13	0.26	
location	*±nr grt*	*adj grt*	*near grt*	*near grt*	*±mtrx rm*	*±mtrx int*	*±mtrx rm*	*int mtrx*	*rm mtrx*	*int mtrx*	*int mtrx*	*int mtrx*	*mtrx ±rm*	*rm mtrx*	*int mtrx*	*rm mtrx*	*mtrx ±rm*

TABLE B-4: Plagioclase Compositions

PC-134D-2

	f1	f1a	f1b	f1c	f2	f2a
WEIGHT PERCENT OXIDES						
SiO2	63.108	62.336	62.530	62.962	62.929	62.813
Al2O3	24.424	24.449	24.738	24.503	24.58:	24.851
FeO	0.234	0.010	0.070	0.000	0.221	0.048
CaO	5.883	5.783	6.104	5.890	5.802	5.716
Na2O	8.832	8.537	8.625	8.744	8.585	8.612
K2O	0.192	0.230	0.219	0.119	0.141	0.276
TOTAL	**102.673**	**101.345**	**102.286**	**102.218**	**102.268**	**102.316**
CATIONS RECALCULATED TO 8 OXYGENS						
Si	2.735	2.732	2.720	2.736	2.734	2.727
Al	1.248	1.263	1.268	1.255	1.259	1.272
Fe	0.008	0.000	0.003	0.000	0.008	0.002
Ca	0.273	0.272	0.285	0.274	0.270	0.266
Na	0.742	0.725	0.727	0.737	0.723	0.725
K	0.011	0.013	0.012	0.007	0.008	0.015
TOTAL	**5.017**	**5.005**	**5.015**	**5.008**	**5.002**	**5.007**
An	0.266	0.269	0.278	0.270	0.270	0.264
Ab	0.723	0.718	0.710	0.724	0.722	0.721
Or	0.010	0.013	0.012	0.006	0.008	0.015
X	67.91	67.02	66.21	65.58	61.99	58.01
Y	-170.06	-168.51	-167.00	-165.49	-169.55	-170.45
x-axis mm	0.00	0.18	0.35	0.51	0.00	0.41
location	*rm mtrx*	*int mtrx*	*int mtrx*	*rm mtrx*	*rm mtrx*	*int mtrx*

TABLE B-5: Quantitative Microprobe Analysis for Muscovite Compositions

	PC-19D										***PC-66A***				***80B sericite***					***PC-83A***	
	M1	**M2**	**M3**	**M4**	**M5**	**M7**	**M8**	**M9**	**M10**	**M11**	**M1**	**M2**	**M3**	**M4**	**fsp1**	**ms?**	**more?**	**6b/fsp**	**9/fsp**	**ms2**	**ms7**
WEIGHT PERCENT OXIDES																					
SiO2	46.217	45.728	45.936	46.522	46.318	46.576	46.176	46.657	45.983	46.081	47.003	46.439	47.000	46.749	45.992	47.424	46.708	46.671	46.623	45.727	46.300
Al2O3	32.530	33.194	34.316	32.644	33.191	33.104	32.529	31.818	33.599	32.785	30.879	29.953	31.582	30.420	37.196	36.256	37.205	35.561	36.099	35.341	35.538
TiO2	0.487	0.58:	0.536	0.367	0.718	0.342	0.383	0.553	0.413	0.645	0.211	0.932	0.844	0.575	0.002	0.000	0.022			0.350	0.498
MgO	0.575	0.576	0.491	0.456	0.552	0.609	0.646	0.748	0.615	0.608	1.005	1.328	0.930	1.276	0.029	0.175	0.021	0.116	0.010	0.462	0.555
FeO	4.053	3.743	3.239	4.357	3.993	4.034	4.314	4.147	4.033	4.078	5.438	6.919	3.844	5.384	0.962	0.686	1.198	0.551	1.004	1.352	1.444
MnO	0.000	0.049	0.049	0.046	0.126	0.000	0.000	0.011	0.000	0.026	0.094	0.060	0.000	0.046	0.039	0.000	0.034			0.069	0.014
CaO	0.024	0.000	0.000	0.007	0.012	0.009	0.000	0.019	0.049	0.019	0.054	0.044	0.024	0.045	0.059	1.579	0.187	0.091	0.252	0.019	0.000
BaO															0.105	0.664	0.155	0.637	0.058		
Na2O	0.325	0.372	0.439	0.397	0.409	0.314	0.284	0.248	0.367	0.226	0.170	0.180	0.162	0.242	0.043	0.624	0.061	0.183	0.033	0.846	0.810
K2O	10.976	10.677	10.733	10.589	10.475	10.529	11.010	10.554	10.648	10.675	10.946	10.726	10.932	10.548	10.606	9.335	10.586	10.544	10.609	10.241	9.935
Cr2O3	0.013	0.044	0.067	0.000	0.000	0.000	0.073	0.000	0.048	0.038	0.027	0.057	0.050	0.015	0.000	0.002	0.011			0.070	0.036
Cl	0.003	0.000	0.000	0.006	0.009	0.015	0.003	0.000	0.012	0.009	0.000	0.024	0.012	0.012	0.001	0.008	0.019			0.000	0.006
F	0.000	0.058	0.069	0.025	0.083	0.031	0.082	0.188	0.053	0.055	0.000	0.209	0.050	0.029	0.033	0.000	0.048			0.003	0.104
TOTAL	*95.203*	*95.031*	*95.875*	*95.416*	*95.886*	*95.563*	*95.500*	*94.943*	*95.820*	*95.245*	*95.827*	*96.871*	*95.430*	*95.341*	*95.067*	*96.753*	*96.255*	*94.354*	*94.688*	*94.480*	*95.240*
-O = Cl	-0.001	0.000	0.000	-0.001	-0.002	-0.003	-0.001	0.000	-0.003	-0.002	0.000	-0.005	-0.003	-0.003	-0.000	-0.002	-0.004			0.000	-0.001
-O = F	0.000	-0.024	-0.029	-0.011	-0.035	-0.013	-0.035	-0.079	-0.022	-0.023	0.000	-0.088	-0.021	-0.012	-0.014	0.000	-0.020			-0.001	-0.044
TOTAL	**95.202**	**95.007**	**95.846**	**95.404**	**95.849**	**95.547**	**95.465**	**94.864**	**95.795**	**95.220**	**95.827**	**96.778**	**95.406**	**95.326**	**95.053**	**96.751**	**96.231**	**94.354**	**94.688**	**94.479**	**95.195**
CATIONS RECALCULATED TO 22 OXYGENS																					
Si	6.266	6.199	6.155	6.286	6.223	6.267	6.256	6.337	6.186	6.238	6.372	6.300	6.347	6.364	6.112	6.200	6.140	6.257	6.216	6.142	6.159
Al	5.198	5.304	5.420	5.199	5.255	5.250	5.194	5.093	5.327	5.230	4.934	4.789	5.026	4.880	5.826	5.586	5.764	5.619	5.672	5.595	5.571
Ti	0.04:	0.060	0.054	0.037	0.073	0.035	0.039	0.057	0.042	0.066	0.021	0.095	0.086	0.059	0.000	0.000	0.002	0.000	0.000	0.035	0.04:
Mg	0.116	0.116	0.098	0.092	0.111	0.122	0.130	0.151	0.123	0.123	0.203	0.269	0.187	0.259	0.006	0.034	0.004	0.023	0.002	0.093	0.110
Fe	0.460	0.424	0.363	0.492	0.449	0.454	0.489	0.471	0.454	0.462	0.617	0.785	0.434	0.613	0.107	0.075	0.132	0.062	0.112	0.152	0.161
Mn	0.000	0.006	0.006	0.005	0.014	0.000	0.000	0.001	0.000	0.003	0.011	0.007	0.000	0.005	0.004	0.000	0.004	0.000	0.000	0.008	0.002
Ca	0.003	0.000	0.000	0.001	0.002	0.001	0.000	0.003	0.007	0.003	0.008	0.006	0.003	0.007	0.008	0.221	0.026	0.013	0.036	0.003	0.000
Ba															0.005	0.034	0.008	0.034	0.003		
Na	0.085	0.098	0.114	0.104	0.107	0.082	0.075	0.065	0.096	0.059	0.045	0.047	0.042	0.064	0.011	0.158	0.016	0.048	0.009	0.220	0.209
K	1.898	1.847	1.835	1.825	1.795	1.807	1.903	1.829	1.827	1.843	1.893	1.856	1.883	1.832	1.798	1.557	1.775	1.803	1.804	1.755	1.686
Cr	0.001	0.005	0.007	0.000	0.000	0.000	0.008	0.000	0.005	0.004	0.003	0.006	0.005	0.002	0.000	0.000	0.001	0.000	0.000	0.007	0.004
TOTAL	**14.077**	**14.059**	**14.052**	**14.042**	**14.028**	**14.018**	**14.093**	**14.007**	**14.068**	**14.031**	**14.107**	**14.160**	**14.015**	**14.084**	**13.879**	**13.865**	**13.871**	**13.859**	**13.854**	**14.009**	**13.951**
Na+K	1.984	1.944	1.949	1.929	1.902	1.889	1.977	1.894	1.923	1.903	1.938	1.904	1.926	1.896	1.809	1.715	1.791	1.851	1.813	1.975	1.895
Na/Na+K	*0.043*	*0.050*	*0.059*	*0.054*	*0.056*	*0.043*	*0.038*	*0.035*	*0.04:*	*0.031*	*0.023*	*0.025*	*0.022*	*0.034*	*0.006*	*0.092*	*0.009*	*0.026*	*0.005*	*0.112*	*0.110*
Alvi	3.463	3.503	3.575	3.485	3.478	3.517	3.450	3.430	3.513	3.468	3.306	3.088	3.373	3.244	3.939	3.785	3.903	3.876	3.888	3.736	3.730
xAlvi	*0.847*	*0.852*	*0.873*	*0.848*	*0.843*	*0.852*	*0.840*	*0.835*	*0.850*	*0.842*	*0.795*	*0.728*	*0.827*	*0.776*	*0.971*	*0.972*	*0.965*	*0.979*	*0.972*	*0.929*	*0.921*
xTi	0.012	0.015	0.013	0.009	0.018	0.008	0.00:	0.014	0.010	0.016	0.005	0.022	0.021	0.014	0.000	0.000	0.001	0.000	0.000	0.009	0.012
xMg	0.028	0.028	0.024	0.022	0.027	0.02:	0.032	0.037	0.02:	0.02:	0.049	0.063	0.046	0.062	0.001	0.009	0.001	0.006	0.000	0.023	0.027
xFe	0.112	0.103	0.089	0.120	0.109	0.110	0.119	0.115	0.110	0.112	0.148	0.185	0.106	0.147	0.026	0.019	0.033	0.016	0.028	0.038	0.03:
Fe/Fe+Mg	0.798	0.785	0.787	0.843	0.802	0.788	0.789	0.757	0.786	0.790	0.752	0.745	0.699	0.703	0.949	0.687	0.970	0.727	0.983	0.621	0.593
X	-61.04	-65.45	-67.53	-54.52	-46.54	-208.20	-49.47	-45.34	-208.09	-48.65	-160.03	-134.23	-174.77	-159.91	56.26	57.30	54.58	-37.61	-57.95	-88.35	-80.72
Y	267.43	213.25	178.23	156.32	156.18	364.34	235.34	248.68	364.06	363.52	-344.67	-353.57	-86.07	-85.76	59.29	56.05	61.21	38.33	10.75	-257.34	
x-axis (mm)															0.00	0.34	0.92				
	near grt	*near grt*	*near grt*	*near grt*	*near grt*	*±nr grt*	*matrix*	*matrix*	*matrix*	*matrix*	*adj grt*	*±nr grt*	*matrix*	*matrix*						*clot*	*clot*

TABLE B-5: Quantitative Microprobe Analysis for Muscovite Compositions

	PC-83A (cont'd)		*PC-84C*									*PC-93A*		*PC-128/10a (looked like green biotite)*						
	ms8	**ms11**	**ms2**	**ms3**	**ms4**	**ms5**	**ms9**	**ms10**	**M1**	**M2**	**ms3**	**2**	**2a**	**3**	**3a**	**4**	**4a**	**5a**	**6**	**6a**
WEIGHT PERCENT OXIDES																				
SiO2	45.345	45.838	44.944	45.469	45.449	45.016	45.041	46.087	47.255	46.669	44.806	45.980	45.796	44.927	45.998	47.584	46.523	44.965	44.389	44.216
Al2O3	35.553	35.802	35.386	35.457	35.674	35.348	35.066	35.527	29.971	30.996	31.455	34.441	34.571	35.745	35.163	34.158	34.385	35.882	35.381	34.952
TiO2	0.671	0.623	0.208	0.286	0.058	0.042	0.467	0.246	0.884	0.915	0.605	0.095	0.004	0.000	0.000	0.041	0.000	0.041	0.062	0.240
MgO	0.522	0.514	0.549	0.517	0.564	0.534	0.435	0.419	1.355	1.076	0.930	0.795	0.939	0.567	0.737	0.764	0.683	0.650	0.551	0.536
FeO	1.530	1.479	1.581	1.513	1.670	1.825	1.560	1.946	4.658	4.335	4.077	2.533	2.363	2.026	2.142	2.245	2.173	2.057	1.909	1.908
MnO	0.000	0.067	0.104	0.014	0.032	0.043	0.012	0.000	0.026	0.000	0.029	0.000	0.034	0.019	0.000	0.124	0.000	0.000	0.023	0.064
CaO	0.000	0.025	0.035	0.000	0.021	0.019	0.037	0.000	0.014	0.031	0.018	0.000	0.061	0.027	0.037	0.044	0.000	0.000	0.037	0.000
BaO																				
Na2O	0.814	0.903	0.600	0.585	0.665	0.724	0.637	0.453	0.190	0.181	0.288	0.464	0.382	0.548	0.326	0.441	0.340	0.444	0.331	0.446
K2O	10.231	10.302	10.46:	9.934	10.769	10.598	10.923	10.775	10.733	10.626	11.210	10.235	11.181	10.793	10.458	9.985	10.842	10.602	10.654	10.894
Cr2O3	0.055	0.011	0.038	0.036	0.015	0.051	0.074	0.000	0.000	0.000	0.019	0.014	0.135	0.014	0.000	0.047	0.027	0.010	0.000	0.139
Cl	0.000	0.015	0.015	0.012	0.003	0.003	0.009	0.000	0.015	0.009	0.000									
F	0.000	0.088	0.098	0.080	0.100	0.128	0.112	0.075	0.030	0.034	0.072	0.000	0.056	0.137	0.156	0.000	0.000	0.072	0.031	0.000
TOTAL	*94.721*	*95.667*	*94.028*	*93.903*	*95.020*	*94.331*	*94.373*	*95.528*	*95.131*	*94.872*	*93.509*	94.557	*95.522*	94.803	95.018	*95.434*	*94.975*	*94.724*	*93.367*	*93.396*
-O = Cl	0.000	-0.003	-0.003	-0.003	-0.001	-0.001	-0.002	0.000	-0.003	-0.002	0.000	0.000	0.000	0.000	0.000	0.000	0.000	0.000	0.000	0.000
-O = F	0.000	-0.037	-0.041	-0.034	-0.042	-0.054	-0.047	-0.032	-0.013	-0.014	-0.030	0.000	-0.024	-0.058	-0.066	0.000	0.000	-0.030	-0.013	0.000
TOTAL	**94.721**	**95.627**	**93.983**	**93.867**	**94.977**	**94.276**	**94.324**	**95.496**	**95.115**	**94.856**	**93.479**	**94.557**	**95.498**	**94.745**	**94.952**	**95.434**	**94.975**	**94.694**	**93.354**	**93.396**
CATIONS RECALCULATED TO 22 OXYGENS																				
Si	6.083	6.095	6.091	6.135	6.102	6.095	6.09:	6.148	6.425	6.348	6.222	6.195	6.149	6.062	6.168	6.320	6.243	6.057	6.065	6.058
Al	5.621	5.611	5.652	5.639	5.645	5.641	5.597	5.586	4.803	4.969	5.148	5.469	5.471	5.684	5.557	5.347	5.438	5.697	5.698	5.644
Ti	0.068	0.062	0.021	0.029	0.006	0.004	0.048	0.025	0.090	0.094	0.063	0.00:	0.000	0.000	0.000	0.004	0.000	0.004	0.006	0.025
Mg	0.104	0.102	0.111	0.104	0.113	0.108	0.088	0.083	0.275	0.218	0.193	0.160	0.188	0.114	0.147	0.151	0.137	0.130	0.112	0.109
Fe	0.172	0.164	0.179	0.171	0.187	0.207	0.177	0.217	0.530	0.493	0.473	0.285	0.265	0.229	0.240	0.249	0.244	0.232	0.218	0.219
Mn	0.000	0.008	0.012	0.002	0.004	0.005	0.001	0.000	0.003	0.000	0.003	0.000	0.004	0.002	0.000	0.014	0.000	0.000	0.003	0.007
Ca	0.000	0.004	0.005	0.000	0.003	0.003	0.005	0.000	0.002	0.005	0.003	0.000	0.009	0.004	0.005	0.006	0.000	0.000	0.005	0.000
Ba																				
Na	0.212	0.233	0.158	0.153	0.173	0.190	0.167	0.117	0.050	0.048	0.078	0.121	0.09:	0.143	0.085	0.114	0.089	0.116	0.088	0.118
K	1.751	1.748	1.810	1.710	1.844	1.831	1.887	1.834	1.862	1.844	1.986	1.759	1.915	1.858	1.789	1.692	1.856	1.822	1.857	1.904
Cr	0.006	0.001	0.004	0.004	0.002	0.005	0.008	0.000	0.000	0.000	0.002	0.001	0.014	0.001	0.000	0.005	0.003	0.001	0.000	0.015
TOTAL	**14.017**	**14.027**	**14.044**	**13.946**	**14.078**	**14.088**	**14.078**	**14.00:**	**14.039**	**14.019**	**14.171**	**14.000**	**14.115**	**14.096**	**13.991**	**13.903**	**14.009**	**14.059**	**14.052**	**14.099**
Na+K	1.963	1.980	1.968	1.863	2.018	2.021	2.054	1.951	1.912	1.892	2.064	1.880	2.015	2.001	1.874	1.806	1.945	1.938	1.945	2.023
Na/Na+K	*0.108*	*0.118*	*0.080*	*0.082*	*0.086*	*0.094*	*0.081*	*0.060*	*0.026*	*0.025*	*0.038*	*0.065*	*0.049*	*0.072*	*0.045*	*0.063*	*0.046*	*0.05:*	*0.045*	*0.059*
Alvi	3.705	3.706	3.743	3.774	3.746	3.736	3.696	3.734	3.228	3.318	3.370	3.664	3.620	3.745	3.724	3.667	3.681	3.754	3.763	3.701
xAlvi	*0.915*	*0.917*	*0.921*	*0.925*	*0.924*	*0.920*	*0.922*	*0.920*	*0.782*	*0.805*	*0.821*	*0.890*	*0.888*	*0.916*	*0.906*	*0.898*	*0.906*	*0.911*	*0.917*	*0.911*
xTi	0.017	0.015	0.005	0.007	0.001	0.001	0.012	0.006	0.022	0.023	0.015	0.002	0.000	0.000	0.000	0.001	0.000	0.001	0.002	0.006
xMg	0.026	0.025	0.027	0.026	0.028	0.027	0.022	0.021	0.067	0.053	0.047	0.039	0.046	0.028	0.036	0.037	0.034	0.032	0.027	0.027
xFe	0.042	0.041	0.044	0.042	0.046	0.051	0.044	0.054	0.128	0.120	0.115	0.069	0.065	0.056	0.058	0.061	0.060	0.056	0.053	0.054
Fe/Fe+Mg	0.622	0.617	0.618	0.621	0.624	0.657	0.668	0.723	0.659	0.693	0.711	0.641	0.585	0.667	0.620	0.623	0.641	0.640	0.660	0.666
X	-47.10	-31.10	80.39	80.39	84.44	72.52	44.33	144.51	179.49	150.91	-158.66									
Y	-294.21	-297.47	-116.68	-118.57	-119.25	-120.44	-234.19	-306.80	226.12	144.20	-328.55									
x-axis (mm)							*parallel*	*leuco*												
	cross	*cross*	*clot*	*clot*	*clot*	*clot*	*foliation*	*adj kfs*	*near grt*	*matrix*	*matrix*	*adj grt*	*adj grt*	*adj grt*	*adj grt*	*adj grt*	*adj grt*	*adj grt*	*adj grt*	*adj grt*

TABLE B-5: Quantitative Microprobe Analysis for Muscovite Compositions

	PC-128/10b									*PC-131/2*		
	ms1	**ms1a**	**ms3**	**ms3a**	**ms4**	**ms4a**	**ms5**	**ms6**	**ms7**	**ms1a**	**ms1b**	**ms2a**
WEIGHT PERCENT OXIDES												
SiO2	45.955	46.208	45.527	45.165	45.498	45.828	45.231	45.149	44.485	45.029	45.248	45.625
Al2O3	36.198	35.761	35.198	35.255	34.515	34.719	35.180	35.107	34.693	33.425	33.204	33.867
TiO2	0.098	0.137	0.219	0.088	1.274	1.179	0.035	0.000	0.050	0.888	0.903	0.901
MgO	0.758	0.763	0.788	0.751	0.690	0.776	0.839	0.976	1.756	0.690	0.666	0.647
FeO	1.581	1.631	1.509	1.517	1.621	1.386	1.672	1.622	2.518	3.503	3.426	3.143
MnO	0.052	0.020	0.017	0.061	0.032	0.009	0.000	0.000	0.000	0.037	0.000	0.000
CaO	0.000	0.019	0.035	0.049	0.018	0.000	0.028	0.030	0.000	0.039	0.000	0.058
BaO												
Na2O	0.650	0.787	0.696	0.769	0.733	0.650	0.643	0.689	0.793	0.584	0.566	0.504
K2O	10.419	10.476	10.687	10.638	10.518	10.713	10.262	10.256	10.112	10.567	10.542	10.350
Cr2O3	0.000	0.045	0.040	0.013	0.000	0.061	0.000	0.042	0.021	0.000	0.000	0.002
Cl	0.000	0.000	0.000	0.000	0.015	0.000	0.000	0.012	0.024	0.003	0.009	0.003
F	0.000	0.102	0.000	0.000	0.078	0.234	0.045	0.038	0.117	0.038	0.061	0.049
TOTAL	*95.711*	*95.949*	*94.716*	*94.306*	*94.992*	*95.555*	*93.935*	*93.921*	*94.569*	*94.803*	*94.625*	*95.149*
-O = Cl	0.000	0.000	0.000	0.000	-0.003	0.000	0.000	-0.003	-0.005	-0.001	-0.002	-0.001
-O = F	0.000	-0.043	0.000	0.000	-0.033	-0.099	-0.019	-0.016	-0.049	-0.016	-0.026	-0.021
TOTAL	**95.711**	**95.906**	**94.716**	**94.306**	**94.956**	**95.456**	**93.916**	**93.902**	**94.514**	**94.786**	**94.597**	**95.128**
CATIONS RECALCULATED TO 22 OXYGENS												
Si	6.097	6.128	6.121	6.102	6.112	6.123	6.121	6.114	6.028	6.122	6.157	6.149
Al	5.660	5.58:	5.577	5.614	5.464	5.467	5.611	5.603	5.541	5.356	5.325	5.380
Ti	0.00:	0.014	0.022	0.009	0.129	0.118	0.004	0.000	0.005	0.091	0.092	0.091
Mg	0.150	0.151	0.158	0.151	0.138	0.155	0.169	0.197	0.355	0.140	0.135	0.130
Fe	0.175	0.181	0.170	0.171	0.182	0.155	0.189	0.184	0.285	0.398	0.390	0.354
Mn	0.006	0.002	0.002	0.007	0.004	0.001	0.000	0.000	0.000	0.004	0.000	0.000
Ca	0.000	0.003	0.005	0.007	0.003	0.000	0.004	0.004	0.000	0.006	0.000	0.008
Ba												
Na	0.167	0.202	0.181	0.201	0.191	0.168	0.169	0.181	0.208	0.154	0.149	0.132
K	1.763	1.772	1.833	1.834	1.802	1.826	1.772	1.772	1.748	1.833	1.82:	1.780
Cr	0.000	0.005	0.004	0.001	0.000	0.006	0.000	0.005	0.002	0.000	0.000	0.000
TOTAL	**14.029**	**14.048**	**14.074**	**14.099**	**14.024**	**14.019**	**14.03:**	**14.059**	**14.173**	**14.103**	**14.078**	**14.025**
Na+K	1.931	1.975	2.014	2.035	1.993	1.994	1.941	1.953	1.957	1.987	1.979	1.911
Na/Na+K	*0.087*	*0.102*	*0.090*	*0.099*	*0.096*	*0.084*	*0.087*	*0.093*	*0.106*	*0.078*	*0.075*	*0.069*
Alvi	3.757	3.718	3.698	3.716	3.576	3.58:	3.733	3.717	3.569	3.477	3.481	3.529
xAlvi	*0.917*	*0.914*	*0.913*	*0.916*	*0.888*	*0.893*	*0.912*	*0.907*	*0.847*	*0.846*	*0.849*	*0.860*
xTi	0.002	0.003	0.005	0.002	0.032	0.029	0.001	0.000	0.001	0.022	0.023	0.022
xMg	0.037	0.037	0.039	0.037	0.034	0.039	0.041	0.048	0.084	0.034	0.033	0.032
xFe	0.043	0.044	0.042	0.042	0.045	0.039	0.046	0.045	0.068	0.097	0.095	0.086
Fe/Fe+Mg	0.539	0.545	0.518	0.531	0.569	0.500	0.528	0.482	0.446	0.740	0.743	0.732
X	166.15	167.08	35.28	34.46	169.33	170.16	79.02	80.58	77.29	135.89	136.59	159.30
Y	360.61	360.77	318.13	320.35	268.37	266.45	200.70	196.43	192.56	257.86	247.18	236.67
x-axis (mm	0.00	0.09	0.00	0.24	0.00	0.21				0.00	1.07	
	adj crd	*adj crd*	*adj crd*	*adj crd*			*adj crd*	*adj crd*	*adj crd*			

TABLE B-6: Quantitative Microprobe Analysis for Hornblende Compositions

PC-80B

	1H1	1H2	1H3	1H4	1H6	1H7	1H8	1H9	1H11	1H12	1HT1a	1HT1b	1HT1c	1HT1d	1HT1e	1HT1f	1HT1g	1HT1h	1HT1i	1HT1j
WEIGHT PERCENT OXIDES																				
SiO2	44.373	43.859	44.516	43.817	44.641	42.711	43.056	44.622	44.098	44.162	45.229	44.556	44.998	44.46:	44.785	44.705	43.793	44.958	44.909	43.440
Al2O3	11.560	11.568	11.301	12.019	11.448	15.226	14.479	12.603	12.885	12.442	10.059	11.450	10.709	12.042	11.249	11.353	11.589	11.266	11.752	12.832
TiO2	0.513	0.673	0.461	0.545	0.476	0.435	0.393	0.635	0.464	0.445	0.508	0.489	0.363	0.396	0.528	0.534	0.628	0.583	0.421	0.417
MgO	7.129	7.047	7.275	7.158	7.154	5.785	6.127	6.998	6.920	6.349	7.736	6.929	6.565	6.458	7.345	6.726	6.867	7.008	7.194	6.774
FeO	21.456	21.948	21.340	21.819	21.724	21.393	22.390	21.329	22.332	23.694	22.902	21.664	22.194	22.342	21.687	22.721	22.376	21.983	21.264	21.166
MnO	0.251	0.163	0.283	0.197	0.193	0.163	0.291	0.197	0.208	0.249	0.279	0.205	0.272	0.124	0.193	0.145	0.215	0.196	0.178	0.231
CaO	11.503	11.387	11.377	11.413	11.562	11.266	11.538	11.174	11.364	11.724	10.366	11.532	11.703	11.566	11.321	11.252	11.503	11.859	11.576	11.561
Na2O	0.807	0.837	0.805	0.728	0.887	0.842	1.017	0.687	0.819	1.074	0.641	0.796	0.720	0.758	0.737	0.652	0.813	0.721	0.649	0.772
K2O	0.509	0.520	0.338	0.515	0.412	0.585	0.504	0.479	0.467	0.507	0.382	0.419	0.342	0.480	0.445	0.441	0.585	0.498	0.432	0.456
Cl	0.000	0.000	0.000	0.011	0.000	0.022	0.014	0.000	0.014	0.017	0.000	0.003	0.013	0.017	0.008	0.010	0.003	0.018	0.007	0.000
F	0.082	0.049	0.064	0.083	0.033	0.045	0.000	0.040	0.053	0.103	0.043	0.083	0.014	0.053	0.084	0.043	0.168	0.074	0.001	0.110
TOTAL	*98.183*	*98.051*	*97.760*	*98.305*	*98.530*	*98.473*	*99.809*	*98.764*	*99.624*	*100.766*	*98.145*	*98.126*	*97.893*	*98.706*	*98.382*	*98.582*	*98.540*	*99.164*	*98.383*	*97.759*
-O = Cl	0.000	0.000	0.000	-0.002	0.000	-0.005	-0.003	0.000	-0.003	-0.004	0.000	-0.001	-0.003	-0.004	-0.002	-0.002	-0.001	-0.004	-0.002	0.000
-O = F	-0.035	-0.021	-0.027	-0.035	-0.014	-0.019	0.000	-0.017	-0.022	-0.043	-0.018	-0.035	-0.006	-0.022	-0.035	-0.018	-0.071	-0.031	-0.000	-0.046
TOTAL	**98.148**	**98.030**	**97.733**	**98.268**	**98.516**	**98.449**	**99.806**	**98.747**	**99.599**	**100.719**	**98.127**	**98.090**	**97.884**	**98.680**	**98.345**	**98.562**	**98.469**	**99.129**	**98.381**	**97.713**
CATIONS RECALCULATED TO 23 OXYGENS																				
Si	6.707	6.657	6.744	6.628	6.722	6.425	6.427	6.670	6.581	6.578	6.848	6.737	6.831	6.699	6.749	6.747	6.642	6.739	6.743	6.58:
Al	2.059	2.06:	2.018	2.143	2.032	2.699	2.547	2.220	2.266	2.184	1.795	2.041	1.916	2.138	1.998	2.019	2.072	1.990	2.07:	2.294
Ti	0.058	0.077	0.053	0.062	0.054	0.049	0.044	0.071	0.052	0.04:	0.058	0.056	0.042	0.045	0.05:	0.061	0.072	0.066	0.048	0.048
Mg	1.606	1.595	1.643	1.614	1.606	1.297	1.363	1.559	1.540	1.410	1.746	1.562	1.486	1.450	1.650	1.513	1.553	1.566	1.610	1.532
Fe	2.712	2.786	2.704	2.760	2.736	2.691	2.795	2.666	2.787	2.952	2.900	2.740	2.818	2.815	2.733	2.868	2.838	2.756	2.670	2.685
Mn	0.032	0.021	0.036	0.025	0.025	0.021	0.037	0.025	0.026	0.031	0.036	0.026	0.035	0.016	0.025	0.019	0.028	0.025	0.023	0.02:
Ca	1.863	1.852	1.847	1.850	1.865	1.816	1.845	1.790	1.817	1.871	1.682	1.868	1.904	1.867	1.828	1.819	1.869	1.905	1.862	1.879
Na	0.236	0.246	0.236	0.214	0.259	0.246	0.294	0.199	0.237	0.310	0.188	0.233	0.212	0.221	0.215	0.191	0.239	0.210	0.189	0.227
K	0.098	0.101	0.065	0.099	0.079	0.112	0.096	0.091	0.089	0.096	0.074	0.081	0.066	0.092	0.086	0.085	0.113	0.095	0.083	0.088
TOTAL	**15.373**	**15.404**	**15.346**	**15.395**	**15.377**	**15.356**	**15.450**	**15.293**	**15.396**	**15.483**	**15.327**	**15.344**	**15.309**	**15.344**	**15.343**	**15.321**	**15.426**	**15.352**	**15.306**	**15.373**
Fe/Fe+Mg	*0.628*	*0.636*	*0.622*	*0.631*	*0.630*	*0.675*	*0.672*	*0.631*	*0.644*	*0.677*	*0.624*	*0.637*	*0.655*	*0.660*	*0.624*	*0.655*	*0.646*	*0.638*	*0.624*	*0.637*
Na+K	0.335	0.347	0.302	0.313	0.338	0.358	0.390	0.290	0.326	0.407	0.262	0.314	0.278	0.314	0.301	0.276	0.352	0.305	0.272	0.315
Al(iv)	1.293	1.343	1.256	1.372	1.278	1.575	1.573	1.330	1.419	1.422	1.152	1.263	1.169	1.301	1.251	1.253	1.358	1.261	1.257	1.410
Al(vi)	0.766	0.727	0.762	0.771	0.754	1.124	0.975	0.891	0.848	0.763	0.644	0.778	0.747	0.837	0.747	0.766	0.714	0.730	0.822	0.884
Na(M4)	*0.137*	*0.148*	*0.153*	*0.150*	*0.135*	*0.184*	*0.155*	*0.210*	*0.183*	*0.129*	*0.318*	*0.132*	*0.096*	*0.133*	*0.172*	*0.181*	*0.131*	*0.095*	*0.138*	*0.121*
X (mm)	59.29	60.12	58.28	50.98	71.45						56.70	58.07	59.56	60.80	62.17	65.00	66.27	67.64	69.00	70.37
Y (mm)	60.99	63.40	69.11	86.65	75.31						74.47	75.09	75.71	76.34	76.96	78.12	78.84	79.39	80.00	80.58
x-axis (mm)											0.00	0.15	0.31	0.45	0.60	0.91	1.05	1.20	1.35	1.50
location	*adj gt*	*±adj gt*	*±adj gt*	*adj gt*	*near gt*	*adj gt*	*±adj gt*	*±adj gt*	*±adj gt*	*adj gt*	*near gt*	*near gt*	*near gt*	*near gt*	*near gt*	*near gt*	*near gt*	*near gt*	*near gt*	*near gt*

TABLE B-6: Quantitative Microprobe Analysis for Hornblende Compositions

PC-80B (continued)										*PC-107F*											
	2H1	**2H2**	**2H3**	**2H4**	**2H5**	**mH1**	**mH2**	**mH4**	**mH5**	**H1**	**H2**	**H3**	**H4**	**H5**	**H6**	**H7**	**H8**	**H9**	**HT1a**	**HT1b**	**HT1c**
WEIGHT PERCENT OXIDES																					
SiO2	45.186	44.880	44.538	43.892	45.492	43.986	43.839	44.996	44.962	40.957	41.742	40.959	40.556	41.006	41.296	40.996	40.935	41.199	40.784	40.628	41.132
Al2O3	10.323	11.594	11.566	11.925	10.749	11.424	11.738	11.710	11.907	12.334	12.077	12.273	12.545	12.844	12.908	12.688	12.763	12.738	12.760	12.244	12.591
TiO2	0.451	0.518	0.764	0.536	0.506	0.674	0.898	0.589	0.507	1.142	1.270	1.274	1.232	1.142	0.936	1.241	1.203	1.189	1.108	1.290	1.308
MgO	7.758	7.181	6.892	7.085	7.513	6.912	6.768	7.050	7.358	5.719	6.003	6.113	5.786	5.572	5.787	5.896	5.833	6.009	5.944	6.191	6.024
FeO	22.844	21.694	21.824	21.319	21.810	22.778	22.504	22.524	22.255	23.679	23.715	23.605	23.843	24.501	23.749	24.274	24.247	23.213	23.398	24.120	23.720
MnO	0.236	0.182	0.214	0.211	0.160	0.224	0.302	0.208	0.324	0.289	0.287	0.292	0.252	0.301	0.291	0.253	0.237	0.331	0.280	0.358	0.301
CaO	10.766	11.567	11.457	11.200	11.494	10.881	11.394	11.433	11.484	11.892	11.802	11.46:	11.872	11.396	11.651	11.651	11.681	11.701	11.786	11.564	11.686
Na2O	0.531	0.803	0.730	0.851	0.827	0.906	0.848	0.824	0.831	1.295	1.184	1.312	1.307	1.297	0.959	1.175	1.179	1.078	1.172	1.374	1.191
K2O	0.418	0.418	0.565	0.518	0.406	0.631	0.782	0.472	0.513	1.153	1.125	1.208	1.076	1.165	1.049	1.102	1.123	1.110	1.149	1.227	1.266
Cl	0.001	0.000	0.006	0.000	0.011	0.011	0.000	0.000	0.050	0.008	0.003	0.014	0.000	0.013	0.000	0.024	0.006	0.000	0.021	0.000	0.010
F	0.079	0.037	0.012	0.125	0.018	0.120	0.073	0.099	0.062	0.036	1.323	0.089	0.000	0.057	0.025	0.085	0.116	0.000	0.063	0.048	0.036
TOTAL	*98.593*	*98.874*	*98.568*	*97.662*	*98.986*	*98.547*	*99.146*	*99.905*	*100.253*	*98.504*	*100.531*	*98.609*	*98.469*	*99.294*	*98.651*	*99.385*	*99.323*	*98.568*	*98.465*	*99.044*	*99.265*
-O = Cl	-0.000	0.000	-0.001	0.000	-0.002	-0.002	0.000	0.000	-0.011	-0.002	-0.001	-0.003	0.000	-0.003	0.000	-0.005	-0.001	0.000	-0.005	0.000	-0.002
-O = F	-0.033	-0.016	-0.005	-0.053	-0.008	-0.051	-0.031	-0.042	-0.026	-0.015	-0.557	-0.038	0.000	-0.024	-0.011	-0.036	-0.049	0.000	-0.027	-0.020	-0.015
TOTAL	**98.560**	**98.858**	**98.562**	**97.609**	**98.976**	**98.494**	**99.115**	**99.863**	**100.216**	**98.487**	**99.973**	**98.568**	**98.469**	**99.267**	**98.640**	**99.344**	**99.273**	**98.568**	**98.434**	**99.024**	**99.248**
CATIONS RECALCULATED TO 23 OXYGENS																					
Si	6.816	6.726	6.707	6.668	6.808	6.671	6.613	6.701	6.671	6.333	6.388	6.324	6.277	6.300	6.347	6.289	6.285	6.332	6.297	6.269	6.305
Al	1.835	2.048	2.053	2.135	1.896	2.042	2.087	2.055	2.082	2.248	2.178	2.233	2.288	2.326	2.338	2.294	2.310	2.307	2.322	2.227	2.275
Ti	0.051	0.058	0.087	0.061	0.057	0.077	0.102	0.066	0.057	0.133	0.146	0.148	0.143	0.132	0.108	0.143	0.139	0.137	0.129	0.150	0.151
Mg	1.744	1.604	1.547	1.605	1.676	1.563	1.522	1.565	1.627	1.318	1.370	1.407	1.335	1.276	1.326	1.348	1.335	1.377	1.368	1.424	1.377
Fe	2.882	2.719	2.749	2.709	2.729	2.889	2.839	2.805	2.761	3.062	3.035	3.048	3.086	3.148	3.053	3.114	3.114	2.984	3.021	3.113	3.041
Mn	0.030	0.023	0.027	0.027	0.020	0.029	0.039	0.026	0.041	0.038	0.037	0.038	0.033	0.039	0.038	0.033	0.031	0.043	0.037	0.047	0.039
Ca	1.740	1.857	1.849	1.823	1.843	1.768	1.842	1.824	1.825	1.970	1.935	1.898	1.969	1.876	1.919	1.915	1.922	1.927	1.950	1.912	1.919
Na	0.155	0.233	0.213	0.251	0.240	0.266	0.248	0.238	0.239	0.388	0.351	0.393	0.392	0.386	0.286	0.350	0.351	0.321	0.351	0.411	0.354
K	0.080	0.07:	0.109	0.100	0.078	0.122	0.150	0.08:	0.097	0.227	0.220	0.238	0.212	0.228	0.206	0.216	0.220	0.218	0.226	0.242	0.248
TOTAL	**15.334**	**15.349**	**15.340**	**15.379**	**15.346**	**15.426**	**15.441**	**15.370**	**15.400**	**15.718**	**15.662**	**15.727**	**15.737**	**15.712**	**15.621**	**15.703**	**15.706**	**15.646**	**15.701**	**15.794**	**15.708**
Fe/Fe+Mg	*0.623*	*0.629*	*0.640*	*0.628*	*0.620*	*0.649*	*0.651*	*0.642*	*0.629*	*0.699*	*0.689*	*0.684*	*0.698*	*0.712*	*0.697*	*0.698*	*0.700*	*0.684*	*0.688*	*0.686*	*0.688*
Na+K	0.236	0.313	0.322	0.351	0.317	0.388	0.398	0.328	0.336	0.616	0.571	0.631	0.605	0.615	0.491	0.565	0.571	0.539	0.577	0.653	0.602
Al(iv)	1.184	1.274	1.293	1.332	1.192	1.329	1.387	1.299	1.329	1.667	1.612	1.676	1.723	1.700	1.653	1.711	1.715	1.668	1.703	1.731	1.695
Al(vi)	0.651	0.773	0.760	0.803	0.703	0.712	0.700	0.756	0.752	0.581	0.567	0.557	0.566	0.626	0.686	0.584	0.595	0.639	0.619	0.496	0.580
Na(M4)	*0.260*	*0.143*	*0.151*	*0.177*	*0.157*	*0.232*	*0.158*	*0.176*	*0.175*	*0.02:*	*0.065*	*0.102*	*0.031*	*0.124*	*0.081*	*0.085*	*0.078*	*0.073*	*0.050*	*0.088*	*0.081*
X (mm)	-115.54	-116.76	-63.68	-63.26	-91.67					-198.97	-203.65	-207.23	-208.32	-210.45	-169.71	-168.48	-168.65	-152.49	-162.48	-162.48	-162.48
Y (mm)	-113.72	-104.31	-118.36	-130.57	-120.14					-124.81	-126.23	-129.74	-133.58	-140.29	-120.99	-118.51	-114.91	-222.31	-131.49	-132.35	-133.07
x-axis (mm)						S-surface	S-surface	C-surface	C-surface										0.00	0.09	0.16
location	*±adj gt*	*near gt*	*near gt*	*near gt*	*incl?*	*matrix*	*matrix*	*matrix*	*matrix*	*±nr gt*	*±matrix*	*matrix*	*matrix*	*matrix*	*matrix*	*matrix*	*matrix*	*matrix*	*±matrix*	*±matrix*	*±matrix*

TABLE B-6: Quantitative Microprobe Analysis for Hornblende Compositions

PC-107F (continued)

	HT1d	HT1e	HT1f	HT1g	HT1h	HT1i	HT1j	HT1k	HT1l	HT1m	HT1n	HT1o	HT1p	HT1q	HT1r	HT1s	HT1t	2H1	2H2	3H1	3H2
WEIGHT PERCENT OXIDES																					
SiO2	40.069	40.945	40.910	40.711	41.291	40.134	40.662	41.270	41.812	41.795	40.563	41.126	40.598	41.083	41.186	41.083	41.139	41.912	41.644	40.102	41.072
Al2O3	12.478	12.537	12.230	12.309	12.484	12.366	12.267	11.736	11.855	11.847	12.274	11.722	12.443	12.426	12.516	12.616	12.673	13.328	13.071	13.996	12.929
TiO2	1.389	1.053	1.328	1.475	1.207	1.297	1.391	1.416	1.225	1.113	1.159	1.327	1.195	1.354	1.313	0.892	1.138	1.032	1.160	0.888	1.043
MgO	5.971	6.172	6.232	6.074	5.910	5.772	5.870	6.242	6.049	6.057	5.913	5.923	5.82:	5.789	5.873	5.821	5.903	5.571	5.569	6.194	5.598
FeO	24.102	23.535	23.876	23.985	23.724	23.955	23.397	23.666	24.152	24.106	24.059	23.907	23.987	23.986	23.714	24.277	23.936	24.069	24.011	25.132	25.025
MnO	0.301	0.236	0.218	0.230	0.300	0.334	0.284	0.269	0.303	0.257	0.245	0.336	0.283	0.334	0.243	0.259	0.243	0.279	0.271	0.212	0.182
CaO	11.498	11.658	11.472	11.591	11.817	11.537	11.689	11.691	11.556	11.781	11.558	11.611	11.464	11.692	11.755	11.807	11.565	11.575	11.589	9.767	11.748
Na2O	1.325	1.389	1.194	1.319	1.264	1.279	1.274	1.204	1.273	1.190	1.155	1.277	1.351	1.222	1.259	1.174	1.103	1.026	1.230	0.785	0.994
K2O	1.411	1.204	1.328	1.309	1.208	1.271	1.281	1.069	0.973	1.202	1.133	1.164	1.127	1.166	1.231	1.030	1.047	1.067	1.092	0.943	1.072
Cl	0.019	0.038	0.010	0.000	0.018	0.000	0.015	0.000	0.011	0.015	0.013	0.008	0.029	0.022	0.014	0.019	0.000	0.000	0.039	0.011	0.000
F	0.030	0.086	0.163	0.127	0.064	0.100	0.000	0.081	0.036	0.055	0.113	0.044	0.061	0.063	0.041	0.026	0.000	0.000	0.066	0.000	0.000
TOTAL	*98.593*	*98.853*	*98.961*	*99.130*	*99.287*	*98.045*	*98.130*	*98.644*	*99.245*	*99.418*	*98.185*	*98.445*	*98.368*	*99.137*	*99.145*	*99.004*	*98.747*	*99.859*	*99.742*	*98.030*	*99.663*
-O = Cl	-0.004	-0.009	-0.002	0.000	-0.004	0.000	-0.003	0.000	-0.002	-0.003	-0.003	-0.002	-0.007	-0.005	-0.003	-0.004	0.000	0.000	-0.009	-0.002	0.000
-O = F	-0.013	-0.036	-0.069	-0.054	-0.027	-0.042	0.000	-0.034	-0.015	-0.023	-0.048	-0.019	-0.026	-0.027	-0.017	-0.011	0.000	0.000	-0.028	0.000	0.000
TOTAL	**98.576**	**98.808**	**98.890**	**99.077**	**99.256**	**98.003**	**98.127**	**98.610**	**99.227**	**99.391**	**98.134**	**98.425**	**98.336**	**99.106**	**99.125**	**98.989**	**98.747**	**99.859**	**99.705**	**98.028**	**99.663**
CATIONS RECALCULATED TO 23 OXYGENS																					
Si	6.223	6.307	6.307	6.274	6.330	6.262	6.309	6.365	6.405	6.402	6.306	6.370	6.297	6.316	6.321	6.322	6.327	6.355	6.341	6.209	6.288
Al	2.284	2.276	2.222	2.236	2.256	2.274	2.243	2.133	2.140	2.139	2.249	2.140	2.274	2.252	2.264	2.288	2.297	2.382	2.346	2.554	2.333
Ti	0.162	0.122	0.154	0.171	0.139	0.152	0.162	0.164	0.141	0.128	0.136	0.155	0.139	0.157	0.152	0.103	0.132	0.118	0.133	0.103	0.120
Mg	1.382	1.417	1.432	1.395	1.351	1.343	1.358	1.435	1.381	1.383	1.370	1.368	1.348	1.327	1.344	1.335	1.353	1.259	1.264	1.430	1.278
Fe	3.130	3.032	3.079	3.091	3.042	3.126	3.036	3.053	3.094	3.088	3.128	3.097	3.111	3.084	3.044	3.124	3.079	3.052	3.057	3.254	3.204
Mn	0.03:	0.031	0.029	0.030	0.039	0.044	0.037	0.035	0.039	0.033	0.032	0.044	0.037	0.044	0.032	0.034	0.032	0.036	0.035	0.028	0.024
Ca	1.913	1.924	1.895	1.914	1.941	1.929	1.943	1.932	1.897	1.933	1.925	1.927	1.905	1.926	1.933	1.947	1.906	1.881	1.891	1.620	1.927
Na	0.399	0.415	0.357	0.394	0.376	0.387	0.383	0.360	0.378	0.353	0.348	0.383	0.406	0.364	0.375	0.350	0.329	0.302	0.363	0.236	0.295
K	0.280	0.237	0.261	0.257	0.236	0.253	0.254	0.210	0.190	0.235	0.225	0.230	0.223	0.229	0.241	0.202	0.205	0.206	0.212	0.186	0.209
TOTAL	**15.812**	**15.759**	**15.736**	**15.763**	**15.709**	**15.769**	**15.725**	**15.689**	**15.667**	**15.695**	**15.720**	**15.713**	**15.741**	**15.698**	**15.704**	**15.707**	**15.660**	**15.58:**	**15.641**	**15.621**	**15.678**
Fe/Fe+Mg	*0.694*	*0.681*	*0.682*	*0.689*	*0.692*	*0.700*	*0.691*	*0.680*	*0.691*	*0.691*	*0.695*	*0.694*	*0.698*	*0.699*	*0.694*	*0.701*	*0.695*	*0.708*	*0.707*	*0.695*	*0.715*
Na+K	0.678	0.651	0.618	0.651	0.612	0.640	0.637	0.56:	0.568	0.588	0.573	0.613	0.629	0.593	0.616	0.553	0.534	0.508	0.575	0.422	0.504
Al(iv)	1.777	1.693	1.693	1.726	1.670	1.738	1.691	1.635	1.595	1.598	1.694	1.630	1.703	1.684	1.679	1.678	1.673	1.645	1.659	1.791	1.712
Al(vi)	0.506	0.582	0.530	0.510	0.586	0.536	0.552	0.499	0.546	0.540	0.555	0.509	0.571	0.568	0.585	0.610	0.624	0.737	0.686	0.763	0.621
Na(M4)	*0.087*	*0.076*	*0.105*	*0.086*	*0.059*	*0.071*	*0.057*	*0.068*	*0.103*	*0.067*	*0.075*	*0.073*	*0.095*	*0.074*	*0.067*	*0.053*	*0.094*	*0.119*	*0.109*	*0.380*	*0.073*
X (mm)	-162.52	-162.48	-162.48	-162.48	-162.48	-162.48	-162.48	-162.48	-162.48	-162.48	-162.48	-162.48	-162.48	-162.48	-162.48	-162.16	-162.48	-162.48	-162.48	-162.16	-162.48
Y (mm)	-134.03	-134.76	-135.60	-136.44	-137.35	-138.13	-139.11	-139.81	-140.65	-141.50	-142.41	-143.18	-144.02	-144.70	-145.71	-146.55	-147.39	-144.70	-145.71	-146.55	-147.39
x-axis (mm	0.25	0.33	0.41	0.50	0.59	0.66	0.76	0.83	0.92	1.00	1.09	1.17	1.25	1.32	1.42	1.51	1.60				
location	*±matrix*	*±matrix*	*±matrix*	*±matrix*	*±matrix*	*±matrix*	*±matrix*	*±matrix*	*±matrix*	*±matrix*	*±matrix*	*±matrix*	*±matrix*	*±matrix*	*±matrix*	*±matrix*	*±matrix*	*adj gt*	*±adj gt*	*adj gt*	*adj gt*

TABLE B-7: Quantitatie Microprobe Analysis for Prehnite and Clinozoisite Compositions

PC-80B PREHNITE ANALYSES

	pr1	pr1a	pr3	pr5	pr6	pr7	pr8	M1	M2
WEIGHT PERCENT OXIDES	*WEIGHT PERCENT OXIDES*								
SiO2	43.270	43.342	42.523	43.288	42.416	42.553	42.678	42.758	42.477
Al2O3	23.416	23.762	22.527	23.116	23.191	23.249	23.163	23.258	22.530
TiO2	0.390	0.584	0.250	0.374	0.397	0.695	0.198	0.409	1.126
Fe2O3	2.904	2.192	4.769	3.114	4.759	2.706	4.760	4.904	4.351
MgO	0.529	0.304	0.581	0.301	0.906	0.212	0.846	1.081	0.719
MnO	0.071	0.014	0.018	0.000	0.023	0.000	0.028	0.000	0.000
CaO	25.184	26.119	25.226	26.026	24.403	26.246	24.370	23.970	25.446
BaO	0.000	0.043	0.070	0.041	0.000	0.000	0.000	0.000	0.024
Na2O	0.054	0.036	0.044	0.029	0.033	0.030	0.015	0.000	0.044
K2O	0.021	0.012	0.019	0.012	0.047	0.014	0.068	0.100	0.062
Cr2O3	0.023	0.000	0.034	0.043	0.027	0.000	0.000	0.000	0.000
TOTAL	**95.862**	**96.408**	**96.061**	**96.344**	**96.202**	**95.705**	**96.126**	**96.480**	**96.779**
CATIONS RECALCULATED TO 22 OXYGENS	*CATIONS RECALCULATED TO 22 OXYGENS*								
Si	5.960	5.939	5.896	5.954	5.854	5.896	5.889	5.874	5.847
Al	3.801	3.837	3.681	3.747	3.772	3.796	3.767	3.766	3.655
Ti	0.040	0.060	0.026	0.039	0.041	0.072	0.021	0.042	0.117
Fe3+	0.301	0.226	0.498	0.322	0.494	0.282	0.494	0.507	0.451
Mg	0.109	0.062	0.120	0.062	0.186	0.044	0.174	0.221	0.148
Mn	0.008	0.002	0.002	0.000	0.003	0.000	0.003	0.000	0.000
Ca	3.717	3.835	3.748	3.835	3.608	3.896	3.603	3.528	3.753
Ba	0.000	0.002	0.004	0.002	0.000	0.000	0.000	0.000	0.001
Na	0.014	0.000	0.012	0.008	0.009	0.008	0.004	0.000	0.012
K	0.004	0.002	0.003	0.002	0.008	0.002	0.012	0.018	0.011
Cr	0.003	0.000	0.004	0.005	0.003	0.000	0.000	0.000	0.000
TOTAL	**13.956**	**13.975**	**13.994**	**13.976**	**13.979**	**13.998**	**13.968**	**13.956**	**13.994**
X (mm)	227.07	228.95	50.63	178.96	210.30	209.64	33.12	209.64	33.12
Y (mm)	381.62	381.49	264.99	102.56	154.76	133.51	328.96	133.51	328.96
Distance	0.00	0.19							
Al(iv)	2.04	2.06	2.10	2.05	2.15	2.10	2.11	2.13	2.15
Al(vi)	1.76	1.78	1.58	1.70	1.63	1.69	1.66	1.64	1.50
6-fold s	2.22	2.13	2.22	2.12	2.35	2.09	2.35	2.41	2.22
Fe/Fe+Alv	0.15	0.11	0.24	0.16	0.23	0.14	0.23	0.24	0.23
Ca+Ba+Na	3.73	3.85	3.77	3.85	3.63	3.91	3.62	3.55	3.78
There is more weight in Fe2O3 than in 2FeO because of the extra oxygen, therefore:									
Fe2O3 recalulated from FeO reported by probe analysis: FeO(MWFe2O3/2MWFeO) = FeO(159.69									
FeO prob	2.613	1.972	4.291	2.802	4.282	2.435	4.283	4.413	3.915
Fe2O3	2.904	2.192	4.769	3.114	4.759	2.706	4.760	4.904	4.351

PC-80B CLINOZOISITE ANALYSES

	czo1	czo2	czo3	czo5	czo6
SiO2	39.295	38.912	38.921	39.257	39.835
Al2O3	31.047	30.301	31.087	31.485	31.264
TiO2	0.013	0.020	0.030	0.000	0.000
Fe2O3	4.547	5.939	4.767	4.272	4.854
MgO	0.000	0.002	0.000	0.005	0.014
MnO	0.037	0.027	0.074	0.000	0.049
CaO	24.072	23.843	24.284	24.046	24.138
BaO	0.000	0.033	0.000	0.066	0.028
Na2O	0.000	0.000	0.033	0.000	0.027
K2O	0.000	0.001	0.000	0.016	0.000
Cr2O3	0.004	0.024	0.010	0.007	0.004
TOTAL	**99.015**	**99.102**	**99.206**	**99.154**	**100.213**
Si	5.973	5.941	5.920	5.955	5.985
Al	5.562	5.453	5.573	5.629	5.536
Ti	0.001	0.002	0.003	0.000	0.000
Fe3+	0.520	0.682	0.546	0.488	0.549
Mg	0.000	0.000	0.000	0.001	0.003
Mn	0.005	0.003	0.000	0.000	0.006
Ca	3.921	3.900	3.958	3.908	3.886
Ba	0.000	0.002	0.000	0.004	0.002
Na	0.000	0.000	0.000	0.000	0.008
K	0.000	0.000	0.000	0.003	0.000
Cr	0.000	0.003	0.001	0.001	0.000
TOTAL	**15.984**	**15.988**	**16.021**	**15.988**	**15.976**
X (mm)	176.58	173.07	24.49	179.61	81.28
Y (mm)	391.16	391.95	269.45	99.89	304.54
Distance					
Al(iv)	2.03	2.06	2.08	2.05	2.02
Al(vi)	3.54	3.39	3.49	3.58	3.52
6-fold s	4.06	4.08	4.05	4.07	4.08
Fe/Fe+Alv	0.13	0.17	0.14	0.12	0.13
Ca+Ba+Na	3.92	3.90	3.97	3.92	3.90
Recalculation of FeO to Fe2O3:					
FeO prob	4.091	5.344	4.289	3.844	4.368
Fe2O3	4.547	5.939	4.767	4.272	4.854

TABLE B-8: Quantitative Microprobe Analysis for Ilmenite Composition

PC-80B				***PC-107F***																			
	I1	**I2**	**I3**	**I1**	**I2**	**I3**	**I4**	**I7**	**I8**	**I9**	**I10**	**I11**	**IT1a**	**IT1b**	**IT1c**	**IT2a**	**IT2b**	**IT3a**	**IT3b**	**IT3c**	**IT4a**	**IT4b**	**IT4c**
WEIGHT PERCENT OXIDES																							
SiO2	0.034	0.007	0.000	0.054	0.040	0.012	0.029	0.088	0.030	0.029	0.032	0.000	0.030	0.042	0.051	0.077	0.146	0.045	0.030	0.001	0.026	0.040	0.049
Al2O3	0.032	0.000	0.005	0.015	0.019	0.000	0.027	0.015	0.022	0.037	0.002	0.000	0.004	0.000	0.000	0.046	0.041	0.007	0.024	0.004	0.000	0.003	0.000
TiO2	51.758	52.226	51.744	49.192	50.235	49.762	50.285	49.852	50.015	49.848	49.663	50.103	49.730	50.029	49.469	50.212	50.087	49.332	49.130	49.46:	49.991	50.471	51.171
Fe2O3	1.692	1.023	1.899	7.700	5.504	6.587	6.244	5.342	5.728	5.748	7.264	5.362	6.064	5.889	6.691	4.854	4.583	6.319	7.377	6.979	5.639	5.080	4.269
MgO	0.047	0.046	0.046	0.012	0.021	0.010	0.024	0.025	0.010	0.019	0.049	0.029	0.036	0.026	0.014	0.018	0.000	0.000	0.000	0.035	0.008	0.028	0.000
FeO	45.109	45.555	45.053	42.413	43.610	43.240	43.647	43.139	43.365	43.056	43.359	43.670	42.979	43.204	42.759	43.408	43.250	42.373	42.638	42.736	43.403	43.980	44.496
MnO	1.356	1.309	1.381	1.788	1.519	1.471	1.526	1.633	1.587	1.737	1.196	1.316	1.657	1.714	1.678	1.723	1.794	1.967	1.538	1.668	1.516	1.340	1.499
TOTAL	**100.03**	**100.17**	**100.13**	**101.17**	**100.95**	**101.08**	**101.78**	**100.09**	**100.76**	**100.47**	**101.56**	**100.48**	**100.50**	**100.90**	**100.66**	**100.34**	**99.90**	**100.04**	**100.74**	**100.89**	**100.58**	**100.94**	**101.48**
CATIONS RECALCULATED TO 3 OXYGENS																							
Si	0.001	0.000	0.000	0.001	0.001	0.000	0.001	0.002	0.001	0.001	0.001	0.000	0.001	0.001	0.001	0.002	0.004	0.001	0.001	0.000	0.001	0.001	0.001
Al	0.001	0.000	0.000	0.000	0.001	0.000	0.001	0.000	0.001	0.001	0.000	0.000	0.000	0.000	0.000	0.001	0.001	0.000	0.001	0.000	0.000	0.000	0.000
Ti	0.983	0.990	0.982	0.926	0.947	0.938	0.941	0.948	0.945	0.944	0.931	0.949	0.942	0.944	0.936	0.952	0.953	0.939	0.929	0.934	0.946	0.951	0.959
Fe3+	0.032	0.019	0.036	0.145	0.104	0.124	0.117	0.102	0.108	0.109	0.136	0.102	0.115	0.111	0.127	0.092	0.087	0.120	0.140	0.132	0.107	0.096	0.080
Mg	0.002	0.002	0.002	0.000	0.001	0.000	0.001	0.001	0.000	0.001	0.002	0.001	0.001	0.001	0.001	0.001	0.000	0.000	0.000	0.001	0.000	0.001	0.000
Fe2+	0.952	0.960	0.951	0.888	0.914	0.906	0.908	0.912	0.911	0.907	0.904	0.920	0.905	0.906	0.899	0.915	0.915	0.897	0.897	0.897	0.913	0.922	0.927
Mn	0.029	0.028	0.029	0.038	0.032	0.031	0.032	0.035	0.034	0.037	0.025	0.028	0.035	0.036	0.036	0.037	0.038	0.042	0.033	0.036	0.032	0.028	0.032
TOTAL	**1.000**	**1.000**	**1.000**	**1.000**	**1.000**	**1.000**	**1.000**	**1.999**	**1.000**	**1.000**	**1.000**	**1.000**	**1.000**	**1.000**	**1.999**	**1.000**	**1.999**	**1.000**	**1.000**	**1.000**	**1.000**	**1.000**	**1.000**
X	69.04	67.14	44.07	-196.58	-195.82	-194.53	-195.98	-191.48	-188.55	-162.15	-161.85	-160.80	-197.24	-197.13	-197.01	-195.31	-195.72	-191.56	-191.39	-191.22	-196.47	-197.17	-197.87
Y	61.10	69.85	76.30	-112.38	-114.28	-116.30	-116.86	-118.37	-120.36	-138.82	-134.72	-131.69	-109.41	-109.75	-110.09	-109.28	-109.37	-109.99	-110.56	-111.13	-116.08	-116.13	-116.19
x-axis mm													0.00	0.04	0.07	0.00	0.04	0.00	0.06	0.12	0.00	0.07	0.14
location	*hb incl*	*hb incl*	*adj gt*	*gt emb*	*gt emb*	*gt incl*	*gt incl*	*gt incl*	*gt emb*	*hb incl*	*adj hb*	*hb incl*	*gt emb*	*gt emb*	*gt emb*	*gt incl*	*gt incl*	*gt incl*	*gt incl*	*gt incl*	*gt emb*	*gt emb*	*gt emb*

APPENDIX C

Garnet Composition Profiles for Pelites and Semi-Pelites

Representative Garnet Profiles for Pelites and Semi-Pelites* (given in order from west to east; see figure A-1, Appendix A for sample locations).

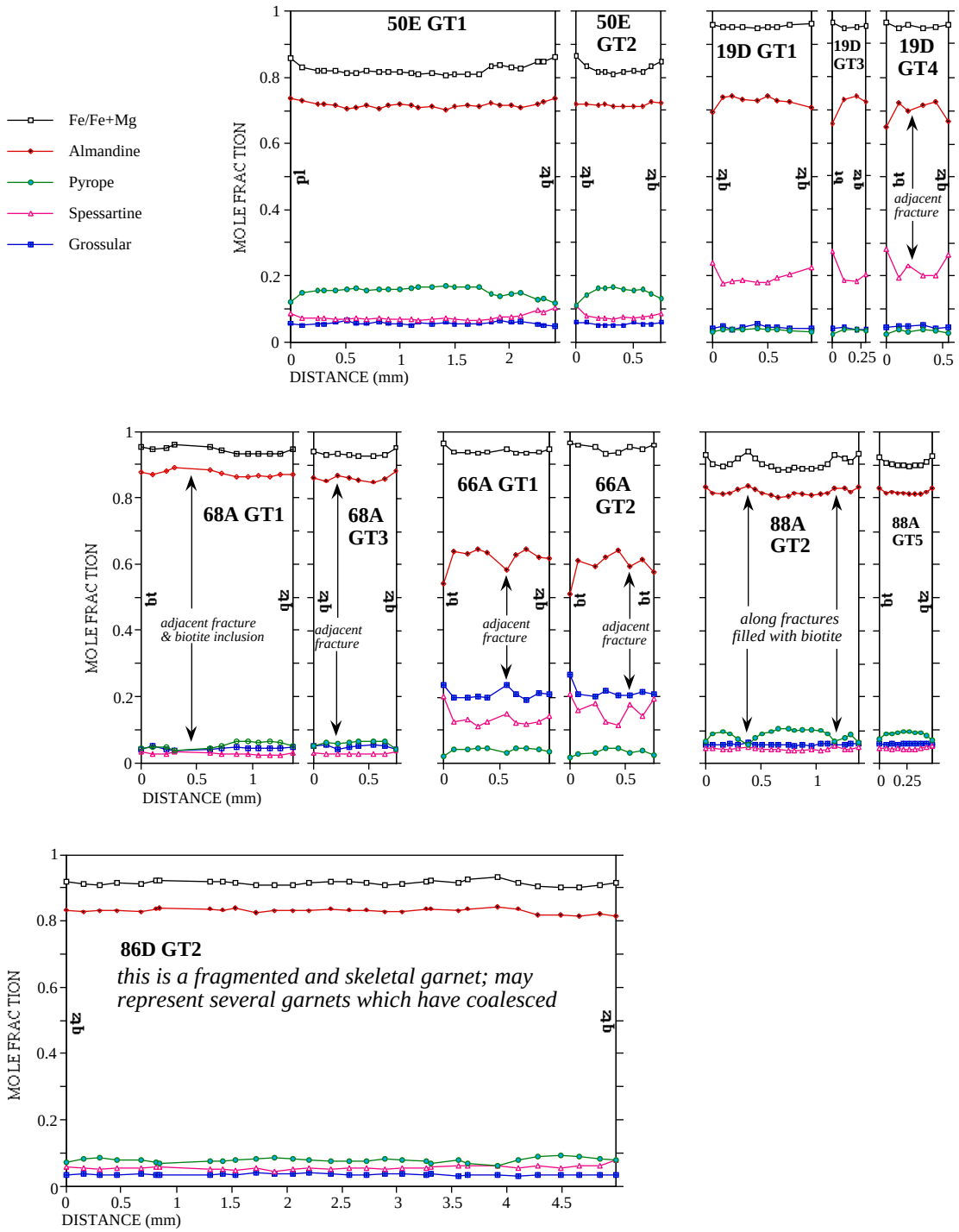

* mineral abbreviations indicate minerals in contact with the garnet rim at the traverse endpoints (qtz=quartz, pl=plagioclase, bt=biotite, crd=cordierite, hole=plucked portion of the thin section).

Representative Garnet Profiles for Pelites and Semi-Pelites* *(continued)*

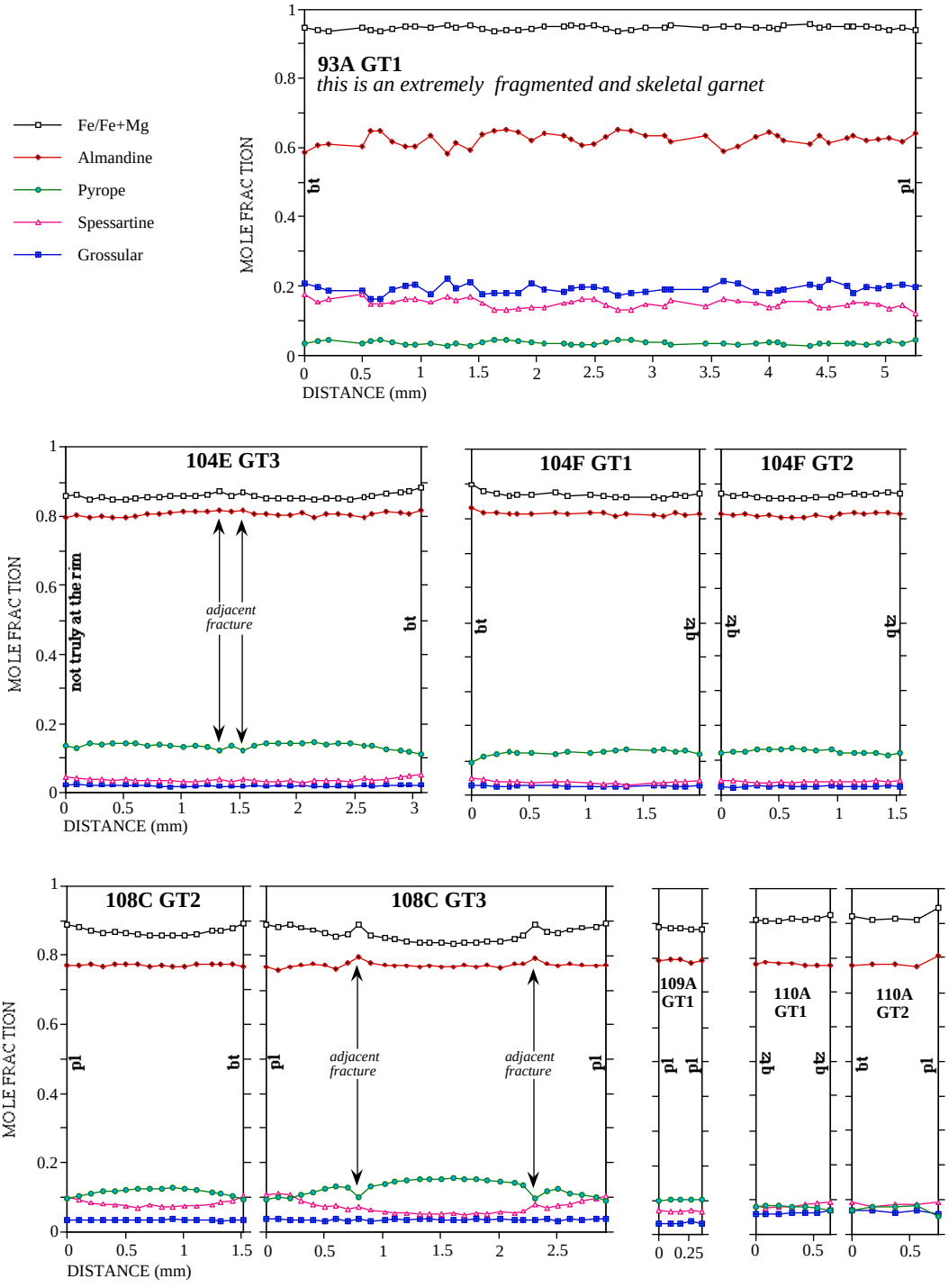

* mineral abbreviations indicate minerals in contact with the garnet rim at the traverse endpoints (qtz=quartz, pl=plagioclase, bt=biotite, crd=cordierite, hole=plucked portion of the thin section).

Representative Garnet Profiles for Pelites and Semi-Pelites* *(continued)*

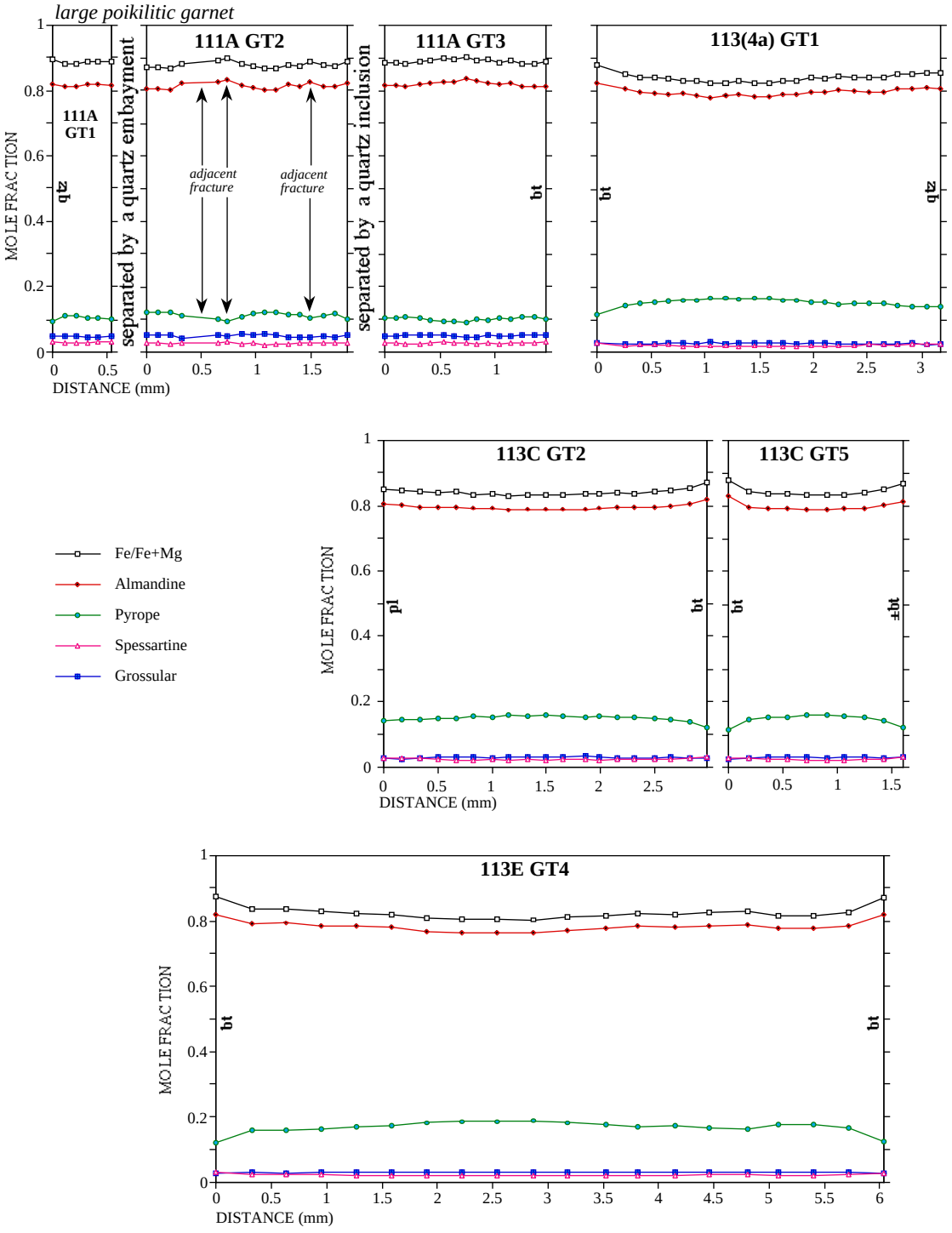

* mineral abbreviations indicate minerals in contact with the garnet rim at the traverse endpoints (qtz=quartz, pl=plagioclase, bt=biotite, crd=cordierite, hole=plucked portion of the thin section).

Representative Garnet Profiles for Pelites and Semi-Pelites* *(continued)*

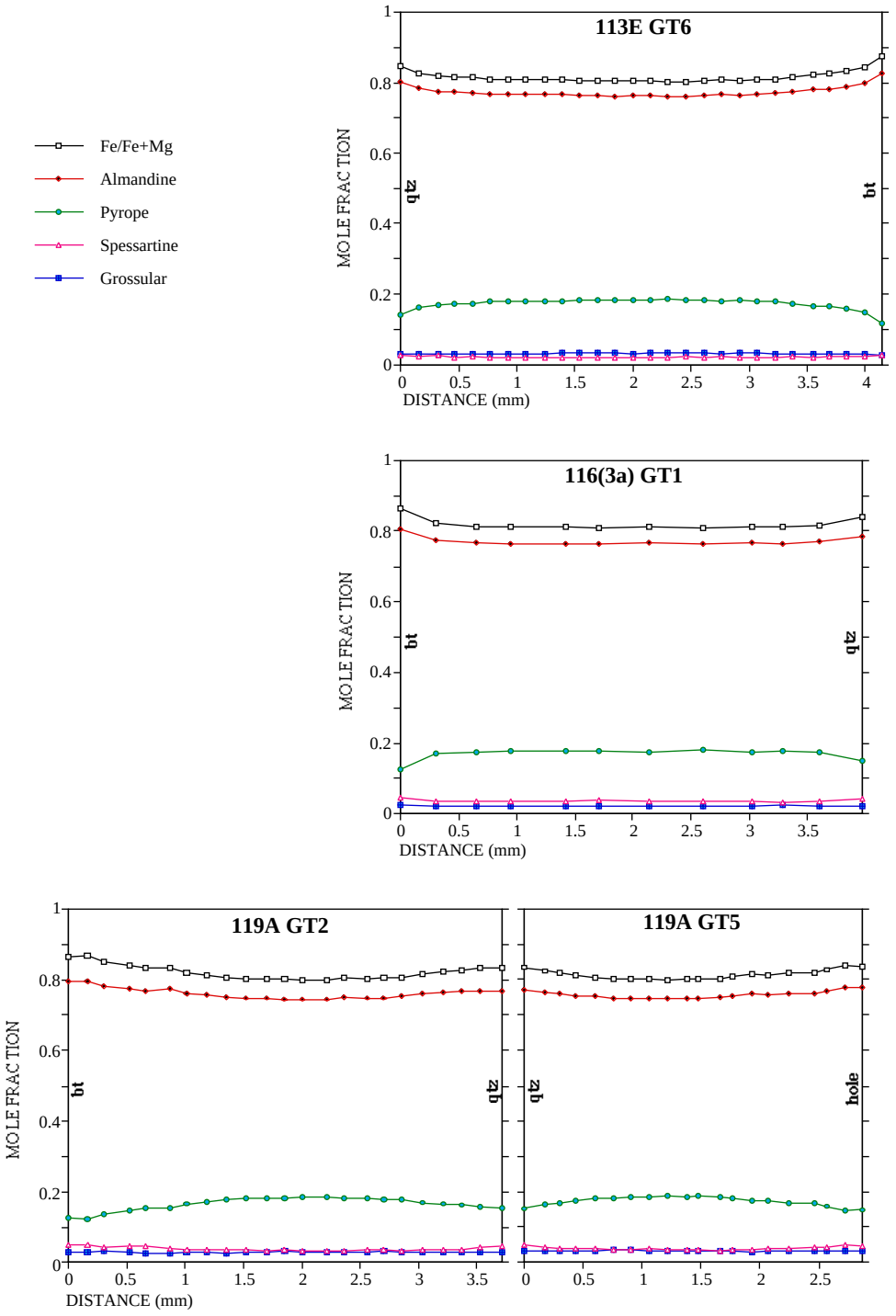

* mineral abbreviations indicate minerals in contact with the garnet rim at the traverse endpoints (qtz=quartz, pl=plagioclase, bt=biotite, crd=cordierite hole=plucked portion of the thin section).

Representative Garnet Profiles for Pelites and Semi-Pelites* *(continued)*

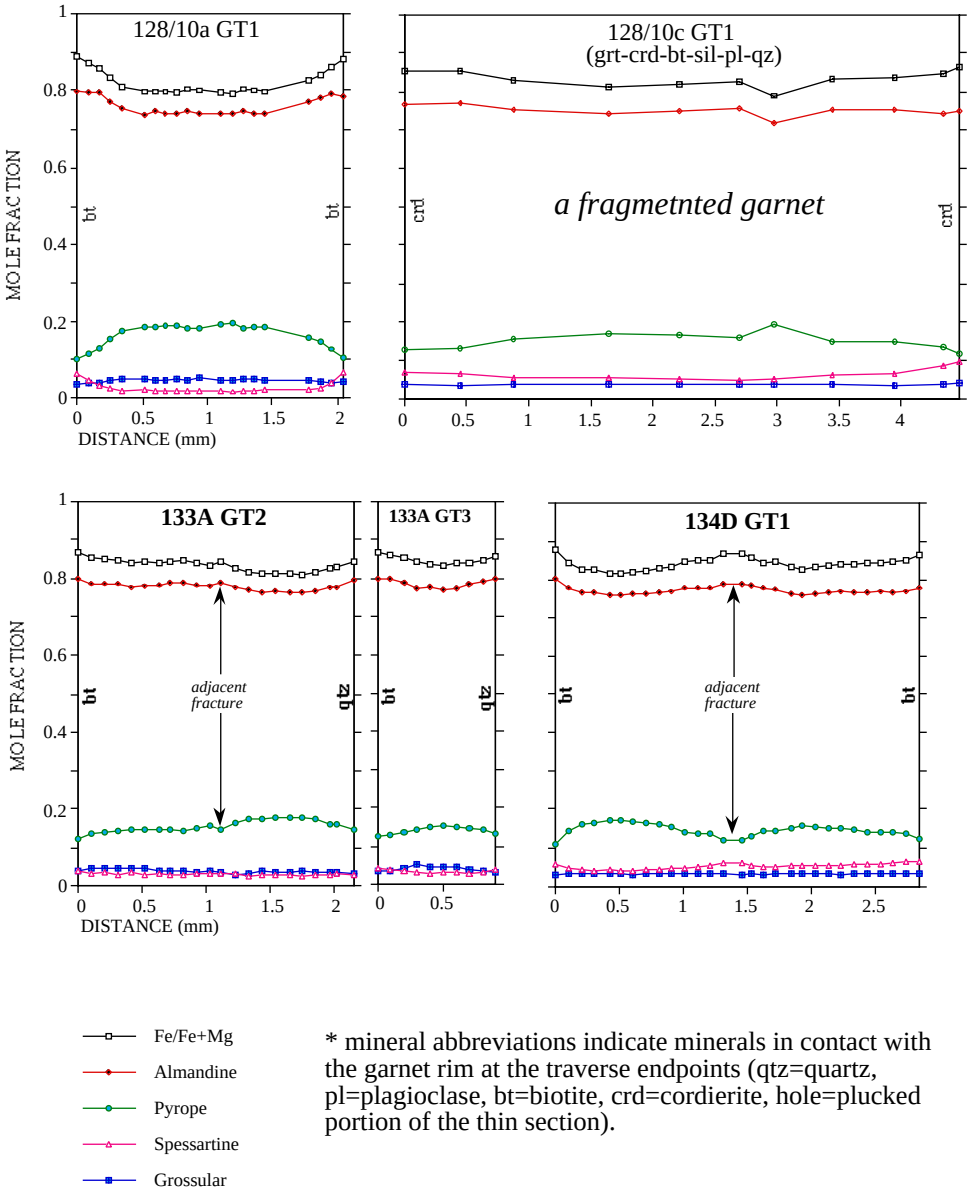

* mineral abbreviations indicate minerals in contact with the garnet rim at the traverse endpoints (qtz=quartz, pl=plagioclase, bt=biotite, crd=cordierite, hole=plucked portion of the thin section).

APPENDIX D

Garnet X-ray Images for Representative Samples*

Pelites and Semi-Pelites

PC-50E

PC-88A

PC-113C

PC-113E

PC-119A

Amphibolites

PC-80B

PC-107F

* Image processing performed using Image (version 1.47), produced by NIH for the Macintosh.

Figure D-1 False color representation of the distribution of Mg, Fe, Mn and Fe concentrations based on X-ray intensities for PC-50E; solid lines represent garnet traverses depicted in the profiles in Appendix C).

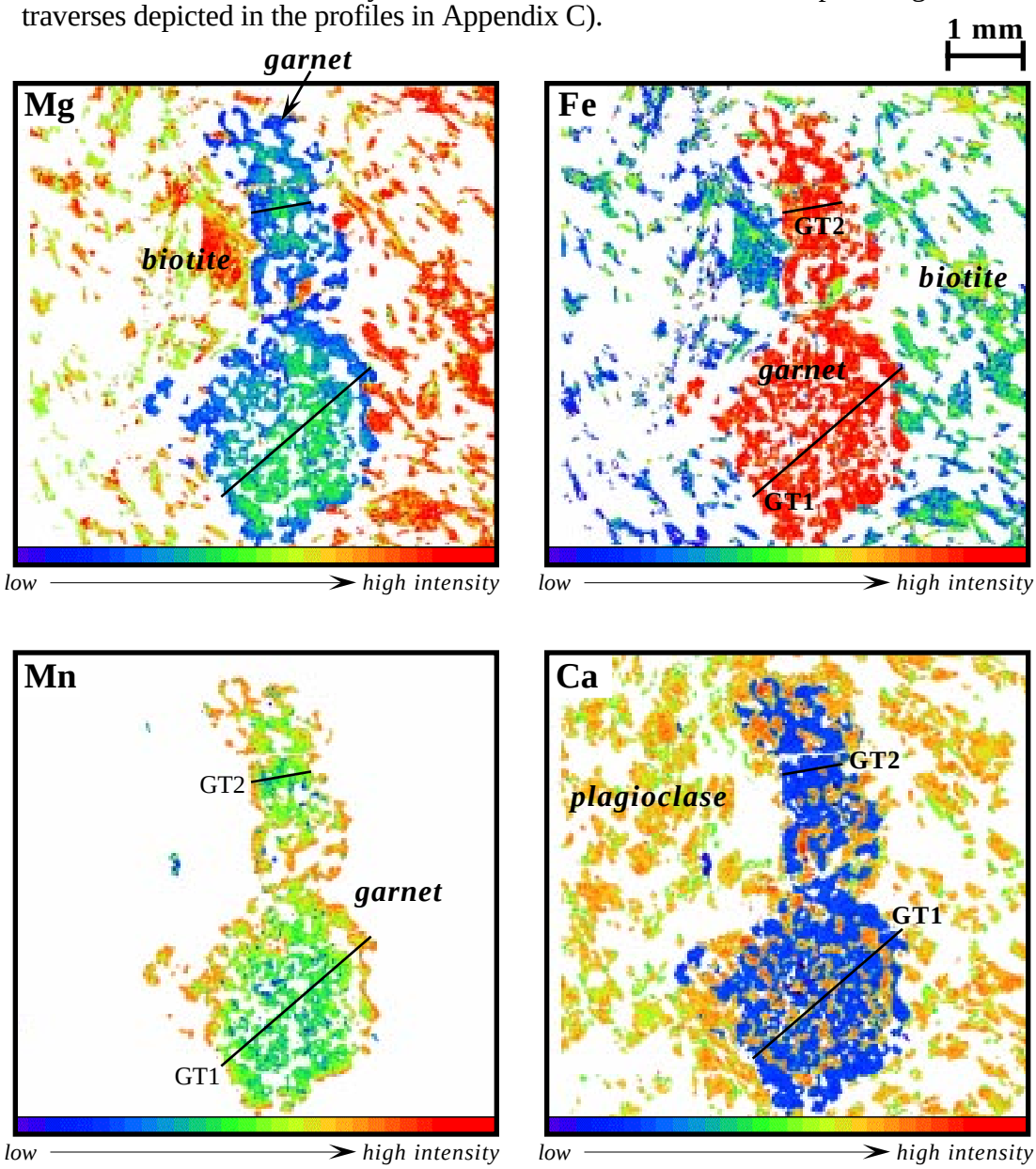

Figure D-2 False color representation of the distribution of Mg, Fe, Mn and Fe concentrations based on X-ray intensities for PC-88A; solid line represents a garnet traverse depicted in Appendix C).

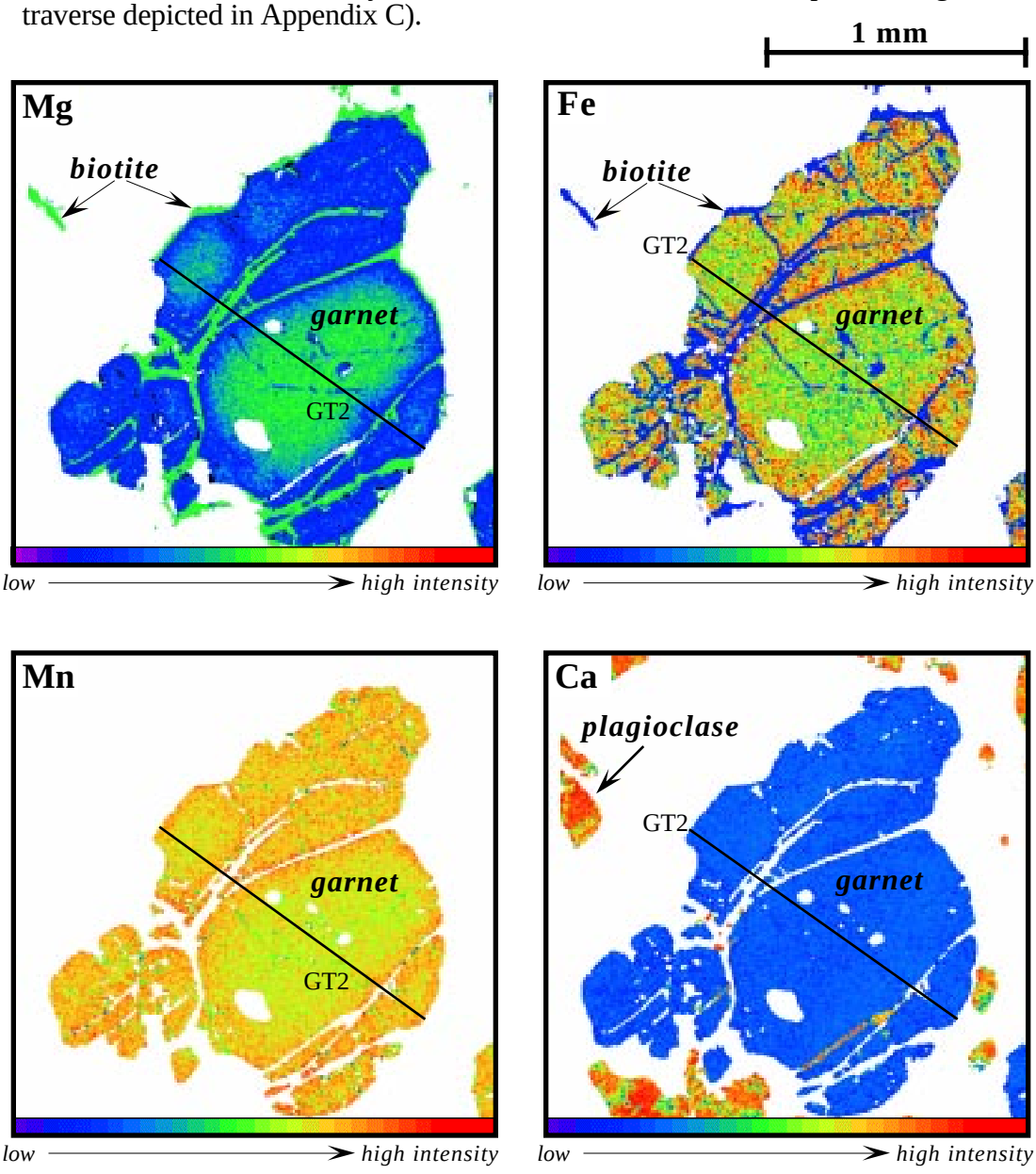

Figure D-3 False color representation of the distribution of Mg, Fe, Mn and Fe concentrations based on X-ray intensities for PC-113C; solid lines represent garnet traverses for profiles depicted in Appendix C).

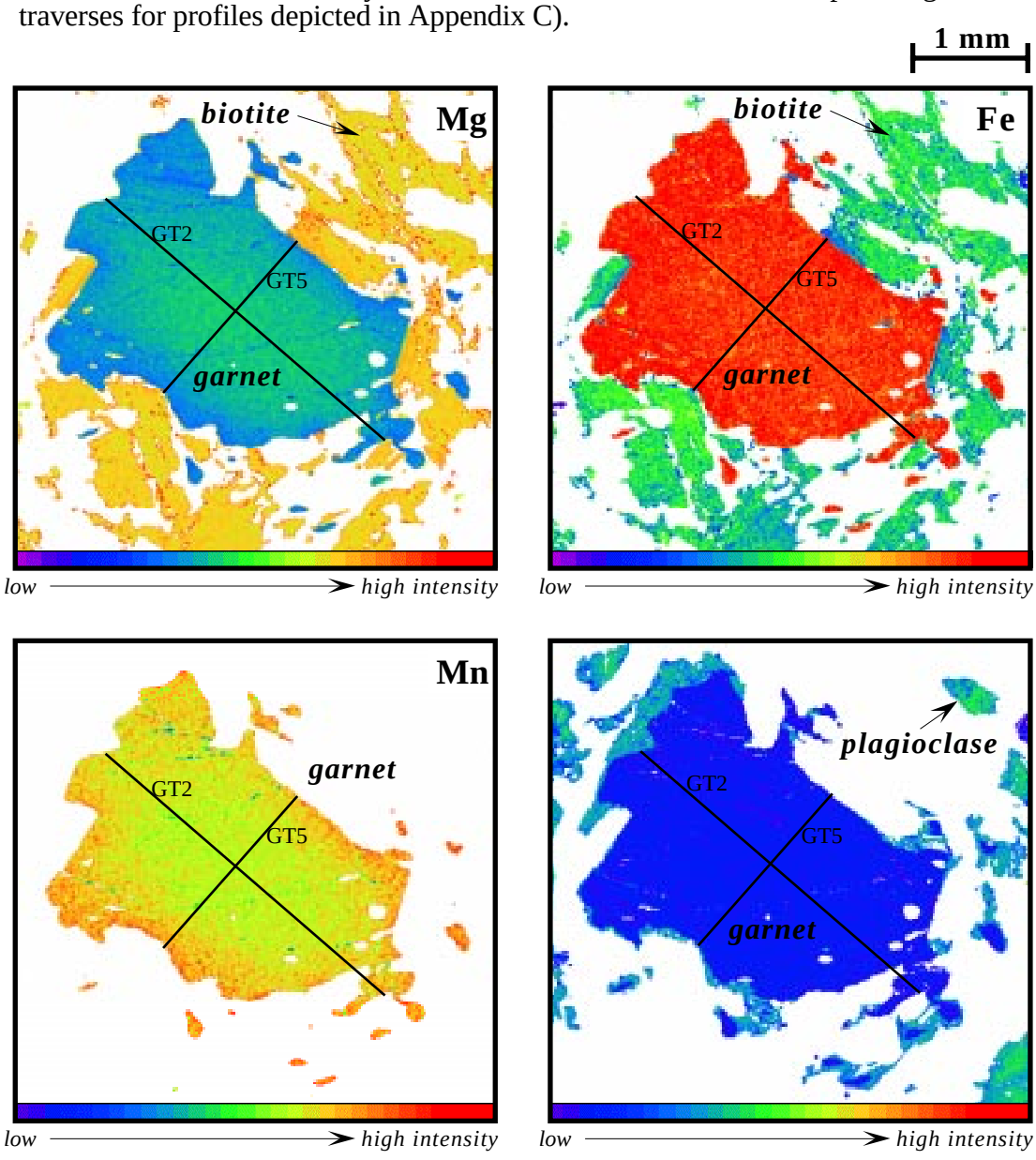

Figure D-4 False color representation of the distribution of Mg, Fe, Mn and Fe concentrations based on X-ray intensities for PC-113E; solid lines represent garnet traverses used to make the profiles in Appendix C).

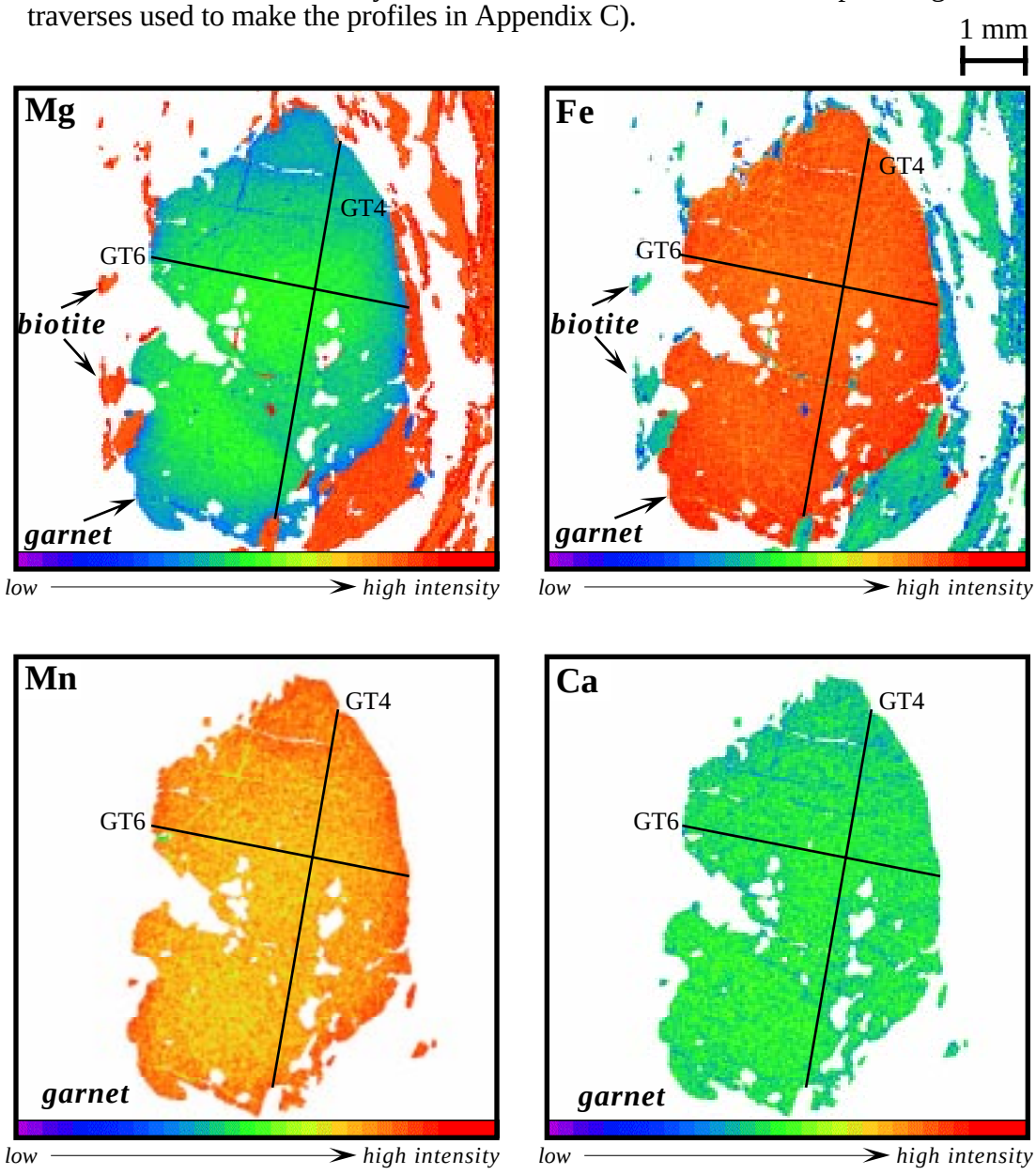

Figure D-5 False color representation of the distribution of Mg, Fe, Mn and Fe concentrations based on X-ray intensities for PC-119A; solid lines represent garnet traverses depicted in the profiles in Appendix C).

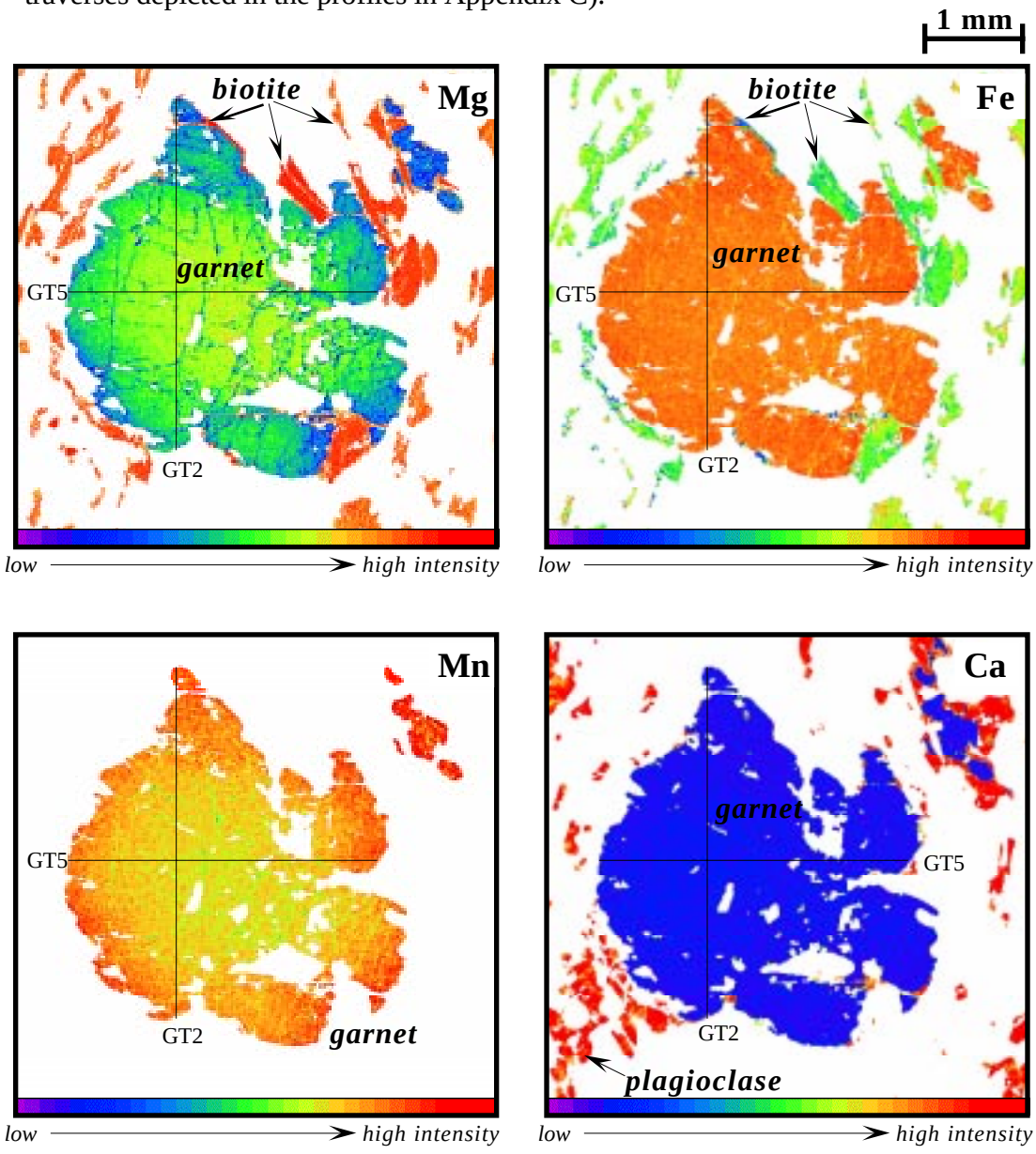

Figure D-6 False color representation of the distribution of Mg, Fe, Mn and Fe concentrations based on X-ray intensities for PC-80B; solid line represents garnet traverse presented in figure 53.

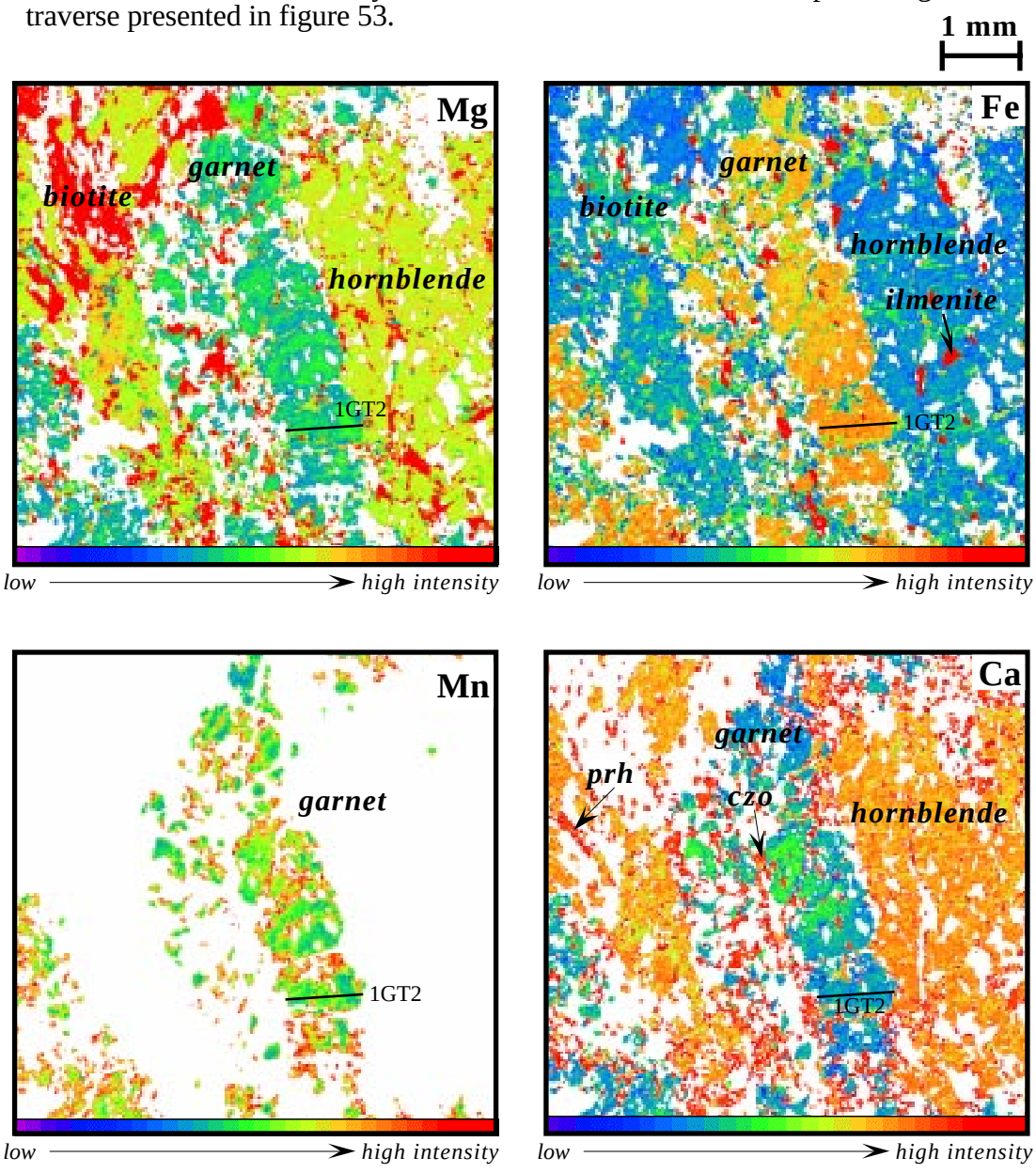

NOTE: the red-colored phases are either prehnite (prh), clinozoisite (czo), or apatite.

Figure D-7 False color representation of the distribution of Mg, Fe, Mn and Fe concentrations based on X-ray intensities for PC-107F; solid lines represent garnet traverses used to make the profiles in figure 53.

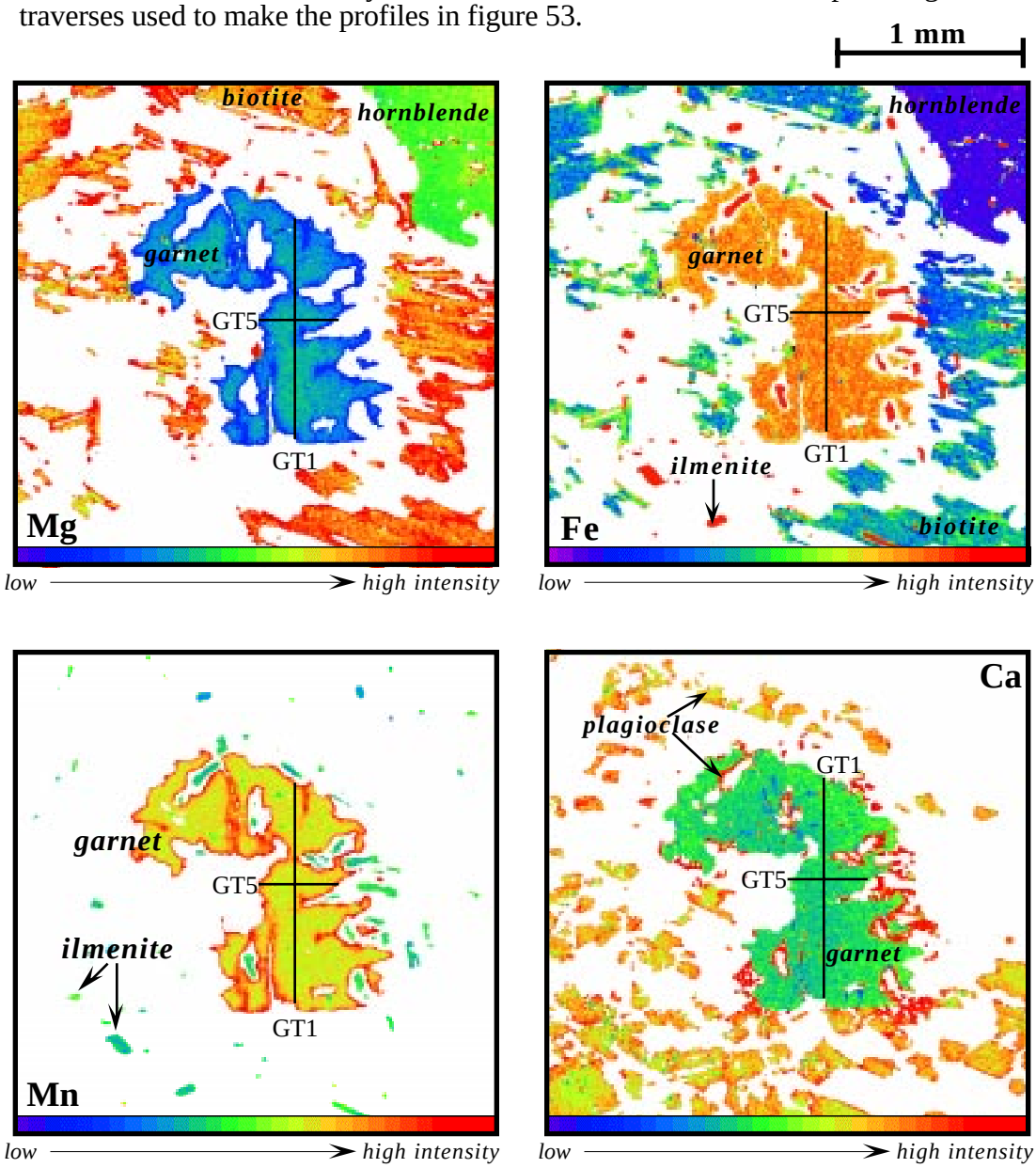

APPENDIX E

Compositions used for thermobarometry

APPENDIX E: Compositions Used for Thermobarometry for Each Sample

Sample #	garnet diameter	garnet choice	biotite choice	plagioclase choice	hbl choice	crd choice
50E	2.5 mm	near rim *GT1b,v,2b,i*	matrix *B1b,3*	interior, matrix *P19c,21b,22b,23*		
19D	1 mm	interior *GT1e*	left side matrix *B9,10,11*	interior, left side matrix *P4b,c*		
68A	1 mm	interior *GT1g,h,i,j,3d,e,f*	matrix *B6,7,8,9,10*	rim, matrix *P1b,2b,3b*		
66A	1-1.5 mm	interior *GT1c,d,h,2d,e*	matrix *B3b,4a,b,c,7*	rim, matrix *P2a,3a,c*		
80B	5 mm	near rim *1GT2b,g*			s-surfaces, matrix *mH1,2*	
86D	*fragmented*	near rim *GT1b, c,as,av,2b,ab,ac*	matrix *B7,BT6a,b,c,d,c,f*	all matrix *PT6b,d,e,7a,c,d,e,8a,b*		
108C	1.5-3 mm	near rim *GT2b,2o,3d,3ab*	matrix *BT3c,4d,5a,6a*	interior, matrix *P1b,2b,3b,4b,c,5b*		
109A	0.5 mm	interior *GT1b,c,2b*	matrix *B2,3a,b,4a,5*	rim, matrix *P1a,d,3a,PT2a,c*		
110A	0.5 mm	interior *GT1b,c,d,e,2b,c,d*	matrix *B1,2a,b,3a,b,BT5b*	all matrix *P3a,b,4a,b, 5a,b,6a,b,c,d*		
88A	0.5-1.5mm	interior,leucosome *GT2j,k,l,m,n,o,3f →k,4f,g,h,5c→h*	host matrix *B14,16,17,BT7b,c, BT8a,c,e*	rim, host matrix *PT7a,8a*		
93A	*fragmented*	interior *GT1o,p,q*	matrix *B4a,b,c, 5,6,7,8,9,10*	interior, matrix *P1b,c 2b,c,3,4,5a,6b,7b,8b*		
104E	1.5-3 mm	near rim *GT2n,3b,c,ab,ac*	matrix *BT2a,b,c d,e,3a,b,c,4b*	rim, matrix *P1a,2a,PT1a,e,2a,c*		
104F	1.5-2 mm	interior *GT1h,i,j, k,l,2e,f,g,h,i*	matrix *BT2b,3b*	all matrix *P3a,b, PT1a,b,c,2a,b,c,d*		
107F	0.5-1 mm	interior *GT1b,c,d, e,f,g,i,5b,c,d,e*		interior, matrix *PT1c,2c*	matrix *H3,5*	
111A	4 mm	near rim *GT3n,4l*	matrix *B2a,b,3b,4b BT1a,b,c,d,e,2a,c,d*	interior, matrix *P1b,2b 3b,4b,PT2b,c,3b,4b,c*		
113/4a	3 mm	near rim *GT2,20*	matrix *B5,5a,6*	rim, matrix *f1,1c,2,3*		
113C	2-3 mm	near rim *GT1b,f, 2b,q,3b,h,4c,i,5b,i*	matrix *BT2a,3,3a, 4,4a,7,7a,b,B14,15*	rim, matrix *F1,1c,5*		
113E	4-7 mm	near rim *GT3i,as,4c,6b,aa*	matrix *B12,13,14, BT4b,5b,c,d,7a,b,c, d,e,8a,b,c,e*	rim, matrix *P7,PT1b,e*		
116/3a	4 mm	near rim *G4,13*	matrix *B3a,4a,5,5a*	rim, matrix *f4,4c,5*		
119A	2-4 mm	near rim *GT1b,f,2f v,3i,4f,5b,r,6b,j*	matrix *B11,12,13*	interior, matrix *mP3,4,8,9*		
128/10a	2 mm	near rim *GT3,24*	matrix *B7,7a,8,8a*	all matrix *P2,P3*		
128/10c	*fragmented*	interior *gar5,8,9,GT7*		interior, matrix *pl1a,2a,3a,b*		matrix *crd8,8a,b*
133a	2 mm	near rim *GT2b,3b,i*	matrix *B2b,BT2b,3b,c*	interior, matrix *P3b,c,4b,5b,6b,c*		
134D	3 mm	near rim *GT1b,ab,ac*	matrix *bt1,1a,3,4*	all matrix *f1,1a,b,c,2,2a*		

APPENDIX F

Pressure-Temperature Plots

APPENDIX F: Pressure-Temperature Plots

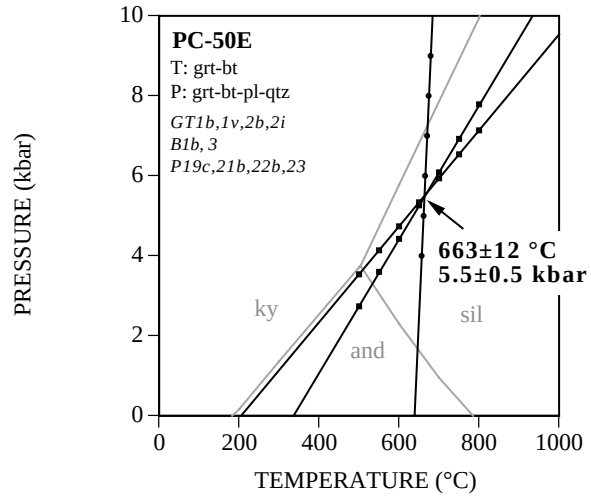

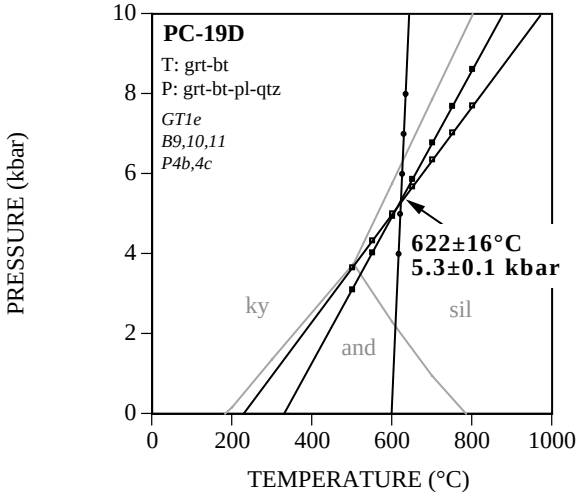

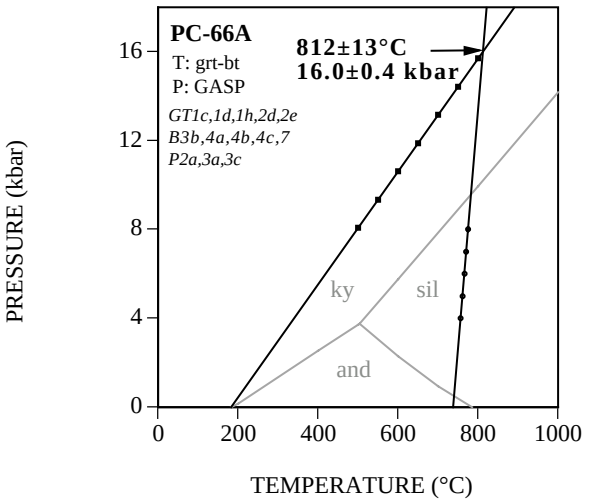

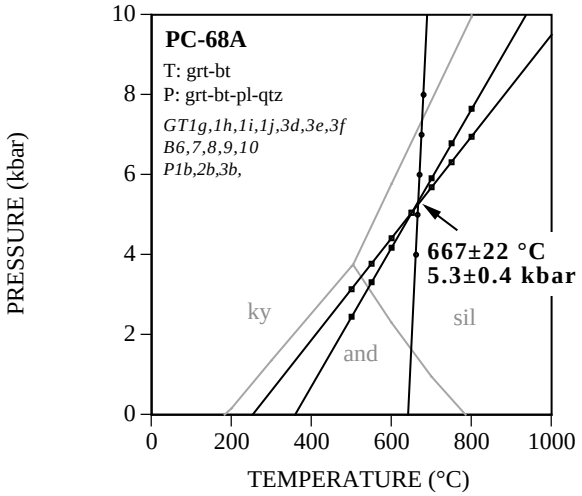

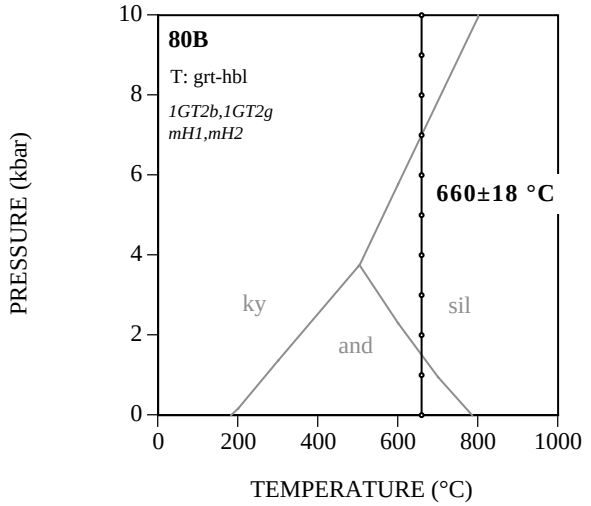

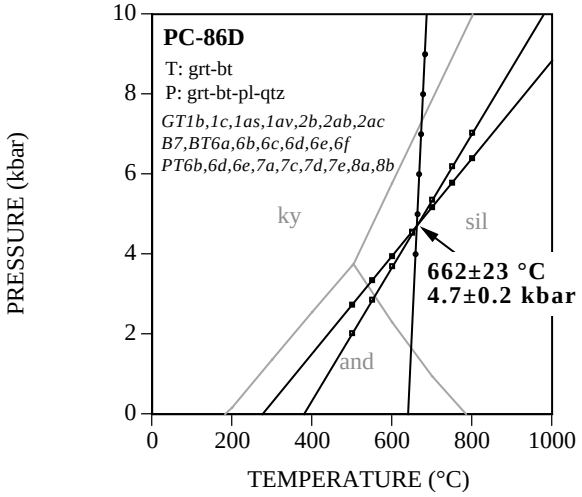

APPENDIX F: Pressure-Temperature Plots (continued)

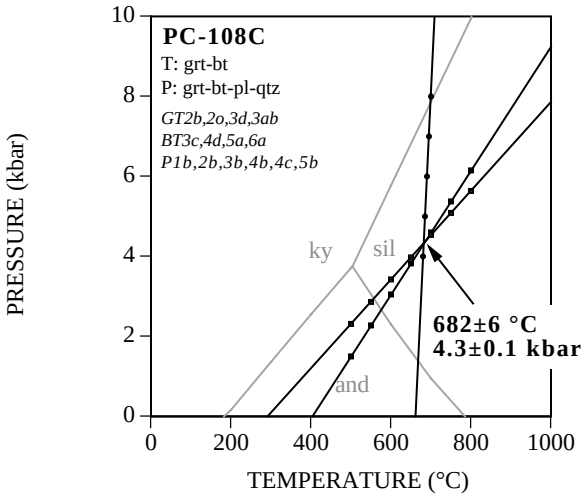

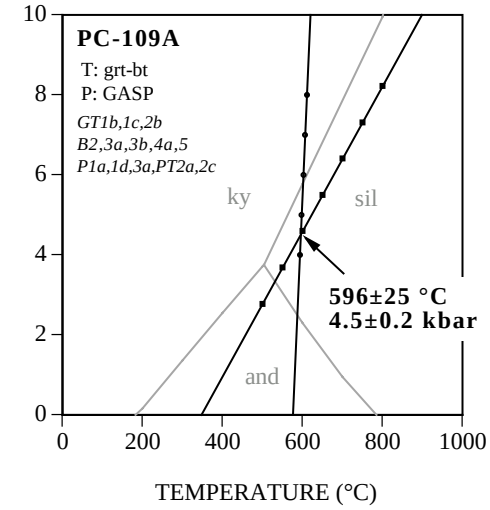

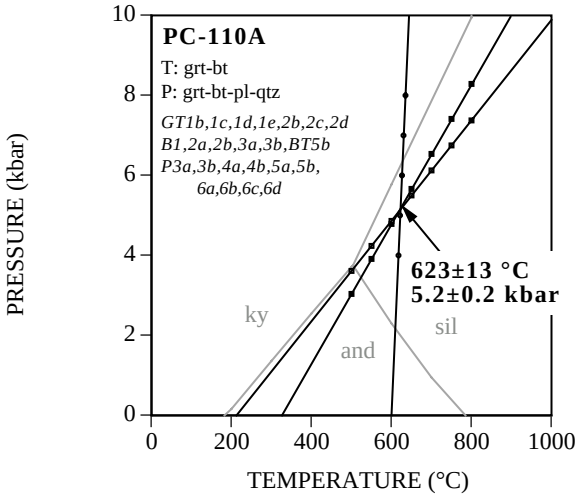

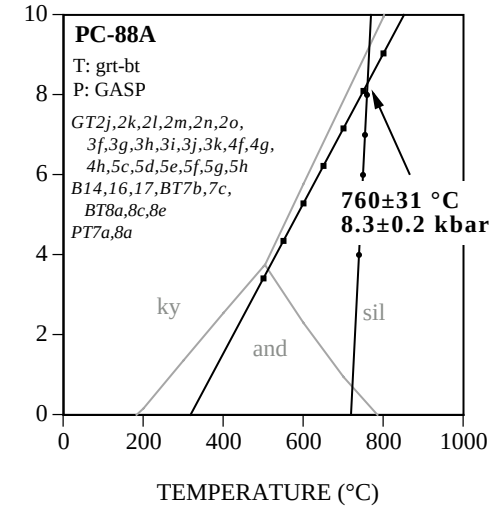

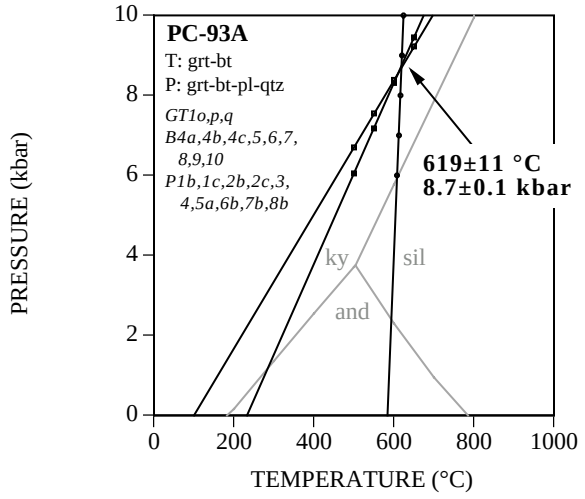

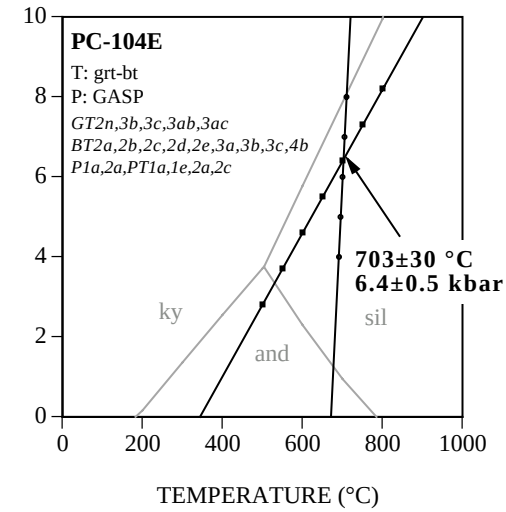

APPENDIX F: Pressure-Temperature Plots (continued)

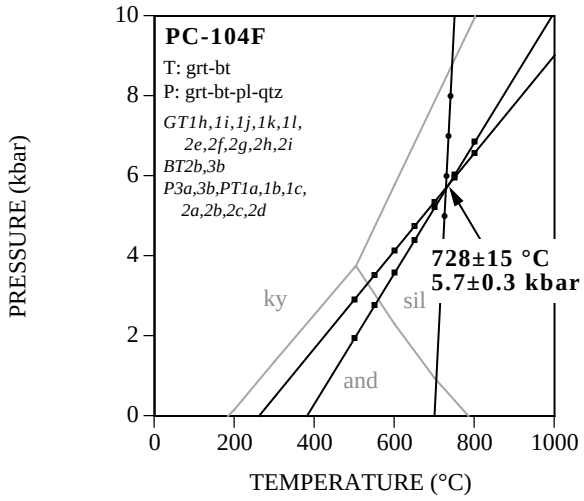

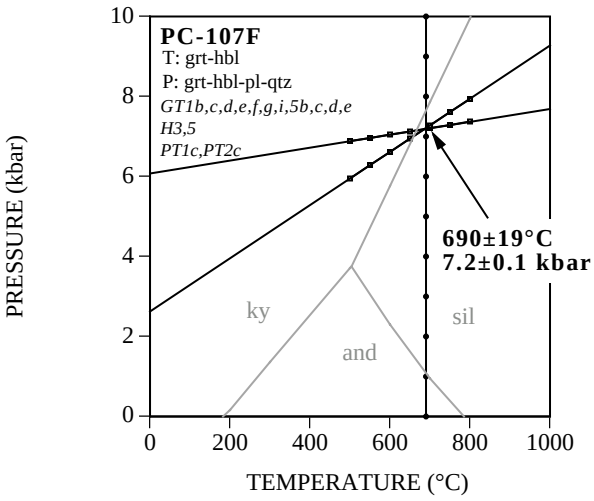

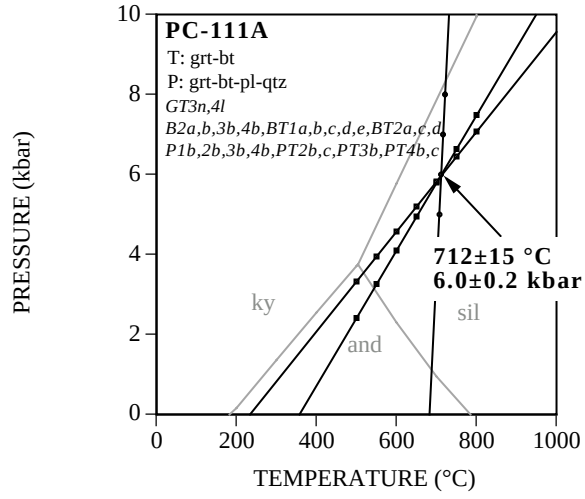

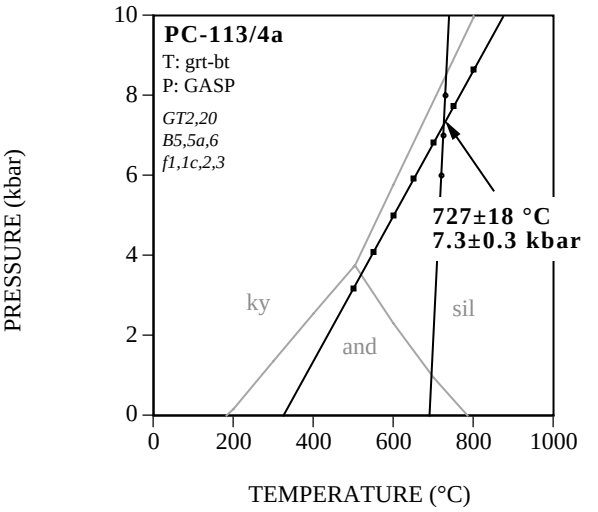

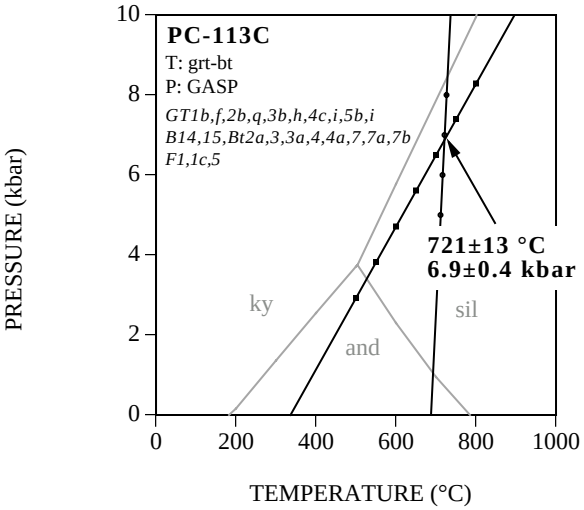

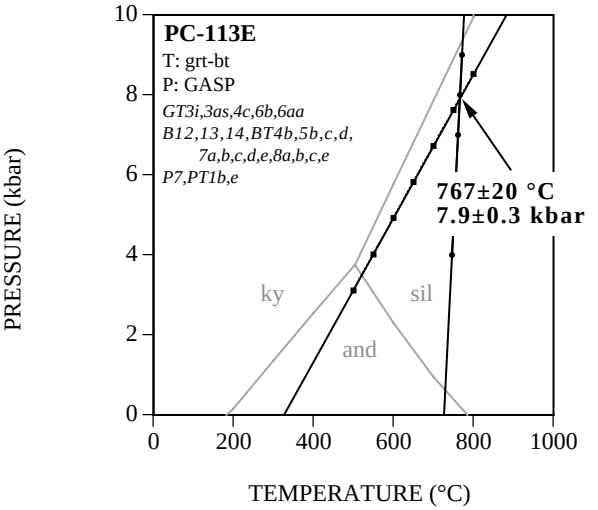

APPENDIX F: Pressure-Temperature Plots (continued)

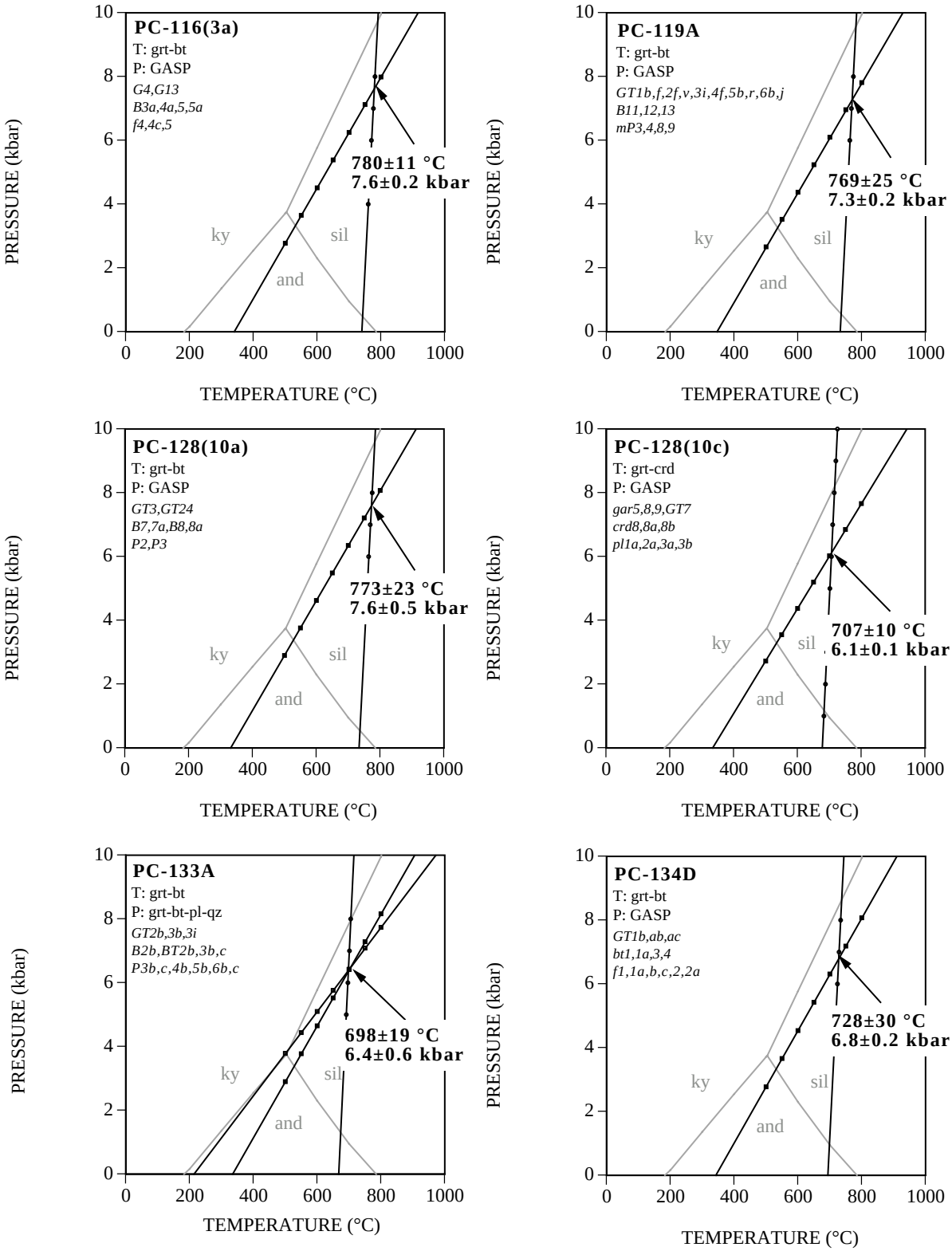

APPENDIX G

The Gibbs' Method Calculations

Appendix G: The Gibbs' Method Calculations

Refer to Spear et al. (1982) for a complete description of the Gibbs' Method

Question: **How does μ_{H_2O} vary as a function of x_{Fe} in outcrop 128?**

Three different pelitic assemblages are observed in this system:

128/10a: grt-bt-sil-qtz-pl-kfs
128/10b: crd-bt-sil-qtz-pl-*(kfs)*
128/10c: grt-crd-bt-sil-qtz-pl-*(kfs)*

There are six system components: K_2O-FeO-MgO-Al_2O_3-SiO_2-H_2O *(ignoring plagioclase)*

There are nine phase components:

garnet (grt)	Fe-grt	$Fe_3Al_2Si_3O_{12}$
	Mg-grt	$Mg_3Al_2Si_3O_{12}$
cordierite (crd)	Fe-crd	$Fe_2Al_4Si_5O_{18}\cdot 0.5H_2O$
	Mg-crd	$Mg_2Al_4Si_5O_{18}\cdot 0.5H_2O$
biotite (bt)	Fe-bt	$KFe_{2.5}Al_{0.5}(Al_{1.5}Si_{2.5}O_{10})(OH)_2$
	Mg-bt	$KMg_{2.5}Al_{0.5}(Al_{1.5}Si_{2.5}O_{10})(OH)_2$
k-feldspar	kfs	$KAlSi_3O_8$
sillimanite	sil	Al_2SiO_5
quartz	qtz	SiO_2

The Gibbs-Duhem equation describes the conditions of homogeneous equilibrium within each phase. There are 6 equations of homogeneous equilibrium for this system:

$$0 = \overline{S}^{grt}dT - \overline{V}^{grt}dP + x^{grt}_{Fe}d\mu^{grt}_{Fe} + x^{grt}_{Mg}d\mu^{grt}_{Mg}$$

$$0 = \overline{S}^{crd}dT - \overline{V}^{crd}dP + x^{crd}_{Fe}d\mu^{crd}_{Fe} + x^{crd}_{Mg}d\mu^{crd}_{Mg}$$

$$0 = \overline{S}^{bt}dT - \overline{V}^{bt}dP + x^{bt}_{Fe}d\mu^{bt}_{Fe} + x^{bt}_{Mg}d\mu^{bt}_{Mg}$$

$$0 = \overline{S}^{kfs}dT - \overline{V}^{kfs}dP + d\mu^{kfs}$$

$$0 = \overline{S}^{sil}dT - \overline{V}^{sil}dP + d\mu^{sil}$$

$$0 = \overline{S}^{qtz}dT - \overline{V}^{qtz}dP + d\mu^{qtz}$$

The number of equations (n) needed to describe the heterogeneous equilibrium is given as: the phase components less the system components. For this system n = 9 - 6, or n = 3.

The 3 equations that describe the heterogeneous equilibria are:

$$0 = 5d\mu_{Fe}^{grt} + 6d\mu_{Mg}^{bt} - 5d\mu_{Mg}^{grt} - 6d\mu_{Fe}^{bt}$$

$$0 = 2d\mu_{Fe}^{grt} + 3d\mu_{Mg}^{crd} - 2d\mu_{Mg}^{grt} - 3d\mu_{Fe}^{crd}$$

$$0 = 5d\mu_{Fe}^{crd} + 4d\mu_{Mg}^{bt} - 5d\mu_{Mg}^{crd} - 4d\mu_{Fe}^{bt}$$

Three reactions were chosen to describe the assemblages observed in each of the 3 pelitic samples from outcrop 128.

Divariant reactions:

1. 128/10a: *2sillimanite + 6biotite + 16quartz → 5garnet + 6K-feldspar + 6H_2O*

2. 128/10b: *16sillimanite + 8biotite + 38quartz → 10cordierite + 8K-feldspar + 3H_2O*

Univariant reaction:

3. 128/10c:

4sillimanite + 4biotite + 14quartz → 2garnet + 2cordierite + 4K-feldspar +3H_2O

The equations (in terms of μ_{Fe} and μ_{H2O}) associated with each of these reactions are:

$$0 = 2d\mu^{sil} + 6d\mu_{Fe}^{bt} + 16d\mu^{qtz} - 5d\mu_{Fe}^{grt} - 6d\mu^{kfs} - 6d\mu_{H2O}$$

$$0 = 16\mu^{sil} + 8d\mu_{Fe}^{bt} + 38d\mu^{qtz} - 10d\mu_{Fe}^{crd} - 8d\mu^{kfs} - 3d\mu_{H2O}$$

$$0 = 4d\mu^{sil} + 4d\mu_{Fe}^{bt} + 14d\mu^{qtz} - 2\mu_{Fe}^{grt} - 2d\mu_{Fe}^{crd} - 4d\mu^{kfs} - 3d\mu_{H2O}$$

Reaction 1 - ***Sample 128/10a***

2sillimanite + 6biotite + 16quartz → 5garnet + 6K-feldspar + 6H_2O

Reaction 1 describes how the grt-sil-bt field shifts in X_{Fe} with changing P,T, and μ_{H2O}; X_{Fe} in garnet is chosen to monitor changes in μ_{H2O}. For garnet, μ_{Fe}- μ_{Mg} is the slope of the tangent to the free energy surface (G-surface) of garnet. The total differential of this slope as a function of P,T, and X_{Fe} gives the change of the slope as it pivots around the G–surface with changing μ_{H2O}, as follows.

$$d(\mu_{Fe}^{grt} - \mu_{Mg}^{grt}) = \left[\frac{\delta(\mu_{Fe}^{grt} - \mu_{Mg}^{grt})}{\delta T}\right]_{P,x_{Fe}^{Grt}} dT + \left[\frac{\delta(\mu_{Fe}^{grt} - \mu_{Mg}^{grt})}{\delta P}\right]_{T,x_{Fe}^{Grt}} dP + \left[\frac{\delta(\mu_{Fe}^{grt} - \mu_{Mg}^{grt})}{\delta x_{Fe}^{Grt}}\right]_{P,T} dx_{Fe}^{grt}$$

From thermodynamics:

$$-\overline{S}_i = \left[\frac{\delta \mu_i}{\delta T}\right]_{P,x}; \quad \overline{V}_i = \left[\frac{\delta \mu_i}{\delta P}\right]_{T,x}; \text{ and } (\mu_{Fe}^{grt} - \mu_{Mg}^{grt})_{P,T} = \left[\frac{\delta \overline{G}^{grt}}{\delta x_{Fe}^{grt}}\right]_{P,T}$$

where: $\overline{G}$ = molar Gibbs Free Energy

$\overline{S}$ = molar entropy

$\overline{V}$ = molar volume

T = temperature

P = pressure

μ = chemical potential

Make the appropriate substitutions:

$$d(\mu_{Fe}^{grt} - \mu_{Mg}^{grt}) = -(\overline{S}_{Fe}^{grt} - \overline{S}_{Mg}^{grt})dT + (\overline{V}_{Fe}^{grt} - \overline{V}_{Mg}^{grt})dP + \left[\frac{\delta^2 \overline{G}^{grt}}{\delta (x_{Fe}^{grt})^2}\right]_{P,T} dx_{Fe}^{grt}$$

Set this equation equal to zero:

$$0 = -(\overline{S}_{Fe}^{grt} - \overline{S}_{Mg}^{grt})dT + (\overline{V}_{Fe}^{grt} - \overline{V}_{Mg}^{grt})dP - d\mu_{Fe}^{grt} + d\mu_{Mg}^{grt} + \left[\frac{\delta^2 \overline{G}^{grt}}{\delta (x_{Fe}^{grt})^2}\right]_{P,T} dx_{Fe}^{grt}$$

Put the equations for reaction 1 (including the homogeneous and heterogeneous equilibria) into matrix form:

$$\begin{bmatrix}
\overline{S}^{grt} & -\overline{V}^{grt} & x_{Fe}^{grt} & x_{Mg}^{grt} & 0 & 0 & 0 & 0 & 0 & 0 & 0 \\
\overline{S}^{bt} & -\overline{V}^{bt} & 0 & 0 & x_{Fe}^{bt} & x_{Mg}^{bt} & 0 & 0 & 0 & 0 & 0 \\
\overline{S}^{kfs} & -\overline{V}^{kfs} & 0 & 0 & 0 & 0 & 1 & 0 & 0 & 0 & 0 \\
\overline{S}^{sil} & -\overline{V}^{sil} & 0 & 0 & 0 & 0 & 0 & 1 & 0 & 0 & 0 \\
\overline{S}^{qtz} & -\overline{V}^{qtz} & 0 & 0 & 0 & 0 & 0 & 0 & 1 & 0 & 0 \\
0 & 0 & 5 & -5 & -6 & 6 & 0 & 0 & 0 & 0 & 0 \\
0 & 0 & -5 & 0 & 6 & 0 & -6 & 2 & 16 & -6 & 0 \\
-(\overline{S}_{Fe}^{grt} - \overline{S}_{Mg}^{grt}) & (\overline{V}_{Fe}^{grt} - \overline{V}_{Mg}^{grt}) & -1 & 1 & 0 & 0 & 0 & 0 & 0 & 0 & \frac{\delta^2 \overline{G}^{grt}}{\delta (x_{Fe}^{grt})^2}
\end{bmatrix} \cdot \begin{bmatrix}
dT \\ dP \\ d\mu_{Fe}^{grt} \\ d\mu_{Mg}^{grt} \\ d\mu_{Fe}^{bt} \\ d\mu_{Mg}^{bt} \\ d\mu^{kfs} \\ d\mu^{kfs} \\ d\mu^{qtz} \\ d\mu_{H2O} \\ x_{Fe}^{grt}
\end{bmatrix} = \begin{bmatrix} 0 \\ 0 \\ 0 \\ 0 \\ 0 \\ 0 \\ 0 \\ 0 \end{bmatrix}$$

To solve for $\left[\frac{d\mu_{H2O}}{dx_{Fe}^{grt}}\right]_{P,T}$, hold P and T constant ($dP = dT = 0$) and divide through by dx_{Fe}^{grt}:

$$\begin{bmatrix} x_{Fe}^{grt} & x_{Mg}^{grt} & 0 & 0 & 0 & 0 & 0 & 0 \\ 0 & 0 & x_{Fe}^{bt} & x_{Mg}^{bt} & 0 & 0 & 0 & 0 \\ 0 & 0 & 0 & 0 & 1 & 0 & 0 & 0 \\ 0 & 0 & 0 & 0 & 0 & 1 & 0 & 0 \\ 0 & 0 & 0 & 0 & 0 & 0 & 1 & 0 \\ 5 & -5 & -6 & 6 & 0 & 0 & 0 & 0 \\ -5 & 0 & 6 & 0 & -6 & 2 & 16 & -6 \\ -1 & 1 & 0 & 0 & 0 & 0 & 0 & 0 \end{bmatrix} \cdot \begin{bmatrix} d\mu_{Fe}^{grt}/dx_{Fe}^{grt} \\ d\mu_{Mg}^{grt}/dx_{Fe}^{grt} \\ d\mu_{Fe}^{bt}/dx_{Fe}^{grt} \\ d\mu_{Mg}^{bt}/dx_{Fe}^{grt} \\ d\mu^{kfs}/dx_{Fe}^{grt} \\ d\mu^{sil}/dx_{Fe}^{grt} \\ d\mu^{qtz}/dx_{Fe}^{grt} \\ d\mu_{H2O}/dx_{Fe}^{grt} \end{bmatrix} = \begin{bmatrix} 0 \\ 0 \\ 0 \\ 0 \\ 0 \\ 0 \\ 0 \\ -\left[\delta^2 \overline{G}^{grt}/\delta(x_{Fe}^{grt})^2\right]_{P,T} \end{bmatrix}$$

This equation written in matrix notation is: $\mathbf{M} \cdot \mathbf{X} = \mathbf{Y}$

To solve for **X** simply calculate the appropriate values for x_{Fe}^{grt}, x_{Mg}^{grt}, x_{Fe}^{bt}, and x_{Mg}^{bt}, invert **M** and multiply: $\mathbf{X} = \mathbf{M}^{-1} \cdot \mathbf{Y}$.

<u>Calculating the appropriate x(Fe,Mg) for co-existing garnet and biotite</u>:

Use the Fe/(Fe+Mg) ratios derived from microprobe analysis to calculate the equilibrium constant (K_D) for peak metamorphic garnet-biotite pairs:

$$\mathbf{K_D} = \frac{[\mathbf{Fe}/(\mathbf{Fe}+\mathbf{Mg})]^{\mathbf{grt}}(\mathbf{Mg}/(\mathbf{Fe}+\mathbf{Mg})]^{\mathbf{bt}}}{[\mathbf{Mg}/(\mathbf{Fe}+\mathbf{Mg})]^{\mathbf{grt}}[\mathbf{Fe}/(\mathbf{Fe}+\mathbf{Mg})]^{\mathbf{bt}}} = \frac{(x_{Fe}^{grt})(x_{Mg}^{bt})}{(x_{Mg}^{grt})(x_{Fe}^{bt})} = \frac{(x_{Fe}^{grt})(1-x_{Fe}^{bt})}{(x_{Mg}^{grt})(x_{Fe}^{bt})} = \frac{x_{Fe}^{grt}}{x_{Mg}^{grt}}\left[\frac{1}{x_{Fe}^{bt}} - 1\right]$$

$$K_D + \frac{x_{Fe}^{grt}}{x_{Mg}^{grt}} = \frac{x_{Fe}^{grt}}{x_{Mg}^{grt}}\left[\frac{1}{x_{Fe}^{bt}}\right] \quad \text{and} \quad x_{Fe}^{bt}\left[\frac{K_D(x_{Mg}^{grt}) + x_{Fe}^{grt}}{x_{Mg}^{grt}}\right] = \frac{x_{Fe}^{grt}}{x_{Mg}^{grt}}$$

$$\mathbf{x_{Fe}^{bt}} = \frac{x_{Fe}^{grt}}{x_{Mg}^{grt}}\left[\frac{x_{Mg}^{grt}}{K_D(x_{Mg}^{grt}) + x_{Fe}^{grt}}\right] = \frac{x_{Fe}^{grt}}{K_D(1-x_{Fe}^{grt}) + x_{Fe}^{grt}} = \frac{\mathbf{x_{Fe}^{grt}}}{\mathbf{K_D} - (\mathbf{K_D}-1)\mathbf{x_{Fe}^{grt}}}$$

Using the K_D, calculate x_{Fe}^{bt} for a series of x_{Fe}^{grt}; $x_{Mg}^{grt} = (1 - x_{Fe}^{grt})$ and $x_{Mg}^{bt} = (1 - x_{Fe}^{bt})$.

Average approximate "peak" Fe/(Fe+Mg) ratios for sample 128/10a:

- garnet just in from the rim (3T and 24T) $\rightarrow$ **0.860**
- matrix biotite (B7,B7a,B8 and B8a) $\rightarrow$ **0.579**

$\mathbf{K_D}$ = (0.860)(0.421)/(0.140)(0.579) = **4.467**

$$x_{Fe}^{bt} = \frac{x_{Fe}^{grt}}{(4.467 - 3.467 x_{Fe}^{grt})}$$

Construct a table for x(Mg,Fe) values:

xFe,grt	**xMg,grt**	**xFe,bt**	**xMg,bt**
0.010	0.990	0.002	0.998
0.100	0.900	0.024	0.976
0.200	0.800	0.053	0.947
0.300	0.700	0.088	0.912
0.400	0.600	0.130	0.870
0.500	0.500	0.183	0.817
0.600	0.400	0.251	0.749
0.700	0.300	0.343	0.657
0.800	0.200	0.472	0.528
0.900	0.100	0.668	0.332
0.990	0.010	0.957	0.043

Place each set of x(Fe,Mg) values in the matrix, M; invert and multiply. The resultant equation is:

$$\left[\frac{d\mu_{H2O}}{dx_{Fe}^{grt}}\right] = a\left[-\frac{\delta^2 \overline{G}}{\delta(x_{Fe}^{grt})^2}\right]_{P,T}$$ where **a** is obtained from the matrix inversion.

To evaluate $\left[\frac{\delta^2 \overline{G}}{\delta(x_{Fe}^{grt})^2}\right]_{P,T}$ assume ideal solution in garnet.

$G^{grt} = G^\circ + \Delta G_{mixing}$

G° = standard state = $x_{Fe}^{grt}\mu_{Fe}^{o} + x_{Mg}^{grt}\mu_{Mg}^{o}$

$\Delta G_{mixing} = RT[\, x_{Fe}^{grt} \ln(x_{Fe}^{grt})^3 + x_{Mg}^{grt} \ln(x_{Mg}^{grt})^3\,]$; multiplicity = 3 for $(Fe,Mg)_3Al_2Si_3O_{12}$

Substitution:

$$\overline{G}^{grt} = \left[x_{Fe}^{grt}\mu^{o}_{Fe} + (1 - x_{Fe}^{grt})\mu^{o}_{Mg} \right] + RT\left[x_{Fe}^{grt}\ln(x_{Fe}^{grt})^3 + (1 - x_{Fe}^{grt})\ln(1 - x_{Fe}^{grt})^3 \right]$$

Take the derivative, holding pressure and temperature constant:

$$\left[\frac{\delta\,\overline{G}^{grt}}{\delta\, x_{Fe}^{grt}}\right]_{P,T} = \mu^{o}_{Fe} - \mu^{o}_{Mg} + RT\left[x_{Fe}^{grt}\cdot\frac{3(x_{Fe}^{grt})^2}{(x_{Fe}^{grt})^3} + \ln(x_{Fe}^{grt})^3 + \frac{(1 - x_{Fe}^{grt})(-3)(1 - x_{Fe}^{grt})^2}{(1 - x_{Fe}^{grt})^3} - \ln(1 - x_{Fe}^{grt})^3 \right]$$

$$= \mu^{o}_{Fe} - \mu^{o}_{Mg} + RT\left[\ln(x_{Fe}^{grt})^3 - \ln(1 - x_{Fe}^{grt})^3 \right]$$

Take the second derivative:

$$\frac{\delta^2\,\overline{G}^{grt}}{\delta(x_{Fe}^{grt})^2} = RT\left[\frac{3(x_{Fe}^{grt})^2}{(x_{Fe}^{grt})^3} - \frac{3(-1)(1 - x_{Fe}^{grt})^2}{(1 - x_{Fe}^{grt})^3}\right] = RT\left[\frac{3(x_{Mg}^{grt} + x_{Fe}^{grt})}{(x_{Fe}^{grt})(x_{Mg}^{grt})}\right] = \frac{3RT}{(x_{Fe}^{grt})(x_{Mg}^{grt})}$$

where: T is in Kelvin and $R = 1.9872\,cal/mol\cdot K$

The relative change in μ_{H2O} is obtained by doing a numerical integration of $d\mu_{H2O}/dx_{Fe}^{grt}$.

Example: Sample 128/10a, $T = 775°C = 1048K$.

$$\frac{\delta^2\,\overline{G}^{grt}}{\delta(x_{Fe}^{grt})^2} = \frac{3(1048K)(1.9872cal/mol\cdot K)}{(x_{Fe}^{grt})(x_{Mg}^{grt})}; \quad \frac{d\mu_{H2O}}{dx_{Fe}^{grt}} = a\cdot\left[-\frac{\delta^2\,\overline{G}^{grt}}{\delta(x_{Fe}^{grt})^2}\right]$$

where a = the value obtained from M^{-1} for each set of x(Fe,Mg) values.

Set up an integration table as follows:

x_{Fe}^{grt}	x_{Fe}^{bt}	a	$\frac{\delta^2 \overline{G}^{grt}}{\delta(x_{Fe}^{grt})^2}$	$\frac{d\mu_{H2O}}{dx_{Fe}^{grt}}$	$\Delta\mu_{H2O}$	$\Sigma\Delta\mu_{H2O}$
0.010	0.002	−0.00645	631087	4072		
0.100	0.024	−0.06311	69420	4381	380	380
0.200	0.053	−0.12250	39048	4783	458	838
0.300	0.088	−0.17704	29751	5267	503	1341
0.400	0.130	−0.22511	26032	5860	556	1897
0.500	0.183	−0.26422	24991	6603	623	2521
0.600	0.251	−0.29050	26032	7562	708	3229
0.700	0.343	−0.29738	29751	8847	820	4049
0.800	0.472	−0.27296	39048	10659	974	5023
0.900	0.668	−0.19307	69420	13402	1203	6226
0.990	0.957	−0.02764	631087	17444	1388	7614

where: $\Delta\mu_{H2O} = \frac{\left[\frac{d\mu_{H2O}}{dx_{Fe}^{grt}}\right]_2 + \left[\frac{d\mu_{H2O}}{dx_{Fe}^{grt}}\right]_1}{2} \cdot \left[(x_{Fe}^{grt})_2 - (x_{Fe}^{grt})_1\right]$

Example : $380 = \left[\frac{4381 + 4072}{2}\right] \cdot (0.100 - 0.010)$

Reaction 2 - ***Sample 128/10b***

16sillimanite + 8biotite + 38quartz → 10cordierite + 8K-feldspar + 3H_2O

Reaction 2 describes how the crd-sil-bt field shifts in x_{Fe} with changing P,T and, μ_{H2O}; x_{Fe} in cordierite is chosen to monitor the changes in μ_{H2O}. Following the logic given for reaction 1, a matrix equation is set up:

$$\begin{bmatrix} x_{Fe}^{crd} & x_{Mg}^{crd} & 0 & 0 & 0 & 0 & 0 & 0 \\ 0 & 0 & x_{Fe}^{bt} & x_{Mg}^{bt} & 0 & 0 & 0 & 0 \\ 0 & 0 & 0 & 0 & 1 & 0 & 0 & 0 \\ 0 & 0 & 0 & 0 & 0 & 1 & 0 & 0 \\ 0 & 0 & 0 & 0 & 0 & 0 & 1 & 0 \\ 5 & -5 & -6 & 6 & 0 & 0 & 0 & 0 \\ -5 & 0 & 6 & 0 & -6 & 2 & 16 & -6 \\ -1 & 1 & 0 & 0 & 0 & 0 & 0 & 0 \end{bmatrix} \cdot \begin{bmatrix} d\mu_{Fe}^{crd}/dx_{Fe}^{crd} \\ d\mu_{Mg}^{crd}/dx_{Fe}^{crd} \\ d\mu_{Fe}^{bt}/dx_{Fe}^{crd} \\ d\mu_{Mg}^{bt}/dx_{Fe}^{crd} \\ d\mu^{kfs}/dx_{Fe}^{crd} \\ d\mu^{sil}/dx_{Fe}^{crd} \\ d\mu^{qtz}/dx_{Fe}^{crd} \\ d\mu_{H2O}/dx_{Fe}^{crd} \end{bmatrix} = \begin{bmatrix} 0 \\ 0 \\ 0 \\ 0 \\ 0 \\ 0 \\ 0 \\ -\left[\delta^2 \overline{G}^{crd}/\delta(x_{Fe}^{crd})^2\right]_{P,T} \end{bmatrix}$$

For sample 128/10b: $K_D = \frac{(x^{crd}_{Fe})\,(x^{bt}_{Mg})}{(x^{crd}_{Mg})\,(x^{bt}_{Fe})}$ and the average approximate "peak"

Fe / (Fe + Mg) ratios are:

- interior cordierite (ct1c,d,e,f,g,h,i)→ **0.273**
- matrix biotite (bt8,9)→ **0.437**

$\mathbf{K_D}$ = (0.273)(0.563)/(0.727)(0.437) = **0.484** and: $x^{crd}_{Fe} = \frac{x^{crd}_{Fe}}{(0.484 + 0.516x^{crd}_{Fe})}$

Construct a table for x(Mg,Fe) values:

xFe,crd	**xMg,crd**	**xFe,bt**	**xMg,bt**
0.010	0.990	0.020	0.980
0.100	0.900	0.187	0.813
0.200	0.800	0.341	0.659
0.300	0.700	0.470	0.530
0.400	0.600	0.579	0.421
0.500	0.500	0.674	0.326
0.600	0.400	0.756	0.244
0.700	0.300	0.828	0.172
0.800	0.200	0.892	0.108
0.900	0.100	0.949	0.051
0.990	0.010	0.995	0.005

Place each set of x(Fe,Mg) values in the matrix; invert, multiply to solve for $d\mu_{H2O}/dx_{Fe,crd}$ and numerically integrate (as done for reaction 1).

Sample 128/10b, T=775°C

x^{crd}_{Fe}	x^{bt}_{Fe}	**a**	$\frac{\delta^2 \overline{G}^{crd}}{\delta(x^{crd}_{Fe})^2}$	$\frac{d\mu_{H2O}}{dx^{crd}_{Fe}}$	$\Delta\mu_{H2O}$	$\Sigma\Delta\mu_{H2O}$
0.010	0.020	0.03478	420724	−14634		
0.100	0.182	0.28881	46280	−13366	−1260	−1260
0.200	0.334	0.46835	26032	−12192	−1278	−2538
0.300	0.463	0.56509	19834	−11208	−1170	−3708
0.400	0.573	0.59758	17355	−10371	−1079	−4787
0.500	0.668	0.57921	16661	−9650	−1001	−5788
0.600	0.751	0.51991	17355	−9023	−934	−6721
0.700	0.824	0.42716	19834	−8472	−875	−7596
0.800	0.889	0.30674	26032	−7985	−823	−8419
0.900	0.948	0.16316	46280	−7551	−777	−9196
0.990	0.995	0.01711	420724	−7198	−664	−9859

Reaction 3: ***Sample 128/10c***

4sillimanite + 4biotite + 14quartz → 2garnet + 2cordierite + 4K-feldspar +3H_2O

Since this is a univariant reaction, these phases only coexist at a single μ_{H2O} for a specified temperature. Therefore, the μ_{H2O} of reaction 3 can be set to zero and used as a reference for the $\Delta\mu_{H2O}$ of reactions 1 and 2.

The average approximate "peak" Fe/(Fe+Mg) ratios for sample 128/10c are:

- garnet interior (gar5,8,9,GT7) → **0.791**
- matrix cordierite (crd8,8a,8b) → **0.296**
- matrix biotite (bt14,15,16) → **0.461**

The garnet, biotite and cordierite loops of the continuous reactions (1 and 2) should intersect these compositions at the μ_{H2O} of discontinuous reaction 3. Since X_{Fe} of biotite lies between that of cordierite and garnet, the μ_{H2O} of biotite with X_{Fe} = 0.461 is set to zero for reactions 1 and 2 and the change in μ_{H2O} from that zero value is calculated as follows:

Sample 128/10a; T = 775°C

X_{Fe}^{crd}	X_{Fe}^{bt}	$\Delta\mu_{H2O}$	$\Sigma\Delta\mu_{H2O}$	$\Delta\mu_{H2O}^{new}$	$\frac{f_1}{f_3}$
0.793	0.461	900	4949	0	1.00
0.800	0.472	74	5023	74	1.04
0.860	0.579	684	5707	758	1.44
0.900	0.668	511	6218	1269	1.84
0.990	0.957	1388	7607	2658	3.58

Sample 128/10b; T = 775°C

X_{Fe}^{crd}	X_{Fe}^{bt}	$\Delta\mu_{H2O}$	$\Sigma\Delta\mu_{H2O}$	$\Delta\mu_{H2O}^{new}$	$\frac{f_2}{f_3}$
0.010	0.020			3628	5.71
0.100	0.187	−1260	−1260	2368	3.12
0.200	0.341	−1278	−2538	1091	1.69
0.273	0.437	−863	−3401	227	1.12
0.293	0.461	−227	−3628	0	1.00

The new values of $\Delta\mu_{H2O}$ (last column in each table above) are then used, along with the univariant data set at μ_{H2O} = 0, to construct the μ_{H2O}-X_{Fe} plot for peak conditions of the pelites observed in sample 128 (Figure 64).

<u>Reaction 4</u>: ***Sample 128/10c*** *(waning stages of metamorphism)*

2 cordierite + 8 biotite + 18 quartz = 8 garnet + 8 K-feldspar + 9 H_2O

Reaction 4 describes how the crd-grt-bt field shifs in X_{Fe} with changing P, T and μ_{H2O}; X_{Fe} in garnet is chosen to monitor the changes in μ_{H2O}. Following the logic given for reaction 1, a matrix equation is set up:

$$\begin{bmatrix} x_{Fe}^{grt} & x_{Mg}^{grt} & 0 & 0 & 0 & 0 & 0 & 0 & 0 \\ 0 & 0 & x_{Fe}^{crd} & x_{Mg}^{crd} & 0 & 0 & 0 & 0 & 0 \\ 0 & 0 & 0 & 0 & x_{Fe}^{bt} & x_{Mg}^{bt} & 0 & 0 & 0 \\ 0 & 0 & 0 & 0 & 0 & 0 & 1 & 0 & 0 \\ 0 & 0 & 0 & 0 & 0 & 0 & 0 & 1 & 0 \\ 5 & -5 & 0 & 0 & -6 & 6 & 0 & 0 & 0 \\ 2 & -2 & -3 & 3 & 0 & 0 & 0 & 0 & 0 \\ -8 & 0 & 2 & 0 & 8 & 0 & -8 & 18 & -9 \\ -1 & 1 & 0 & 0 & 0 & 0 & 0 & 0 & 0 \end{bmatrix} \bullet \begin{bmatrix} d\mu_{Fe}^{grt}/dx_{Fe}^{grt} \\ d\mu_{Mg}^{grt}/dx_{Fe}^{grt} \\ d\mu_{Fe}^{crd}/dx_{Fe}^{grt} \\ d\mu_{Mg}^{crd}/dx_{Fe}^{grt} \\ d\mu_{Fe}^{bt}/dx_{Fe}^{grt} \\ d\mu_{Mg}^{bt}/dx_{Fe}^{grt} \\ d\mu^{kfs}/dx_{Fe}^{grt} \\ d\mu^{qtz}/dx_{Fe}^{grt} \\ d\mu_{H2O}/dx_{Fe}^{grt} \end{bmatrix} = \begin{bmatrix} 0 \\ 0 \\ 0 \\ 0 \\ 0 \\ 0 \\ 0 \\ 0 \\ -[\delta^2 G/\delta(x_{Fe}^{grt})^2]_{P,T} \end{bmatrix}$$

For reaction 4 in sample 128/10c: $K_{D1} = \dfrac{(x_{Fe}^{grt})(x_{Mg}^{bt})}{(x_{Mg}^{grt})(x_{Fe}^{bt})}$ and $K_{D2} = \dfrac{(x_{Fe}^{grt})(x_{Mg}^{crd})}{(x_{Mg}^{grt})(x_{Fe}^{crd})}$

The Fe/(Fe+Mg) ratios for the waning stages of metamorphism are:

- garnet near rim (grt1c) → **0.838**
- cordierite rim adjacent garnet (crd1) → **0.334**
- biotite adjacnet garnet and cordierite (bt11) → **0.499**

K_{D1} = (0.838)(0.501)/(0.162)(0.499) = **5.194** and: $x_{Fe}^{bt} = \dfrac{x_{Fe}^{grt}}{(5.194 + 4.194 x_{Fe}^{grt})}$

K_{D2} = (0.838)(0.666)/(0.162)(0.334) = **10.315** and: $x_{Fe}^{crd} = \dfrac{x_{Fe}^{grt}}{(10.315 + 9.315 x_{Fe}^{grt})}$

Construct a table for x(Fe,Mg) values:

xFe,grt	xMg,grt	xFe,crd	xMg,crd	xFe,bt	xMg,bt
0.010	0.990	0.001	0.999	0.002	0.998
0.100	0.900	0.011	0.989	0.021	0.979
0.200	0.800	0.024	0.976	0.046	0.954
0.300	0.700	0.040	0.960	0.076	0.924
0.400	0.600	0.061	0.939	0.114	0.886
0.500	0.500	0.088	0.912	0.161	0.839
0.600	0.400	0.127	0.873	0.224	0.776
0.700	0.300	0.184	0.816	0.310	0.690
0.800	0.200	0.279	0.721	0.435	0.565
0.900	0.100	0.466	0.534	0.634	0.366
0.990	0.010	0.906	0.094	0.950	0.050

Place each set of x(Fe,Mg) values in the matrix; invert and multiply to solve for $d\mu_{H2O}/dx_{Fe,grt}$; numerically integrate (as done for reaction 1).

Sample 128/10c (reaction 4), T= 775°C

x_{Fe}^{grt}	x_{Fe}^{crd}	x_{Fe}^{bt}	a	$\frac{\delta^2 \overline{G}^{grt}}{\delta (x_{Fe}^{grt})^2}$	$\frac{d\mu_{H_2O}}{dx_{Fe}^{grt}}$	$\Delta\mu_{H_2O}$	$\Sigma\Delta\mu_{H_2O}$
0.010	0.001	0.002	– 0.00731	631087	4611		
0.100	0.011	0.021	– 0.07179	69420	4984	432	432
0.200	0.024	0.046	– 0.14025	39048	5477	523	955
0.300	0.040	0.076	– 0.20429	29751	6078	578	1533
0.400	0.061	0.114	– 0.26229	26032	6828	645	2178
0.500	0.088	0.161	– 0.31175	24991	7791	731	2909
0.600	0.127	0.224	– 0.34853	26032	9073	843	3752
0.700	0.184	0.310	– 0.36526	29751	10867	997	4749
0.800	0.279	0.435	– 0.34743	39048	13567	1222	5971
0.900	0.466	0.634	– 0.26127	69420	18137	1585	7556
0.990	0.906	0.950	– 0.04201	631087	26514	2009	9565

The garnet, biotite, and coridiertie loop of reaction 4 should intersect the compositions of discontinuous reaction 3 (at $\Delta\mu_{H2O} = 0$). Because X_{Fe} of biotite lies between that of cordierite and garnet, the μ_{H2O} of biotite with $X_{Fe} = 0.461$ is set to zero and the change in μ_{H2O} from that zero value is calculated as follows:

Sample 128/10c; T = 775°C

X_{Fe}^{grt}	X_{Fe}^{crd}	X_{Fe}^{bt}	$\Delta\mu_{H2O}$	$\Sigma\Delta\mu_{H2O}$	$\Delta\mu_{H2O}^{new}$	$\frac{f_4}{f_3}$
0.816	0.301	0.461	222	6192	0	1.00
0.838	0.334	0.499	320	6513	– 320	0.86
0.900	0.466	0.634	1027	7540	– 1347	0.52
0.990	0.906	0.950	2009	9549	– 3357	0.20

The new values of $\Delta\mu_{H2O}$ are used to construct the μ_{H2O}-X_{Fe} plot shown in Figure 66.

APPENDIX H

Quantitative Analysis for Migmatite Feldspar Compositions

Plagioclase
K-Feldspar

Abbreviations used for analysis location:

grt	*garnet*
host	*region surrounding leucosome*
incl	*inclusion*
interior	*plagioclase interior*
kfs	*K-feldspar*
leuco	*leucosome*
nr	*near*
plag	*plagioclase*
rim	*plagioclase rim*

TABLE H-1: Quantitative Microprobe Analysis for Plagioclase Compositions

PC-13G

leucosome									*host*							
	PL4	**PL4a**	**PL4b**	**PL4d**	**PL4e**	**PL4f**	**PL5**	**PL5a**	**PH1**	**PH1a**	**PH1b**	**PH1c**	**PH2**	**PH2a**	**PH2b**	**PH3**
WEIGHT PERCENT OXIDES																
SiO2	61.70	60.98	60.80	62.25	62.26	61.40	61.33	60.88	62.56	63.78	63.63	62.88	62.03	60.90	60.67	60.61
Al2O3	24.41	25.27	24.48	24.45	24.69	24.67	24.92	25.17	24.24	23.82	23.71	23.68	24.20	25.32	24.62	25.20
FeO	0.00	0.07	0.12	0.18	0.05	0.20	0.05	0.00	0.25	0.10	0.00	0.34	0.19	0.05	0.20	0.13
CaO	4.51	5.17	5.28	4.72	4.97	4.84	4.91	5.19	3.98	3.31	3.33	3.46	4.73	4.98	5.60	5.21
Na2O	9.55	9.00	8.82	8.97	9.01	9.39	9.30	8.59	9.77	10.36	10.25	10.21	9.30	9.36	8.65	8.92
K2O	0.14	0.20	0.29	0.19	0.20	0.14	0.18	0.32	0.13	0.14	0.18	0.18	0.18	0.09	0.17	0.15
TOTAL	**100.31**	**100.69**	**99.78**	**100.76**	**101.18**	**100.64**	**100.67**	**100.16**	**100.92**	**101.51**	**101.11**	**100.75**	**100.62**	**100.71**	**99.90**	**100.22**
CATIONS RECALCULATED TO 8 OXYGENS																
Si	2.731	2.694	2.712	2.740	2.731	2.714	2.709	2.701	2.750	2.782	2.785	2.770	2.739	2.691	2.704	2.691
Al	1.273	1.316	1.287	1.269	1.276	1.286	1.297	1.316	1.256	1.224	1.223	1.229	1.259	1.318	1.293	1.318
Fe	0.000	0.003	0.005	0.007	0.002	0.007	0.002	0.000	0.009	0.004	0.000	0.012	0.007	0.002	0.007	0.005
Ca	0.214	0.245	0.252	0.223	0.233	0.229	0.232	0.247	0.187	0.155	0.156	0.163	0.224	0.236	0.267	0.248
Na	0.820	0.771	0.762	0.766	0.767	0.805	0.796	0.739	0.833	0.876	0.870	0.872	0.796	0.802	0.747	0.768
K	0.008	0.011	0.016	0.010	0.011	0.008	0.010	0.018	0.007	0.008	0.010	0.010	0.010	0.005	0.010	0.009
TOTAL	**5.046**	**5.039**	**5.034**	**5.014**	**5.020**	**5.049**	**5.046**	**5.020**	**5.042**	**5.048**	**5.044**	**5.056**	**5.035**	**5.054**	**5.028**	**5.038**
An	0.21	0.24	0.24	0.22	0.23	0.22	0.22	0.25	0.18	0.15	0.15	0.16	0.22	0.23	0.26	0.24
Ab	0.79	0.75	0.74	0.77	0.76	0.77	0.77	0.74	0.81	0.84	0.84	0.83	0.77	0.77	0.73	0.75
Or	0.01	0.01	0.02	0.01	0.01	0.01	0.01	0.02	0.01	0.01	0.01	0.01	0.01	0.01	0.01	0.01
X	-169.20	-168.77	-168.07	-165.40	-165.25	-164.79	-187.85	-189.60	-214.82	-215.81	-216.62	-217.66	-106.34	-107.13	-106.69	-100.34
Y	-206.00	-203.24	-199.22	-195.89	-193.60	-189.98	-175.51	-176.05	-161.62	-161.81	-161.63	-161.63	-181.92	-181.99	-180.20	-183.22
x-axis mm	0.00	0.28	0.69	1.11	1.34	1.71	0.00	0.18	0.00	0.10	0.18	0.29	0.00	0.08	0.26	0.00
	rim	*interior*	*interior*	*interior*	*interior*	*rim*	*rim*	*interior*	*rim*	*interior*	*interior*	*rim*	*rim*	*±interior*	*interior*	*±interior*
location	leuco	leuco	leuco	leuco	leuco	leuco	leuco	leuco	host	host	host	host	host	host	host	host

TABLE H-1: Quantitative Microprobe Analysis for Plagioclase Compositions (continued)

PC-13G (continued)					***PC-13G-1***											
host					*leucosome*											
	PH3a	**PH3b**	**PH4**	**PH4a**	**P1**	**P1a**	**P1b**	**P1c**	**P1d**	**P1e**	**P2**	**P2a**	**P3a**	**P3b**	**P3c**	**P3cc**
WEIGHT PERCENT OXIDES																
SiO2	62.94	62.35	61.15	61.59	64.69	64.27	63.15	62.47	62.53	65.52	65.19	62.68	61.62	62.10	60.84	62.00
Al2O3	23.37	24.42	25.48	25.28	23.06	24.60	24.41	24.26	24.27	23.31	22.04	23.49	24.11	24.23	24.51	24.36
FeO	0.14	0.15	0.00	0.00	0.10	0.00	0.00	0.20	0.02	0.21	0.17	0.00	0.12	0.05	0.00	0.00
CaO	3.40	3.58	4.73	5.01	3.98	5.33	5.20	5.16	5.16	3.59	2.93	4.84	4.79	4.74	5.29	5.18
Na2O	9.92	9.43	9.16	8.68	9.59	8.62	8.95	9.17	8.90	9.73	9.94	8.88	8.96	8.86	8.79	8.79
K2O	0.04	0.16	0.24	0.22	0.12	0.22	0.24	0.10	0.21	0.00	0.10	0.15	0.16	0.15	0.14	0.20
TOTAL	**99.81**	**100.08**	**100.74**	**100.77**	**101.53**	**103.04**	**101.95**	**101.36**	**101.08**	**102.36**	**100.36**	**100.04**	**99.77**	**100.13**	**99.57**	**100.53**
CATIONS RECALCULATED TO 8 OXYGENS																
Si	2.788	2.755	2.696	2.711	2.815	2.761	2.748	2.739	2.745	2.823	2.861	2.774	2.740	2.747	2.715	2.736
Al	1.220	1.272	1.324	1.311	1.182	1.246	1.252	1.254	1.255	1.183	1.140	1.225	1.264	1.263	1.289	1.267
Fe	0.005	0.006	0.000	0.000	0.004	0.000	0.000	0.007	0.001	0.007	0.006	0.000	0.005	0.002	0.000	0.000
Ca	0.162	0.169	0.223	0.236	0.185	0.245	0.242	0.242	0.242	0.166	0.138	0.229	0.228	0.225	0.253	0.245
Na	0.852	0.808	0.783	0.741	0.809	0.718	0.755	0.780	0.757	0.812	0.845	0.762	0.773	0.760	0.761	0.752
K	0.002	0.009	0.013	0.012	0.006	0.012	0.013	0.005	0.012	0.000	0.006	0.008	0.009	0.009	0.008	0.011
TOTAL	**5.029**	**5.018**	**5.040**	**5.010**	**5.002**	**4.982**	**5.010**	**5.027**	**5.012**	**4.992**	**4.995**	**4.999**	**5.019**	**5.006**	**5.025**	**5.012**
An	0.16	0.17	0.22	0.24	0.19	0.25	0.24	0.24	0.24	0.17	0.14	0.23	0.23	0.23	0.25	0.24
Ab	0.84	0.82	0.77	0.75	0.81	0.74	0.75	0.76	0.75	0.83	0.86	0.76	0.76	0.77	0.74	0.75
Or	0.00	0.01	0.01	0.01	0.01	0.01	0.01	0.01	0.01	0.00	0.01	0.01	0.01	0.01	0.01	0.01
X	-99.14	-99.26	-56.56	-56.46	140.03	141.97	143.88	146.84	149.61	152.27	151.18	151.12	136.87	138.79	141.13	140.65
Y	-181.96	-181.90	-179.33	-181.05	321.26	321.26	321.54	322.13	321.87	323.27	302.08	299.81	291.20	289.73	288.76	288.35
x-axis mm	0.17	0.19	0.00	0.17	0.00	0.19	0.39	0.69	0.97	1.27	0.00	0.23	0.00	0.24	0.50	0.56
	rim	*rim*	*rim*	*interior*	*rim*	*interior*	*interior*	*interior*	*interior*	*rim*	*rim*	*interior*	*rim*	*interior*	*interior*	*interior*
location	host	host	host	host	leuco	leuco	leuco	leuco	leuco	leuco	leuco	leuco	leuco	leuco	leuco	leuco

TABLE H-1: Quantitative Microprobe Analysis for Plagioclase Compositions (continued)

PC-13G-1 (continued)											***PC-13I***					
host		*leucosome/host*		*host*							*leucosome*					
	P3d	**P4**	**P4a**	**P5**	**P5a**	**P5b**	**P6**	**P6a**	**P7**	**P7a**	**PL1**	**PL1b**	**PL1c**	**PL1d**	**PL1e**	**PL1f**
WEIGHT PERCENT OXIDES																
SiO2	61.61	62.11	63.20	62.51	61.73	63.34	63.14	62.69	62.11	62.37	58.48	59.48	59.18	59.45	59.33	58.88
Al2O3	24.60	23.92	24.00	23.45	23.95	24.17	23.77	24.32	23.76	23.88	26.58	26.60	27.21	26.81	27.80	27.74
FeO	0.08	0.21	0.06	0.09	0.26	0.10	0.00	0.03	0.18	0.06	0.23	0.09	0.04	0.05	0.04	0.04
CaO	5.24	4.64	5.06	4.45	5.07	5.17	4.70	5.10	5.01	5.02	7.05	7.24	7.49	7.03	7.25	7.23
Na2O	9.16	9.44	8.77	9.07	8.95	8.53	9.34	9.06	9.01	9.07	7.66	7.84	7.86	7.59	7.49	7.36
K2O	0.22	0.13	0.07	0.08	0.17	0.19	0.10	0.18	0.13	0.10	0.06	0.11	0.08	0.07	0.11	0.07
TOTAL	**100.91**	**100.45**	**101.16**	**99.64**	**100.13**	**101.50**	**101.04**	**101.36**	**100.20**	**100.51**	**100.07**	**101.35**	**101.86**	**100.99**	**102.02**	**101.31**
CATIONS RECALCULATED TO 8 OXYGENS																
Si	2.717	2.747	2.765	2.776	2.740	2.763	2.768	2.744	2.752	2.753	2.611	2.622	2.599	2.624	2.595	2.592
Al	1.279	1.247	1.237	1.227	1.253	1.242	1.229	1.255	1.241	1.242	1.399	1.382	1.408	1.394	1.433	1.439
Fe	0.003	0.008	0.002	0.003	0.010	0.004	0.000	0.001	0.007	0.002	0.009	0.003	0.002	0.002	0.001	0.001
Ca	0.247	0.220	0.237	0.212	0.241	0.242	0.221	0.239	0.238	0.237	0.337	0.342	0.352	0.333	0.340	0.341
Na	0.783	0.809	0.744	0.781	0.770	0.721	0.794	0.769	0.774	0.776	0.663	0.670	0.669	0.650	0.635	0.628
K	0.013	0.007	0.004	0.005	0.010	0.011	0.005	0.010	0.007	0.006	0.004	0.006	0.005	0.004	0.006	0.004
TOTAL	**5.042**	**5.038**	**4.990**	**5.003**	**5.023**	**4.982**	**5.017**	**5.018**	**5.019**	**5.017**	**5.023**	**5.025**	**5.034**	**5.006**	**5.010**	**5.005**
An	0.24	0.21	0.24	0.21	0.24	0.25	0.22	0.23	0.23	0.23	0.34	0.34	0.34	0.34	0.35	0.35
Ab	0.75	0.78	0.76	0.78	0.75	0.74	0.78	0.76	0.76	0.76	0.66	0.66	0.65	0.66	0.65	0.65
Or	0.01	0.01	0.00	0.00	0.01	0.01	0.01	0.01	0.01	0.01	0.00	0.01	0.00	0.00	0.01	0.00
X	160.08	120.63	118.99	107.82	109.72	111.01	95.60	96.85	58.77	59.88	-116.94	-116.88	-116.95	-117.03	-117.71	-117.71
Y	290.14	279.67	279.94	188.26	188.82	189.73	181.49	181.49	179.05	179.34	246.95	244.72	243.46	242.76	241.21	239.85
x-axis mm	2.51	0.00	0.17	0.00	0.20	0.36	0.00	0.13	0.00	0.11	0.00	0.22	0.35	0.42	0.59	0.72
	interior	*rim*	*interior*	*rim*	*interior*	*rim*	*rim*	*interior*	*rim*	*interior*	*rim*	*interior*	*interior*	*interior*	*interior*	*interior*
location	leuco	leuco/host	leuco/host	host	host	host	host	host	host	host	leuco	leuco	leuco	leuco	leuco	leuco

TABLE H-1: Quantitative Microprobe Analysis for Plagioclase Compositions (continued)

PC-13I (continued)

leucosome																*host*
	PL1g	**PL2**	**PL2a**	**PL2b**	**PL2c**	**PL3**	**PL3a**	**PL3b**	**PL4**	**PL4a**	**PL6**	**PL6a**	**PL6b**	**PL6c**	**PL6d**	**PH2**
WEIGHT PERCENT OXIDES																
SiO2	58.83	59.29	59.59	59.03	58.41	59.46	59.58	59.48	59.11	58.95	58.77	57.93	58.01	58.84	59.08	61.28
Al2O3	27.67	27.31	27.39	26.73	26.36	27.06	27.92	27.17	27.30	27.24	27.04	27.10	27.10	27.37	27.04	27.49
FeO	0.12	0.22	0.00	0.04	0.05	0.26	0.13	0.08	0.07	0.12	0.30	0.11	0.00	0.00	0.05	0.12
CaO	7.14	7.27	7.20	7.00	7.48	7.05	6.98	7.16	7.05	7.20	7.06	7.32	7.67	7.68	7.29	6.66
Na2O	7.85	7.77	7.69	7.88	7.87	7.84	7.62	8.38	7.79	8.06	8.08	7.54	7.61	7.66	7.69	7.85
K2O	0.06	0.06	0.08	0.16	0.05	0.10	0.15	0.25	0.10	0.19	0.11	0.16	0.18	0.12	0.07	0.10
TOTAL	**101.67**	**101.92**	**101.94**	**100.83**	**100.21**	**101.77**	**102.38**	**102.53**	**101.43**	**101.75**	**101.36**	**100.16**	**100.55**	**101.68**	**101.22**	**103.50**
CATIONS RECALCULATED TO 8 OXYGENS																
Si	2.586	2.600	2.608	2.615	2.609	2.611	2.596	2.600	2.602	2.594	2.597	2.587	2.584	2.589	2.607	2.635
Al	1.434	1.412	1.413	1.395	1.387	1.400	1.434	1.400	1.416	1.413	1.408	1.427	1.422	1.420	1.406	1.393
Fe	0.004	0.008	0.000	0.001	0.002	0.009	0.005	0.003	0.003	0.004	0.011	0.004	0.000	0.000	0.002	0.004
Ca	0.336	0.342	0.338	0.332	0.358	0.331	0.326	0.335	0.333	0.339	0.334	0.350	0.366	0.362	0.344	0.307
Na	0.669	0.660	0.652	0.677	0.682	0.668	0.644	0.710	0.665	0.688	0.692	0.653	0.657	0.653	0.658	0.655
K	0.004	0.004	0.004	0.009	0.003	0.006	0.008	0.014	0.006	0.011	0.006	0.009	0.010	0.007	0.004	0.006
TOTAL	**5.033**	**5.026**	**5.014**	**5.030**	**5.040**	**5.026**	**5.013**	**5.062**	**5.025**	**5.049**	**5.049**	**5.030**	**5.039**	**5.031**	**5.021**	**4.999**
An	0.33	0.34	0.34	0.33	0.34	0.33	0.33	0.32	0.33	0.33	0.32	0.35	0.35	0.35	0.34	0.32
Ab	0.66	0.66	0.66	0.66	0.65	0.66	0.66	0.67	0.66	0.66	0.67	0.64	0.64	0.64	0.65	0.68
Or	0.00	0.00	0.00	0.01	0.00	0.01	0.01	0.01	0.01	0.01	0.01	0.01	0.01	0.01	0.00	0.01
X	-117.51	-119.30	-118.22	-115.02	-113.16	-98.48	-98.26	-97.93	-102.08	-100.38	-152.96	-149.43	-145.47	-142.19	-139.25	-54.88
Y	239.02	242.09	241.58	240.51	239.57	237.36	238.35	239.01	235.16	234.95	236.45	236.45	236.94	237.72	241.12	227.10
x-axis mm	0.81	0.00	0.12	0.46	0.67	0.00	0.10	0.18	0.00	0.17	0.00	0.35	0.75	1.09	1.54	0.00
location	*rim* leuco	*rim* leuco	*interior* leuco	*interior* leuco	*rim* leuco	*rim* leuco	*interior* leuco	*interior* leuco	*rim* leuco	*interior* leuco	*rim* leuco	*interior* leuco	*interior* leuco	*interior* leuco	*rim* leuco	*rim* host

TABLE H-1: Quantitative Microprobe Analysis for Plagioclase Compositions (continued)

PC-13I (continued)								***PC-13I-1***								
host								*leucosome*					*host*			
	PH2a	**PH4**	**PH4a**	**PH5**	**PH5a**	**PH6**	**PH6a**	**P1**	**P1a**	**P1b**	**P1c**	**P1d**	**P2**	**P2a**	**P2b**	**P3**
WEIGHT PERCENT OXIDES																
SiO2	60.41	59.29	58.47	57.67	58.93	59.61	58.73	59.89	59.95	59.64	60.06	60.40	60.54	60.52	60.30	60.28
Al2O3	28.12	26.61	25.96	26.46	25.51	26.57	26.49	26.01	25.78	25.55	25.57	25.21	25.72	25.65	25.89	26.02
FeO	0.00	0.03	0.02	0.32	0.00	0.33	0.04	0.25	0.07	0.14	0.05	0.11	0.12	0.12	0.04	0.14
CaO	6.98	7.07	7.53	7.54	7.19	7.15	7.53	7.08	7.12	7.05	7.16	6.43	6.96	6.93	7.05	6.98
Na2O	7.57	8.05	8.12	7.76	8.28	8.05	7.38	7.84	7.66	7.79	7.69	8.22	7.78	7.77	7.72	7.98
K2O	0.11	0.11	0.24	0.16	0.16	0.14	0.19	0.12	0.13	0.14	0.18	0.16	0.11	0.16	0.12	0.09
TOTAL	**103.20**	**101.15**	**100.34**	**99.91**	**100.06**	**101.85**	**100.35**	**101.19**	**100.71**	**100.31**	**100.70**	**100.52**	**101.22**	**101.15**	**101.12**	**101.49**
CATIONS RECALCULATED TO 8 OXYGENS																
Si	2.606	2.619	2.614	2.591	2.637	2.620	2.615	2.644	2.655	2.654	2.661	2.678	2.665	2.667	2.658	2.650
Al	1.430	1.385	1.368	1.401	1.345	1.376	1.390	1.353	1.345	1.340	1.335	1.318	1.335	1.332	1.345	1.348
Fe	0.000	0.001	0.001	0.012	0.000	0.012	0.002	0.009	0.003	0.005	0.002	0.004	0.005	0.004	0.002	0.005
Ca	0.323	0.335	0.361	0.363	0.345	0.337	0.359	0.335	0.338	0.336	0.340	0.305	0.328	0.327	0.333	0.329
Na	0.634	0.689	0.704	0.676	0.718	0.686	0.637	0.671	0.658	0.672	0.660	0.706	0.664	0.663	0.659	0.680
K	0.006	0.006	0.014	0.009	0.009	0.008	0.011	0.007	0.007	0.008	0.010	0.009	0.006	0.009	0.007	0.005
TOTAL	**4.999**	**5.036**	**5.061**	**5.051**	**5.054**	**5.039**	**5.014**	**5.019**	**5.005**	**5.016**	**5.007**	**5.021**	**5.002**	**5.003**	**5.003**	**5.018**
An	0.34	0.33	0.33	0.35	0.32	0.33	0.36	0.33	0.34	0.33	0.34	0.30	0.33	0.33	0.33	0.32
Ab	0.66	0.67	0.65	0.65	0.67	0.67	0.63	0.66	0.66	0.66	0.65	0.69	0.67	0.66	0.66	0.67
Or	0.01	0.01	0.01	0.01	0.01	0.01	0.01	0.01	0.01	0.01	0.01	0.01	0.01	0.01	0.01	0.01
X	-55.68	-167.71	-168.08	-166.20	-166.96	-203.25	-205.24	-44.30	-42.13	-38.83	-36.27	-35.50	-75.02	-75.24	-76.29	-91.51
Y	226.46	227.93	225.56	242.11	242.17	236.35	236.86	244.98	243.75	243.36	242.96	242.50	246.67	247.97	249.36	254.70
x-axis mm	0.10	0.00	0.24	0.00	0.08	0.00	0.21	0.00	0.25	0.58	0.84	0.93	0.00	0.13	0.31	0.00
	interior	*rim*	*interior*	*rim*	*interior*	*rim*	*interior*	*rim*	*interior*	*interior*	*int nr rim*	*rim*	*rim*	*interior*	*interior*	*rim*
location	host	host	host	host	host	host	host	leuco	leuco	leuco	leuco	leuco	host	host	host	host

TABLE H-1: Quantitative Microprobe Analysis for Plagioclase Compositions (continued)

PC-13I-1 (continued)									***PC-111I***						
host									*leucosome/host*						
	P3a	**P4**	**P4a**	**P4b**	**P5**	**P5a**	**P6**	**P6a**	**P1**	**P2**	**P2a**	**P2b**	**P3**	**P4**	**P4a**
WEIGHT PERCENT OXIDES															
SiO2	59.91	59.95	59.99	60.19	60.46	60.29	60.02	59.38	62.35	61.84	62.88	63.28	62.79	62.92	63.16
Al2O3	25.60	26.17	25.43	25.94	25.94	25.45	25.84	25.36	23.65	23.91	23.71	23.69	23.92	23.95	24.00
FeO	0.12	0.15	0.11	0.03	0.30	0.09	0.00	0.01	0.01	0.11	0.00	0.09	0.14	0.02	0.00
CaO	7.01	7.01	6.96	7.00	7.16	6.98	7.06	6.98	4.32	4.08	4.43	4.09	4.32	4.56	4.67
Na2O	7.76	7.91	7.66	7.81	7.78	7.70	7.67	7.65	9.33	9.56	9.09	9.55	9.50	9.41	9.00
K2O	0.17	0.13	0.10	0.13	0.11	0.13	0.09	0.20	0.14	0.10	0.26	0.13	0.18	0.05	0.27
TOTAL	**100.57**	**101.31**	**100.25**	**101.11**	**101.74**	**100.65**	**100.67**	**99.57**	**99.80**	**99.61**	**100.37**	**100.82**	**100.84**	**100.91**	**101.09**
CATIONS RECALCULATED TO 8 OXYGENS															
Si	2.658	2.642	2.667	2.654	2.653	2.669	2.656	2.660	2.767	2.752	2.773	2.778	2.761	2.762	2.767
Al	1.339	1.359	1.332	1.348	1.342	1.328	1.348	1.339	1.237	1.254	1.232	1.226	1.240	1.239	1.239
Fe	0.004	0.005	0.004	0.001	0.011	0.003	0.000	0.000	0.001	0.004	0.000	0.003	0.005	0.001	0.000
Ca	0.333	0.331	0.331	0.331	0.336	0.331	0.335	0.335	0.205	0.195	0.209	0.193	0.203	0.214	0.219
Na	0.667	0.676	0.660	0.668	0.662	0.661	0.658	0.664	0.803	0.825	0.778	0.812	0.810	0.801	0.764
K	0.009	0.007	0.005	0.007	0.006	0.007	0.005	0.011	0.008	0.006	0.014	0.007	0.010	0.003	0.015
TOTAL	**5.011**	**5.020**	**5.000**	**5.009**	**5.010**	**5.001**	**5.002**	**5.009**	**5.020**	**5.036**	**5.007**	**5.019**	**5.029**	**5.020**	**5.003**
An	0.33	0.33	0.33	0.33	0.34	0.33	0.34	0.33	0.20	0.19	0.21	0.19	0.20	0.21	0.22
Ab	0.66	0.67	0.66	0.66	0.66	0.66	0.66	0.66	0.79	0.80	0.78	0.80	0.79	0.79	0.77
Or	0.01	0.01	0.01	0.01	0.01	0.01	0.00	0.01	0.01	0.01	0.01	0.01	0.01	0.00	0.01
X	-92.61	-112.71	-112.98	-112.98	-150.54	-151.13	-176.37	-175.89	-73.88	-76.56	-75.77	-76.22	-53.78	-56.57	-55.63
Y	255.07	238.48	239.92	240.87	240.92	242.17	226.48	228.21	-340.58	-346.79	-345.20	-342.38	-357.20	-359.54	-356.16
x-axis mm	0.12	0.00	0.15	0.24	0.00	0.14	0.00	0.18		0.00	0.18	0.46		0.00	0.35
	interior	*rim*	*interior*	*interior*	*rim*	*interior*	*rim*	*interior*	*rim*	*rim*	*interior*	*interior*	*rim*	*rim*	*interior*
location	host	host	host	host	host	host	host	host	leuco/host	leuco/host	leuco/host	leuco/host	leuco/host	leuco/host	leuco/host

TABLE H-1: Quantitative Microprobe Analysis for Plagioclase Compositions (continued)

PC-111I (continued)						***PC-111I-1A***										
leucosome						*leucosome?*										*host*
	P5	**P5a**	**P6**	**P6a**	**P7a**	**P6**	**P6a**	**P7**	**P7a**	**P7b**	**P7c**	**P7d**	**P7e**	**P8**	**P8a**	**P1**
WEIGHT PERCENT OXIDES																
SiO2	67.66	62.15	67.93	62.94	63.31	64.80	64.27	64.79	64.00	63.82	63.97	64.80	64.55	62.81	63.78	62.85
Al2O3	20.30	23.71	20.41	23.62	23.36	24.17	24.14	23.91	23.91	24.00	24.00	23.72	24.48	23.95	24.38	23.85
FeO	0.07	0.01	0.00	0.01	0.07	0.00	0.04	0.11	0.02	0.00	0.00	0.05	0.07	0.01	0.08	0.19
CaO	0.53	4.34	0.53	4.42	4.09	4.29	4.57	4.36	4.49	4.41	4.63	4.05	4.35	4.12	4.51	4.09
Na2O	11.45	9.06	11.31	9.08	9.38	9.40	9.28	9.39	9.08	9.47	9.16	9.44	9.62	9.35	9.31	9.81
K2O	0.06	0.28	0.08	0.25	0.29	0.15	0.35	0.19	0.39	0.34	0.26	0.29	0.24	0.12	0.24	0.11
TOTAL	**100.07**	**99.55**	**100.25**	**100.33**	**100.50**	**102.81**	**102.65**	**102.74**	**101.90**	**102.03**	**102.01**	**102.35**	**103.30**	**100.35**	**102.29**	**100.90**
CATIONS RECALCULATED TO 8 OXYGENS																
Si	2.958	2.765	2.961	2.777	2.789	2.785	2.774	2.789	2.780	2.772	2.776	2.798	2.768	2.768	2.762	2.763
Al	1.046	1.243	1.049	1.228	1.212	1.224	1.228	1.213	1.224	1.228	1.227	1.207	1.237	1.244	1.244	1.236
Fe	0.003	0.000	0.000	0.000	0.003	0.000	0.001	0.004	0.001	0.000	0.000	0.002	0.003	0.000	0.003	0.007
Ca	0.025	0.207	0.025	0.209	0.193	0.198	0.211	0.201	0.209	0.205	0.215	0.187	0.200	0.195	0.209	0.193
Na	0.971	0.782	0.956	0.777	0.801	0.783	0.776	0.784	0.765	0.798	0.771	0.790	0.799	0.799	0.781	0.836
K	0.003	0.016	0.004	0.014	0.016	0.008	0.019	0.010	0.022	0.019	0.014	0.016	0.013	0.007	0.013	0.006
TOTAL	**5.006**	**5.012**	**4.994**	**5.005**	**5.014**	**4.998**	**5.010**	**5.001**	**5.001**	**5.022**	**5.003**	**5.001**	**5.020**	**5.012**	**5.013**	**5.041**
An	0.03	0.21	0.02	0.21	0.19	0.20	0.21	0.20	0.21	0.20	0.22	0.19	0.20	0.19	0.21	0.19
Ab	0.97	0.78	0.97	0.78	0.79	0.79	0.77	0.79	0.77	0.78	0.77	0.80	0.79	0.80	0.78	0.81
Or	0.00	0.02	0.00	0.01	0.02	0.01	0.02	0.01	0.02	0.02	0.01	0.02	0.01	0.01	0.01	0.01
X	-223.29	-224.61	-121.72	-119.40	-71.67	59.82	60.83	43.98	42.91	41.92	40.58	38.68		31.92	32.92	187.44
Y	-219.89	-223.05	-273.41	-275.33	-126.78	-352.34	-353.84	-338.85	-338.34	-337.24	-335.07	-333.59		-312.69	-315.49	-226.24
x-axis mm	0.00	0.34	0.00	0.30		0.00	0.18	0.00	0.12	0.27	0.52	0.76		0.00	0.30	0.00
	rim	*interior*	*rim*	*interior*	*interior*	*rim*	*interior*	*rim*	*interior*	*interior*	*interior*	*interior*	*rim*	*rim*	*interior*	*rim*
location	leuco	leuco	incl in kfs	incl in kfs	leuco	leuco?	leuco?	leuco?	leuco?	leuco?	leuco?	leuco?	leuco?	leuco?	leuco?	host

TABLE H-1: Quantitative Microprobe Analysis for Plagioclase Compositions (continued)

PC-111I-1A (continued)											***PC-113B***					
host											*leucosome*					
	P1a	**P1b**	**P2**	**P2a**	**P3**	**P3a**	**P4**	**P4a**	**P5**	**P5a**	**P1**	**P1a**	**P2**	**P2a**	**P3**	**P3a**
WEIGHT PERCENT OXIDES																
SiO2	62.36	63.36	63.22	63.50	63.54	63.67	63.72	64.56	64.20	63.56	63.66	61.57	62.80	62.44	62.87	62.66
Al2O3	24.05	23.90	24.40	24.16	23.92	24.08	23.90	24.28	23.97	24.15	23.60	24.25	23.74	24.25	23.87	24.07
FeO	0.06	0.08	0.00	0.10	0.17	0.06	0.03	0.00	0.06	0.00	0.00	0.00	0.06	0.03	0.00	0.06
CaO	4.58	4.36	4.46	4.62	4.66	4.43	4.55	4.52	4.27	4.69	4.52	5.73	4.49	5.06	4.59	4.81
Na2O	9.21	9.40	9.47	9.04	9.08	9.10	9.51	9.29	9.09	9.21	9.10	8.31	9.40	9.00	9.41	8.97
K2O	0.26	0.10	0.20	0.24	0.09	0.22	0.13	0.21	0.06	0.23	0.04	0.26	0.08	0.26	0.10	0.19
TOTAL	**100.52**	**101.20**	**101.74**	**101.66**	**101.47**	**101.56**	**101.83**	**102.87**	**101.65**	**101.83**	**100.91**	**100.13**	**100.56**	**101.04**	**100.84**	**100.74**
CATIONS RECALCULATED TO 8 OXYGENS																
Si	2.752	2.771	2.754	2.766	2.772	2.773	2.772	2.776	2.788	2.765	2.787	2.731	2.767	2.743	2.763	2.756
Al	1.251	1.232	1.253	1.240	1.230	1.236	1.225	1.230	1.227	1.238	1.217	1.268	1.233	1.256	1.236	1.248
Fe	0.002	0.003	0.000	0.004	0.006	0.002	0.001	0.000	0.002	0.000	0.000	0.000	0.002	0.001	0.000	0.002
Ca	0.217	0.204	0.208	0.216	0.218	0.207	0.212	0.208	0.199	0.218	0.212	0.272	0.212	0.238	0.216	0.227
Na	0.788	0.797	0.800	0.764	0.768	0.768	0.802	0.775	0.765	0.776	0.773	0.714	0.803	0.767	0.801	0.765
K	0.015	0.006	0.011	0.013	0.005	0.012	0.007	0.012	0.003	0.013	0.002	0.015	0.004	0.015	0.006	0.011
TOTAL	**5.024**	**5.014**	**5.025**	**5.002**	**5.000**	**4.999**	**5.020**	**5.002**	**4.983**	**5.011**	**4.991**	**5.000**	**5.020**	**5.020**	**5.023**	**5.008**
An	0.21	0.20	0.20	0.22	0.22	0.21	0.21	0.21	0.21	0.22	0.21	0.27	0.21	0.23	0.21	0.23
Ab	0.77	0.79	0.78	0.77	0.78	0.78	0.79	0.78	0.79	0.77	0.78	0.71	0.79	0.75	0.78	0.76
Or	0.01	0.01	0.01	0.01	0.01	0.01	0.01	0.01	0.00	0.01	0.00	0.01	0.00	0.01	0.01	0.01
X	188.78	188.74	219.19	218.32	231.03	231.63	159.27	160.25	141.02	140.71	39.95	41.62	52.91	55.67	101.74	103.01
Y	-224.50	-221.21	-243.52	-243.88	-240.71	-240.36	-227.57	-227.78	-255.27	-251.80	132.61	129.65	132.59	131.71	21.93	22.18
x-axis mm	0.22	0.55	0.00	0.09	0.00	0.07	0.00	0.10	0.00	0.35	0.00	0.34	0.00	0.29	0.00	0.13
	interior	*rim*	*rim*	*interior*	*rim*	*interior*	*rim*	*interior*	*rim*	*interior*	*rim*	*interior*	*rim*	*interior*	*rim*	*interior*
location	host	host	host	host	host	host	host	host	host	host	leuco	leuco	leuco	leuco	leuco	leuco

TABLE H-1: Quantitative Microprobe Analysis for Plagioclase Compositions (continued)

	PC-113B (continued) *host*													***PC-113M-2*** *leucosome*		
	P4	**P4a**	**P5**	**P5a**	**P6**	**P6a**	**P7**	**P7a**	**P7b**	**P8**	**P8a**	**P9**	**P9a**	**PL2**	**PL2b**	**PL3a**
WEIGHT PERCENT OXIDES																
SiO2	63.13	61.91	62.93	61.41	62.86	61.81	62.50	61.96	62.24	63.83	61.80	61.94	61.32	59.99	60.81	60.31
Al2O3	24.10	24.76	23.89	24.56	23.79	24.84	24.06	24.51	24.14	23.07	24.90	24.15	24.20	25.01	26.05	25.69
FeO	0.06	0.06	0.25	0.00	0.08	0.02	0.01	0.00	0.01	0.18	0.10	0.23	0.03	0.14	0.04	0.12
CaO	4.87	5.51	4.28	5.81	4.57	5.55	5.11	5.00	4.87	4.01	5.46	4.64	5.18	5.01	5.49	5.26
Na2O	9.04	8.77	9.50	8.43	9.16	8.60	8.83	8.74	8.90	9.31	8.79	9.42	8.79	9.29	8.60	8.75
K2O	0.12	0.22	0.09	0.17	0.10	0.18	0.20	0.19	0.14	0.09	0.21	0.09	0.15	0.13	0.16	0.14
TOTAL	**101.33**	**101.24**	**100.94**	**100.38**	**100.55**	**101.00**	**100.71**	**100.39**	**100.30**	**100.49**	**101.25**	**100.46**	**99.67**	**99.56**	**101.15**	**100.27**
CATIONS RECALCULATED TO 8 OXYGENS																
Si	2.760	2.719	2.764	2.718	2.768	2.718	2.752	2.736	2.750	2.806	2.714	2.739	2.731	2.685	2.673	2.675
Al	1.242	1.281	1.236	1.281	1.235	1.287	1.249	1.275	1.257	1.195	1.288	1.258	1.270	1.319	1.349	1.343
Fe	0.002	0.002	0.009	0.000	0.003	0.001	0.000	0.000	0.000	0.007	0.004	0.008	0.001	0.005	0.002	0.005
Ca	0.228	0.259	0.201	0.275	0.216	0.261	0.241	0.237	0.230	0.189	0.257	0.220	0.247	0.240	0.258	0.250
Na	0.766	0.747	0.809	0.723	0.782	0.733	0.754	0.748	0.762	0.794	0.748	0.808	0.759	0.806	0.733	0.752
K	0.007	0.012	0.005	0.010	0.005	0.010	0.011	0.011	0.008	0.005	0.012	0.005	0.009	0.007	0.009	0.008
TOTAL	**5.006**	**5.020**	**5.025**	**5.008**	**5.008**	**5.010**	**5.007**	**5.006**	**5.007**	**4.996**	**5.022**	**5.038**	**5.017**	**5.063**	**5.023**	**5.033**
An	0.23	0.25	0.20	0.27	0.22	0.26	0.24	0.24	0.23	0.19	0.25	0.21	0.24	0.23	0.26	0.25
Ab	0.77	0.73	0.80	0.72	0.78	0.73	0.75	0.75	0.76	0.80	0.74	0.78	0.75	0.77	0.73	0.74
Or	0.01	0.01	0.00	0.01	0.01	0.01	0.01	0.01	0.01	0.00	0.01	0.01	0.01	0.01	0.01	0.01
X	168.41	169.02	173.08	173.09	153.55	153.44	78.70	75.87	74.63	122.30	124.16	156.05	156.05	117.34	118.62	127.24
Y	281.17	278.77	282.24	279.82	258.42	256.60	351.93	337.59	350.17	392.66	393.59	377.49	376.15	86.57	85.51	86.81
x-axis mm	0.00	0.25	0.00	0.24	0.00	0.18	0.00	1.46		0.00	0.21	0.00	0.13	0.00	0.17	0.00
location	*rim* host	*interior* host	*rim* host	*interior* host	*rim* host	*interior* host	*adj grt*	*adj grt*	*adj grt*	*rim* host	*interior* host	*rim* host	*interior* host	*rim* leuco	*interior* leuco	*interior* leuco

TABLE H-1: Quantitative Microprobe Analysis for Plagioclase Compositions (continued)

PC-113M-2			*PC-113M-2 (continued)*							*PC-134E-1*								
leucosome			*leucosome*	*host*						*leucosome*								
PL2	**PL2b**	**PL3a**		**PL3b**	**PH1**	**PH1a**	**PH2**	**PH2a**	**PH3**	**PH3a**	**P1a**	**P1b**	**P2**	**P2a**	**P2b**	**P2c**	**P7**	**P7a**	**P7b**
			WEIGHT PERCENT OXIDES																
59.99	60.81	60.31	SiO2	61.01	60.96	59.85	60.75	60.23	61.40	60.98	61.75	61.53	62.21	60.69	61.95	62.66	62.73	61.84	61.71
25.01	26.05	25.69	Al2O3	25.04	24.98	25.44	25.04	25.19	25.08	26.03	24.53	24.52	24.13	24.92	24.87	23.98	24.40	24.69	24.28
0.14	0.04	0.12	FeO	0.06	0.19	0.07	0.00	0.03	0.13	0.00	0.00	0.07	0.00	0.02	0.00	0.03	0.02	0.06	0.00
5.01	5.49	5.26	CaO	4.45	4.66	5.58	5.06	5.57	4.75	4.94	5.63	5.73	4.71	5.81	5.93	5.14	5.08	5.52	5.65
9.29	8.60	8.75	Na2O	9.40	9.10	8.99	9.01	9.30	9.27	8.97	8.44	8.43	9.08	8.24	8.27	8.66	8.96	8.55	8.45
0.13	0.16	0.14	K2O	0.10	0.15	0.24	0.09	0.16	0.08	0.19	0.26	0.28	0.11	0.29	0.34	0.11	0.21	0.22	0.26
99.56	**101.15**	**100.27**	**TOTAL**	**100.06**	**100.04**	**100.17**	**99.94**	**100.48**	**100.71**	**101.10**	**100.61**	**100.55**	**100.23**	**99.97**	**101.36**	**100.57**	**101.39**	**100.88**	**100.36**
			CATIONS RECALCULATED TO 8 OXYGENS																
2.685	2.673	2.675	Si	2.707	2.707	2.666	2.700	2.675	2.708	2.679	2.726	2.720	2.750	2.700	2.716	2.759	2.744	2.723	2.731
1.319	1.349	1.343	Al	1.310	1.307	1.336	1.312	1.319	1.304	1.348	1.276	1.278	1.257	1.306	1.285	1.244	1.258	1.281	1.266
0.005	0.002	0.005	Fe	0.002	0.007	0.003	0.000	0.001	0.005	0.000	0.000	0.003	0.000	0.001	0.000	0.001	0.001	0.002	0.000
0.240	0.258	0.250	Ca	0.211	0.222	0.267	0.241	0.265	0.224	0.233	0.266	0.271	0.223	0.277	0.279	0.242	0.238	0.260	0.268
0.806	0.733	0.752	Na	0.809	0.784	0.777	0.776	0.801	0.793	0.764	0.723	0.723	0.778	0.711	0.703	0.739	0.760	0.730	0.725
0.007	0.009	0.008	K	0.006	0.008	0.013	0.005	0.009	0.004	0.010	0.015	0.016	0.006	0.016	0.019	0.006	0.012	0.012	0.015
5.063	**5.023**	**5.033**	**TOTAL**	**5.045**	**5.035**	**5.061**	**5.034**	**5.070**	**5.038**	**5.034**	**5.005**	**5.010**	**5.014**	**5.011**	**5.002**	**4.992**	**5.012**	**5.008**	**5.006**
0.23	0.26	0.25	An	0.21	0.22	0.25	0.24	0.25	0.22	0.23	0.27	0.27	0.22	0.28	0.28	0.25	0.24	0.26	0.27
0.77	0.73	0.74	Ab	0.79	0.77	0.74	0.76	0.75	0.78	0.76	0.72	0.72	0.77	0.71	0.70	0.75	0.75	0.73	0.72
0.01	0.01	0.01	Or	0.01	0.01	0.01	0.00	0.01	0.00	0.01	0.01	0.02	0.01	0.02	0.02	0.01	0.01	0.01	0.01
117.34	118.62	127.24	X	128.99	36.97	37.35	39.28	38.50	43.90	42.78	221.40	221.69	197.96	199.50	201.14	201.67	62.00	61.60	62.05
86.57	85.51	86.81	Y	84.15	335.64	336.87	322.77	322.77	188.77	188.12	-128.85	-133.87	-134.58	-127.61	-124.15	-117.88	-226.32	-222.98	-216.60
0.00	0.17	0.00	x-axis mm	0.32	0.00	0.13	0.00	0.08	0.00	0.13	0.16	0.66	0.00	0.71	1.10	1.73	0.00	0.34	0.98
rim	*interior*	*interior*	*location*	*rim*	*rim*	*interior*	*rim*	*interior*	*rim*	*interior*	*interior*	*interior*	*rim*	*interior*	*interior*	*rim*	*rim*	*interior*	*interior*
leuco	leuco	leuco		leuco	host	host	host	host	host	host	leuco	leuco	leuco	leuco	leuco	leuco	leuco	leuco	leuco

TABLE H-1: Quantitative Microprobe Analysis for Plagioclase Compositions (continued)

PC-134E-1 (continued)													***PC-134E-2***			
leucosome					*host/leucosome*				*host*				*leucosome*			
	P7c	**P8**	**P8a**	**P8b**	**P3**	**P3a**	**P4**	**P4a**	**P5**	**P5a**	**P6**	**P6a**	**P3**	**P3a**	**P3b**	**P3c**
WEIGHT PERCENT OXIDES																
SiO2	60.99	62.46	61.41	61.28	63.28	61.80	62.84	61.00	62.98	61.77	62.88	62.00	62.72	62.73	63.11	62.59
Al2O3	25.20	23.89	24.95	24.90	24.11	24.80	24.00	24.74	24.71	24.73	24.52	24.78	24.49	24.95	25.17	25.16
FeO	0.00	0.06	0.13	0.08	0.38	0.00	0.08	0.00	0.36	0.05	0.06	0.06	0.26	0.18	0.00	0.08
CaO	5.86	4.96	6.00	5.95	4.71	5.57	4.88	5.70	5.36	5.63	5.17	5.58	5.10	6.00	6.00	5.76
Na2O	8.22	9.02	8.35	8.28	9.33	8.36	8.99	8.38	8.96	8.37	9.05	8.47	8.60	8.73	8.69	8.33
K2O	0.25	0.12	0.25	0.26	0.10	0.19	0.11	0.19	0.14	0.24	0.07	0.21	0.25	0.24	0.32	0.38
TOTAL	**100.52**	**100.50**	**101.09**	**100.76**	**101.91**	**100.72**	**100.91**	**100.00**	**102.51**	**100.79**	**101.75**	**101.10**	**101.42**	**102.83**	**103.29**	**102.30**
CATIONS RECALCULATED TO 8 OXYGENS																
Si	2.697	2.756	2.703	2.705	2.756	2.722	2.759	2.710	2.731	2.721	2.741	2.723	2.743	2.716	2.718	2.718
Al	1.313	1.242	1.295	1.296	1.238	1.288	1.242	1.295	1.263	1.284	1.260	1.282	1.262	1.273	1.278	1.288
Fe	0.000	0.002	0.005	0.003	0.014	0.000	0.003	0.000	0.013	0.002	0.002	0.002	0.009	0.007	0.000	0.003
Ca	0.278	0.235	0.283	0.281	0.220	0.263	0.230	0.271	0.249	0.266	0.242	0.263	0.239	0.278	0.277	0.268
Na	0.704	0.771	0.713	0.709	0.788	0.714	0.766	0.722	0.753	0.715	0.765	0.721	0.729	0.733	0.726	0.701
K	0.014	0.007	0.014	0.014	0.005	0.011	0.006	0.011	0.008	0.014	0.004	0.012	0.014	0.013	0.017	0.021
TOTAL	**5.006**	**5.012**	**5.013**	**5.009**	**5.021**	**4.997**	**5.006**	**5.009**	**5.017**	**5.001**	**5.013**	**5.003**	**4.997**	**5.020**	**5.015**	**4.999**
An	0.28	0.23	0.28	0.28	0.22	0.27	0.23	0.27	0.25	0.27	0.24	0.26	0.24	0.27	0.27	0.27
Ab	0.71	0.76	0.71	0.71	0.78	0.72	0.76	0.72	0.75	0.72	0.76	0.72	0.74	0.72	0.71	0.71
Or	0.01	0.01	0.01	0.01	0.01	0.01	0.01	0.01	0.01	0.01	0.00	0.01	0.01	0.01	0.02	0.02
X	67.52	64.98	68.28	71.77	225.31	222.61	230.06	230.06	36.41	33.75	45.28	45.28	57.84	59.62	62.34	65.37
Y	-211.32	-228.96	-228.77	-228.77	-110.02	-107.18	-157.36	-159.33	-215.46	-216.70	-253.63	-251.34	290.30	288.11	284.60	279.50
x-axis mm	1.74	0.00	0.33	0.68	0.00	0.39	0.00	0.20	0.00	0.29	0.00	0.23	0.00	0.28	0.73	1.32
	interior	*rim*	*interior*	*interior*	*rim*	*interior*	*rim*	*interior*	*rim*	*interior*	*rim*	*interior*	*rim*	*interior*	*interior*	*interior*
location	leuco	leuco	leuco	leuco	host/leuco	host/leuco	host/leuco	host/leuco	host	host	host	host	leuco	leuco	leuco	leuco

TABLE H-1: Quantitative Microprobe Analysis for Plagioclase Compositions (continued)

PC-134E-2 (continued)

leucosome															*host*	
	P3d	**P3e**	**P3f**	**P3g**	**P3h**	**P3i**	**P3j**	**P4**	**P4a**	**P5**	**P5a**	**P5b**	**P5c**	**P5d**	**P1**	**P1a**
WEIGHT PERCENT OXIDES																
SiO2	62.48	62.37	61.98	61.91	61.74	61.81	62.19	62.63	62.75	63.10	61.15	61.79	62.13	62.38	62.05	61.73
Al2O3	24.75	25.13	25.22	24.90	24.77	25.22	24.09	24.22	25.17	24.67	25.36	25.13	25.20	25.29	24.44	24.86
FeO	0.00	0.01	0.29	0.00	0.01	0.14	0.02	0.02	0.00	0.00	0.05	0.04	0.03	0.27	0.07	0.00
CaO	5.79	6.08	6.19	5.93	6.09	5.99	5.05	4.91	5.94	5.22	5.95	5.89	5.97	6.12	4.94	5.98
Na2O	8.47	8.12	7.95	8.24	8.29	8.25	9.09	8.82	8.15	8.73	8.41	8.09	8.24	8.26	8.62	8.21
K2O	0.41	0.38	0.41	0.40	0.37	0.26	0.13	0.10	0.24	0.16	0.36	0.37	0.35	0.42	0.12	0.26
TOTAL	**101.90**	**102.08**	**102.05**	**101.38**	**101.27**	**101.67**	**100.58**	**100.69**	**102.25**	**101.88**	**101.28**	**101.30**	**101.92**	**102.74**	**100.24**	**101.04**
CATIONS RECALCULATED TO 8 OXYGENS																
Si	2.726	2.715	2.704	2.715	2.713	2.704	2.744	2.753	2.722	2.744	2.689	2.710	2.710	2.705	2.741	2.714
Al	1.272	1.289	1.297	1.287	1.283	1.300	1.253	1.255	1.287	1.264	1.314	1.299	1.295	1.292	1.273	1.288
Fe	0.000	0.000	0.011	0.000	0.000	0.005	0.001	0.001	0.000	0.000	0.002	0.001	0.001	0.010	0.003	0.000
Ca	0.271	0.283	0.289	0.278	0.287	0.281	0.239	0.231	0.276	0.243	0.281	0.277	0.279	0.284	0.234	0.282
Na	0.716	0.685	0.673	0.701	0.706	0.699	0.777	0.752	0.685	0.736	0.717	0.688	0.697	0.694	0.738	0.700
K	0.023	0.021	0.023	0.022	0.020	0.014	0.008	0.005	0.013	0.009	0.020	0.021	0.019	0.023	0.007	0.014
TOTAL	**5.008**	**4.994**	**4.996**	**5.004**	**5.009**	**5.003**	**5.022**	**4.998**	**4.984**	**4.996**	**5.022**	**4.995**	**5.001**	**5.008**	**4.995**	**4.999**
An	0.27	0.29	0.29	0.28	0.28	0.28	0.23	0.23	0.28	0.25	0.28	0.28	0.28	0.28	0.24	0.28
Ab	0.71	0.69	0.68	0.70	0.70	0.70	0.76	0.76	0.70	0.75	0.70	0.70	0.70	0.69	0.75	0.70
Or	0.02	0.02	0.02	0.02	0.02	0.01	0.01	0.01	0.01	0.01	0.02	0.02	0.02	0.02	0.01	0.01
X	69.33	73.44	80.56	84.41	91.73	95.39	98.34	225.28	219.63	204.52	201.08	193.04	185.30	179.63	46.54	47.64
Y	276.60	271.84	266.27	261.81	256.29	252.73	250.66	239.50	235.10	263.18	262.57	259.09	255.15	256.12	242.11	244.29
x-axis mm	1.81	2.44	3.34	3.93	4.85	5.36	5.72	0.00	0.72	0.00	0.35	1.23	2.09	2.67	0.00	0.24
location	*interior* leuco	*interior* leuco	*interior* leuco	*interior* leuco	*interior* leuco	*interior* leuco	*rim* leuco	*rim* leuco	*interior* leuco	*rim* leuco	*interior* leuco	*interior* leuco	*interior* leuco	*interior* leuco	*rim* host	*interior* host

TABLE H-1: Quantitative Microprobe Analysis for Plagioclase Compositions (continued)

PC-134E-2 (cont'd)			***PC-134E-2A***													
host			*host*													
	P2	**P2a**	**P1**	**P1a**	**P1b**	**P1c**	**P1d**	**P2**	**P2a**	**P2b**	**P3**	**P3a**	**P4**	**P4a**	**P5**	**P6**
WEIGHT PERCENT OXIDES																
SiO2	62.43	62.82	63.22	62.00	61.49	60.67	61.92	62.04	61.08	61.48	62.86	62.96	62.78	60.99	62.64	63.47
Al2O3	24.42	24.94	24.65	24.96	25.10	25.29	25.06	24.62	25.07	25.12	24.48	24.49	24.72	25.45	24.38	23.91
FeO	0.01	0.00	0.12	0.03	0.00	0.00	0.16	0.15	0.00	0.00	0.04	0.10	0.27	0.06	0.00	0.00
CaO	5.18	5.87	4.81	5.64	5.82	5.74	5.47	4.98	5.67	5.82	4.87	5.05	5.20	5.64	5.18	4.23
Na2O	8.69	8.50	8.86	8.43	8.23	8.40	8.63	8.81	8.14	8.48	8.84	8.88	9.02	8.40	9.00	9.24
K2O	0.14	0.22	0.19	0.27	0.28	0.26	0.13	0.17	0.14	0.19	0.11	0.17	0.13	0.22	0.13	0.08
TOTAL	**100.87**	**102.36**	**101.85**	**101.33**	**100.93**	**100.35**	**101.36**	**100.78**	**100.09**	**101.09**	**101.20**	**101.65**	**102.12**	**100.77**	**101.32**	**100.93**
CATIONS RECALCULATED TO 8 OXYGENS																
Si	2.743	2.725	2.749	2.717	2.707	2.689	2.713	2.731	2.707	2.703	2.750	2.746	2.731	2.690	2.742	2.779
Al	1.264	1.275	1.263	1.289	1.302	1.321	1.294	1.277	1.310	1.302	1.262	1.259	1.268	1.323	1.258	1.233
Fe	0.000	0.000	0.004	0.001	0.000	0.000	0.006	0.006	0.000	0.000	0.001	0.004	0.010	0.002	0.000	0.000
Ca	0.244	0.273	0.224	0.265	0.274	0.272	0.257	0.235	0.269	0.274	0.228	0.236	0.242	0.267	0.243	0.199
Na	0.740	0.715	0.747	0.716	0.703	0.722	0.733	0.752	0.699	0.723	0.750	0.751	0.760	0.719	0.764	0.784
K	0.008	0.012	0.010	0.015	0.016	0.015	0.007	0.010	0.008	0.011	0.006	0.009	0.007	0.012	0.007	0.004
TOTAL	**4.999**	**5.001**	**4.998**	**5.004**	**5.001**	**5.019**	**5.010**	**5.011**	**4.992**	**5.012**	**4.997**	**5.005**	**5.019**	**5.014**	**5.014**	**4.999**
An	0.25	0.27	0.23	0.27	0.28	0.27	0.26	0.24	0.28	0.27	0.23	0.24	0.24	0.27	0.24	0.20
Ab	0.75	0.71	0.76	0.72	0.71	0.72	0.74	0.75	0.72	0.72	0.76	0.75	0.75	0.72	0.75	0.79
Or	0.01	0.01	0.01	0.01	0.02	0.01	0.01	0.01	0.01	0.01	0.01	0.01	0.01	0.01	0.01	0.00
X	50.17	48.74	-35.58	-36.18	-36.47	-36.92	-38.09	-43.29	-44.58	-46.36	-161.36	-160.76	-124.36	-127.53	-234.69	-149.18
Y	256.24	254.45	127.68	128.84	130.59	132.14	133.20	121.62	122.39	120.20	77.80	80.07	67.05	67.29	121.95	168.13
x-axis mm	0.00	0.23	0.00	0.13	0.31	0.47	0.63	0.00	0.15	0.43	0.00	0.23	0.00	0.32		0.00
	rim	*interior*	*rim*	*interior*	*interior*	*interior*	*rim*	*rim*	*interior*	*interior*	*rim*	*interior*	*rim*	*interior*	*rim*	*rim*
location	host	host	host	host	host	host	host	host	host	host	host	host	host	host	host	host

TABLE H-1: Quantitative Microprobe Analysis for Plagioclase Compositions (continued)

PC-134E-2A (cont'd)				***PC-134M-1***												
host				*leucosome*											*host*	
	P6a	**P7**	**P7a**	**P5**	**P5a**	**P5b**	**P5c**	**P5d**	**P5e**	**P7**	**P7a**	**P7b**	**P6**	**P6a**	**P1**	**P2**
WEIGHT PERCENT OXIDES																
SiO2	61.49	63.28	61.07	61.96	60.88	60.94	61.37	61.71	61.39	60.46	60.23	61.34	61.52	61.32	60.64	61.76
Al2O3	24.94	24.32	25.52	24.82	25.20	24.95	25.33	25.01	25.18	24.58	24.78	24.57	24.91	25.00	25.12	23.77
FeO	0.00	0.00	0.00	0.23	0.05	0.02	0.10	0.06	0.17	0.14	0.12	0.07	0.11	0.02	0.32	0.21
CaO	5.57	5.16	5.96	5.49	6.01	6.10	5.98	5.83	5.77	5.83	5.86	5.84	5.85	5.82	5.85	4.63
Na2O	8.37	9.06	8.33	8.77	8.15	8.11	8.16	8.37	8.35	8.41	8.37	8.22	8.32	8.31	8.44	9.09
K2O	0.26	0.14	0.21	0.13	0.33	0.35	0.36	0.31	0.22	0.18	0.31	0.30	0.18	0.31	0.18	0.14
TOTAL	**100.63**	**101.96**	**101.08**	**101.40**	**100.62**	**100.48**	**101.30**	**101.30**	**101.08**	**99.60**	**99.68**	**100.34**	**100.88**	**100.77**	**100.54**	**99.60**
CATIONS RECALCULATED TO 8 OXYGENS																
Si	2.713	2.752	2.687	2.717	2.692	2.699	2.695	2.709	2.701	2.702	2.692	2.717	2.710	2.705	2.687	2.751
Al	1.297	1.247	1.323	1.282	1.313	1.302	1.311	1.294	1.305	1.295	1.306	1.283	1.293	1.300	1.312	1.248
Fe	0.000	0.000	0.000	0.009	0.002	0.001	0.004	0.002	0.006	0.005	0.005	0.002	0.004	0.001	0.012	0.008
Ca	0.263	0.240	0.281	0.258	0.285	0.290	0.282	0.274	0.272	0.279	0.281	0.277	0.276	0.275	0.278	0.221
Na	0.716	0.764	0.710	0.745	0.699	0.697	0.695	0.712	0.712	0.729	0.726	0.706	0.711	0.711	0.725	0.785
K	0.015	0.008	0.012	0.007	0.019	0.020	0.020	0.018	0.012	0.010	0.018	0.017	0.010	0.017	0.010	0.008
TOTAL	**5.004**	**5.011**	**5.013**	**5.018**	**5.010**	**5.008**	**5.007**	**5.009**	**5.009**	**5.020**	**5.027**	**5.003**	**5.004**	**5.009**	**5.024**	**5.021**
An	0.26	0.24	0.28	0.26	0.28	0.29	0.28	0.27	0.27	0.27	0.27	0.28	0.28	0.27	0.27	0.22
Ab	0.72	0.75	0.71	0.74	0.70	0.69	0.70	0.71	0.71	0.72	0.71	0.71	0.71	0.71	0.72	0.77
Or	0.01	0.01	0.01	0.01	0.02	0.02	0.02	0.02	0.01	0.01	0.02	0.02	0.01	0.02	0.01	0.01
X	-148.04	-159.51	-157.04	114.33	116.48	118.86	121.62	124.64	126.48	164.39	166.56	167.93	142.05	139.99	63.08	46.37
Y	164.89	177.88	178.18	200.69	200.14	198.99	198.80	196.90	196.77	269.44	267.46	266.22	239.04	239.42	234.32	223.09
x-axis mm	0.34	0.00	0.25	0.00	0.22	0.49	0.76	1.12	1.30	0.00	0.29	0.48	0.00	0.21		0.00
	interior	*rim*	*interior*	*rim*	*interior*	*interior*	*interior*	*interior*	*rim*	*rim*	*interior*	*interior*	*rim*	*interior*	*rim*	*rim*
location	host	host	host	leuco	leuco	leuco	leuco	leuco	leuco	leuco	leuco	leuco	±leuco	±leuco	host	host

TABLE H-1: Quantitative Microprobe Analysis for Plagioclase Compositions (continued)

PC-134M-1 (continued)					***PC-134M-1A***											
host					*host*											
	P2a	**P3a**	**P4**	**P4a**	**P1**	**P1a**	**P2**	**P2a**	**P2b**	**P2c**	**P3**	**P3a**	**P4**	**P4a**	**P5**	**P5a**
WEIGHT PERCENT OXIDES																
SiO2	61.20	61.45	61.62	60.56	60.44	61.71	61.56	62.01	61.91	62.12	61.24	61.76	61.74	61.71	61.46	61.51
Al2O3	24.65	25.00	24.79	24.93	24.96	25.11	24.95	25.04	25.25	25.07	25.00	24.53	25.21	24.92	24.74	24.74
FeO	0.13	0.05	0.00	0.17	0.17	0.26	0.05	0.00	0.11	0.13	0.02	0.20	0.00	0.01	0.10	0.03
CaO	5.74	5.90	5.78	5.90	5.55	5.56	6.16	5.63	5.80	5.84	5.70	5.89	5.95	6.00	5.89	5.77
Na2O	8.22	8.39	8.31	8.28	8.32	8.29	8.34	8.42	8.28	8.34	8.49	7.95	8.36	8.23	8.48	8.37
K2O	0.20	0.24	0.19	0.25	0.28	0.29	0.20	0.26	0.29	0.25	0.13	0.28	0.16	0.30	0.21	0.36
TOTAL	**100.14**	**101.03**	**100.69**	**100.09**	**99.72**	**101.21**	**101.25**	**101.36**	**101.64**	**101.76**	**100.58**	**100.62**	**101.43**	**101.17**	**100.88**	**100.77**
CATIONS RECALCULATED TO 8 OXYGENS																
Si	2.715	2.705	2.717	2.694	2.696	2.709	2.705	2.716	2.707	2.713	2.705	2.726	2.704	2.711	2.710	2.714
Al	1.289	1.297	1.288	1.307	1.312	1.300	1.292	1.293	1.301	1.290	1.302	1.276	1.302	1.290	1.286	1.286
Fe	0.005	0.002	0.000	0.006	0.006	0.009	0.002	0.000	0.004	0.005	0.001	0.007	0.000	0.000	0.004	0.001
Ca	0.273	0.278	0.273	0.281	0.265	0.261	0.290	0.264	0.272	0.273	0.270	0.279	0.279	0.282	0.278	0.273
Na	0.707	0.716	0.710	0.714	0.720	0.706	0.710	0.715	0.702	0.707	0.727	0.680	0.710	0.701	0.725	0.716
K	0.011	0.013	0.011	0.014	0.016	0.016	0.011	0.015	0.016	0.014	0.007	0.016	0.009	0.017	0.012	0.020
TOTAL	**5.000**	**5.011**	**4.999**	**5.017**	**5.016**	**5.002**	**5.010**	**5.002**	**5.001**	**5.002**	**5.012**	**4.984**	**5.005**	**5.002**	**5.015**	**5.011**
An	0.28	0.28	0.27	0.28	0.27	0.27	0.29	0.27	0.27	0.28	0.27	0.29	0.28	0.28	0.27	0.27
Ab	0.71	0.71	0.71	0.71	0.72	0.72	0.70	0.72	0.71	0.71	0.72	0.70	0.71	0.70	0.71	0.71
Or	0.01	0.01	0.01	0.01	0.02	0.02	0.01	0.01	0.02	0.01	0.01	0.02	0.01	0.02	0.01	0.02
X	46.82	50.72	97.88	98.43	-194.42	-195.65	-212.30	-210.28	-208.13	-205.35	-205.86	-207.97	-222.18	-219.33	-215.54	-215.54
Y	221.68	206.20	207.89	205.84	-47.28	-47.51	-24.34	-22.56	-20.94	-19.45	10.08	11.68	-65.65	-64.86	-81.44	-82.83
x-axis mm	0.15		0.00	0.21	0.00	0.13	0.00	0.27	0.54	0.85	0.00	0.26	0.00	0.30	0.00	0.14
	interior	*interior*	*rim*	*interior*	*rim*	*interior*	*rim*	*interior*	*interior*	*rim*	*rim*	*interior*	*rim*	*interior*	*rim*	*interior*
location	host	host	host	host	host	host	host	host	host	host	host	host	host	host	host	host

TABLE H-1: Quantitative Microprobe Analysis for Plagioclase Compositions (continued)

PC-134M-1A (continued)									***PC-134M-2***							
host									*leucosome*							
	P6	**P6a**	**P7**	**P7a**	**P8**	**P8a**	**P9**	**P9a**	**P1**	**P1a**	**P1b**	**P2**	**P2a**	**P3**	**P3a**	**P3b**
WEIGHT PERCENT OXIDES																
SiO2	62.01	61.56	62.11	62.17	62.07	61.88	61.41	62.43	61.74	61.58	61.25	61.35	61.49	61.79	60.77	60.80
Al2O3	25.05	24.96	25.11	24.66	24.84	24.99	24.92	24.83	24.75	24.91	24.66	24.56	24.67	24.90	25.13	25.05
FeO	0.24	0.05	0.08	0.10	0.12	0.00	0.00	0.00	0.00	0.08	0.08	0.00	0.05	0.00	0.13	0.19
CaO	5.79	6.00	5.73	5.69	6.03	5.81	5.77	5.85	5.45	5.93	5.97	5.78	6.00	5.72	6.06	6.02
Na2O	8.18	8.21	8.58	8.29	8.32	8.63	8.56	8.29	8.54	8.11	8.24	8.34	8.19	8.51	8.14	8.16
K2O	0.26	0.35	0.22	0.36	0.21	0.31	0.20	0.32	0.36	0.31	0.31	0.24	0.31	0.30	0.30	0.37
TOTAL	**101.52**	**101.13**	**101.83**	**101.26**	**101.58**	**101.60**	**100.85**	**101.73**	**100.84**	**100.93**	**100.51**	**100.27**	**100.70**	**101.22**	**100.53**	**100.60**
CATIONS RECALCULATED TO 8 OXYGENS																
Si	2.714	2.707	2.711	2.727	2.716	2.709	2.707	2.725	2.720	2.712	2.711	2.718	2.715	2.714	2.691	2.693
Al	1.292	1.294	1.292	1.275	1.281	1.289	1.295	1.277	1.285	1.293	1.286	1.283	1.284	1.289	1.312	1.307
Fe	0.009	0.002	0.003	0.004	0.004	0.000	0.000	0.000	0.000	0.003	0.003	0.000	0.002	0.000	0.005	0.007
Ca	0.272	0.283	0.268	0.267	0.283	0.272	0.273	0.274	0.257	0.280	0.283	0.274	0.284	0.269	0.288	0.286
Na	0.694	0.700	0.726	0.705	0.706	0.733	0.731	0.702	0.730	0.693	0.707	0.717	0.701	0.724	0.699	0.701
K	0.014	0.020	0.012	0.020	0.012	0.017	0.011	0.018	0.020	0.017	0.017	0.014	0.017	0.017	0.017	0.021
TOTAL	**4.995**	**5.005**	**5.012**	**4.998**	**5.002**	**5.021**	**5.017**	**4.996**	**5.012**	**4.997**	**5.008**	**5.006**	**5.002**	**5.013**	**5.011**	**5.014**
An	0.28	0.28	0.27	0.27	0.28	0.27	0.27	0.28	0.26	0.28	0.28	0.27	0.28	0.27	0.29	0.28
Ab	0.71	0.70	0.72	0.71	0.71	0.72	0.72	0.71	0.72	0.70	0.70	0.71	0.70	0.72	0.70	0.70
Or	0.01	0.02	0.01	0.02	0.01	0.02	0.01	0.02	0.02	0.02	0.02	0.01	0.02	0.02	0.02	0.02
X	-217.09	-218.01	-206.35	-204.57	-203.34	-206.38	-206.83	-207.59	-229.86	-229.17	-228.55	-209.95	-208.01	-197.35	-196.00	-190.39
Y	-123.33	-122.25	-145.81	-146.66	-196.99	-197.65	-211.45	-212.76	318.93	316.13	312.93	318.55	313.09	316.01	317.67	325.52
x-axis mm	0.00	0.14	0.00	0.20	0.00	0.31	0.00	0.15	0.00	0.29	0.61	0.00	0.58	0.00	0.21	1.18
	rim	*interior*	*rim*	*interior*	*rim*	*interior*	*rim*	*interior*	*rim*	*interior*	*interior*	*rim*	*interior*	*rim*	*interior*	*interior*
location	host	host	host	host	host	host	host	host	leuco	leuco	leuco	leuco	leuco	leuco	leuco	leuco

TABLE H-1: Quantitative Microprobe Analysis for Plagioclase Compositions (continued)

PC-134M-2 (continued)

leucosome									*host?*		*host*		
	P5	**P5a**	**P6**	**P6a**	**P7**	**P7a**	**P7b**	**P8**	**P8a**	**P9**	**P9a**	**P4**	**P4a**
WEIGHT PERCENT OXIDES													
SiO2	61.01	60.79	62.12	60.21	60.81	61.53	61.25	60.82	61.63	61.19	60.85	61.69	61.68
Al2O3	24.97	24.69	24.67	25.18	24.96	24.61	24.85	24.60	24.59	24.79	24.74	24.58	24.73
FeO	0.00	0.00	0.09	0.00	0.10	0.09	0.10	0.26	0.07	0.21	0.05	0.00	0.01
CaO	5.94	5.84	5.00	5.97	5.65	5.75	5.72	5.58	5.61	5.81	5.94	5.57	5.83
Na2O	8.13	8.23	8.44	8.08	8.40	8.30	8.17	8.43	8.46	8.38	8.21	8.34	8.21
K2O	0.26	0.32	0.36	0.34	0.15	0.30	0.32	0.21	0.28	0.22	0.27	0.16	0.27
TOTAL	**100.32**	**99.88**	**100.67**	**99.77**	**100.07**	**100.58**	**100.41**	**99.90**	**100.62**	**100.61**	**100.07**	**100.34**	**100.74**
CATIONS RECALCULATED TO 8 OXYGENS													
Si	2.703	2.707	2.735	2.685	2.701	2.719	2.711	2.709	2.721	2.706	2.705	2.727	2.719
Al	1.304	1.296	1.280	1.323	1.307	1.282	1.296	1.291	1.280	1.292	1.296	1.281	1.285
Fe	0.000	0.000	0.003	0.000	0.004	0.003	0.004	0.010	0.003	0.008	0.002	0.000	0.000
Ca	0.282	0.279	0.236	0.285	0.269	0.272	0.271	0.266	0.265	0.275	0.283	0.264	0.275
Na	0.698	0.711	0.721	0.699	0.724	0.711	0.701	0.728	0.724	0.719	0.707	0.715	0.702
K	0.015	0.018	0.020	0.019	0.009	0.017	0.018	0.012	0.015	0.013	0.015	0.009	0.015
TOTAL	**5.002**	**5.010**	**4.995**	**5.012**	**5.012**	**5.004**	**5.001**	**5.016**	**5.008**	**5.013**	**5.008**	**4.995**	**4.997**
An	0.28	0.28	0.24	0.28	0.27	0.27	0.27	0.26	0.26	0.27	0.28	0.27	0.28
Ab	0.70	0.71	0.74	0.70	0.72	0.71	0.71	0.72	0.72	0.71	0.70	0.72	0.71
Or	0.01	0.02	0.02	0.02	0.01	0.02	0.02	0.01	0.02	0.01	0.02	0.01	0.02
X	-104.51	-105.20	-112.22	-108.30	-97.39	-93.98	-92.89	-71.25	-69.21	-33.17	-32.73	-227.11	-224.52
Y	132.59	130.05	160.21	163.13	168.58	166.34	163.92	177.48	176.62	156.29	157.39	279.73	278.69
x-axis mm	0.00	0.26	0.00	0.49	0.00	0.41	0.67	0.00	0.22	0.00	0.12	0.00	0.28
	rim	*interior*	*rim*	*interior*	*rim*	*interior*	*interior*	*rim*	*interior*	*rim*	*interior*	*rim*	*interior*
location	leuco	leuco	leuco	leuco	leuco	leuco	leuco	small leuco	small leuco	host?	host?	host	host

TABLE H-2: Quantitative Microprobe Analysis for K-Feldspar Compositions

PC-13G										***PC-13G-1***						
leucosome					*host*					*leucosome*				*host*		
	K1	**K2**	**K3**	**K4**	**K5**	**K6**	**K7**	**K8**	**K9**	**k1**	**k2**	**k3**	**k4**	**k5**	**k6**	**k7**
WEIGHT PERCENT OXIDES																
SiO2	64.22	63.91	64.38	63.71	64.21	65.16	63.92	64.88	65.11	64.40	64.30	64.45	62.84	64.43	63.61	62.42
Al2O3	18.89	18.78	18.79	19.01	19.06	19.08	19.11	19.08	19.10	18.89	19.17	18.62	18.74	18.73	18.84	18.81
FeO	0.13	0.08	0.06	0.00	0.00	0.00	0.17	0.00	0.07	0.00	0.05	0.18	0.00	0.00	0.00	0.09
CaO	0.03	0.03	0.08	0.04	0.02	0.01	0.09	0.00	0.03	0.09	0.02	0.05	0.04	0.00	0.01	0.00
BaO	0.24	0.29	0.29	0.34	0.42	0.24	0.17	0.26	0.38	0.23	0.33	0.26	0.30	0.41	0.40	0.45
Na2O	0.70	0.69	0.90	0.77	0.83	0.71	0.88	0.70	0.71	0.91	0.68	0.82	0.60	1.10	0.90	0.71
K2O	15.98	15.78	15.78	16.00	15.97	15.96	15.68	16.14	16.16	15.93	15.91	15.73	15.90	15.69	15.59	15.65
TOTAL	**100.18**	**99.55**	**100.26**	**99.88**	**100.52**	**101.16**	**100.01**	**101.06**	**101.56**	**100.45**	**100.46**	**100.11**	**98.43**	**100.36**	**99.34**	**98.13**
CATIONS RECALCULATED TO 8 OXYGENS																
Si	2.971	2.973	2.974	2.960	2.964	2.978	2.960	2.973	2.973	2.971	2.965	2.981	2.963	2.976	2.967	2.954
Al	1.030	1.029	1.023	1.041	1.037	1.028	1.043	1.031	1.028	1.027	1.042	1.015	1.041	1.019	1.036	1.049
Fe	0.005	0.003	0.002	0.000	0.000	0.000	0.007	0.000	0.003	0.000	0.002	0.007	0.000	0.000	0.000	0.003
Ca	0.001	0.002	0.004	0.002	0.001	0.000	0.004	0.000	0.002	0.004	0.001	0.003	0.002	0.000	0.000	0.000
Ba	0.004	0.005	0.005	0.006	0.008	0.004	0.003	0.005	0.007	0.004	0.006	0.005	0.006	0.007	0.007	0.008
Na	0.062	0.062	0.080	0.069	0.075	0.063	0.079	0.062	0.063	0.081	0.061	0.073	0.054	0.099	0.081	0.065
K	0.943	0.936	0.930	0.949	0.941	0.931	0.926	0.944	0.941	0.937	0.936	0.928	0.956	0.925	0.928	0.945
TOTAL	**5.017**	**5.011**	**5.019**	**5.028**	**5.025**	**5.005**	**5.022**	**5.014**	**5.016**	**5.025**	**5.013**	**5.012**	**5.022**	**5.026**	**5.020**	**5.026**
An	0.00	0.00	0.00	0.00	0.00	0.00	0.00	0.00	0.00	0.00	0.00	0.00	0.00	0.00	0.00	0.00
Ab	0.06	0.06	0.08	0.07	0.07	0.06	0.08	0.06	0.06	0.08	0.06	0.07	0.05	0.10	0.08	0.06
Or	0.94	0.94	0.92	0.93	0.93	0.94	0.92	0.94	0.94	0.92	0.94	0.92	0.94	0.90	0.92	0.94
X	-121.25	-119.02	-114.62	-98.62	-74.84	-58.94	-192.74	-211.51	-227.51	211.64	179.47	185.63	128.10	98.97	78.29	57.24
Y	224.44	222.77	230.80	173.31	171.77	194.59	206.63	218.45	190.08	145.54	222.61	269.37	269.95	185.80	183.12	176.73
location	*leuco*	*leuco*	*leuco*	*leuco*	*host*	*host*	*host*	*host*	*host*	*leuco*	*leuco*	*leuco*	*leuco/host*	*host*	*host*	*host*

TABLE H-2: Quantitative Microprobe Analysis for K-Feldspar Compositions (continued)

PC-13I								***PC-13I-1***					***PC-111I***					
host					*leucosome*			*leuco*	*host*				*leucosome*					
	'PH1'	**K1**	**K2**	**K3**	**K4**	**K5**	**K6**	**K1**	**K2**	**K3**	**K4**	**K5**	**K1**	**K2**	**K3**	**K4**	**K5**	**K6**
WEIGHT PERCENT OXIDES																		
SiO2	64.85	63.68	65.18	64.66	63.44	65.25	63.78	64.14	64.03	63.95	62.98	63.88	64.47	64.42	63.90	63.47	63.17	64.29
Al2O3	20.78	18.64	18.63	18.94	18.53	18.97	19.06	18.67	18.69	18.48	18.95	18.77	19.62	19.50	19.10	19.09	19.16	19.11
FeO	0.39	0.00	0.01	0.16	0.01	0.04	0.00	0.12	0.10	0.02	0.03	0.11	0.06	0.06	0.05	0.14	0.03	0.14
CaO	0.04	0.00	0.02	0.03	0.00	0.01	0.03	0.02	0.03	0.02	0.02	0.04	0.31	0.26	0.18	0.04	0.15	0.12
BaO		0.83	0.59	0.64	0.59	0.64	0.63	0.75	0.75	0.79	0.81	0.76	0.30	0.39	0.40	0.46	0.38	0.45
Na2O	0.53	0.72	0.68	0.74	0.66	1.21	0.75	0.77	0.64	0.70	0.79	0.69	3.38	3.30	1.96	1.39	1.83	2.27
K2O	15.84	16.07	15.75	15.98	15.96	15.40	16.09	14.85	15.08	14.83	14.73	14.95	11.40	11.45	13.22	14.22	13.34	12.70
TOTAL	**102.42**	**99.95**	**100.85**	**101.15**	**99.18**	**101.51**	**100.33**	**99.32**	**99.32**	**98.77**	**98.30**	**99.19**	**99.53**	**99.36**	**98.81**	**98.80**	**98.06**	**99.07**
CATIONS RECALCULATED TO 8 OXYGENS																		
Si	2.924	2.969	2.992	2.971	2.973	2.978	2.958	2.985	2.983	2.991	2.964	2.978	2.953	2.957	2.967	2.962	2.958	2.971
Al	1.104	1.024	1.008	1.026	1.023	1.020	1.042	1.024	1.026	1.019	1.051	1.032	1.059	1.055	1.045	1.050	1.058	1.041
Fe	0.015	0.000	0.000	0.006	0.000	0.001	0.000	0.005	0.004	0.001	0.001	0.004	0.002	0.002	0.002	0.005	0.001	0.005
Ca	0.002	0.000	0.001	0.001	0.000	0.000	0.001	0.001	0.002	0.001	0.001	0.002	0.015	0.013	0.009	0.002	0.008	0.006
Ba		0.015	0.011	0.011	0.011	0.011	0.011	0.014	0.014	0.014	0.015	0.014	0.005	0.007	0.007	0.008	0.007	0.008
Na	0.046	0.065	0.061	0.066	0.060	0.107	0.067	0.069	0.058	0.063	0.072	0.062	0.300	0.294	0.176	0.125	0.166	0.204
K	0.911	0.956	0.923	0.937	0.954	0.897	0.952	0.881	0.896	0.885	0.884	0.889	0.666	0.670	0.783	0.847	0.797	0.749
TOTAL	**5.002**	**5.029**	**4.995**	**5.018**	**5.022**	**5.014**	**5.031**	**4.979**	**4.981**	**4.974**	**4.989**	**4.981**	**5.001**	**4.998**	**4.990**	**4.999**	**4.995**	**4.984**
An	0.00	0.00	0.00	0.00	0.00	0.00	0.00	0.00	0.00	0.00	0.00	0.00	0.02	0.01	0.01	0.00	0.01	0.01
Ab	0.05	0.06	0.06	0.07	0.06	0.11	0.07	0.07	0.06	0.07	0.08	0.07	0.31	0.30	0.18	0.13	0.17	0.21
Or	0.95	0.94	0.94	0.93	0.94	0.89	0.93	0.93	0.94	0.93	0.92	0.93	0.68	0.69	0.81	0.87	0.82	0.78
X	-57.68	-173.53	-180.71	-218.20	-95.58	-93.98	-140.15	-30.74	-89.31	-99.45	-119.26	-143.62	-77.39	-87.09	-225.03	-126.73	-128.57	-96.05
Y	235.61	-203.85	-230.80	-214.92	-205.74	-220.94	-119.27	270.87	240.74	255.73	224.78	240.92	-248.78	-209.28	-218.13	-274.96	-259.36	-133.59
location	*host*	*host*	*host*	*host*	*leuco*	*leuco*	*leuco*	*leuco*	*host*	*host*	*host*	*host*	*leuco*	*leuco*	*leuco*	*leuco*	*leuco*	*leuco*

TABLE H-2: Quantitative Microprobe Analysis for K-Feldspar Compositions (continued)

PC-111I-1A						***PC-113B***								***PC-113M-2***				
host					*leucosome*	*leucosome*								*leucosome*			*host*	
	k1	**k2**	**k3**	**k4**	**k5**	**K1**	**K2**	**K3**	**K4**	**K5**	**K6**	**K7**	**K8**	**K1**	**K2**	**K3**	**K4**	**K5**
WEIGHT PERCENT OXIDES																		
SiO2	64.21	64.08	64.48	65.57	64.24	63.61	63.46	63.81	64.80	64.12	63.44	63.64	64.14	64.42	63.37	63.83	64.82	64.08
Al2O3	19.49	19.32	19.29	19.42	19.53	18.92	19.29	19.22	19.43	19.18	18.97	19.04	19.01	18.87	18.82	19.16	18.85	19.25
FeO	0.00	0.05	0.00	0.18	0.10	0.00	0.00	0.02	0.08	0.00	0.00	0.00	0.03	0.12	0.00	0.00	0.02	0.09
CaO	0.09	0.05	0.06	0.07	0.03	0.04	0.03	0.06	0.36	0.07	0.04	0.04	0.05	0.20	0.04	0.14	0.02	0.06
BaO	0.72	0.71	0.50	0.49	0.69	0.59	0.67	0.47	0.33	0.50	0.72	0.59	0.58	0.28	0.38	0.32	0.64	0.62
Na2O	1.59	1.48	1.21	1.75	1.58	1.21	1.02	1.21	3.13	1.68	1.22	1.65	1.60	2.50	1.69	2.90	1.94	3.07
K2O	15.10	14.68	14.86	14.50	14.94	14.33	14.37	13.99	11.53	13.96	14.17	13.78	13.70	12.27	13.68	12.21	13.03	11.62
TOTAL	**101.19**	**100.36**	**100.40**	**101.99**	**101.12**	**98.69**	**98.85**	**98.77**	**99.65**	**99.50**	**98.55**	**98.74**	**99.09**	**98.66**	**97.97**	**98.55**	**99.32**	**98.79**
CATIONS RECALCULATED TO 8 OXYGENS																		
Si	2.945	2.955	2.965	2.966	2.946	2.972	2.961	2.969	2.964	2.966	2.969	2.967	2.975	2.981	2.972	2.962	2.990	2.964
Al	1.053	1.050	1.045	1.035	1.055	1.042	1.061	1.054	1.047	1.045	1.046	1.046	1.039	1.029	1.040	1.048	1.025	1.049
Fe	0.000	0.002	0.000	0.007	0.004	0.000	0.000	0.001	0.003	0.000	0.000	0.000	0.001	0.005	0.000	0.000	0.001	0.004
Ca	0.004	0.002	0.003	0.004	0.002	0.002	0.001	0.003	0.018	0.003	0.002	0.002	0.002	0.010	0.002	0.007	0.001	0.003
Ba	0.013	0.013	0.009	0.009	0.012	0.011	0.012	0.008	0.006	0.009	0.013	0.011	0.010	0.005	0.007	0.006	0.012	0.011
Na	0.142	0.132	0.108	0.154	0.141	0.110	0.093	0.109	0.278	0.151	0.111	0.149	0.144	0.224	0.153	0.260	0.173	0.275
K	0.883	0.864	0.872	0.837	0.874	0.854	0.855	0.830	0.673	0.824	0.846	0.819	0.811	0.724	0.819	0.723	0.767	0.686
TOTAL	**5.041**	**5.018**	**5.002**	**5.011**	**5.034**	**4.989**	**4.983**	**4.974**	**4.988**	**4.999**	**4.987**	**4.994**	**4.983**	**4.979**	**4.993**	**5.006**	**4.968**	**4.992**
An	0.00	0.00	0.00	0.00	0.00	0.00	0.00	0.00	0.02	0.00	0.00	0.00	0.00	0.01	0.00	0.01	0.00	0.00
Ab	0.14	0.13	0.11	0.15	0.14	0.11	0.10	0.12	0.29	0.15	0.12	0.15	0.15	0.23	0.16	0.26	0.18	0.29
Or	0.86	0.87	0.89	0.84	0.86	0.88	0.90	0.88	0.69	0.84	0.88	0.84	0.85	0.76	0.84	0.73	0.82	0.71
X	198.29	197.96	224.88	238.74	29.08	70.46	74.19	41.03	105.47	93.20	64.33	132.03	141.67	-112.40	-129.57	-127.61	-41.85	-40.23
Y	-215.22	-223.03	-237.22	-240.36	-325.07	116.00	141.19	91.01	29.94	33.82	349.79	389.55	378.78	-66.52	-86.98	-153.26	-312.86	-302.01
location	*host*	*host*	*host*	*host*	*leuco?*	*leuco*	*leuco*	*leuco*	*leuco*	*leuco*	*near grt host*	*host*	*host*	*leuco*	*leuco*	*leuco*	*host?*	*host?*

TABLE H-2: Quantitative Microprobe Analysis for K-Feldspar Compositions (continued)

PC-113M-2 cont'd			*PC-134E-1*				*PC-134E-2*			*PC-134E-2A*					
leucosome				*leucosome*		*host*	*leucosome*			*host*					
	K6	**K7**	**K1**	**K2**	**K3**	**K4**	**K1**	**K2**	**K3**	**K1**	**K2**	**K3**	**K4**	**K5**	**'P3'**
WEIGHT PERCENT OXIDES															
SiO2	63.03	64.17	63.91	64.59	63.31	64.36	64.66	65.18	64.53	63.33	64.25	64.49	63.59	63.35	65.76
Al2O3	19.12	19.01	19.06	19.49	19.19	18.84	19.26	19.27	19.02	19.01	19.36	19.32	19.21	19.40	19.26
FeO	0.05	0.06	0.06	0.00	0.06	0.08	0.01	0.00	0.02	0.00	0.03	0.00	0.14	0.00	0.13
CaO	0.13	0.14	0.04	0.37	0.06	0.04	0.00	0.05	0.17	0.07	0.03	0.07	0.01	0.04	0.06
BaO	0.29	0.45	0.81	0.48	0.54	0.55	0.73	1.04	0.53	0.52	0.43	0.72	0.70	0.85	0.59
Na2O	2.26	1.93	1.19	2.97	1.64	1.58	1.37	1.02	1.44	1.22	2.16	1.75	1.66	1.43	1.43
K2O	12.85	13.34	14.07	11.72	13.69	13.73	15.33	14.94	14.86	15.06	13.52	14.25	14.69	14.93	14.73
TOTAL	**97.74**	**99.09**	**99.13**	**99.62**	**98.50**	**99.18**	**101.34**	**101.51**	**100.57**	**99.21**	**99.78**	**100.59**	**99.99**	**99.99**	**101.97**
CATIONS RECALCULATED TO 8 OXYGENS															
Si	2.957	2.973	2.972	2.960	2.958	2.982	2.960	2.973	2.967	2.957	2.959	2.961	2.949	2.942	2.976
Al	1.057	1.038	1.045	1.053	1.057	1.029	1.039	1.036	1.031	1.046	1.051	1.045	1.050	1.062	1.027
Fe	0.002	0.002	0.002	0.000	0.003	0.003	0.000	0.000	0.001	0.000	0.001	0.000	0.005	0.000	0.005
Ca	0.006	0.007	0.002	0.018	0.003	0.002	0.000	0.002	0.009	0.004	0.001	0.003	0.000	0.002	0.003
Ba	0.005	0.008	0.015	0.009	0.010	0.010	0.013	0.019	0.010	0.009	0.008	0.013	0.013	0.016	0.010
Na	0.205	0.173	0.107	0.264	0.149	0.142	0.121	0.090	0.128	0.111	0.193	0.155	0.149	0.129	0.126
K	0.769	0.788	0.834	0.685	0.816	0.812	0.895	0.869	0.871	0.897	0.795	0.835	0.869	0.884	0.851
TOTAL	**5.002**	**4.989**	**4.977**	**4.988**	**4.995**	**4.980**	**5.029**	**4.989**	**5.017**	**5.024**	**5.009**	**5.012**	**5.035**	**5.034**	**4.998**
An	0.01	0.01	0.00	0.02	0.00	0.00	0.00	0.00	0.01	0.00	0.00	0.00	0.00	0.00	0.00
Ab	0.21	0.18	0.11	0.27	0.15	0.15	0.12	0.09	0.13	0.11	0.20	0.16	0.15	0.13	0.13
Or	0.78	0.81	0.88	0.71	0.84	0.85	0.88	0.90	0.86	0.89	0.80	0.84	0.85	0.87	0.87
X	-86.84	-167.77	229.40	87.77	106.06	36.69	77.65	169.01	89.61	-20.71	-153.34	-124.41	-177.22	-156.95	-155.68
Y	-265.48	-282.41	-154.66	-215.51	-164.55	-173.39	92.66	84.36	357.28	112.43	83.04	82.30	171.46	162.31	85.76
			incl in pl												
location	*leuco*	*leuco*	*host/leuco*	*leuco*	*leuco*	*host*	*leuco*	*leuco*	*leuco*	*host*	*host*	*host*	*host*	*host*	*host*

APPENDIX I

Heating and Freezing Measurements

TABLE I-1: PC-113M Aqueous Fluid Inclusion Data

LEUCOSOME								HOST							
Fracture Number	**Sample Number**	**approx. Te (°C)**	**Tm ice (°C)**	**Th L (°C)**	**Tm salt (°C)**	**Td (°C)**	**Size (microns)**	**Fracture Number**	**Sample Number**	**approx. Te (°C)**	**Tm ice (°C)**	**Th L (°C)**	**Tm salt (°C)**	**Td (°C)**	**Size (microns)**
1-3a	2/1a	-65	-32.2	-	-	-	10	8-1	1	-90	-44.0	152	180	486	11
	2/2a	-	-31.2	-	-	482	4	9-4	a	-74	-41.9	-	-	-	12
	average:	*-65*	*-31.7*						b	-75	-42.6	165	182	-	7
1-3b	3/1a	-63	-32.6	393	-	-	12		c	-68	-44.4	175	186	-	3
	3/1b	-	-31.2	-	-	-	4		*average:*	*-72*	*-43.0*	*170*	*184*		
	average:	*-63*	*-31.9*	*393*				9-7	7	-40	-11.4	151	-	-	3
1-4	4/3c	-24	-10.5	-	-	-	10	10-3	3	-	-	148	191	-	5
	4/4c	-22	-10.4	230	-	-	10	10-4	4	-	-	140	196	-	
	4/5c	-	-	230	-	-	8	*cluster*	10-1a	-	-	153	184	-	12
	average:	*-23*	*-10.5*	*230*					10-1b	-	-	148	179	-	6
1-5	5/2a	-40	-24.5	decrep?	-	-	5		*average:*			*151*	*181*		
	5/1b	-	-23.2	370	-	-	5	*cluster?*	10-2	-	-22.0	139	194	-	3
	average:	*-40*	*-23.9*	*370*				*isolated*	9-2	-41	-11.6	150	-	-	6
1-6	7/1a	-22	-9.5	232	-	-	9								
	7/1b	-25	-10.5	-	-	-	12								
	average:	*-24*	*-10.0*	*232*				*NOTE:*	*The gas flow stage was not recently calibrated prior to use.*						
2-1	a	-43	10.5	63	-	-	3		*A second gas flow stage in the same room was more recently*						
2-2	a	-52	-22.7	157	-	-	6		*calibrated and it read from 0.7 to 1.1°C higher at room temperature.*						
2-4	a	-22	-17.4	172	-	-	3		*Therefore, these reading may be about 1° too low.*						
2-5	a	-	-6.6	391	-	-	10								
2-8	a	-67	-32.7	138	-	-	4								
2-9	a	-29	-16.7	193	-	-	3								
2-7	e	-45	-31.7	177	-	-	12								
	8/b	-	-33.0	166	-	-	4								
	average:	*-45*	*-32.4*	*172*											
3-1	a	50	-25.3	79	-	-	3								
	b	49	-24.1	84	-	-	3								
	average:	*49*	*-24.7*	*84*											
3-2	a	-3	0.0	273	-	-	4								
	b	-5	-1.0	-	-	-	5								
	average:	*-4*	*-0.5*	*273*											
3-3	a	-32	-24.0	-	-	-	6								
	b	-27	-22.4	-	-	448	6								
	average:	*-30*	*-23.2*												
4-1	a	-66	-39.4	131	167	-	3								
	b	-	-	119	-	-	3								
	average:	*-66*	*-39.4*	*125*											
4-3	a	-56	-21.4	98	-	-	5								
4-4	a	-55	-22.1	139	-	-	6								
4-6	a	-69	-22.4	151	-	-	6								
cluster	2-9a/a	-25	-9.9	386	-	-	10								
cluster	2-9b/a	-27	-12.2	235	-	-	6								
isolated	2-2b	-28	-17.5	decrep	354	-	10								
isolated	2-8a	-37	-17.3	384	-	-	4								
isolated	2-10a	-36	-14.5	243	-	-	6								

TABLE I-2: PC-113M CO2 Fluid Inclusion Data										
LEUCOSOME						HOST				
Fracture	**Sample**	**Tm**	**Th L**	**Th V**	**Size**	**Fracture**	**Sample**	**Tm**	**Th L**	**Size**
Number	**Number**	**(°C)**	**(°C)**	**(°C)**	**(microns)**	**Number**	**Number**	**(°C)**	**(°C)**	**(microns)**
1-1	1/1	-57.5	22.2		10	6-3	a	-57.4	26.4	7
	1/2	-57.6	22.8		6		b	-57.4	26.4	6
	1/3	-57.6	22.3		5		d	-57.4	26.6	9
	1/4	-57.1	22.4		5		*Average:*	*-57.4*	*26.5*	
	1/5	-57.2	22.7		5	7-4	4a	-57.5	25.5	8
	Average:	*-57.4*	*22.5*				4b	-57.6	26.6	6
1-2	3/4a	-57.3	22.7		8		*Average:*	*-57.6*	*26.1*	
	3/5a	-57.3	22.8		9	*isolated*	6-2	-57.7	12.6	4
	4/3a	-57.5	22.3		12					
	4/1c	-57.4	23.5		8					
	4/2c	-57.3	23.6		9					
	8/1a	-57.3	22.7		9	*NOTE:*	*The gas flow stage was not recently*			
	8/2a	-57.3	22.5		8		*calibrated prior to use. A second gas*			
	Average:	*-57.3*	*22.9*				*flow stage in the same room was more*			
2-6	6a	-56.9	28.8		5		*recently calibrated and it read from 0.7*			
	6b	-57.1	27.5		3		*to 1.1°C higher at room temperature.*			
	6c	-57.2	27.3		10		*Therefore, these reading may be about*			
	7/a	-57.2	27.4		8		*1° too low.*			
	7/b	-57.1	28.4		3					
	Average:	*-57.1*	*27.9*							
2-10	a	-57.0	25.2		3					
2-11	a	-57.0	28.7		4					
	b	-57.0	28.6		3					
	Average:	*-57.0*	*28.7*							
3-4	4a	-57.2	28.3		6					
	4b	-57.0	27.9		5					
	5a	-57.1	29.3		8					
	Average:	*-57.1*	*28.5*							
4-2	a	-57.0	25.8		3					
	b	-56.9	28.0		4					
	Average:	*-57.0*	*26.9*							
isolated	1-1/6	-57.6	11.6		12					
isolated	1-6/1a	-57.4		28.0						
isolated	2-2a	-57.1	12.4		10					
isolated	2-5a	-56.8		21.7						
isolated	2-7a	-57.0	23.5		6					
isolated	2-10b	-57.3	16.2		15					

TABLE I-3: PC-113M H20-CO2 Fluid Inclusion Data								
Fracture Number	**Sample Number**	**TmCO2 (°C)**	**TmH2O (°C)**	**Tm clathrate (°C)**	**ThCO2 L (°C)**	**Th(total) L (°C)**	**Td (°C)**	**Size (microns)**
LEUCOSOME								
isolated	2-11a	-59.6	-1.2	10.2	9.7	-	±390	30
HOST								
isolated	6-1	-57.2	-11.3	not observed	not observed	400.1		5

TABLE I-4: PC-13I Aqueous Fluid Inclusion Data

Chip #	Sample Number	~ Te (°C)	Tm ice (°C)	Th L (°C)	Tm DM (°C)	Td (°C)	Size (microns)
Z2E-1	2A	-78	-15.9	161	-	-	3
	2B	-71	-15.8	140	-	-	3
	2C	-72	-17.4	144	-	-	3
	2D	-75	-18.7	162	-	-	4
	average:	*-74*	*-17.0*	*152*			
	5B	-71	-21.3	142	-	-	3
	5C	-	-21.9	152	-	-	3
	average:	*-71*	*-21.6*	*147*			
	6A	-48	-9.0	128	-	-	3
	6B	-	-	113	-	-	3
	average:	*-48*	*-9.0*	*120*			
	7B	-67	-25.7	177	-	-	5
	7C	-67	-23.7	172	-	-	5
	average:	*-67*	*-24.7*	*174*			
	8A	-	-	159	-	-	6
	8B	-62	-24.6	159	175	-	3
	8C	-48	-24.1	157	180	-	6
	average:	*-55*	*-24.4*	*158*	*177*		
	9A	-	-20.8	168	-	-	3
Z2E-2	1B	-	-8.5	169	not observed		4
	1E	-	-	169	not observed		8
	average:		*-8.5*	*169*			
	3A	-40	-8.0	186	-	-	5
	3B	-34	-8.4	-	-	-	5
	average:	*-37*	*-8.2*	*186*			
	4A	-38	-8.2	179	-	-	5
	4B	-35	-9.1	-	-	-	5
	4B-1	-	-	171	-	-	3
	4B-2	-	-	180	-	-	2
	average:	*-36*	*-8.7*	*176*			
	5A	-	-	174	-	-	5
	5B	-27	-10.3	173	-	-	4
	average:	*-27*	*-10.3*	*174*			
	6B	-44	-13.2	125	-	-	3
	7A	-25	-10.5	186	-	-	5
	7C	-29	-8.5	175	-	-	5
	average:	*-27*	*-9.5*	*180*			*5*
	8A	-40	-8.1	183	-	-	4
	8B	-46	-8.5	175	-	-	8
	average:	*-43*	*-8.3*	*179*			

Chip #	Sample Number	~ Te (°C)	Tm ice (°C)	Th L (°C)	Tm DM (°C)	Td (°C)	Size (microns)
Z2E-2	9A	-52	-6.5	201	-	-	4
cont'd	9B	-44	-9.1	186	-	-	5
	average:	*-48*	*-7.8*	*193*			
	10A	-67	-26.3	183	-	-	5
	10B	-65	-27.5	178	-	-	6
	10C	-68	-26.7	183	-	-	7
	average:	*-67*	*-26.8*	*181*			
	11A	-54	-	167	not observed		4
	11B	-	-30.6	166	169		3
	11C	-71	-	171	not observed		4
	average:	*-63*	*-30.6*	*168*	*169*		
	12A	-67	-23.9	182	-	-	5
Z2W	1A	-26	-8.5	163	-	-	3
	1B	-26	-6.5	181	-	-	5
	1D	-30	-9.5	183	-	-	2
	1F	-	-9.5	183	-	-	3
	1H	-34	-8.5	174	-	-	2
	1K	-	-10.0	168	-	-	2
	1L	-42	-9.0	176	-	-	2
	1M	-38	-11.5	181	-	-	2
	average:	*-33*	*-9.1*	*176*			
	3A	-49	-15.0	158	-	-	4
	3B	-50	-14.0	-	-	-	5
	3C	-51	-15.0	178	-	-	4
	3E	-62	-17.0	169	-	-	3
	3F	-58	-15.0	181	-	-	4
	3H	-52	-14.0	154	-	-	3
	average:	*-54*	*-15.0*	*168*			
	4D	-52	-12.5	168	-	-	2
	4E	-59	-15.0	158	-	-	2
	4F	-65	-15.5	-	-	-	7
	4G	-44	-14.5	-	-	-	3
	4H	-50	-12.0	159	-	-	2
	4I	-58	-14.5	-	-	-	4
	4J	-45	-13.0	178	-	-	3
	4K	-55	-14.0	177	-	-	4
	average:	*-53*	*-13.9*	*168*			
Y2W	2A	-	-	91	-	-	3
	2B	-	-	106	-	-	4
	2C	-41	-6.5	110	-	-	5
	average:	*-41*	*-6.5*	*102*			

TABLE I-4 (continued): PC-13I Aqueous Fluid Inclusion Data

Chip #	Sample Number	~ Te (°C)	Tm ice (°C)	Th L (°C)	Tm DM (°C)	Td (°C)	Size (microns)
Y2W	3A	-34	-15.0	144	-	-	3
cont'd	3B	-	-	149	-	-	6
	3C	-	-17.0	159	-	-	3
	3D	-	-	137	-	-	4
	average:	*-34*	*-16.0*	*147*			
	4A	-40	-15.0	173	-	-	6
	4B	-42	-18.0	175	-	-	4
	average:	*-41*	*-16.5*	*174*			
Y2C	1A	-	-0.5	186	-	-	5
	1B	-	-	195	-	-	6
	average:		*-0.5*	*191*			
	2A	-	-	176	-	-	3
	2B	-	-	176	-	-	4
	2D	-	-	173	-	-	3
	3B	-	-	175	-	-	3
	average:			*175*			
	4A	-40	-13.0	190	-	-	4
	5B	-	0.0	163	-	-	3
	6C	-	-	156	-	-	3
	average:		*0.0*	*160*			
	10A	-	-	171	-	-	1
	10B	-	-	184	-	-	3
	average:			*178*			
	11A	-	-	162	178		5
	11B	-	-	167	-		4
	average:			*165*	*178*		
	13A	-	-	176	-	-	7
	13B	-	-	173	-	-	4
	13C	-	-	174	-	-	5
	13D	-	-	174	-	-	6
	average:			*174*			
W2W-E1/2	1A	-	-10.0	177	166	-	4
	2A	-	-	165	-	-	2
	2B	-63	-25.5	180	-	-	4
	average:	*-63*	*-25.5*	*173*			
	4A	-	-	187	-	-	7
	4C	-55	-15.0	185	-	-	3
	average:	*-55*	*-15.0*	*186*			
	5A	-41	-13.5	182	-	-	4
	5B	-	-	184	-	-	4
	average:	*-41*	*-13.5*	*183*			
W2W-E1/2	6A	-40	-22.0	191	-	-	6
cont'd	6B	-	-	194	-	-	2
	average:	*-40*	*-22.0*	*193*			
	7A	-	-	181	192	-	4
	7B	-34	-15.0	176	-	-	3
	7C	-	-18.0	175	-	-	4
	average:	*-34*	*-16.5*	*177*	*192*		
	8B	-	-24?	185	185	-	3
	8D	-	-	186	-	-	5
	average:		*-24?*	*186*	*185*		
	9A	-39	-17.0	194	-	-	3
	9B	-	-	183	-	-	3
	average:	*-39*	*-17.0*	*189*			
	13A	-	-	174	150	-	8
	13B	-	-	175	163	-	5
	13C	-	-6.0	172	150	-	4
	average:		*-6.0*	*174*	*154*		
V2W	4A	-	-18.0	157	-	-	5
	4B	-	-	159	-	-	4
	4C	-	-	163	-	-	10
	4D	-37	-19.0	152	-	-	3
	average:	*-37*	*-18.5*	*158*			
	5A	-51	-16.5	169	-	-	4
	5C	-	-	163	-	-	3
	5D	-	-	168	-	-	8
	5F	-	-	155	-	-	2
	average:	*-51*	*-16.5*	*164*			
	7A	-60	-11.0	169	-	-	4
	7B	-	-	166	-	-	4
	7C	-	-	170	-	-	4
	7D	-	-	163	-	-	3
	average:	*-60*	*-11.0*	*167*			
	8A	-51	-6.5	169	-	-	3
	8B	-	-	168	-	-	2
	average:	*-51*	*-6.5*	*169*			
	9A	-44	-22.5	156	-	-	5
	9B	-	-	174	-	-	3
	average:	*-44*	*-22.5*	*165*			
	10A	-	-	154	-	-	6
	10B	-52	-11	174	-	-	4
	average:	*-52*	*-11.0*	*164*			

TABLE I-5: PC-13I CO2 Fluid Inclusion Data						
	Chip	**Sample**	**Tm**	**Th L**	**Size**	
	Number	**Number**	**(°C)**	**(°C)**	**(microns)**	
	Y2C	9A	-56.2	25.0	4	
		9B	-56.6	22.0	3	
		Average:	*-56.4*	*23.5*		
		12A	-56.2	22.0	4	
		14A	-56.0	22.0	6	
	V2W	1A	-56.6	30.0	3	
		2A	-56.2	29.0	4	
		2B	-56.6	28.0	4	
		Average:	*-56.4*	*28.5*		
		3A	-56.6	29.0	2	

BARBARA J. MUNN

Geography & Earth Sciences
Shippensburg University
Shippensburg, PA 17257

Office (717) 532-1310
e-mail: bjmunn@ark.ship.edu

WORK EXPERIENCE

Shippensburg University
Shippensburg, Pennsylvania — **Assistant Professor** — 9/96-Present
teaching responsibilities:
Introduction to Geology
Historical Geology
Oceanography
Mineral and Rock Resources

The Richard Stockton College of New Jersey
Pomona, New Jersey — **Instructor of Geology** — 9/94-5/96
teaching responsibilities:
The Earth
Mineralogy
Igneous & Metamorphic Petrology

Virginia Polytechnic Institute
Blacksburg, Virginia — **Teaching Assistant** — 8/89 - 6/94

Leighton and Associates
Carlsbad, California — **Staff Geologist** — 1/87 - 5/89

Santa Fe Soils
San Diego, California — **Staff Geologist** — 9/86 - 12/86

Exxon Company, USA
New Orleans, Louisiana — **Exploration Geologist** — 11/85 - 7/86

EDUCATIONAL BACKGROUND

PhD **Virginia Polytechnic Institute** *Blacksburg, Virginia* 1997
Dissertation topic: Migmatization in the Northern Front Range, Colorado.

MS **Boston College** *Chestnut Hill, Massachusetts* 1987
Master's thesis title: Bedrock Geology at the Western Boundary of the Nashoba Block, East-Central Massachusetts.

University of Illinois *Urbana, Illinois* 1979
Geology Field Camp in the British Isles

BA **Wellesley College** *Wellesley, Massachusetts* 1979
Geology and Anthropology; Wellesley Scholar, Freshman Honors

University of New Mexico *Albuquerque, New Mexico* 1977-1978
Academic Honors, Visiting Student

PUBLICATIONS & ABSTRACTS

Munn, B.J., Tracy, R.J. and Jenks, P.J., 1995, A collaborative approach to petrology field trips: Journal Geological Education, 43, p.381-384.

Munn, B.J., Jenks, P.J., Tracy, R.J. and Miller, S.J., 1994, A collaborative approach to petrology field trips: Geological Society America Abstracts/Programs, 26, p.A-327.

Martino, R., Munn, B., Kraemer, P., Escayola, M. and Guereschi, A., 1994, Thermobarometry at 32°00'S in the Pampean Ranges near Cordoba, Argentina: Geological Society America Abstracts/Programs, 26, p.A-226.

Munn, B.J. and Tracy, R.J., 1994, Migmatite Genesis in Basement Rocks of the Northern Front Range, Colorado: EOS, Transactions, American Geophysical Union, p.360 (invited paper).

Munn, B. J., Tracy, R. J. and Armstrong, T. R., 1993, Thermobarometric clues to Proterozoic tectonism in the northern Front Range, Colorado: Geological Society America Abstracts/Programs, 25, p.A-424.

Munn, B.J. and Tracy, R.J., 1992, Thermobarometry in a migmatitic terrane, northern Front Range, Colorado: Geological Society America Abstracts/Programs, 24, p.A264-A265.

Munn, B.J., 1989, Metamorphic history of the western margin of the Nashoba Block, east-central Massachusetts: Geological Society America Abstracts/Programs, 21, p.54.

Hepburn, J. and Munn, B., 1984, A geologic traverse across the Nashoba Block, eastern Massachusetts, *in* Hanson, L., ed., Geology of the Coastal Lowlands Boston, Massachusetts to Kennebunk, Maine: 76th Annual NEIGC, p.103-123.